Fusing low-valent Germanium with Silicon: From Double Bonds to Polymers and Clusters

Dissertation

Zur Erlangung des Grades
des Doktors der Naturwissenschaften
der Naturwissenschaftlich-Technischen Fakultät
der Universität des Saarlandes

von

M. Sc. Lukas Klemmer

Saarbrücken

2021

Tag des Kolloquiums:	23. Juli 2021
Dekan:	Prof. Dr. Jörn Eric Walter
Berichterstatter:	Prof. Dr. David Scheschkewitz Dr. André Schäfer Prof. Dr. Lars Wesemann
Vorsitz:	Prof. Dr. Gregor Jung
Akademischer Mitarbeiter:	Dr. Bernd Morgenstern

Für meine Familie

The present dissertation was prepared in the time between January 2017 and March 2021 at the Institute for General and Inorganic Chemistry of the Faculty of Natural Science and Engineering at the Saarland University under the supervision of Prof. Dr. David Scheschkewitz.

Die vorliegende Dissertation wurde in der Zeit zwischen Januar 2017 und März 2021 am Institut für Allgemeine und Anorganische Chemie der Naturwissenschaftlich-Technischen Fakultät an der Universität des Saarlandes unter der Aufsicht von Prof. Dr. David Scheschkewitz erstellt.

„The philosopher may very justly be delighted with the extent of his views, and the artificer with the readiness of his hands;

but let the one remember that, without mechanical performances, refined speculation is an empty dream;

and the other that, without theoretical reasoning, dexterity is little more than a brute instinct.”

Samuel Johnson (1709–1784)

Abstract

Low-valent species of silicon and germanium play a pivotal role in the chemical vapor deposition of the bulk elements and their alloys for semiconductor applications. The transition from molecular intermediates to extended unsaturated cluster motifs incorporated into the bulk is of particular interest and stable model compounds for these species are intensively sought. This thesis investigates the structural behavior of such low-valent germanium and germanium-silicon compounds in comparison to their well-established silicon congeners. An anionic Si_4Ge_2 siliconoid is synthesized by reduction of a Si_4Ge_2 benzene and the position of the germanium atoms in the scaffold allows mechanistic insight in E_6-cluster rearrangements in general (E = Group 14 element). The first examples of heavy germanium-containing Group 14 allyl chlorides and α,β-unsaturated ketones are now accessible from a lithium digermenide and show extraordinary resilience against cyclization, a rearrangement mode commonly observed for the analogue silicon compounds. The same digermenide is used for synthesis of targeted designed asymmetric digermenes, able to undergo heavy olefin metathesis by a dissociation-association rearrangement. Two symmetric digermenes are synthesized that way and the lack of demand for any catalyst is a first in olefin metathesis in general. Extension of the concept now allows Heavy Acyclic Metathesis (HADMET) polymerization of a α,ω-bis(digermene) to the first example of a poly(digermene).

Zusammenfassung

Niedervalente Silizium- und Germaniumspezies spielen eine entscheidende Rolle in der chemischen Gasphasenabscheidung beider Elemente für Halbleiteranwendungen. Der Übergang von molekularen Intermediaten zu ungesättigten Cluster-Motiven, die im Festkörper verbleiben, ist von besonderem Interesse und stabile Modellverbindungen dieser Spezies werden intensiv gesucht. Die vorliegende Arbeit untersucht das strukturelle Verhalten solcher niedervalenter Ge- und Si/Ge-Verbindungen im Vergleich zu ihren wohlbekannten Si-analoga. Ein anionisches Si_4Ge_2 Silicoid wird durch Reduktion eines Si_4Ge_2 Benzols hergestellt und die Position der Ge-Atome im Gerüst gibt mechanistische Einblicke in E_6-Cluster Umlagerungen im Allgemeinen (E= Gruppe 14 Element). Die ersten Beispiele für schwere Ge-haltige Gruppe-14 Allylchloride sowie α,β-ungesättigte Ketone sind nun von einem Lithiumdigermenid aus zugänglich und zeigen erstaunliche Resilienz gegen Cyclisierung, eine Umlagerungsart, die häufig bei den analogen Si-verbindungen auftritt. Dasselbe Digermenid wird für die Synthese zielgerichtet gestalteter, asymmetrischer Digermene verwendet, die durch eine Dissoziations-Assoziations-Umlagerung eine schwere Olefin Metathese durchzumachen. Zwei symmetrische Digermene wurden so hergestellt und der mangelnde Bedarf an Katalysator ist eine Premiere für Olefin-Metathesen. Erweiterung des Konzepts erlaubt nun Schwere Acylische Dien Metathese (HADMET) Polymerisierung von α,ω-Bis(digermenen) zum Poly(digermen).

List of Publications

As part of the present dissertation:

- L. Klemmer, V. Huch, A. Jana, D. Scheschkewitz, An anionic heterosiliconoid with two germanium vertices. *Chem. Commun*. **2019**, *55*, 10100−10103. https://doi.org/10.1039/c9cc04576g.

- L. Klemmer*, Y. Kaiser*, V. Huch, M. Zimmer, D. Scheschkewitz, Persistent digermenes with acyl and α-chlorosilyl functionalities. *Chem. Eur. J.* **2019**, *25*, 12187−12195. https://doi.org/10.1002/chem.201902553.
  *These authors contributed equally.

- L. Klemmer, A.-L. Thömmes, M. Zimmer, V. Huch, B. Morgenstern, D. Scheschkewitz, Metathesis of Ge=Ge double bonds. *Nat. Chem.* **2021**, https://doi.org/10.1038/s41557-021-00639-9.

Others:

- N. M. Obeid, L. Klemmer, D. Maus, M. Zimmer, J. Jeck, I. Bejan, A. J. P. White, V. Huch, G. Jung, D. Scheschkewitz, (Oligo)aromatic species with one or two conjugated Si=Si bonds: near-IR emission of anthracenyl-bridged tetrasiladiene. *Dalton Trans*. **2017**, *46*, 8839−8848. https://doi.org/10.1039/c7dt00397h

- D. Nieder, L. Klemmer, Y. Kaiser, V. Huch, D. Scheschkewitz, Isolation and reactivity of a digerma analogue of vinyllithiums: a lithium digermenide. *Organometallics* **2018**, *37*, 632−635. https://doi.org/10.1021/acs.organomet.7b00470

- D. Mandal, D. Dhara, A. Maiti, L. Klemmer, V. Huch, M. Zimmer, H. S. Rzepa, D. Scheschkewitz, A. Jana, Mono- and dicoordinate Germanium(0) as a Four-Electron Donor. *Chem. Eur. J.* **2018**, *24*, 2873−2878.
  https://doi.org/10.1002/chem.201800071

- H. Zhao, K. Leszczyńska, L. Klemmer, V. Huch, M. Zimmer, D. Scheschkewitz, Disilenyl silylene reactivity of a cyclotrisilene. *Angew. Chem. Int. Ed.* **2018**, *57*, 2445−2449; *Angew. Chem.* **2018**, *130*, 2470−2474.
  English version: https://doi.org/10.1002/anie.201711833
  German version: https://doi.org/10.1002/ange.201711833

- H. Zhao, L. Klemmer, M. J. Cowley, M. Majumdar, V. Huch, M. Zimmer, D, Scheschkewitz, phenylene-bridged cross-conjugated 1,2,3-trisilacyclopenta-dienes. *Chem. Commun*. **2018**, *54*, 8399−8402.
  https://doi.org/10.1039/c8cc03297a

- H. Zhao, L. Klemmer, M. J. Cowley, V. Huch, M. Zimmer, D, Scheschkewitz, Reactivity of a peraryl cyclotrisilene (c-Si_3R_4) toward chalcogens. *Z. Anorg. Allg. Chem.* **2018**, *644*, 999−1005.
  http://dx.doi.org/10.1002/zaac.201800182

- A.-C. Andres, J. Beckmann, L. Klemmer, S. Muth, D. Scheschkewitz, M. Springborg, Structure and stability of propellane-like $E_2E'_2E''_2H_6$. *J. Mol. Model*. **2018**, *24*:190.
  https://doi.org/10.1007/s00894-018-3713-9

- A. Maiti, D. Mandal, I. Omlor, D. Dhara, L. Klemmer, V. Huch, M. Zimmer, D. Scheschkewitz, A. Jana, Equilibrium coordination of NHCs to Si(IV) species and donor exchange in donor-acceptor stabilized Si(II) and Ge(II) compounds. *Inorg. Chem.* **2019**, *58*, 4071−4075.
  https://doi.org/10.1021/acs.inorgchem.9b00246

- Y. Heider, P. Willmes, D. Mühlhausen, L. Klemmer, M. Zimmer, V. Huch, D. Scheschkewitz, A three-membered cyclic phosphasilene. *Angew. Chem. Int. Ed.* **2019**, *58*, 1939−1944; *Angew. Chem.* **2019**, *131*, 1958−1964.

  English version: https://doi.org/10.1002/anie.201811944

  German version: https://doi.org/10.1002/ange.201811944

Acknowledgements/Danksagung

Ich möchte mich zunächst besonders bei **Prof. Dr. David Scheschkewitz** für das in mich gesetzte Vertrauen bedanken, mir die niedervalente Germaniumchemie als ein ebenso anspruchsvolles wie interessantes Thema anzuvertrauen. Seine fordernde sowie fördernde Art hat mich stets inspiriert und es mir ermöglicht mich wissenschaftlich weiterzuentwickeln. Unsere zahlreichen, intensiven Diskussionen werde ich genauso positiv in Erinnerung behalten, wie die gemeinsamen Tagungsbesuche und Wanderungen mit der Arbeitsgruppe.

Dr. André Schäfer möchte ich an dieser Stelle herzlich für die Begutachtung dieser Arbeit danken.

A special thanks goes to **Dr. Diego M. Andrada** for being my mentor in terms of computational chemistry who never backed out of any discussion and who helped to gain various insights. I further wish to thank **Dr. Anukul Jana** for his support in my siliconoid project and his always cheerful and helpful nature.

Ich möchte mich außerdem besonders herzlich bei **Bianca Iannuzzi** und **Dr. Carsten Präsang** für ihre Unterstützung und Hilfsbereitschaft bedanken, sei es administrativer oder wissenschaftlicher Natur.

Ein großes Dankeschön geht an **Dr. Volker Huch** und **Dr. Bernd Morgenstern** für die Durchführung von Kristallstrukturanalyen, an **Dr. Michael Zimmer** für seine Unterstützung bei allerlei NMR-Experimenten und an **Susanne Harling** für die Durchführung von Elementaranalysen.

Ich möchte mich außerdem beim Team des AK Kickelbick und insbesondere bei **Dr. Nils Steinbrück**, **Bastian Oberhausen** und **Max Briesenick** für die Hilfestellung bei verschiedensten Festkörper-Analytikverfahren bedanken.

I want to thank **Dr. Naim Obeid**, **Dr. Hui Zhao** and **Dr. Kinga Leszczynska** for the nice and successful collaborations within their research projects.

Ich möchte mich bei allen (ehemaligen) Mitarbeitern des AK Scheschkewitz u.a., **Andreas Adolf, Eveline Altmeyer, Britta Schreiber, Sylvia Beetz, Nadine Poitiers, Andreas Kell, Marc Hunsicker, Daniel Mühlhausen, Felix Gerlach, Dr. Andreas Rammo, Dr. Paresh K. Majhi, Dr. Harinath Adimulam, Dr. Cem Yildiz, Isabell Omlor, Marcel Lambert, Ramona Cullmann** und **Lena Pesch** für die tolle Arbeitsatmosphäre und den großen Zusammenhalt im Team bedanken.

Ein großes Dankeschön verdient **Anna-Lena Thömmes**, die durch ihre ambitionierte und fleißige Art einen wichtigen Teil zu meiner Arbeit beigetragen hat und mit der es immer Spaß gemacht hat im Labor zusammenzuarbeiten.

Ich möchte mich besonders herzlich bei **Dr. David Nieder** und **Dr. Philipp Willmes** bedanken, die mich vor einer gefühlten Ewigkeit für die niedervalente Hauptgruppenchemie begeistert haben, von denen ich einerseits unglaublich viel lernen konnte, mit denen die Zusammenarbeit andererseits immer sehr viel Spaß gemacht hat und dir mir bis heute mit Rat zur Seite stehen.

Ein ganz herzliches Dankeschön möchte ich an **Alexander „Sascha“ Grandjean**, **Thomas Büttner, Dr. Yannic Heider** und **Yvonne Kaiser** richten, dafür, dass wir seit dem ersten Semester zu guten Freunden geworden sind, uns immer tatkräftig unterstützt haben und eine super Zeit mit vielen schönen Erinnerungen miteinander verbracht haben. Ohne euch hätte ich es nicht geschafft! **Yvonne** und **Yannic** gilt ein besonderer Dank, für mannigfaltige, aufschlussreiche fachliche Diskussionen, sehr unterhaltsame Kaffeepausen und feuchtfröhliche Abende während unserer gemeinsamen Promotionszeit.

Es fällt mir schwer meinen Dank für **Inga Bischoff** in Worte zu fassen, denn ihre bodenständige und geduldige Art, ihre bedingungslose Unterstützung und Liebe haben aus jedem Tief schnell wieder ein Hoch gemacht und sie hat mir immer den Rückhalt gegeben mich ganz und gar dieser Arbeit widmen zu können. Ich liebe dich!

Und wie gewohnt, kommt das Beste zum Schluss:

Ich möchte meinen Eltern **Petra** und **Peter Klemmer** und meiner Schwester **Michelle Klemmer** meine endlose Dankbarkeit ausdrücken, dafür, dass sie mich seit jeher unterstützen, mich ermutigen, wenn ich Hilfe brauche und mich am Boden halten, wenn ich drohe abzuheben. Ohne euch wäre ich nicht der, der ich bin. Danke, dass ihr immer für mich da seid, ich liebe euch!

Content

List of Abbreviations

ADMET	Acylic diene metathesis
BDE	Bond dissociation energy
BJT	Bipolar junction transistor
cAAC	cyclic Alkylaminocarbene
cal	Calory
cat.	Catalytic
cf.	*conferatur*
CGMT	Carter-Goddard-Malrieu-Trinquier
Cp	Cyclopentadienyl, -C_5H_5
Cp*	Pentamethylcyclopentadienyl, -C_5Me_5
CP/MAS	Cross-polarization/Magic angle spinning
CVD	Chemical vapor deposition
Dep	2,6-Diethylphenyl, -2,6-$Et_2C_6H_3$
DFT	Density functional theory
Dip	2,6-Diisopropylphenyl, -2,6-$^{i}Pr_2C_6H_3$
DLS	Dynamic light scattering
DMAP	4-Dimethylaminopyridine
dme	Dimethoxyethane
DSC	Differential scanning calorimetry
e.g.	*exempli gratia*
EPR	Electron paragmagnetic resonance
eq.	equivalents
Et	Ethyl, -C_2H_5
et al.	*et alii*
eV	Electronvolt
exc.	Excess
FTIR	Fourier-transform infrared
g	Gram
GPC	Gel permeation chromatography
h	Hour
HADMET	Heavy cyclic diene metathesis

HBT	Heterojunction transistor
HMDS	Hexamethyldisilazane
HOMO	Highest occupied molecular orbital
Hz	Hertz
i.e.	*id est*
IC	Integrated circuit
^{i}Pr	Isopropyl, -C_3H_7
IR	Infrared
K	Kelvin
L	Liter
LA	Lewis-acid
LB	Lewis-base
LHMDS	Lithiumhexamethyldisilazane
LUMO	Lowest unoccupied molecular orbital
m	Meter
m.p.	Melting point
Me	Methyl, -CH_3
Mes	Mesityl (2,4,6-trimethyphenyl), -$Me_3C_6H_2$
min	Minute
MOSFET	Metal-oxide semiconductor field-effect transistor
nbd	Norbornadiene
^{n}Bu	*n*-Butyl, -C_4H_9
NHC	*N*-Heterocyclic Carbene
NHGe	*N*-Heterocyclic Germylene
NHSi	*N*-Heterocyclic Silylene
NICS	Nucleus-independent chemical shift
NMR	Nuclear megnetic resonance
NP	Nanoparticle
PES	Potential energy surface
Ph	Phenyl, -C_6H_5
ppm	Parts per million
PTOE	Periodic table of elements
r.t.	Room temperature
s	Second

^{t}Bu	*tert*.-Butyl, -C_4H_9
TD-DFT	Time-dependent density functional theory
Tf	Triflate, -SO_3CF_3
TFT	Thin-film transistor
TGA	Thermogravimetric analysis
thf	Tetrahydrofurane
Tip	2,4,6-Triisopropylphenyl, -$^{i}Pr_3C_6H_2$
TMS	Trimethylsilane
UV/vis	Ultraviolet/visible
VSEPR	Valence shell electron pair repulsion
VT-NMR	Variable temperature nuclear magnetic resonance
Xyl	Xylyl (2,6-Dimethylphenyl), -$Me_2C_6H_3$

List of Figures

List of Schemes

List of Tables

Preface

The roles of the two archetypical semiconductors silicon and germanium for the Information Age could not vary more widely, despite both being part of Group 14 in the periodic table of elements (PTOE): With 28.2% the second most abundant element in earth's crust,[1] silicon and its compounds constitute the workhorses of modern technology, with far reaching applications in semiconductors, photovoltaics, construction materials, ceramics and glasses to name just a few.[2,3] This unsurpassed impact on today's society is also reflected in the term "Silicon Age" for the late 20th and early 21st century.[4]

Germanium on the other side leads a modest but therefore all the more specialized existence: Discovered only in 1886 as eka-silicon (atomic number: 32) by Clemens Winkler, it gave first proof for the predictive power of the then just emerging PTOE.[5–7] Winkler named the new element after his homeland Germany where it was found for the first time in argyrodite, a rare mineral from the "*Himmelsfürst Fundgrube Freiberg"*. The low natural abundance (1.5 ppm)[1] of germanium prevented its earlier discovery as there are only 26 defined, extremely rare germanium minerals and the remaining germanium is found in minute amounts as impurities in sulfides such as sphalerite and wurtzite.[8–10] As a result, the worldwide annual production of germanium amounted to manageable 106 to 160 tons between 2016 and 2019.[11–14] Despite its scarcity, germanium was the element of choice for the first transistor developed by Bardeen[15] because it exhibits superior electronic properties (band gap 0.67 eV, highest hole-mobility of any known semiconductor[16]). Nowadays, germanium finds use in high-tech applications like fiber optics, infrared optics, polymerization catalysis, semiconductors, and photovoltaics. This combination of rarity and lack of alternatives for important modern and future applications (e.g. spintronics[17,18]) makes germanium a so-called "technology-critical element".[19–21] Synergies with silicon in materials like alloys or thin films of hydrogenated amorphous a-Si/Ge:H give access to promising technologies like thin-film solarcells,[22–24], photonics,[25] high performance transistors[26–29] and quantum computing.[30–32] It is therefore of high importance to deepen our understanding of germanium chemistry to be able to extract the full potential of the element, its compounds, and materials in the future.

Introduction

1. Silicon and Germanium: Surface and Bulk Features

The transistor ranks among the most important inventions in human history, being an electronic component that allows to switch an electric current between two of their contacts (“Collector” and “Emitter” or “Source” and “Drain”) by applying voltage to a third (“Base” or “Gate”) (Figure 1). Since its first fabrication by Bardeen and Brattain[15] in 1947, we witness the far-reaching consequences of this simple property everywhere: Realization of logic gates in electric systems formed the basis of the combination of numerous transistors into integrated circuits (IC) and enabled electronic computations. Development of the metal-oxide-semiconductor field-effect transistor (MOSFET)[33] allowed for a stepwise miniaturization of ICs following Moore’s Law, which roughly predicts doubling of transistors per area unit on a microchip every two years and analogous shrinkage of MOSFETs.[34] The accuracy of this empirical prediction condenses in the triumph of ever smaller electronic devices with continually higher computing power, from archaic digital calculators to cutting-edge high-end smartphones. By this means, the astonishing number of approximately $1.3 \cdot 10^{22}$ MOSFETs was manufactured until 2018, making it the most frequently produced device in human history.[35] Furthermore, the rise of the internet since the 1990s has left deep marks in science, politics, industry and culture, still coining society in an unprecedented manner and leaving the transistor as the building block of the Information Age.

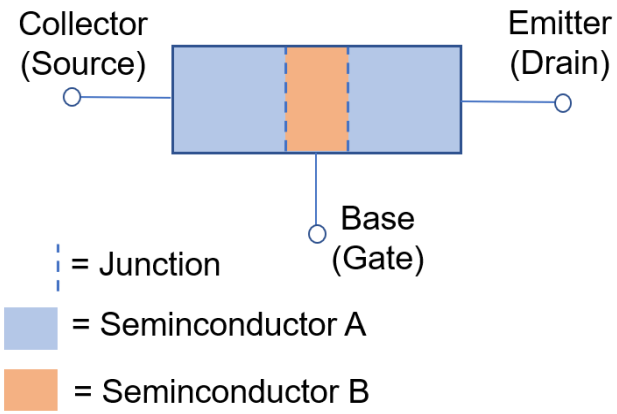

transistor	junction	materials
BJT	n-p	α-Si, α-Ge
MOSFET	n-p	α-Si
HBT	hetero	α-Si, α-Ge, α-SiGe
TFT	hetero	a-Si, a-Ge, a-SiGe

α = crystalline a = amorphous

Figure 1: Left: Schematic view of a generalized transistor. Terms at the contacts refer to those of a BJT; those in parentheses to those of a MOSFET. Semiconductor A and B either refer to oppositely doped versions of the same material (n-p junction) or two different materials (heterojunction). Right: Overview of junction types used in different transistor architectures.

Since Bardeen's seminal work dozens of transistor architectures have been conceived, united by one operating principle: the exclusively electric switching by exploiting the unique electronic properties of semiconductors. The first transistor, for instance, was a bipolar junction transistor (BJT) in which two interfaces, called p-n junctions, between oppositely doped (p- and n-) areas of germanium are crucial to its functioning (Figure 1).[36] While MOSFETs also utilize p-n junctions, the heterojunction bipolar transistor (HBT) possesses heterojunctions between two entirely different semiconductors, allowing band gap tuning and high switching frequencies for application in telecommunication. Thin-film transistors (TFT) possess another heterojunction-based architecture related to thin-film solar-cells; the flat design makes them well suited for application in displays or small devices. Figure 1 summarizes the different transistor architectures and the most used Group 14 semiconductors. Note that crystalline α-Si, α-Ge and α-SiGe are omnipresent in conventional transistors, whereas their amorphous counterparts (a-Si, a-Ge and a-SiGe) are indispensable for thin-film applications.

The sheer unlimited availability and simple processability of silicon makes it the material of choice in most standard semiconductor applications where economic factors dominate performance issues. Germanium on the contrary is rare and expensive but exhibits the highest hole mobility of all known semiconductors and a band gap in the IR,[16] making it suitable for high-end applications like X-Ray imaging[37,38] and IR sensors[39] in which cost is of secondary importance. Mixing both elements to crystalline or amorphous SiGe not only enhances the performance with respect to silicon but the resulting materials can even surpass germanium: Transistors based on silicon-germanium alloys (α-SiGe) for example, target the Terahertz clocking regime and are expected to play a pivotal role in future high-speed internet applications and state-of-the-art sensors.[40–45] The spectacular discovery of stable hexagonal $Si_{0.2}Ge_{0.8}$ which is the first Group 14 semiconductor to efficiently emit light due to a direct bandgap, opens the door for integrated optoelectronics and emphasizes the potential impact of SiGe alloys on prospective technologies.[25] The same applies to amorphous SiGe (a-SiGe) the bandgap of which can be fine-tuned to the solar spectrum by adjusting the Ge-content.[46,47] Its higher carrier mobility further allows for the development of competitive thin-film transistors.[48]

Semiconductive layers are usually fabricated by chemical vapor deposition (CVD). During CVD, a volatile, thermally unstable precursor is evaporated and then decomposed either directly in the gas phase or by contact with the hot substrate. For depositing silicon and germanium layers, silanes or germanes (EH_4, E_2H_6) are the precursors of choice; SiGe can be deposited from parallel CVD of both silanes and germanes.[43,47,49,50] The substrates for CVD are mostly wafers of α-Si, α-Ge or α-SiGe making their surface characteristics crucial for the deposition behavior. Similarly, the junctions in transistors highly depend on interface characteristics of semiconductors and in the highly miniaturized MOSFETs the surface atoms are no longer a negligible perturbation of the bulk but become the dominant structural feature. It is therefore insightful to examine the surface features of crystalline silicon and germanium in the following and see how molecular model compounds can help to unravel their reactivity.

1.1. Surface features of crystalline α-Si and α-Ge

Substrates for epitaxial CVD are produced by cutting along the (100) plane of an α-$Si_{1-x}Ge_x$ ($0 \leq x \leq 1$) crystal, leaving two unpaired electrons with each surface atom which are located in highly reactive "dangling" bonds. To decrease free energy, the surface undergoes reconstruction by pairing up surface atoms under formation of a *cis*-bent double-bonded dimer. The dimer tilts in accordance with a Jahn-Teller distortion and an uneven structural feature is left on the surface which is referred to as the "buckled dimer" and the reconstructed surface as E(100)-c(4x2) (Scheme 1).[51,52]

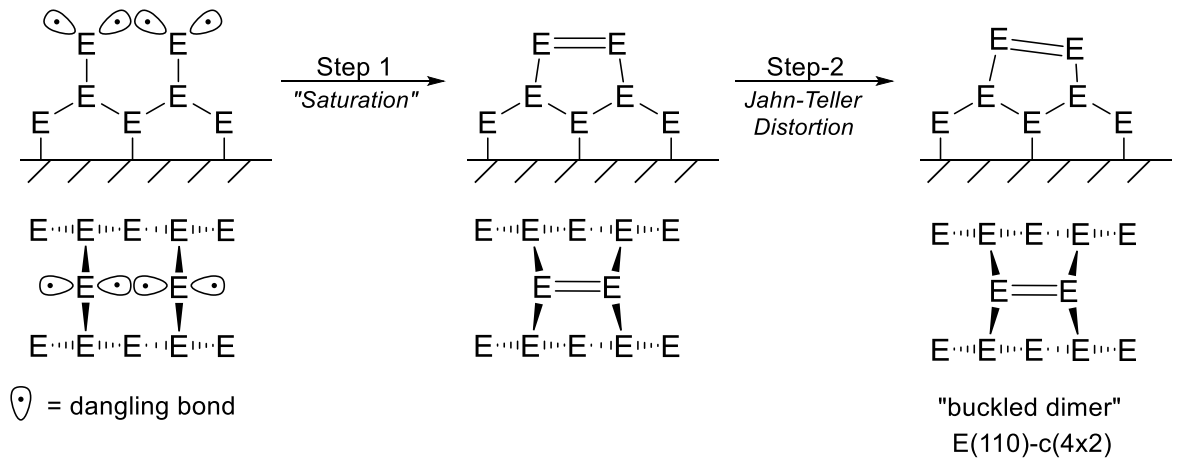

Scheme 1: Surface reconstruction processes on the (100) surface of α-Si and α-Ge. Top: View along the [-110] vector; Bottom: View along the [001] vector (E = Si, Ge).

At room temperature, the buckled dimers on the α-Si- and α-Ge surface are subject to a rapid wiggle motion (Scheme 2)[53,54] which is only quenched in proximity of surface defects, due to a higher local anisotropy and therefore higher energetic discrimination of one orientation against the other.[52] The rate of the wiggle motion on the α-Si surface exceeds that on the α-Ge surface, hinting towards differing activation energies.[54]

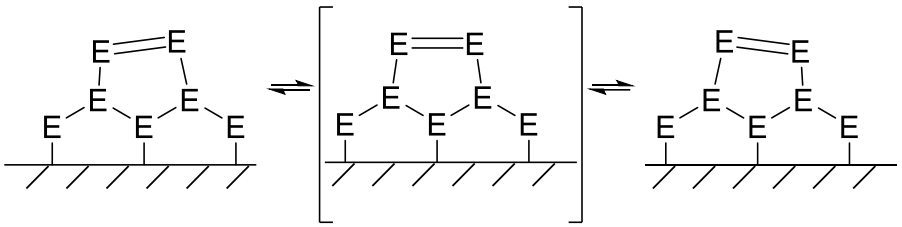

Scheme 2: Dynamic behavior of buckled dimers on the surface of α-Si and α-Ge (E = Si, Ge).

Structurally, the buckled dimer resembles *cis*-bent heavy alkenes. Approximations to this bonding situation in the molecular case were reported for both silicon[55] and germanium.[56] The different kinetics of the dynamic behavior on the α-Si and α-Ge(100) surfaces fits this interpretation: While disilenes exhibit a shallow Potential Energy Surface (PES) and therefore readily undergo conformational changes, the *trans*-bent structure is clearly favored for digermenes, rendering them less fluxionary (cf. Section 3.1).[57–59] The structural similarities between surfaces and molecular model systems translate directly into parallel chemical behavior as has been investigated for germanium by the group of Baines: In close resemblance to what has been reported for the Ge(100)-(4x2) surface,[60,61] digermene **1a** reacts with carboxylic acids[62] and the highly-functionalized acetylene **3**[63] to the saturated digermanes **2a-c** and the diradical intermediate **4**, respectively (Scheme 3).

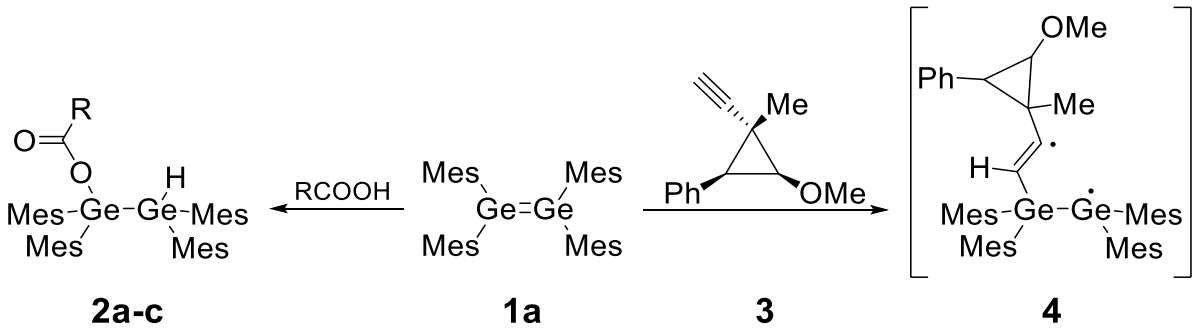

Scheme 3: Reactivity of digermene **1a** with carboxylic acids to digermanes **2a-c** and with highly functionalized acetylene **3** to the intermediate diradical **4** (**2a**: R = ^{t}Bu; **2b**: R = Mes; **2c**: R = *trans*-2-phenylcyclopropyl).

Treatment of **1a** with isocyanides,[64] gives intermediate donor-acceptor complexes **5a-c**, which undergo subsequent reactions to digermane **6** or cyclotrigermane **7**, depending on the isocyanide (Scheme 4). The formation of structures analogous to **6** had never been proposed in reactions of isocyanides with Ge(100)-(4x2) but is reasonably assumed based on FTIR data.[65] Likewise, treating **1a** with nitriles[66] resolves the mechanism of Ge(100) functionalization with acrylonitriles,[67,68] demonstrating the suitability of digermenes to help gain insight to the surface chemistry of germanium.[69,70]

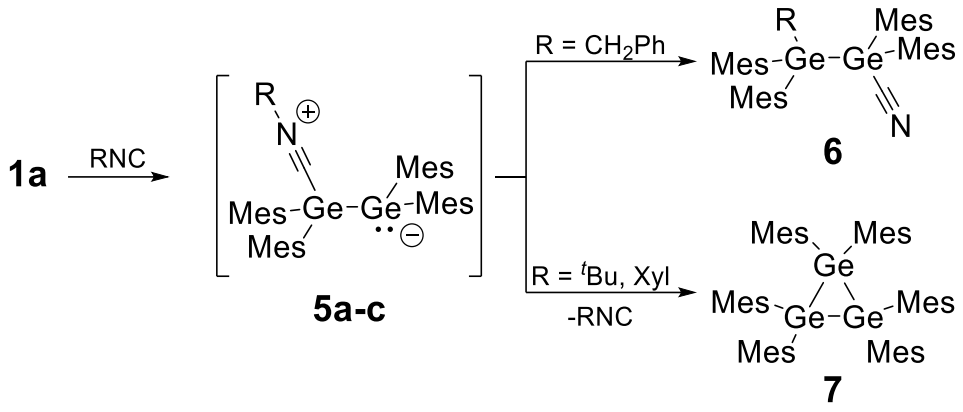

Scheme 4: Reaction of digermene **1a** with isonitriles to the intermediate donor-acceptor complexes **5a-c** and subsequent reactions to digermane **6** and cyclotrigermane **7** (**5a**: R = benzyl; **5b**: R = ^{t}Bu; **5c**: R = Xyl).

1.2. Nanoclusters in amorphous Si, Ge and SiGe

Like their crystalline counterparts, amorphous a-Si, a-Ge and a-SiGe are processed *via* CVD but their immanent disorder renders their properties susceptible to the deposition conditions. Detailed knowledge of the processes in both the gas-phase and at the substrate surface are therefore required to gain control over short-range structures in the bulk as for example dangling bonds on the surfaces of internal voids (Figure 2).[71–73] These generate defined states in the band-gap which dictate the electronic and optic properties of the material and in fact deteriorate the semiconducting behavior due to accelerated charge carrier recombination.[47] Significant performance improvement can be reached by introducing hydrogen to the bulk (Figure 2) as it eliminates states from the pseudo band-gap by partially saturating the dangling bonds.[74,75] The resulting semiconductors (a-Si:H, a-Ge:H & a-SiGe:H) are in fact the materials used in industrial thin-film applications as they in particular exhibit desirable electronic properties.[37–39,46,48,76–78]

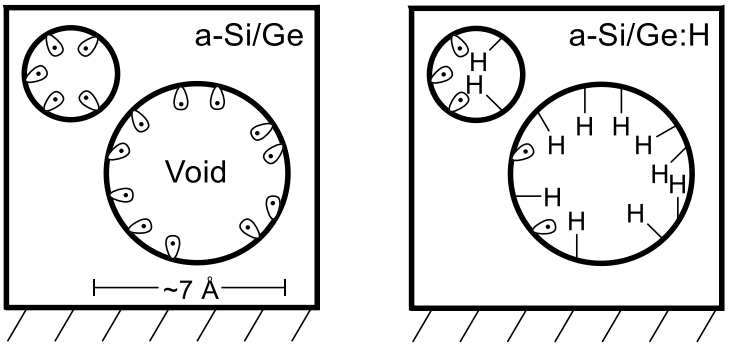

Figure 2: Left: Schematic view of a non-hydrogenated amorphous semiconductor with dangling bonds on the internal surfaces of randomly distributed voids. Right: Schematic view of a hydrogenated amorphous semiconductor. Dangling bonds are partially saturated.

Other structural features found in a-Si:H, a-Ge:H and a-SiGe:H are partially-hydrogenated, unsaturated nanoclusters randomly distributed in the bulk.[79–81] Theoretical investigations on the silicon system show a dependency between the optical properties of such clusters and their size, structure, and hydrogen-content, suggesting that these factors play a pivotal role for the material characteristics.[82–84] High hydrogen content, for instance, leads to saturated nano-crystallites, while lower degrees of hydrogenation induce the presence of unsaturated clusters that exhibit higher photoluminescence intensity.[82] Consequently, a hydrogen-content of 10 to 15% in a-Ge:H was found to yield optimal optoelectronic properties.[85] Complete removal of hydrogen leaves silicon nanoclusters covered by dangling bonds, leading to inferior optical properties.[82] Based on solid-state simulations, unsaturated silicon clusters were proposed as structural features of a-Si as high concentrations of three- and five-fold coordinated Si atoms were found in the near-surface domains.[86] Experimental validation of these suggestions remains difficult at present, due to limited characterization methods of local features in amorphous materials.

Decomposition of silane or germane precursors in the gas-phase during CVD to highly unstable anions,[87,88] radicals,[89–92] cations[93–96] or carbene analogues[87,89,90,97–106] is presumably followed by subsequent insertion, elimination and aggregation reactions that step by step build larger structures of various compositions. Both silicon and germanium clusters of different sizes and hydrogenation degrees have been experimentally detected in the gas phase by applying manifold decomposition techniques,[87,88,105–112] while structural suggestions exclusively rely on theoretical results.[113–122] Adsorption of all occurring species to the substrate surface is then followed by decomposition and finally film growth (Scheme 5).

Detailed knowledge of mechanistic processes and occurring species is therefore crucial to control the formed clusters and properties of the deposited material.

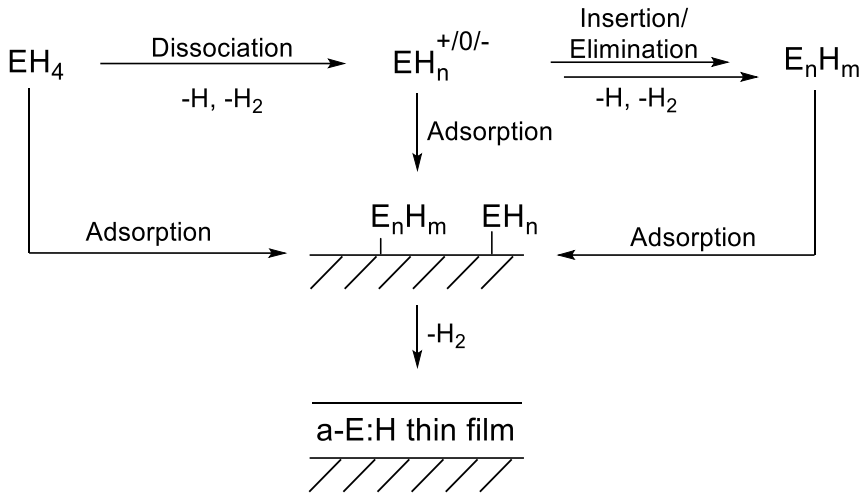

Scheme 5: Simplified processes during the CVD of silanes and germanes to a-Si:H, a-Ge:H and a-SiGe:H thin films over intermediate partially hydrogenated clusters (E = Si, Ge).

1.3. The bottom-up approach to Si and Ge materials

High instability of the low-valent Group 14 intermediates in CVD and the consequential unselective nature of the occurring reactions set boundaries for controlling the deposited semiconductor's properties. Taming their reactivity usually requires sterically demanding and chemically inert substituents which protect the low-valent center from possible reactants. This "kinetic stabilization" was proposed by Jutzi in 1975[123] and has become the key in isolating most low-valent Group 14 species. Another important stabilization technique that admittedly interferes heavily with the electronic structure of the stabilized species, is the saturation of electron-deficient centers with strong donors (Scheme 6).

Scheme 6: Stabilization techniques in low-valent Group 14 chemistry, depicted on tetrylenes. Left: Kinetic stabilization *via* sterically demanding substituents: Right: Electronic stabilization of electron-deficient centers with strong donors (E = heavy group 14 element, D = donor).

Interestingly, many of these species are accessible by systematic coupling of smaller low-valent Group 14 units to build larger molecules and finally crossing the threshold to unsaturated cluster motifs (cf. Chapter 6) known from CVD and amorphous semiconductors. This bottom-up approach promises better control over the deposited structures and thus the properties of the final material. Hence, the following chapters will systematically review low-valent germanium species with increasing number of unsaturated Ge centers from germylenes to clusters. Additionally, mixed species that contain both low-valent silicon and germanium will be covered as conceptual bridge to a-SiGe. The amount of hydrogen induces extraordinary structural changes to the cluster cores, which is why every chapter dedicated to a number of "core" atoms will be subdivided into sections of number of substituents (Table 1). Silicon species will be covered if the heavier congeners are unknown. Explicitly not included are non-conjugated anions, radicals, or cations with the general formula $GeR_3^{+/0/-}$.

Table 1: Ordering of low-valent germanium-containing molecules, as they will be presented in the following chapters. The last chapter does not include an additional subdivision (E = Si, Ge).

Ge_1	**Ge_2 & SiGe**	**E_3**	**E_4**	**Clusters**
GeR_2	Ge_2R_4	E_3R_6	E_4R_6	
GeR	Ge_2R_3	E_3R_5	E_4R_5	
Ge(0)	Ge_2R_2	E_3R_4	E_4R_4	
	$Ge_2(0)$	E_3R_3		
	$GeSiR_4$	E_3R_2		
	$GeSiR_2$	$E_3(0)$		

2. Ge_1-Systems

Group 14 elements typically occur in the two oxidation states +IV and +II, with an increasing tendency for the latter when going down the group as exemplified by the element halides: CCl_2 and $SiCl_2$ are highly reactive intermediates,$GeCl_2$ can only be isolated when stabilized by donors while $SnCl_2$ and $PbCl_2$ represent the more stable oxidation state of tin and lead chlorides. This ordering is found to be reversed for the tetrachlorides, rendering CCl_4 stable and $PbCl_4$ extremely prone to disproportionation (Scheme 7).

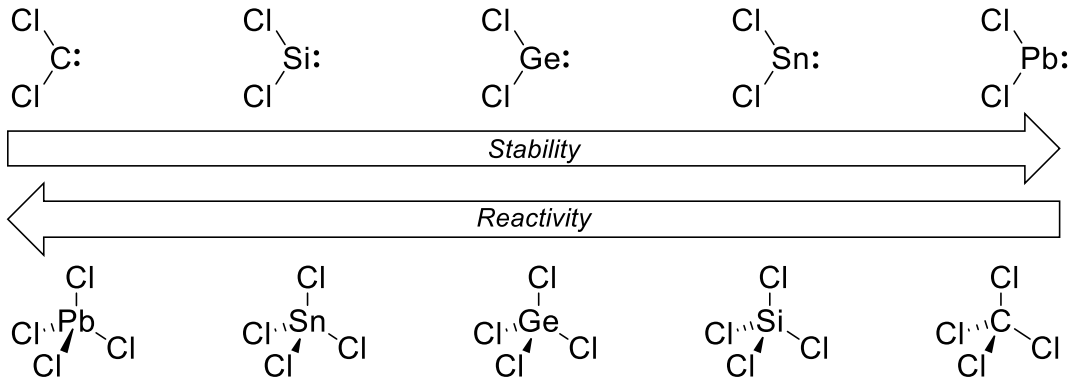

Scheme 7: Group 14 (II)- and (IV)-halides arranged according to their reactivity/stability.

This trend is rationalized by the “inert-pair effect”, stating that in the lower rows of the PTOE the valence s-orbital becomes less involved in bonding (“inert”) and hence the tetravalent bonding mode is increasingly destabilized compared to the divalent one.[124] Of several explanations,[125,126] according to Kutzelnigg the 2s-orbital expands further from the nucleus to maintain orthogonality to the 1s orbital, while the 2p-orbitals are unperturbed. As p-orbitals are localized further from the nucleus than s-orbitals, the 2p-orbitals overlap effectively with the expanded 2s-orbital, allowing significant mixing and hybridization. The np-orbitals in lower rows, however, need to avoid their energetically lower congeners, which restores the mismatch in orbital size between ns and np orbitals, decreasing the ns-orbital’s tendency towards hybridization.[127] One consequence of the inert-pair effect is the decrease in X-E-X bonding angles for E = C to Pb (Table 2). The decrease in angles for electronegative halides is explained by Bent’s Rule, stating that electronegative substituents favor p-orbitals in their bonds.[128] The degree of bending of heavier tetrylenes has been rationalized by a second-order Jahn-Teller effect:[129–131] the lowering of symmetry from $D_{\infty h}$ to C_{2v} enables favorable orbital interactions due to mixing of previously immiscible orbitals. The extent of this deformation is therefore reciprocally related to the HOMO-LUMO gap.

Table 2: Experimental X-E-X values of Group 14 dihalides determined in the gas-phase (E = C, Si, Ge, Sn, Pb; X = F, Cl, Br).[132–140]

X-E-X [°]	**C**	**Si**	**Ge**	**Sn**	**Pb**
F	105	101	97.2	94	90
Cl	108	105	100.2		98.7
Br		109			

Group 14 (II) compounds are referred to as carbenes, silylenes, germylenes, stannylenes and plumbylenes, or more general as tetrylenes which electronic structure is in between two borderline cases, the idealized triplet and singlet state (Figure 3).

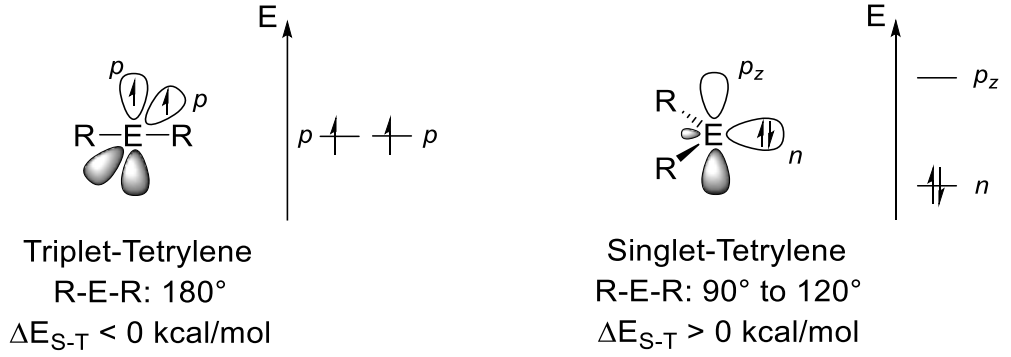

Figure 3: Idealized structure of tetrylenes in the triplet and singlet state.

The highly reactive, linear triplet state possesses two singly occupied, degenerate p-orbitals with the s-orbital being utilized in the E-R single bonds, requiring extraordinarily effective hybridization between s- and p-orbitals only seen in the second row of the PTOE. Hence, the parent carbene, despite still being bent with a HCH angle of 134°, possesses a triplet ground state,[141–144] whereas the singlet state is increasingly favored for heavier parent tetrylenes (Table 3).[59,145–148] In this case, the electrons occupy a non-bonding orbital and the remaining vacant p-orbital leaves singlet tetrylenes Lewis-amphoteric. The singlet-triplet character also depends on the substituents: Bulky substituents force the molecule into an arrangement closer to linearity and hence stabilize the triplet state,[149–151] as has been observed for sterically extremely encumbered silylenes.[152,153] Similarly, σ-donating substituents decrease the s-character of the tetrylene lone-pair according to Bent's Rule and therefore stabilize the triplet state.[150,154] The opposite is true for σ-acceptors and for π-donors: their lone-pair stabilizes singlet tetrylenes *via* donation into the vacant p_z-orbital.

Table 3: Calculated singlet-triplet gaps for parent tetrylenes (numbers in parentheses include relativistic effects).

$\Delta E_{S\rightarrow T}$ [kcal/mol]	**C**	**Si**	**Ge**	**Sn**	**Pb**
	−12.7	16.7	21.8	24.8	34.8
	(−10.6)	(16.8)	(24.1)	(23.7)	(39.1)

2.1. GeR_2: Germylenes

The intermediate position of germanium in Group 14 renders the oxidations state +II stable enough to isolate germylenes as air and moisture sensitive compounds by using suitable substituents or Lewis-bases. Hence, early isolated examples of germylenes were germanium(II) halide complexes **8a,b** which were synthesized by thermal treatment of trihalogermanes in the presence of 1,4-dioxane (Scheme 8).[155,156] Dichlorogermylene **8a** undergoes ligand exchange with thf to the corresponding complex **8c**.[157] Reaction with triflic acid leads to elimination of HCl and the formation of the germanium(II) triflate **9**.[158] A range of other base-stabilized dichlorogermylenes are accessible by ligand exchange and several other weak donors have been reported to undergo complex formation with germylenes.[159–164]

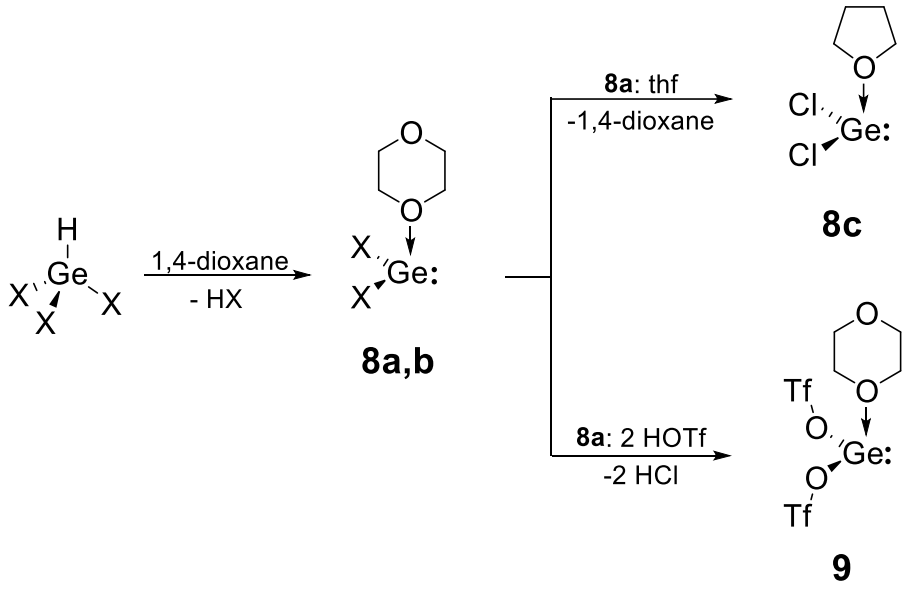

Scheme 8: Synthesis of donor-stabilized germanium(II) halides **8a,b** and examples of typical germylene reactivity for **8a** with donor-exchange to **8c** and salt metathesis to **9** (**8a**: X = Cl; **8b**: X = Br).

Synthesis of the first isolable N-heterocyclic carbenes (NHC) **10a-h** and **11a,b** by Arduengo *et al.* in the 1990s,[165–169] broadened the scope of applicable Lewis-bases significantly. NHCs are singlet carbenes and extraordinarily strong σ-donors. The π-donating endocyclic nitrogen atoms stabilize the vacant p-orbital at the carbene center efficiently and their σ-accepting character increases the singlet character of the carbene, further enhancing its stability (Scheme 9). In addition, unsaturated NHCs **10a-h** experience a certain amount of 6π-aromaticity in the five-membered ring.[170,171]

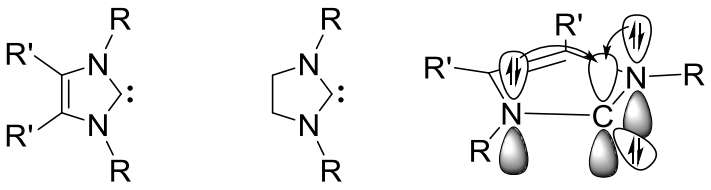

10a-h **11a,b**

Scheme 9: Unsaturated NHCs **10a-h**, saturated NHCs **11a,b** and the electronic structure of **10a** (**10a**: R = 1-Ad, R' = H; **10b**: R = R' = Me; **10c**: R = Me, R' = H; **10d**: R = ^{i}Pr, R' = Me; **10e**: R = Mes, R' = H; **10f**: R = Dip, R' = H; **10g**: R = 4-MeC_6H_4, R' = H; **10h**: R = 4-Cl-C_6H_4, R' = H; **11a**: R = Mes; **11b**: R = Dip).

Since the discovery of NHCs several germylene-NHC complexes have been reported: Ligand exchange in germanium(II) dichloride × dioxane complex **8a** with NHCs **10d** or **10f** gives the NHC-stabilized germanium(II) dihalides **12a,b** (Scheme 10) and complexation of GeI_2 with **10e** the corresponding diiodide.[172–175]

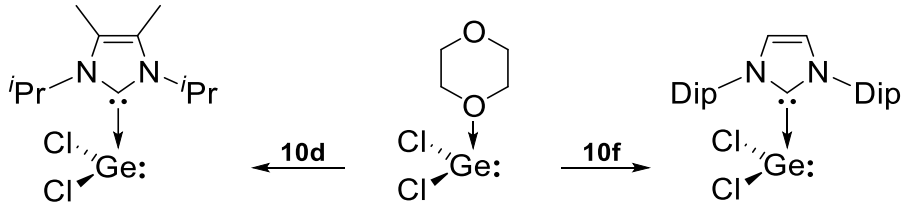

12a **8a** **12b**

Scheme 10: Germanium(II) dichloride NHC complexes **12a,b** synthesized *via* ligand exchange.

Just like dioxane-stabilized **8a, 12a** is a valuable precursor in low-valent germanium chemistry: the complexes **12c-h**, which all bear strongly electronegative functionalities at the germanium center can be obtained *via* substitution of the chlorides in **12a** (Scheme 11).[173,176] Furthermore, treatment of **12a** with metal organic reagents in a 1:1 or 1:2 ratio gives the base-stabilized germylenes **13** and **14** with one and two substituents, respectively, *via* salt metathesis (Scheme 11).[176,177]

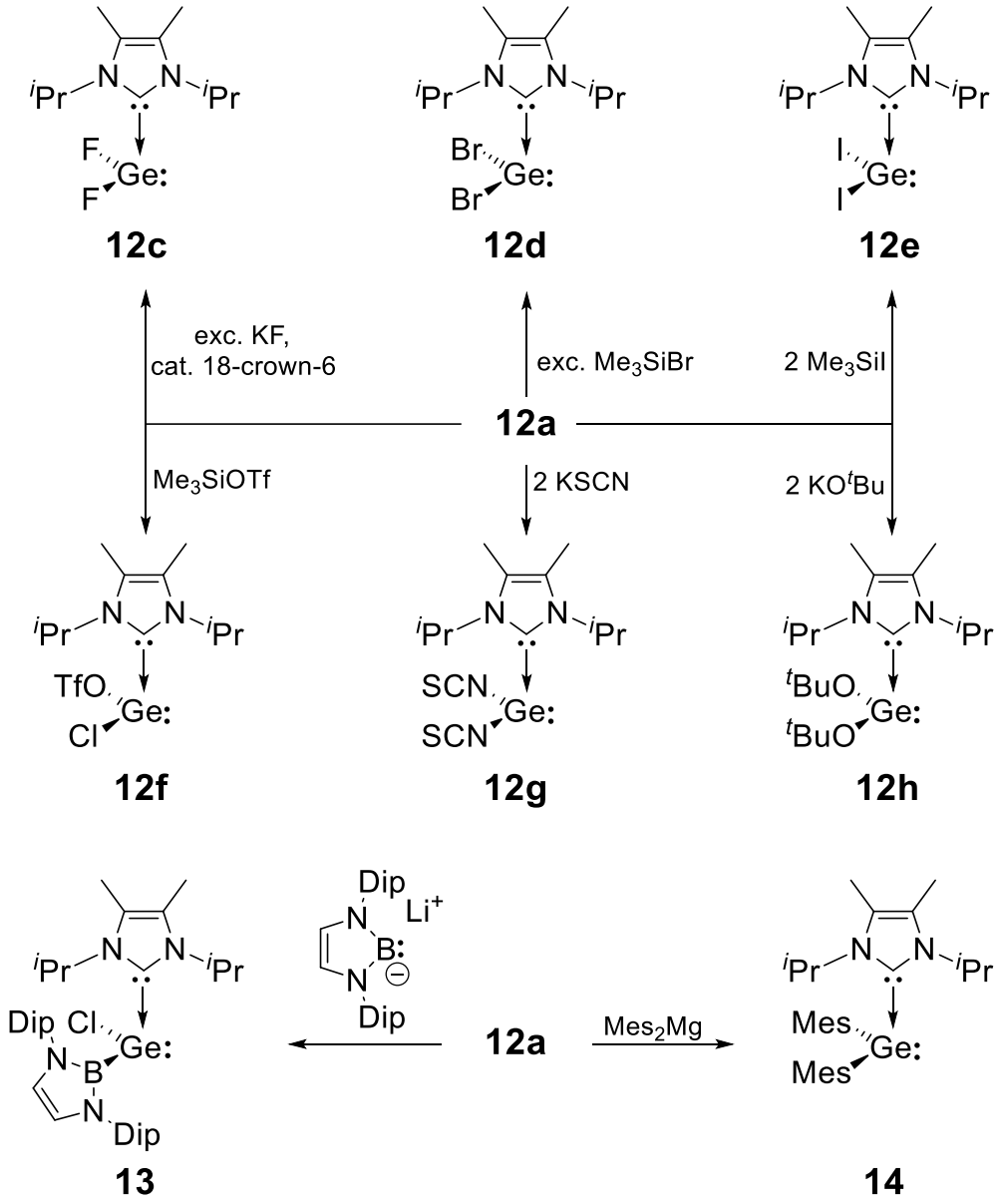

Scheme 11: Synthesis of Ge(II) halide-NHC complexes **12c-h** with strongly electronegative functionalities from **12a** and salt metathesis of **12a** to **13** and **14**.

Diarylgermylene **14** is also accessible *via* NHC mediated cleavage of digermene **1a**. Similarly, addition of NHC **10d** induces splitting of functionalized digermene **15** to the cyclic germylene **16**. While **15** can be reversibly recovered by addition of triphenylborane under formation of the NHC-borane adduct, **14** itself reacts as a Lewis base with borane to give the donor-acceptor stabilized germylene **17** (Scheme 12).[178,179] NHC mediated deconstruction of a tetragermacyclobutane to four equivalents of the corresponding NHC-stabilized germylene has been reported as well.[180]

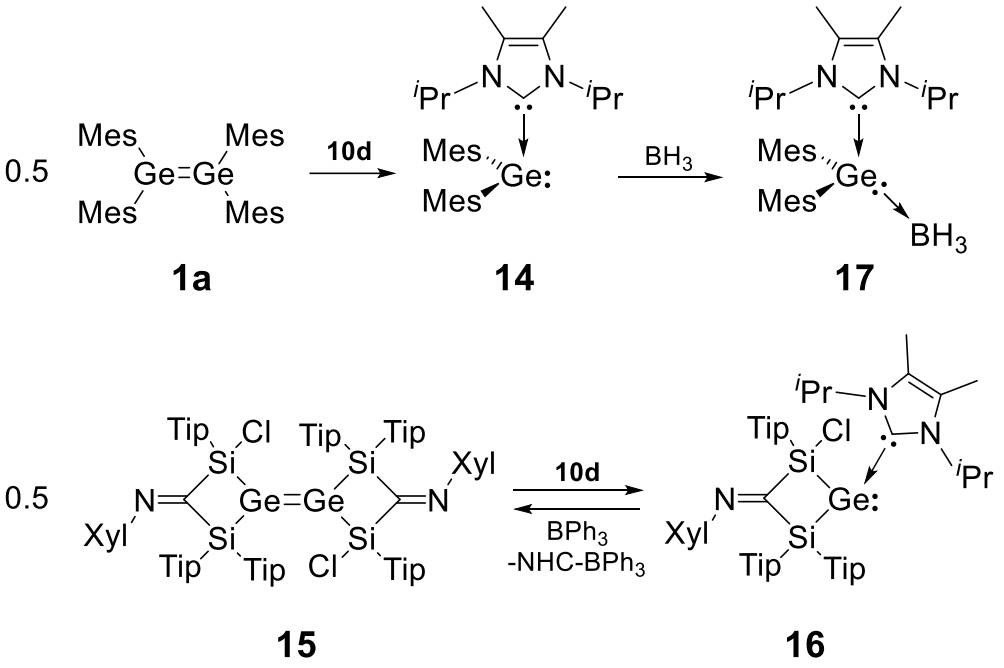

Scheme 12: Cleavage of digermenes **1a** and **15** to the NHC-stabilized germylenes **14** and **16** and their diverging reactivity towards boranes to donor-acceptor stabilized germylene **17** and digermene **15**.

Employing the same stabilization technique, the group of Rivard succeeded in isolating the parent-germylene complex **18a** by treatment of **12b** with lithium borohydride and could deposit elemental germanium nano-particles from complex **18b**, in which a weaker bonded phosphorus ylide stabilizes the germylene (Scheme 13).[175,181]

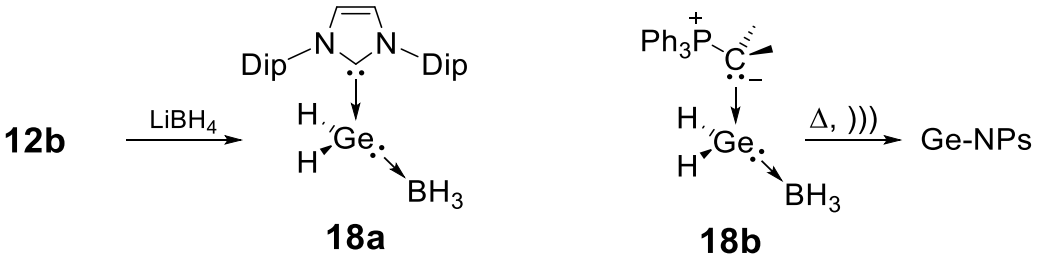

Scheme 13: Synthesis of donor-acceptor stabilized parent-germylenes **18a** from germanium(II) chloride NHC complex **12b** and deposition of **18b** to give Ge-nanoparticles.

Instead of external Lewis-bases, it is also possible to utilize intramolecular donors to stabilize germylenes: The earliest application of this strategy made use of the rigid acac-ligand and allowed isolation of germylenes **19a,b** and **20**.[182,183] The germylenes **21a,b** and **22a-d** are similarly stabilized by a tropolone and calix[4]arene-based ligand, respectively (Scheme 14).[182,184]

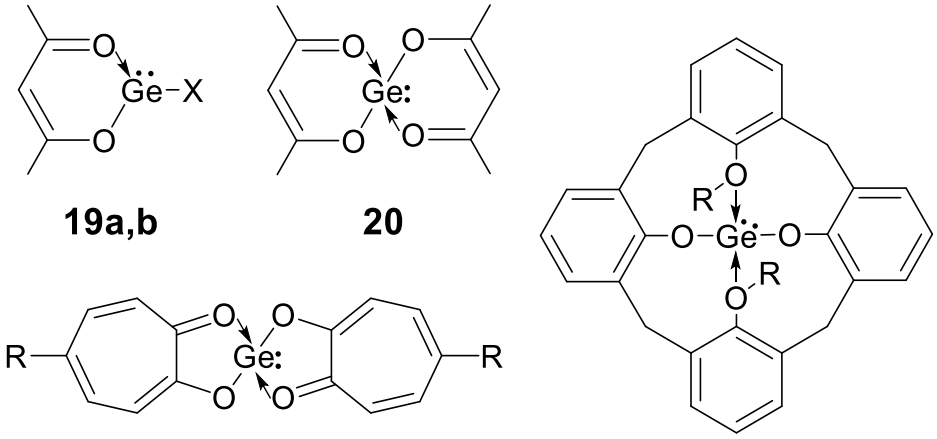

Scheme 14: Germylenes **19-22**, stabilized by chelating O-ligands. (**19a**: X = Cl; **19b**: X = I; **21a**: R = H; **21b**: R = ^{i}Pr; **22a**: R = $SiMe_3$; **22b**: R = $Si^{i}Pr_3$; **22c**: R = Me; **22d**: R = CH_2Ph).

Examples with nitrogen-based ligands include the β-diketiminatogermylene **23-26**,[185–194] the amidinato and guanidinatogermylenes **27a,b**[195] as well as **28** and **29a-c** in which the germylene is incorporated into five-membered rings (Scheme 15).[196,197]

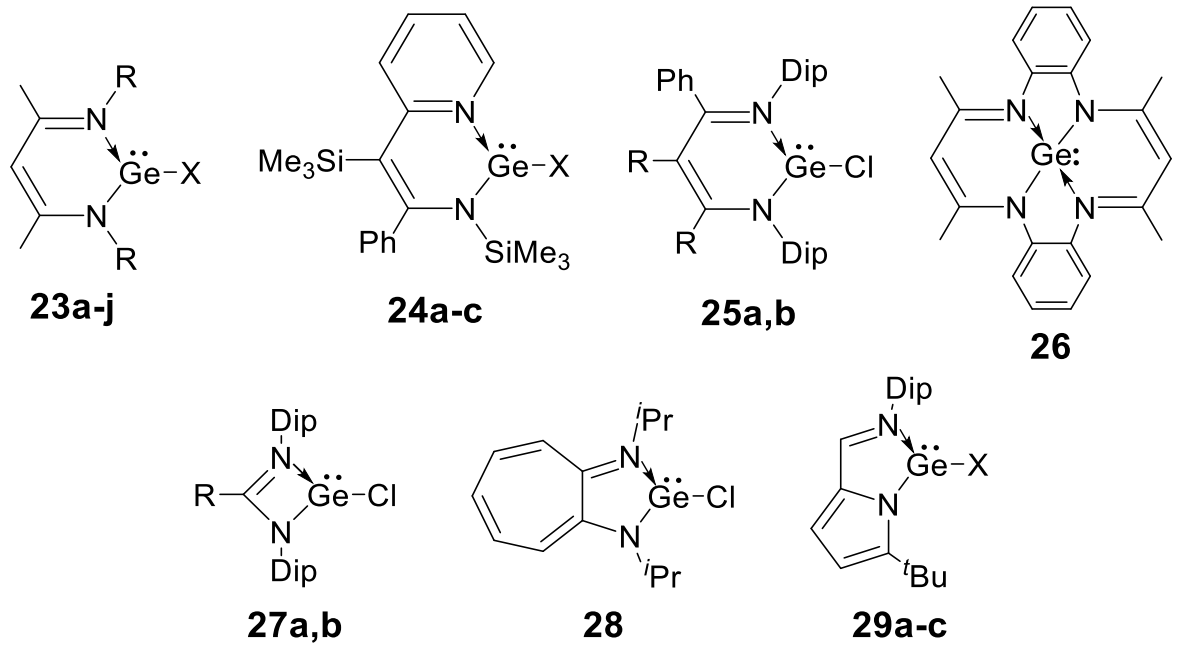

Scheme 15: Germylenes **23-29**, stabilized by chelating N-ligands (**23a**: X = Cl, R = Ph; **23b**: X = I, R = Ph; **23c**: X = Cl, R = Mes; **23d**: X = N_3, R = Mes; **23e**: X = H, R = Dip; **23f**: X = F, R = Dip; **23g**: X = Cl, R = Dip; **23h**: X = Me, R = Dip; **23i**: X = ^{n}Bu, R = Dip; **23j**: X = OH, R = Dip; **24a**: X = Cl, **24b**: X = ^{t}Bu; **24c**: X = -C≡CPh; **25a**: R = Ph; **25b**: R = ^{t}Bu; **27a**: R = ^{t}Bu; **27b**: R = $N^{i}Pr_2$; **29a**: X = Cl; **29b**: X = O^{t}Bu; **29c**: X = N(H)Dip).

Germylenes **19-29** owe their stability to electron delocalization across their ligand backbone with contributions of zwitterionic resonance formulae as depicted in Scheme 16 for acac-, β-diketiminato- and amidinato-stabilized systems.

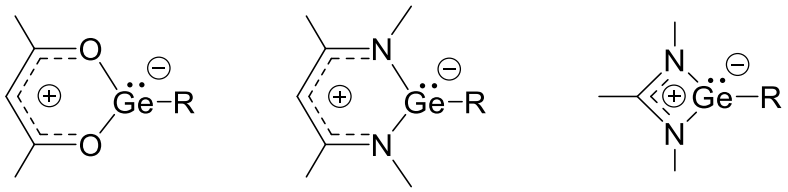

Scheme 16: Zwitterionic resonance structures of acac-, β-diketiminato- and amidinato-stabilized germylenes.

Chelating ligands interfere with the electronic structure of the original germylene, rendering the employment of more innocent donor-substituents advantageous when the Ge(II) characteristics are to be preserved. Attachment of a donor to a flexible tether as in germylenes **30a-e** and **31a-c** allows dynamic interaction with the germylene and retains stabilization (Scheme 17).[158,198–203] The coordination behavior of compounds **30a-e** and **31a-c** can be experimentally validated in solution by NMR.

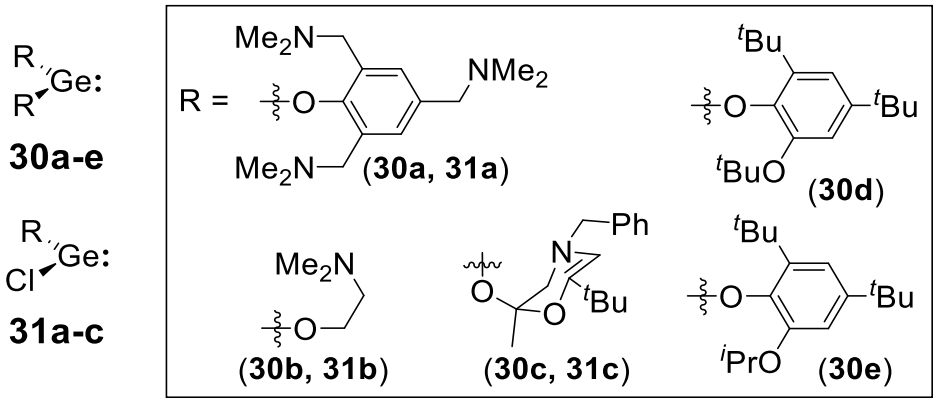

Scheme 17: Donor stabilized germylenes **30a-e** and **31a-c**.

Germylene **32** undergoes adduct formation with borane to complex **33** (Scheme 18).[204,205] While **33** exhibits labile coordination of the nitrogen donor to Ge(II), the carbene-germylene bonds in NHC-germylene complexes **17** and **18a** (Scheme 12, Scheme 13) are formed irreversibly.

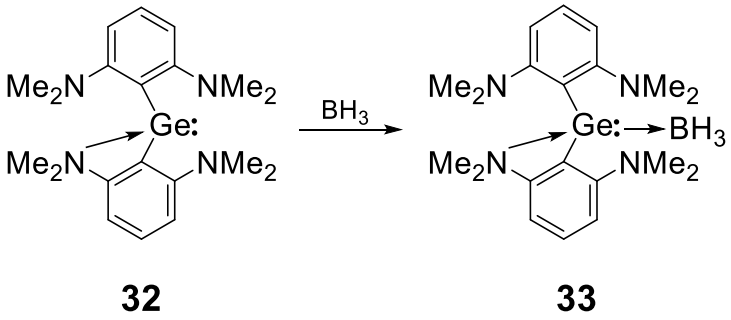

32 **33**

Scheme 18: Complexation of borane by n-donor stabilized germylene **32** to the complex **33**.

Kinetic stabilization is the strategy for expanding the lifetime of Ge(II) species that interferes least with the electronic structure. The first isolable diorganogermanium(II) species free of external donors was germanocene Cp_2Ge. The eponymous compound class is not covered here due to the non-classical η^2-bonding of each Cp group.[206] In 1974 the group of Lappert isolated the first stable donor-free, divalent germylene **34** *via* salt metathesis of **8a** and two equivalents of LHMDS (Scheme **19**).[207,208]

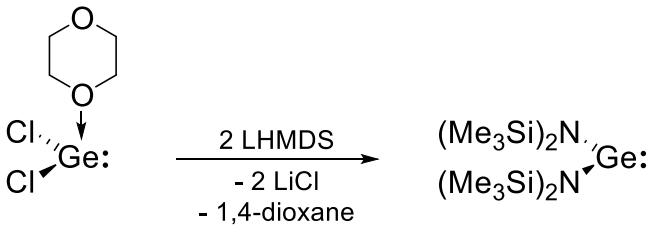

8a **34**

Scheme 19: Synthesis of the first donor-free germylene **34** *via* transmetallation.

The singlet character of **34** was validated by photoelectron spectroscopy[209] and its structure was elucidated in the gas-phase[210] and in the solid state:[211]. Structurally similar diaminogermylenes show π-donation from the nitrogen lone pairs to the adjacent germanium p-orbital, [208,209,212–214] explaining the monomeric nature of **34**, as isoelectronic dialkylgermylene **35**, which is obtained from **8a** or **34** (Scheme 20), undergoes dimerization to a digermene in the solid state (cf. Section 3.1).[209,215–219]

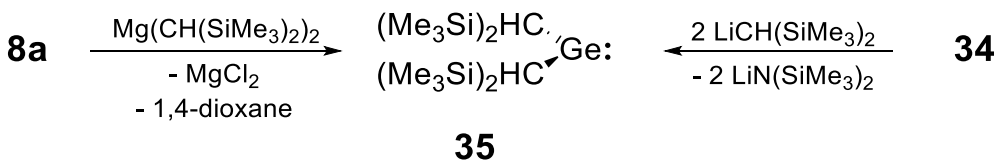

35

Scheme 20: Synthesis of dialkylgermylene **35** from **34** or **8a** *via* transmetallation.

The reactivity of **35** in solution however, is prototypical of germylenes (Scheme 21):[217] The most common reaction type is the insertion into σ-bonds, like for instance, the reaction of **35** with methyliodide to **36**. The other dominant reaction type is coordination to electrophiles to form complexes such as **37** (cf. formation of **17** and **33**).

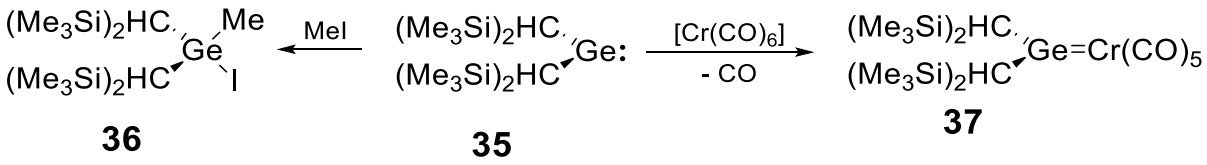

Scheme 21: Reactions of germylene **35**: Insertion to iodogermane **36** and complex formation to **37**.

Since the isolation of **34** and **35**, a vast number of stable germylenes has been reported (Scheme 22): dialkylgermylenes **38** and **39** that remain monomeric in the solid state,[220,221] amino-, oxo- and thio-germylenes **40a-c**,[222–224] and phosphino- as well as silyl-substituted **41** and **42**.[225,226]

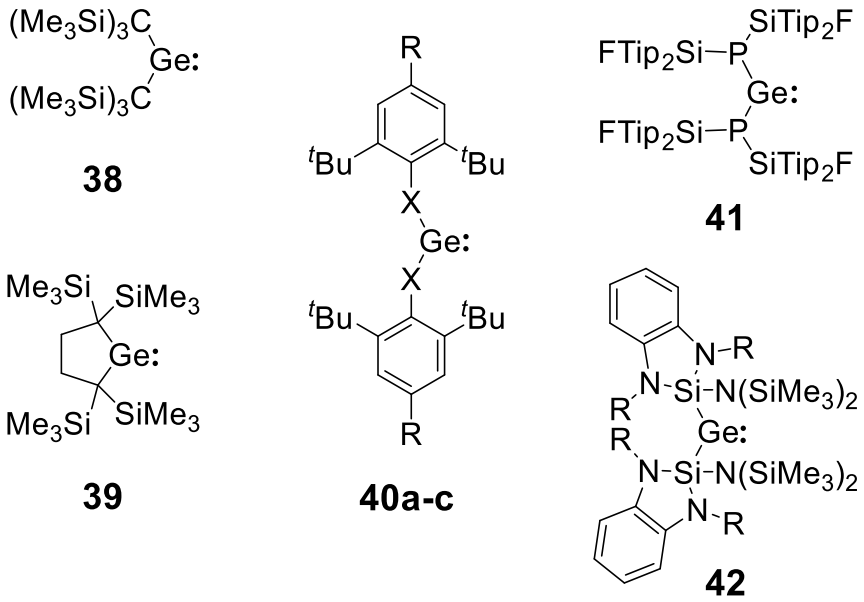

Scheme 22: Isolated germylenes **38-42** with different main group substituents (**40a**: X = O, R = Me; **40b**: X = NH, R = ^{t}Bu; **40c**: X = S, R = ^{t}Bu; **42**: R = $CH_2{}^t$Bu).

Aryl-substituted germylenes require larger substituents for efficient steric protection (Scheme 23). While **43a** decomposes at room temperature, **43b** was fully characterized and is stable for several weeks.[227–230] **44** is stabilized by intramolecular through-space interactions between fluorine and germanium.[231] Utilization of sterically very demanding terphenyl groups by Power allowed for the isolation of **45a-d**.[232–234]

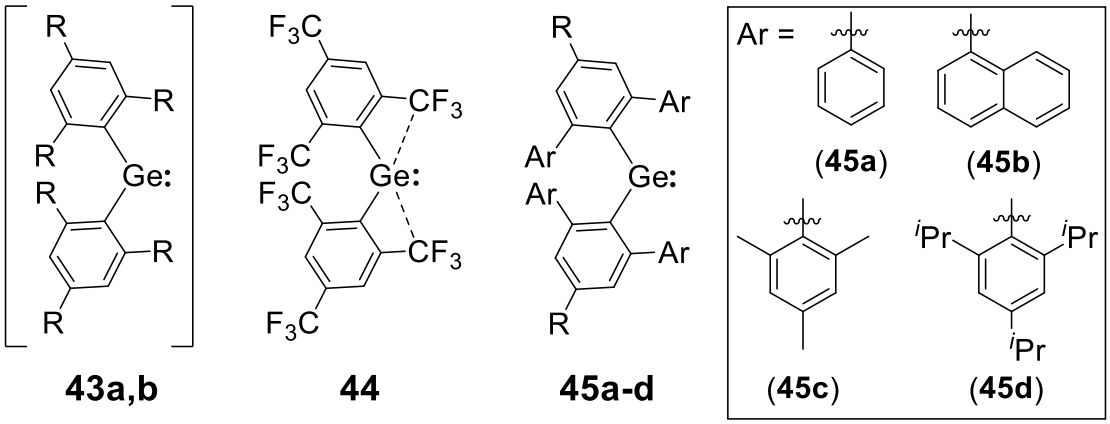

Scheme 23: Aryl substituted germylenes **43-45** (**43a**: R = Me; **43b**: R = ^{t}Bu; **45a**: R = Ph; **45b**, **45c**, **45d**: R = H).

The use of sterically very demanding groups also enabled the synthesis of monochlorogermylenes **46** and **47a-c** of which the latter dimerize in the solid state to the corresponding digermenes (cf. Section 3.1), a consequence of the reduced steric repulsion of only one substituent (Scheme 24).[232,235–237] Chlorogermylenes **48**-**50** that remain monomeric in the solid state were reported by Jones and carry even bulkier substituents.[164,180,238] **47a-c**, **49a,b** and **50a-d** serve as precursors for digermynes (cf. Section 3.3), germyliumylidenes and germanylidenides (cf. Section 2.2).

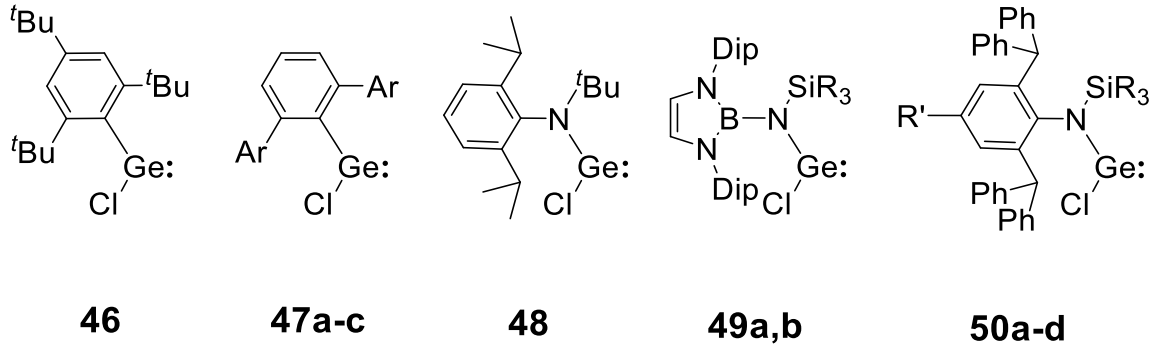

Scheme 24: Monochlorogermylenes **46-50** with sterically demanding substituents (**47a**: Ar = Mes; **47b**: Ar = Dip; **47**: Ar = Tip; **49a**: R = Me; **49b**: R = Ph; **50a**: SiR_3 = $SiMe_3$, R' = Me; **50b**: SiR_3 = $SiMe_2Ph$, R' = Me; **50c**: SiR_3 = $SiPh_3$, R' = Me; **50d**: SiR_3 = $Si^{i}Pr_3$, R' = ^{i}Pr;).

Similar behavior is found for hydridogermylenes: **52** is in equilibrium with digermene **51** and only stabilized by DMAP to form complex **53**. Larger substituents, however, allow for the isolation of monomeric hydridogermylenes **54a,b** (Scheme 25).[164,239]

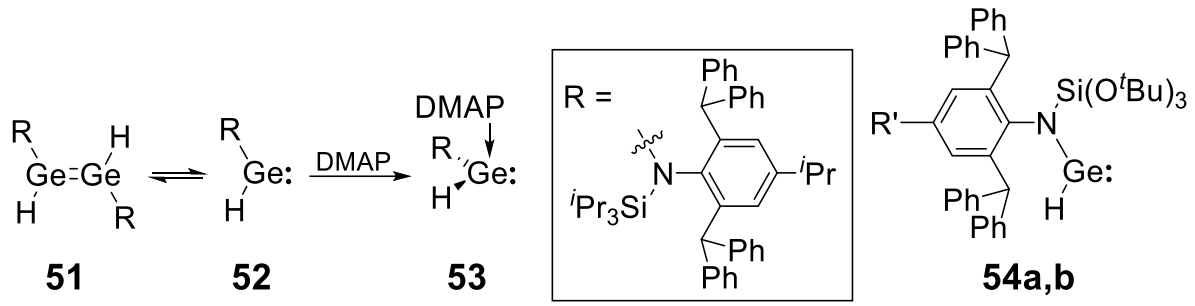

Scheme 25: Equilibrium between dihydridodigermene **51** and hydridogermylene **52** and synthesis of donor-stabilized germylene complex **53** as well as isolable hydridogermylenes **54a,b** (**54a**: R' = Me; **54b**: R' = ^{i}Pr).

Stabilization of germylenes with adjacent π-donors is most effective in planar molecules with maximal overlap of the orbitals involved in π backdonation. Planarity can be enforced by incorporation into a ring (Scheme 26). The first example of cyclic germylenes of this sort was reported by Veith *et al.* with the four-membered ring **55**.[240] Since then, NHGes **56**, **57a-f** and **58** have been reported[241–247] and dehydrochlorination of β-diketiminato chelated chlorogermylene **23g** gives germylene **59**.[248]

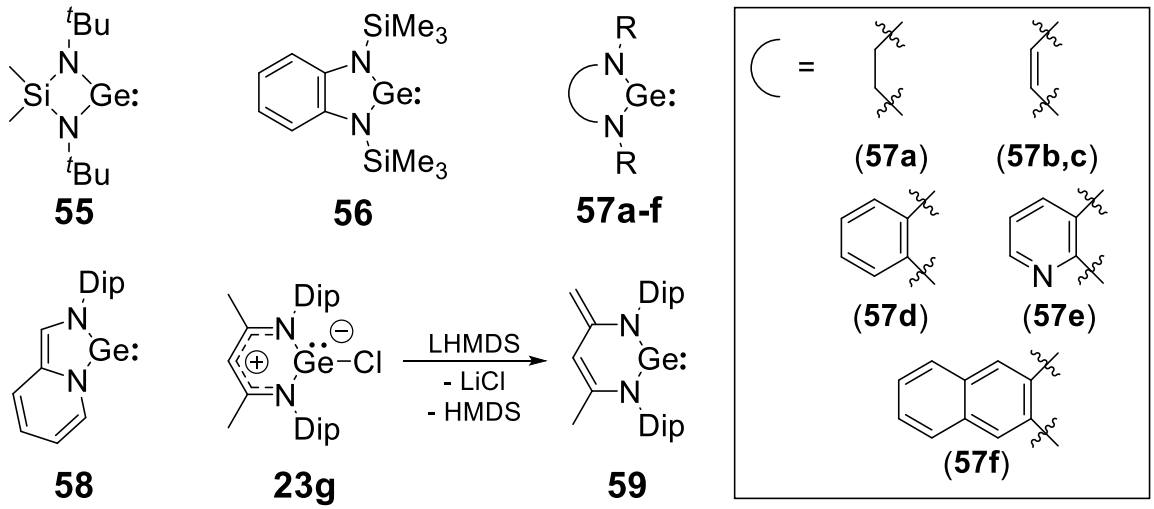

Scheme 26: Stable cyclic germylene **55**, NHGes **56**-**58** and synthesis of six-membered ring germylene **59** from **23g** (**57a**, **57b**: R = ^{t}Bu; **57c-f**: R = $CH_2{}^{t}$Bu).

Regarding the construction of extended inorganic structures and chelating ligands, bisgermylenes are attractive synthetic targets and have been realized as **60**-**63** (Scheme 27).[222,249–254] Bis-NHGes **63a-h** are particularly interesting as NHGes are strong σ-donors and therefore potential ligands in coordination chemistry and catalysis. For example, **63h** forms the chelate-complex **64** upon treatment with a

molybdenum complex.[254] Other examples of bisgermylenes were synthesized by reaction of digermynes with unsaturated organic compounds.[255,256]

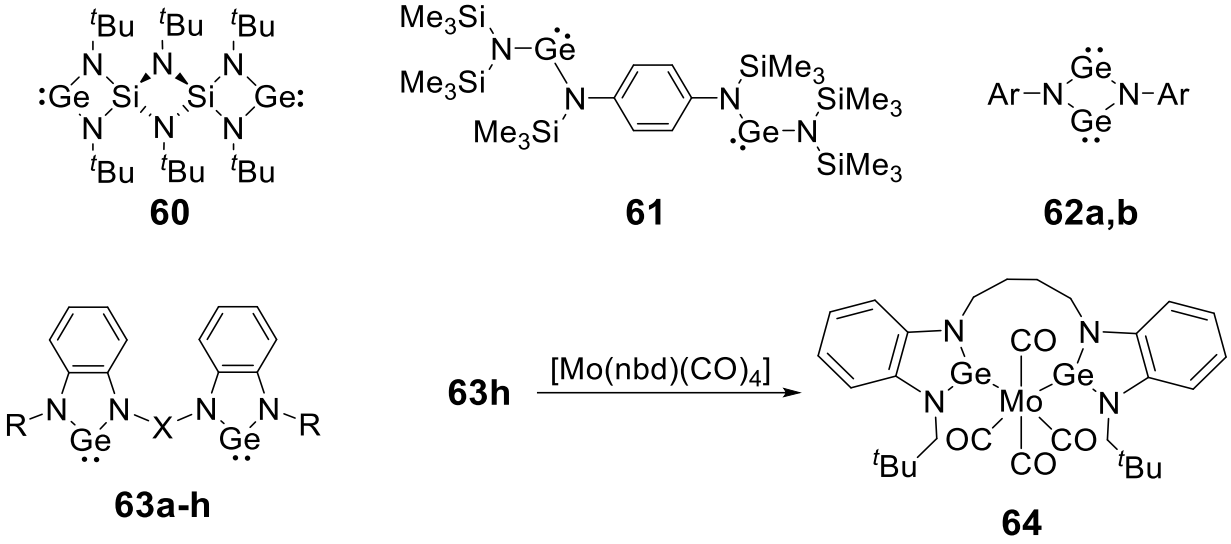

Scheme 27: Bisgermylenes **60-63** and chelate complex **64** (**62a**: Ar = 2,4,6-$Me_3C_6H_2$; **62b**: Ar = 2,4,6-$(CF_3)_3C_6H_2$; **63a**: R = $CH_2{}^tBu$, X = -$C(CH_3)_2$-; **63b**: R = $CH_2{}^tBu$, X = -$(CH_2)_2$-; **63c**: R = $CH_2{}^tBu$, X = -$(CH_2)_3$-; **63d**: R = $CH_2{}^tBu$, X = *o*-C_6H_4-; **63e**: R = $CH_2{}^tBu$, X = *m*-C_6H_4-; **63f**: R = Et, X = -$(CH_2)_2$-; **63g**: R = Et, X = -$(CH_2)_3$-; **63h**: R = $CH_2{}^tBu$, X = -$(CH_2)_5$-).

2.2. GeR: Germyliumylidenes & Germanylidenides

The parent compounds of monosubstituted germanium species have been observed during CVD (cf. Section 1.2.).[87–96] GeH^+ (germyliumylidene) and GeH^- (germanylidenide) are isolobal to borylene and phosphinidene, respectively, while the GeH radical represents a germanium(I) species (Figure 4). Sufficient stabilization of such species necessarily requires enormous steric bulk at the single substituent of $GeR^{+/0/-}$ or Lewis-base coordination to the otherwise extremely reactive low-valent germanium centers.

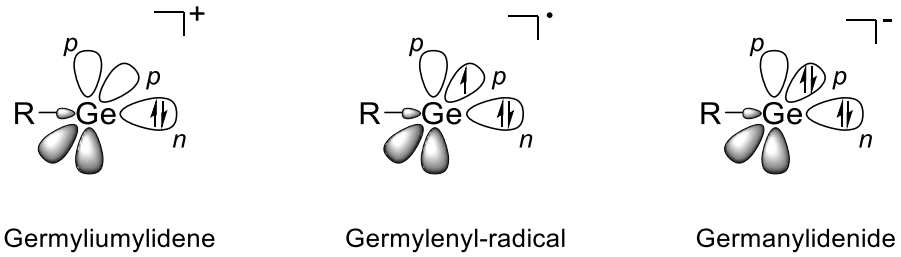

Figure 4: Electronic structure of $GeR^{+/0/-}$- species.

Early examples of chlorogermyliumylidenes $GeCl^+$ were obtained by chloride abstraction from $GeCl_2$ dioxane with $AlCl_3$ and $GeCl_2$, respectively and stabilized by polydentate [2.2.2]-paracyclophane or crown ethers.[257,258] Highly nucleophilic, chelating ligands themselves can induce dismutation of **8a** into $GeCl_3^-$ and $GeCl^+$, a strategy employed in the syntheses of **65a-f** (Scheme 28).[259–264] Analogously, NHC **10d** expels the triflate group as an anion from **12g** to form **65g**.[265] Chlorogermyliumylidenes are frequently encountered as the chloride substituent stabilizes the singlet state shown in Figure 4 and therefore facilitates coordination of ligands. They furthermore serve as precursors for mononuclear Ge(0) species, the so-called germylones (cf. Section 2.3).

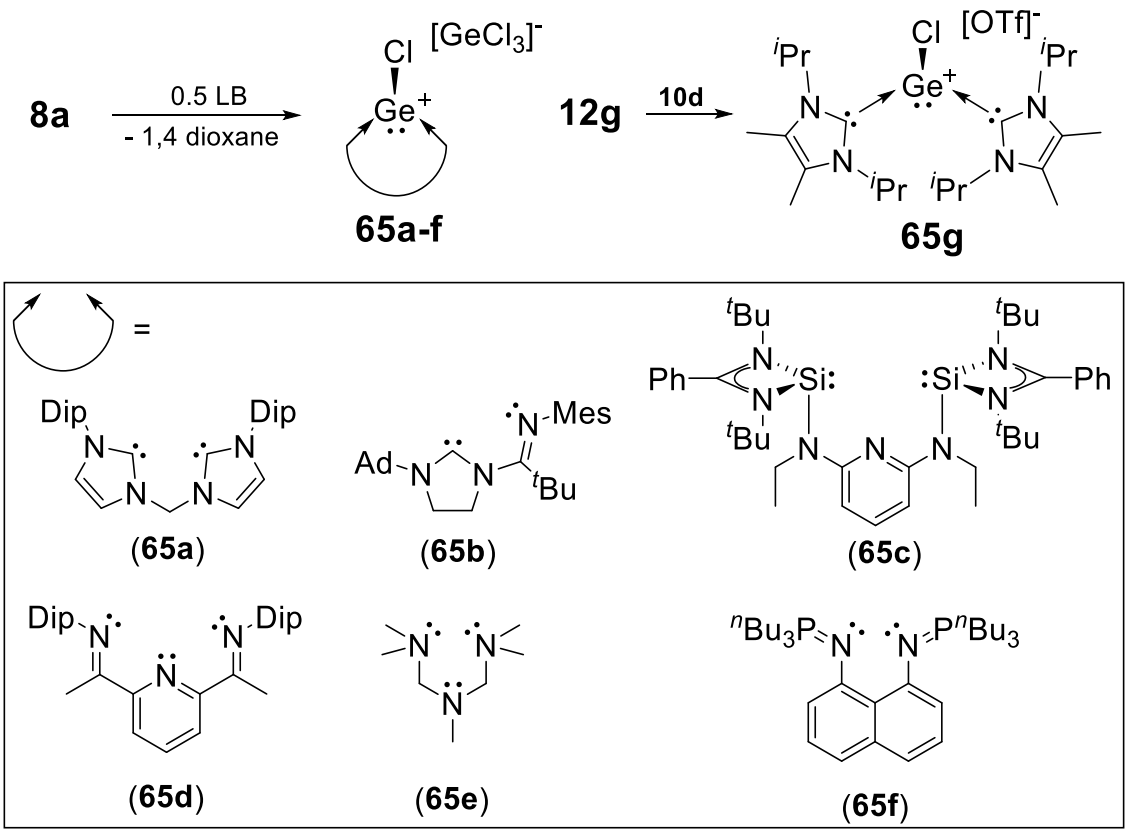

Scheme 28: Synthesis of chlorogermyliumylidenes **65a-f** by dismutation of **8a** and synthesis of **65g** *via* nucleophilic substitution of triflate-functionalized chlorogermylene **12g** with NHC **10d**. Atoms with drawn lone-pairs participate in coordination to $GeCl^+$.

Exchange of chloride in base-stabilized chlorogermylenes against weakly coordinating anions gives access to germyliumylidenes **67-69** by treatment of **66a,b** with $Na[BAr^f_4]$ (Ar^f = 3,5-$(CF_3)_2$-C_6H_3), **28** with AgOTf and **50a** with $Li[Al\{OC(CF_3)_3\}_4]$, respectively. **69** is further coordinated by DMAP (Scheme 29).[196,266–269]

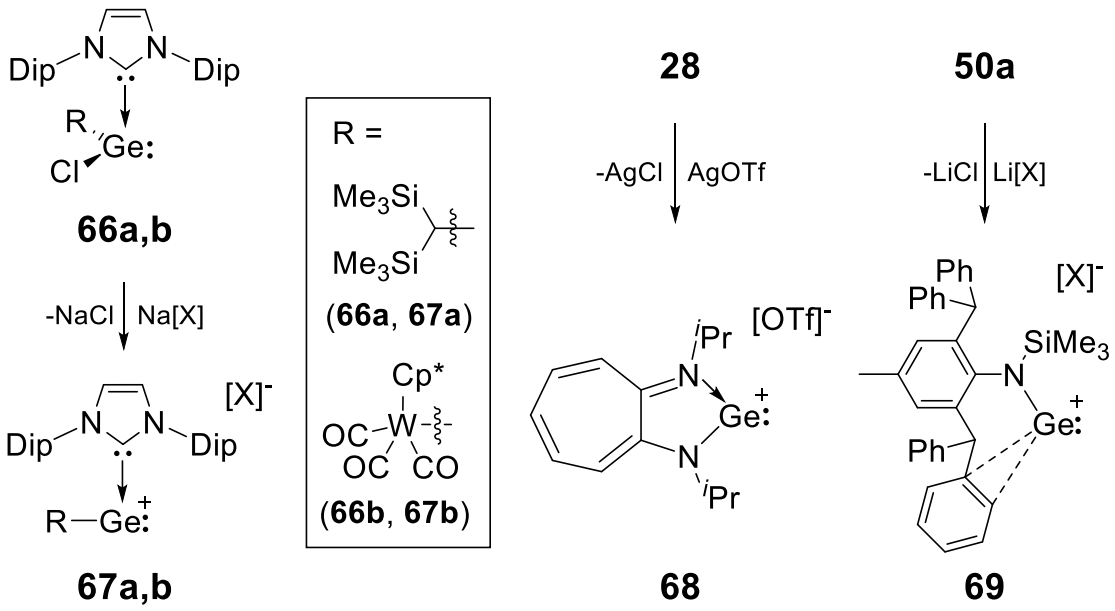

Scheme 29: Synthesis of donor-stabilized germyliumylidenes **67-69** by dechlorination of chlorogermylenes **66a,b**, **28** and **50a** (**66a,b**, **67a,b**: $[X]^- = [BAr^f_4]^-$ (Ar^f = 3,5-$(CF_3)_2$-C_6H_3); **69**: $[X]^- = [Al\{OC(CF_3)_3\}_4]^-$).

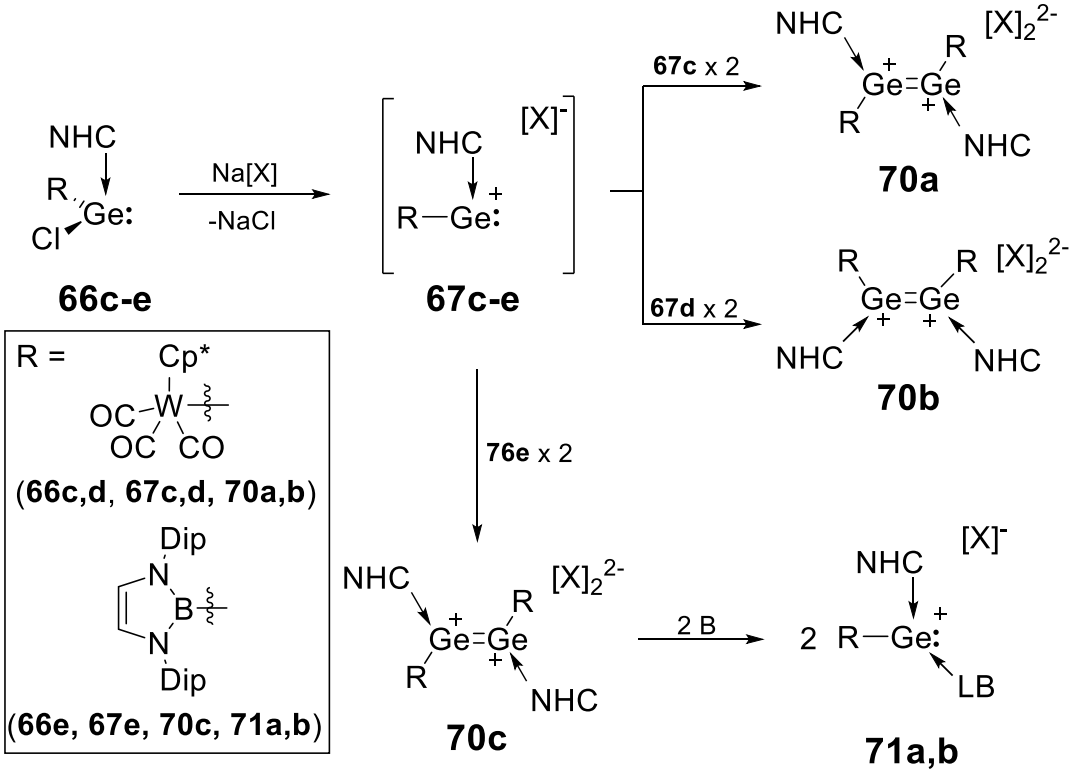

Scheme 30: Dimerization of intermediate germyliumylidenes **67c-e** to dicationic digermynes **70a-c** and base-induces cleavage of **70c** to germyliumylidenes **71a,b** ($[X]^- = [BAr^f_4]^-$ (Ar^f = 3,5-$(CF_3)_2$-C_6H_3); **66c**, **67c**, **70a**: NHC = **10b**; **66d,e**, **67d,e**, **70b,c**: NHC = **10d**; **71a**: NHC = **10d**, B = thf; **71b**: NHC = **10d**, B = pyridine).

When the same reaction conditions are applied to chlorogermylenes **66c-e** with sterically less demanding NHCs than those in **66a,b**, dimerization of the intermediate germyliumylidenes **67c-e** to the digermyne dications **70a-c** takes place (Scheme 30).[268,270] **70c** was reported to dissociate back into its germyliumylidene monomers **71a,b** upon addition of weak donors such as thf or pyridine. Theoretical investigations as well as solid-state X-ray analysis hint towards a significant delocalization of the positive charges into the NHC backbones of **67b-e** and **70a-c**, which can therefore also be described as germylenes and digermenes with cationic substituents.

β-Diketiminato stabilized **23g** can be either oxidized to cationic germyliumylidene **72** or reduced to the ring-contracted anionic germanylidenide **73** under concomitant release of one equivalent of **74**. Cationic **72** can then be deprotonated to get the cyclic germylene **59** (Scheme 31).[248,271,272]

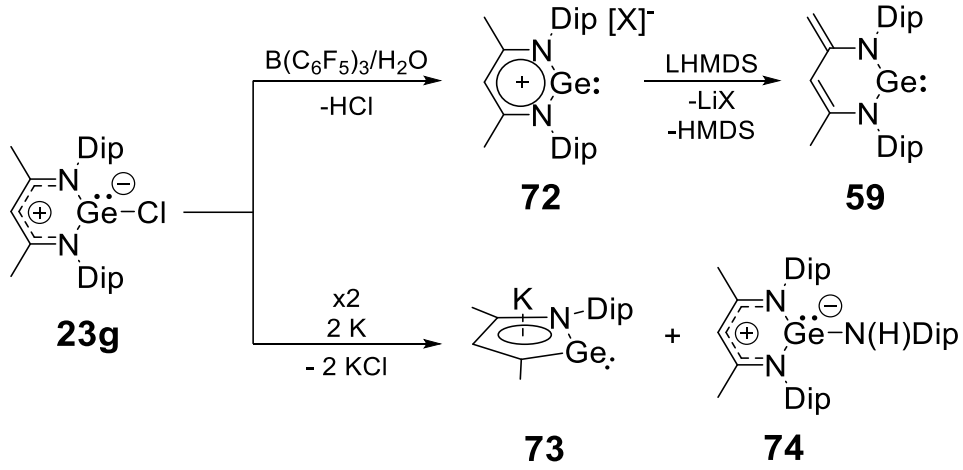

Scheme 31: Synthesis of germyliumylidenes **72** and germanylidenide **73** from **23g** ($[X]^-$ = $[HO(B(C_6F_5)_4)_2]^-$).

The related chlorogermylene **23k** undergoes reversible one-electron reduction to the monovalent radical **75** (Scheme 32).[273] The open-chained monovalent radical **76** and the germanylidene **77** are stabilized by the coordination of cyclic alkylaminocarbenes (cAACs). EPR measurements and DFT calculations, however, suggest considerable spin-density at the carbene center of **76**. Similarly, according to theoretical results **77** is best described as germenide anion **77'**.[274,275]

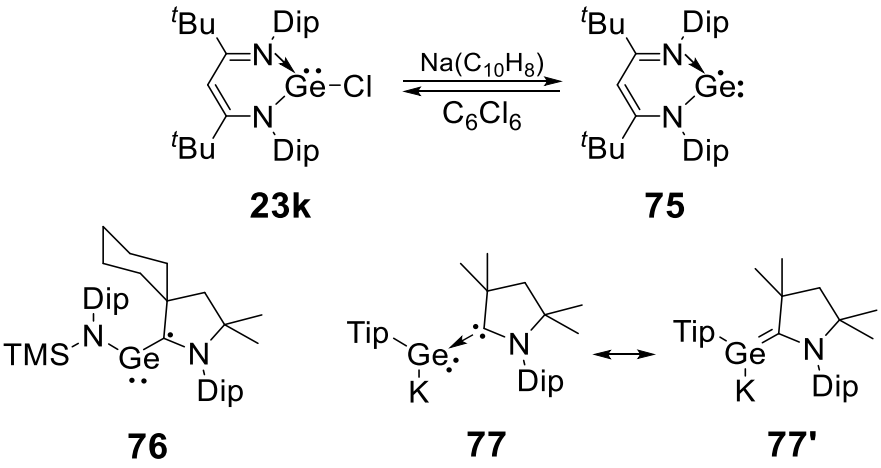

Scheme 32: Reversible one-electron reduction of **23k** to **75** (top) and germylene radical and anion **76** and **77** stabilized by cyclic alkylaminocarbenes.

2.3. Ge(0): Germylones

The concept of ligand-stabilized Ge(0) atoms was proposed by Arduengo *et al.* in 1994 based on photoelectron spectroscopy and bonding analysis of the homologous series of N-heterocyclic tetrylenes. According to this study, NHGe **57b** might be better described as diazabutadiene-stabilized Ge(0) **57b'** (Scheme 33).[276] Indeed, **57** turns out to be an efficient precursor for the deposition of amorphous Ge-layers in CVD,[277] and transfers Ge(0) to other 1,4-diazabutadienes.[278]

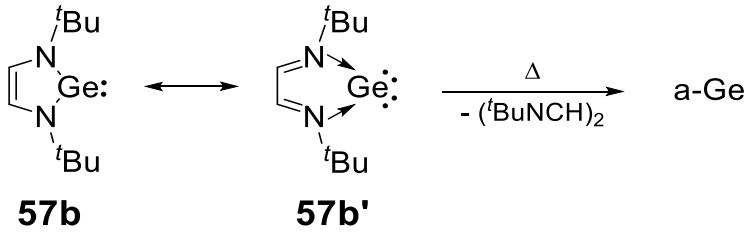

Scheme 33: Representation of **57b** as germylone **5b'** and its deposition to amorphous germanium.

Instead of two covalently bonded substituents Ge(0) complexes experience donation of two donors into their two vacant p orbitals. The remaining s and p orbital are fully occupied and non-bonding. The presence of one lone-pair each of π and σ-symmetry is comparable to the familiar orbital structure of H_2O. Hence, in 2014 Frenking *et al.* suggested the term “germylone” for the germanium case and more general “tetrylones” for any Group 14 derivative of this structural motif in contrast to tetrylenes.

In the same contribution, it was proposed that heavy Group 14 allenes (cf. Section 4.3) might also be regarded as tetrylones.[279] Ge(0) species **78a-d** stabilized by chelating ligands are synthetically accessible by reduction of chlorogermyliumylidenes **65a-d** (Scheme 34).[262–264,280] Note that **65d** needs to be coordinated to an $Fe(CO)_4$ fragment, in order to attain sufficient stability for isolation. The reactivity of germylones has been reviewed, including their capability to act as 4-electron donors.[281–283]

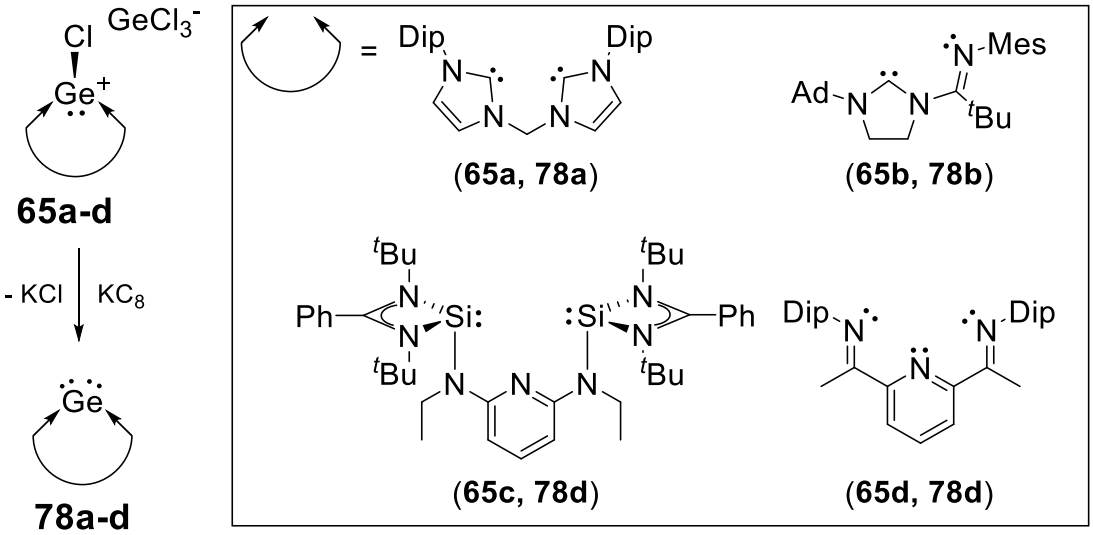

Scheme 34: Synthesis of germylones **78a-d** by reduction of chlorogermyliumylidenes **65a-d**.

In analogy to the synthesis of germyliumylidenes *via* base-induced cleavage of one substituent from a germylene, removal of both substituents gives access to unsubstituted $Ge(II)^{2+}$ species (Scheme 35). In this manner, the NHC-stabilized dication **79** was obtained by reaction of **12f** with **10d** as well as the analogous crown-ether and cryptand-coordinated Ge^{2+} dications.[173,258,265]

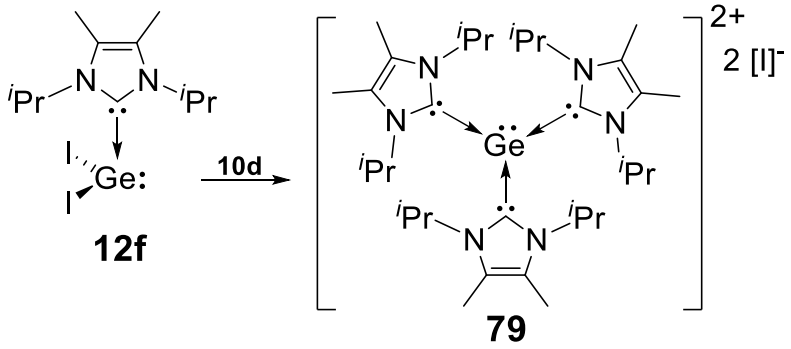

Scheme 35. Synthesis of $Ge(II)^{2+}$ complex **79**.

3. Ge_2- and SiGe Systems

In total, six isomers exist on the E_2H_4 hypersurface (Scheme 36): The double-bonded species **I** and **II** of which the former has a planar D_{2h} symmetry and the second a *trans*-bent geometry, the tetryltetrylene **III**, the mono-bridged **IV** and the double-bridged **V** and **VI** in *cis*- and *trans*-orientation, respectively.[284,285] Although the non-interacting tetrylenes **VII** are only a saddle point in the parent systems, they can be stabilized using strategies as reviewed in the previous chapter (cf. Section 2.1).

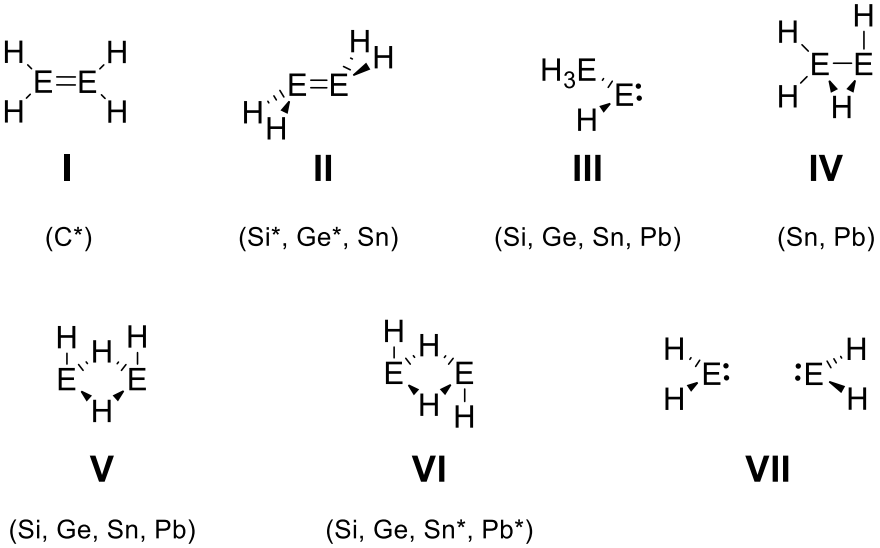

Scheme 36: Minimum structures **I-VI** on the PES of homonuclear E_2H_4 and the non-minmum structure **VII** (E = C, Si, Ge, Sn, Pb; elements in parentheses indicate local minima on the PES; an asterisk marks the global minimum).

Even though the planarity of olefins is almost dogmatic and entangled with fundamental concepts like hybridization or the VSEPR model, isomer **I** is a saddle point for every Group 14 element except carbon. Instead, *trans*-bent **II** is the global minimum on the silicon and germanium PES. In line with these results, isolated heavy double bonds indeed show two deviations from the classical planar double bond geometry (Figure 5): out-of-plane bending of the substituents, the so-called *trans*-bending and the dihedral distortion of the substituents, referred to as twisting. The *trans*-bent angle θ is defined as the angle between the double bond vector and the R-E-R plane while the twist angle τ is defined as the angle between the two R-E-R planes. While *trans*-bending is an intrinsic property of heavy double bonds in general, twisting is a direct consequence of the required bulky substituents' repulsion.

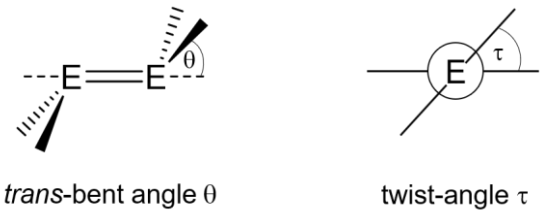

Figure 5: Non-classical deviations of double bonds, *trans*-bent θ and twist τ.

Rationalizations for *trans*-bending[286] reach from a resonating lone-pair,[287] over the second-order Jahn Teller effect,[288] to favorable orbital mixing as a consequence of smaller HOMO-LUMO gaps.[58,289,290] The most popular explanation, however, is given by the model of Carter, Goddard, Malrieu and Trinquier (CGMT) in which olefins are described as dimers of the corresponding tetrylene fragments (Figure 6).[59,289,291–294]

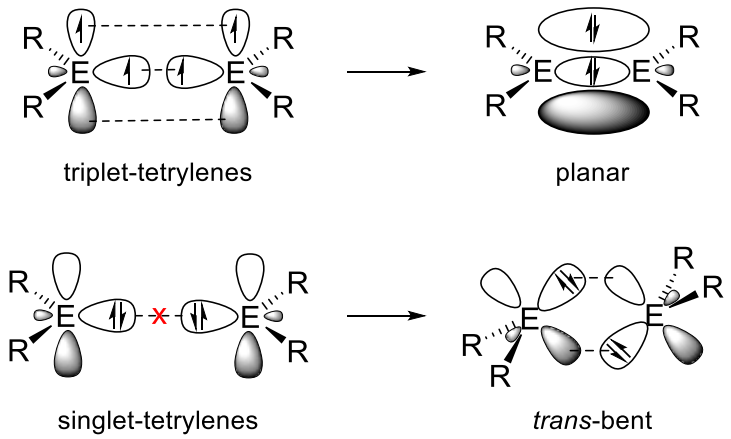

Figure 6: Dimerization of triplet and singlet tetrylenes to planar and *trans*-bent double bonds according to the CGMT model.

While triplet tetrylenes can approach each other directly to form a planar double bond, such an orbital interaction is impossible for singlet tetrylenes. The tilting of the bonding planes against each other, however, allows for a double donor-acceptor interaction between the lone-pairs and the vacant p-orbitals. Hence, the geometry of a double bond is determined by the singlet-triplet gaps $\Delta E_{S\rightarrow T}$ of the constituting fragments. Trinquier and Malrieu showed that the relation between $\Sigma\Delta E_{S\rightarrow T}$ and the double bond energy $E_{\sigma\text{-}\pi}$ can be taken as a predictive indicator for the double bond geometry (Figure 7):[292,293] If $\Sigma\Delta E_{S\rightarrow T} < 0.5\ E_{\sigma+\pi}$, a classical planar double bond results; *trans*-bent structures are encountered if $0.5\ E_{\sigma+\pi} < \Sigma\Delta E_{S\rightarrow T} < E_{\sigma+\pi}$ and for $\Sigma\Delta E_{S\rightarrow T} > E_{\sigma+\pi}$ no double bond is formed at all. These relationships are of general

validity and include asymmetric double bonds but also triply bonded species (in this case, characterized by their doublet-quartet splitting).

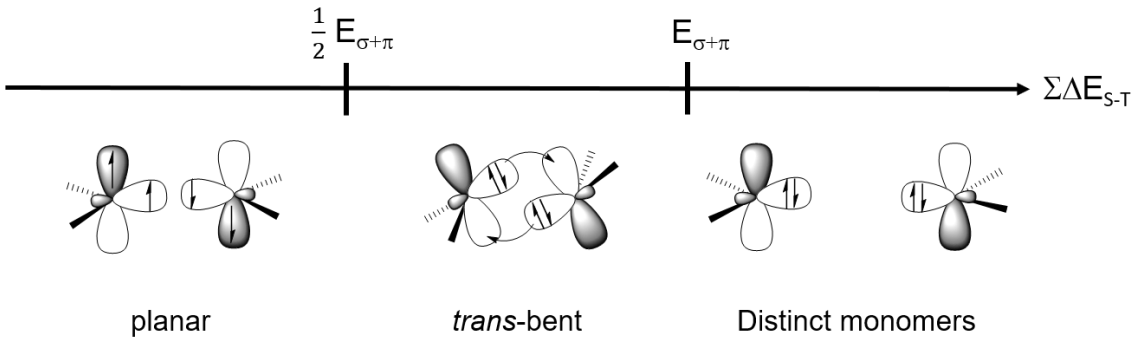

Figure 7: Dependence of the double bond geometry on $\Sigma\Delta E_{S\rightarrow T}$ according to the CGMT model.

The CGMT model rationalizes the global minima on the E_2R_4 hypersurfaces. Planar double bonds **I** are formed by non-stabilized carbenes as they predominantly possess a triplet ground state (negative $\Sigma\Delta E_{S\rightarrow T}$). The inert-pair effect accounts for increasing $\Sigma\Delta E_{S\rightarrow T}$ values when descending Group 14, leading to *trans*-bent disilenes and digermenes **II**, while stannylenes and plumbylenes do not form double bonds at all but bridged species **V** and **VI** which is reinforced by highly polarized E-H bonds with significant electrostatic contributions.[295] Similarly, germylenes with strongly electron-withdrawing substituents rather dimerize to bridged **VI** than *trans*-bent **II** like observed in the gas-phase for GeF_2,[296] and in the solid state for alkoxygermylenes.[207] Bent's rule accounts for substituent effects on the singlet-triplet gap $\Sigma\Delta E_{S\rightarrow T}$ of the carbene-like fragments and with that on the double bond geometry as electronegative substituents induce *trans*-bent or even dissociation while electropositive moieties planarize the double bond.[294,297–299] Most recent theoretical studies indicate stabilization of some double bonds by dispersion between the large substituents.[300,301]

3.1. Ge_2R_4: Digermenes

In accordance with their description as adducts of germylenes in the CGMT model, digermenes are usually synthesized by dimerization of germylenes, which are in turn obtained from different precursors (Scheme 37). The majority of isolated digermenes is thus symmetric, in the sense of being composed of two identical germylene fragments.

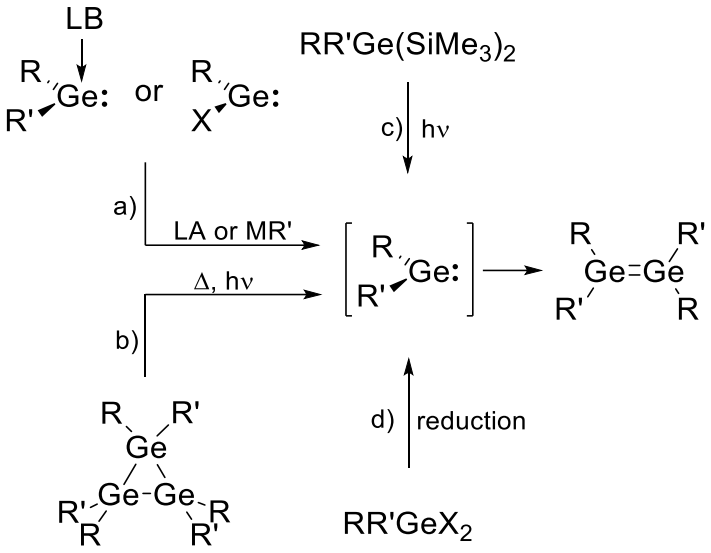

Scheme 37: Syntheses of digermenes by dimerization of unstable germylenes from stable (a) germylenes, (b) cyclotrigermanes, (c) bis(trimethylsilyl)germanes and (d) dichlorogermanes.

Pathway a) is encountered in the dimerization of Lappert's germylene **35** and synthesis of digermene **15** from **16** *via* removal of stabilizing NHC (Scheme 12).[179,215,217] The dimerization behavior, however, is markedly different, as **35** is stable in solution and only dimerizes in the solid state whereas **15** is immediately formed in solution while the donor-free version of **16** cannot be observed. Solution stable digermenes **1a-d** are accessible *via* pathways b) and c) (Scheme 38). Cyclotrigermanes **80a-c** undergo [2+1] cycloreversion to digermenes **1a-c** and germylenes **81a-c**, which in turn dimerize to another half equivalent of **1a-c**.[302–304] Photolysis of the bis(trisilyl)germanes **82a-e** allowed matrix isolation and spectroscopic characterization of germylenes **81a-e** and digermenes **1a-e**.[62,305–307]

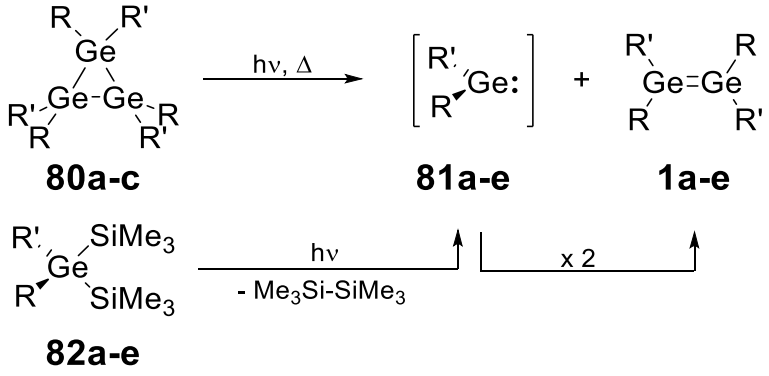

Scheme 38: Syntheses of digermenes **1a-e** by cleavage of cyclotrigermanes **80a-c** or bis(trimethylsilyl)germanes **82a-e** (**1a**, **80a**, **81a**, **82a**: R = R' = Mes; **1b**, **80b**, **81b**, **82b**: R = R' = Xyl; **1c**, **82c**, **83c**: R = R' = Dep; **1d**, **81d**, **82d**: R = Mes, R' = ^{t}Bu; **1e, 80e**, **81e**, **82e**: R = R' = Tip).

The homoleptic triisopropylphenyl-substituted digermene **1e** is also accessible *via* pathway d), the reductive coupling of dichlorogermane **83a**, a method that is employed as well for the synthesis of **1f-h** from **83b-d** (Scheme 39).[308–311] Just as their less sterically congested analogues **1a-e, 1f-h** do not dissociate in solution and **1h** exhibits *E-Z* isomerism in solution, presumably through rotation about the Ge-Ge bond.[312]

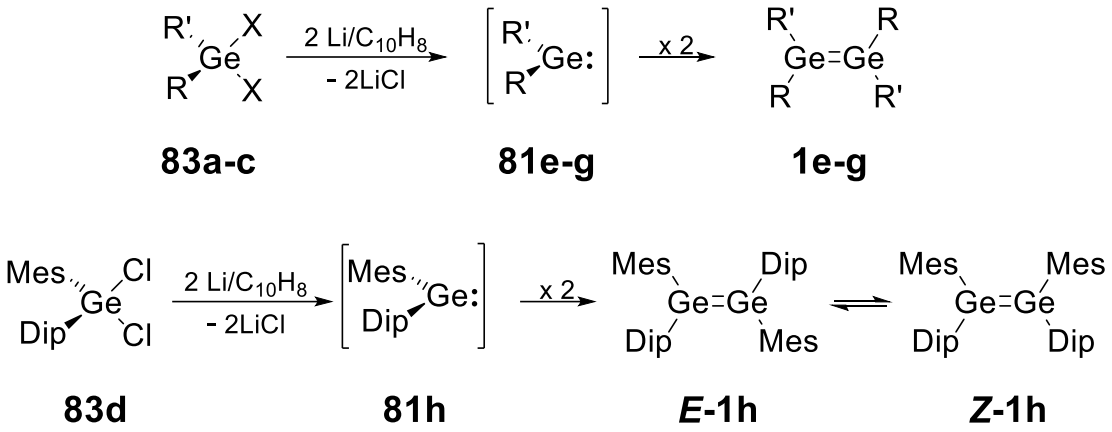

Scheme 39: Synthesis of digermenes **1e-h** *via* reductive coupling of dichlorogermanes **83a-d** (**83a**: X = Cl, R = R' = Tip; **83b**: X = Cl, R = R' = Tip; **83c**: X = Br, R = Tip, R' = ferrocenyl; **81e**, **1e**: R = R'= Tip; **81f**, **1f**: R = R'= Dip; **81g**, **1g**: R = Tip, R' = ferrocenyl).

A different behavior is observed in the digermenes **1i-k** (Scheme 40): The sterically less encumbered **1i** retains its structure, whereas **1j** dissociates into germylene **81j**.[313,314] The extremely bulky digermene **1k** is in equilibrium with its germylene **81k**.[315,316]

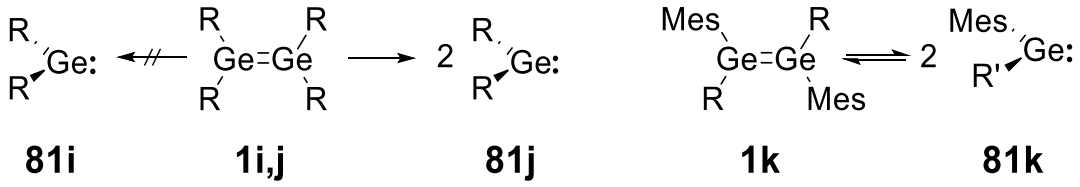

Scheme 40: Aryldigermenes **1i-k** and their differing dissociation behavior in solution (**1i**, **81i**: R = 2,5-^{t}Bu$_2$C$_6$H$_3$; **1j**, **81j**: R = 6-^{t}Bu-2,3,4-Me$_3$C$_6$H; **1k**, **81k**: R = 2,4,6-((Me$_3$Si)$_2$HC)$_3$C$_6$H$_2$).

The non-trivial relationship between the steric bulk of the substituents and the structural characteristics of the resulting digermene becomes obvious in Table 4. None of the structural features (Ge-Ge distance, *trans*-bent angle θ, or twist angle τ) nor the dissociation behavior in solution follow any obvious trend, making the choice of substituents crucial when designing digermenes.

Table 4: Structural parameters and dissociation behavior of selected digermenes.

	R	Ge-Ge [Å]	θ [°]	τ [°]	Dissociates?
1a	Mes	2.2856(8)	33.4	2.9	no
1c	Dep	2.213	12.4	10.8	no
1e	Tip	2.2894(6)	12.3	13.7	no
***Z*-1h**	Mes/Dip	2.3011(9)	36.3	3.4	no
1i	2,5-^{t}Bu$_2$C$_6$H$_3$	2.3643(4)	47.7	10.9	no
1j	2-^{t}Bu-4,5,6-Me$_3$C$_6$H	2.252	0	20.4	yes
1k	Mes/2,4,6-(CH(SiMe$_3$)$_2$)$_3$C$_6$H$_2$	2.416(2)	21.4	9.0	yes

This is also exemplified by digermenes **87a-c**, which are synthesized from NHGes **57a,g,h** and NHSi **84** (Scheme 41). Initial formation of germasilenes **85a-c** is followed by 1,3-shift to the thermodynamically favorable silylgermylene **86a-c** (cf. Section 3.5). Depending on the substituent at the NHGe, dimerization to either the *Z*-digermene **87a** (R = ^{t}Bu, Ge-Ge: 2.454(2) Å, θ = 41.3°, τ = 22.3°), the *E*-isomer **87b** (R = ^{i}Pr, Ge-Ge: 2.460(1) Å, θ = 47°, τ = 63°) or the weakly bonded germylene dimer **87c** (R = Xyl, Ge-Ge: 4.10 Å) occurs.[317,318]

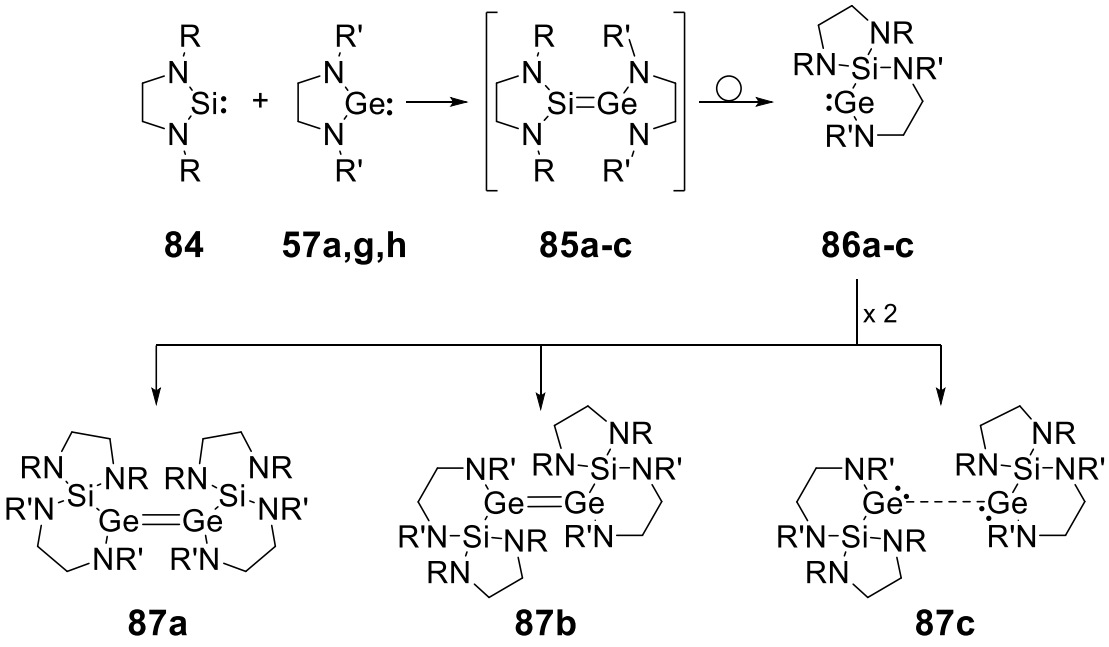

Scheme 41:Structurally different digermenes **87a-c** from NHSi **84** and NHGes **57a,g,h** (R = ^{t}Bu; **57a**, **85a**, **86a**, **87a**: R' = ^{t}Bu; **57g**, **85b**, **86b**, **87b**: R' = ^{i}Pr; **57h**, **85c**, **86c**, **87c**: R' = Xyl).

In a similar manner as the silyl-substituted digermenes **15** and **87a,b** mentioned previously, compounds **88a-d** (Scheme 42) are obtained by reduction of the corresponding dichloro precursors. Whereas **88a,c** are reported to exhibit no twisting about the double bond at all, **88d** exhibits a significantly reduced HOMO-LUMO gap due to substantial twisting, resulting in its blue color.[319–323] The sterically less encumbered digermene **88e** is only stable when coordinated to a transition metal center under formation of complexes **89a-c**.[324,325] All digermenes **88a-d** show no sign of dissociation in solution, as expected on grounds of the CGMT model.

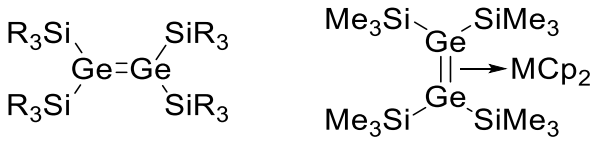

88a-e **89a-c**

Scheme 42: Silyl substituted digermenes **88a-e** and Tetrakis(trimethylsilyl)digermene complexes **89a-c** (**88a**: SiR_3 = $SiMe_2{}^iPr$; **88b**: SiR_3 = $SiMe_2{}^tBu$; **88c**: SiR_3 = Si^iPr_3; **88d**: SiR_3 = $SiMe^tBu_2$; **88e**: SiR_3 = $SiMe_3$; **89a**: M = Ti; **89b**: M = Zr; **89c**: M = Hf).

A whole class of digermenes has been reported by Power *et al.*, which contain a large terphenyl-group at germanium that allows for smaller and more reactive groups at the second binding site (Scheme 43). In this way, dihalodigermenes **90a-c**,[162,232,236] dialkyldigermenes **91a-c**,[162] diacetylenyldigermenes **92a,b** and dihydridodigermene **93** were isolated.[326–328] They were synthesized by dimerization of *in situ* generated germylenes and remain intact in solution except for the dichloro-derivatives **90a-c**, which dissociate into germylenes **47a-c** (Scheme 24). All these digermenes adopt *E*-geometry in the solid state.

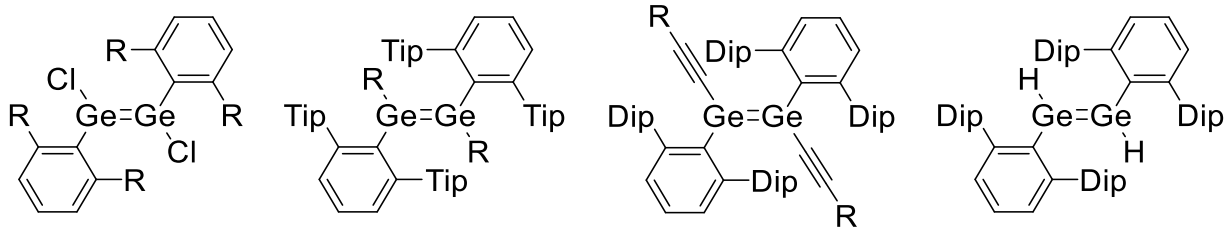

90a-c **91a-c** **92a,b** **93**

Scheme 43: Terphenyl-protected digermenes **90a-c**, **91a-c**, **92a,b** and **93** (**90a**: R = Mes; **90b**: R = Dip; **90c**: R = Tip; **91a**: R = Me; **91b**: R = Et; **91c**: R = Ph; **92a**: R = ^{t}Bu; **92b**: R = $SiMe_3$).

The terphenyl group is not the only extremely bulky substituent that is capable of stabilizing dihalodigermenes: Matsuo *et al.* isolated **94a-c** by employing the rigid hydrindacen-4-yl groups Eind and Mind and Tokitoh *et al.* synthesized **95a,b** with sterically demanding aryl groups (Scheme 44). In solution, **95a,b** are in equilibrium with bromogermylenes **96a,b** while **94a-c** completely dissociate.[339–332]

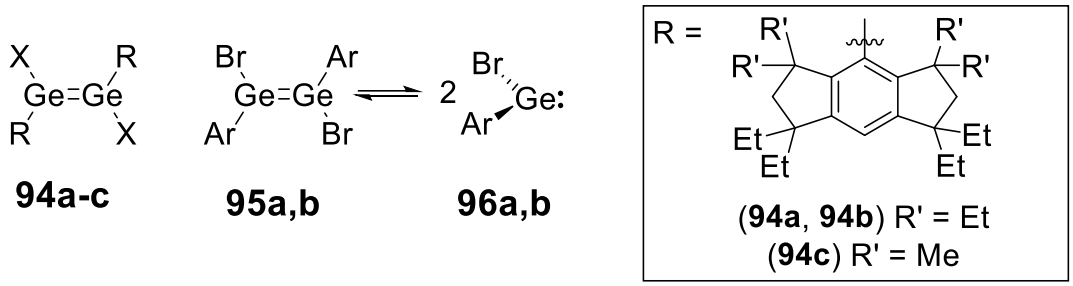

Scheme 44: Dihalodigermenes **94a-c** and **95a,b** (**94a**: X = Cl, **94b**: X = Br; **94c**: X = Cl; **95a**, **96a**: Ar = 2,4,6-$((Me_3Si)_2HC)_3C_6H_2$; **95b**, **96b**: Ar = 2,6-$((Me_3Si)_2HC)_2$-4-$((Me_3Si)_3C)$-C_6H_2).

Dihydridodigermenes are accessible *via* hydrogenation of chlorogermylenes and by reaction of the corresponding digermynes with molecular H_2 (cf. Section 3.3).[164,180,256,327,328] Parent digermene and tetrachlorodigermene were furthermore obtained using the donor-acceptor approach already employed in the case of complex **18a**.[333,334] The chloro derivative undergoes growth reactions with $GeCl_2$, giving insight into CVD gas-phase processes.

Only three unsymmetrically substituted digermenes are known (Scheme 45): Digermene **97** is obtained by hydrogermylation of cyclopentene with **93** [335] and two silyldigermenes can be isolated *via* salt elimination of a lithium digermenide (cf. Section 3.2) with the corresponding chlorosilanes.[336]

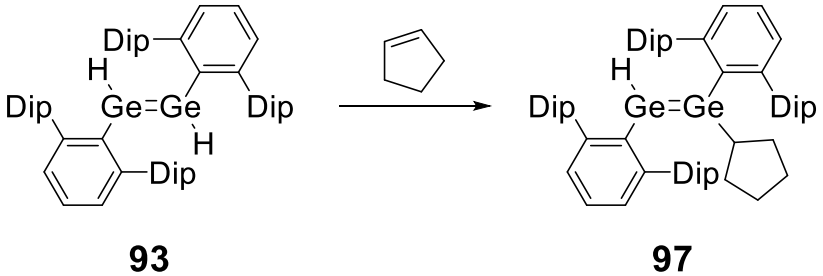

Scheme 45: Synthesis of unsymmetric digermene **97** by hydrogermylation of pentene with **93**.

The only compound that features conjugation between a Ge-Ge bond and another heavy multiple bond is tetragermabutadiene **99** (Scheme 46), which was obtained by

Weidenbruch *et al.* by oxidative coupling of digermenide **98a**. The two digermenes adopt a *s*-cis conformation and the π-systems of the two double bonds interact efficiently according to the pronounced bathochromic shift in the UV/vis spectrum compared to all-Tip substituted digermene **1e**.[337]

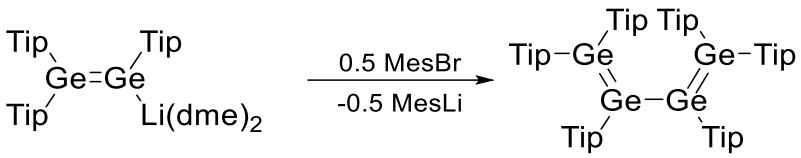

98a **99**

Scheme 46: Synthesis of the conjugated tetragermabutadiene **99** from digermenide **98a**.

In general, compounds with conjugated heavy main group double bonds are rare. Several disilenes with large aromatic groups have been reported that exhibit interesting spectroscopic properties like electroluminescence or near-IR emission.[338–340] Tetrasilabutadienes have been isolated as well as bridged derivatives.[340–342] Higher oligomeric species are only known for disilenes (number of E=E repeat units, *n* = 4),[343] phosphenes (*n* = 21)[344] and diphosphenes (*n* = 26).[345] Naturally the class of poly(ditetrenes) is of extraordinary interest due to the potential applications when combining conductive polymers with semiconductive properties of silicon and germanium.

Not only acyclic digermenes have been isolated, also a reasonable number of cyclic digermenes is known (Scheme 47). Cyclotrigermene **100a** was the first of its kind and due to their unique chemistry, the cyclotrigermenes will be covered in a later chapter (cf. Section 4.3).[346] Bicyclic compound **101** is inasmuch remarkable as it exhibits an inverted double bond geometry, making it resemble the hemispheroidally coordinated atoms that are defining for siliconoids (cf. Chapter 6).[120] Theoretical investigations further show that its bonding situation is quite unusual as it presumably possesses a Ge-Ge π-bond but no corresponding σ-bond. Four-membered ring analogues can be roughly divided into cyclobutene analogues **102a-g** and cyclobutadiene analogues **103a,b**.[256,310,330,347–350] Five-membered rings are the chalcogenides **104a-c** and the bicyclic system **105**.[310,351,352] Finally, the three-dimensional cage structure **106** as well as the digermabenzene analogues **107** and **108** form the group of known six-membered ring digermenes.[255,352,353] Species with more low-valent silicon and germanium atoms in the ring will be discussed in the corresponding chapters.

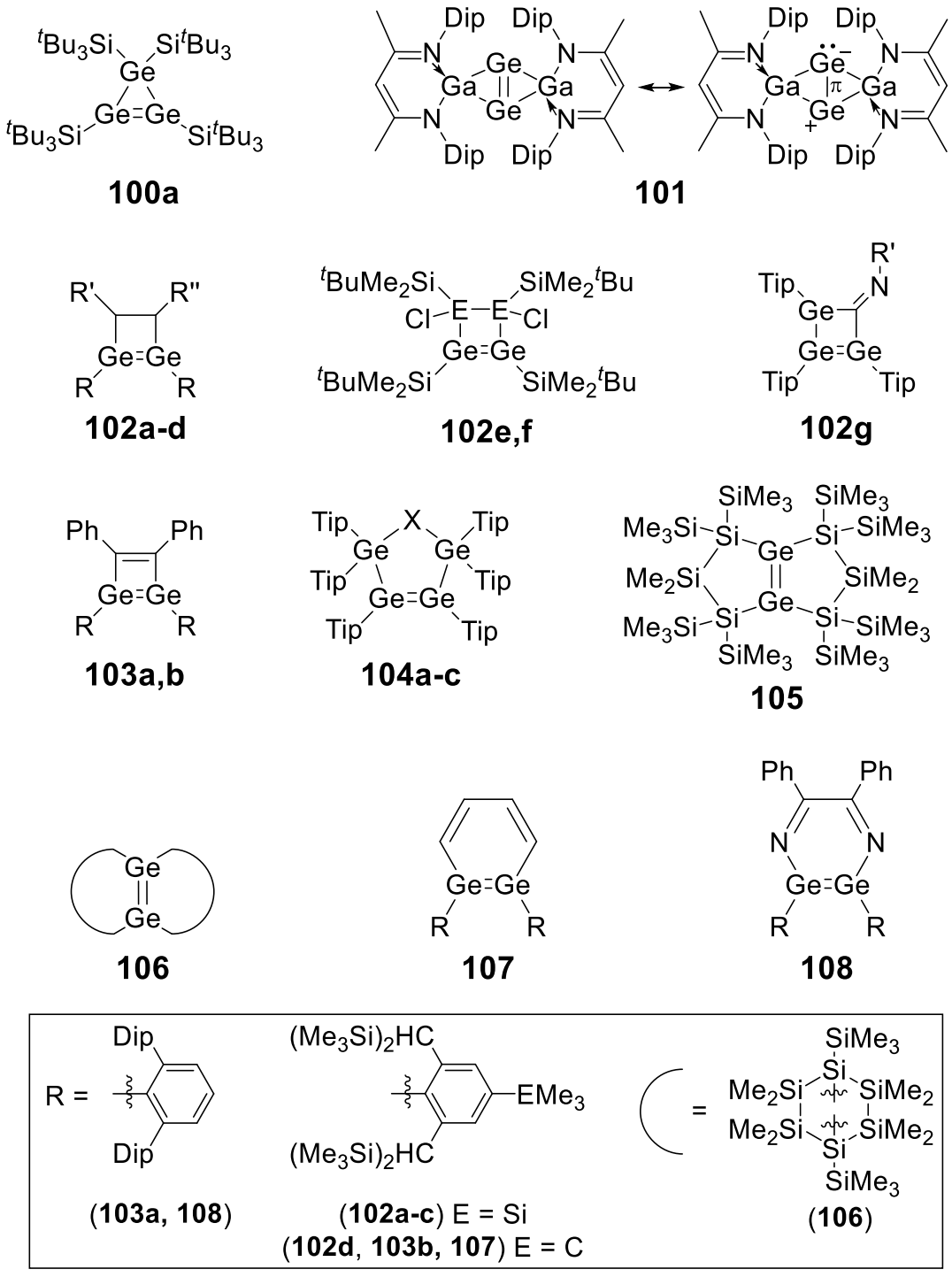

Scheme 47: Reported cyclic digermenes: Three-membered rings **100a**,**101**; Four-membered rings **102a-g**,**103a,b**; Five-membered rings **104a-c**,**105**; Six-membered rings **106-108** (**102a**: R' = R'' = H; **102b**: R' = H, R'' = Ph; **102c**: R' = H, R'' = ^{n}Bu; **102d**: R' = H, R'' = Ph; **102e**: E = Ge; **102f**: E = Si; **102g**: R' = 2-MeO-C_6H_4; **104a**: X = O; **104b**: X = S; **104c**: X = Se).

Neither compounds **102g**, **103a,b** nor **108** show conjugation between their double bonds and digermabenzene **107** exhibits only weak aromaticity based on a non-planar structure and NICS calculations. The π-conjugation between light double bonds and digermenes is presumably disfavored due to the size difference between the p-orbitals.

The reactivity of digermenes is determined by their constitution in solution. Thus, digermenes that dissociate exhibit typical germylene reactivity (cf. Section 2.1), and in fact, whether a digermene cleaves in solution is often decided based on this reactivity. For example, the dissociation of sterically encumbered **1k** was assumed based on the trapping of fragment **81k** with both 2,3-dimethylbutadiene and triethylsilane (reagents that typically do not react with Ge=Ge bonds) to yield germanes **109a** and **110a** (Scheme 48). In contrast, the *E*-*Z* isomerization of **103h** does not appear to proceed through germylene **102h**, as no reaction with 2,3-dimethylbutadiene occurs. Instead the rearrangement may occur through the migration of the substituents. In case of digermene **1a** the 1,2-shift to germylgermylene **111** was proven by the isolation of trapping products **109b** and **110b**.[62,354] The same was found for bis(ferrocenyl)digermene **1g**.[311]Occasionally, germylenes can also be trapped by coordination of bases, for instance, DMAP in case of dihydridodigermene **64** (Scheme 25) and pyridine for dichlorodigermene **60c**.[162,164]

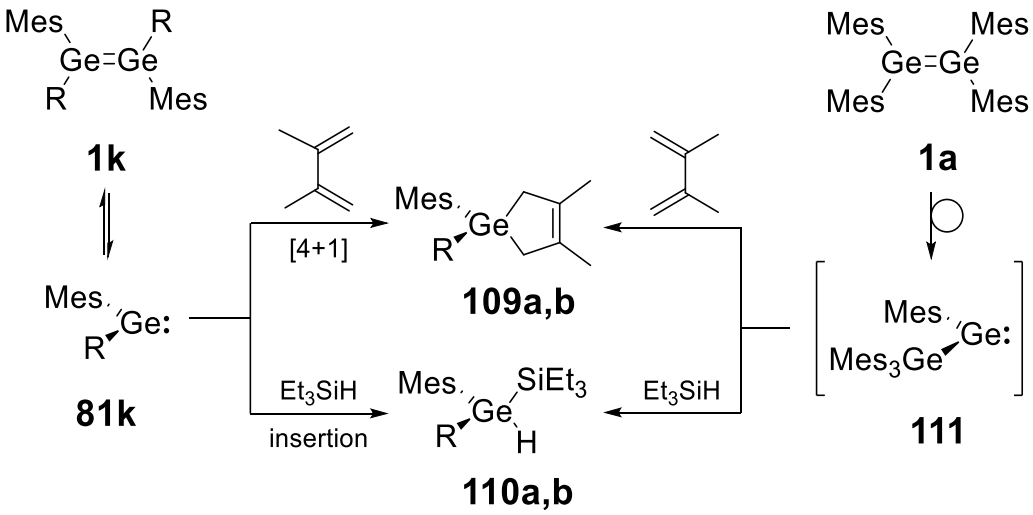

Scheme 48: Germylene reactivity of bulky **1k** with 2,3-dimethylbutadiene and triethylsilane to germanes **109** and **110** and 1,2-shift of digermene **1a** to germylgermylene **111** with subsequent trapping to digermanes **109b** and **110b**. (**1k**, **81k**, **109a**, **110a**: R = 2,4,6-$((Me_3Si)_2HC)_3C_6H_2$; **109b**, **110b**: R = $GeMes_3$).

Cleavage of otherwise stable digermenes can also be induced by NHCs as in the cases of **1a**, **15** or **70c**, which form NHC-germylene complexes **14**, **16** and **71a,b** (Scheme 12, Scheme 30).[178,179,270] Similar reactivity is observed when **1a** is treated with an anionic NHGa. Interestingly, the treatment of **1a** with isocyanides mediates the cleavage of the Ge=Ge bond under formation of the corresponding cyclotrigermane

without isocyanide incorporation (Scheme 4), while **88d** eliminates isoprene under these conditions to form a germyl isocyanide.[64,163,321]

Digermenes that retain the Ge=Ge bond in solution show typical alkene reactivity: Several 1,2-additions with polar reagents (e.g. methanol) have been reported[62,302,303,308,355–358] and various cycloadditions to carbonyl compounds,[66,304,359] C-C multiple bonds,[353,360–362] nitrogen compounds,[64,309,363,364] oxygen,[311,316,317] and heavier chalcogens[308,365,366] are known.

A wide range of different anionic motifs is obtained when digermenes are reduced (Scheme 49): From dianions **112** and **113** and digermenides **98a,b** (cf. Section 3.2) to the four-membered ring system **114** (cf. Section 4.2), which in turn serve as precursors for more complex structures.[308,321,337,367]

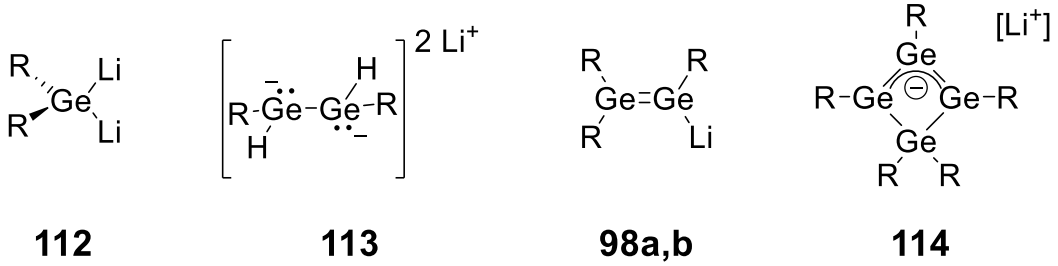

112 **113** **98a,b** **114**

Scheme 49: Anionic species **98a,b** and **112-114** obtainable *via* reduction of digermenes (**112**: R = $SiMe^tBu_2$; **113**: R = 2,6-$Dip_2C_6H_3$; **98a**,**114**: R = Tip; **98b**: R = Dip).

3.2. E_2R_3: Digermenides & Disilenides

First evidence for a heavy vinyl anion was reported in 1989 by Masamune (Scheme 50).[308] Reduction of digermene **1f** with an excess of lithium/naphthalene in dme yields a red microcrystalline substance, which was identified as digermenide **98b** based on NMR and UV/Vis spectroscopy as well as trapping with methanol to give methoxydigermane **115**. In analogous manner, reduction of very similar digermene **1e** with two equivalents lithium powder in dme gives the proposed intermediate **98a**, which is then coupled oxidatively to tetragermabutadiene **99** upon treatment with mesityl bromide.[337] The isolation of **98a** was achieved in 2018, by reaction of the dichlorogermane **83b** with 3.3 equivalents of lithium powder and catalytic amounts of naphthalene in dme. Digermenide **98a** was obtained as extremely air-sensitive orange-red crystals. Its capability to transfer the digermenyl moiety to substrates was

established in proof-of-principle reactions with chlorosilanes to yield asymmetric silyldigermenes **116a,b**.[336] The further reactivity of **98a** remains largely unexplored but the comparison to its disilicon congener **117** allows a glimpse on its synthetic potential.

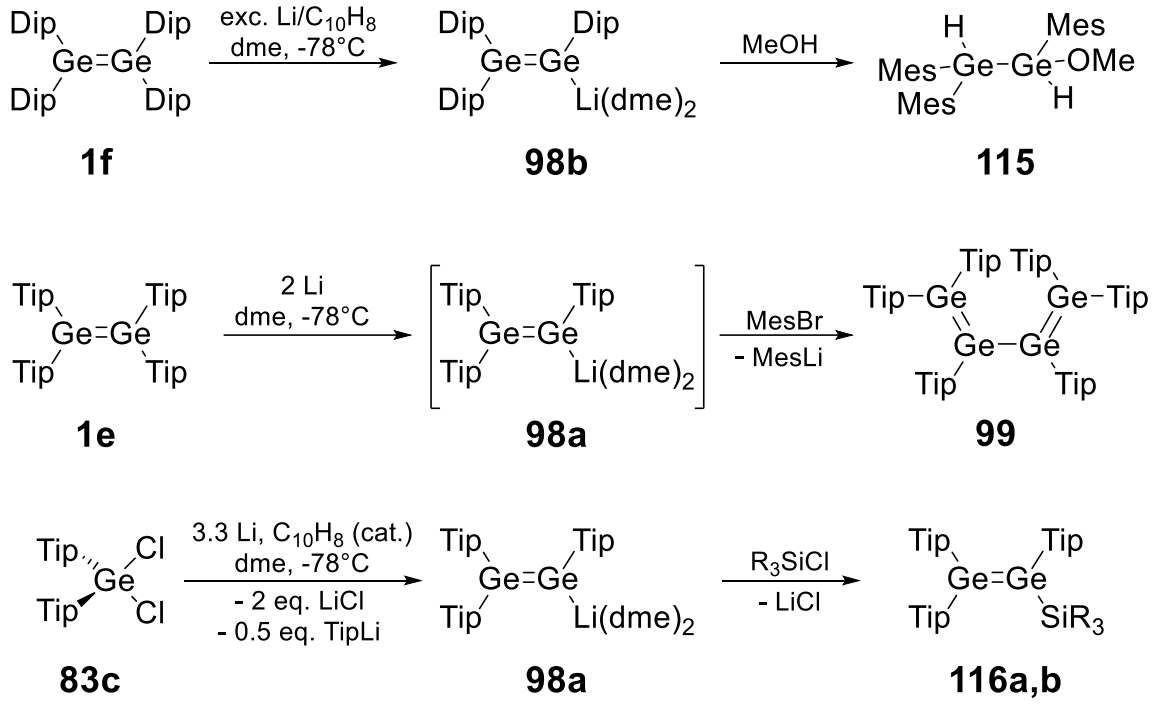

Scheme 50: Syntheses of digermenides **98a,b** and reported reactivity: addition of methanol to digermane **115**, oxidation to tetragermabutadiene **99** and substitution to digermenes **116a,b.**

Like **98a**, disilenide **117** was first postulated as intermediate in the synthesis of a heavy butadiene and is synthesized from the corresponding dichlorosilane (Scheme 51).[368,369] Since then, several disilenides were reported, none of which, however, had the synthetic impact of the Tip-substituted **117**.[370–375]

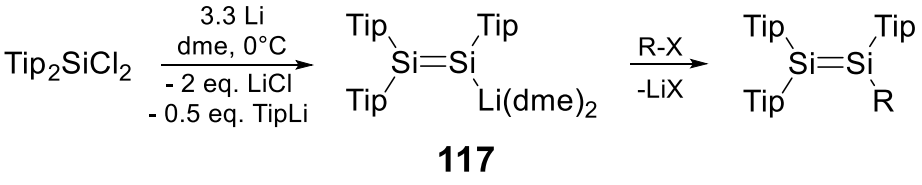

Scheme 51: Synthesis of disilenide **117** and general reactivity towards unfunctionalized element halides (X = halogen, R = silyl-, stannyl-, phosphino-, aryl).

Basic reactivity of **117** includes transmetallation of lithium to other metals,[376,377] and direct attachment of unfunctionalized silyl,[369] stannyl,[378] phosphino,[379] and aryl groups *via* salt elimination.[340,380–382] Reaction with aryldihalides makes bridged

tetrasilabutadienes **118a-e** accessible of which **118a** can be used to construct hybrid polymer **119** by treatment with 1,4-diethynylbenzene (Scheme 52).[340,342,381,383]

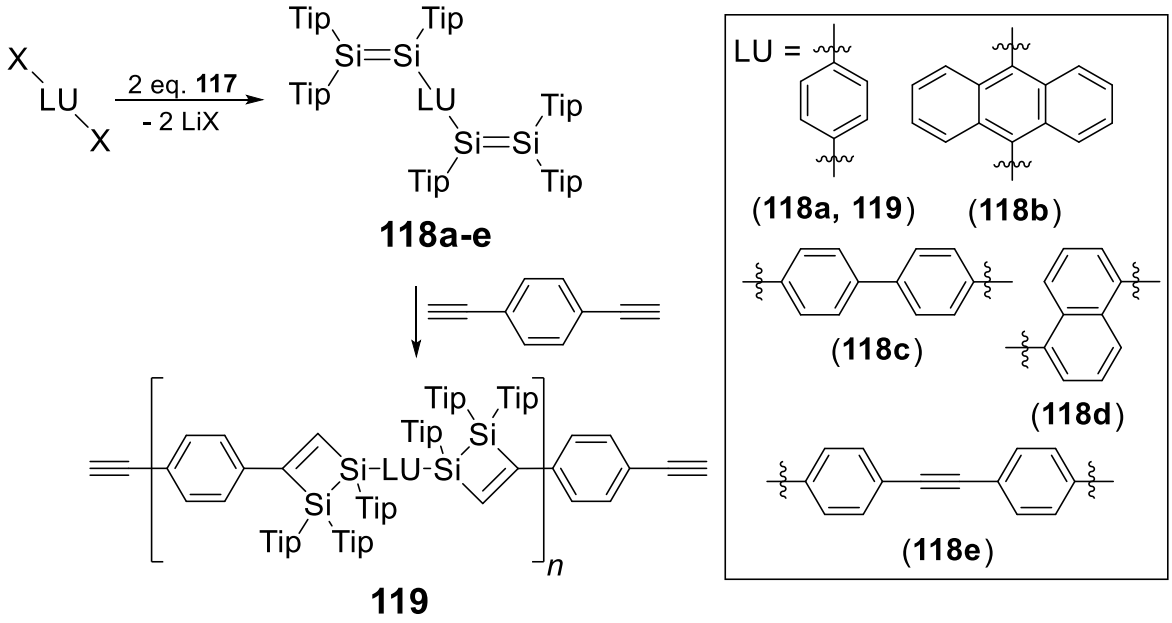

Scheme 52: Synthesis of bridged tetrasilabutadienes **118a-e** from disilenide **117** and polyaddition of **118a** with 1,4-diethynylbenzene to hybridpolymer **119** (X = Br, I).

The high stability of bonds between silicon and electronegative elements like oxygen or chlorine can be exploited to build cyclic structures (Scheme 53). Although chlorosilyldisilenes **120a,b** can be isolated they readily rearrange to cyclotrisilanes **121a,b** upon heating. Conversely, the postulated but unobserved disilene intermediates **120c,d** as well as acyl and vinyl disilenes **122a-d** appear to rearrange immediately to **121b,c** and the cyclic silenes **123a-d**, respectively.[378,380,384–386] An analogous strategy is applied for the synthesis of acyclic and cyclic phosphasilenes from **117**.[387–389] Besides this already astounding variety of structural motifs, disilenide **117** also enables the construction of larger low-valent structures of silicon and germanium that may arise as intermediates during CVD, as for example, cyclopropenes, vinylidenes, cyclopropylidenes and vinyltetrylenes (cf. Section 4.3) as well as siliconoids with between 5 and 11 vertices (cf. Chapter 6). Using a common precursor, a preparative connection between electron-precise low-valent SiGe species and cluster compounds is established. Digermenide **98a** may therefore play a similarly pivotal role to further develop the chemistry of mixed silicon-germanium systems through the isolation of molecules with hitherto unrealized Si:Ge ratios.

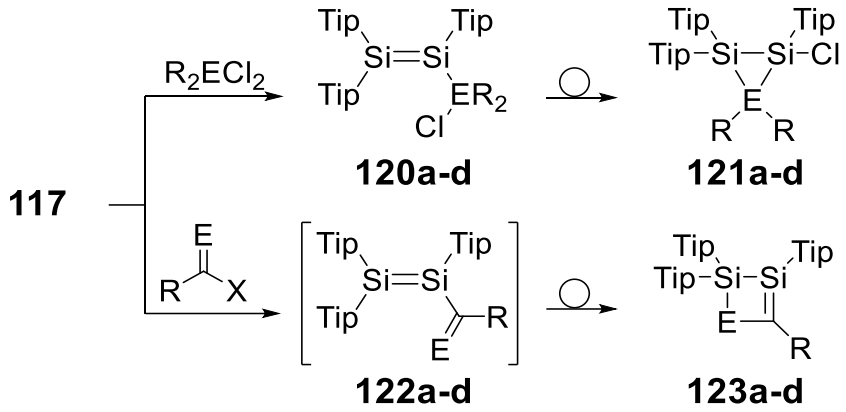

Scheme 53: Cyclization of chlorosilyl-, acyl- and vinyldisilenes **120a-d** and **122a-d** (**120a**, **121a**: E = Si, R = Me; **120b**, **121b**: E = Si, R = Ph; **121c**, **121c**: E = Sn, R = Me; **120d**, **121d**: E = Si, R = Cl; **122a**, **123a**: E = O, R = ^{t}Bu; **122b**, **123b**: E = O, R = 1-Ad, **122c**, **123c**: E = CH_2, R = Ph; **122d**, **123d**: E = CH_2, R = $SiMe_3$).

3.3. Ge_2R_2: Digermynes and Digermavinylidenes

The Ge_2H_2 hypersurface exhibits three minima of which derivatives have been isolated (Scheme 54): the double bridged butterfly structure **VIII** is presumably the global minimum and has been detected in the gas-phase.[390] The digermavinylidene **IX** is slightly higher in energy and the *trans*-bent digermyne **X** the energetically least favorable.[391,392]

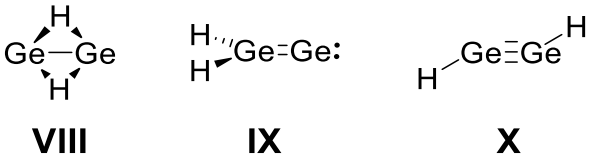

Scheme 54: Minima on the Ge_2H_2 PES: double bridged butterfly **VIII**, vinylidene **IX**, and *trans*-bent alkyne **X**.

The first neutral digermynes **124a,b** were prepared by reduction of chlorogermylenes **47b,c** (Scheme 55). Further terphenyl derivatives were obtained in an analogous manner. Their reaction with unsaturated compounds yields for example cyclic digermenes **103a** and **108**.[255,335,393–395] Both **124a**,**b** undergo scrambling reactions with Mo-Mo triple bonds to the corresponding germylenyl-molybdenum complexes **125a,b**.[396] A landmark achievement was the activation of dihydrogen by **124a** to form species with varying hydrogenation degree, dihydridodigermene **93**, tetrahydrodigermane **126** and trihydridogermane **127**.[328] Non-terphenyl digermynes

with bulky alkylated aryl substituents act as catalysts in the trimerization of carbon-based alkynes to substituted benzenes.[347,397,398]

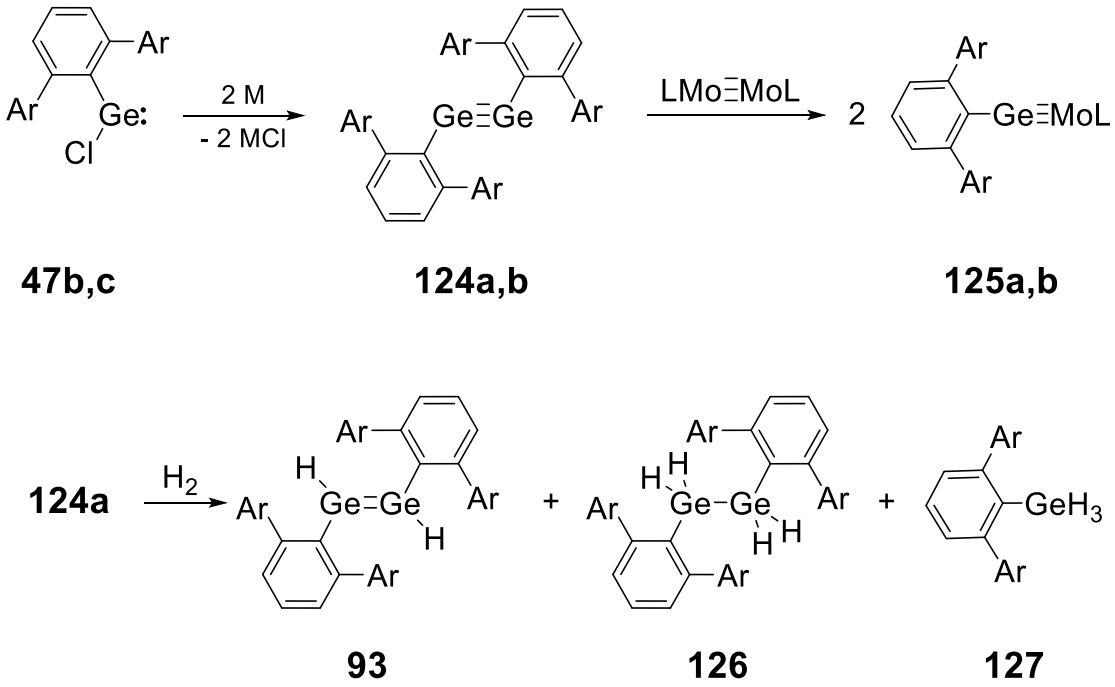

Scheme 55: Synthesis of digermynes **124a,b** from chlorogermylenes **47b,c**, metathesis with Mo-Mo triple bonds to complexes **125a,b** and hydrogenation of **124a** to **93**, **126** and **127** (M = Li, Na, K; L = $Cp(CO)_2$; **47b**, **93**, **124a**, **125a**, **126**, **127**: Ar = Dip; **47c**, **124b, 125b**: Ar = Tip).

The suitability of digermynes for small molecule activation and catalysis was rationalized by diradicaloid contributions to the electronic structure (Figure 8).[399]

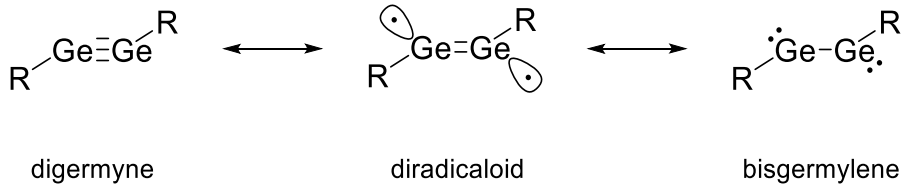

Figure 8: Resonance forms of digermynes.

The remaining known digermynes are best described as bisgermylenes based on structural arguments (acute R-Ge-Ge angles), reactivity and coordination behavior. For example, **128a,b** are coordinated by two equivalents of DMAP to form bisgermylene complexes **129a,b** (Scheme 56).[256] **128a,b** and their boryl-substituted derivatives further add dihydrogen in either 1,1- or 1,2-fashion.[164,180,400] Base coordination of *tert*.-butylisocyanide to digermyne **124a** has been reported as well.[255]

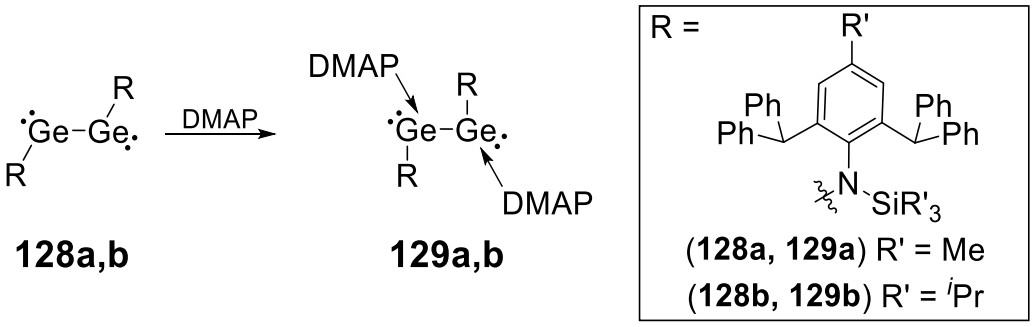

Scheme 56: Reaction of bisgermylenes **128a,b** with DMAP to complexes **129a,b**.

Reduction of chlorogermylene **66e** yields dianionic digermyne **130** or base-stabilized digermyne **131** (Scheme 57).[177] As expected, **131** can be further reduced to **130**, the oxidation of which provides access to digermavinylidene **132**, stabilized by intramolecular π-coordination. Reduction or addition of NHC **10d** to **132** recovers digermynes **130** and **131**, respectively. Transfer of the terminal Ge(0) atom was reported for an intramolecularly phosphino-stabilized digermavinylidene[401] and overreduction of chlorogermylenes **47a-c** also yields mono- and dianionic digermynes, stabilized by π-interaction, similar to **130**.[236,402,403] Conversely, dications **70a-c** require stabilization through NHC coordination (Scheme 30).

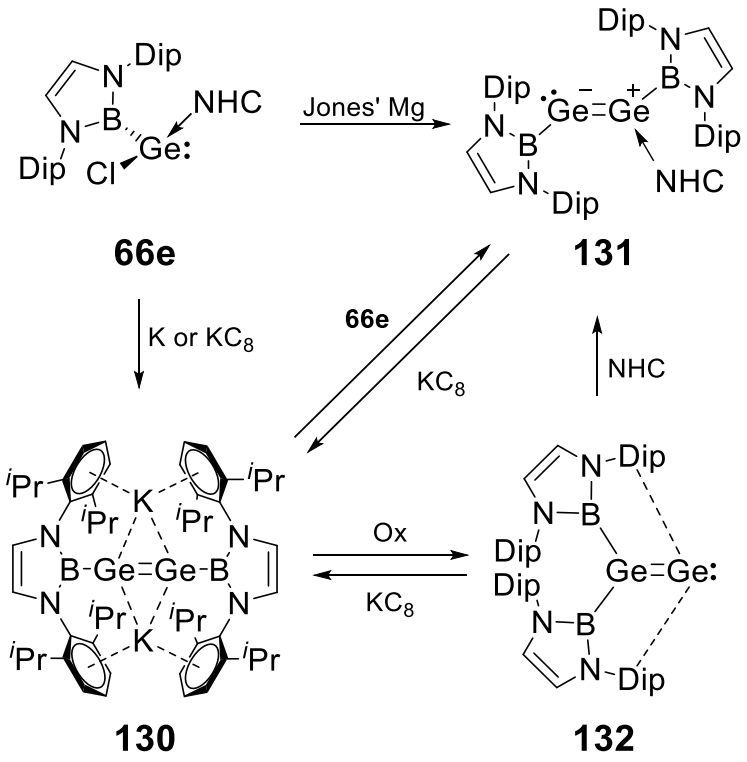

Scheme 57: Synthesis of digermynes **130**, **131** and digermavinylidene **132** (NHC = **10d**; Ox = $[Cp_2Fe][BAr^f_4]$ (Ar^f = 3,5-$(CF_3)_2$- C_6H_3) and $[Ph_3C][B(C_6F_5)_4]$).

3.4. $Ge(0)_2$

In the sequence from digermenes ($R_2Ge=GeR_2$) to digermavinylidenes ($R_2Ge=Ge$:), the consequent next step is a $Ge(0)_2$ dumbbell, on the way towards bulk germanium. Base-stabilized examples **135a-c** were synthesized from the corresponding coordinated dichlorogermylenes **12b**, **133** and **134** (Scheme 58).[174,404,405] While **135a,b** experience donor stabilization exclusively, **135c** is further stabilized by both σ- and π-coordination of the $Ge(0)_2$ moiety to iron tetracarbonyl fragments.

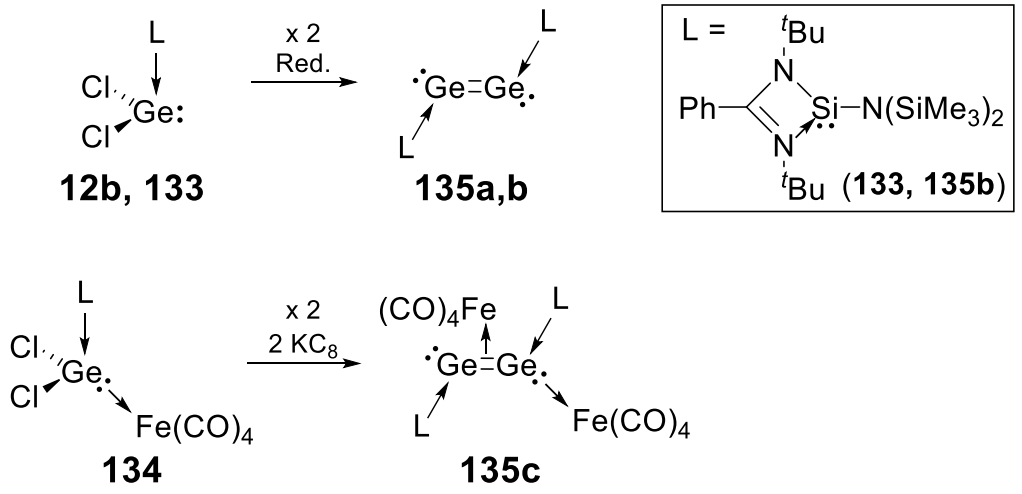

Scheme 58: Synthesis of $Ge(0)_2$ **135a-c** from germylenes **12b**, **133** and 1**34** (Red. = Jones' Mg or KC_8; **12b**, **135a**: L = **10f**; **134**, **135c**: L = **10d**).

3.5. $GeSiR_4$: Germasilenes

Only few germasilenes **136-138** are known (Scheme 59),[406–411], which may be due to the fact that the global minimum of $GeSiH_4$ is silylgermylene.[412,413] 2-Disilagermirene **137** is obtained *via* thermal rearrangement of the corresponding 1-disilagermirene; its treatment with phenylacetylene yields the heavier cyclopentadiene analogue **138**.

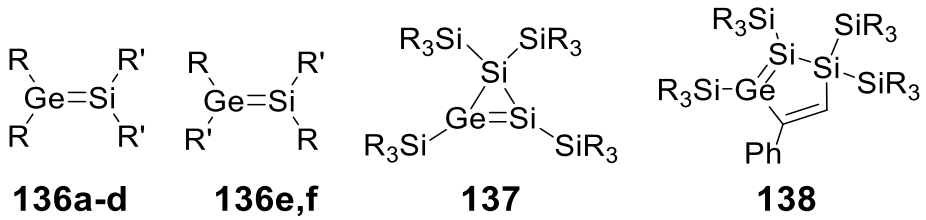

Scheme 59: Germasilenes **136-138** (**136a**: R = Mes, R' = $SiMe^tBu_2$; **136b**: R' = $SiMe^tBu_2$, R' = Mes; **136c**: R = R' = $SiMe^tBu_2$; **136d,e**: R = Mes, R' = Si^tBu_3; **136f**: R = R' = Mes; **137, 138**: SiR_3 = $SiMe^tBu_2$).

Transient germasilene **136f** has been trapped as methoxy silane **139** and undergoes 1,2-shift of a mesityl substituent more readily than its digerma congener **1a** to form silylgermylene **140**, which can be trapped with 2,3-dimethylbutadiene to silylgermane **141** (Scheme 60).[355,414] Similar rearrangements are probably preceding the formation of **109a-c** (Scheme 41). In analogy to the parent digermene and the tetrachloro derivative, their SiGe analogues were isolated by employing donor-acceptor stabilization.[415]

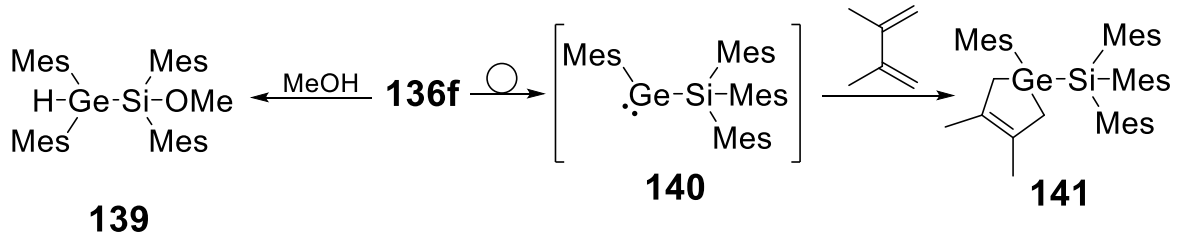

139 **140** **141**

Scheme 60: Trapping of silagermene **136f** as methoxysilane **139** and 1,2-aryl shift to silylgermylene **140** and subsequent trapping as silylgermane **141**.

3.6. $GeSiR_2$: Germasilynes and Silagermenylidenes

The parent silagermenylidene was predicted to be lower in energy than the germasilyne.[416,417] Two representatives of $GeSiR_2$ are known, both requiring donor stabilization: Germasilyne **142** and silagermenylidene **143** (Scheme 61).[193,418]

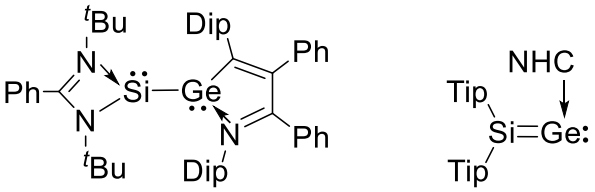

142 **143**

Scheme 61: Isolated Derivatives of the $GeSiR_2$ hypersurface: silagermyne **142** and silagermenylidene **143** (NHC = **10d**).

The higher stability of silylgermylene and silagermenylidene in comparison to their double and triple bonded isomers, respectively is a direct consequence of the inert-pair effect as the molecules adopt geometries that lower the oxidation state of germanium and increase the oxidation state of silicon. This observation is of general validity and will be encountered in the following chapters as well, where the element to substituent ratio will constantly decrease.

4. E_3-Systems

4.1. E_3R_6: Heavy Propenes & Cyclopropanes

Conceivable E_3R_6 isomers **XI-XIV** (Scheme 62), either belong to previous categories (**XI, XII**: tetrylenes; **XIII**: ditetrene) or are saturated in the first place (**XIV**).

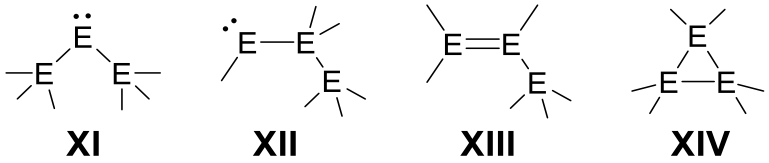

Scheme 62: E_3R_6 isomers: tetrylenes **XI, XII**, heavy propene **XIII** and heavy cyclopropane **XIV**.

Transient disilanylsilylenes **144a,b** are proposed as intermediates during the rearrangement of silyldisilenes **120a,b** to cyclotrisilanes **121a,b** (Scheme 63). The intermediacy of **144b** received additional support from the isolation of a CH insertion product.[385]

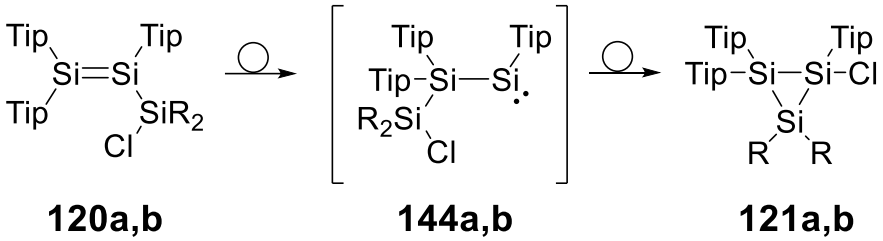

Scheme 63: Rearrangement of disilenes **120a,b** to cyclotrisilanes **121a,b** *via* intermediary disilanylsilylenes **144a,b** (**120a**, **121a**, **144a**: R = Me; **120b**, **121b**, **144b**: R = Ph).

While several other stable silyldisilenes are known,[369,373,419–421] Si-Ge species are limited to germasilene **138**, bissilylgermylenes **16, 145** and **147** as well as disilanylgermylenes **146** and **148** (Scheme 64).[179,406,422] Note that the carbene analogues require NHC stabilization, as silylgermylenes usually dimerize to digermenes (Scheme 42). The only examples of unsaturated $SiGe_2R_6$ motifs are the silyldigermenes **116a,b** (Scheme 50) while pergerma compounds are unknown.[336]

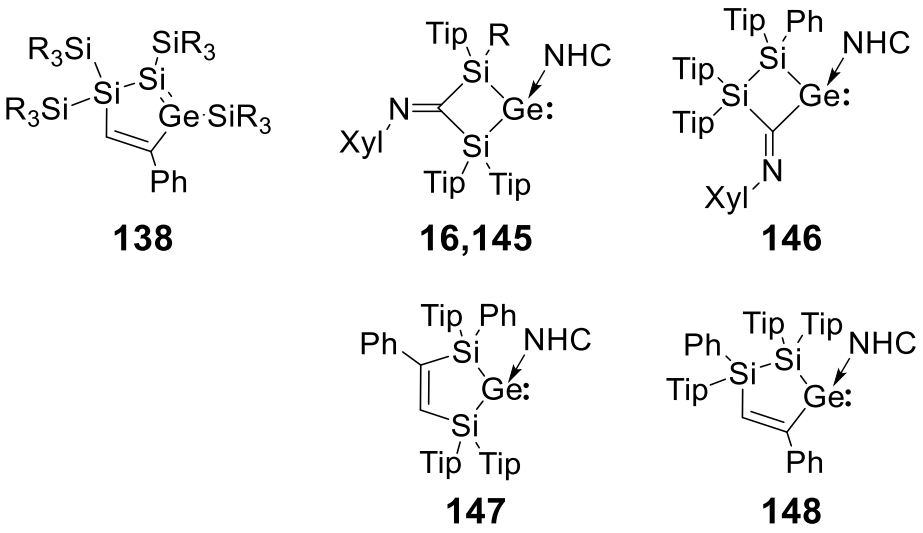

Scheme 64: Reportes species of the type Si_2GeR_6:Silylgermasilene **138**, bissilylgermylenes **16**, **145** and **147** as well as disilanylgermylene **146** and **148** (NHC = **10d**; SiR_3 = $SiMe^tBu_2$; **16**: R = Cl; **145**: R = Ph).

4.2. E_3R_5: Heavyl Allyl cations, radicals & anions

Open-chained heavy allyl cations, radicals and anions are unknown, as their saturated three-membered ring isomers are predicted to be lower in energy.[423,424] Incorporation of the allyl moiety into ring systems, however, renders such isomerizations unfavorable as the formation of strained bicyclic systems would be required. Reduction of cyclic germasilene **138** thus yields the heavy cyclopentadienide **149** (Scheme 65).[425]

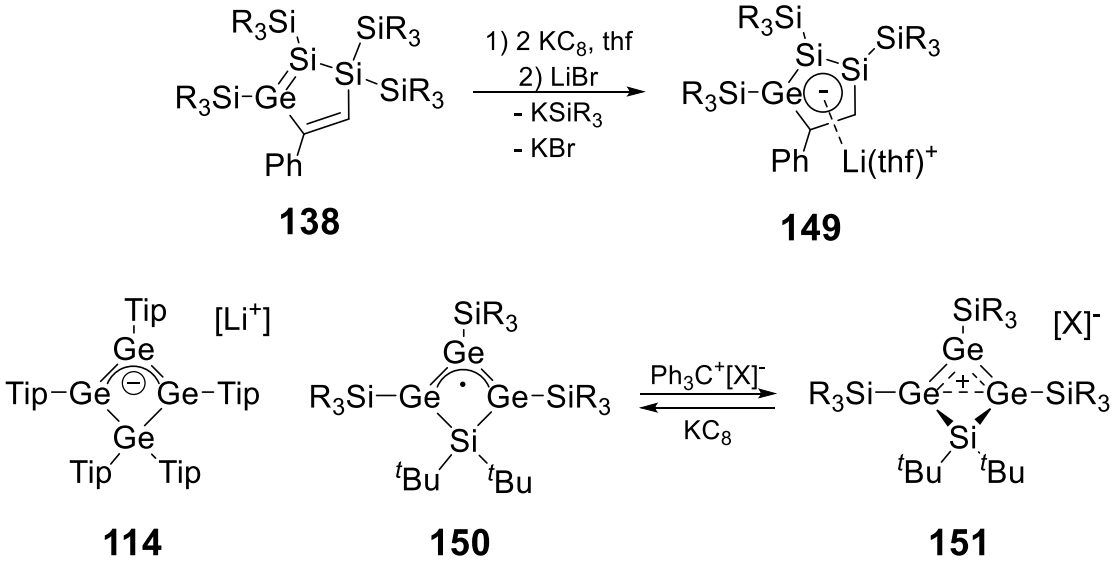

Scheme 65: Synthesis of heavy cyclopentadienide 1**49** from germasilene **138** as well as Ge_3-allyl anion **114**, -radical **150** and cation **151** (SiR_3 = $SiMe^tBu_2$; $[X]^-$ = $B[(C_6F_5)_4]^-$).

Similarly, the planar four-membered Ge_4-ring allyl anion **114** and the isostructural radical **150** are sufficiently stable for isolation (Scheme 65).[337,426] The radical **150** is furthermore reversibly converted into the corresponding allyl cation **151**,[427] which possesses a remarkable electronic structure with a homoaromatic Ge_3 unit in which the two "terminal" Ge atom interact through space in a similar manner as the transannular interaction in heavy bicyclobutanes (cf. Section 5.1).

4.3. E_3R_4: Heavy Allenes, Cyclopropenes, Cyclopropylidenes, Vinylidenes & Vinylcarbenes

The E_3R_4 hypersurface shows a rich structural diversity (16 conceivable isomers) of which the five most frequently observed (**XV-XIX**, Scheme 66) are in a narrow 8.9 kcal/mol energy range in the silicon case.[428,429]

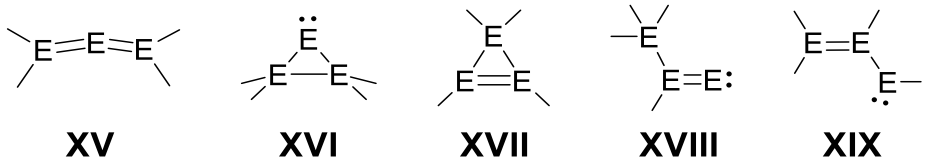

Scheme 66: E_3R_4 isomers **XV-XIX** ordered by increasing relative energy in the Si_3 system.

The heavy allenes **152-154** are bent (Scheme 67),[430–434] which has been attributed to a pronounced tetrylone character of the central atom by Frenking *et al.*,[279] but is equally well rationalized invoking the CGMT model for heavier double bonds. Theoretical results suggest a barrierless transition between parent allenes and cyclopropylidenes *via* bond-stretch isomerism similar to the transannular interaction in **151**.[435]

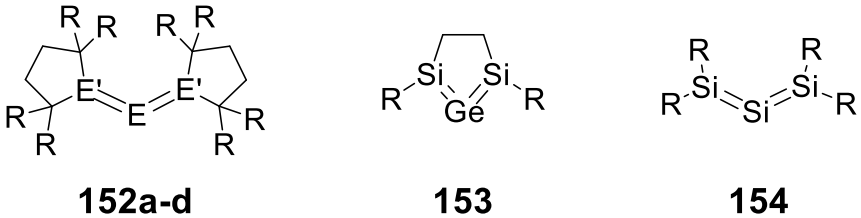

Scheme 67: Heavy allenes **152-154** (**152a**: E = E' = Ge, R = $SiMe_3$; **152b**: E = Si, E' = Ge, R = $SiMe_3$; **152c**: E = Ge, E' = Si, R = $SiMe_3$; **152d**: E = E' = Si, R = $SiMe_3$; **153**: R = 2,6-$(CH(SiMe_3)_2)_2$-4-$C(SiMe_3)_3$-C_6H_2; **154**: R = $SiMe^tBu_2$).

The symmetrically substituted cyclotrigermene **100a** can be oxidized to the corresponding cyclopropenylium cation (cf. Section 4.4), which in turn serves as precursor for functionalized cyclotrigermenes **155a-f** (Scheme 68).[56,346,436–438] The halo-substituted **155d-f** display a rapid shift of the halogen across the three different positions in the ring. In case of **155f**, the conversion into an unsaturated cationic Ge_{10} cluster (cf. Chapter 6) is achieved by treatment with potassium iodide in the presence of weakly coordinating borate salt.

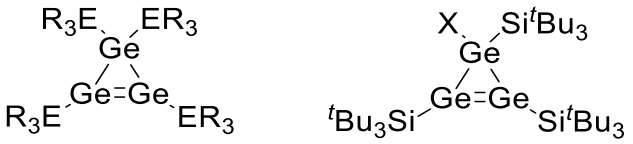

100a-c **155a-f**

Scheme 68: Cyclotrigermenes **100a-c** and **155a-f** (**100a**: $ER_3 = Si^tBu_3$; **100b**: $ER_3 = Ge^tBu_3$; **100c**: $ER_3 = SiMe^tBu_2$; **155a**: X = $Si(SiMe_3)_3$; **155b**: X = $Ge(SiMe_3)_3$; **155c**: X = Mes; **155d**: X = Cl; **155e**: X = Br; **155f**: X = I).

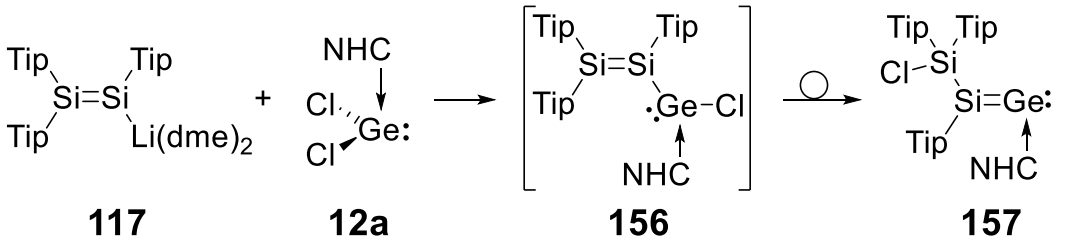

117 **12a** **156** **157**

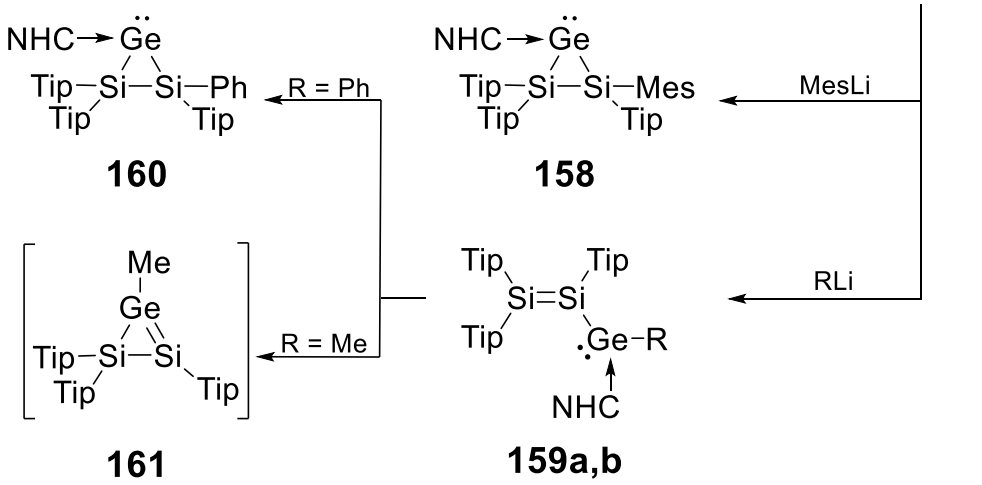

160 **158** **161** **159a,b**

Scheme 69: Synthesis of silagermenylidene **157** from reaction of disilenide **117** and **12a** to intermediate disilenylgermylene **156** and its reactivity towards organolithium reagents under formation of cyclopropylidenes **158** & **160**, disilenylgermylene **159a,b** and cyclopropene analogue **161** (NHC = **10d**).

Silylsilagermenylidene **157** constitutes the only example of type **XVIII** and is obtained from disilenide **117** and $GeCl_2$·NHC complex **12a** *via* the suggested intermediate disilenylgermylene **156** (Scheme 69).[439] **117** also serves as precursor for cyclotrisilenes, persilacyclopropylidenes and a disilenylsilylene.[440–444] Reaction of **157** with MesLi gives access to cyclopropylidene **158** while treatment with sterically less demanding PhLi or MeLi gives the disilenylgermylenes **159a,b**, respectively.[422,443,445] Open-chained isomers **159a,b** undergo subsequent rearrangement to either cyclopropylidene **160** or the cyclopropene **161** (Scheme 69). The latter can only be isolated as the saturated head-to-head or head-to-tail dimerization products as the stabilizing NHC spontaneously dissociates. Treatment of **157** with the small NHC **10b** induces ligand exchange to the chlorosubstituted cyclopropylidene.[443]

4.4. E_3R_3, ER_3R_2 & $E(0)_3$

Cyclotrigermenyliumcations **162a-g** are synthesized from the corresponding cyclotrigermenes **100a,b** *via* oxidation with trityl cations. They show an aromatic delocalization of the 2π system across the three-membered ring (Scheme 70).[436,446–448] Similar conjugation is found in the stable cyclotrigermenyl radical **163**.[449] Isomeric $GeSi_2$ and Si_3 analogues of **163** are postulated to rapidly dimerize to heavy benzenes isomers (cf. Chapter 6).[386,450]

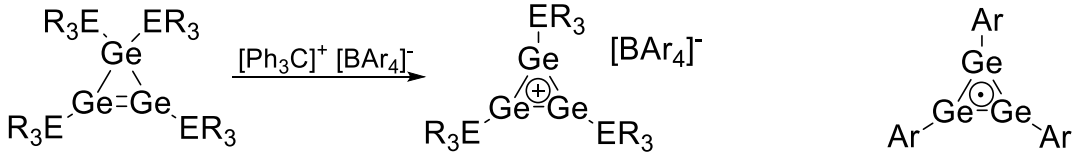

100a,b **162a-g** **163**

Scheme 70: Delocalized cyclotrigermenylium cations **162a-g** and cyclotrigermenylradical **161** (**100a**: E = Si; **100b**: E = Ge; **162a**: E = Si, Ar = Ph; **162b**: E = Si, Ar = 3,5-$(CF_3)_2C_6H_3$; **162c**: E = Ge, Ar = 3,5-$(CF_3)_2C_6H_3$; **162d**: E = Si, Ar = C_6F_5; **162e**: E = Ge, Ar = C_6F_5; **162f**: E = Si, Ar = 4-(^{t}BuMe$_2$Si)C_6F_4; **162g**: E = Ge, Ar = 4-(^{t}BuMe$_2$Si)C_6F_4; **163**: Ar = 2,6-$Mes_2C_6H_3$).

Further reduction of **163** gives the unusual allyl-like anion **164** (Scheme 71).[449] The related neutral Ge_3R_2 species **165** is formally a trisgermylene, although the electronic nature of the central germanium is unclear and might as well be described as a germene or a germylone.[451] A triatomic Si(0) species is known as well.[452]

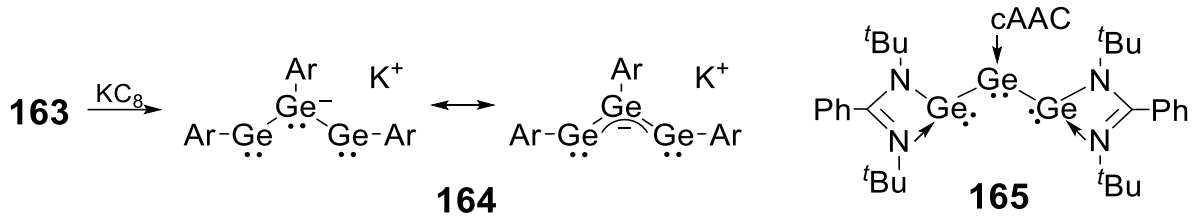

Scheme 71: Trigermaallyl anion **164** and the base-stabilized tritetrylene **165** (Ar = 2,6-$Mes_2C_6H_3$).

5. E_4-Systems

5.1. E_4R_6: Heavy butadienes, cyclobutenes & bicyclobutanes

The homonuclear E_4H_6 hypersurface exhibits at least 60 possible minimum structures. Butadiene **XX**, cyclobutene **XXI** and bicyclobutane **XXII** constitute the usually encountered motifs (Scheme 72);[453] their interconversions have been studied in most detail in the carbon case.[454–456] For both Si_4 and Ge_4, the parent system favors **XXII** over **XXI** and **XX** while sterically demanding groups reverse this order.[457,458]

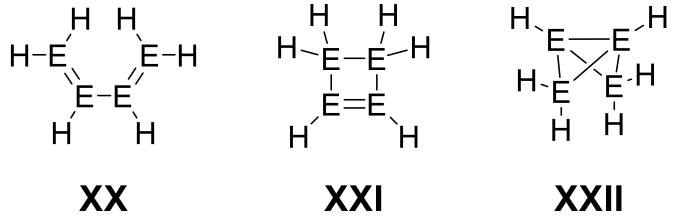

Scheme 72: E_4H_6 isomers butadiene **XX**, cyclobutene **XXI** and bicyclobutane **XXII**.

Tetragermabutadiene **99** (Scheme 46) was discussed in Section 3.1. The two germanium-containing cyclobutenes **102e,f** were obtained by treating cyclotrigermene **100c** and cyclic silagermene **137**, respectively, with germylene **8a** (Scheme 73).[348,349]

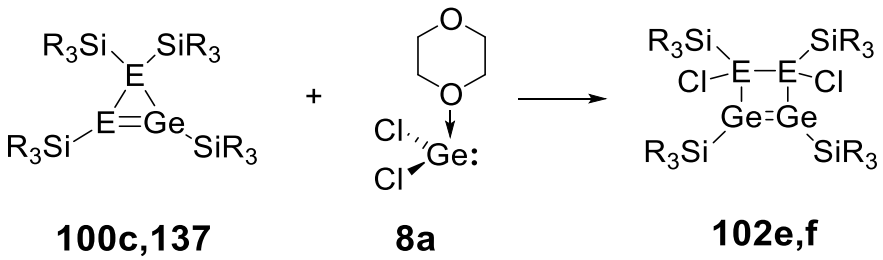

Scheme 73: Synthesis of Ge-containing cyclobutenes **102e,f** from heavy cyclopropenes **100c**, **137** and $GeCl_2$ dioxane **8a** (SiR_3 = $SiMe^tBu_2$; **100c**, **102e**: E = Ge; **102f**, **137**: E = Si).

Tetragermabicyclobutanes were predicted to exhibit bond-stretch isomerism to **XXII'** (Scheme 74) with the central Ge-Ge bond replaced by a singlet diradical(oid) interaction, closely resembling the through-space interaction in propellane and benzpolarene, examples of siliconoids (cf. Chapter 6). The bridgehead germanium atoms in **XXII'** are furthermore hemispheroidally coordinated, another structural property of siliconoids. Tetragermabicyclobutanes therefore manifest the transition from electron precise molecules to unsaturated cluster compounds.

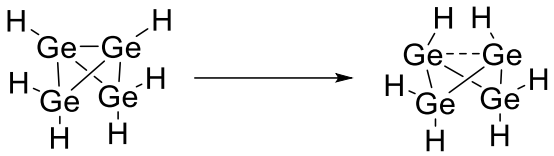

XXII **XXII'**

Scheme 74: Bond-stretch isomerization of tetragermacylobutane **XXII** to the diradicaloid **XXII'**.

The energy gain from bond-stretching increases going down Group 14 from Si_4H_6 to Sn_4H_6, with Pb_4H_6 only exhibiting a minimum as **XXII'**.[459] Nonetheless, several examples of bicyclobutanes with Si_4-cores have been synthetically realized and possess extremely reactive central Si-Si bonds that in two cases even show π-character without an underlying σ-bond, comparable to **101** (Scheme 47), suggesting the validity of the so far merely theoretical predictions in the Ge case.[460–464]

5.2. E_4R_4: Tetrahedranes, Cyclobutadienes & their dianions

E_4R_4 structures range from the three-dimensional cluster tetrahedrane **XXIII** to the planar cyclobutadiene **XXVI** by successive σ-bond cleavage to structures **XXIV** and **XXV** (Scheme 75).

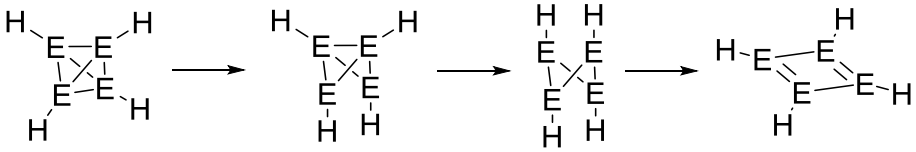

XXIII **XXIV** **XXV** **XXVI**

Scheme 75: Isomers **XXIII-XVI** of E_4H_4.

Tetragermatetrahedrane **167** with bulky supersilyl substituents was obtained by reduction of tetrachlorodigermane **166** although the corresponding parent species is not a minimum on the Ge_4H_4 PES (Scheme 76).[465]

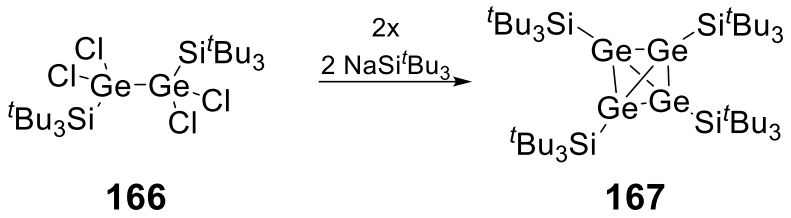

166 **167**

Scheme 76: Synthesis of tetrahedrane **167** *via* reductive coupling of tetrachlorodigermane **166**.

The zwitterionic butterfly compound **168** was synthesized from chlorogermylene **48** and exhibits two trivalent germanium atoms with opposing charges in the solid states. In solution, the structure is fluxional and thus highly symmetric on the NMR timescale, due to breaking and rebuilding of the central Ge-Ge bond.[180] The only example of type **XXV** constitutes cluster **169**,[120] in which all four Ge atoms are hemispheroidally coordinated.

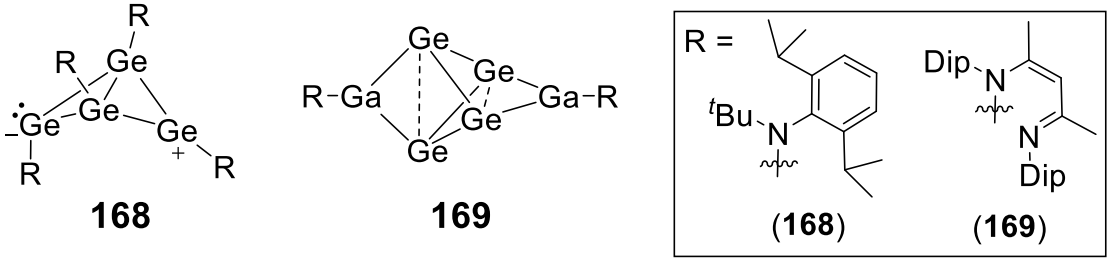

168 **169**

Scheme 77: Zwitterionic Ge_4-butterfly **168** and mixed cluster **169**.

Germanium derivatives of cyclobutadiene avoid antiaromaticity by Jahn-Teller distortion to rhombic, charge separated systems as in **170a-c** (Scheme 78).[332,466,467] NICS calculations confirmed the non-aromatic nature of the ring system in **170b**. An isostructural Si_3Ge analogue of **170c** has been reported as well.[468] Cyclobutadiene dianions **171a,b** were obtained by reduction of dichlorocyclobutenes **102e,f** (Scheme 79).[349,469,470] NICS values and structural arguments exclude the presence of aromatic ring currents in **171a,b**, which are consequently classified as non-aromatic. Nonetheless, **171a,b** coordinate to transition-metals in a η^4-fashion as for example in the cobalt complexes **172a,b**.[470] Reduction of **102f** with alkaline earth metals yields bicyclobutane dianions **175a-c** (Scheme 79).[471] The mechanism for the formation of

175a-c was proposed to proceed through the intermediates **173a-c** and **174a-c**, in analogy to the archetypal cyclobutene-butadiene-bicyclobutane rearrangement known from carbon. A similar rearrangement was found for the formal heavy butadiene **138** (cf. Section 3.5), which is presumably formed from a transient cyclobutene isomer and rearranges to the corresponding bicyclobutane upon heating.[407,472] **175a-c** can alternatively be prepared by transmetallation of **171b** with the appropriate alkaline earth metal halides.

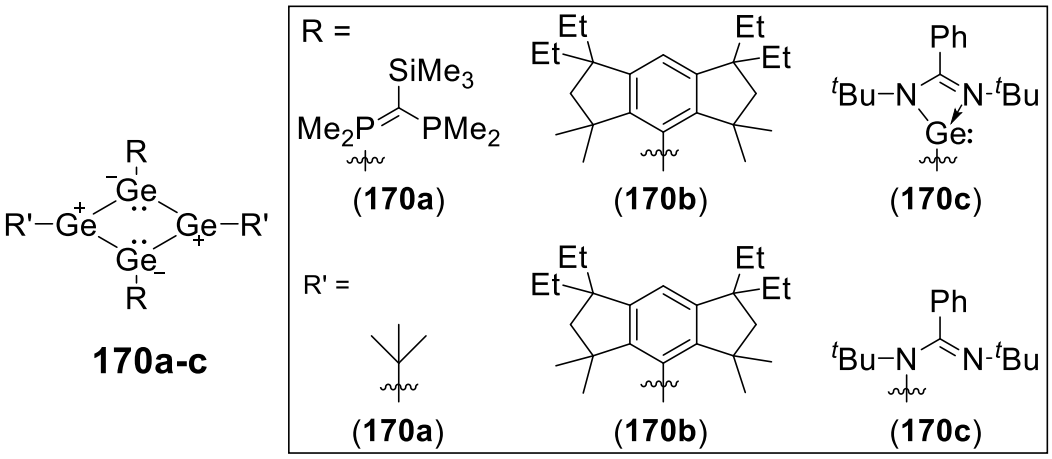

Scheme 78: Tetragermacyclobutadienes **170a-c**.

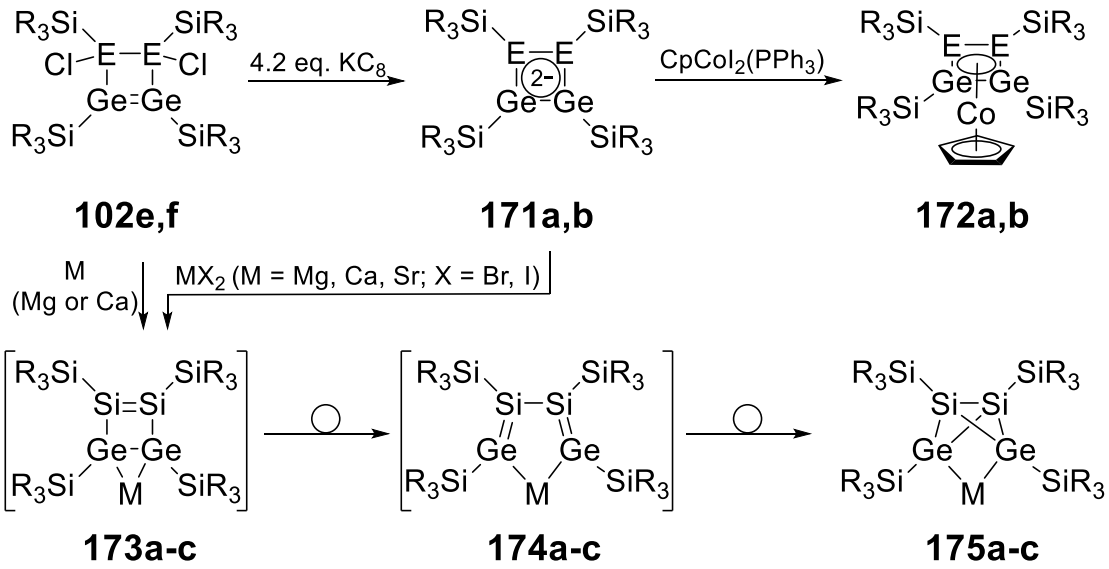

Scheme 79: Reduction of dichlorocyclobutenes **102e,f** to cyclobutadiene dianions **171a,b** and subsequent coordination to complexes **172a,b** as well as reduction of 1**02f** to bicyclobutane dianion **175a-c** over the intermediates **173a-c** and 1**74a-c** (SiR_3 = $SiMe^tBu_2$; **102e**, **171a**, **172a**: E = Ge; **102f**, **171b**, **172b**: E = Si; **173a, 174a, 175a**: M = Mg; **173b, 174b, 175b**: M = Ca; **173c, 174c, 175c**: M = Sr).

6. Unsaturated Cluster compounds

A cluster refers in general to a “group of things of the same type that grow or appear close together”.[473] In a chemical context no strict definition for clusters exists. Cotton suggested that the presence of more metal-metal bonds than metal-ligand bonds is the defining characteristic of a cluster.[474] According to this definition, tetrahedranes **167** and **169** can be regarded clusters. Germanium clusters are classically divided into three major groups: 1) saturated, polycyclic germanes; 2) unsaturated clusters with element to substituent ratios below 1:1, so-called metalloid clusters, and finally 3) Zintl-anions (Scheme 80). Polyhedral oligogermanes have the general composition Ge_nR_m, with $n \leq m$, as in tricyclic **176**, the heavy benzene isomer prismane **177** or the highly symmetric tetrahedrane **167** and cubane **178** with platonic bodies as cluster scaffolds.[465,475–477] If $n > m$, clusters are classified as metalloid and consequently exhibit an average oxidation state of the cluster vertices between zero and +1,[478] as in the cases of cubic **179a,b** and anionic **180**.[479–481] In contrast to oligogermanes, metalloid clusters are unsaturated, exhibit non-classical bonding situations and unsubstituted, or “naked”, cluster vertices. Formal removal of all substituents from a cluster under retention of a few negative charges leads to Zintl-anions, polyanionic clusters that typically are confined in the corresponding Zintl-phases, e.g. is the crystal structure of $Na_{12}Ge_{17}$ that contains both **181** and **182** in the anionic lattice.[482]

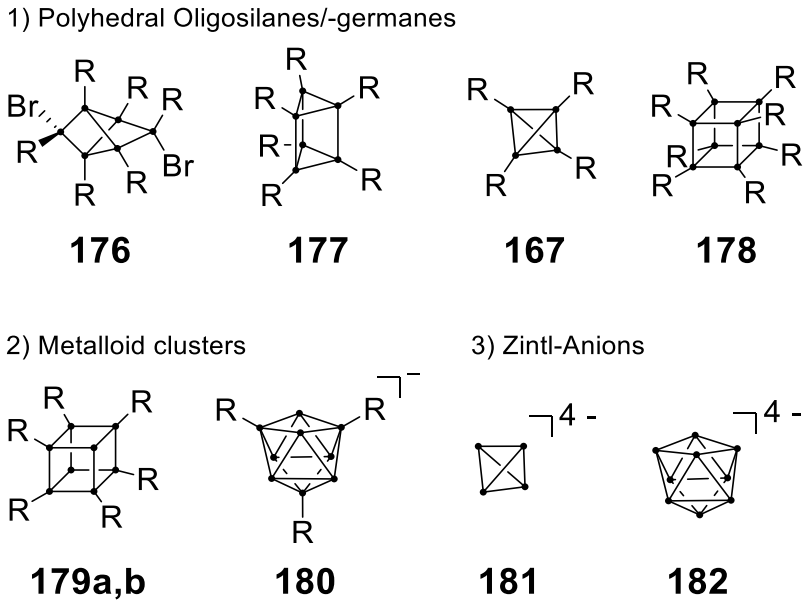

Scheme 80: Examples of the three classes of germanium clusters (● = Ge; **167**: R = Si^tBu_3; **176**: R = $Mn(CO)_5$; **177**: R = $CH(SiMe_3)_2$; **178**: R = Dep; **179a**: R = $N(SiMe_3)_2$; **179b**: R = 2,6-$^tBuO_2C_6H_3$; **180**: R = $Si(SiMe_3)_3$).

Metalloid germanium clusters are known from Ge_5 to Ge_{18} motifs and with increasing number of core atoms the resemblance to crystalline Ge-phases becomes more pronounced. While Ge_5 **183a,b** and **184** possess (more or less deviated) tetragonal pyramid structures,[483,484] Ge_6 **185**, Ge_8 **179a,b** and Ge_9 **180** resemble octahedra, cubes and tricapped trigonal prisms, respectively (Scheme 81).[479,480,485] The structure of Ge_6 cluster **186** is in between that of a trigonal prism and an octahedron with the two unsubstituted vertices being reminiscent of the buckled dimer on the Ge(001)-(4x2) surface (cf. Scheme 1).[486] Anionic cluster **180** was also reported with other substituents, dianionic, and coordinated to several transition metals.[487–494] **183a,b** resemble butterfly structure **168** (cf. Section 5.2) but show no dynamic behavior in solution. In contrast, **183c** undergoes fast flipping of the Ge_4-base, through the transition state structure **184**, which could be isolated in the solid state.

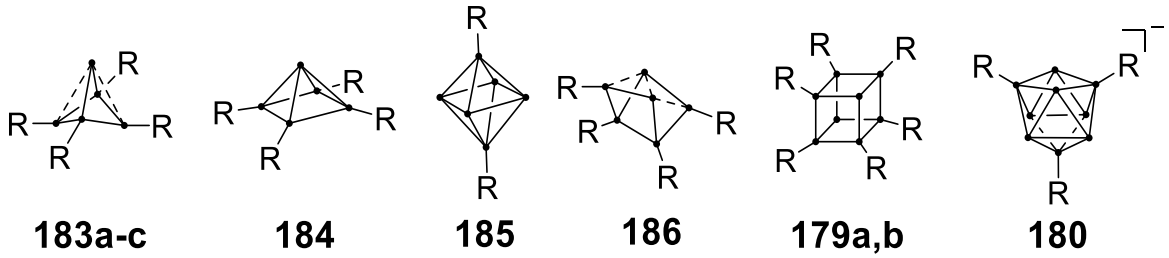

Scheme 81: Metalloid Ge-clusters **179a,b**, **180** and **183-186** that form regular and distorted polyhedra (● = Ge; dashed bonds indicate transannular interactions in bond-stretch bicyclobutane motifs; **179a**: R = $N(SiMe_3)_2$; **179b**: R = 2,6-^{t}Bu$O_2C_6H_3$; **180**: R = $Si(SiMe_3)_3$; **183a**: R = $CH(SiMe_3)_2$; **183b**: R = 2,6-$Mes_2C_6H_3$; **183c**: R = SiMe^tBu$_2$; **184**: R = SiMe^tBu$_2$; **185**: R = 2,6-$Dip_2C_6H_3$; **186**: R = $N(SiMe_3)$Dip).

Increasing the number of core germanium atoms beyond *n* = 9 leads to drastic changes in the structural characteristics: Instead of regular polyhedra, the larger clusters are less symmetric (i.e. more anisotropic) and their scaffold is often formally composed from the chimeric combination of smaller polyhedra. Ge_{10} clusters **187** and **188** only exhibit C_s symmetry and their structures show some resemblance to cutouts from the α-Ge diamond-lattice (Scheme 82).[495,496] In contrast, Ge_{12} cluster **189** shows the arrangement of the high-pressure phase [Ge(*tI*4)] (Scheme 82) with the central Ge_4 ring resembling the biradicaloid bond-stretch isomers of hypothetical tetragermabicyclobutanes.[497] The Ge_{14} clusters **190a,b** even possess three such moieties, rendering them hexaradicaloids.[498,499] Strongly deviated versions of the bond-stretch bicyclobutane are encountered in **183a-c** and **186**.

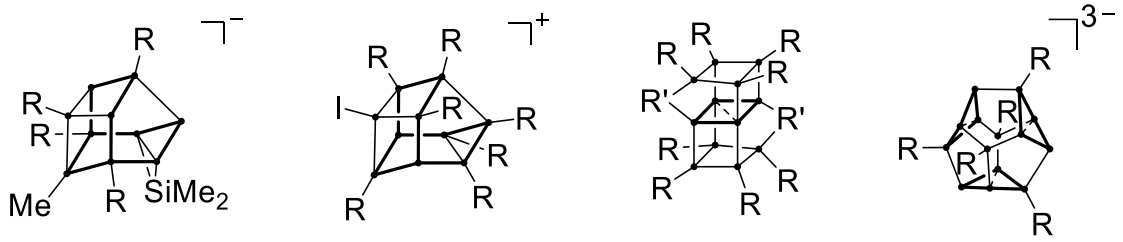

187 **188** **189** **190a,b**

Scheme 82: Ge_{10}-Ge_{14} clusters **187**-**190** (● = Ge; dashed bonds indicate transannular interactions in bond-stretch bicyclobutane motifs; bonds that are part of a diamond-lattice cutout or of bond-stretch bicyclobutanes are emphasized in bold; **187**: R = $Si(SiMe_3)_3$; **188**: R = Si^tBu_3; **189**: R = $FeCp(CO)_2$, R' = FeCp(CO); **190a**: R = $Ge(SiMe_3)_3$; **190b**: R = $Si(SiMe_3)_3$).

Metalloid germanium clusters are commonly obtained *via* two different routes: The clusters in Scheme 81 are synthesized by reduction of Ge(II) halides or treatment of metastable Ge(I) halides with nucleophiles at low temperatures. A second approach is the employment of soluble, germanium based Zintl-anions as nucleophiles. With this method, functionalization,[493,500–506] linkange,[505,507–512] and catenation[513–516] of metalloid germanium clusters were achieved.

Germanium clusters **191-193** exhibit intriguing electronic properties (Scheme 83): The [1.1.1]propellanes **191a,b** possess two unsubstituted Ge vertices, the nature of their interaction still being disputed. CASSCF calculations predict only a small biradicaloid character, whereas experimental studies revealed some examples for biradicaloid reactivity. A similar bond and furthermore three-dimensional cluster currents are found in the heavy heteronuclear benzene isomer **192**, a structural motif that has been christened “benzpolarene” to reflect the immense electronic anisotropy that extends over the cluster scaffold.

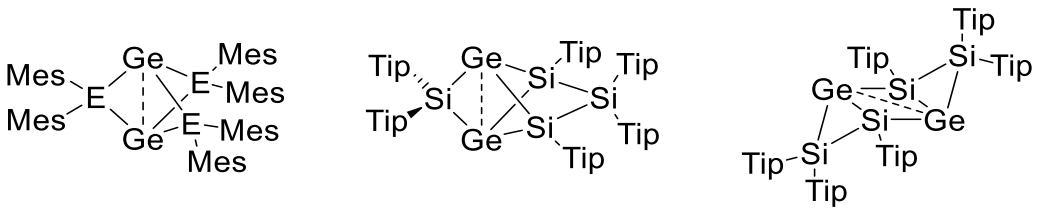

191a,b **192** **193**

Scheme 83: Unsaturated SiGe clusters **191-193** which do not count as metalloid clusters (E = Si, Ge; dashed bonds indicate transannular interactions in bond-stretch bicyclobutane motifs).

Benzpolarene **192** is synthesized by thermal rearrangement of benzene isomer **193** (that formally contains a bond-stretch bicyclobutane), which is in turn obtained by reduction of the transient disilenylchlorogermylene **194**, formed upon treatment of lithium disilenide **117** with germanium dichloride × dioxane **8a** (Scheme 84). **193** exhibits a unique type of six-electron delocalization over its central Si_2Ge_2 ring referred to as dismutational aromaticity, because of the variable oxidation state of the six vertices. The unsubstituted vertices in both **193** and **192** are occupied by germanium atoms, as would be expected in the light of the inert-pair effect. The analogous persila-systems are more thoroughly investigated and can be functionalized in manifold ways, inter alia: substitution in different cluster positions, expansion to Si_7 and Si_8 clusters, reduction to mono- and dianionic clusters, and even incorporation of dopant atoms into the cluster scaffold.[386,517–524]

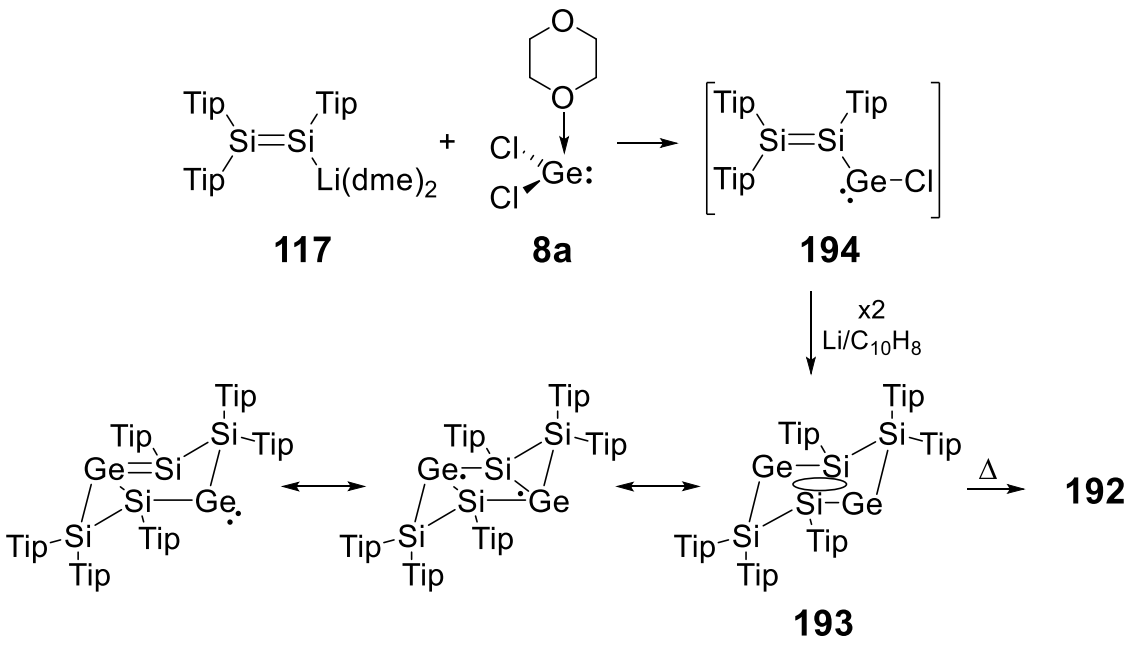

Scheme 84: Synthesis of germanoids **192** and **193** from disilenide **117** and germanium dichloride dioxane **8a**.

The reference to the average oxidation state for the classification of clusters as metalloid ignores local metalloid characteristics. This becomes obvious in the clusters **191-193** which all possess unsaturated vertices, and thus potential diradicaloid character (Scheme 83), but do not concur with the definition of metalloid clusters due to their average oxidation state equal or greater than +1.[450,525,526]

In order to address this shortcoming, the hemispheroidality criterion was established in case of silicon-clusters, with those that fit the criterion being referred to as “siliconoids”.[527] One may consequently call the analogous germanium clusters “germanoids”. For a cluster to qualify as a siliconoid or germanoid, it needs to possess at least one unsubstituted vertex that is hemispheroidally coordinated. A quantitative criterion for hemispheroidal coordination is defined as follows (Figure 9): The three atoms bonded to the vertex in question with the sum of angles closest to 360° define a reference plane. The closest distance between the fourth atom (given by the normal vector) is defined as negative when the fourth atom resides on the other side of the reference plane and otherwise as positive. The thus obtained value is the hemispheroidality ϕ. A positive value for ϕ indicates hemispheroidal coordination while a negative value indicates (distorted) tetrahedral coordination. By this definition, the compounds in Scheme 83 as well as all of the above-mentioned metalloid clusters are in fact germanoids. Note however, that some cases that meet the criterion of an average oxidation state below 1 do not feature any hemispheroidal vertex, as for example *spiro*-bis(cyclotrigermene).[528] The hemispheroidality criterion is also met for the atoms of the buckled dimer on Si(100) and Ge(100) and therefore directly links the siliconoids and germanoids with surface and bulk characteristics of elemental silicon and germanium.

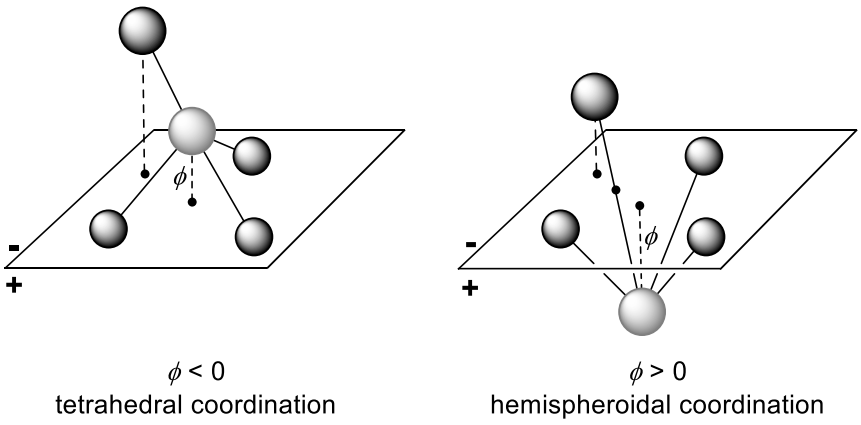

Figure 9: Definition of the hemispheroidality ϕ.

When comparing hypothetical bicyclobutane **XXII’** with propellanes **191a,b** and benzpolarene **192**, the structural similarities are obvious (Scheme 85): In all four structures, a non-classical interaction between hemispheroidally coordinated germanium atoms is found and the fact that bond-stretch bicyclobutane,

[1.1.1]propellane and benzpolarene are the global minima of the corresponding hypersurfaces is no coincidence, in the light of findings for the analogous silicon compounds:[529–537] In fact, the inert-pair effect leads to a destabilization of bond angles different from 90° as they require significant hybridization between the perpendicular p-orbitals and the s-orbital. Consequently, germanium prefers four-membered rings with endocyclic 90° angles and the compounds in Scheme 85 simply maximize the number of endohedral four-membered rings with one in **XXII'**, three in **191a,b** and four in **192** with the non-classical bond as a direct consequence of this pursuit.

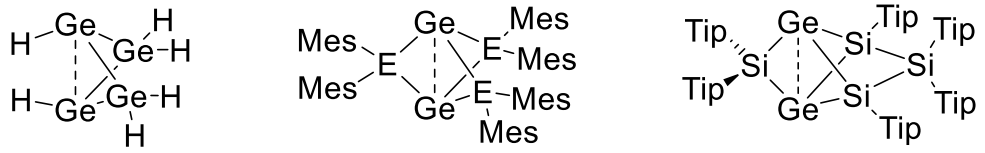

XXII' **191a,b** **192**

Scheme 85: Bicyclobutane **XXII'** and germanoids **191a,b & 192** with non-classical interactions between hemispheroidally coordinated Ge-atoms.

Metalloid clusters **189** and **190a,b**, which contain the bond-stretch bicyclobutane once and three times respectively, presumably gain stability by this effect as well, inducing hexaradicaloid character in **190a,b**. The presence of dangling bonds on the surface of crystalline germanium and in the bulk of amorphous germanium can be therefore traced back to intrinsic atomic properties of germanium, with the bent germylenes, *trans*-bent digermenes, preference of silagermenylidene over germasilanylidene and frequent encounters with bicyclobutanes in unsaturated clusters as molecular manifestations on the way to the bulk.

Aims & Scope

As outlined in the introduction, low-valent germanium containing systems of varying size are highly susceptible to constitutional isomerizations due to the usually flat potential energy surfaces. Especially, the reduction of the dismutational Si_4Ge_2 isomer **193** to the anticipated anionic heterosiliconoid (or germanoid) **198** isostructural to benzpolarenide **197** (Scheme 86) promises insight into rearrangement processes of heavy benzene isomers in general: The positions of the germanium atoms in the resulting cluster scaffold should allow for mechanistic conclusions that might be extended to the all-silicon systems and facilitate design of homo-and heteronuclear siliconoids in the future. Hence, isolation and characterization of the reduction product of **193** is a first goal of this work, in order to promote targeted cluster design.

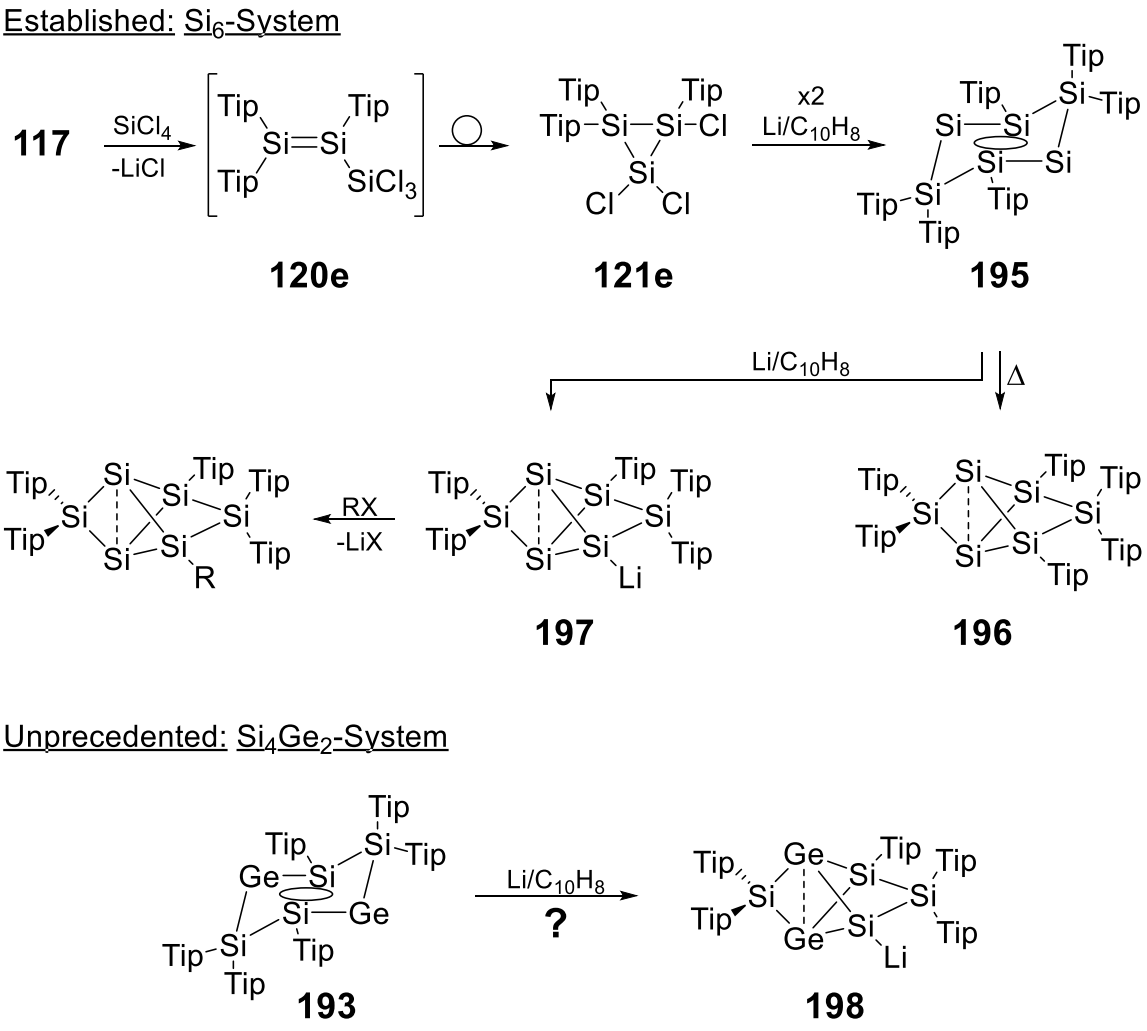

Scheme 86: Top: Synthetic pathway from disilenide **117** to hexasilabenzene isomer **195** *via* intermediate cyclotrisilane **121e** and its two rearrangements to benzpolarenes **196** and **197**. Anionic **197** can be utilized to attach a variety of substituents to the cluster scaffold. Bottom: Hypothetical reduction product **198** of dismutational benzene isomer **193**.

The pivotal role of disilenide **117** in the construction of both homo- and heteronuclear siliconoids emerges from Scheme 86 and raises the question if its heavy analogue digermenide **98a** could grant access to cluster compounds with unprecedented Si/Ge ratios or even pure germanoids. Digermenide **98a** has recently been employed for the straightforward synthesis of asymmetric digermenes but its reactivity remains unexplored otherwise.[538–540] A second goal of this work is therefore a comparison between the isomerization behavior of reported functionalized disilenes obtained from disilenide **117** (cf. Scheme 53) with analogous digermenes accessible from digermenide **98a**. If the digermenes retain an open-chained structure, they will constitute unprecedented peripherally functionalized Ge-Ge double bonds with potential synthetic value. In case of similar reactivity, the resulting germacycles (particularly chloro-substituted cyclopropane analogues) would pave the way for unprecedented germanoids, in analogy to the silicon case.

The third major objective of this work is the establishment of a metathesis protocol for asymmetric digermenes: Digermenide **98a** gives exclusive access to Ge-Ge double bonds consisting of two different germylene fragments. As digermenes in general are relatively prone towards cleavage of the Ge-Ge double bond, this might allow for an unprecedented reaction type in which an unsymmetric digermene splits into the corresponding germylenes which then could homocouple to yield two symmetric digermenes (Scheme 87). This metathesis reaction might furthermore be exploited for the polymerization of suitable α,ω-bis(digermenes) to poly(digermenes), a class of compounds which is sought extensively and which would constitute one of the first examples of polymers with heavy multiple bonds in the repeating unit in general.

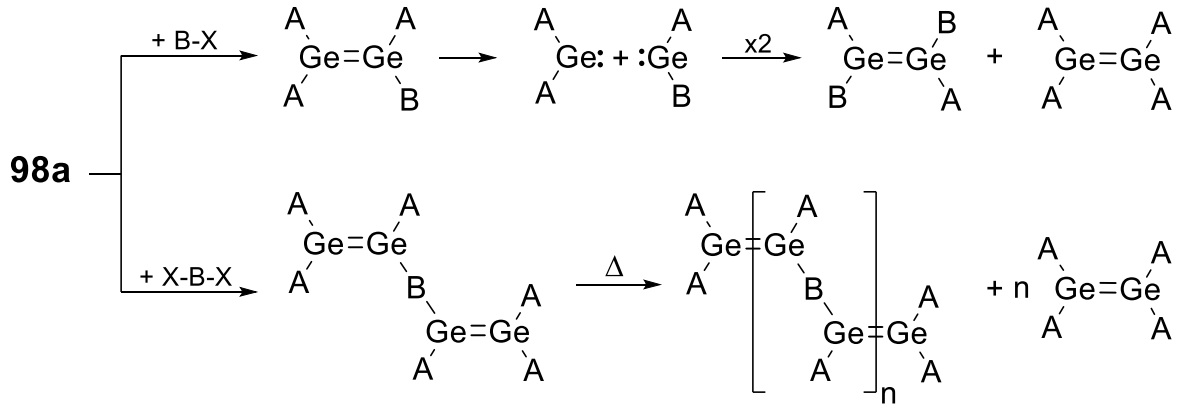

Scheme 87: Proposed metathesis of asymmetric digermenes and suggested polymerization of α,ω-bis(digermenes) to unprecedented poly(digermenes).

Results and Discussion

An anionic heterosiliconoid with two germanium vertices

L. Klemmer, V. Huch, A. Jana, D. Scheschkewitz, *Chem. Commun*. **2019**, *55*, 10100−10103.
https://doi.org/10.1039/c9cc04576g.

The results described within this article are additionally concluded and put into context in the Conclusion and Outlook chapter.

Contributions of the Authors:

Lukas Klemmer: Lead: Conceptualization, Visualization, Investigation, Methodology, Data Curation, Formal Analysis, Writing ─ Review and Editing of the supporting information, Theoretical studies, Synthesis, and characterization of heterosiliconoids; Supporting: Writing ─ Review and Editing of the manuscript.

Volker Huch: Lead: X-ray analysis.

Anukul Jana: Lead: Writing ─ Review and Editing of the manuscript; Supporting: Project administration, Supervision, Acquisition of funding and resources.

David Scheschkewitz: Lead: Project administration, Supervision, Acquisition of funding and resources; Supporting: Conceptualization, Writing ─ Review and Editing.

ChemComm

COMMUNICATION

View Article Online
View Journal | View Issue

Cite this: *Chem. Commun.*, 2019, 55, 10100

Received 14th June 2019,
Accepted 23rd July 2019

DOI: 10.1039/c9cc04576g

rsc.li/chemcomm

An anionic heterosiliconoid with two germanium vertices†

Lukas Klemmer,[a] Volker Huch,[a] Anukul Jana[b] and David Scheschkewitz*[a]

The two-electron reduction of the dismutational isomer of a 1,4-digermatetrasilabenzene cleaves one of the aryl groups in *ligato*-position and thus yields an unsaturated anionic Ge_2Si_4 cluster (digermatetrasila-benzpolarenide) with the negative charge at a Ge center. The regioselective positioning of the germanium centers in one *nudo*- and one *ligato*-position provides insight into the rearrangement of the Si_4E_2-scaffold of the dismutational isomers of hexatetrelbenzenes under reductive conditions with concomitant aryl group cleavage (E = Si and Ge).

The chemistry of stable siliconoids has seen remarkable progress in recent years.[1] The most striking feature of siliconoids is the presence of one or more unsubstituted vertices, which is reminiscent of surface characteristics of silicon in the bulk and at the nano scale.[2] The groups of Scheschkewitz,[3] Breher (**I**),[4] Wiberg (**II**),[5] Iwamoto (**III**),[6] and Kyushin[7] reported neutral siliconoids of varying nuclearity (Si_5 to Si_{11}, see Chart 1 for selected examples). In addition, we reported the isolation of anionic Si_6 siliconoids that serve as synthons for further variously functionalized silicon clusters.[8] Notably, anionic siliconoids can also be employed for the systematic and stepwise expansion of the cluster core by additional silicon vertices.[9]

Since very recently, the selective functionalization of silicon-based Zintl anions offers a complementary approach to (anionic) siliconoids, thus closing the conceptual gap between Zintl phases and neutral unsaturated molecular clusters.[10] While binary Zintl anions of heteronuclear heavier Group 14 elements[10a,11] and homonuclear germanium and tin-based metalloids are well-known,[12] the number of heteronuclear siliconoids of heavier Group 14 elements (**IV**, **V**) are limited (Chart 1).[13] In 2013, we

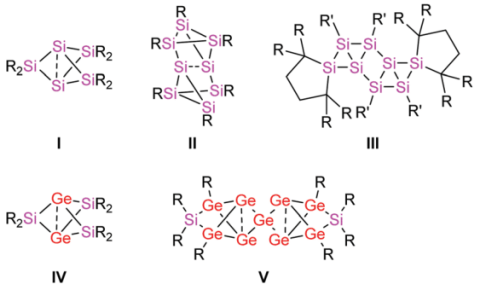

Chart 1 Selected homo- (**I–III**) and heteronuclear (**IV–V**) siliconoids.

reported the synthesis of dismutational and global minimum isomers of 1,4-digermatetrasilabenzene and the global minimum isomer of distannatetrasilabenzene.[14] In analogy to the anionic Si_6 siliconoid, we assumed that an anionic heterosiliconoid should be accessible by reduction of the dismutational isomer of 1,4-digermatetrasilabenzene.

Indeed, treatment of **1** in diethylether with two equivalents of freshly prepared Li/$C_{10}H_8$ in THF leads to the cleavage of one of the Tip substituents[15] to yield a crystalline product of uniform appearance in isolated yields of 47% (from THF) and 64% (from DME) (Scheme 1).[16] We tentatively assigned the structure of the anionic unsaturated Si_4Ge_2 cluster **2** as its lithium salt on the basis of the characteristically wide distribution of chemical shifts in the $^{29}Si\{^1H\}$ NMR spectrum.[3d,8]

Single crystal X-ray diffraction analyses of both the THF-coordinated contact ion pair **2Li**·$(THF)_2$ and solvent-separated

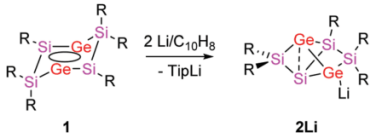

Scheme 1 Synthesis of anionic Ge_2Si_4 heterosiliconoid **2Li** (R = 2,4,6-$iPr_3C_6H_2$).

[a] *Krupp-Chair of General and Inorganic Chemistry, Saarland University, 66123 Saarbrücken, Germany. E-mail: scheschkewitz@mx.uni-saarland.de*
[b] *Tata Institute of Fundamental Research Hyderabad, Gopanpally, Hyderabad-500107, India*

† Electronic supplementary information (ESI) available: Experimental details, NMR and X-ray crystallographic data. CCDC 1921154 (**2Li**·$(THF)_2$) and 1921153 (**2** [Li$(DME)_3$]). For ESI and crystallographic data in CIF or other electronic format see DOI: 10.1039/c9cc04576g

ion pair **2**[Li(DME)$_3$] confirm the connectivity of **2** and thus the rearrangement of the Si_4Ge_2 scaffold from a dismutational isomer to a global minimum isomer (Fig. 1 and 2). We recently proposed the term benzpolarene for the six-membered tricyclic scaffold of bridged propellane-type global minimum isomers of the (mostly hypothetic) heavier benzenes.[8b] For the facile identifications of the inequivalent vertices of benzpolarenes, we introduced the descriptors *nudo*, *privo*, *ligato* and *remoto*.[8b] This nomenclature will be applied to the here reported di germa-substituted derivatives in the following.

Unexpectedly, the germanium atoms of Si_4Ge_2 benzpolarenide **2** do not occupy the two *nudo* positions as previously observed[14] for the neutral Si_4Ge_2 benzpolarene. Instead, the unsubstituted vertices of **2Li** are occupied by one silicon and one germanium atom, while the second germanium atom is exclusively located at the anionic *ligato* vertex. As the formal exchange of silicon and germanium atoms at the *nudo* positions results in energetically degenerate enantiomeric species, equal occupation would be anticipated. The lifting of the degeneracy by symmetry breaking through the differing orientations of the substituents, however, results in ratios of 64 : 36 for **2Li**·(THF)$_2$ and 55 : 45 for **2**[Li(DME)$_3$] (see ESI† for the molecular structures including the positions of the minor isomers). Further evidence for this interpretation is given by DFT calculations on both enantiomers of the isolated $Tip_5Ge_2Si_4^-$ anion with identically oriented Tip groups. Optimization at the (BP86-D3/def2SVP) level of theory retains the differing ligand shells for the two mirror images of the Si_4Ge_2 core (see ESI† for a comparison of the structures) and reveals a difference in free enthalpy of ΔG = 0.24 kcal mol^{-1}. Although such a small energy difference has to be treated with caution, the resulting 60 : 40 Boltzmann distribution corresponds well to the solid-state occupations found for **2Li**·(THF)$_2$ and **2**[Li(DME)$_3$]. Essentially, the two enantiomers are differentiated by the ligand conformation although it should be noted that the achiral point groups $C2/c$ for **2Li**·(THF)$_2$ and $P2_1/c$ for **2**[Li(DME)$_3$] obviously result in overall racemic mixtures of the two rotameric species.

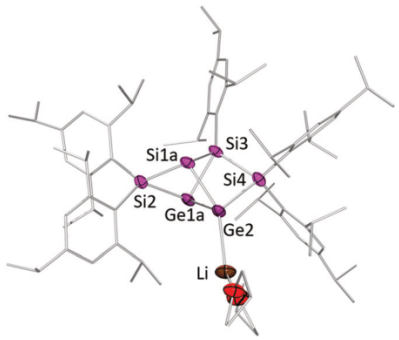

Fig. 1 Molecular structure of the major isomer (64%) of **2Li**·(THF)$_2$ in the solid state (thermal ellipsoids at 50% probality level; disordered *nudo*-Si1b and *nudo*-Ge2b, hydrogen atoms and co-crystallized half molecule of naphthalene are omitted for clarity). Selected interatomic distances (Å): Si1a···Ge1a 2.670(8), Si1a–Si2 2.344(8), Si1a–Si3 2.347(8), Si1a–Ge2 2.432(8), Ge1a–Si2 2.454(2), Ge1a–Si3 2.428(2), Ge1a–Ge2 2.557(2), Si3–Si4 2.347(2), Ge2–Si4 2.458(1), Ge2–Li 2.594(8).

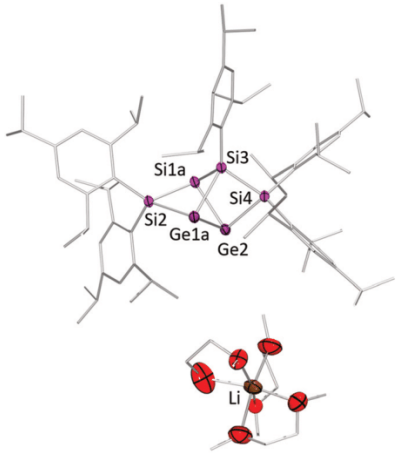

Fig. 2 Molecular structure of the major isomer (55%) of **2**[Li(DME)$_3$] in the solid state (thermal ellipsoids at 50% probality level; disordered *nudo*-Si1b and *nudo*-Ge2b, hydrogen atoms and co-crystallized solvent *n*-hexane are omitted for clarity). Selected interatomic distances (Å): Si1a···Ge1a 2.674(7), Ge2···Li 7.607(9), Si1a–Si2 2.339(8), Si1a–Si3 2.343(8), Si1a–Ge2 2.467(8), Ge1a–Si2 2.450(3), Ge1a–Si3 2.414(3), Ge1a–Ge2 2.559(2), Si3–Si4 2.344(1), Ge2–Si4 2.480(9).

Even in solution, the crystallized products show two sets of four ^{29}Si resonances at room temperature (Table 1), which we attribute to the preservation of the broken symmetry by hindered rotation of the Tip groups due to sufficiently high rotational barriers as previously discussed for the all-silicon species.[8a] The ^{29}Si NMR spectra of **2Li**·(THF)$_2$ in C_6D_6 and **2**[Li(DME)$_3$] in thf-d_8 are almost identical except for the different ratios between the two rotamers (**2Li**·(THF)$_2$: 61 : 39; **2**[Li(DME)$_3$]: 56 : 44), which are reasonably close to the ratios determined by X-Ray crystallography.

In **2Li**·(THF)$_2$ (Fig. 1), the distance of 2.594(8) Å between Ge and Li is at the lower end of the typical range of Ge–Li bond lengths (2.55 to 2.91 Å).[17] In the case of the solvent-separated ion pair **2**[Li(DME)$_3$] (Fig. 2), the shortest distance between Ge and Li is 7.607(9) Å, hence excluding any significant interaction.

Table 1 Comparison of NMR spectroscopic and structure data of lithiated benzpolarenides **2Li**·(THF)$_2$ and **2**[Li(DME)$_3$]

	2Li·(THF)$_2$		**2**[Li(DME)$_3$]	
	Major	Minor	Major	Minor
δ^{29} Si1 [ppm]	−182.6	−177.8	−181.1	−183.9
δ^{29} Si2 [ppm]	172.8	168.5	171.4	172.4
δ^{29} Si3 [ppm]	60.9	65.4	36.1	37.2
δ^{29} Si4 [ppm]	7.4	9.2	5.6	6.2
Si1–Ge1 [Å]	2.670(8)	2.656(9)	2.674(7)	2.669(7)
Ge2–Li [Å]	2.594(8)	2.594(8)	7.607(9)	7.607(9)
ϕ_{Si1} [Å]^a	1.2387	1.2494	1.2540	1.2553
ϕ_{Ge1} [Å]^a	1.4302	1.4069	1.4200	1.4130

^{a} The hemispheroidality ϕ is the distance of a naked cluster vertex from the plane spanned by its three substituents. Its value is taken as a measure for the degree of hemispheroidality of the vertex. For a detailed explanation see ref. 1.

The unsubstituted bridgehead atoms (Si and Ge) of the two rotamers of **2Li**·$(THF)_2$ are 2.670(8) Å (major) and 2.656(9) Å (minor) apart, which is closer than the corresponding distances of Si_6Tip_6 (Si···Si 2.707 Å)[3d] and of $Si_4Ge_2Tip_6$ (Ge···Ge 2.782 Å),[14] but farther than that of $Si_6Tip_5Li(12\text{-crown-}4)_2$ (Si···Si 2.5506(9) Å).[8a] The separation of Li^+ from the anion **2** by coordination of three molecules of DME does not entail any drastic structural changes: in **2**$[Li(DME)_3]$, the *nudo* positions in the major and minor isomer are 2.674(7) Å and 2.669(7) Å apart, respectively.

The observed rearrangement of the Si_4Ge_2 scaffold with the resulting relocation of the two Ge atoms into a *nudo* and a *ligato* position during the reductive cleavage of one Tip group requires some reflections regarding the mechanism. Considering the often similar chemical properties of silicon and germanium, the formation of **2Li** can be regarded as a labelling experiment to also shed light on the formation of benzpolarene scaffolds in general (Scheme 2).

Notably, while the Ge atoms exclusively occupy the *nudo* positions after thermal isomerisation of dismutational Si_4Ge_2 isomer **1** to the neutral heteronuclear siliconoid **3** (Scheme 2a),[14] a similar positional rearrangement as in the present case occurs during the formation of the recently reported saturated Si_4Ge_2 derivative **5** (Scheme 2b),[18] which we now propose to be termed benzpolarane (with the replacement of the letter "e" in the suffix by an "a" indicating saturation).

As already postulated for the formation of **7Li** (Scheme 2c),[8b] the first step in the formation of **2Li** presumably consists of the addition of two electrons to the unsubstituted vertices of **1**. The thus formed dianionic intermediate [**8**] is structurally related to the Si_4Ge_2 tricyclohexane **4**. The elimination of an aryl anion R^- would result in the doubly-bridged cyclobutenide analogue [**9**] with allylic delocalization of the negative charge. Due to its high ring strain, [**9**] would then rearrange to butadienide [**10**] and finally to the corresponding bicyclobutanide, *i.e.* the benzpolarenide **2** (Scheme 3). It is well established for carbon as well as hetero-substituted systems such as B_2P_2 that the two internal doubly-bonded atoms of the butadiene system end up as the bridgehead atoms of the isomeric bicyclobutane.[19] Based on these considerations, it can be speculated that the rearrangement of the neutral species **1** (as well as of the corresponding Si_6 derivative) may initially result in a benzpolarene scaffold with adjacent *nudo* positions.

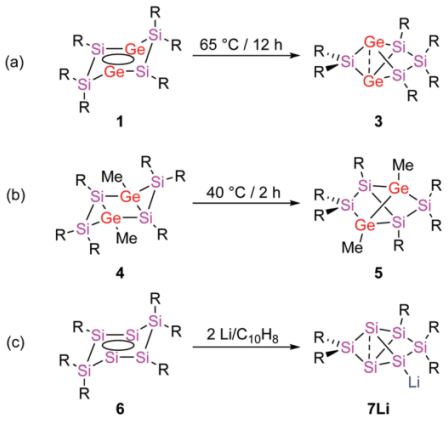

Scheme 2 Previously reported thermal rearrangements of (a) 1,4-digermatetrasilabenzene **1** and (b) tetrasiladigermatricyclohexane **4**; (c) chemical rearrangement of dismutational isomer of hexasilabenzene **6** (R = 2,4,6-$iPr_3C_6H_2$).

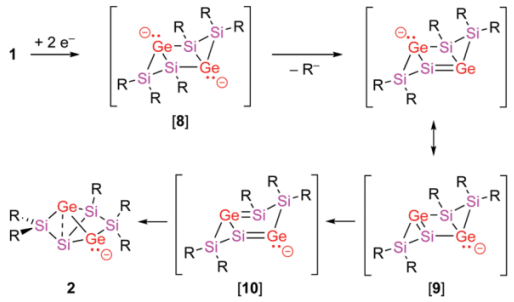

Scheme 3 Proposed mechanism for the formation of **2Li** from **1** (R = 2,4,6-$iPr_3C_6H_2$).

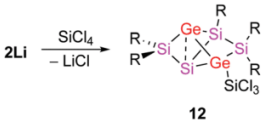

Scheme 4 Synthesis of **12** (R = 2,4,6-$iPr_3C_6H_2$).

Finally, in order to address the nucleophilic properties of the anionic unsaturated germanium centre[20] of **2Li**, we treated **2Li**·$(THF)_2$ with $SiCl_4$ in toluene (Scheme 4). After workup, the Si_4Ge_2 benzpolarene **12** with trichlorosilyl substituent in *ligato* position is obtained as a viscous red oil and characterized by solution state $^{29}Si\{^1H\}$ NMR spectroscopy. As in the case of **2Li**, two sets of five widely dispersed resonances are observed in the $^{29}Si\{^1H\}$ NMR spectrum in a 68 : 32 ratio (δ (major) = 202.9, 47.7, 27.2, 11.4, −222.9 ppm; δ (minor) = 204.6, 49.3, 26.2, 12.1, −225.0 ppm). The preservation of the non-degeneracy of the two rotamers provides a strong indication that the positions of the germanium atoms are the same as in **2Li**.

In summary, we have isolated the first hetero-benzpolarenide $Si_4Ge_2LiTip_5$ as its lithium salt with germanium atoms in one *nudo* and one *ligato* position by reductive cleavage of an aryl group from the dismutational isomer of 1,4-digermatetrasilabenzene. The different positions of the germanium atoms in the anionic Si_4Ge_2 scaffold compared to the corresponding neutral Si_4Ge_2 benzpolarene provide evidence for the plausible mechanistic scenario regarding the formation of the former *via* a cyclobutene – butadiene – bicyclobutane rearrangement. The negative charge in heteronuclear siliconoid resides at the germanium centre so that a certain relationship exists to the GeC_5 analogue of a phenyl anion recently reported by the Tokitoh group.[21] As shown theoretically by Boldyrev *et al.*, the benzpolarene structure becomes more and more competitive with increasing content of heavier Group 14 elements.[22] Finally, we have also demonstrated the nucleophilic character of anionic heteronuclear siliconoid by the exemplary reaction with a silicon-based electrophile such as $SiCl_4$.

This work was supported by the Deutsche Forschungsgemeinschaft (DFG SCHE 906/4-2), the Research Group Linkage Programme of the Alexander von Humboldt Foundation, Germany, and Saarland University, Germany. AJ is grateful to the Alexander von Humboldt Foundation for the sponsoring of a renewed research stay.

Conflicts of interest

There are no conflicts to declare.

References

1 Y. Heider and D. Scheschkewitz, *Dalton Trans.*, 2018, **47**, 7104–7112.
2 H. N. Waltenburg and J. T. Yates, Jr., *Chem. Rev.*, 1995, **95**, 1589–1673.
3 (*a*) D. Scheschkewitz, *Angew. Chem., Int. Ed.*, 2005, **44**, 2954–2956; (*b*) K. Leszczyńska, K. Abersfelder, M. Majumdar, B. Neumann, H.-G. Stammler, H. S. Rzepa, P. Jutzi and D. Scheschkewitz, *Chem. Commun.*, 2012, **48**, 7820–7822; (*c*) K. Abersfelder, A. J. P. White, H. S. Rzepa and D. Scheschkewitz, *Science*, 2010, **327**, 564–566; (*d*) K. Abersfelder, A. J. P. White, R. J. F. Berger, H. S. Rzepa and D. Scheschkewitz, *Angew. Chem., Int. Ed.*, 2011, **50**, 7936–7939; (*e*) K. Abersfelder, A. Russell, H. S. Rzepa, A. J. P. White, P. R. Haycock and D. Scheschkewitz, *J. Am. Chem. Soc.*, 2012, **134**, 16008–16016.
4 D. Nied, R. Köppe, W. Klopper, H. Schnöckel and F. Breher, *J. Am. Chem. Soc.*, 2010, **132**, 10264–10265.
5 G. Fischer, V. Huch, P. Mayer, S. K. Vasisht, M. Veith and N. Wiberg, *Angew. Chem., Int. Ed.*, 2005, **44**, 7884–7887.
6 T. Iwamoto, N. Akasake and S. Ishida, *Nat. Commun.*, 2014, **5**, 5353.
7 (*a*) A. Tsurusaki, C. Iizuka, K. Otsuka and S. Kyushin, *J. Am. Chem. Soc.*, 2013, **135**, 16340–16343; (*b*) S. Ishida, K. Otsuka, Y. Toma and S. Kyushin, *Angew. Chem., Int. Ed.*, 2013, **52**, 2507–2510.
8 (*a*) P. Willmes, K. Leszczyńska, Y. Heider, K. Abersfelder, M. Zimmer, V. Huch and D. Scheschkewitz, *Angew. Chem., Int. Ed.*, 2016, **55**, 2907–2910; (*b*) Y. Heider, N. E. Poitiers, P. Willmes, K. I. Leszczyńska, V. Huch and D. Scheschkewitz, *Chem. Sci.*, 2019, **10**, 4523–4530.
9 K. Leszczyńska, V. Huch, C. Präsang, J. Schwabedissen, R. J. F. Berger and D. Scheschkewitz, *Angew. Chem., Int. Ed.*, 2019, **58**, 5124–5128.
10 (*a*) T. Henneberger, W. Klein and T. F. Fässler, *Z. Anorg. Allg. Chem.*, 2018, **644**, 1018–1027; (*b*) C. Lorenz, F. Hastreiter, K. Hioe, N. Lokesh, S. Gärtner, N. Korber and R. M. Gschwind, *Angew. Chem., Int. Ed.*, 2018, **57**, 12956–12960; (*c*) L. Schiegerl, A. J. Karttunen, W. Klein and T. F. Fässler, *Chem. – Eur. J.*, 2018, **24**, 19171–19174; (*d*) F. Hastreiter, C. Lorenz, J. Hioe, S. Gärtner, N. Lokesh, N. Korber and R. M. Gschwind, *Angew. Chem., Int. Ed.*, 2019, **58**, 3133–3137.
11 (*a*) M. Waibel, G. Raudaschl-Sieber and T. F. Fässler, *Chem. – Eur. J.*, 2011, **17**, 13391–13394; (*b*) M. Waibel and T. F. Fässler, *Inorg. Chem.*, 2013, **52**, 5861–5866.
12 (*a*) A. Schnepf, *Chem. Soc. Rev.*, 2007, **36**, 745–758; (*b*) C. Schenk, F. Henke and A. Schnepf, *Angew. Chem., Int. Ed.*, 2013, **52**, 1834–1838; (*c*) A. Sekiguchi, Y. Ishida, Y. Kabe and M. Ichinohe, *J. Am. Chem. Soc.*, 2002, **124**, 8776–8777; (*d*) B. E. Eichler and P. P. Power, *Angew. Chem., Int. Ed.*, 2001, **40**, 796–797; (*e*) L. R. Sita, *Acc. Chem. Res.*, 1994, **27**, 191–197; (*f*) C. P. Sindlinger and L. Wesemann, *Chem. Sci.*, 2014, **5**, 2739–2746; (*g*) N. Zapp, K. Rohe, R. Ye, D. Scheschkewitz and M. Springborg, *Comput. Theor. Chem.*, 2017, **1102**, 5–14.
13 (*a*) D. Nied, P. Oña-Burgos, W. Klopper and F. Breher, *Organometallics*, 2011, **30**, 1419–1428; (*b*) Y. Ito, V. Y. Lee, H. Gornitzka, C. Goedecke, G. Frenking and A. Sekiguchi, *J. Am. Chem. Soc.*, 2013, **135**, 6670–6673; (*c*) A.-C. Andres, J. Beckmann, L. Klemmer, S. Muth, D. Scheschkewitz and M. Springborg, *J. Mol. Model.*, 2018, **29**, 190.
14 A. Jana, V. Huch, M. Repisky, R. J. F. Berger and D. Scheschkewitz, *Angew. Chem., Int. Ed.*, 2014, **53**, 3514–3518.
15 (*a*) D. Scheschkewitz, *Angew. Chem., Int. Ed.*, 2004, **43**, 2965–2967; (*b*) M. Ichinohe, K. Sanuki, S. Inoue and A. Sekiguchi, *Organometallics*, 2004, **23**, 3088–3090; (*c*) S. Inoue, M. Ichinohe and A. Sekiguchi, *Chem. Lett.*, 2005, **34**, 1564–1565; (*d*) C. Strohmann, D. Schildbach and D. Auer, *J. Am. Chem. Soc.*, 2005, **127**, 7968–7971; (*e*) D. Nieder, L. Klemmer, Y. Kaiser, V. Huch and D. Scheschkewitz, *Organometallics*, 2018, **37**, 632–635.
16 See the ESI† for the details of experimental work.
17 (*a*) R. West, H. Sohn, D. R. Powell, T. Müller and Y. Apeloig, *Angew. Chem., Int. Ed. Engl.*, 1996, **35**, 1002–1004; (*b*) C. Seow, H.-W. Xi, Y. Li and C.-W. So, *Organometallics*, 2016, **35**, 1060–1063.
18 D. Nieder, C. B. Yildiz, A. Jana, M. Zimmer, V. Huch and D. Scheschkewitz, *Chem. Commun.*, 2016, **52**, 2799–2802.
19 (*a*) J. L. Buechele, E. Weitz and F. D. Lewis, *J. Am. Chem. Soc.*, 1981, **103**, 3588–3589; (*b*) K. A. Nguyen and M. S. Gordon, *J. Am. Chem. Soc.*, 1995, **117**, 3835–3847; (*c*) S. Sakai, *Chem. Phys. Lett.*, 2000, **319**, 687–694; (*d*) D. Scheschkewitz, H. Amii, H. Gornitzka, W. W. Schoeller, D. Bourissou and G. Bertrand, *Science*, 2002, **295**, 1880–1881; (*e*) D. Scheschkewitz, H. Amii, H. Gornitzka, W. W. Schoeller, D. Bourissou and G. Bertrand, *Angew. Chem., Int. Ed.*, 2004, **43**, 585–587; (*f*) A. Rodriguez, R. A. Olsen, N. Ghaderi, D. Scheschkewitz, F. S. Tham, L. J. Mueller and G. Bertrand, *Angew. Chem., Int. Ed.*, 2004, **43**, 4880–4883; (*g*) J.-B. Bourg, A. Rodriguez, D. Scheschkewitz, H. Gornitzka, D. Bourissou and G. Bertrand, *Angew. Chem., Int. Ed.*, 2007, **46**, 5741–5745.
20 (*a*) D. Nieder, L. Klemmer, Y. Kaiser, V. Huch and D. Scheschkewitz, *Organometallics*, 2018, **37**, 632–635; (*b*) F. S. Geitner, W. Klein and T. F. Fässler, *Angew. Chem., Int. Ed.*, 2018, **57**, 14509–14513.
21 Y. Mizuhata, S. Fujimori, T. Sasamori and N. Tokitoh, *Angew. Chem., Int. Ed.*, 2017, **56**, 4588–4592.
22 A. S. Ivanov and A. I. Boldyrev, *J. Phys. Chem. A*, 2012, **116**, 9591–9598.

Persistent digermenes with acyl and α-chlorosilyl functionalities

L. Klemmer*, Y. Kaiser*, V. Huch, M. Zimmer, D. Scheschkewitz, *Chem. Eur. J.* **2019**, *25*, 12187−12195.
https://doi.org/10.1002/chem.201902553.
*These authors contributed equally.

The results described within this article are additionally concluded and put into context in the Conclusion and Outlook chapter.

Contributions of the Authors:

Lukas Klemmer: Lead: Conceptualization, Visualization, Writing – Review and Editing, Investigation, Methodology, Data Curation, Formal Analysis, Theoretical studies, Synthesis and characterization of silyldigermenes; Supporting: Characterization of acyldigermenes, VT-NMR.

Yvonne Kaiser: Lead: Synthesis and characterization of acyldigermenes; Supporting: Conceptualization, Visualization, Writing – Review and Editing, Investigation, Methodology, Data Curation, Formal Analysis.

Volker Huch: Lead: X-Ray analysis.

Michael Zimmer: Lead: CP/MAS NMR and VT-NMR.

David Scheschkewitz: Lead: Project administration, Supervision, Acquisition of funding and resources; Supporting: Conceptualization, Writing – Review and Editing.

ChemPubSoc Europe
DOI: 10.1002/chem.201902553
CHEMISTRY A European Journal Full Paper

Inorganic Chemistry | *Hot Paper*

Persistent Digermenes with Acyl and α-Chlorosilyl Functionalities

Lukas Klemmer[+], Yvonne Kaiser[+], Volker Huch, Michael Zimmer, and David Scheschkewitz*[a]

Abstract: We report the preparation of α-chlorosilyl- and acyl-substituted digermenes. Unlike the corresponding transient disilenes, these species with a Ge=Ge double bond show an unexpectedly low tendency for cyclization, but in turn are prone to thermal Ge=Ge bond cleavage. Triphenylsilyldigermene has been isolated as a crystalline model compound, and is the first fully characterized example of a neutral digermene with an A_2GeGeAB substitution pattern. Spectroscopic and computational evidence prove the constitution of 1-adamantoyldigermene as a first persistent species with a heavy double bond conjugated with a carbonyl moiety.

Introduction

The discovery of the first alkene analogue in 1976, Lappert's distannene,[1] led to a rapid growth in interest in the chemistry of multiple bonds between heavier Group 14 elements. This resulted in the isolation of stable doubly and eventually triply bonded species of both silicon and germanium,[2] which have since been proven to be useful synthons in preparative chemistry. For example, Si- and Ge-based ring systems are accessible by their cycloaddition to unsaturated organic substrates such as ketones (**I**),[3] alkenes (**II**),[4] and acetylenes (**III**)[3e,5] (Scheme 1).

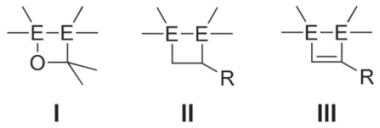

Scheme 1. Small ring systems (E = Si, Ge) derived from [2+2] cycloadditions of disilenes or digermenes to ketones (**I**), alkenes (**II**), and acetylenes (**III**).

The synthetic application of disilenes gained further momentum with the advent of functionalized derivatives, most notably disilenides as analogues of vinyllithium.[6] The anionic, nucleophilic silicon center in these species enables targeted peripheral functionalization of the uncompromised Si=Si moiety, as documented by various examples.[7] In some cases, however, these functional disilenes rearrange to cyclic isomers, a process that is thermodynamically driven by replacement of the weak π bond by stronger bonds (Scheme 2). In particular, disilenides

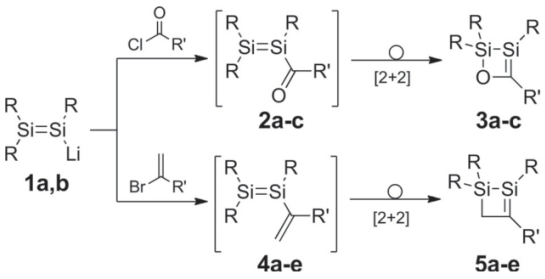

Scheme 2. Synthesis of cyclic silenes **3a–c** and **5a–e** (**1a**: R = Tip = 2,4,6-$iPr_3C_6H_2$; **1b**: R = SiMe*t*Bu$_2$; **2a**, **3a**: R = Tip, R′ = *t*Bu; **2b**, **3b**: R = Tip, R′ = 1-adamantyl; **2c**, **3c**: R = SiMe*t*Bu$_2$, R′ = 1-adamantyl; **4a**, **5a**: R = Tip, R′ = Ph; **4b**, **5b**: R = Tip, R′ = SiMe$_3$; **4c**, **5c**: R = SiMe*t*Bu$_2$, R′ = H; **4d**, **5d**: R = SiMe*t*Bu$_2$, R′ = Ph; **4e**, **5e**: R = SiMe*t*Bu$_2$, R′ = SiMe$_3$).[8,9]

1a,b undergo quantitative reactions with carboxylic acid chlorides to afford cyclic Brook-type silenes **3a–c**.[8] The plausible intermediates, acyl disilenes **2a–c**, could not be detected by NMR spectroscopy, even at low temperature. Documented examples of acyl-substituted species with double bonds between heavier main group elements are still unknown, both experimentally and theoretically. Likewise, disilenides **1a,b** react with various vinyl bromides to afford 1,2-disilacyclobut-2-enes **5a–e**, without spectroscopic evidence for the putative intermediates, vinyldisilenes **4a–e**.[9] The electronic structure of the latter has been investigated theoretically for the parent species.[10] Experimentally, however, 1,2-disilabutadienes are as yet unknown, except for the recently reported 1,2,3-trisilacyclopentadienes, in which cyclization is hindered by incorporation of the butadiene motif into the five-membered ring.[11]

[a] *L. Klemmer,[+] Y. Kaiser,[+] Dr. V. Huch, Dr. M. Zimmer, Prof. Dr. D. Scheschkewitz*
Krupp Chair of General and Inorganic Chemistry
Saarland University, 66123 Saarbrücken, (Germany)
E-mail: scheschkewitz@mx.uni-saarland.de
[+] *These authors contributed equally to this work.*
Supporting information and the ORCID identification number(s) for the author(s) of this article can be found under: https://doi.org/10.1002/chem.201902553.

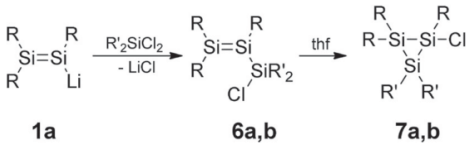

Scheme 3. Synthesis of α-chlorosilyldisilenes **6a,b** and cyclotrisilanes **7a,b** (R = Tip; **6a**, **7a**: R′ = Me; **6b**, **7b**: R′ = Ph).[12]

Conversely, α-chlorosilyldisilenes **6a,b**, prepared from the reaction of **1a** with dichlorosilanes, have been isolated, although they readily rearrange to cyclotrisilanes **7a,b** (Scheme 3).[12] Specifically, the dimethyl-substituted trisilaallyl chloride **6a** spontaneously cyclizes to cyclotrisilane **7a**, even at room temperature in the absence of a donor solvent, whereas the corresponding diphenyl derivative **6b** is stable in a hydrocarbon solvent for several weeks and needs elevated temperature or the addition of THF to promote isomerization to **7b**.

Compared to the versatile syntheses, reactions, and applications of disilenes, the chemistry of digermenes is still in its infancy. We recently reported the isolation of the first lithium digermenide **8** as well as proof-of-principle experiments for its reactivity as a nucleophile in salt metathesis reactions with monochlorosilanes (Scheme 4).[13] Single-crystal X-ray diffraction data for the resulting unsymmetrically substituted digermenes **9a,b** could only be obtained for a partially hydrolyzed sample of **9b**, which were of limited value in terms of the determination of pertinent bonding parameters.

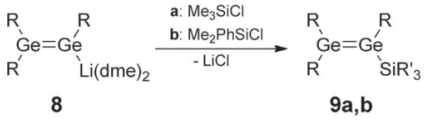

Scheme 4. Previously reported synthesis of unsymmetrically substituted digermenes **9a,b** (R = Tip = 2,4,6-*i*Pr$_3$C$_6$H$_2$; **9a**: SiR′$_3$ = SiMe$_3$; **9b**: SiR′$_3$ = SiMe$_2$Ph).[13]

Considering the vast synthetic possibilities offered by the availability of disilenides and the lack of simple synthetic protocols for digermasilacyclopropanes[14] and cyclic Brook-type germenes, we investigated the reactivity of **8** towards dichlorosilanes and acyl chlorides in order to prepare the digerma analogues of previously reported silacycles **3** and **7**.

Results and Discussion

Triphenylsilyldigermene 10

Reaction of Ph_3SiCl with digermenide **8** in toluene at room temperature yielded triphenylsilyldigermene **10** of NMR spectroscopic purity. Crystallization from a concentrated solution in hexane afforded single crystals of **10** as yellow plates in 52% yield (Scheme 5).

The ^{29}Si NMR spectrum of **10** features one singlet at δ = 1.89 ppm, in the expected range for a tetracoordinate silicon center, which compares well to the signals observed for **9a** (δ = 1.87 ppm) and **9b** (δ = 0.25 ppm).[13] The longest wavelength absorption in the UV/Vis spectrum is located in the typical region for heavier alkene homologues at λ_{max} = 426 nm (ε = 20845 L mol^{-1} cm^{-1}) and is thus slightly blue-shifted compared to the value reported for digermenide **8** (λ_{max} = 435 nm).[13] Single-crystal X-ray diffraction analysis confirmed the constitution of **10** as a silyl-substituted digermene (Figure 1). The *trans*-bent angles θ (defined as the angle between the R-E-R′ plane normal and the E-E bond vector) in **10** [θ(Ge1) = 23.7°; θ(Ge2) = 21.3°] are substantially larger than those in **8** [θ(GeTipLi) = 12.8°, θ(GeTip$_2$) = 7.1°] or the symmetrically substituted Tip$_2$Ge=GeTip$_2$ [θ(GeTip$_2$) = 12°]. In contrast, the twist angle τ (defined as the angle between the R-E-R′ plane normals) of **10** (τ = 13.6°) is similar to that in Tip$_2$Ge=GeTip$_2$ (τ = 14°) and thus smaller than that in **8** (τ = 19.9°).[13,15,16] In agreement with the increased *trans* bending, the Ge–Ge distance of 2.3279(4) Å is elongated compared to those in both **8** (2.284 Å) and Tip$_2$Ge=GeTip$_2$ (2.213 Å).[13,15,16] The Ge1–Si bond of 2.3984(8) Å is slightly shorter than those in persilyl-substituted digermenes (*i*Pr$_2$MeSi)$_2$Ge=Ge(SiMe*i*Pr$_2$)$_2$ (2.400 Å) and (*i*Pr$_3$Si)$_2$Ge=Ge(Si*i*Pr$_3$)$_2$ (2.427 Å).[17]

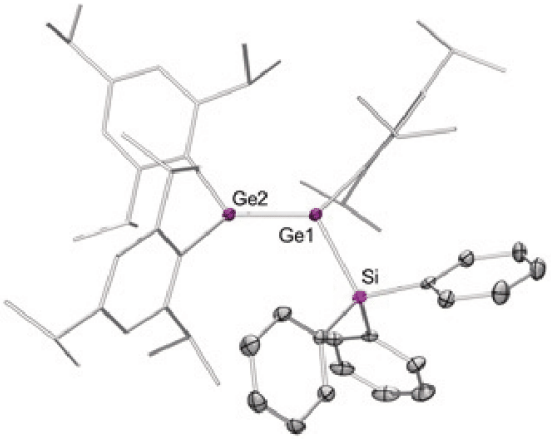

Figure 1. Molecular structure of triphenylsilyl digermene **10** in the solid state (hydrogen atoms omitted for clarity; thermal ellipsoids drawn at 50% probability). Selected bond lengths [Å] and angles [°]: Ge1–Ge2 2.3279(4), Ge1–Si 2.3984(8); Ge2–Ge1–Si 119.09(8), Σ°(Ge1) 346.53, Σ°(Ge2) 345.24, θ(Ge1) 23.7, θ(Ge2) 21.3, τ 13.6. Σ°(E) refers to the sum of angles around atom E.

Reaction of digermenide 8 with dichlorosilanes

Treatment of **8** with 1.5 equivalents of Me_2SiCl_2 at −78 °C in toluene resulted in an immediate color change to bright-

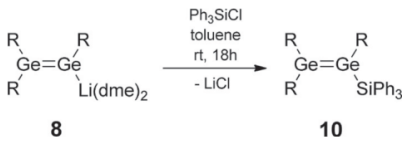

Scheme 5. Synthesis of triphenylsilyl digermene **10** (R = Tip = 2,4,6-*i*Pr$_3$C$_6$H$_2$).

ChemPubSoc Europe

CHEMISTRY A European Journal Full Paper

orange. The ^{1}H NMR spectrum of the reaction mixture showed full conversion to a single product, which was identified as silyl digermene **11 a** based on the following spectroscopic observations.

Three sharp singlets in the aryl region at $\delta = 7.12$, 7.09, and 7.01 ppm suggest the presence of three chemically inequivalent Tip groups that rotate rapidly on the NMR time scale and are therefore relatively unhindered. The singlet at $\delta = 0.58$ ppm with a relative intensity corresponding to six H atoms is assigned to the Si-bonded methyl groups. The identical chemical environment of the two methyl groups virtually excludes a three-membered Si_2Ge ring as the presence of the asymmetric Ge center in the hypothetical heavy cyclopropane **12 a** would cause diastereotopic splitting of the corresponding signals. Comparison with the NMR data of silyl disilene **6 a** and its isomeric cyclotrisilane **7 a** underpins this interpretation (Table 1).[11]

Table 1. NMR spectroscopic data for α-chlorosilyldigermenes **11 a–c** in comparison with those of α-chlorosilyldisilenes **6 a,b**, cyclotrisilanes **7 a,b**, and silyldigermenes **9 a,b** and **10**.

	δ ^{29}Si [ppm]	δ $^{1}H_{Tip\text{-}H}$ [ppm]	δ $^{1}H_{ortho\text{-}iPr\text{-}CH}$ [ppm]
11 a	31.5	7.12, 7.09, 7.02	3.89, 3.75, 3.59
11 b	23.7	7.12, 7.03, 7.03	3.92, 3.76, 3.62
11 c	15.2	masked by Ph signals	3.58, 3.54, 3.34
6 a	26.2	7.09, 7.06, 6.99	4.29, 4.00, 3.78
6 b	11.8	masked by Ph signals	4.15, 3.97, 3.74
7 a	−35.4	7.20, 7.18, 7.15, 7.02, 6.95	4.21, 4.09, 3.74, 3.61, 3.43
7 b	−54.8	masked by Ph signals	4.04, 3.96, 3.89, 3.55
9 a	1.87	7.11, 7.10, 7.02	3.84, 3.83, 3.65
9 b	0.25	7.09, 7.06, 7.05	3.85, 3.82, 3.67
10	1.89	7.06, 7.01, 6.95	3.86, 3.76, 3.72

Consistent evidence is provided by the ^{13}C NMR spectrum of **11 a**, with twelve signals between 153.1 and 122.0 ppm that satisfyingly match, in number and chemical shifts, the corresponding signals of silyl disilene **6 a**, while being in stark contrast to the eighteen signals in this range for cyclotrisilane **7 a**.[12] The ^{29}Si NMR signal at $\delta = 31.5$ ppm is typical of a terminal silyl group (**6 a**: $\delta = 26.2$ ppm, **9 a**: $\delta = 1.87$ ppm, **9 b**: $\delta = 0.25$ ppm), unambiguously excluding the presence of an endocyclic Si atom (**7 a**: $\delta = -35.4$ ppm).[12,13] The slightly lower field ^{29}Si NMR shift of **11 a** compared to **6 a** can be rationalized in terms of the higher electronegativity of germanium compared to silicon. The UV/Vis spectrum of a freshly prepared and filtered solution shows the longest-wavelength absorption at $\lambda_{max} = 435$ nm ($\varepsilon = 11110\ L\,mol^{-1}\,cm^{-1}$), close to the values for silyldisilenes and digermenes (**7 b**: 427 nm,[12] **10**: 426 nm), strongly supporting the presence of an uncompromised Ge=Ge moiety. Based on the accumulated spectroscopic evidence, we are confident in assigning the connectivity of α-chlorosilyldigermene **11 a** to the main product of the reaction of digermenide **8** with Me_2SiCl_2 (Scheme 6). Despite various attempts at crystallization from concentrated solutions in hexane, pentane, benzene, toluene, mesitylene, fluorobenzene, or THF, single crystals of **11 a** could not be obtained.

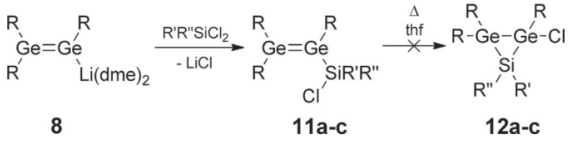

Scheme 6. Synthesis of α-chlorosilyl digermenes **11 a–c** (R = Tip = 2,4,6-$iPr_3C_6H_2$; **11 a**, **12 a**: R′ = R″ = Me; **11 b**, **12 b**: R′ = Me, R″ = Ph; **11 c**, **12 c**: R′ = R″ = Ph).

In an analogous manner to Me_2SiCl_2, the sterically more demanding dichlorosilanes $MePhSiCl_2$ and Ph_2SiCl_2 reacted with digermenide **8** at −78 °C in toluene to afford the α-chlorosilyldigermenes **11 b** and **11 c**, which were characterized by multinuclear NMR spectroscopy, but again eluded crystallization. In principle, the same arguments for structure identification hold as in the case of **11 a** (Table 1): the ^{29}Si NMR signals of **11 b,c** (**11 b**: $\delta = 23.7$ ppm; **11 c**: $\delta = 15.2$ ppm) are detected at significantly lower field than expected for three-membered rings (**7 a**: $\delta = -35.4$ ppm; **7 b**: $\delta = -54.8$ ppm). Three chemically distinct Tip groups give rise to the minimum number of signals in the ^{1}H and ^{13}C NMR spectra, indicating free rotation about the Ge–C bond. Unfortunately, redox processes become competitive during the synthesis of **11 b** and **11 c**, resulting in increasing amounts of the intensely green 1,3-tetragermabutadiene $Tip_2Ge{=}Ge(Tip){-}(Tip)Ge{=}GeTip_2$[18] as a side product (**11 b**: < 0.5 %; **11 c**: 2 %, as determined by ^{1}H NMR). Presumably, the increasing number of electron-withdrawing phenyl groups renders the dichlorosilane reagents more prone to reduction by digermenide **8**, which is oxidatively coupled to the tetragermabutadiene in the process.

As reported previously, isomerization of the related disilenes **6 a,b** to the corresponding cyclotrisilanes is induced by heating or the addition of THF as a donor solvent. At higher temperatures or upon addition of THF, however, all silyldigermenes eventually decompose to product mixtures dominated by the homoleptic $Tip_2Ge{=}GeTip_2$[15] as the only identifiable product. Digermenes in general are known to be readily cleaved into their constituent germylene fragments. Thermally induced dissociation of the Ge=Ge double bond of **10** and **11 a–c** and subsequent dimerization of the resulting $Tip_2Ge{:}$ fragments plausibly explains the formation of Tip_4Ge_2. The concomitantly formed $Tip(R_2ClSi)Ge{:}$ fragments seem to be highly unstable and presumably decompose via various pathways to a variety of unknown products.

Accordingly, α-chlorosilyldigermenes **11 a–c** are much less prone to cyclization to heavy cyclopropanes **12 a–c** compared to the disilene congeners **6 a,b**, but rather dissociate into their germylene fragments under thermal treatment or in the presence of *n*-donating solvents.

Reactions of digermenide 8 with acyl chlorides

In the light of the above observations, we anticipated that the use of acyl chlorides as substrates for the reaction with **8** might allow the isolation of the first stable compounds with acyl-substituted heavier double bonds. Upon addition of

1 equivalent of either pivaloyl chloride, 2,2-dimethylbutyryl chloride, or 1-adamantoyl chloride to digermenide **8** at room temperature in C_6D_6, the reaction mixture instantly turned dark-red and precipitation of a white solid was observed (Scheme 7).

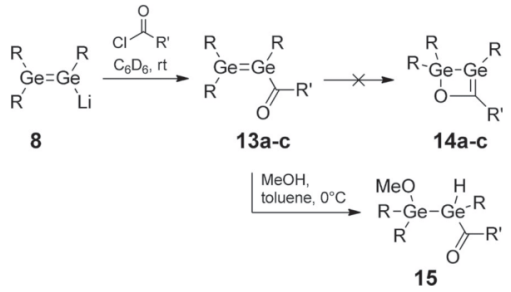

Scheme 7. Synthesis of acyl digermenes **13a–c** and trapping with methanol to afford **15** (R = Tip = 2,4,6-*i*Pr$_3$C$_6$H$_2$; **13a**, **14a**: R′ = *t*Bu; **13b**, **14b**: R′ = 2-methylbutan-2-yl; **13c**, **14c**, **15**: R′ = 1-adamantyl).

The ^{1}H NMR spectra of the crude products after five minutes indicated very clean conversion to single products in all cases. During the reported reactions of disilenide **1** with carboxylic acid chlorides, an initially occurring red color[8] might be attributed to transient yet undetected acyl disilenes. In the present case, the red color persisted at room temperature for up to several hours (**13a**,**b**) or days (**13c**). The ^{1}H and ^{13}C NMR signals of **13a–c** (see the Supporting Information) are of limited diagnostic value in distinguishing them from hypothetical cyclic germenes **14a–c** as the cyclic Brook silenes **3a**,**b** have been reported to show rapid inversion at the Si=C silicon atom at room temperature, leading to apparent C_s symmetry in solution and hence a lower number of signals for the Tip substituents than might otherwise be expected.[8]

Monitoring samples of **13a–c** by ^{1}H NMR revealed that conversion to homoleptic Tip$_2$Ge=GeTip$_2$ and various unidentified side products takes place even at room temperature, in analogy to what was observed for α-chlorosilyldigermenes **11a–c**. Whereas the reaction mixtures obtained from digermenide **8** and pivaloyl chloride or 2,2-dimethylbutyryl chloride largely decomposed in the course of one night, the 1-adamantoyl-substituted **13c** persisted to about 95% even after 18 h in reaction mixtures at the original concentration. The decomposition rate, however, increased at higher concentrations, which prevented the removal of 1,2-dimethoxyethane (liberated from **8**) from the reaction mixture as well as crystallization attempts from concentrated solutions. The similarity to the decomposition behavior of digermenes **11a–c**, however, suggests that the reaction products may indeed be the unprecedented acyldigermenes **13a–c**. Due to its superior stability in solution, we limit the following discussion to the 1-adamantoyl derivative **13c** (see the Supporting Information for spectra of **13a**,**b**).

The ^{13}C NMR spectrum of **13c** at 300 K features two signals at $\delta = 232.4$ and 238.7 ppm, in the typical range for carbonyl C atoms, which we attribute to the s-*cis* and s-*trans* isomers of the Ge=Ge–C=O system. Theoretical calculations on their relative thermodynamic stabilities at the M06-2X(D3)/def2-TZVPP//BP86(D3)def2-SVP level of theory predicted the s-*cis* isomer (dihedral angle $\phi = 51.64°$) to be 10.9 kcal mol^{-1} more stable than the s-*trans* form ($\phi = -149.13°$). The IR band at 1649 cm^{-1} validates the presence of a C=O bond attached to germanium in **13c**, and is in acceptable agreement with the calculated value of 1690 cm^{-1} for the s-*cis* isomer. A shift of around 70 cm^{-1} to lower wavenumbers compared to fully organic ketones is well known for acylsilanes and -germanes, and has been rationalized in terms of lowering of the C–O bond order due to the σ donating character of the tetryl moiety.[19] In the UV/Vis spectrum of **13c**, two bands at $\lambda_{max} = 476$ nm and $\lambda = 386$ nm further support the proposed open-chain structure: the longest-wavelength absorption maximum falls within the typical absorption range of digermenes and shows a substantial bathochromic shift compared to the bands observed for **8** ($\lambda_{max} = 435$ nm), **9b** ($\lambda_{max} = 424$ nm), and **10** ($\lambda_{max} = 426$ nm), presumably due to strong polarization of the Ge=Ge moiety by the attached C–O double bond.[13] In contrast, the longest-wavelength absorptions of the cyclic Brook germenes **3a–c** ($\lambda_{max} = 351$, 355, and 354 nm) have been reported to be significantly blue-shifted compared to the corresponding peaks for disilenide **1**.[8] Even the second absorption of **13c** at $\lambda_{max} = 386$ nm is red-shifted compared to the bands of **3a–c**. The excellent agreement with λ_{max} of reported germyl-substituted ketones Et$_3$GeCOMe ($\lambda_{max} = 380$ nm) and Ph$_3$GeCOMe ($\lambda_{max} = 380$ nm) corroborates the presence of a C=O double bond in **13c**.[19b] The bathochromic shift observed in comparison to all-organic ketones (which typically absorb in the UV region) can be explained in terms of mixing of the oxygen-centered lone pair with the Ge–C bond.[19b,e,f,20]

Further support for the assignment was sought by performing time-dependent DFT calculations on **13c** at the M06-2X(D3)/def2-SVP level of theory. The predicted longest-wavelength absorption at $\lambda_{Ge=Ge,calc.} = 468$ nm is in excellent agreement with the experimental value $\lambda_{Ge=Ge,exp.} = 476$ nm and is mainly due to the HOMO→LUMO transition. The second-longest absorption wavelength $\lambda_{C=O,calc.} = 401$ nm also exhibits satisfactory agreement with the experimental value $\lambda_{C=O,exp.} = 386$ nm and stems from a complex transition with HOMO−1→LUMO as its main component. The HOMO−1 resembles the π-symmetric nonbonding orbital of an isolated carbonyl group, whereas the HOMO is the π orbital of the Ge=Ge double bond (Figure 2).[21] The two orbitals are only marginally intermixed, providing little evidence of conjugation. In contrast, the LUMO

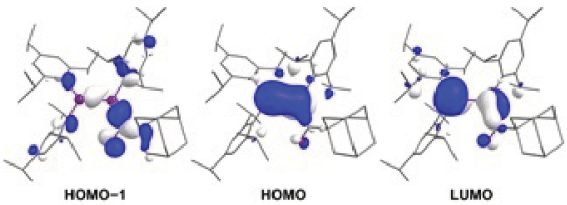

Figure 2. Selected Kohn–Sham orbitals of **13c** at the M06-2X(D3)/def2-SVP level of theory.

ChemPubSoc Europe

CHEMISTRY A European Journal Full Paper

is clearly a shared π* orbital of the conjugated Ge=Ge–C=O system resulting from substantial antibonding contributions of both the Ge=Ge double bond and the carbonyl group. Overestimation of this mixing between HOMO−1 and HOMO accounts for both the blue-shift of $\lambda_{Ge=Ge}$ and the red-shift of $\lambda_{C=O}$ in the calculated UV/Vis spectrum. The tendency of DFT methods to overvalue conjugation is well known.[22]

The strongest evidence for the existence of a persistent acyldigermene **13c** was finally provided by quenching with methanol. It should be noted that the cyclic adamantyl-substituted Brook silene **3b** has been reported to be inert towards MeOH in the absence of a base. The cyclic structure is retained, however, after base-catalyzed addition of MeOH to the Si=C moiety of **3b**.[8] In contrast, the reaction of **13c** with MeOH in toluene proceeds even at 0 °C and results in the formation of acyldigermane **15**, which can be isolated as pale-yellow crystals in 60% yield from a filtered and concentrated solution in hexane.

Single-crystal X-ray diffraction analysis confirmed the constitution of **15** as the 1,2-addition product of methanol to the Ge=Ge bond of **13c** (Figure 3). The Ge1–Ge2 distance of 2.4694(5) Å is in the expected range for Ge–Ge single bonds. The CO double-bond length of 1.215(3) Å is also unremarkable. The IR spectrum of **15** shows the expected bands for the Ge–H (2037 cm^{-1}) and C=O (1647 cm^{-1}) stretching modes, and the carbonyl moiety gives rise to a signal at $\delta = 238.6$ ppm in the ^{13}C NMR spectrum, similar to that of the acyldigermene starting material **13c**. The similarity of the ^{13}C NMR shifts and IR bands of α,β-unsaturated **13c** and saturated **15** confirms that π-conjugation between the Ge=Ge moiety and the carbonyl group in acyldigermene **13c** is insignificant and that solely the inductive effect of the digermanium moiety accounts for the observed differences to organic ketones. Conversely, the electron-withdrawing carbonyl moiety induces strong polarization of the Ge–Ge double bond towards the acyl-substituted terminus, as is evident from the regioselective addition of methanol.

The sum of available evidence leaves no doubt that we have prepared the first persistent acyldigermenes **13a–c**, which, unlike the acyldisilenes (only proposed as intermediates), show no tendency for cyclization at room temperature but instead readily decompose by facile dissociation of the Ge=Ge bond. As similar conclusions apply to α-silyldigermenes **11a–c** (see above), the electronic structures and thermodynamic properties vary substantially between functionalized disilenes and digermenes. We therefore sought to shed some light on the underlying reasons by performing DFT calculations.

Theoretical results

In order to rationalize the strongly differing inclinations of digermenes **11a–c** and **13a–c** towards cyclization compared to their lighter silicon analogues **2a–c** and **6a,b**, we took a closer look at the thermodynamics of these rearrangements (Scheme 8). To enable comparison, we restricted our investiga-

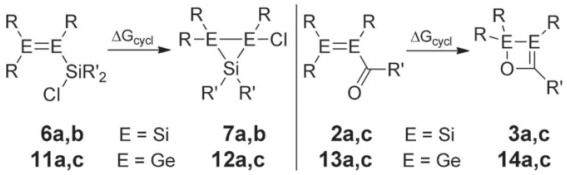

Scheme 8. Theoretically investigated cyclizations of α-chlorosilyldimetallenes **6a,b** and **11a,c** as well as acyldimetallenes **2a,c** and **13a,c** (R = Tip = 2,4,6-$iPr_3C_6H_2$; **6a**, **7a**: E = Si, R′ = Me; **6b**, **7b**: E = Si, R′ = Ph; **11a**, **12a**: E = Ge, R′ = Me; **11c**, **12c**: E = Ge, R′ = Ph; **2a**, **3a**: E = Si, R′ = *t*Bu; **2c**, **3c**: E = Si, R′ = 1-adamantyl; **13a**, **14a**: E = Ge, R′ = *t*Bu; **13c**, **14c**: E = Ge, R′ = 1-adamantyl).

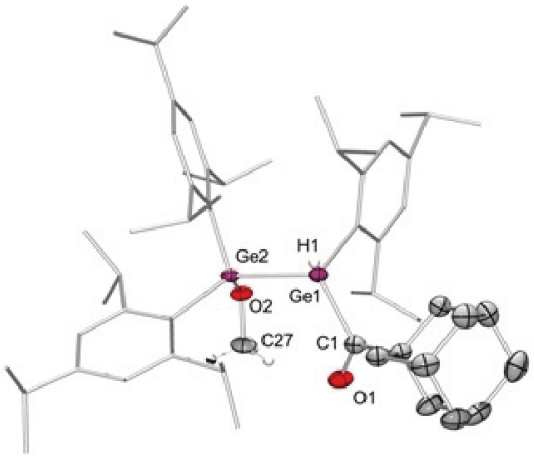

Figure 3. Molecular structure of acyldigermane **15** in the solid state (carbon-bonded hydrogen atoms omitted for clarity; thermal ellipsoids drawn at 50% probability). Selected bond lengths (Å) and angles (°): Ge1–Ge2 2.4694(5), Ge1–C1 2.041(3), C1–O1 1.215(3), Ge2–O2 1.8189(17); Ge1–C1–O1 118.7(2).

tions to those systems for which both the disilene and digermene are now known. In the case of the adamantyl-substituted acyldigermene **13c**, the s-*cis* conformer is thermodynamically favored over the s-*trans* conformer (see the Supporting Information) and we generalized these findings for the remaining acylmetallenes without further verification. The calculated free enthalpies of cyclization ΔG_{cycl} at the M06-2X(D3)/def2-TZVPP//BP86(D3)/def2-SVP level of theory for α-chlorosilyldigermenes **11a,c**, the corresponding disilenes **6a,b**, the s-*cis* acyldigermenes **13a,c**, and their silicon analogues **2a,c** show a clear trend (Table 2).

While the acyclic digermenes **11a,c** and **13a,c** show slightly endergonic or exergonic ΔG_{cycl} values near 0 kcal mol^{-1}, the corresponding disilenes **6a,b** and **2a,c** exhibit far more negative cyclization enthalpies ranging from −5.1 to −17.9 kcal mol^{-1}, in line with the observed trend for the formation of small rings **7a,b** and **3a,c**. Geometric ring parameters of cyclic silicon systems and their germanium analogues do not differ significantly (see the Supporting Information), and so differences in ring strain are unlikely to be a destabilizing factor. Therefore, to a first approximation, ΔG_{cycl} can be taken as a measure of the bond dissociation energy (BDE) balance of the cycliza-

Table 2. Calculated free reaction enthalpies ΔG_{cycl} at the M06-2X(D3)/def2-TZVPP//BP86(D3)/def2-SVP level of theory.

	E	R′	ΔG_{cycl} [kcal mol^{-1}]
11a/12a	Ge	Me	+2.6
11c/12c	Ge	Ph	+0.02
6a/7a	Si	Me	−7.6
6b/7b	Si	Ph	−5.1
13a/14a	Ge	*t*Bu	−2.5
13c/14c	Ge	1-Ad	−3.1
2a/3a	Si	*t*Bu	−17.9
2c/3c	Si	1-Ad	−16.9

tion. While an Si–Cl bond appears in both the starting material and the product during the formation of cyclotrisilanes **7a**,**b** and hence is unlikely to exert a pronounced influence on ΔG_{cycl}, the difference in BDEs of Si–Cl (ca. 100 kcal mol^{-1})[23] and Ge–Cl (ca. 93 kcal mol^{-1})[23] of about 7 kcal mol^{-1} is apparently responsible for the higher ΔG_{cycl} values of **12a**,**c**. Similarly, the much more negative ΔG_{cycl} values of acyldisilenes compared to digermenes can be rationalized in terms of the higher BDE of Si–O bonds (ca. 191 kcal mol^{-1}) compared to Ge–O bonds (ca. 158 kcal mol^{-1}).[23]

Conclusions

Functionalized digermenes, namely α-chlorosilyldigermenes **11a–c** and acyldigermenes **13a–c**, have been synthesized and their stability has been studied. The rich cyclization chemistry of the corresponding functional disilenes appears not to be reflected by the analogous germanium systems. None of the systems shows a detectable tendency towards cyclization; instead, they slowly decompose under ambient conditions to the homoleptic $Tip_2Ge{=}GeTip_2$ and unidentified side products. Chlorosilyldisilenes **13a–c** have been identified by detailed comparison of their NMR spectra with those of their silicon analogues. In addition, the newly synthesized triphenylsilyldigermene **10** has been fully characterized as the first neutral digermene with an $A_2Ge{=}GeAB$ substitution pattern. IR and UV/Vis spectra of **13c** as well as trapping with methanol to yield digermane **15** provide evidence for the synthesis of acyldigermenes **13a–c**, which, to the best of our knowledge, are the first isolated examples of acyldimetallenes of any heavier main group element. Considering the wide scope of reactions that α,β-unsaturated ketones are known for in organic chemistry, our current focus is on exploring the synthetic potential of **13a–c**.

Experimental Section

All reactions were carried out under a protective argon atmosphere using the Schlenk technique or gloveboxes. Pentane was heated to reflux with sodium/benzophenone and distilled prior to use. Hexane and toluene were taken directly from a solvent purification system (Innovative Technology PureSolv MD7). Deuterated benzene was heated to reflux over potassium and distilled prior to use. NMR spectra were recorded at 300 K on a Bruker Avance III 300 (^{1}H: 300.13 MHz, ^{7}Li: 116.59 MHz, ^{29}Si: 59.6 MHz) or Bruker Avance III HD 400 instrument (^{1}H: 400.13 MHz, ^{13}C: 100.61 MHz, ^{29}Si: 79.5 MHz). Chemical shifts are reported relative to $SiMe_4$. UV/Vis spectra were measured on a Shimadzu UV-2600 spectrometer from solutions in quartz cells with a path length of 1 mm. Fourier-transform IR spectra were acquired on a Bruker Vertex 70 spectrometer in attenuated total reflectance (ATR) mode. Elemental analyses were carried out on an Elementar Vario Micro Cube and show slightly suppressed carbon and hydrogen contents for digermenes **10**, **11a**, and **13a–c** as a result of their extraordinary sensitivity towards oxygen. Methanol, dichlorodimethylsilane, dichloromethylphenylsilane, dichlorodiphenylsilane, pivaloyl chloride, and 2,2-dimethylbutyryl chloride were boiled over magnesium and distilled prior to use. 1-Adamantoyl chloride was recrystallized from hexane prior to use. Chlorotriphenylsilane was dried in vacuo and stored under argon prior to use. Digermenide **8** was prepared according to our published procedure.[13] For theoretical data, crystallographic details, and plots of spectra, see the Supporting Information. CCDC 1920322 (**10**) and 1920323 (**15**) contain the supplementary crystallographic data for this paper. These data are provided free of charge by The Cambridge Crystallographic Data Center.

Synthesis and characterization

$Tip_2Ge{=}Ge(Tip)SiPh_3$ (10): Digermenide **8** (600 mg, 0.58 mmol) and chlorotriphenylsilane (171 mg, 0.58 mmol, 1 equiv.) were mixed as solids in a Schlenk flask and toluene (6 mL) was added by means of a syringe. The reaction mixture was stirred overnight at room temperature, whereupon a white precipitate was formed. After removal of the solvent in vacuo, hexane (10 mL) was added, and the mixture was filtered through a cannula to remove insoluble material. Reducing the volume to approximately 1.5 mL gave a dark-red solution, from which 308 mg (52%) of digermene **10** was obtained as crystalline yellow plates (m.p. 177 °C; dec.). ^{1}H NMR (400 MHz, C_6D_6, 300 K, TMS): $\delta = 7.75$ (d, $^3J = 6.88$ Hz, 6H; *m*-Ph-*H*), 7.06 (s, 2H; Tip-*H*), 7.05 (br, 3H; *p*-Ph-*H*), 7.01 (s, 2H; Tip-*H*), 6.99 (s, 3H; *o*-Ph-*H*), 6.97 (s, 3H; *o*-Ph-*H*), 6.95 (s, 2H; Tip-*H*), 3.85 (sept, $^3J = 6.61$ Hz, 2H; *i*Pr-C*H*), 3.80–3.69 (m, 4H; *i*Pr-C*H*), 2.73 (sept, $^3J = 6.90$ Hz, 3H; *i*Pr-C*H*), 1.26 (br d, 6H; *i*Pr-CH_3), 1.20, 1.17, 1.14 (each d, $^3J = 6.94$ Hz, 6H each; *i*Pr-CH_3), 1.10–0.84 (d & v br, $^3J = 6.54$ Hz, altogether 24H; *i*Pr-CH_3), 0.74 ppm (br d, 6H; *i*Pr-CH_3); ^{13}C NMR (100.61 MHz, C_6D_6, 300 K, TMS): $\delta = 153.2$, 152.9, 151.9, 149.8, 149.4, 149.2, 146.4, 143.9, 139.7 (each s; Tip-*C*), 136.9, 136.0, 129.1, 127.5 (each s; Ph-*C*), 122.3, 122.0, 121.4 (each s; Tip-*C*), 38.3, 37.1, 37.0, 34.3, 34.2, 34.1 (each s; *i*Pr-CH), 24.8, 24.4, 24.1, 23.9, 23.9, 23.7 ppm (each s, *i*Pr-CH_3); ^{29}Si{^{1}H} NMR (79.5 MHz, C_6D_6, 300 K, TMS): $\delta = 1.9$ ppm; UV/Vis (hexane): $\lambda_{max} = 425$ nm ($\varepsilon = 20843$ L mol^{-1} cm^{-1}); elemental analysis calcd (%) for $C_{63}H_{84}Ge_2Si$ (1014.71): C 74.57, H 8.34; found: C 73.26, H 8.02.

$Tip_2Ge{=}Ge(Tip)SiMe_2Cl$ (11a): Digermenide **8** (212 mg, 0.2 mmol) was dissolved in toluene (8 mL) and the solution was cooled to −60 °C. Dropwise addition to a solution of dichlorodimethylsilane (53 mg, 50 μL, 0.41 mmol, 2 equiv.) in toluene (2 mL) at −60 °C led to an immediate color change to bright-orange. The reaction mixture was stirred overnight and allowed to reach room temperature. After removal of the solvent and volatiles in vacuo, hexane (6 mL) was added and the mixture was filtered. Although formation of **11a** and the purity of the orange-red filtrate were confirmed by NMR spectroscopy, no crystals could be obtained under any conditions. ^{1}H NMR (400.13 MHz, C_6D_6, 300 K, TMS): $\delta = 7.12$, 7.09, 7.02 (each s, 2H each, altogether 6H; Tip-*H*), 3.89, 3.75, 3.59 (each sept, $^3J = 6.75$ Hz, 2H each, altogether 6H; Tip-Pr-C*H*), 2.85–2.63 (m, 3H; Tip-Pr-C*H*), 1.33 (d, $^3J = 6.47$ Hz, 12H; Tip-Pr-CH_3), 1.27 (br d, $^3J = 6.07$ Hz, 9H; Tip-Pr-CH_3), 1.21, 1.18 (each d, $^3J = 6.85$ Hz, 9H each;

ChemPubSoc Europe

CHEMISTRY A European Journal Full Paper

Tip-Pr-CH_3), 1.11 (d, ^3J=6.85 Hz, 6H; Tip-Pr-CH_3), 0.99 (d, ^3J=6.85 Hz, 9H; Tip-Pr-CH_3), 0.58 ppm (s, 6H; Si-CH_3); ^{13}C NMR (100.61 MHz, C_6D_6, 300 K, TMS): δ=153.1, 153.4, 152.5, 150.9, 150.1, 149.8, 145.8, 143.7, 139.3, 122.6, 122.4, 122.0 (Tip-Ar-*C*), 38.7, 37.6, 37.5, 34.8, 34.7, 34.4 (Tip-Pr-*C*H), 25.3, 25.0, 24.6, 24.3, 24.2, 24.0 (Tip-Pr-CH_3), 7.4 ppm (Si-CH_3); ^{29}Si{^{1}H} NMR (79.5 MHz, 300 K, C_6D_6, TMS): δ=31.5 ppm; UV/Vis (hexane): λ_{max}=435 nm (ε=11 080 L mol^{-1} cm^{-1}); elemental analysis calcd (%) for $C_{47}H_{75}ClGe_2Si$ (848.91): C 66.50, H 8.91; found: C 65.60, H 8.55.

Tip$_2$Ge=Ge(Tip)SiMePhCl (11 b): Digermenide **8** (265 mg, 0.26 mmol) was dissolved in toluene (8 mL) and the solution was cooled to −60 °C. Dropwise addition to a solution of dichloromethylphenylsilane (59 mg, 50 μL, 0.31 mmol, 1.2 equiv.) in toluene (2 mL) at −60 °C led to an immediate color change to bright-orange. The reaction mixture was allowed to reach room temperature, whereupon it turned yellow-green due to the formation of a small amount of tetragermabutadiene (not detectable in the ^{1}H NMR spectrum). After removal of the solvent and volatiles in vacuo at 60 °C, hexane (8 mL) was added and the mixture was filtered. Although formation of **11 b** and the purity of the product solution were confirmed by NMR spectroscopy, no crystals could be obtained under any conditions. ^{1}H NMR (400.13 MHz, C_6D_6, 300 K, TMS): δ=7.74 (d, *J*=6.58 Hz, 2H; Si-Ph-*H*), 7.12 (s, 2H; Tip-*H*), 7.03 (s, 2H; Tip-*H*), 7.03 (s, 2H; Tip-*H*), 7.00–6.90 (m, 3H, overlapping with MePhSiCl_2; Si-Ph-*H*), 3.92 (sept, ^3J=7.05 Hz, 2H; Tip-*i*Pr-C*H*), 3.76 (sept, ^3J=7.05 Hz, 2H; Tip-*i*Pr-C*H*), 3.62 (sept, ^3J=6.35 Hz, 2H; Tip-*i*Pr-C*H*), 2.79–2.63 (m, 3H; Tip-*i*Pr-C*H*), 1.28 (d, ^3J=6.30 Hz, 12H; Tip-*i*Pr-CH_3), 1.20, 1.17 (each d, ^3J=7.16 Hz, altogether 18H; Tip-*i*Pr-CH_3), 1.11 (d, ^3J=6.77 Hz, 12H; Tip-*i*Pr-CH_3), 1.04 (d, ^3J=6.77 Hz, 6H; Tip-*i*Pr-CH_3), 0.96 (d, ^3J=6.37 Hz, 6H; Tip-*i*Pr-CH_3), 0.81 ppm (s, 3H, Si-CH_3); ^{13}C NMR (100.61 MHz, C_6D_6, 300 K, TMS): δ=154.2, 154.2, 152.5, 150.9, 150.2, 149.9, 146.0, 144.0, 138.0 (Tip-Ar-*C*), 134.7 (Si-Ph-*C*), 133.7 (Cl_2MeSiPh-*C*), 133.5 (Si-Ph-*C*), 133.4, 131.7 (Cl_2MeSiPh-*C*), 131.2, 130.2 (Si-Ph-*C*), 128.6 (Cl_2MeSiPh-*C*), 122.7, 122.4, 122.1 (Tip-Ar-*C*), 37.7, 37.6, 34.7, 34.7, 34.4 (Tip-*i*Pr-*C*H), 24.9, 24.6, 24.6, 24.2, 24.2, 24.0, 24.0 (Tip-*i*Pr-CH_3), 6.8 (Si-CH_3), 5.1 ppm (Cl_2PhSi-CH_3); ^{29}Si{^{1}H} NMR (79.5 MHz, 300 K, C_6D_6, TMS): δ=23.7 ppm.

Tip$_2$Ge=Ge(Tip)SiPh$_2$Cl (11 c): Digermenide **8** (246 mg, 0.24 mmol) was dissolved in toluene (5 mL) and the solution was cooled to −70 °C. Dropwise addition to a solution of dichlorodiphenylsilane (60.4 mg, 50 μL, 0.24 mmol, 1 equiv.) in toluene (2 mL) at −70 °C led to an immediate color change to dark-red-orange. The reaction mixture was allowed to reach room temperature, whereupon it turned deep-green due to the formation of tetragermabutadiene (ca. 2%, as determined by ^{1}H NMR spectroscopy). After removal of the solvent and volatiles in vacuo, hexane (8 mL) was added, the mixture was filtered, and the filtrate was concentrated to a volume of 1 mL. At −26 °C, traces of tetragermabutadiene crystallized, which could be filtered off from the orange mother liquor. Although the formation of **11 c** was confirmed by NMR spectroscopy, no crystals could be obtained under any conditions due to the presence of side products. ^{1}H NMR (400.13 MHz, C_6D_6, 300 K, TMS): *Due to strong overlap with the signals of Tip$_4$-digermene, tetragermabutadiene, toluene, and remaining Ph$_2$SiCl$_2$, detailed assignment and integration of the signals was only possible to a limited extent.* δ=7.65 (dd, ^3J=7.91 Hz, ^4J=1.53 Hz, 4H; Ph-*H*), 7.07–6.97 (m, 8H; Tip-*H* & Ph-*H*, masked by signals of side products), 6.90 (t, ^3J=7.51 Hz, 4H; Ph-*H*), 3.87–3.73 (m, 4H; Tip-*i*Pr-C*H*), 3.59 (sept, ^3J=6.44 Hz, 2H; Tip-*i*Pr-C*H*), 2.77–2.65 (m, 3H; Tip-*i*Pr-C*H*, overlapping with signals of side products), 1.21–1.17 (m, 18H; Tip-*i*Pr-CH_3, overlapping with signals of side products), 1.13–1.08 (m, 24H; Tip-*i*Pr-CH_3, overlapping with signals of side products), 0.99 ppm (d, ^3J=6.54 Hz, 12H; Tip-*i*Pr-CH_3); ^{13}C NMR (100.61 MHz, C_6D_6, 300 K, TMS): δ=154.0, 153.3, 152.2, 150.7, 150.1, 149.8, 146.4, 144.2, 138.7 (Tip-Ar-*C*), 137.8 (Tol-Ar-*C*), 136.5, 135.9, 134.5, 134.4, 132.2, 131.8, 130.3 (Ph-Ar-*C*), 129.2, 128.5 (Tol-Ar-*C*), 128.5 (Ph-Ar-*C*), 125.6 (Tol-Ar-*C*), 122.7, 122.3, 121.8 (Tip-Ar-*C*), 38.8, 38.0, 37.3, 34.6, 34.5, 34.3 (Tip-*i*Pr-*C*H), 24.9, 24.5, 24.2, 24.1, 24.0, 23.9 (Tip-*i*Pr-CH_3), 7.4 ppm (toluene-CH_3); ^{29}Si{^{1}H} NMR (79.5 MHz, 300 K, C_6D_6, TMS): δ=15.2 ppm.

Tip$_2$Ge=Ge(Tip)-CO-*t*Bu (13 a): Pivaloyl chloride (4.0 μL, 0.032 mmol, 1 equiv.) was added at room temperature to a solution of digermenide **8** (30 mg, 0.032 mmol) in C_6D_6 (0.5 mL). The solution instantly turned dark-red and ^{1}H NMR confirmed the selective formation of acyldigermene **13 a**. In an attempted crystallization, digermenide **8** (402 mg, 0.389 mmol) was suspended in pentane (8 mL) and pivaloyl chloride (48 μL, 0.389 mmol, 1 equiv.) was added, which again afforded a dark-red solution. Insoluble material was filtered off after stirring for 15 min at room temperature, and the filtrate was concentrated. Crystals of **13 a** could not be obtained. ^{1}H NMR (300 MHz, C_6D_6, 300 K, TMS): δ=7.10 (s, 2H; Tip-*H*), 7.07 (s, 4H; Tip-*H*), 3.97 (sept, ^3J=6.74 Hz, 2H; Tip-*i*Pr-C*H*), 3.70 (sept, ^3J=6.78 Hz, 4H; Tip-*i*Pr-C*H*), 3.33, 3.13 (each s, altogether 20H; dme), 2.77–2.68 (m, 3H; Tip-*i*Pr-C*H*), 1.24–1.15 ppm (m, 63H; Tip-*i*Pr-CH_3, *t*Bu-CH_3); ^{13}C NMR (75 MHz, C_6D_6, 300 K, TMS): δ=154.3, 153.4, 150.4, 150.3, 142.4, 141.6, 122.5, 122.0 (Tip-Ar-*C*), 72.2 (dme), 58.7 (dme), 38.4, 36.2, 34.7, 34.6 (Tip-*i*Pr-*C*H), 28.0, 25.2, 25.0 (Tip-*i*Pr-CH_3), 24.5 (*t*Bu-*C*), 24.2 (Tip-*i*Pr-CH_3), 24.1 ppm (*t*Bu-CH_3); UV/Vis (hexane): λ_{max}=472 (4770), 383 nm (2750 L mol^{-1} cm^{-1}); IR (powder): ν(CO)=1652 cm^{-1}; elemental analysis calcd (%) for $C_{50}H_{78}Ge_2O$ (840.43): C 71.46, H 9.36; found: C 70.61, H 9.03.

Tip$_2$Ge=Ge(Tip)-CO-*t*Pent (13 b): 2,2-Dimethylbutyryl chloride (4.0 μL, 0.029 mmol) was added at room temperature to a solution of digermenide **8** (30 mg, 0.029 mmol) in C_6D_6 (0.5 mL). The solution instantly turned dark-red and ^{1}H NMR confirmed the selective formation of acyldigermene **13 b**. In an attempted crystallization, digermenide **8** (383 mg, 0.406 mmol) was suspended in pentane (6.5 mL) and 2,2-dimethylbutyryl chloride (56 μL, 0.406 mmol, 1 equiv.) was added, which again afforded a dark-red solution. After stirring for 15 min at room temperature, insoluble material was filtered off, and the filtrate was concentrated. A second crystallization attempt was made from hexane instead of pentane, but in neither case were crystals of **13 b** obtained. ^{1}H NMR (300 MHz, C_6D_6, 300 K, TMS): δ=7.13 (s, 2H; Tip-*H*), 7.09 (s, 4H; Tip-*H*), 4.03 (sept, ^3J=7.30 Hz, 2H; Tip-*i*Pr-C*H*), 3.75 (sept, ^3J=7.30 Hz, 4H; Tip-*i*Pr-C*H*), 3.34, 3.13 (each s, altogether 30H; dme), 2.75–2.73 (m, 3H; Tip-*i*Pr-C*H*), 1.65 (quart, ^3J=7.63 Hz, 2H; *t*pentyl-CH_2), 1.24, 1.23 (each d, ^3J=6.80 Hz, altogether 36H; Tip-*i*Pr-CH_3), 1.18–1.15 (m, 24H; Tip-*i*Pr-CH_3, *t*pentyl-CH_3), 0.79 ppm (t, ^3J=7.30 Hz, 3H; *t*pentyl-CH_2-CH_3); ^{13}C NMR (75 MHz, C_6D_6, 300 K, TMS): δ=154.4, 153.5, 150.4, 150.3, 142.6, 122.5, 121.9 (Tip-Ar-*C*), 72.3 (dme), 58.7 (dme), 38.4, 35.8, 34.7, 34.6 (Tip-*i*Pr-CH), 25.3, 25.0 (Tip-*i*Pr-CH_3), 24.9 ($C_{quart.}$), 24.1, 24.1 (*i*Pr-CH_3, *t*pentyl-CH_3), 8.9 ppm (*t*pentyl-CH_3); UV/Vis (hexane): λ_{max}=474 (4820), 382 nm (2780 L mol^{-1} cm^{-1}); IR (powder): ν(CO)=1653 cm^{-1}; elemental analysis calcd (%) for $C_{51}H_{80}Ge_2O$ (854.46): C 71.69, H 9.44; found: C 70.94, H 9.08.

Tip$_2$Ge=Ge(Tip)-CO-1-Ad (13 c): 1-Adamantoyl chloride (6.4 mg, 0.032 mmol, 1.0 equiv.) in C_6D_6 (0.25 mL) was added at room temperature to a solution of digermenide **8** (30 mg, 0.032 mmol) in C_6D_6 (0.25 mL). The solution instantly turned dark-red and ^{1}H NMR confirmed the selective formation of acyldigermene **13 c**. In an attempted crystallization, pentane (5 mL) was added to a mixture of digermenide **8** (300 mg, 0.318 mmol) and 1-adamantoyl chloride (63 mg, 0.318 mmol, 1.0 equiv.), which again afforded a dark-red solution. After stirring for 15 min at room temperature, insoluble material was filtered off, and the filtrate was concentrated. A

second crystallization attempt was made using hexane instead of pentane, but in neither case were crystals of **13c** obtained. ^{1}H NMR (300 MHz, C_6D_6, 300 K, TMS): $\delta = 7.13$ (s, 2H; Tip-*H*), 7.09 (s, 4H; Tip-*H*), 4.04 (sept, $^3J = 7.11$ Hz, 2H; Tip-*i*Pr-C*H*), 3.76 (br sept, $^3J = 6.56$ Hz, 4H; Tip-*i*Pr-C*H*), 3.34, 3.13 (each s, altogether 20H; dme), 2.74 (sept, $^3J = 6.85$ Hz, 3H; Tip-*i*Pr-C*H*), 2.01 (s, 6H; Ad-α-CH_2), 1.79 (s, 3H; Ad-β-C*H*), 1.50 (s, 6H; Ad-γ-CH_2), 1.28–1.23 (m, 36H; Tip-*i*Pr-CH_3), 1.18–1.15 ppm (m, 18H; Tip-*i*Pr-CH_3); ^{13}C NMR (100.61 MHz, C_6D_6, 300 K, TMS): $\delta = 232.4$ (C=O), 154.4, 153.4, 150.4, 150.2, 142.5, 141.4 (Tip-Ar-*C*), 127.9 (Tip-Ar-*C*, masked by solvent), 122.5, 121.9 (Tip-Ar-*C*), 72.3, 58.7 (dme), 51.5 (br; Ad-C_{quart}), 40.5 (br; Ad-α-CH_2), 38.5, 37.0 (Tip-*i*Pr-CH), 36.0 (br; Ad-γ-CH_2), 34.6 (Tip-*i*Pr-CH), 28.7 (Ad-β-C*H*), 25.3, 25.1, 24.1 ppm (Tip-*i*Pr-CH_3); UV/Vis (hexane): $\lambda_{max} = 476$ (4140), 385 nm (2240 L mol^{-1} cm^{-1}); IR (powder): ν(CO) = 1649 cm^{-1}; elemental analysis calcd (%) for $C_{55}H_{82}Ge_2O$ (918.55): C 73.23, H 9.22; found: C 72.22, H 9.15.

Tip$_2$(OMe)Ge–GeH(Tip)-CO-1-Ad (15): 1-Adamantoyl chloride (50.7 mg, 0.26 mmol, 1.0 equiv.) and digermenide **8** (240 mg, 0.26 mmol) were combined in a flask and toluene (5 mL) was added. The reaction mixture immediately turned dark-orange and was then cooled to −60 °C. Neat MeOH (12 μL, 9.8 mg, 0.31 mmol, 1.2 equiv.) was added to the cold reaction mixture and the cooling bath was removed. After reaching room temperature, all volatiles were removed from the green solution in vacuo and the remaining solid was redissolved in hexane (10 mL). The solution was filtered through a cannula. The green filtrate was concentrated to about 1 mL and stored at room temperature overnight, whereupon digermane **15** crystallized as 146 mg (60%) of pale-yellow needles. ^{1}H NMR (400.13 MHz, C_6D_6, 300 K, TMS): *The crystalline sample of* **15** *contained approximately 10% of the regioisomer* Tip$_2$HGe–Ge(OMe)(Tip)-CO-1-Ad **15′**, *which could not be removed by purification methods due to the chemical similarity between* **15** *and* **15′**. *Hence, integrals are overestimated in the spectrum.* $\delta = 7.22$ (d, 1H; Tip-*H*), 7.16 (br, masked by signal of C_6D_5H, 1H; Tip-*H*), 7.08 (d, 1H; Tip-*H*), 7.02 (d, 1H; Tip-*H*), 6.98 (d, 1H; Tip-*H*), 6.89 (d, 1H; Tip-*H*), 6.46 (s, 1H; Ge-*H*), 3.90 (s, 3H; OCH_3), 3.80 (sept, 1H; Tip-*i*Pr-C*H*), 3.61 (sept, 1H; Tip-*i*Pr-C*H*), 3.50 (sept, 1H; Tip-*i*Pr-C*H*), 3.38 (sept, 1H; Tip-*i*Pr-C*H*), 3.24 (sept, 1H; Tip-*i*Pr-C*H*), 2.94 (sept, 1H; Tip-*i*Pr-C*H*), 2.83–2.64 (m, 3H; Tip-*i*Pr-C*H*), 2.08 (br d, 3H; Ad-α-CH_2), 1.90 (br d, 3H; Ad-α-CH_2), 1.76 (br, 3H; Ad-β-C*H*), 1.63 (d, 3H; Tip-*i*Pr-CH_3), 1.55, 1.53 (each d, altogether 6H; Tip-*i*Pr-CH_3), 1.43 (br, 6H; Ad-γ-CH_2), 1.41 (d, 3H; Tip-*i*Pr-CH_3), 1.35 (d, 6H; Tip-*i*Pr-CH_3), 1.31 (d, 3H; Tip-*i*Pr-CH_3), 1.22 (d, 3H; Tip-*i*Pr-CH_3), 1.20 (d, 3H; Tip-*i*Pr-CH_3), 1.18–1.12 (m, 15H; Tip-*i*Pr-CH_3), 0.47 (d, 6H; Tip-*i*Pr-CH_3), 0.39 (d, 3H; Tip-*i*Pr-CH_3), 0.33 ppm (d, 3H; Tip-*i*Pr-CH_3); ^{13}C NMR (100.61 MHz, C_6D_6, 300 K, TMS): $\delta = 238.6$ (C=O), 155.8, 155.3, 155.1, 153.6, 153.5, 152.1, 150.7, 150.4, 150.0, 137.2, 136.8, 132.5, 123.3, 123.1, 122.8, 122.6, 122.2, 121.9 (Tip-Ar-*C*), 55.4 (Ad-C_{quat}), 53.9 (OCH_3), 38.4, 36.8, 36.3, 35.6, 35.5, 34.6, 33.1, 32.4 (Tip-*i*Pr-CH, Ad-CH, and Ad-CH_2), 28.3, 27.5, 26.9, 25.7, 25.1, 24.9, 24.9, 24.6, 24.3, 24.2, 24.2, 24.1, 24.0, 24.0, 23.9, 23.4, 23.1, 22.9 ppm (Ad-CH_2 and Tip-*i*Pr-CH_3); IR (powder): $\nu = 1647$ (CO), 2037 cm^{-1} (Ge–H); m.p. > 220 °C; elemental analysis calcd (%) for $C_{57}H_{88}Ge_2O_2$ (950.59): C 72.02, H 9.33; found: C 72.17, H 8.99.

Acknowledgements

Support of this study by the Deutsche Forschungsgemeinschaft (DFG SCHE906/5-1) is gratefully acknowledged.

Conflict of interest

The authors declare no conflict of interest.

Keywords: cycloaddition · digermenes · double bonds · germanium · isomerization

[1] D. E. Goldberg, D. H. Harris, M. F. Lappert, K. M. Thomas, *J. Chem. Soc. Chem. Commun.* **1976**, *227*, 261.
[2] a) R. West, M. J. Fink, *Science* **1981**, *214*, 1343–1344; b) P. B. Hitchcock, M. F. Lappert, S. J. Miles, A. J. Thorne, *J. Chem. Soc. Chem. Commun.* **1984**, 480–482; c) M. Stender, A. D. Phillips, R. J. Wright, P. P. Power, *Angew. Chem. Int. Ed.* **2002**, *41*, 1785–1787; *Angew. Chem.* **2002**, *114*, 1863–1865; d) A. Sekiguchi, R. Kingo, M. Ichinohe, *Science* **2004**, *305*, 1755–1757.
[3] a) N. Wiberg, W. Niedermayer, K. Polborn, P. Mayer, *Chem. Eur. J.* **2002**, *8*, 2730–2739; b) A. D. Fanta, D. J. DeYoung, J. Belzner, R. West, *Organometallics* **1991**, *10*, 3466–3470; c) A. D. Fanta, J. Belzner, D. R. Powell, R. West, *Organometallics* **1993**, *12*, 2177–2181; d) M. J. Fink, D. J. DeYoung, R. West, J. Michl, *J. Am. Chem. Soc.* **1983**, *105*, 1070–1071; e) S. A. Batcheller, S. Masamune, *Tetrahedron Lett.* **1988**, *29*, 3383–3384.
[4] a) M. Weidenbruch, E. Kroke, H. Marsmann, S. Pohl, W. Saak, *J. Chem. Soc. Chem. Commun.* **1994**, 1233–1234; b) C. E. Dixon, H. W. Liu, C. M. Vander Kant, K. M. Baines, *Organometallics* **1996**, *15*, 5701–5705; c) C. E. Dixon, J. A. Cooke, K. M. Baines, *Organometallics* **1997**, *16*, 5437–5440; d) T. Sasamori, T. Sugahara, T. Agou, K. Sugamata, J. D. Guo, S. Nagase, N. Tokitoh, *Chem. Sci.* **2015**, *6*, 5526–5530.
[5] a) D. J. De Young, R. West, *Chem. Lett.* **1986**, *15*, 883–884; b) N. Wiberg, W. Niedermayer, K. Polborn, *Z. Anorg. Allg. Chem.* **2002**, *628*, 1045–1052; c) S. E. Gottschling, K. K. Milnes, M. C. Jennings, K. M. Baines, *Organometallics* **2005**, *24*, 3811–3814; d) S. E. Gottschling, M. C. Jennings, K. M. Baines, *Can. J. Chem.* **2005**, *83*, 1568–1576; e) K. K. Milnes, M. C. Jennings, K. M. Baines, *J. Am. Chem. Soc.* **2006**, *128*, 2491–2501; f) M. Majumdar, I. Bejan, V. Huch, A. J. P. White, G. R. Whittell, A. Schäfer, I. Manners, D. Scheschkewitz, *Chem. Eur. J.* **2014**, *20*, 9225–9229; g) A. T. Henry, J. L. Bourque, I. Vacirca, D. Scheschkewitz, K. M. Baines, *Organometallics* **2019**, *38*, 1622–1626; h) M. Weidenbruch, A. Hagedorn, K. Peters, *Angew. Chem. Int. Ed. Engl.* **1995**, *34*, 1085–1086; *Angew. Chem.* **1995**, *107*, 1187–1188; i) K. L. Hurni, K. M. Baines, *Chem. Commun.* **2011**, *47*, 8382–8384; j) K. K. Milnes, L. C. Pavelka, K. M. Baines, *Chem. Soc. Rev.* **2016**, *45*, 1019–1035.
[6] a) D. Scheschkewitz, *Angew. Chem. Int. Ed.* **2004**, *43*, 2965–2967; *Angew. Chem.* **2004**, *116*, 3025–3028; b) M. Ichinohe, K. Sanuki, S. Inoue, A. Sekiguchi, *Organometallics* **2004**, *23*, 3088–3090.
[7] a) D. Scheschkewitz, *Chem. Eur. J.* **2009**, *15*, 2476–2485; b) D. Scheschkewitz, *Chem. Lett.* **2011**, *40*, 2–11; c) C. Präsang, D. Scheschkewitz, *Chem. Soc. Rev.* **2016**, *45*, 900–921; d) A. Rammo, D. Scheschkewitz, *Chem. Eur. J.* **2018**, *24*, 6866–6885.
[8] I. Bejan, D. Güclü, S. Inoue, M. Ichinohe, A. Sekiguchi, D. Scheschkewitz, *Angew. Chem. Int. Ed.* **2007**, *46*, 3349–3352; *Angew. Chem.* **2007**, *119*, 3413–3416.
[9] I. Bejan, S. Inoue, M. Ichinohe, A. Sekiguchi, D. Scheschkewitz, *Chem. Eur. J.* **2008**, *14*, 7119–7122.
[10] a) I. Fernández, G. Frenking, *Chem. Eur. J.* **2006**, *12*, 3617–3629; b) H.-W. Xi, M. Karni, Y. Apeloig, *J. Phys. Chem. A* **2008**, *112*, 13066–13079.
[11] H. Zhao, L. Klemmer, M. J. Cowley, M. Majumdar, V. Huch, M. Zimmer, D. Scheschkewitz, *Chem. Commun.* **2018**, *54*, 8399–8402.
[12] K. Abersfelder, D. Scheschkewitz, *J. Am. Chem. Soc.* **2008**, *130*, 4114–4121.
[13] D. Nieder, L. Klemmer, Y. Kaiser, V. Huch, D. Scheschkewitz, *Organometallics* **2018**, *37*, 632–635.
[14] a) K. M. Baines, J. A. Cooke, *Organometallics* **1991**, *10*, 3419–3421; b) G. M. Kollegger, W. G. Stibbs, J. J. Vittal, K. M. Baines, *Main Group Met. Chem.* **1996**, *17*, 317–330; c) V. Ya. Lee, H. Yasuda, M. Ichinohe, A. Sekiguchi, *Angew. Chem. Int. Ed.* **2005**, *44*, 6378–6381; *Angew. Chem.* **2005**, *117*, 6536–6539; d) V. Ya. Lee, H. Yasuda, M. Ichinohe, A. Sekiguchi, *J. Organomet. Chem.* **2007**, *692*, 10–19.

ChemPubSoc Europe

CHEMISTRY
A European Journal
Full Paper

[15] H. Schäfer, W. Saak, M. Weidenbruch, *Organometallics* **1999**, *18*, 3159 – 3163.
[16] R. C. Fischer, P. P. Power, *Chem. Rev.* **2010**, *110*, 3877 – 3923.
[17] M. Kira, T. Iwamoto, T. Maruyama, C. Kabuto, H. Sakurai, *Organometallics* **1996**, *15*, 3767 – 3769.
[18] H. Schäfer, W. Saak, M. Weidenbruch, *Angew. Chem. Int. Ed.* **2000**, *39*, 3703 – 3705; *Angew. Chem.* **2000**, *112*, 3847 – 3849.
[19] a) K. Yates, F. Agolini, *Can. J. Chem.* **1966**, *44*, 2229 – 2231; b) A. G. Brook, J. M. Duff, P. F. Jones, N. R. Davis, *J. Am. Chem. Soc.* **1967**, *89*, 431 – 434; c) A. Castel, P. Rivière, J. Satagé, D. Desor, M. Ahbala, C. Abdenadher, *Inorg. Chim. Acta* **1993**, *212*, 51 – 55; d) D. A. Bravo-Zhivotovskii, S. D. Pigarev, I. D. Kalikhman, O. A. Vyazankina, N. S. Vyazankin, *J. Organomet. Chem.* **1983**, *248*, 51 – 60; e) G. J. D. Peddle, *J. Organomet. Chem.* **1966**, *5*, 486 – 488; f) A. G. Brook, J. B. Pierce, *Can. J. Chem.* **1964**, *42*, 298 – 304.
[20] B. G. Ramsey, A. Brook, A. R. Bassindale, H. Bock, *J. Organomet. Chem.* **1974**, *74*, C41 – 45.
[21] M. K. Orloff, N. B. Colthup, *J. Chem. Educ.* **1973**, *50*, 400 – 401.
[22] a) M. Korth, *Angew. Chem. Int. Ed.* **2017**, *56*, 5396 – 5398; *Angew. Chem.* **2017**, *129*, 5482 – 5484; b) B. G. Janesko, E. Proynov, J. Kong, G. Scalmani, M. J. Frisch, *J. Phys. Chem. Lett.* **2017**, *8*, 4314 – 4318.
[23] Y.-R. Luo, *Comprehensive Handbook of Chemical Bond Energies*, Taylor & Francis, **2007**.

Manuscript received: June 4, 2019
Revised manuscript received: July 12, 2019
Accepted manuscript online: July 15, 2019
Version of record online: August 28, 2019

Metathesis of Ge=Ge double bonds

L. Klemmer, A.-L. Thömmes, M. Zimmer, V. Huch, B. Morgenstern, D. Scheschkewitz, *Nat. Chem.* **2021**, https://doi.org/10.1038/s41557-021-00639-9.

The results described within this article are additionally concluded and put into context in the Conclusion and Outlook chapter.

Contributions of the Authors:

Lukas Klemmer: Lead: Conceptualization, Visualization, Writing – Review and Editing, Investigation, Methodology, Data Curation, Formal Analysis, Theoretical studies, Synthesis and Characterization of molecular compounds, Synthesis and characterization of polymers.

Anna-Lena Thömmes: Supporting: Synthesis and characterization of bis(digermene), Synthesis and characterization of polymers, Writing – Review and Editing.

Michael Zimmer: Lead: CP/MAS NMR.

Volker Huch: Lead: X-Ray analysis.

Bernd Morgenstern: Supporting: X-Ray analysis

David Scheschkewitz: Lead: Project administration, Supervision, Acquisition of funding and resources; Supporting: Conceptualization, Writing – Review and Editing.

nature chemistry

ARTICLES

https://doi.org/10.1038/s41557-021-00639-9

Metathesis of Ge=Ge double bonds

Lukas Klemmer, Anna-Lena Thömmes, Michael Zimmer, Volker Huch, Bernd Morgenstern and David Scheschkewitz ✉

The metathesis of carbon–carbon double bonds—the 'reshuffling' of their constituting carbene fragments—is a tremendously important preparative tool in industry and academia. Metathesis of heavier alkene homologues is restricted to occasional unproductive examples in phosphorus chemistry and cross-metathesis to mixed heavier alkynes. We now report the thermally induced, transition-metal-free metathesis of purpose-built unsymmetrically substituted digermenes. The $A_2Ge{=}GeAB$ starting materials are thus converted to symmetrically substituted derivatives of the $A_2Ge{=}GeA_2$ and $ABGe{=}GeAB$ types. The use of tethered auxiliary donors (dimethylaniline groups) in substituents B ensures intramolecular donor–acceptor stabilization of the transient germylene fragments, the intermediacy of which is proven by trapping experiments. Density functional theory calculations shed light on the thermodynamic driving force of the metathesis and validate the crucial role of the tethered donor. With an analogously equipped bridged tetragermadiene precursor ($A_2Ge{=}GeB\text{-}X\text{-}BGe{=}GeA_2$), heavier acyclic diene metathesis polymerization occurs, in analogy to the widespread acyclic diene metathesis (ADMET) polymerization in the carbon case, yielding a polydigermene.

Since its discovery in the 1960s[1], olefin metathesis has developed into one of the most prominent reactions in organic synthesis[2,3] and is widely used in industry[4]. An early example is the equilibrium conversion of propylene to ethylene and 2-butene on a heterogeneous molybdena-alumina catalyst (160 °C and 30 bar), reported as 'olefin disproportionation'[5]. Homogeneous transition-metal catalysts operate under milder conditions, in particular ambient pressure, and convert terminal alkenes selectively and completely if the ethylene by-product is removed[6,7]. In this manner, α,ω-dienes are routinely polymerized by acyclic diene metathesis (ADMET)[8].

The considerably weaker double bonds between heavier group 14 elements[9] suggest a more facile interchange of the constituting fragments, possibly even in the absence of catalysts. Nonetheless, virtually all results supporting the principal feasibility of heavier main group metathesis concern phosphorus species: Mes*P=PMes^F equilibrates with Mes*P=PMes* and Mes^{F}P=PMes^F in the presence of a tungsten catalyst (Mes*, 2,4,6-tri-*tert*-butylphenyl; Mes^F, 2,4,6-tris(trifluoromethyl)phenyl)[10]. Similarly, the photolysis of the heteroleptic diphosphene MesP=PMes* (Mes, 2,4,6-trimethylphenyl) results in symmetric Mes*P=PMes*, with the fate of the MesP fragment being unclear[11]. Recently, the thermal scrambling of a molybdenum–molybdenum triple bond with group 14 alkyne homologues has been reported[12]. Still, despite the vast number of stable heavier alkenes[9], preparatively useful metathesis reactions remain elusive.

Regarding group 14 alkene homologues, digermenes may be particularly suitable for heavier alkene metathesis as they readily cleave into their germylene fragments in many cases. $R_2Ge{=}GeR_2$ (R = $CH(SiMe_3)_2$), for example, is stable as a solid but completely dissociates in solution[13]. Tbt(Mes)Ge=Ge(Mes)Tbt exists in equilibrium with the Tbt(Mes)Ge fragment (Tbt, 2,4,6-tris[bis(trimethylsilyl)methyl]phenyl)[14]. Conversely, $Mes_2Ge{=}GeMes_2$ is only cleaved by addition of a base, coordinating to the otherwise unstable Mes_2Ge fragments[15]. Notably, all cases of spontaneous or induced dissociation concern symmetrically substituted digermenes ($A_2Ge{=}GeA_2$ or $ABGe{=}GeBA$)[16], preventing productive metathesis reactions.

We now report on the design and preparation of unsymmetrically substituted Ge=Ge systems of the $A_2Ge{=}GeAB$ type with a purpose-built ligand B featuring a pending auxiliary donor ligand. We show that these systems readily undergo productive heavier alkene metathesis to produce 'reshuffled' molecular species and even polymers with Ge=Ge repeat units.

Results and discussion

Design and synthesis of suitable ligands 3a,b. We recently reported digermenide **1**[17] and its use for the synthesis of unsymmetrically substituted digermenes of the $A_2Ge{=}GeAB$ type[18]. In solution, decomposition of these digermenes to the known homoleptic digermene **2** occurs[19], presumably through initial dissociation of the Ge=Ge bond and dimerization of the A_2Ge fragment. The concomitantly formed germylenes ABGe remained undetected due to their unselective and rapid decomposition.

The pronounced formation tendency of **2** could nevertheless act as a driving force for metathesis and thus assume a similar role as the evolution of ethylene $H_2C{=}CH_2$ in carbon-based alkene metathesis. We therefore focused on increasing the lifetime of a transient germylene ABGe sufficiently for dimerization to occur by incorporation of a substituent B with a tethered donor group (Fig. 1a). The 2-*N*,*N*-dimethylanilino group (Dma) with a monoatomic linking unit should form a relatively unstrained five-membered ring with the electron-deficient germanium centre. For ease of synthesis, we selected an SiR_2 moiety (R = Me, Ph) for this purpose, because digermenide **1** usually reacts selecs[17,18]. The chlorosilanes $DmaR_2SiCl$ **3a**,**b** were thus prepared following an adapted protocol[20].

Synthesis and metathesis of asymmetric digermene 4a. Reaction of **3a** with digermenide **1** affords a product with NMR spectroscopic data strongly supporting the constitution of the targeted **4a**: the signal distributions and the multiplicities in the ^{1}H and ^{13}C NMR spectra resemble those of previously reported monosilyl-substituted digermenes[17,18]. The ^{29}Si NMR spectrum shows a single resonance (δ = 2.7 ppm) close to those of digermenes $Tip_2Ge{=}GeTipR$ (R = $SiMe_3$, 1.87 ppm; R = $SiMe_2Ph$, 0.25 ppm; R = $SiPh_3$, 1.89 ppm)[17,18].

Krupp Chair of General and Inorganic Chemistry, Saarland University, Saarbrücken, Germany. ✉e-mail: scheschkewitz@mx.uni-saarland.de

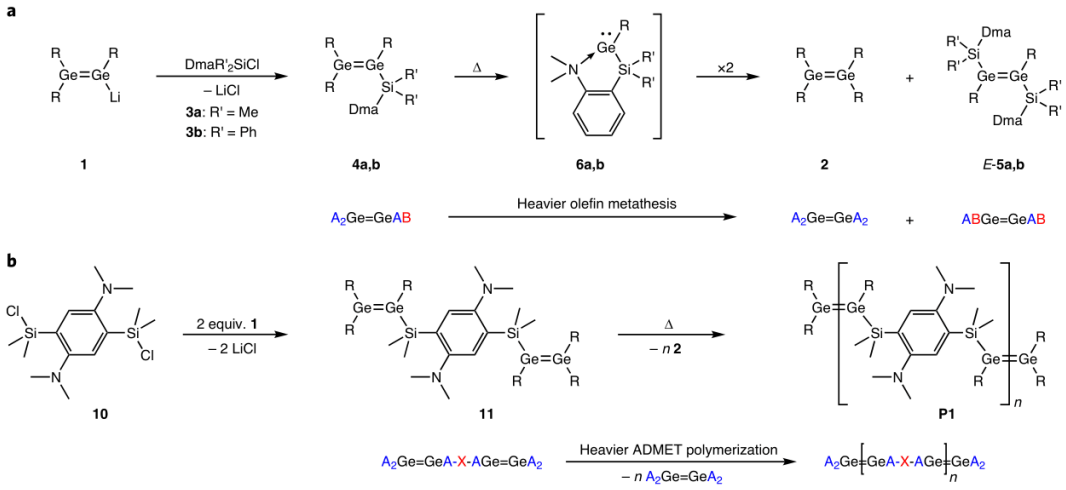

Fig. 1 | Metathesis of digermenes. a, Synthesis of digermenes **4a**,**b** and metathesis to homoleptic digermene **2** and symmetric ***E*-5a**,**b** (R = Tip = 2,4,6-$^{i}Pr_3C_6H_2$; Dma = 2-$Me_2NC_6H_4$). **b**, Synthesis of α,ω-tetragermadiene **11** and metathesis to poly(digermene) **P1** (R = Tip = 2,4,6-$^{i}Pr_3C_6H_2$). In both cases, the general reaction schemes of the heavier metathesis (**a**) and the heavier acyclic diene metathesis (ADMET) polymerization (**b**) are shown.

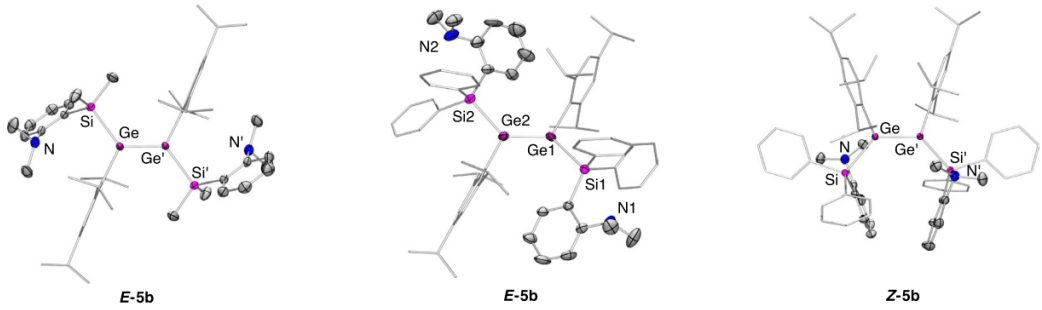

Fig. 2 | Molecular structures of *E*-5a, *E*-5b and *Z*-5b in the solid state. Germanium, purple; silicon, magenta; nitrogen, blue; carbon, grey; Tip and phenyl groups shown in stick representation, remaining atoms depicted with thermal ellipsoids. Hydrogen atoms omitted for clarity, thermal ellipsoids at 50% probability.

To prompt Ge=Ge metathesis, we heated a solution of **4a** in benzene at 65 °C for 18 h. ^{1}H NMR reaction control indeed showed uniform conversion to digermene **2**[19] and a second product, which was isolated from hexane as yellow crystals in 81% yield. Single-crystal X-ray diffraction revealed the constitution of digermene ***E*-5a** with the silyl groups in a *trans* relationship (Fig. 2).

The solid-state structure of ***E*-5a** exhibits an inversion centre between the two germanium atoms, and the Ge–Ge bond distance of 2.2576(5) Å is within the typical range for digermenes[19,21]. As in known persilyl-substituted digermenes[21], the Ge–Ge double bond of ***E*-5a** is completely untwisted, with a twist angle of $\tau = 0.0°$ (defined as the angle between the two R–Ge–R′ normals). The substituents are bent away from the Ge–Ge bond vector, as routinely observed for Ge=Ge systems (*trans*-bent angles $\theta(\mathrm{Ge}) = 21.5°$, where the *trans*-bent angle θ is defined as the angle between the R–Ge–R′ plane and the Ge–Ge bond vector)[17,19]. The Ge–N distance of 4.074(1) Å is longer than the sum of the van der Waals radii of germanium and nitrogen (3.66 Å), rendering a donor–acceptor interaction unlikely. The low number of signals in the NMR spectra of ***E*-5a** reflects its symmetric structure in solution and the ^{29}Si NMR resonance at −2.7 ppm is in the expected range for tetracoordinate silicon and similar to the signal observed for **4a**. In line with a relatively stable Ge=Ge bond, ***E*-5a** does not react with Et_3SiH up to 70 °C, which is known to readily undergo oxidative addition to germylenes but not to digermenes[14,22]. By contrast, **6a** is trapped in situ as triethylsilylgermane **7a** by reaction of **4a** with Et_3SiH at 65 °C (Fig. 3 and Supplementary Methods), an observation that supports metathesis via dissociation and association of germylenes. A singlet at 4.22 ppm in the ^{1}H NMR spectrum is in the diagnostic range for Ge–H and shows cross-peaks in the ^{29}Si/^{1}H spectrum to two resonances at 5.56 ppm and −11.90 ppm, which is in line with the expected trapping product **7a**. A second singlet at 5.57 ppm in the ^{1}H NMR is attributed to the Et_3SiH trapping product of Tip_2Ge **8**, the silylgermane **9**, as it couples to only one ^{29}Si resonance at 5.01 ppm. We note in passing that the disilene corresponding to **4a** is obtained by treatment of $Tip_2Si{=}Si(Tip)Li$[23] with **3a** (Supplementary Methods), but—in contrast to **4a**—does not engage in metathesis.

Synthesis and metathesis of digermene 4b. Increased steric demand at the silyl tether should further facilitate dissociation of the

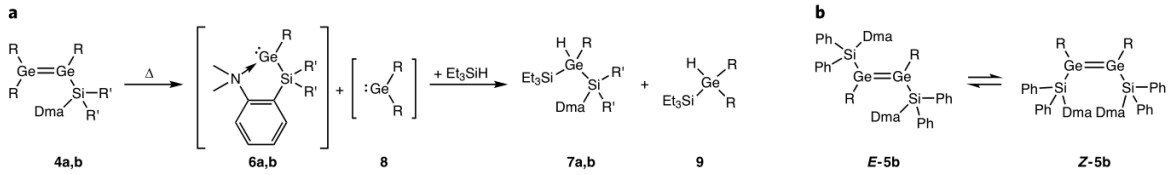

Fig. 3 | Trapping of germylenes 6a,b and equilibrium between digermenes *E*-5b and *Z*-5b in solution. a, Heating of **4a** results in fragmentation to germylenes, which react with Et_3SiH to **7a** and **9**. **b**, Room-temperature equilibrium between stereoisomeric digermenes ***E*-5b** and ***Z*-5b** (R = Tip = 2,4,6-$^iPr_3C_6H_2$; Dma = 2-$Me_2NC_6H_4$; **4a**, **6a**, **7a**: R′ = Me; **4b**, **6b**, **7b**: R′ = Ph).

Ge=Ge bond[14]. Phenyl derivative **4b** is indeed destabilized to such an extent that Ge=Ge bond cleavage starts even before complete conversion, hence preventing its isolation. Heating of the reaction mixture overnight at 65 °C, however, results in a mixture of two species in a 78:22 ratio (aside from the homoleptic **2**), as indicated by ^{29}Si NMR signals at −2.4 and −4.7 ppm. Crystallization from hexane yields orange crystals in 66% yield, which were characterized as digermene ***E*-5b** by X-ray diffraction (Fig. 2). In contrast to ***E*-5a**, the solid-state structure of ***E*-5b** does not possess an inversion centre or symmetry axis, making the two halves of the molecule inequivalent. The Ge1–Ge2 distance of 2.2604(6) Å is almost identical to that in ***E*-5a** (2.2576(5) Å), although the increased size of the silyl substituents gives rise to substantial twisting of the Ge=Ge double bond (τ = 20.1° versus τ = 0° for ***E*-5a**) at the expense of less pronounced *trans* bending (θ(Ge1) = 15.2°; θ(Ge2) = 5.9° versus θ(Ge) = 21.5° in ***E*-5a**). The Ge–N distances are, with 5.310(3) Å and 5.471(3) Å, significantly longer than in ***E*-5a**. The UV–vis longest-wavelength absorption at λ_{max} = 438 nm (ε = 11,925 l mol^{-1} cm^{-1}) confirms the existence of a Ge=Ge bond in solution[24]. The broken symmetry in the solid state is reflected in the appearance of two signals in the ^{29}Si cross-polarization magic angle spinning (CP/MAS) NMR at 2.6 ppm and −0.3 ppm, close to the solution ^{29}Si NMR signal at −2.4 ppm. ***E*-5b** is identified as the major component of the 78:22 equilibrium mixture in solution by ^{1}H NMR spectroscopy of a crystallized sample of ***E*-5b** directly after its dissolution in C_6D_6. The longer acquisition times of ^{13}C and ^{29}Si NMR result in the gradual formation of the second equilibrium component, and the 78:22 composition of the initial reaction mixture is re-established after 12 h.

Trapping of germylene 6b and isolation of *Z*-5b. We initially suspected that germylene **6b** may represent the minor component of the observed equilibrium in solution (Fig. 3). Treatment of ***E*-5b** with an excess of Et_3SiH, however, requires heating to 65 °C for conversion. Two ^{29}Si NMR signals at δ = 5.2 ppm and δ = −12.5 ppm dominating the reaction mixture obtained after 15 h are in line with the successful trapping of germylene **6b** (**6a**: 5.6 ppm and −11.9 ppm). The ^{1}H NMR singlet at δ = 4.79 ppm exhibits cross-peaks of similar intensity to both the $SiEt_3$ group and the Dma-carrying silyl group in the ^{29}Si/^{1}H spectrum, confirming the formation of bis(silyl) germane **7b**. In an attempt to obtain single crystals of **6b**, **4b** was heated to 65 °C without stirring. Surprisingly, X-ray diffraction on the resulting orange crystals revealed the formation of digermene ***Z*-5b** instead (Fig. 2). The *cis* relationship of the Tip groups of ***Z*-5b** may result from the apparent π-stacking interaction[25]. The Ge–Ge′ distance of 2.2909(6) Å in ***Z*-5b** (crystallographic C_2 symmetry) is significantly longer than that of ***E*-5b** (2.2604(6) Å) and the deviation from planarity is more pronounced with *trans* bending of θ(Ge) = 26.0° and twisting of τ = 23.9°. In addition to increased steric strain, the stronger interaction between the Dma donors and the germanium centres in ***Z*-5b** (N–Ge 3.597(1) Å) compared to ***E*-5b** (N1–Ge1 5.310(3) Å; N2–Ge2 5.4711(3) Å) contributes to the overall weaker Ge=Ge double bond. Upon dissolution of ***Z*-5b**, the 78:22 equilibrium is reinstated almost instantly and thus much faster than upon dissolution of ***E*-5b**, in line with ***Z*-5b** representing the minor, higher-energy component. The ^{29}Si CP/MAS NMR signal (δ = −9.7 ppm) of ***Z*-5b** is indeed only shifted by $\Delta\delta$ = 5 ppm from the minor signal of the equilibrium in solution.

DFT calculations. To understand the thermodynamic driving force of the metathesis and corroborate our conclusions regarding the equilibrium between ***E*-5b** and ***Z*-5b**, we optimized the involved digermenes and germylenes at the BP86(D3)/def2-SVP-level of theory. More accurate energies were calculated at the M06-2X(D3)/def2-TVPP level (see the DFT section in the Supplementary Information). The dimerization of germylene **8** to digermene **2** is strongly exergonic (ΔG_{Dim} = −28.6 kcal mol^{-1}) confirming our assumption that formation of **8** is contributing to the driving force of the reaction. The formation of ***E*-5a** and ***E*-5b** from the corresponding donor-stabilized germylenes is less exergonic in both cases (***E*-5a**, ΔG_{Dim} = −24.3 kcal mol^{-1}; ***E*-5b**, ΔG_{Dim} = −20.3 kcal mol^{-1}), presumably due to the intramolecular stabilization of the monomeric germylenes **6a**,**b**. Although the increased steric bulk in ***E*-5b** slightly lowers the free dimerization enthalpy ΔG_{Dim}, it is still far too high for the spectroscopic observation of **6b**. By contrast, the free enthalpy difference between ***Z*-5b** and ***E*-5b** is only 2.3 kcal mol^{-1} in favour of ***Z*-5b** (Supplementary Table 11) fully in line with the simultaneous observation of both compounds.

The stabilizing effect of intramolecular coordination of the amino groups to the vacant orbital at germanium was estimated by comparison of the free energies of **6a**,**b** with those of the conformers **6a**,**b**′ in which the anilino moiety is turned away from the germanium centres by 180° (**6a** versus **6a**′, ΔG_{stab} = −17.0 kcal mol^{-1}; **6b** versus **6b**′, ΔG_{stab} = −15.7 kcal mol^{-1}). Second-order perturbation analysis even gives values of −45.6 kcal mol^{-1} for ***E*-5a** and −41.7 kcal mol^{-1} for ***E*-5b**, which are substantially higher as they do not account for the entropy penalty of ring formation.

Synthesis of tetragermadiene 11 and HADMET polymerization to polygermene P1. To enlarge the scope of our heavier metathesis towards heavier ADMET (HADMET) polymerization, we synthesized bis(chlorosilyl)benzene **10** (Supplementary Methods) and treated it with 2 equiv. of **1** (Fig. 1b). The reaction resulted in the selective formation of a single product (^{29}Si NMR 4.3 ppm). X-ray diffraction on single crystals grown from a concentrated benzene solution confirmed its constitution as α,ω-tetragermadiene **11** (Fig. 4). The Ge–Ge distances of 2.3038(4) Å lie between the longer Ge–Ge bond of the unsymmetrically substituted Tip_2Ge=GeTipSiPh$_3$ (2.3279(4) Å)[18] and the significantly shorter Ge–Ge distance in symmetrically substituted ***E*-5a** (2.2576(5) Å). Both *trans* bending (θ(Ge1) = 31.9°; θ(Ge2) = 24.9°) and twisting (τ = 18.0°) in **11** are more pronounced than the corresponding values of Tip_2Ge=GeTipSiPh$_3$ (θ(GeTip$_2$) = 21.3°; θ(GeSiTip) = 23.7°; τ = 13.6)[18]. The longest-wavelength UV–vis absorption at λ_{max} = 426 nm (ε = 17,580 l mol^{-1} cm^{-1}) is only marginally redshifted compared to **4a** (λ_{max} = 421 nm).

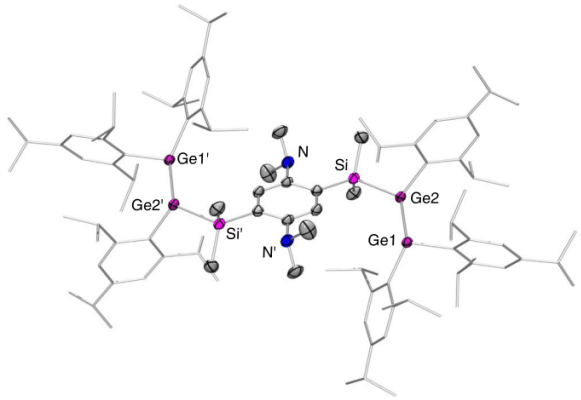

Fig. 4 | Molecular structure of 11 in the solid state. Germanium, purple; silicon, magenta; nitrogen, blue; carbon, grey; Tip groups are shown in stick representation and the remaining atoms with thermal ellipsoids. Hydrogen atoms and co-crystallized benzene are omitted for clarity; thermal ellipsoids are at 50%.

In the solid state, **11** is stable for at least 30 days at 25 °C in the absence of air and moisture. By contrast, in benzene solution at 60 °C a viscous gel is formed after 48 h, as is typically observed during polymerization processes[26]. Drying in vacuum results in an insoluble, yellow solid **P1** (Fig. 1b). The supernatant liquid shows only the ^{1}H NMR signals of the homoleptic digermene **2**, indicating a selective metathesis reaction. The ^{13}C and ^{29}Si CP-MAS NMR signals of the insoluble part are broadened but otherwise a near-perfect match with both the solution and solid-state NMR spectra of the model system ***E*-5a** (Supplementary Figs. 11–14, 52 and 53). The presence of $GeTip_2$ end groups in **P1** was deduced from the deviation of the ^{13}C CP-MAS NMR integral values of the Tip-^{i}PrCH_3 signals in comparison to the Me_2Si signals from the expected ratio of 3:1. The observed ratio of 3.275:1 indicates an average degree of polymerization of $\bar{X}_n = 21$. The quantitative nature of the ^{13}C CP-MAS NMR was confirmed by the almost perfect ratio of integrals of the corresponding signals in the solid-state spectrum of ***E*-5a** (Supplementary Fig. 13). Differential scanning calorimetry (DSC) of **P1** reveals a reversible glass transition at 72 °C, in line with its polymeric nature. Owing to the insolubility of **P1**, solution methods for the determination of the degree of polymerization could not be applied. Given the essentially side-product-free reaction, however, the released amount of digermene **2** allows for an independent approximation of the degree of polymerization (Supplementary Table 1 and Supplementary Figs. 57 and 58). The estimation of the number-average degree of polymerization to $\bar{X}_n = 23$ using Carothers' equation[27] agrees with the results from endgroup analysis and compares favourably to the few known species with repeating heavy double bonds prepared by reductive coupling or condensation techniques ($\bar{X}_n = 4$ for Si=Si[28], $\bar{X}_n = 4.5$ to 6.5 for P=P[29], $\bar{X}_n = 5$ to 21 for P=C[30]). This indirect method also provides the mass-average degree of polymerization $\bar{X}_w$ and the dispersity $Đ$ of **P1** ($\bar{X}_w = 45$, $Đ = 1.95$). Dynamic light scattering (DLS) on supernatant colloidal suspensions of **P1** after centrifugation gave hydrodynamic radii between $R_h = 12.8$ and 15.4 nm, in agreement with average degrees of polymerization $\bar{X}_n$ between 26 and 31, assuming a rod-like arrangement of the polymer chain and repeating units with length of 0.98 nm (value taken from the X-ray structure of **11**).

Conclusions

With the help of purpose-designed stabilizing ligands, a preparatively useful heavier olefin metathesis has been achieved. Simply by heating, and in the absence of catalysts, the obtained asymmetrically substituted digermenes are 'reshuffled' to the symmetrically substituted products. Trapping experiments provide solid evidence for the intermediacy of intramolecularly stabilized germylenes. A polymer with Ge–Ge double bonds in the repeating unit is obtained from the corresponding α,ω-tetragermadiene through a process that we suggest be referred to as heavier acyclic diene metathesis (HADMET) polymerization. Future work will focus on increasing the solubility to explore the full potential of this new class of materials.

Online content

Any methods, additional references, Nature Research reporting summaries, source data, extended data, supplementary information, acknowledgements, peer review information; details of author contributions and competing interests; and statements of data and code availability are available at https://doi.org/10.1038/s41557-021-00639-9.

Received: 20 May 2020; Accepted: 12 January 2021;
Published online: 01 March 2021

References

1. Truett, W. L., Johnson, D. R., Robinson, I. M. & Montague, B. A. Polynorbornene by coordination polymerization. *J. Am. Chem. Soc.* **82**, 2337–2340 (1960).
2. Grubbs, R. H. & Chang, S. Recent advances in olefin metathesis and its application in organic synthesis. *Tetrahedron* **54**, 4413–4450 (1998).
3. Grubbs, R. H. Olefin metathesis. *Tetrahedron* **60**, 7117–7140 (2004).
4. Mol, J. C. Industrial applications of olefin metathesis. *J. Mol. Catal. A Chem.* **213**, 39–45 (2004).
5. Banks, R. L. & Bailey, G. C. Olefin disproportionation. *Ind. Eng. Chem. Prod. Res. Dev.* **3**, 170–173 (1964).
6. Schrock, R. R. An 'alkylcarbene' complex of tantalum by intramolecular α-hydrogen abstraction. *J. Am. Chem. Soc.* **96**, 6796–6797 (1974).
7. Schwab, P., France, M. B., Ziller, J. W. & Grubbs, R. H. A series of well-defined metathesis catalysts—synthesis of $[RuCl_2(=CHR')(PR_3)_2]$ and its reactions. *Angew. Chem. Int. Ed.* **34**, 2039–2041 (1995).
8. Wagener, K. B., Boncella, J. M. & Nel, J. G. Acyclic diene metathesis (ADMET) polymerization. *Macromolecules* **24**, 2649–2657 (1991).
9. Fischer, R. C. & Power, P. P. π-Bonding and the lone pair effect in multiple bonds involving heavier main group elements: developments in the new millennium. *Chem. Rev.* **110**, 3877–3923 (2010).
10. Dillon, K. B., Gibson, V. C. & Sequeira, L. J. Transition-metal catalyzed metathesis of phosphorus–phosphorus double bonds. *J. Chem. Soc. Chem. Commun.* **23**, 2429–2430 (1995).
11. Yoshifuji, M., Sato, T. & Inamoto, N. Photoreaction of (*E*)-1-mesityl-2-(2,4,6-tri-*t*-butylphenyl)diphosphene. *Bull. Chem. Soc. Jpn* **62**, 2394–2395 (1989).
12. Queen, J. D., Phung, A. C., Fettinger, J. C. & Power, P. P. Metathetical exchange between metal–metal triple bonds. *J. Am. Chem. Soc.* **142**, 2233–2237 (2020).
13. Davidson, P. J., Harris, D. H. & Lappert, M. F. Subvalent group 4B metal alkyls and amides. Part I. The synthesis and physical properties of kinetically stable bis[bis(trimethysilyl)methyl]-germanium(II), -tin(II) and -lead(II). *J. Chem. Soc. Dalton Trans.* **21**, 2268–2274 (1976).
14. Kishikawa, K., Tokitoh, N. & Okazaki, R. The first spectroscopic observation of an equilibrium between a digermene and germylenes and experimental determination of a bond dissociation energy of a Ge–Ge double bond. *Chem. Lett.* **27**, 239–240 (1998).
15. Rupar, P. A., Jennings, M. C., Ragogna, P. J. & Baines, K. M. Stabilization of a transient diorganogermylene by an N-heterocyclic carbene. *Organometallics* **26**, 4109–4111 (2007).
16. Jana, A., Huch, V., Rzepa, H. S. & Scheschkewitz, D. A multiply functionalized base-coordinated Ge^{II} compound and its reversible dimerization to the digermene. *Angew. Chem. Int. Ed.* **54**, 289–292 (2015).
17. Nieder, D., Klemmer, L., Kaiser, Y., Huch, V. & Scheschkewitz, D. Isolation and reactivity of a digerma analogue of vinyllithiums: a lithium digermenide. *Organometallics* **37**, 632–635 (2018).
18. Klemmer, L., Kaiser, Y., Huch, V., Zimmer, M. & Scheschkewitz, D. Persistent digermenes with acyl and α-chlorosilyl functionalities. *Chem. Eur. J.* **25**, 12187–12195 (2019).
19. Schäfer, H., Saak, W. & Weidenbruch, M. Azadigermiridines by addition of diazomethane or trimethylsilyldiazomethane to a digermene. *Organometallics* **18**, 3159–3163 (1999).

20. Wetzel, T. G. & Roesky, P. W. A functionalized cyclooctatetraene as ligand in organolanthanide chemistry. *Organometallics* **17**, 4009–4013 (1998).
21. Kira, M., Iwamoto, T., Maruyama, T., Kabuto, C. & Sakurai, H. Tetrakis(trialkylsilyl)-digermenes. Salient effects of trialkylsilyl substituents on planarity around the Ge=Ge bond and remarkable thermochromism. *Organometallics* **15**, 3767–3769 (1996).
22. Iwamoto, T., Okita, J., Yoshida, N. & Kira, M. Structure and reactions of an isolable Ge=Si doubly bonded compound, tetra(*t*-butyldimethylsilyl) germasilene. *Silicon* **2**, 209–216 (2010).
23. Scheschkewitz, D. A silicon analogue of vinyllithium: structural characterization of a disilenide. *Angew. Chem. Int. Ed.* **43**, 2965–2967 (2004).
24. Ando, W., Itoh, H., Tsumuraya, T. & Yoshida, H. Spectroscopic characterization of diarylgermylene complexes with heteroatom-containing substrates. *Organometallics* **7**, 1880–1882 (1988).
25. Kobayashi, M. et al. (*Z*)-1,2-di(1-pyrenyl)disilene: synthesis, structure, and intramolecular charge-transfer emission. *J. Am. Chem. Soc.* **138**, 758–761 (2016).
26. Moritz, H. U. Increase in viscosity and its influence on polymerization processes. *Chem. Eng. Technol.* **12**, 71–87 (1989).
27. Carothers, W. H. Polymers and polyfunctionality. *Trans. Faraday Soc.* **32**, 39–49 (1936).
28. Li, L. et al. Coplanar oligo(*p*-phenylenedisilenylene)s as Si=Si analogues of oligo(*p*-phenylenevinylene)s: evidence for extended π-conjugation through the carbon and silicon π-frameworks. *J. Am. Chem. Soc.* **137**, 15026–15035 (2015).
29. Smith, R. C. & Protasiewicz, J. D. Conjugated polymers featuring heavier main group element multiple bonds: a diphosphene-PPV. *J. Am. Chem. Soc.* **126**, 2268–2269 (2004).
30. Wright, V. A. & Gates, D. P. Poly(*p*-phenylenephospaalkene): a π-conjugated macromolecule containing P=C bonds in the main chain. *Angew. Chem. Int. Ed.* **41**, 2389–2392 (2002).

Methods

General. All reactions were carried out under a protective argon atmosphere and using Schlenk techniques or a glovebox. Benzene and pentane were refluxed with sodium/benzophenone and distilled before use. Hexane, toluene and tetrahydrofuran were taken directly from a solvent purification system (Innovative Technology PureSolv MD7). Deuterated benzene was refluxed over potassium and distilled before use. NMR spectra were recorded at 300 K on a Bruker Avance III HD 400 system (^{1}H, 400.13 MHz; ^{13}C{^{1}H}, 100.61 MHz; ^{29}Si{^{1}H}, 79.5 MHz). Chemical shifts are reported relative to $SiMe_4$. Solid-state CP/MAS NMR spectra were acquired on a Bruker AV400 WB spectrometer. UV–vis spectra were measured using a Shimadzu UV-2600 spectrometer in quartz cells with a path length of 1 mm. Elemental analyses were carried out on an Elementar Vario Micro Cube system. DLS measurements were carried out by non-invasive backscattering on an ALV/CGS-3 compact goniometer system with an ALV/LSE-5003 and multiple tau correlator at a wavelength of 632.8 nm (He–Ne laser) and a goniometer angle of 90°. Determination of particle size was carried out by analysis of the correlation function using the g2(t) method followed by a linearized number-weighting of the distribution function. Thermogravimetric analyses were performed on a Netzsch Iris TG 209C instrument in alumina crucibles with heating to 1,000 °C under nitrogen, with a rate of 10 K min^{-1}. DSC was performed with a Netzsch DSC 204 F1 Phoenix calorimeter with aluminium crucibles with pierced lids under nitrogen (100 ml min^{-1}), with a heating rate of 20 K min^{-1} from −120 to 260 °C and a cooling rate of 15 K min^{-1} from 260 °C to −120 °C. Lithium digermenide **1**[17] and 2-(chlorodimethylsilyl)-*N*,*N*-dimethylaniline **3a**[20] were prepared according to literature procedures. Syntheses of chlorosilanes **3b** and **11**, trapping reactions and spectroscopic data are supplied in the extended Methods section of the Supplementary Information.

2-(Dimethyl(1,2,2-tris(2,4,6-triisopropylphenyl)digermenyl)-silyl)-*N*,*N*-dimethylaniline 4a. Digermenide **1** (400 mg, 0.42 mmol) and 2-(chlorodimethylsilyl)-*N*,*N*-dimethylaniline **3a** (90.7 mg, 0.42 mmol, 1.0 equiv.) were mixed as solids in a Schlenk flask and 10 ml of toluene were added at room temperature. Stirring for 2 h was followed by removal of volatile species in vacuo and the residual solid was digested in 10 ml of hexane. Filtration via cannula yielded a yellow filtrate, which was dried in vacuo, giving 231 mg (60%) **4a** as a yellow powder.

Note that, as **4a** could not be crystallized and not be purified using other techniques, small traces digermene **2** were present, as seen from ^{1}H NMR spectroscopy and deviations in the elemental analysis.

^{1}H NMR (400.13 MHz, C_6D_6, 300 K, TMS): δ = 8.03 (dd, ^3J = 7.46 Hz, ^4J = 1.48 Hz, 1H, Me_2N-Ph-*H*), 7.15 (s, 2H, Tip-*H*), 7.07 to 7.02 (m, 1H, Me_2N-Ph-*H*), 7.04 (s, 2H, Tip-*H*), 7.01 (s, 2H, Tip-*H*), 6.99 to 6.95 (m, 1H, Me_2N-Ph-*H*), 6.56 (dt, ^3J = 7.31 Hz, ^4J = 1.05 Hz, 1H, Me_2N-Ph-*H*), 3.95 (sept., ^3J = 6.67 Hz, 1 Hz, 2H, Tip-^{i}Pr-C*H*), 3.88 (sept., ^3J = = 6.67 Hz, 2H, Tip-^{i}Pr-C*H*), 3.69 (sept., ^3J = 6.67 Hz, 2H, Tip-^{i}Pr-C*H*), 2.85 to 2.67 (m, 3H, Tip-^{i}Pr-C*H*), 2.40 (s, 6H, N-CH_3), 1.34 (d, ^3J = 6.71 Hz. 12H, Tip-^{i}Pr-CH_3), 1.23, 1.21 (each d, ^3J = 6.86 Hz, altogether 15H, Tip-^{i}Pr-CH_3), 1.15 (d, ^3J = 6.93 Hz, 6H, Tip-^{i}Pr-CH_3), 1.10 (br. d, ^3J = 5.92 Hz, 9H, Tip-^{i}Pr-CH_3), 1.01 (d, ^3J = 6.60 Hz, 12H, Tip-^{i}Pr-CH_3), 0.84 (s, 6H, Si-CH_3) ppm.

^{13}C{^{1}H} NMR (100.61 MHz, C_6D_6, 300 K, TMS): δ = 161.4 (Ph-*C*), 153.9, 153.2, 152.3, 150.0, 149.4, 149.2, 146.9, 145.4, 141.4 (Tip-*C*), 139.3, 136.5, 131.1, 125.3 (Ph-*C*), 122.5, 122.2, 121.9 (Tip-*C*), 47.1 (N-CH_3), 38.4, 37.5, 37.1, 34.8, 34.7, 34.4 (Tip-^{i}Pr-*C*H), 25.2, 24.6, 24.3, 24.3, 24.1 (Tip-^{i}Pr-CH_3), 3.9 (Si-CH_3) ppm.

^{29}Si{^{1}H} NMR (79.5 MHz, C_6D_6, 300 K, TMS): δ = 2.7 ppm.

UV–vis (hexane): λ_{max} (ε) = 421 nm (ε = 16,900 l mol^{-1} cm^{-1}), 323 nm (ε = 4,000 l mol^{-1} cm^{-1}).

Elemental analysis: Calcd. for $C_{55}H_{85}Ge_2NSi$ (933.64): C, 70.76; H, 9.18; N, 1.50. Found: C, 69.87; H, 9.26; N, 1.40.

(*E*)-2,2′-((1,2-bis(2,4,6-triisopropylphenyl)digermene-1,2-diyl)bis(dimethylsilanediyl))-bis(*N*,*N*-dimethylaniline) *E*-5a. Digermenide **1** (250 mg, 0.27 mmol) and 2-(chlorodimethylsilyl)-*N*,*N*-dimethylaniline **3a** (56.7 mg, 0.27 mmol, 1.0 equiv.) were mixed as solids in a Schlenk tube and 5 ml of toluene were added at room temperature. Stirring overnight afforded a red reaction mixture that was dried in vacuo and filtered from 5 ml of hexane. The filtrate was evaporated to dryness in vacuo and the remaining solid redissolved in 5 ml of benzene. The red solution was then heated to 65 °C for 18 h, during which time it turned pale orange. Removal of the solvent in vacuo yielded a yellow foam, which was dissolved in 5 ml of hexane. Concentration to ~1 ml and storage at −26 °C overnight yielded small yellow crystals of ***E*-5a** that were contaminated with ~15% digermene **2**. Subsequent recrystallization from 1 ml of hexane gave 41 mg (34%) ***E*-5a** as small yellow crystals (melting point of 175 °C), which were suitable for X-ray crystallography. Aminosilyldigermene **4a** (57.5 mg, 0.06 mmol) was dissolved in 2 ml of benzene and the resulting solution was heated to 65 °C for 18 h. NMR spectroscopy of the reaction indicated clean conversion to **2** and ***E*-5a**, where the latter crystallized from a concentrated hexane solution as 21 mg (81%) of yellow crystals contaminated with ~10% of **2**.

^{1}H NMR (400.13 MHz, C_6D_6, 300 K, TMS): δ = 7.60 (dd, ^3J = 7.44 Hz, ^3J = 1.51 Hz, 2H, Me_2N-Ph-*H*), 7.13 (s, 4H, Tip-*H*), 7.08 (m, 2H, Me_2N-Ph-*H*), 6.93 to 6.85 (m, 4H, Me_2N-Ph-*H*), 3.85 (sept., ^3J = 6.90 Hz, 4H, Tip-^{i}Pr-C*H*), 2.83 (sept., ^3J = 6.83 Hz, 2H, Tip-^{i}Pr-C*H*), 2.17 (s, 12H, N-CH_3), 1.48 (d, ^3J = 6.80 Hz 12H, Tip-^{i}Pr-CH_3), 1.26 (d, ^3J = 6.96 Hz, 12H, Tip-^{i}Pr-CH_3), 1.18 (d, ^3J = 6.84 Hz, 12H, Tip-^{i}Pr-CH_3), 0.61 (s, 12H, Si-CH_3) ppm.

^{13}C{^{1}H} NMR (100.61 MHz, C_6D_6, 300 K, TMS): δ = 161.1 (Ph-*C*), 153.8, 149.6, 141.3 (Tip-*C*), 136.8, 136.4, 130.5, 124.9, 121.3 (Ph-*C*), 121.2 (Tip-*C*), 46.7 (N-CH_3), 37.8, 34.8 (Tip-^{i}Pr-CH), 24.6, 24.4, 24.4 (Tip-^{i}Pr-CH_3), 2.6 (Si-CH_3) ppm.

^{29}Si{^{1}H} NMR (79.5 MHz, C_6D_6, 300 K, TMS): δ = −2.7 ppm.

^{13}C{^{1}H} CP/MAS NMR (100.61 MHz, 300 K, 13 kHz, TMS): δ = 161.8, 153.3, 150.1, 141.3, 137.2, 134.8, 130.7, 125.6, 128.7, 121.9, 119.7 (Tip-*C* & Ph-*C*), 47.3 (N-CH_3), 37.6, 36.0 (Tip-^{i}Pr-CH), 26.8, 25.3, 24.2 (together, 12H, Tip-^{i}Pr-CH_3), 5.5, −1.4 (together 4H, Si-CH_3) ppm.

^{29}Si{^{1}H} CP/MAS NMR (79.5 MHz, 300 K, 13 kHz, TMS): δ = −4.9 ppm.

UV–vis (hexane): λ_{max} (ε) = 411 nm (ε = 28,400 l mol^{-1} cm^{-1}), 322 nm (ε = 6,300 l mol^{-1} cm^{-1}), 250 nm (ε = 58,500 l mol^{-1} cm^{-1}).

Elemental analysis: Calcd. for $C_{50}H_{78}Ge_2N_2Si_2$ (908.62): C, 66.09; H, 8.65; N, 3.08. Found: C, 66.50; H, 8.85; N, 2.87.

(*E*)-2,2′-((1,2-bis(2,4,6-triisopropylphenyl)digermene-1,2-diyl)bis(diphenylsilanediyl))-bis(*N*,*N*-dimethylaniline) *E*-5b. Digermenide **1** (500 mg, 0.54 mmol) and 2-(chlorodiphenylsilyl)-*N*,*N*-dimethylaniline **3b** (154.2 mg, 0.54 mmol, 1.0 equiv.) were mixed as solids in a Schlenk tube and 5 ml of benzene was added. Stirring for six days at room temperature afforded a dark yellow reaction mixture, which was dried in vacuo and filtered from 15 ml of hexane. The filtrate was evaporated to dryness in vacuo and the remaining solid was redissolved in 5 ml of benzene. The dark yellow solution was then heated to 65 °C for 18 h, during which it turned red. Removal of the solvent in vacuo yielded an orange foam, which was digested in 3 ml of hexane. Heating of the suspension to 70 °C and immediate filtration washed out $Tip_2Ge{=}GeTip_2$ **2**, with 91 mg (33%) of ***E*-5b** remaining as an orange solid. Storage of the filtrate at room temperature gave a second crop of ***E*-5b** as 87 mg (33%, overall 66%) of small orange crystals (melting point of 186 °C), which were suitable for X-ray crystallography.

Note that, in solution, digermene ***E*-5b** is in equilibrium with its isomer ***Z*-5b**, which is consequently observed in long-term solution spectra at room temperature.

^{1}H NMR (400.13 MHz, C_6D_6, 300 K, TMS): δ = 8.09 (dd, ^3J = 7.41 Hz, ^4J = 1.53 Hz, 2H, Me_2N-Ph-*H*), 7.70 (dd, ^3J = 7.70 Hz, ^4J = 1.78 Hz 8H, Ph-*H*), 7.18 to 7.04 (m, 14H, Ph-*H* & Me_2N-Ph-*H*, overlapping with solvent signal), 7.00 (s, 4H, Tip-*H*), 6.98 to 6.93 (m, 2H, Me_2N-Ph-*H*), 6.56 (td, ^3J = 7.31 Hz, ^4J = = 0.82 Hz, 2H, Me_2N-Ph-*H*), 3.80 (sept., ^3J = 6.65 Hz, 4H, Tip-^{i}Pr-C*H*), 2.86 (sept., ^3J = 6.90 Hz, 2H, Tip-^{i}Pr-C*H*), 1.93 (s, 12H, N-CH_3), 1.34 (d, ^3J = 6.87 Hz, 12H, Tip-^{i}Pr-CH_3), 1.15 (d, ^3J = 6.70 Hz 12H, Tip-^{i}Pr-CH_3), 0.72 (d, ^3J = 6.67 Hz, 12H, Tip-^{i}Pr-CH_3) ppm.

^{13}C{^{1}H} NMR (100.61 MHz, C_6D_6, 300 K, TMS): δ = 161.4 (Me_2N-Ph-*C*), 153.9, 149.4, 141.5 (Tip-*C*), 140.8 (Me_2N-Ph-*C*), 137.1, 137.0 (Ph-*C*), 132.8, 131.7 (Me_2N-Ph-*C*), 128.9, 127.5 (Ph-*C*), 125.4, 122.5 (Me_2N-Ph-*C*), 121.6 (Tip-*C*), 46.2 (N-CH_3), 38.4, 34.9 (Tip-^{i}Pr-CH), 25.0, 24.6, 23.8 (Tip-^{i}Pr-CH_3) ppm.

^{29}Si{^{1}H} NMR (79.5 MHz, C_6D_6, 300 K, TMS): δ = −2.4 ppm.

^{29}Si{^{1}H} CP/MAS NMR (79.5 MHz, 300 K, 13 kHz, TMS): δ = 2.6, −0.3 ppm.

UV–vis (hexane): λ_{max} (ε) = 438 nm (ε = 11,900 l mol^{-1} cm^{-1}), 336 nm (ε = 4,900 l mol^{-1} cm^{-1}), 276 nm (ε = 35,900 l mol^{-1} cm^{-1}).

Elemental analysis: Calcd. for $C_{70}H_{86}Ge_2N_2Si_2$ (1,156.90): C, 72.67; H, 7.49; N, 2.42. Found: C, 72.34; H, 7.48; N, 2.25.

(*Z*)-2,2′-((1,2-bis(2,4,6-triisopropylphenyl)digermene-1,2-diyl)bis(diphenylsilanediyl))-bis(*N*,*N*-dimethylaniline) *Z*-5b. Digermenide **1** (1.17 g, 1.0 mmol) and 2-(chlorodiphenylsilyl)-*N*,*N*-dimethylaniline **3b** (353 mg, 1.0 mmol, 1.0 equiv.) were mixed as solids in a Schlenk tube and 5 ml of benzene was added. Stirring for six days at room temperature afforded a dark yellow reaction mixture, which was dried in vacuo and filtered from 15 ml of hexane. Heating of the solution to 65 °C overnight without stirring gave 102 mg (17%) of bis-silyldigermene ***Z*-5b** as orange blocks (melting point of 176 °C; dec.). Reducing the mother liquor to around 5 ml and heating for another night at 65 °C gave a second crop of ***Z*-5b** as 103 mg (17%) of yellow-orange microcrystalline precipitate (overall yield, 34%).

Note that ***Z*-5b** instantly equilibrates in solution with its isomer ***E*-5b**, which is consequently observed in solution spectra at room temperature, so only solid-state techniques can be employed for obtaining spectra of pure ***Z*-5b**.

^{1}H NMR (400.13 MHz, C_6D_6, 300 K, TMS): δ = 8.17 (d, ^3J = 7.11 Hz, 1H, Me_2N-Ph-*H*), 7.50 (dd, ^3J = 7.82 Hz, ^4J = 1.33 Hz, 4H, Si-Ph-*H*), 7.26 (dt, ^3J = 7.88 Hz, ^4J = 1.66 Hz, 1H, Me_2N-Ph-*H*), 7.12 (d, ^3J = 7.32 Hz, 1H, Me_2N-Ph-*H*), 7.06 to 6.93 (m, 9H, Tip-*H*, Me_2N-Ph-*H*, Si-Ph-*H*), 3.69 (sept., ^3J = 6.78 Hz, 2H, Tip-^{i}Pr-C*H*), 2.75 (sept., ^3J = 6.70 Hz, 1H, Tip-^{i}Pr-C*H*), 2.07 (s, 6H, N-CH_3), 1.20 (d, ^3J = 6.91, Hz, 6H, Tip-^{i}Pr-CH_3), 1.02 (d, ^3J = 6.64 Hz, 6H, Tip-^{i}Pr-CH_3), 0.88 (d, ^3J = 6.70 Hz, 6H, Tip-^{i}Pr-CH_3) ppm.

^{13}C{^{1}H} NMR (100.61 MHz, C_6D_6, 300 K, TMS): δ = 161.8 (Me_2N-Ph-*C*), 152.9, 149.4, 143.6 (Tip-*C*), 140.4 (Me_2N-Ph-*C*), 137.1, 136.9 (Ph-*C*), 136.1, 131.9 (Me_2N-Ph-*C*), 128.7, 127.5 (Me_2N-Ph-*C*), 125.8, 123.1 (Me_2N-Ph-*C*), 121.6 (Tip-*C*), 46.7 (N-CH_3), 37.9, 34.7 (Tip-^{i}Pr-CH), 24.9, 24.3, 23.9 (Tip-^{i}Pr-CH_3) ppm.

^{29}Si{^{1}H} NMR (79.5 MHz, C_6D_6, 300 K, TMS): δ = −4.7 ppm.

^{29}Si{^{1}H} CP/MAS NMR (79.5 MHz, 300 K, 13 kHz, TMS): δ = −9.7 ppm.

Elemental analysis: Calcd. for $C_{70}H_{86}Ge_2N_2Si_2$(1,156.90): C, 72.67; H, 7.49; N, 2.42. Found: C, 72.03; H, 7.15; N, 2.30.

2,5-Bis(dimethyl(1,2,2-tris(2,4,6-triisopropylphenyl)digermenyl)silyl)-*N*^{1},*N*^{1},*N*^{4},*N*^{4}-tetramethylbenzene-1,4-diamine 11. Bis-silylphenylenediamine **10** (278 mg, 0.80 mmol, 0.5 equiv.) and digermenide **1** (1.5 g, 1.60 mmol) were mixed as solids in a Schlenk tube and 10 ml of benzene was added. Stirring overnight at room temperature in a glovebox led to precipitation of lithium chloride, which was filtered off via cannula. The dark red filtrate was concentrated to ~1.5 ml, and storage overnight at room temperature gave 768.4 mg (56%) of **11** as orange blocks (melting point, >360 °C, decomposition with formation of **2**) that were suitable for X-ray diffraction.

^{1}H NMR (400.13 MHz, C_6D_6, 300 K, TMS): δ = 8.26 (s, 2H, Ph-*H*), 7.11, 7.02, 7.01 (each s, each 4H, altogether 12H, Tip-*H*), 3.89 (sept., ^3J = 6.64 Hz, 4H, Tip-^{i}Pr-C*H*), 3.79 (sept., ^3J = 6.70 Hz 4H, Tip-^{i}Pr-C*H*), 3.65 (sept., ^3J = 6.61 Hz, 4H, Tip-^{i}Pr-C*H*), 2.83 to 2.67 (m, 6H, Tip-^{i}Pr-C*H*), 2.24 (s, 12H, N-CH_3), 1.26 (d, ^3J = 6.82 Hz, 24H, Tip-^{i}Pr-CH_3), 1.21 (d, ^3J = 6.82 Hz 12H, Tip-^{i}Pr-CH_3), 1.18 to 1.13 (m, 30H, Tip-^{i}Pr-CH_3), 1.11 (br., 18H, Tip-^{i}Pr-CH_3), 0.96 (d, 24H, ^3J = 6.82 Hz, Tip-^{i}Pr-CH_3), 0.77 (s, 12H, Si-CH_3) ppm.

^{13}C{^{1}H} NMR (100.61 MHz, C_6D_6, 300 K, TMS): δ = 158.6 (Ph-*C*), 153.9, 153.0, 152.4, 149.8, 149.6, 149.4, 146.3, 145.2, 141.5 (Tip-Ar-*C*), 139.5, 132.7 (Ph-*C*), 122.4, 122.3, 121.7 (Tip-Ar-*C*), 46.9 (N-CH_3), 37.9, 37.5, 37.1, 34.8, 34.6, 34.5 (Tip-^{i}Pr-*C*H), 25.0 to 24.5 (br., Tip-^{i}Pr-*C*H_3) 24.3, 24.3, 24.2, 24.1 (Tip-^{i}Pr-*C*H_3), 3.7 (Si-*C*H_3) ppm

^{29}Si{^{1}H} NMR (79.5 MHz, C_6D_6, 300 K, TMS): δ = 4.3 ppm.

UV–vis (hexane): λ_{max} (ε) = 426 nm (ε = 17,600 l mol^{-1} cm^{-1}), 320 nm (ε = 5,400 l mol^{-1} cm^{-1}).

Elemental analysis: Calcd. for $C_{104}H_{146}Ge_4N_2Si_2$ (1,789.16): C, 69.82; H, 9.24; N, 1.57. Found: C, 69.85; H, 8.83; N, 1.20.

Polymerization of 11 to P1. Tetragermadiene **11** (646.8 mg, 0.36 mmol) was dissolved in 8 ml benzene and the resulting dark red solution was stirred at 65 °C for 48 h, leading to formation of a gel. Heating was stopped and the now yellow reaction mixture was allowed to reach room temperature before volatile species were removed in vacuo. The remaining solid was suspended in 20 ml of hexane, allowed to settle for 12 h, then the supernatant was separated by filtration. This washing procedure was repeated twice before the remaining solid was thoroughly dried in vacuo to give 263.9 mg (84%) of polydigermene **P1** as a yellow-orange brittle solid, which was ground to a powder. The combined supernatants were freed from solvent in vacuum and the remaining yellow solid was identified as the homoleptic digermene **2** by ^{1}H NMR spectroscopy.

Note that, due to the non-solubility of **P1** in all common solvents, only solid-state characterization techniques were applied. The broad low-intensity signals observed in the reaction mixture solution ^{1}H NMR spectrum probably stem from soluble oligomers from the lighter part of the molecular weight distribution that do not redissolve once dried. The low solubility of **P1** together with its high sensitivity towards air and moisture prevent a determination of the degree of polymerization and the mean molecular weight by standard techniques such as gel permeation chromatography. We therefore determined the mean molecular weight indirectly from ^{1}H NMR spectra (see below) and directly by endgroup analysis through integration of ^{13}C CP-MAS spectra.

^{1}H NMR (400.13 MHz, C_6D_6, 300 K, TMS): δ = 7.22, 7.13 (both br, 1H each, together 2H, Ph-*H*), 7.11 to 7.03 (br, 4H, Tip-*H*), 4.02 to 3.89 (br, 4H, Tip-^{i}Pr-C*H*), 2.90 to 2.75 (br, partially overlapping with Tip-^{i}Pr-C*H* signal of **2**, 2H, Tip-^{i}Pr-C*H*), 2.49 to 2.05 (br m, 12H, N-CH_3), 1.59 to 1.45, 1.29 to 1.20, 1.14 to 1.03 (each br, altogether 36H, Tip-^{i}Pr-CH_3), 0.69 to 0.50 (br, 12H, Si-CH_3) ppm.

^{13}C{^{1}H} CP/MAS NMR (100.61 MHz, 300 K, 13 kHz, TMS): δ = 157.0 (Ph-*C*), 153.3, 149.6 (Tip-*C*), 140.76 (Tip-*C* & Ph-*C*), 128.7 (Ph-*C*), 121.2 (Tip-*C*), 46.9 (N-CH_3), 37.6, 35.0 (Tip-^{i}Pr-*C*H), 24.8 (13.1H, Tip-^{i}Pr-*C*H_3), 3.7 (4H, Si-*C*H_3) ppm.

^{29}Si{^{1}H} CP/MAS NMR (79.5 MHz, 300 K, 13 kHz, TMS): δ = −4.4 ppm.

DLS (hexane): R_h = 13.5 nm.

Data availability

Crystallographic data for the structures in this Article have been deposited at the Cambridge Crystallographic Data Centre under deposition nos. CCDC 1948744 (**3b**), 1948745 (***E*-5a**), 1948746 (***E*-5b**),1948747 (***Z*-5b**), 1995973 (**10**) and 1995974 (**11**). Copies of data can be obtained free of charge from www.ccdc.cam.ac.uk/structures/. All other data supporting the findings of this study are available within the Article and its Supplementary Information.

Acknowledgements

We acknowledge Deutsche Forschungsgemeinschschaft (SCHE906/5-1) for funding. We thank B. Oberhausen, T. Klein and G. Kickelbick for assistance with DSC, thermogravimetric analysis and DLS measurements.

Author contributions

L.K. and D.S. conceived and designed the experiments. L.K. and A.-L.T. synthesized and characterized all compounds. M.Z. performed solid-state NMR experiments. V.H. and B.M. carried out single-crystal X-ray structure determinations. L.K. analysed the data. L.K. performed and analysed the DFT calculations. L.K. and D.S. co-wrote the manuscript. D.S. acquired funding.

Competing interests

The authors declare no competing interests.

Additional information

Supplementary information The online version contains supplementary material available at https://doi.org/10.1038/s41557-021-00639-9.

Correspondence and requests for materials should be addressed to D.S.

Peer review information *Nature Chemistry* thanks the anonymous reviewers for their contribution to the peer review of this work.

Reprints and permissions information is available at www.nature.com/reprints.

Conclusion & Outlook

Just before the start of the experimental work towards this PhD thesis, reduction of Si_6-benzpolarene **196** was carried out in our lab and instead of **197** a positional isomer was isolated.[519,541] To differentiate between both isomers, our group established a nomenclature for the four positions in the benzpolarene scaffold (Scheme 88): the *nudo* position refers to the two unsubstituted ('naked') vertices, *privo* ('empty') to the bridging SiR_2 moiety between the *nudo*-vertices, indicating the strong electronic deshielding this position is exposed to, *ligato* ('bound') to the SiR groups and *remoto* ('remote') to the remaining bridging SiR_2 tether.[527] The diverging reduction products of **195** and **196** excluded **196** as an intermediate in the synthesis of *ligato*-**197** and indicated that **196** and *ligato*-**197** are formed from **195** *via* different mechanisms.

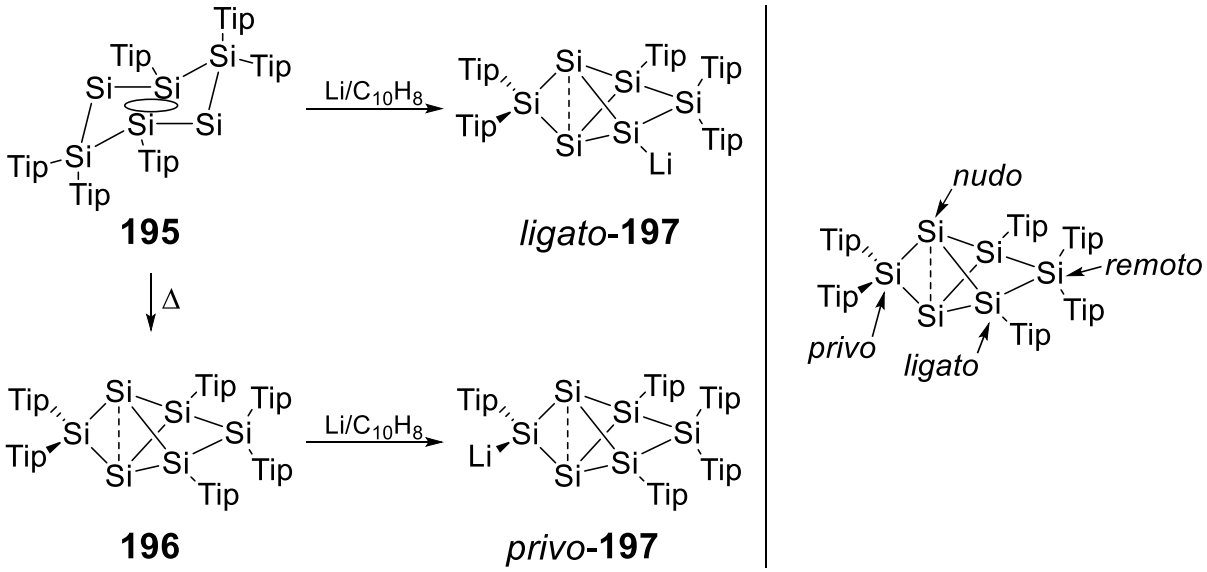

Scheme 88: Left: reduction of siliconoids **195** and **196** to two regioisomers of **197**. Right: Nomenclature for the benzpolarene vertices on the example of **196**.

During the thermal rearrangement of Si_4Ge_2 isomers **193** to **192**, the germanium atoms in the dismutational isomer end up in the *nudo* positions of the benzpolarene scaffold, hence maintaining their unsubstituted character. The two-electron reduction of **193** was therefore topic of the first part of this PhD thesis and surprisingly the isolated and characterized *ligato*-benzpolarenide anion **199** (being the first anionic heterosiliconoid) exhibits a different positioning of the germanium atoms than the neutral **192** (Scheme 89): Instead of both *nudo*-positions, germanium occupies one *nudo*-vertex and the anionic *ligato* position.

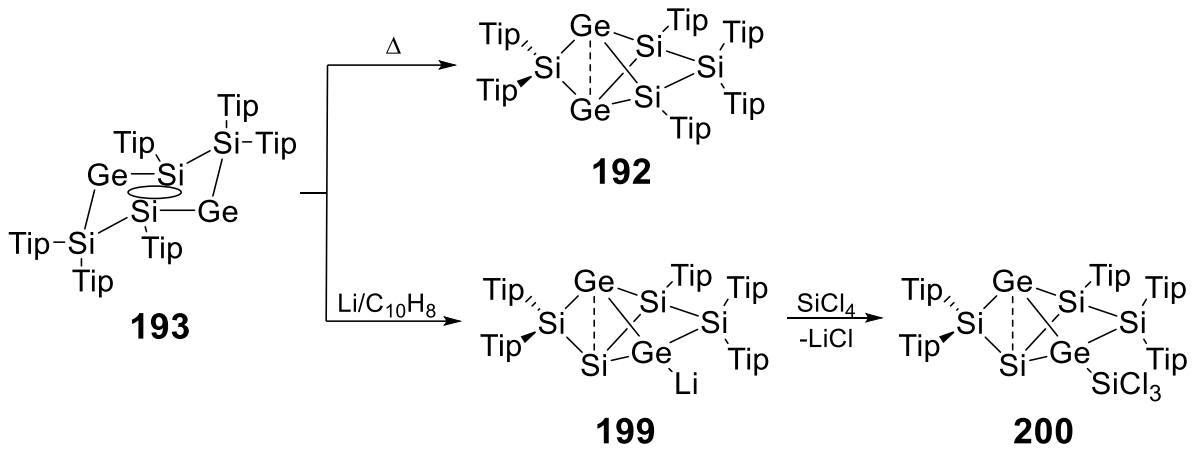

Scheme 89: Reduction of dismutational Si_4Ge_2 isomer **193** to anionic heterosiliconoid **199** with different germanium occupation than **192** and subsequent functionalization to silyl-substituted germanoid **200**.

Formation of **199** *via* a cyclobutene-butadiene-bicyclobutane rearrangement (cf. Section 5.1) is another example for the guiding effect of subunits on the structure of siliconoids (and germanoids) as outlined in the introduction: the bicyclobutane motif is favored for heavy Group 14 elements and the central Si_2Ge_2 unit in **199** even resembles the bond-stretch isomer **XXII'** (Scheme 85). The usage of germanium atoms as mechanistic probes in siliconoid chemistry is further established beyond the synthesis of **192** by this work. Recent investigations in our group strive for insight into formation of larger clusters by employing this technique. The proof-of-principle reaction of **199** with $SiCl_4$ to yield the trichlorosilylsubstituted germanoid **200** is furthermore a first step towards the construction of larger unsaturated Si/Ge clusters.

(S_a)-**199** (R_a)-**199**

Scheme 90: Enantiomers of **199** from the chiral axis through the *privo* and *remoto* position.

Another interesting property of **199** is the inherent axial chirality of its cluster core which was also observed in saturated benzpolarane scaffolds and leads to the existence of two enantiomers of **199** (Scheme 90).[389,445] Heterosiliconoid **199** is thus "chiral-at-cage", a feature that is particularly sought after in the case of carboranes.[542] Even though **199** is obtained as racemic mixture and its reactivity

was examined towards $SiCl_4$ only, it still provides an outlook towards application of chiral siliconoids in stereoselective conversions and even catalysis.[523]

Considering the vast follow-up chemistry that disilenide **117** continues to bring to the forth (cf. Introduction and the first part of this thesis), the further development of the chemistry of digermenide **98a** was a logical step, after only proof-of-principle reactions had been carried out previously (Scheme 50). Especially salt metathesis with halogen bearing compounds was expected to act as a tool for introducing various substituents to the Ge-Ge double bond periphery, similar to the silicon congener. As described in the second part of this thesis, it was possible by this procedure to isolate the first digermenes with $A_2Ge{=}GeAB$ substitution pattern **201** and to functionalize digermenes with α-chlorosilyl as well as acyl groups, rendering the compounds **202a-c** and **203a-c** as the first reported heavy Group 14 analogues of allylchlorides and α,β-unsaturated ketones, respectively (in collaboration with Yvonne Kaiser from our group; Scheme 91).

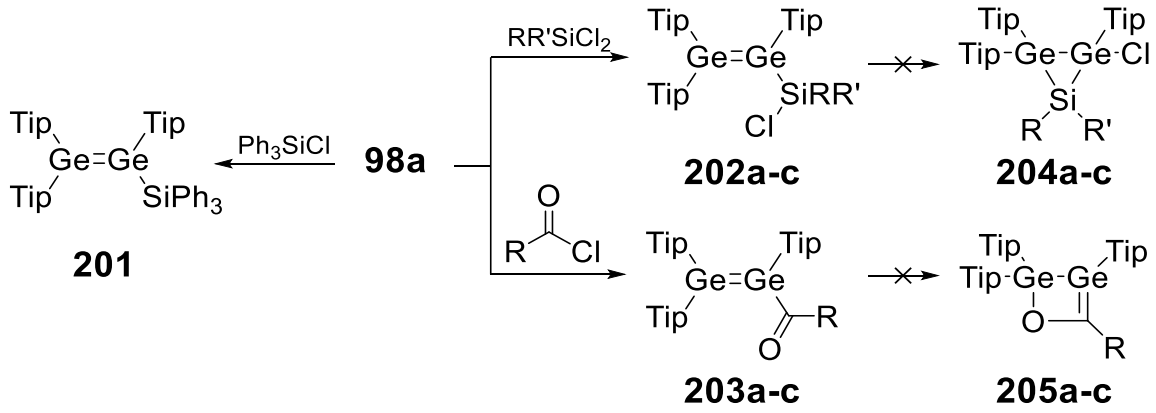

Scheme 91: Synthesis of asymmetric digermene **201** and persistent α-chlorosilyldigermenes **202a-c** and acyldigermenes **203a-c** which do not undergo cyclization to the corresponding cyclopropanes **204a-c** or cyclic Brook germenes **205a-c** (**202a**, **204a**: R = R' = Me; **202b, 204b**: R = Me, R' = Ph; **202c**, **204c**: R = R' = Ph; **203a**, **205a**: R = ^{t}Bu;, **203b**, **205b**: R = 2-methylbutan-2-yl; **203c**, **205c**: 1-Ad).

Their relationship with these prominent organic functionalities makes **202a-c** and **203a-c** attractive targets for future reactivity studies: The chloride group in **202a-c** might undergo subsequent salt metathesis or be removed reductively/oxidatively to form the corresponding allyl anions and cations, respectively. Acyldigermenes **203a-c** could furthermore be treated with the entire toolbox of carbonyl chemistry, as for instance the Wittig-reaction and their strong polarization and high reactivity might enable them to activate otherwise unreactive small molecules.

The results of this part of the thesis reveal several important consequences for the further development of digermenide chemistry and its use for the synthesis of germanoids: First, the inherent lower tendency towards cyclization is restricting the synthesis of germanium analogues of cyclotrisilane **121e**, a vital precursor in the synthesis of benzpolarene **196** (Scheme 86). This might be circumvented by other synthetic pathways, as Si_4Ge_2 benzene **193** is synthesized *via* the intermediate disilenylgermylene **194** (Scheme 84). Second, digermenide **98a** is extraordinarily redox active and forms tetragermabutadiene **99** upon reaction with a lot of different reagents (including atmospheric oxygen), instead of undergoing salt metathesis. This represents an even greater challenge for the synthesis of germanoid precursors which require highly halogenated reagents with accordingly low-lying LUMOs. The suitability of **98a** for the synthesis of germanoids is therefore at least questionable without novel synthetic approaches as preliminary results with $SiCl_4$ hint towards unselective reaction. Third and last, the observation that all solution samples of **201-203** contained the homoleptic digermene **1e** after several days, despite their entirely different electronic structure, strengthened our assumption that asymmetrically substituted digermenes in general should qualify for metathesis reactions and the olefin disproportionation in particular, as **1e** was apparently formed through dissociation of diarylgermylene **81e** from **201-203** (Scheme 92). In these cases, however, the functionalized germylene fragments decomposed due to their immanent instability.

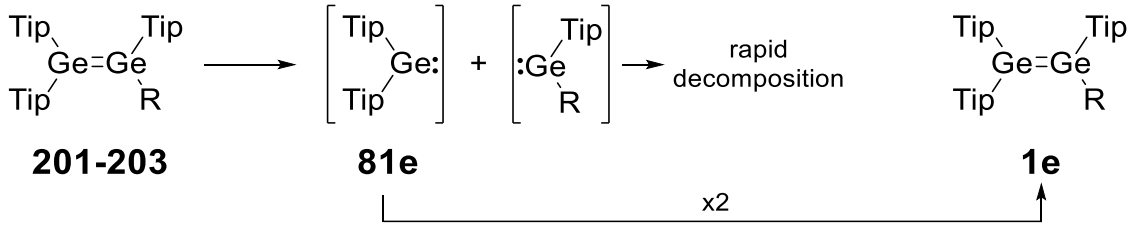

Scheme 92: Formation of homoleptic digermene **1e** from asymmetric digermenes **201-203** via Ge-Ge double bond cleavage (R = chlorosilyl, acyl).

The third part of this thesis therefore aimed at the design of a substituent that would stabilize the otherwise elusive functionalized germylene fragment to enable the first example of heavy olefin metathesis. Our strategy of choice employed intramolecular n-donation to the vacant p-orbital of germanium as outlined in Section 2.1. Based on the observation from the second part of this thesis that digermenide reacts selectively with monochlorosilanes (isolation of **201**) we designed 2-(*N*,*N*-dimethylanillino)dimethylchlorosilane and 2-(*N*,*N*-dimethylanillino)diphenylchloro-

silane as suitable reagents that indeed reacted selectively with digermenide **98a** to the asymmetric digermenes **206a,b**. Metathesis to **1e** and the symmetric digermenes *E*-**207a,b** is triggered thermally and was shown to proceed over germylene intermediates **208a,b** , just as anticipated (Scheme 93).

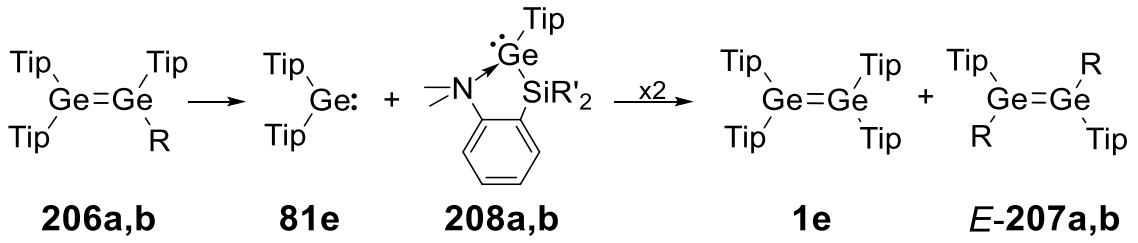

Scheme 93: Olefin Metathesis of asymmetric **206a,b** via intermediate germylene **81e** and **208a,b** to symmetric digermenes **1e** and *E*-**207a,b** (**206a**, *E*-**207a**: R = 2-(*N*,*N*-$Me_2C_6H_3$)Me_2Si-; **206b**, *E*-**207b**: R = 2-(*N*,*N*-$Me_2C_6H_3$)Ph_2Si-; **208a**: R' = Me; **208b**: R' = Ph).

The metathesis of **206a,b** does not only constitute the first example of a synthetically useful metathesis of heavy double bonds, it is also the first olefin metathesis in general which does require on the presence of a catalyst. The employed strategy of stabilizing the intermediate germylene with a tethered donor group might therefore also be expanded towards organic olefin metathesis and help to get rid of transition metal catalysts in specific cases. Both synthesis of Tip_2Ge=GeTipR-type digermenes *via* salt metathesis from **98a** and metathesis of exactly those to symmetric digermenes provide unprecedented synthetic routes to digermenes and add significantly to the accessible set of functionalized Ge-Ge double bonds. *E*-**207b** furthermore equilibrates with its isolable isomer *Z*-**207b** and both compounds represent the only reported example of a fully characterized *E*-*Z*-isomer couple of digermenes.

The extension of the successful metathesis approach towards α,ω-bis(digermene) **209** culminated in the synthesis of poly(digermene) **210** (Scheme 94) which is the first Heavy Group 14 polyene and one of only a handful reported examples for polymers with heavy doubly bonds in their repeating unit. Due to the conceptional similarity with the organic Acyclic Diene Metathesis (ADMET) we coined the term Heavy ADMET or HADMET for this type of metathesis polymerization.

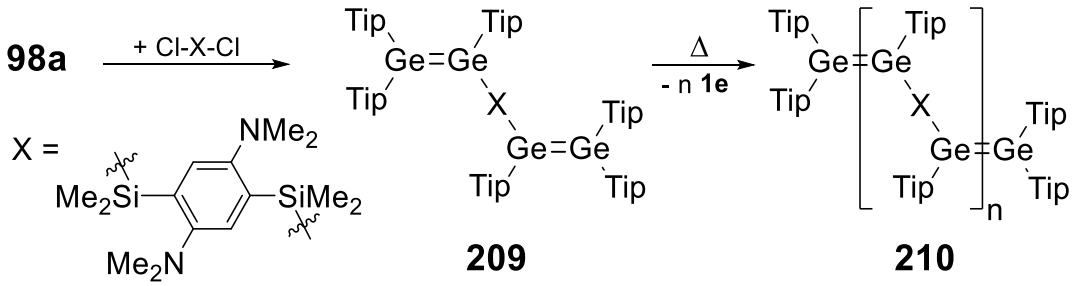

Scheme 94: HADMET polymerization of α,ω-bis(digermene) **209** to polydigermene **210**.

Poly(digermene) **210** proved challenging to analyze with standard polymer analytics due to its poor solubility hence several new methods were developed in order to determine its polymerization degree: Quantification of the released amount of **1e** *via* ^{1}H NMR spectroscopy gave X_n = 23 indirectly while end-group analysis in a ^{13}C CP/MAS NMR of isolated **210** estimated X_n= 21. The latter method was priorly evaluated on the molecular test compound *E*-**207a**. Both values compare well with the degree of polymerization determined from DLS which is between X_n = 26 and X_n = 31. Future studies will focus on increasing the solubility of **210** to provide more analytical data which should allow optimization of the polymerisation process and properties. For this target either post-functionalization of the polymer or designed spacers with solubility mediating alkyl groups might be suitable and further allow longer chain lengths due to delayed chain termination by precipitation. In a long-term perspective the material properties of **210** and related polymers should be of high interest as no comparable materials are known and they constitute a first step in combining the properties of organic conductive polymers with semiconductor characteristics. In this context incorporation of dopant atoms like boron and phosphorus as well as electrochemical investigations promise further advancement.

It is interesting to note that while the first part of this thesis was built primarily on the chemical similarity between silicon and germanium in order to gain mechanistic insight, the second part demonstrated the consequences of their subtle differences as diverging reactivities. The third part then made use of exactly these differences to employ germanium-based compounds in reactions that were not possible with the corresponding silicon analogues. Hence, the present thesis makes use of a wide spectrum of germanium-silicon interactions in low-valent compounds and it will be crucial for future developments to deepen the understanding of especially the differences between both elements in order to unfold their full synthetic potential.

References

[1] D. R. Lide, G. Baysinger, L. I. Berger, R. N. Goldberg, H. V. Kehiaian, K. Kuchitsu, G. Rosenblatt, D. L. Roth, D. L. Zwillinger, *CRC Handbook of Chemistry and Physics, Internet Version 2005*, CRC Press, Boca Raton, FL, **2005**.

[2] E. K. Schnebele, *U.S. Geol. Surv. Miner. Yearb. – 2017,* **2020**, 67.1−67.14.

[3] T. P. Dolley, *U.S. Geol. Surv. Miner. Yearb. – 2016,* **2019**, 66.1−66.15.

[4] L. C. Feldman, in *Fundam. Asp. Silicon Oxid.* (Ed.: Y.J. Chabal), Springer Science & Business Media, **2001**, pp. 1–11.

[5] D. Mendelejew, in *Justus Liebigs Ann. Der Chemie Und Pharm. VIII. Suppl.*, **1872**, pp. 133–229.

[6] C. Winkler, *Ber. Deutsch. Chem. Ges.* **1886**, *19*, 210–211.

[7] C. Winkler, *J. Prakt. Chemie* **1886**, *34*, 177–229.

[8] L. R. Bernstein, *Geochim. Cosmochim. Acta* **1985**, *49*, 2409–2422.

[9] R. R. Moskalyk, *Miner. Eng.* **2004**, *17*, 393–402.

[10] R. Höll, M. Kling, E. Schroll, *Ore Geol. Rev.* **2007**, *30*, 145–180.

[11] A. C. Tolcin, *U.S. Geol. Surv. Miner. Commod. Summ. – 2019,* **2020**, 68–69.

[12] C. L. Thomas, *U.S. Geol. Surv. Miner. Commod. Summ. – 2018,* **2019**, 68–69.

[13] C. L. Thomas, *U.S. Geol. Surv. Miner. Commod. Summ. – 2017,* **2018**, 68–69.

[14] D. E. Guberman, *U.S. Geol. Surv. Miner. Commod. Summ. – 2016,* **2017**, 70–71.

[15] J. Bardeen, W. H. Brattain, *Phys. Rev.* **1948**, *71*, 230–231.

[16] R. Pillarisetty, *Nature* **2011**, *479*, 324–328.

[17] C. Shen, T. Trypiniotis, K. Y. Lee, S. N. Holmes, R. Mansell, M. Husain, V. Shah, X. V. Li, H. Kurebayashi, I. Farrer, C. H. de Groot, D. R. Leadley, G. Bell, E. H. C. Parker, T. Whall, D. A. Ritchie, C. H. W. Barnes, *Appl. Phys. Lett.* **2010**, *97*, 1–4.

[18] A. J. Sigillito, R. M. Jock, A. M. Tyryshkin, J. W. Beeman, E. E. Haller, K. M. Itoh, S. A. Lyon, *Phys. Rev. Lett.* **2015**, *115*, 1–5.

[19] H. Elsner, F. Melcher, U. Schwarz-Schampera, P. Buchholz, *Commod. Top News* **2010**, *33*, 1–13.

[20] A. Cobelo-García, M. Filella, P. Croot, C. Frazzoli, G. Du Laing, N. Ospina-Alvarez, S. Rauch, P. Salaun, J. Schäfer, S. Zimmermann, *Environ. Sci. Pollut. Res.* **2015**, *22*, 15188–15194.

[21] L. Grandell, M. Höök, *Sustain.* **2015**, *7*, 11818–11837.

[22] B. A. Andersson, *Prog. Photovoltaics Res. Appl.* **2000**, *8*, 61–76.

[23] C. Eisele, M. Berger, M. Nerding, H. P. Strunk, C. E. Nebel, M. Stutzmann, *Thin Solid Films* **2003**, *427*, 176–180.

[24] K. V. Maydell, K. Grunewald, M. Kellermann, O. Sergeev, P. Klement, N. Reininghaus, T. Kilper, *Energy Procedia* **2014**, *44*, 209–215.

[25] E. M. T. Fadaly, A. Dijkstra, J. R. Suckert, D. Ziss, M. A. J. van Tilburg, C. Mao, Y. Ren, V. T. van Lange, K. Korzun, S. Kölling, M. A. Verheijen, D. Busse, C. Rödl, J. Furthmüller, F. Bechstedt, J. Stangl, J. J. Finley, S. Botti, J. E. Heverkort, E. P. A. M. Bakkers, *Nature* **2020**, *580*, 205–209.

[26] J.-S. Rieh, B. Jagannathan, H. Chen, K. T. Schonenberg, D. Angell, A. Chinthakindi, J. Florkey, F. Golan, D. Greenberg, S. J. Jeng, M. Khater, F. Pagette, C. Schnabel, P. Smith, A. Stricker, K. Vaed, R. Volant, D. Ahlgren, G. Freeman, K. Stein, S. Subbanna, *Tech. Dig. - Int. Electron Devices Meet.* **2002**, 771–774.

[27] J. D. Cressler, *Proc. IEEE* **2005**, *93*, 1559–1582.

[28] R. Krithivasan, Y. Lu, J. D. Cressler, J.-S. Rieh, M. H. Khater, D. Ahlgren, G. Freeman, *IEEE Electron Device Lett.* **2006**, *27*, 567–569.

[29] P. Chevalier, T. F. Meister, B. Heinemann, *Proc. IEEE BCTM,* **2011**.

[30] R. Rahman, S. H. Park, T. B. Boykin, G. Klimeck, S. Rogge, L. C. L. Hollenberg, *Phys. Rev. B - Condens. Matter Mater. Phys.* **2009**, *80*, 1–5.

[31] R. Vrijen, E. Yablonovitch, K. Wang, H. W. Jiang, A. Balandin, V. Roychowdhury, T. Mor, D. DiVincenzo, *Phys. Rev. A - At. Mol. Opt. Phys.* **2000**, *62*, 1–10.

[32] W. M. Witzel, R. Rahman, M. S. Carroll, *Phys. Rev. B - Condens. Matter Mater. Phys.* **2012**, *85*, 1–5.

[33] K. Dawon, *Electric Field Controlled Semiconductor Device*, US-Patent 3102230, **1963**.

[34] G. E. Moore, *Electronics* **1965**, *38*.

[35] D. Laws, “13 sextillion & counting: the long & winding road to the most frequently manufactured human artifact in history” can be found online under https://computerhistory.org/blog/13-sextillion-counting-the-long-winding-road-to-the-most-frequently-manufactured-human-artifact-in-history/, **2018**.

[36] R. A. Lefever, *J. Chem. Educ.* **1953**, *30*, 554–556.

[37] X. Niu, V. L. Dalal, *J. Appl. Phys.* **2005**, *98*, 1–4.

[38] E. L. Hull, R. H. Pehl, *Nucl. Instrum. Methods Phys. Res. A.* **2005**, *538*, 651–656.

[39] J. Zhu, V. L. Dalal, M. A. Ring, J. J. Gutierrez, J. D. Cohen, *J. Non. Cryst. Solids* **2004**, *338–340*, 651–654.

[40] S. S. Iyer, G. L. Patton, J. M. Stork, B. S. Meyerson, D. L. Harame, *IEEE Trans. Electron Devices* **1989**, *36*, 2043–2064.

[41] A. Mai, I. Garcia Lopez, P. Rito, R. Nagulapalli, A. Awny, M. Elkhouly, M. Eissa, M. Ko, A. Malignaggi, M. Kucharski, H. J. Ng, K. Schmalz, D. Kissinger, *Int. J. High Speed Electron. Syst.* **2017**, *26*, 1–22.

[42] M. Bosi, G. Attolini, *Prog. Cryst. Growth Charact. Mater.* **2010**, *56*, 146–174.

[43] T. E. Whall, E. H. C. Parker, *J. Mater. Sci. Mater. Electron.* **1995**, *6*, 249–264.

[44] D. L. Harame, S. J. Koester, G. Freeman, P. Cottrel, K. Rim, G. Dehlinger, D. Ahlgren, J. S. Dunn, D. Greenberg, A. Joseph, F. Anderson, J.-S. Rich, S. A. S. T. Onge, D. Coolbaugh, V. Ramachandran, J. D. Cressler, S. Subbanna, *Appl. Surf. Sci.* **2004**, *224*, 9–17.

[45] C. W. Leitz, M. T. Currie, M. L. Lee, Z. Y. Cheng, D. A. Antoniadis, E. A. Fitzgerald, *J. Appl. Phys.* **2002**, *92*, 3745–3751.

[46] A. Gordijn, R. J. Zambrano, J. K. Rath, R. E. I. Schropp, *IEEE Trans. Electron Devices* **2002**, *49*, 949–952.

[47] W. Paul, R. A. Street, S. Wagner, *J. Electron. Mater.* **1993**, *22*, 39–48.

[48] M. Dominguez, P. Rosales, A. Torres, *Solid. State. Electron.* **2012**, *76*, 44–47.

[49] P. Rivière, M. Rivière-Baudet, J. Satgé, *Compr. Organomet. Chem.* **1995**, *2*, 137–216.

[50] X. Ji, H. Y. Cheng, A. J. Grede, A. Molina, D. Talreja, S. E. Mohney, N. C. Giebink, J. V. Badding, V. Gopalan, *APL Mater.* **2018**, *6*, 046105-1−046105-8.

[51] C. B. Duke, *Chem. Rev.* **1996**, *96*, 1237–1259.

[52] J. A. Kubby, J. J. Boland, *Surf. Sci. Rep.* **1996**, *26*, 61–204.

[53] R. A. Wolkow, *Phys. Rev. Lett.* **1992**, *68*, 2636–2639.

[54] T. Sato, M. Iwatsuki, H. Tochihara, *J. Electron Microsc.* **1999**, *48*, 1–7.

[55] H. Kobayashi, T. Iwamoto, M. Kira, *J. Am. Chem. Soc.* **2005**, *127*, 15376–15377.

[56] A. Sekiguchi, N. Fukaya, M. Ichinohe, *J. Am. Chem. Soc.* **1999**, *121*, 11587–11588.

[57] T. Fjeldberg, A. Haaland, M. F. Lappert, B. E. R. Schilling, R. Seip, A. J. Thorne, *J. Chem. Soc. Chem. Commun.* **1982**, *4*, 1407–1408.

[58] D. E. Goldberg, P. B. Hitchcock, M. F. Lappert, K. Mark Thomas, A. J. Thorne, A. Haaland, B. E. R. Schilling, *J. Chem. Soc. Dalton Trans.* **1986**, 2387–2394.

[59] G. Trinquier, J.-P. Malrieu, *J. Phys. Chem.* **1990**, *94*, 6184–6196.

[60] M. A. Filler, J. A. Van Deventer, A. J. Keung, S. F. Bent, *J. Am. Chem. Soc.* **2006**, *128*, 770–779.

[61] X. Lu, M. Zhu, X. Wang, Q. Zhang, *J. Phys. Chem. B* **2004**, *108*, 4478–4484.

[62] K. L. Hurni, P. A. Rupar, N. C. Payne, K. M. Baines, *Organometallics* **2007**, *26*, 5569–5575.

[63] K. L. Hurni, K. M. Baines, *Chem. Commun.* **2011**, *47*, 8382–8384.

[64] N. Y. Tashkandi, E. E. Cook, J. L. Bourque, K. M. Baines, *Chem. - A Eur. J.* **2016**, *22*, 14006–14012.

[65] B. Shong, K. T. Wong, S. F. Bent, *J. Am. Chem. Soc.* **2014**, *136*, 5848–5851.

[66] J. A. Hardwick, K. M. Baines, *Angew. Chem. Int. Ed.* **2015**, *54*, 6600–6603.

[67] C. Mui, M. A. Filler, S. F. Bent, C. B. Musgrave, *J. Phys. Chem. B* **2003**, *107*, 12256–12267.

[68] M. A. Filler, C. Mui, C. B. Musgrave, S. F. Bent, *J. Am. Chem. Soc.* **2003**, *125*, 4928–4936.

[69] J. M. Buriak, *Chem. Rev.* **2002**, *102*, 1271.

[70] J. S. Kachian, K. T. Wong, S. F. Bent, *Acc. Chem. Res.* **2010**, *43*, 346–355.

[71] S. C. Moss, J. F. Graczyk, *Phys. Rev. Lett.* **1969**, *23*, 1167–1171.

[72] W. Paul, G. A. N. Connell, R. J. Temkin, *Adv. Phys.* **1973**, *22*, 531–580.

[73] R. J. Temkin, W. Paul, G. A. N. Connell, *Adv. Phys.* **1973**, *22*, 581–641.

[74] G. A. N. Connell, J. R. Pawlik, *Phys. Rev. B* **1976**, *13*, 787–805.

[75] T. D. Moustakas, W. Paul, *Phys. Rev. B* **1977**, *16*, 1564–1576.

[76] S. DeWolf, A. Descoeudres, Z. C. Holman, C. Ballif, *Green* **2012**, *2*, 7–24.

[77] T. Yamaguchi, Y. Ichihashi, T. Mishima, N. Matsubara, T. Yamanishi, *IEEE J. Photovolt.* **2014**, 15–17.

[78] K. Yoshikawa, H. Kawasaki, W. Yoshida, T. Irie, K. Konishi, K. Nakano, T. Uto, D. Adachi, M. Kanematsu, H. Uzu, K. Yamamoto, *Nat. Energy* **2017**, *2*, 17032-1−17032-8.

[79] T. V. Torchynska, *J. Non. Cryst. Solids* **2006**, *352*, 2484–2487.

[80] T. V. Torchynska, A. L. Quintos Vazquez, G. Polupan, Y. Matsumoto, L. Khomenkova, L. Shcherbyna, *J. Non. Cryst. Solids* **2008**, *354*, 2186–2189.

[81] Y. S. Shcherbyna, T. V. Torchynska, *Thin Solid Films* **2010**, *518*, S204–S207.

[82] M. Hirao, T. Uda, *Surf. Sci.* **1994**, *306*, 87–92.

[83] G. Onida, W. Andreoni, *Chem. Phys. Lett.* **1995**, *243*, 183–189.

[84] M. Rohlfing, S. G. Louie, *Phys. Rev. Lett.* **1998**, *80*, 3320–3323.

[85] D. Martin, B. Schroeder, M. Leidner, H. Oechsner, *J. Non. Cryst. Solids* **1989**, *114*, 537–539.

[86] G. Hadjisavvas, G. Kopidakis, P. Kelires, *Phys. Rev. B* **2001**, *64*, 125413.

[87] P. Antoniotti, L. Operti, R. Rabezzana, G. A. Vaglio, A. Guarini, *Rapid Commun. Mass Spectrom.* **2002**, *16*, 185–191.

[88] J. M. Riveros, *Int. J. Mass Spectrom.* **2002**, *221*, 177–190.

[89] J. Jasinski, B. S. Meyerson, B. A. Scott, *Annu. Rev. Phys. Chem* **1987**, *38*, 109-140.

[90] J. M. Jasinski, R. Becerra, R. Walsh, *Chem. Rev.* **1995**, *95*, 1203–1228.

[91] R. Robertson, A. Gallagher, *J. Appl. Phys.* **1986**, *59*, 3402–3411.

[92] R. Robertson, D. Hils, H. Chatham, A. Gallagher, *Appl. Phys. Lett.* **1983**, *43*, 544–546.

[93] K. Raghavachari, *J. Chem. Phys.* **1991**, *95*, 7373–7388.

[94] K. Raghavachari, *J. Chem. Phys.* **1992**, *96*, 4440–4448.

[95] K. Raghavachari, *J. Chem. Phys.* **1990**, *92*, 452–465.

[96] G. Trinquier, *J. Am. Chem. Soc.* **1992**, *114*, 6807–6820.

[97] A. Arrais, P. Benzi, E. Bottizzo, C. Demaria, *J. Phys. D. Appl. Phys.* **2009**, *42*, 10540-1−10540-6.

[98] A. J. Adamczyk, M. F. Reyniers, G. B. Marin, L. J. Broadbelt, *ChemPhysChem* **2010**, *11*, 1978–1994.

[99] W. O. Filtvedt, A. Holt, P. A. Ramachandran, M. C. Melaaen, *Sol. Energy Mater. Sol. Cells* **2012**, *107*, 188–200.

[100] C. G. Newman, J. Dzarnoski, M. A. Ring, H. E. O'Neal, *Int. J. Chem. Kinet.* **1980**, *12*, 661–670.

[101] C. J. Giunta, R. J. McCurdy, J. D. Chapple-Sokol, R. G. Gordon, *J. Appl. Phys.* **1990**, *67*, 1062–1075.

[102] S. M. Gates, C. M. Greenlief, D. B. Beach, *J. Chem. Phys.* **1990**, *93*, 7493–7503.

[103] J. Simon, R. Feurer, A. Reynes, R. Morancho, *J. Anal. Appl. Pyrolysis* **1992**, *24*, 51–59.

[104] D. C. Marra, E. A. Edelberg, R. L. Naone, E. S. Aydil, *J. Vac. Sci. Technol. A* **1998**, *16*, 3199–3210.

[105] S. D. Chambreau, J. Zhang, *Chem. Phys. Lett.* **2002**, *351*, 171–177.

[106] J. M. Lemieux, S. D. Chambreau, J. Zhang, *Chem. Phys. Lett.* **2008**, *459*, 49–53.

[107] I. Haller, *Appl. Phys. Lett.* **1980**, *37*, 282–284.

[108] T. P. Martin, H. Schaber, *J. Chem. Phys.* **1985**, *83*, 855–858.

[109] M. L. Mandich, *J. Vac. Sci. Technol. B* **1989**, *7*, 1295.

[110] H. Murakami, T. Kanayama, *Appl. Phys. Lett.* **1995**, *67*, 2341.

[111] W. M. M. Kessels, M. C. M. Van De Sanden, D. C. Schram, *Appl. Phys. Lett.* **1998**, *72*, 2397–2399.

[112] S. D. Chambreau, L. Wang, J. Zhang, *J. Phys. Chem. A* **2002**, *106*, 5081–5087.

[113] K. Raghavachari, *J. Chem. Phys.* **1986**, *84*, 5672–5686.

[114] V. Meleshko, Y. Morokov, V. Schweigert, *Chem. Phys. Lett.* **1999**, *300*, 118–124.

[115] D. K. Yu, R. Q. Zhang, S. T. Lee, *J. Appl. Phys.* **2002**, *92*, 7453–7458.

[116] C. P. Li, X. J. Li, J. C. Yang, *J. Phys. Chem. A* **2006**, *110*, 12026–12034.

[117] R. Singh, *J. Phys. Condens. Matter* **2008**, *20*, 045226-1−045226-14.

[118] D. Bandyopadhyay, P. Sen, *J. Phys. Chem. A* **2010**, *114*, 1835–1842.

[119] A. J. Adamczyk, M. F. Reyniers, G. B. Marin, L. J. Broadbelt, *Theor. Chem. Acc.* **2011**, *128*, 91–113.

[120] A. Doddi, C. Gemel, M. Winter, R. A. Fischer, C. Goedecke, H. S. Rzepa, G. Frenking, *Angew. Chem. Int. Ed.* **2013**, *52*, 450–454.

[121] Y. Choi, A. J. Adamczyk, *J. Phys. Chem. A* **2018**, *122*, 9851–9868.

[122] L. Wang, L. Zhang, Y. Jiang, P. Li, J. Li, X. Li, *Mol. Phys.* **2020**, *118*, 1−11.

[123] P. Jutzi, *Angew. Chem. Int. Ed. Engl.* **1975**, *14*, 232–245.

[124] N. V. Sidgwick, W. Wardlaw, O. B. E. Whytlaw-Gray, *Annu. Rep. Prog. Chem.* **1933**, *30*, 82–132.

[125] K. S. Pitzer, *Acc. Chem. Res.* **1978**, 35–43.

[126] P. Pyykkö, J. P. Desclaux, *Acc. Chem. Res.* **1979**, *12*, 276–281.

[127] W. Kutzelnigg, *Angew. Chem. Int. Ed. Engl.* **1984**, *23*, 272–295.

[128] H. A. Bent, *Chem. Rev.* **1961**, *61*, 275–311.

[129] R. F. W. Bader, *Can. J. Chem.* **1962**, *40*, 1164–1175.

[130] R. G. Pearson, *J. Am. Chem. Soc.* **1969**, *91*, 4947–4955.

[131] R. G. Pearson, *J. Mol. Struct.* **1983**, *103*, 25–34.

[132] W. D. Kirchhoff, D. R. Lide, F. X. Powell, *J. Mol. Spectrosc.* **1973**, *47*, 491–498.

[133] A. K. Maltsev, R. G. Mikaelian, O. M. Nefedov, R. H. Hauge, J. L. Margrave, *Proc. Natl. Acad. Sci.* **1971**, *68*, 3238–3241.

[134] V. M. Rao, R. F. Curl, P. L. Timms, J. L. Margrave, *J. Chem. Phys.* **1965**, *43*, 2557–2558.

[135] G. Maass, R. H. Hauge, J. L. Margrave, *Z. .Anorg. Allg. Chem.* **1972**, *302*, 295–302.

[136] H. Takeo, R. F. Curl, P. W. Wilson, *J. Mol. Spectrosc.* **1971**, *38*, 464–475.

[137] H. Takeo, R. F. Curl, *J. Mol. Spectrosc.* **1972**, *43*, 21–30.

[138] E. V. Hargittai, M. Kolonits, K. Ujszaszy, J. Tamas, *J. Organomet. Chem.* **1976**, *105*, 33–44.

[139] R. H. Hauge, J. W. Hastie, J. L. Margrave, *J. Mol. Spectrosc.* **1973**, *45*, 420–427.

[140] I. Hargittai, J. Tremmel, E. Vajda, A. A. Ishchenko, A. A. Ivanov, L. S. Ivashkevich, V. P. Spiridonov, *J. Mol. Struct.* **1977**, *42*, 147–151.

[141] G. Herzberg, J. W. C. Johns, *J. Chem. Phys.* **1971**, *54*, 2276–2278.

[142] P. Jensen, P. R. Bunker, A. R. Hoy, *J. Chem. Phys.* **1982**, *77*, 5370–5374.

[143] P. R. Bunker, P. Jensen, *J. Chem. Phys.* **1983**, *79*, 1224–1228.

[144] A. R. W. McKellar, P. R. Bunker, T. J. Sears, K. M. Evenson, R. J. Saykally, S. R. Langhoff, *J. Chem. Phys.* **1983**, *79*, 5251–5264.

[145] I. Dubois, G. Herzberg, R. D. Verma, *J. Chem. Phys.* **1967**, *47*, 4262–4263.

[146] J. Berkowitz, J. P. Greene, H. Cho, B. Ruscic, *J. Chem. Phys.* **1987**, *86*, 1235.

[147] J. Karolczak, W. W. Harper, R. S. Grev, D. J. Clouthier, *J. Chem. Phys.* **1995**, *103*, 2839–2849.

[148] N. Matsunaga, S. Koseki, M. S. Gordon, *J. Chem. Phys.* **1996**, *104*, 7988–7996.

[149] M. S. Gordon, *Chem. Phys. Lett.* **1985**, *114*, 348–352.

[150] M. S. Gordon, M. W. Schmidt, *Chem. Phys. Lett.* **1986**, *132*, 294–298.

[151] R. S. Grev, H. F. Schaefer, P. P. Gaspar, *J. Am. Chem. Soc.* **1991**, *113*, 5638–5643.

[152] P. Jiang, P. P. Gaspar, *J. Am. Chem. Soc.* **2001**, *123*, 8622–8623.

[153] A. Sekiguchi, T. Tanaka, M. Ichinohe, K. Akiyama, S. Tero-Kubota, *J. Am. Chem. Soc.* **2003**, *125*, 4962–4963.

[154] K. Krogh-Jespersen, *J. Am. Chem. Soc.* **1985**, *107*, 537–543.

[155] S. P. Kolesnikov, V. I. Shiryaev, O. M. Nefedov, *Izv. Akad. Nauk SSSR, Seriya Khimicheskaya* **1966**, 584.

[156] T. K. Gar, N. A. Viktorov, S. N. Gurkova, A. I. Gusev, N. V. Alkseev, *J. Crystallogr. Spectrosc. Res.* **1987**, *17*, 143–145.

[157] X. Tian, T. Pape, N. W. Mitzel, *Heteroat. Chem.* **2005**, *16*, 361–363.

[158] J. Barrau, G. Rima, T. El Amraoui, *Inorganica Chim. Acta* **1996**, *241*, 9–10.

[159] P. Jutzi, H. J. Hoffmann, D. J. Brauer, C. Krüger, *Angew. Chem. Int. Ed. Engl.* **1973**, *12*, 1002–1003.

[160] P. Jutzi, H. J. Hoffmann, K.-H. Wyes, *J. Organomet. Chem.* **1974**, *81*, 341–350.

[161] B. Gehrhus, P. B. Hitchcock, M. F. Lappert, *J. Chem. Soc. Dalton Trans.* **2000**, *2*, 3094–3099.

[162] M. Stender, L. Pu, P. P. Power, *Organometallics* **2001**, *20*, 1820–1824.

[163] P. A. Rupar, M. C. Jennings, K. M. Baines, *Can. J. Chem.* **2007**, *85*, 141–147.

[164] T. J. Hadlington, M. Hermann, J. Li, G. Frenking, C. Jones, *Angew. Chem. Int. Ed.* **2013**, *52*, 10199–10203.

[165] A. J. Arduengo, R. L. Harlow, M. Kline, *J. Am. Chem. Soc.* **1991**, *113*, 361–363.

[166] A. J. Arduengo, H. V. R. Dias, R. L. Harlow, M. Kline, *J. Am. Chem. Soc.* **1992**, *114*, 5530–5534.

[167] A. J. Arduengo, J. R. Goerlich, W. J. Marshall, *J. Am. Chem. Soc.* **1995**, *117*, 11027–11028.

[168] A. J. Arduengo, R. Krafczyk, R. Schmutzler, H. A. Craig, J. R. Goerlich, W. J. Marshall, M. Unverzagt, *Tetrahedron* **1999**, *55*, 14523–14534.

[169] N. Kuhn, T. Kratz, *Synthesis* **1993**, 561–562.

[170] C. Heinemann, W. Thiel, *Chem. Phys. Lett.* **1994**, *217*, 11–16.

[171] C. Boehme, G. Frenking, *J. Am. Chem. Soc.* **1996**, *118*, 2039–2046.

[172] A. J. Arduengo, H. V. R. Dias, J. C. Calabrese, F. Davidson, *Inorg. Chem.* **1993**, *32*, 1541–1542.

[173] P. A. Rupar, V. N. Staroverov, P. J. Ragogna, K. M. Baines, *J. Am. Chem. Soc.* **2007**, *129*, 15138–15139.

[174] A. Sidiropoulos, C. Jones, A. Stasch, S. Klein, G. Frenking, *Angew. Chem. Int. Ed.* **2009**, *48*, 9701–9704.

[175] K. C. Thimer, S. M. I. Al-Rafia, M. J. Ferguson, R. McDonald, E. Rivard, *Chem. Commun.* **2009**, *112*, 7119–7121.

[176] P. A. Rupar, M. C. Jennings, K. M. Baines, *Organometallics* **2008**, *27*, 5043–5051.

[177] A. Rit, J. Campos, H. Niu, S. Aldridge, *Nat. Chem.* **2016**, *8*, 1022–1026.

[178] P. A. Rupar, M. C. Jennings, P. J. Ragogna, K. M. Baines, *Organometallics* **2007**, *26*, 4109–4111.

[179] A. Jana, V. Huch, H. S. Rzepa, D. Scheschkewitz, *Angew. Chem. Int. Ed.* **2015**, *54*, 289–292.

[180] J. A. Kelly, M. Juckel, T. J. Hadlington, I. Fernández, G. Frenking, C. Jones, *Chem. - A Eur. J.* **2019**, *25*, 2773–2785.

[181] T. K. Purkait, A. K. Swarnakar, G. B. De Los Reyes, F. A. Hegmann, E. Rivard, J. G. C. Veinot, *Nanoscale* **2015**, *7*, 2241–2244.

[182] A. Rodgers, S. R. Stobart, *J. Chem. Soc. Chem. Commun.* **1976**, 52–53.

[183] S. R. Stobart, M. Rowen, J. Hollander, J. Youngs, *J. Chem. Soc. Chem. Commun.* **1979**, 911–912.

[184] T. Hascall, K. Pang, G. Parkin, *Tetrahedron* **2007**, *63*, 10826–10833.

[185] A. Akkari, J. J. Byrne, I. Saur, G. Rima, H. Gornitzka, J. Barrau, *J. Organomet. Chem.* **2001**, *622*, 190–198.

[186] A. E. Ayers, T. M. Klapötke, H. V. Rasika Dias, *Inorg. Chem.* **2001**, *40*, 1000–1005.

[187] Y. Ding, H. Hao, H. W. Roesky, M. Noltemeyer, H.-G. Schmidt, *Organometallics* **2001**, *20*, 4806–4811.

[188] Y. Ding, H. W. Roesky, M. Noltemeyer, H.-G. Schmidt, P. P. Power, *Organometallics* **2001**, *20*, 1190–1194.

[189] Y. Ding, Q. Ma, H. W. Roesky, R. Herbst-Irmer, I. Usón, M. Noltemeyer, H.-G. Schmidt, *Organometallics* **2002**, *21*, 5216–5220.

[190] L. W. Pineda, V. Jancik, H. W. Roesky, D. Neculai, A. M. Neculai, *Angew. Chem. Int. Ed.* **2004**, *43*, 1419–1421.

[191] L. W. Pineda, V. Jancik, K. Starke, R. B. Oswald, H. W. Roesky, *Angew. Chem. Int. Ed.* **2006**, *45*, 2602–2605.

[192] W.-P. Leung, C. W. So, K. H. Chong, K. W. Kan, H. S. Chan, T. C. W. Mak, *Organometallics* **2006**, *25*, 2851–2858.

[193] Y. Qin, G. Zheng, Y. Guo, F. Gao, J. Ma, W. Sun, G. Xie, S. Chen, Y. Wang, H. Sun, A. Li, W. Wang, *Chem. - A Eur. J.* **2020**, *5*, 6122–6125.

[194] D. A. Atwood, V. O. Atwood, A. H. Cowley, J. L. Atwood, E. Román, *Inorg. Chem.* **1992**, *31*, 3871–3872.

[195] S. P. Green, C. Jones, P. C. Junk, K. A. Lippert, A. Stasch, *Chem. Commun.* **2006**, *174*, 3978–3980.

[196] H. V. R. Dias, Z. Wang, *J. Am. Chem. Soc.* **1997**, *119*, 4650–4655.

[197] Y. Yang, N. Zhao, H. Zhu, H. W. Roesky, *Organometallics* **2012**, *31*, 1958–1964.

[198] J. Barrau, G. Rima, *Coord. Chem. Rev.* **1998**, *178–180*, 593–622.

[199] M. Driess, N. Dona, K. Merz, *Dalton Trans.* **2004**, *3*, 3176–3177.

[200] N. N. Zemlyansky, I. V. Borisova, M. G. Kuznetsova, V. N. Khrustalev, Y. A. Ustynyuk, M. S.

Nechaev, V. V. Lunin, J. Barrau, G. Rima, *Organometallics* **2003**, *22*, 1675–1681.

[201] N. N. Zemlyansky, I. V. Borisova, V. N. Khrustalev, M. Y. Antipin, Y. A. Ustynyuk, M. S. Nechaev, V. V. Lunin, *Organometallics* **2003**, *22*, 5441–5446.

[202] V. N. Khrustalev, I. A. Portnyagin, N. N. Zemlyansky, I. V. Borisova, M. S. Nechaev, Y. A. Ustynyuk, M. Y. Antipin, V. Lunin, *J. Organomet. Chem.* **2005**, *690*, 1172–1177.

[203] P. Jutzi, S. Keitemeyer, B. Neumann, A. Stammler, H.-G. Stammler, *Organometallics* **2001**, *20*, 42–46.

[204] C. Drost, P. B. Hitchcock, M. F. Lappert, L. J.-M. Pierssens, *Chem. Commun.* **1997**, *2*, 1141–1142.

[205] C. Drost, P. B. Hitchcock, M. F. Lappert, *Organometallics* **1998**, *17*, 3838–3840.

[206] J. V. Scibelli, M. D. Curtis, *J. Am. Chem. Soc.* **1973**, *95*, 924–925.

[207] M. Grenz, E. Hahn, W.-W. du Mont, J. Pickardt, *Angew. Chem. Int. Ed. Engl.* **1984**, *23*, 61–63.

[208] D. H. Harris, M. F. Lappert, *J. Chem. Soc. Chem. Commun.* **1974**, 895–896.

[209] D. H. Harris, M. F. Lappert, J. B. Pedley, G. J. Sharp, *J. Chem. Soc. Dalton Trans.* **1976**, 945–950.

[210] T. Fjeldberg, H. Hope, M. F. Lappert, P. P. Power, A. J. Thorne, *J. Chem. Soc. Chem. Commun.* **1983**, 639–641.

[211] R. W. Chorley, P. B. Hitchcock, B. S. Jolly, M. F. Lappert, G. A. Lawless, *J. Chem. Soc. Chem. Commun.* **1991**, 1302–1303.

[212] M. J. S. Gynane, D. H. Harris, M. F. Lappert, P. P. Power, P. Rivière, M. Rivière-Baudet, *J. Chem. Soc. Dalton Trans.* **1977**, *1*, 2004–2009.

[213] M. F. Lappert, P. P. Power, M. J. Slade, L. Hedberg, K. Hedberg, V. Schomaker, *J. Chem. Soc. Chem. Commun.* **1979**, 369–370.

[214] M. F. Lappert, M. J. Slade, J. L. Atwood, M. J. Zaworotko, *J. Chem. Soc. Chem. Commun.* **1980**, 621–622.

[215] D. E. Goldberg, D. H. Harris, M. F. Lappert, K. M. Thomas, *J. Chem. Soc. Chem. Commun.* **1976**, *227*, 261.

[216] P. J. Davidson, D. H. Harris, M. F. Lappert, *J. Chem. Soc. Dalton Trans.* **1976**, *21*, 2268–2274.

[217] P. B. Hitchcock, M. F. Lappert, S. J. Miles, A. J. Thorne, *J. Chem. Soc. Chem. Commun.* **1984**, 480–482.

[218] T. Fjeldberg, A. Haaland, B. E. R. Schilling, H. V. Volden, M. F. Lappert, A. J. Thorne, *J. Organomet. Chem.* **1985**, *280*, 43–46.

[219] T. Fjeldberg, A. Haaland, B. E. R. Schilling, M. F. Lappert, A. J. Thorne, *J. Chem. Soc. Dalton Trans.* **1986**, 1551–1556.

[220] P. Jutzi, A. Becker, H.-G. Stammler, B. Neumann, *Organometallics* **1991**, *10*, 1647–1648.

[221] M. Kira, S. Ishida, T. Iwamoto, M. Ichinohe, C. Kabuto, L. Ignatovich, H. Sakurai, *Chem. Lett.* **1999**, 263–264.

[222] P. B. Hitchcock, M. F. Lappert, A. J. Thorne, *J. Chem. Soc. Chem. Commun.* **1990**, 1587–1589.

[223] B. Cetinkaya, I. Gümrükcü, M. F. Lappert, J. L. Atwood, R. Shakir, *J. Am. Chem. Soc.* **1980**, *102*, 2088–2089.

[224] P. B. Hitchcock, M. F. Lappert, B. J. Samways, E. L. Weinberg, *J. Chem. Soc. Chem. Commun.* **1983**, 1492–1494.

[225] M. Driess, R. Janoschek, H. Pritzkow, S. Rell, U. Winkler, *Angew. Chem. Int. Ed. Engl.* **1995**, *34*, 1614–1616.

[226] B. Gehrhus, P. B. Hitchcock, M. F. Lappert, *Angew. Chem. Int. Ed. Engl.* **1997**, *36*, 2514–2516.

[227] L. Lange, B. Meyer, W.-W. du Mont, *J. Organomet. Chem.* **1987**, *329*, C17–C20.

[228] K. Mochida, A. Fujii, N. Tsuchiya, K. Tohji, Y. Udagawa, *Organometallics* **1987**, *6*, 1811–1812.

[229] P. Jutzi, H. Schmidt, B. Neumann, H.-G. Stammler, *Organometallics* **1996**, *15*, 741–746.

[230] N. P. Toltl, W. J. Leigh, G. M. Kollegger, W. G. Stibbs, K. M. Baines, *Organometallics* **1996**, *15*, 3732–3736.

[231] J. E. Bender IV, M. M. B. Holl, J. W. Kampf, *Organometallics* **1997**, *16*, 2743–2745.

[232] R. S. Simons, L. Pu, M. M. Olmstead, P. P. Power, *Organometallics* **1997**, *16*, 1920–1925.

[233] G. L. Wegner, R. J. F. Berger, A. Schier, H. Schmidbaur, *Organometallics* **2001**, *20*, 418–423.

[234] G. H. Spikes, Y. Peng, J. C. Fettinger, P. P. Power, *Z. Anorg. Allg. Chem.* **2006**, *632*, 1005–1010.

[235] L. Pu, M. M. Olmstead, P. P. Power, B. Schiemenz, *Organometallics* **1998**, *17*, 5602–5606.

[236] L. Pu, A. D. Phillips, A. F. Richards, M. Stender, R. S. Simons, M. M. Olmstead, P. P. Power, *J. Am. Chem. Soc.* **2003**, *125*, 11626–11636.

[237] P. Jutzi, C. Leue, *Organometallics* **1994**, *13*, 2898–2899.

[238] J. Li, A. Stasch, C. Schenk, C. Jones, *Dalton Trans.* **2011**, *40*, 10448–10456.

[239] T. J. Hadlington, B. Schwarze, E. I. Izgorodina, C. Jones, *Chem. Commun.* **2015**, *51*, 6854–6857.

[240] M. Veith, M. Grosser, *Zeitschrift für Naturforsch.* **1982**, *37b*, 1375–1381.

[241] J. Pfeiffer, W. Maringgele, M. Noltemeyer, A. Meller, *Chem. Ber.* **1989**, *122*, 245–252.

[242] W. A. Herrmann, M. Denk, J. Behm, W. Scherer, F. Klingan, H. Bock, B. Solouki, M. Wagner, *Angew. Chem. Int. Ed. Engl.* **1992**, *31*, 1485–1488.

[243] J. Heinicke, A. Oprea, M. K. Kindermann, T. Karpati, L. Nyulászi, T. Veszprémi, *Chem. - A Eur. J.* **1998**, *4*, 541–545.

[244] J. Heinicke, A. Oprea, *Heteroat. Chem.* **1998**, *9*, 439–444.

[245] O. Kühl, P. Lönnecke, J. Heinicke, *Polyhedron* **2001**, *20*, 2215–2222.

[246] Y. Li, K. C. Mondal, P. Stollberg, H. Zhu, H. W. Roesky, R. Herbst-Irmer, D. Stalke, H. Fliegl, *Chem. Commun.* **2014**, *50*, 3356–3358.

[247] I. L. Fedushkin, A. A. Skatova, V. A. Chudakova, N. M. Khvoinova, A. Y. Baurin, S. Dechert, M. Hummert, H. Schumann, *Organometallics* **2004**, *23*, 3714–3718.

[248] M. Driess, S. Yao, M. Brym, C. Van Wüllen, *Angew. Chem. Int. Ed.* **2006**, *45*, 4349–4352.

[249] M. Veith, R. Lisowsky, *Angew. Chem. Int. Ed. Engl.* **1988**, *27*, 1087–1089.

[250] S. Kobayashi, S. Cao, *Chem. Lett.* **1994**, 941–944.

[251] H. Braunschweig, P. B. Hitchcock, M. F. Lappert, L. J.-M. Pierssens, *Angew. Chem. Int. Ed. Engl.* **1994**, *33*, 1156–1158.

[252] J.-T. Ahlemann, H. W. Roesky, R. Murugavel, E. Parisini, M. Noltemeyer, H.-G. Schmidt, O. Miillef, R. Herbst-Irmer, L. N. Markovskii, Y. G. Shermolovich, *Chem. Ber.* **1997**, *130*, 1113–1121.

[253] A. V. Zabula, F. E. Hahn, T. Pape, A. Hepp, *Organometallics* **2007**, *26*, 1972–1980.

[254] F. E. Hahn, A. V. Zabula, T. Pape, A. Hepp, *Z. Anorg. Allg. Chem.* **2008**, *634*, 2397–2401.

[255] C. Cui, M. M. Olmstead, J. C. Fettinger, G. H. Spikes, P. P. Power, *J. Am. Chem. Soc.* **2005**, *127*, 17530–17541.

[256] T. J. Hadlington, J. Li, M. Hermann, A. Davey, G. Frenking, C. Jones, *Organometallics* **2015**, *34*, 3175–3185.

[257] T. Probst, O. Steigelmunn, J. Riede, H. Schmidbaur, *Angew. Chem. Int. Ed.* **1990**, *29*, 1397–1398.

[258] P. A. Rupar, R. Bandyopadhyay, B. F. T. Cooper, M. R. Stinchcombe, P. J. Ragogna, C. L. B. Macdonald, K. M. Baines, *Angew. Chem. Int. Ed.* **2009**, *48*, 5155–5158.

[259] F. Cheng, J. M. Dyke, F. Ferrante, A. L. Hector, W. Levason, G. Reid, M. Webster, W. Zhang, *Dalton Trans.* **2010**, *39*, 847–856.

[260] A. P. Singh, H. W. Roesky, E. Carl, D. Stalke, J. P. Demers, A. Lange, *J. Am. Chem. Soc.*

2012, *134*, 4998–5003.

[261] Y. Xiong, S. Yao, S. Inoue, A. Berkefeld, M. Driess, *Chem. Commun.* **2012**, *48*, 12198–12200.

[262] Y. Xiong, S. Yao, G. Tan, S. Inoue, M. Driess, *J. Am. Chem. Soc.* **2013**, *135*, 5004–5007.

[263] B. Su, R. Ganguly, Y. Li, R. Kinjo, *Angew. Chem. Int. Ed.* **2014**, *53*, 13106–13109.

[264] Y. P. Zhou, M. Karni, S. Yao, Y. Apeloig, M. Driess, *Angew. Chem. Int. Ed.* **2016**, *55*, 15096–15099.

[265] P. A. Rupar, V. N. Staroverov, K. M. Baines, *Science* **2009**, *322*, 1360–1363.

[266] A. E. Ayers, H. V. R. Dias, *Inorg. Chem.* **2002**, *41*, 3259–3268.

[267] J. Li, C. Schenk, F. Winter, H. Scherer, N. Trapp, A. Higelin, S. Keller, R. Pöttgen, I. Krossing, C. Jones, *Angew. Chem.* **2012**, *124*, 9695–9699.

[268] K. Inomata, T. Watanabe, H. Tobita, *J. Am. Chem. Soc.* **2014**, *136*, 14341–14344.

[269] A. Rit, R. Tirfoin, S. Aldridge, *Angew. Chem.* **2016**, *128*, 386–390.

[270] R. J. Mangan, A. Rit, C. P. Sindlinger, R. Tirfoin, J. Campos, J. Hicks, K. E. Christensen, H. Niu, S. Aldridge, *Chem. - A Eur. J.* **2020**, *26*, 306–315.

[271] M. Stender, A. D. Phillips, P. P. Power, *Inorg. Chem.* **2001**, *40*, 5314–5315.

[272] W. Wang, S. Yao, C. Van Wüllen, M. Driess, *J. Am. Chem. Soc.* **2008**, *130*, 9640–9641.

[273] W. D. Woodul, E. Carter, R. Müller, A. F. Richards, A. Stasch, M. Kaupp, D. M. Murphy, M. Driess, C. Jones, *J. Am. Chem. Soc.* **2011**, *133*, 10074–10077.

[274] M. M. Siddiqui, S. K. Sarkar, S. Sinhababu, P. N. Ruth, R. Herbst-Irmer, D. Stalke, M. Ghosh, M. Fu, L. Zhao, D. Casanova, G. Frenking, B. Schwederski, W.Kaim, H. W. Roesky, *J. Am. Chem. Soc.* **2019**, *141*, 1908–1912.

[275] M. M. Siddiqui, S. Sinhababu, S. Dutta, S. Kundu, P. N. Ruth, A. Münch, R. Herbst-Irmer, D. Stalke, D. Koley, H. W. Roesky, *Angew. Chem. Int. Ed.* **2018**, *57*, 11776–11780.

[276] A. J. Arduengo, D. A. Dixon, N. L. Jones, H. Bock, H. Chen, M. Denk, R. West, J. C. Green, M. Wagner, W. A. Herrmann, *J. Am. Chem. Soc.* **1994**, *116*, 6641–6649.

[277] S. Vepřek, J. Prokop, F. Glatz, R. Merica, F.-R. Klingan, W. A. Herrmann, *Chem. Mater.* **1996**, *8*, 825–831.

[278] T. Gans-Eichler, D. Gudat, K. Nättinen, M. Nieger, *Chem. - A Eur. J.* **2006**, *12*, 1162–1173.

[279] G. Frenking, R. Tonner, S. Klein, N. Takagi, T. Shimizu, A. Krapp, K. K. Pandey, P. Parameswaran, *Chem. Soc. Rev.* **2014**, *43*, 5106–5139.

[280] T. Chu, L. Belding, A. Van Der Est, T. Dudding, I. Korobkov, G. I. Nikonov, *Angew. Chem. Int. Ed.* **2014**, *53*, 2711–2715.

[281] Y. Xiong, S. Yao, M. Karni, A. Kostenko, A. Burchert, Y. Apeloig, M. Driess, *Chem. Sci.* **2016**, *7*, 5462–5469.

[282] S. Yao, Y. Xiong, M. Driess, *Acc. Chem. Res.* **2017**, *50*, 2026–2037.

[283] P. K. Majhi, T. Sasamori, *Chem. - A Eur. J.* **2018**, *24*, 9441–9455.

[284] G. Trinquier, *J. Am. Chem. Soc.* **1990**, *112*, 2130–2137.

[285] G. Trinquier, *J. Am. Chem. Soc.* **1991**, *113*, 144–151.

[286] P. P. Power, *Organometallics* **2020**, DOI 10.1021/acs.organomet.0c00200.

[287] L. Pauling, *Proc. Natl. Acad. Sci.* **1983**, *80*, 3871–3872.

[288] H. B. Wedler, P. Wendelboe, P. P. Power, *Organometallics* **2018**, *37*, 2929–2936.

[289] G. Trinquier, J.-P. Malrieu, P. Rivière, *J. Am. Chem. Soc.* **1982**, *104*, 4529–4533.

[290] S. Nagase, T. Kudo, *J. Mol. Struct. THEOCHEM* **1983**, *103*, 35–44.

[291] E. A. Carter, W. A. Goddard, *J. Phys. Chem.* **1986**, *90*, 998–1001.

[292] G. Trinquier, J.-P. Malrieu, *J. Am. Chem. Soc.* **1987**, *109*, 5303–5315.

[293] J.-P. Malrieu, G. Trinquier, *J. Am. Chem. Soc.* **1989**, *111*, 5916–5921.

[294] M. Karni, Y. Apeloig, *J. Am. Chem. Soc.* **1990**, *112*, 8589–8590.

[295] G. Trinquier, J. C. Barthelat, *J. Am. Chem. Soc.* **1990**, *112*, 9121–9130.

[296] H. Huber, E. P. Kündig, G. A. Ozin, A. Vander Voet, *Can. J. Chem.* **1974**, *52*, 95–99.

[297] J. Kalcher, A. F. Sax, *J. Mol. Struct. THEOCHEM* **1992**, *253*, 287–302.

[298] C. Liang, L. C. Allen, *J. Am. Chem. Soc.* **1990**, *112*, 1039–1041.

[299] S. Samavat, R. Ghiasi, B. Mohtat, *J. Chinese Chem. Soc.* **2020**, 1–8.

[300] J. D. Guo, D. J. Liptrot, S. Nagase, P. P. Power, *Chem. Sci.* **2015**, *6*, 6235–6244.

[301] R. Sedlak, O. A. Stasyuk, C. Fonseca Guerra, J. Řezáč, A. Růžička, P. Hobza, *J. Chem. Theory Comput.* **2016**, *12*, 1696–1704.

[302] S. Masamune, Y. Hanzawa, D. J. Williams, *J. Am. Chem. Soc.* **1982**, *104*, 6136–6137.

[303] J. T. Snow, S. Murakami, S. Masamune, D. J. Williams, *Tetrahedron Lett.* **1984**, *25*, 4191–4194.

[304] W. Ando, T. Tsumuraya, *J. Chem. Soc. Chem. Commun.* **1989**, 770–772.

[305] W. Ando, H. Itoh, T. Tsumuraya, H. Yoshida, *Organometallics* **1988**, *7*, 1880–1882.

[306] W. Ando, H. Itoh, T. Tsumuraya, *Organometallics* **1989**, *8*, 2759–2766.

[307] W. Ando, T. Tsumuraya, A. Sekiguchi, *Chem. Lett.* **1987**, 317–318.

[308] J. Park, S. A. Batcheller, S. Masamune, *J. Organomet. Chem.* **1989**, *367*, 39–45.

[309] H. Schäfer, W. Saak, M. Weidenbruch, *Organometallics* **1999**, *18*, 3159–3163.

[310] G. Ramaker, W. Saak, D. Haase, M. Weidenbruch, *Organometallics* **2003**, *22*, 5212–5216.

[311] T. Sasamori, H. Miyamoto, H. Sakai, Y. Furukawa, N. Tokitoh, *Organometallics* **2012**, *31*, 3904–3910.

[312] S. A. Batcheller, T. Tsumuraya, O. Tempkin, W. M. Davis, S. Masamune, *J. Am. Chem. Soc.* **1990**, *112*, 9394–9395.

[313] M. Weidenbruch, M. Stürmann, H. Kilian, S. Pohl, W. Saak, *Chem. Ber.* **1997**, *130*, 735–738.

[314] B. Pampuch, W. Saak, M. Weidenbruch, *J. Organomet. Chem.* **2006**, *691*, 3540–3544.

[315] K. Kishikawa, N. Tokitoh, R. Okazaki, *Chem. Lett.* **1998**, 239–240.

[316] N. Tokitoh, K. Kishikawa, R. Okazaki, T. Sasamori, N. Nakata, N. Takeda, *Polyhedron* **2002**, *21*, 563–577.

[317] A. Schäfer, W. Saak, M. Weidenbruch, H. Marsmann, G. Henkel, *Chem. Ber.* **1997**, *130*, 1733–1737.

[318] A. Schäfer, W. Saak, M. Weidenbruch, *Z. Anorg. Allg. Chem.* **1998**, *624*, 1405–1408.

[319] M. Kira, T. Iwamoto, T. Maruyama, C. Kabuto, H. Sakurai, *Organometallics* **1996**, *15*, 3767–3769.

[320] A. Sekiguchi, R. Izumi, S. Ihara, M. Ichinohe, V. Y. Lee, *Angew. Chem. Int. Ed.* **2002**, *41*, 1598–1600.

[321] V. Y. Lee, K. McNeice, Y. Ito, A. Sekiguchi, *Chem. Commun.* **2011**, *47*, 3272–3274.

[322] V. Y. Lee, K. McNiece, Y. Ito, A. Sekiguchi, N. Geinik, J. Y. Becker, *Heteroat. Chem.* **2014**, *25*, 313–319.

[323] R. R. Aysin, S. S. Bukalov, L. A. Leites, V. Y. Lee, A. Sekiguchi, *J. Organomet. Chem.* **2019**, *892*, 18–23.

[324] Y. Apeloig, D. Bravo-Zhivotovskii, I. Zharov, V. Panov, W. J. Leigh, G. W. Sluggett, *J. Am. Chem. Soc.* **1998**, *120*, 1398–1404.

[325] M. Zirngast, M. Flock, J. Baumgartner, C. Marschner, *J. Am. Chem. Soc.* **2009**, *131*, 15952–15962.

[326] H. Lei, J. C. Fettinger, P. P. Power, *Organometallics* **2010**, *29*, 5585–5590.

[327] A. F. Richards, A. D. Phillips, M. M. Olmstead, P. P. Power, *J. Am. Chem. Soc.* **2003**, *125*, 3204–3205.

[328] G. H. Spikes, J. C. Fettinger, P. P. Power, *J. Am. Chem. Soc.* **2005**, *3173*, 12232–12233.

[329] T. Sasamori, Y. Sugiyama, N. Takeda, N. Tokitoh, *Organometallics* **2005**, *24*, 3309–3314.

[330] T. Sugahara, J.-D. Guo, T. Sasamori, Y. Karatsu, Y. Furukawa, A. E. Ferao, S. Nagase, N. Tokitoh, *Bull. Chem. Soc. Jpn.* **2016**, *89*, 1375–1384.

[331] N. Hayakawa, T. Sugahara, Y. Numata, H. Kawaai, K. Yamatani, S. Nishimura, S. Goda, Y. Suzuki, T. Tanikawa, H. Nakai, D. Hashizume, T. Sasamori, M. Tokitoh, T. Matsuo, *Dalton Trans.* **2018**, *47*, 814–822.

[332] K. Suzuki, Y. Numata, N. Fujita, N. Hayakawa, T. Tanikawa, D. Hashizume, K. Tamao, H. Fueno, K. Tanaka, T. Matsuo, *Chem. Commun.* **2018**, *54*, 2200–2203.

[333] S. M. I. Al-Rafia, M. R. Momeni, M. J. Ferguson, R. McDonald, A. Brown, E. Rivard, *Organometallics* **2013**, *32*, 6658–6665.

[334] S. M. I. Al-Rafia, M. R. Momeni, R. McDonald, M. J. Ferguson, A. Brown, E. Rivard, *Angew. Chem. Int. Ed.* **2013**, *52*, 6390–6395.

[335] O. T. Summerscales, C. A. Caputo, C. E. Knapp, J. C. Fettinger, P. P. Power, *J. Am. Chem. Soc.* **2012**, *134*, 14595–14603.

[336] D. Nieder, L. Klemmer, Y. Kaiser, V. Huch, D. Scheschkewitz, *Organometallics* **2018**, *37*, 632–635.

[337] H. Schäfer, W. Saak, M. Weidenbruch, *Angew. Chem. Int. Ed.* **2000**, *39*, 3703–3705.

[338] M. Kobayashi, T. Matsuo, T. Fukunaga, D. Hashizume, H. Fueno, K. Tanaka, K. Tamao, *J. Am. Chem. Soc.* **2010**, *132*, 15162–15163.

[339] K. Tamao, M. Kobayashi, T. Matsuo, S. Furukawa, H. Tsuji, *Chem. Commun.* **2012**, *48*, 1030.

[340] N. M. Obeid, L. Klemmer, D. Maus, M. Zimmer, J. Jeck, I. Bejan, A. J. P. White, V. Huch, G. Jung, D. Scheschkewitz, *Dalton Trans.* **2017**, *46*, 8839–8848.

[341] A. Fukazawa, Y. Li, S. Yamaguchi, H. Tsuji, K. Tamao, *J. Am. Chem. Soc.* **2007**, *129*, 14164–14165.

[342] I. Bejan, D. Scheschkewitz, *Angew. Chem. Int. Ed.* **2007**, *46*, 5783–5786.

[343] L. Li, T. Matsuo, D. Hashizume, H. Fueno, K. Tanaka, K. Tamao, *J. Am. Chem. Soc.* **2015**, *137*, 15026–15035.

[344] V. A. Wright, D. P. Gates, *Angew. Chem. Int. Ed.* **2002**, *41*, 2389–2392.

[345] R. C. Smith, J. D. Protasiewicz, *J. Am. Chem. Soc.* **2004**, *126*, 2268–2269.

[346] A. Sekiguchi, H. Yamazaki, C. Kabuto, H. Sakurai, S. Nagase, *J. Am. Chem. Soc.* **1995**, *117*, 8025–8026.

[347] T. Sasamori, T. Sugahara, T. Agou, K. Sugamata, J.-D. Guo, S. Nagase, N. Tokitoh, *Chem. Sci.* **2015**, *6*, 5526–5530.

[348] V. Y. Lee, K. Takanashi, M. Ichinohe, A. Sekiguchi, *J. Am. Chem. Soc.* **2003**, *125*, 6012–6013.

[349] V. Y. Lee, Y. Ito, H. Yasuda, K. Takanashi, A. Sekiguchi, *J. Am. Chem. Soc.* **2011**, *133*, 5103–5108.

[350] T. Sugahara, J. D. Guo, T. Sasamori, S. Nagase, N. Tokitoh, *Chem. Commun.* **2018**, *54*, 519–522.

[351] G. Ramaker, A. Schäfer, W. Saak, M. Weidenbruch, *Organometallics* **2003**, *22*, 1302–1304.

[352] J. Hlina, J. Baumgartner, C. Marschner, L. Albers, T. Müller, V. V. Jouikov, *Chem. - A Eur. J.* **2014**, *20*, 9357–9366.

[353] T. Sasamori, T. Sugahara, T. Agou, J.-D. Guo, S. Nagase, R. Streubel, N. Tokitoh, *Organometallics* **2015**, *34*, 2106–2109.

[354] K. M. Baines, J. A. Cooke, J. J. Vittal, *J. Chem. Soc. Chem. Commun.* **1992**, 1484–1485.

[355] K. M. Baines, J. A. Cooke, C. E. Dixon, H. W. Liu, M. R. Netherton, *Organometallics* **1994**, *13*, 631–634.

[356] C. E. Dixon, M. R. Netherton, K. M. Baines, *J. Am. Chem. Soc.* **1998**, *120*, 10365–10371.

[357] M. S. Samuel, M. C. Jennings, K. M. Baines, *Organometallics* **2001**, *20*, 590–592.

[358] K. L. Fujdala, D. W. K. Gracey, E. F. Wong, K. M. Baines, *Can. J. Chem.* **2002**, *80*, 1387–1392.

[359] S. A. Batcheller, S. Masamune, *Tetrahedron Lett.* **1988**, *29*, 3383–3384.

[360] M. S. Samuel, K. M. Baines, *J. Am. Chem. Soc.* **2003**, *125*, 12702–12703.

[361] K. L. Hurni, K. M. Baines, *Chem. Commun.* **2011**, *47*, 8382.

[362] K. K. Milnes, L. C. Pavelka, K. M. Baines, *Chem. Soc. Rev.* **2016**, *45*, 1019–1035.

[363] T. Tsumuraya, S. Sato, W. Ando, *Organometallics* **1990**, *9*, 2061–2067.

[364] N. Y. Tashkandi, F. Parsons, J. Guo, K. M. Baines, *Angew. Chem. Int. Ed.* **2015**, *54*, 1612–1615.

[365] T. Tsumuraya, Y. Kabe, W. Ando, *J. Chem. Soc. Chem. Commun.* **1990**, 1159–1160.

[366] T. Sugahara, T. Sasamori, N. Tokitoh, *Chem. Lett.* **2018**, *47*, 719–722.

[367] A. F. Richards, M. Brynda, P. P. Power, *J. Am. Chem. Soc.* **2004**, *126*, 10530–10531.

[368] M. Weidenbruch, S. Willms, W. Saak, G. Henkel, *Angew. Chem. Int. Ed. Engl.* **1997**, *36*, 2503–2504.

[369] D. Scheschkewitz, *Angew. Chem. Int. Ed.* **2004**, *43*, 2965–2967.

[370] M. Ichinohe, K. Sanuki, S. Inoue, A. Sekiguchi, *Organometallics* **2004**, *23*, 3088–3090.

[371] S. Inoue, M. Ichinohe, A. Sekiguchi, *Chem. Lett.* **2005**, *34*, 1564–1565.

[372] R. Kinjo, M. Ichinohe, A. Sekiguchi, *J. Am. Chem. Soc.* **2007**, *129*, 26–27.

[373] H. Yasuda, V. Y. Lee, A. Sekiguchi, *J. Am. Chem. Soc.* **2009**, *131*, 6352–6353.

[374] T. Iwamoto, M. Kobayashi, K. Uchiyama, S. Sasaki, S. Nagendran, H. Isobe, M. Kira, *J. Am. Chem. Soc.* **2009**, *131*, 3156–3157.

[375] M. Tian, J. Zhang, H. Yang, C. Cui, *J. Am. Chem. Soc.* **2020**, 0–4.

[376] T.-L. Nguyen, D. Scheschkewitz, *J. Am. Chem. Soc.* **2005**, *127*, 10174–10175.

[377] M. J. Cowley, K. Abersfelder, A. J. P. White, M. Majumdar, D. Scheschkewitz, *Chem. Commun.* **2012**, *48*, 6595.

[378] K. Abersfelder, T.-L. Nguyen, D. Scheschkewitz, *Z. Anorg. Allg. Chem.* **2009**, *635*, 2093–2098.

[379] M. Hartmann, A. Haji-Abdi, K. Abersfelder, P. R. Haycock, A. J. P. White, D. Scheschkewitz, *Dalton Trans.* **2010**, *39*, 9288–9295.

[380] I. Bejan, D. Güclü, S. Inoue, M. Ichinohe, A. Sekiguchi, D. Scheschkewitz, *Angew. Chem. Int. Ed.* **2007**, *46*, 3349–3352.

[381] J. Jeck, I. Bejan, A. J. P. White, D. Nied, F. Breher, D. Scheschkewitz, *J. Am. Chem. Soc.* **2010**, *132*, 17306–17315.

[382] A. Meltzer, M. Majumdar, A. J. P. White, V. Huch, D. Scheschkewitz, *Organometallics* **2013**, *32*, 6844–6850.

[383] M. Majumdar, I. Bejan, V. Huch, A. J. P. White, G. R. Whittell, A. Schäfer, I. Manners, D. Scheschkewitz, *Chem. - A Eur. J.* **2014**, *20*, 9225–9229.

[384] I. Bejan, S. Inoue, M. Ichinohe, A. Sekiguchi, D. Scheschkewitz, *Chem. - A Eur. J.* **2008**, *14*, 7119–7122.

[385] K. Abersfelder, D. Scheschkewitz, *J. Am. Chem. Soc.* **2008**, *130*, 4114–4121.

[386] K. Abersfelder, A. J. P. White, H. S. Rzepa, D. Scheschkewitz, *Science* **2010**, *327*, 564–566.

[387] P. Willmes, M. J. Cowley, M. Hartmann, M. Zimmer, V. Huch, D. Scheschkewitz, *Angew. Chem. Int. Ed.* **2014**, *53*, 2216–2220.

[388] P. Willmes, L. Junk, V. Huch, C. B. Yildiz, D. Scheschkewitz, *Angew. Chem. Int. Ed.* **2016**, *55*, 10913–10917.

[389] Y. Heider, P. Willmes, D. Mühlhausen, L. Klemmer, M. Zimmer, V. Huch, D. Scheschkewitz, *Angew. Chem. Int. Ed.* **2019**, *58*, 1939–1944.

[390] X. Wang, L. Andrews, G. P. Kushto, *J. Phys. Chem. A* **2002**, *106*, 5809–5816.

[391] R. S. Grev, B. J. Deleeuw, H. F. Schaefer, *Chem. Phys. Lett.* **1990**, *165*, 257–264.

[392] Z. Palágyi, H. F. Schaefer, E. Kapuy, *J. Am. Chem. Soc.* **1993**, *115*, 6901–6903.

[393] Y. Peng, R. C. Fischer, W. A. Merrill, J. Fischer, L. Pu, B. D. Ellis, J. C. Fettinger, R. H. Herber, P. P. Power, *Chem. Sci.* **2010**, *1*, 461–468.

[394] C. Cui, M. M. Olmstead, P. P. Power, *J. Am. Chem. Soc.* **2004**, *126*, 5062–5063.

[395] O. T. Summerscales, J. C. Fettinger, P. P. Power, *J. Am. Chem. Soc.* **2011**, *133*, 11960–11963.

[396] J. D. Queen, A. C. Phung, C. A. Caputo, J. C. Fettinger, P. P. Power, *J. Am. Chem. Soc.* **2020**, *142*, 2233–2237.

[397] Y. Sugiyama, T. Sasamori, Y. Hosoi, Y. Furukawa, N. Takagi, S. Nagase, N. Tokitoh, *J. Am. Chem. Soc.* **2006**, *128*, 1023–1031.

[398] T. Sugahara, J.-D. Guo, T. Sasamori, S. Nagase, N. Tokitoh, *Angew. Chem. Int. Ed.* **2018**, *57*, 3499–3503.

[399] Y. Jung, M. Brynda, P. P. Power, M. Head-Gordon, *J. Am. Chem. Soc.* **2006**, *128*, 7185–7192.

[400] J. Li, C. Schenk, C. Goedecke, G. Frenking, C. Jones, *J. Am. Chem. Soc.* **2011**, *133*, 18622–18625.

[401] K. M. Krebs, D. Hanselmann, H. Schubert, K. Wurst, M. Scheele, L. Wesemann, *J. Am. Chem. Soc.* **2019**, *141*, 3424–3429.

[402] L. Pu, M. O. Senge, M. M. Olmstead, P. P. Power, *J. Am. Chem. Soc.* **1998**, *120*, 12682–12683.

[403] A. F. Richards, M. Brynda, P. P. Power, *Chem. Commun.* **2004**, *4*, 1592–1593.

[404] Y. L. Shan, W. L. Yim, C. W. So, *Angew. Chem. Int. Ed.* **2014**, *53*, 13155–13158.

[405] A. Jana, V. Huch, H. S. Rzepa, D. Scheschkewitz, *Organometallics* **2015**, *34*, 2130–2133.

[406] V. Y. Lee, M. Ichinohe, A. Sekiguchi, N. Takagi, S. Nagase, *J. Am. Chem. Soc.* **2000**, *122*, 9034–9035.

[407] V. Y. Lee, M. Ichinohe, A. Sekiguchi, *J. Am. Chem. Soc.* **2000**, *122*, 12604–12605.

[408] M. Ichinohe, Y. Arai, A. Sekiguchi, N. Takagi, S. Nagase, *Organometallics* **2001**, *20*, 4141–4143.

[409] A. Sekiguchi, R. Izumi, S. Ihara, M. Ichinohe, V. Y. Lee, *Angew. Chem. Int. Ed.* **2002**, *41*, 1598–1600.

[410] M. Igarashi, M. Ichinohe, A. Sekiguchi, *Heteroat. Chem.* **2008**, *19*, 649–653.

[411] T. Iwamoto, J. Okita, N. Yoshida, M. Kira, *Silicon* **2010**, *2*, 209–216.

[412] R. S. Grev, H. F. Schaefer III, K. M. Baines, *J. Am. Chem. Soc.* **1990**, *112*, 9458–9467.

[413] R. S. Grev, H. F. Schaefer, *Organometallics* **1992**, *11*, 3489–3492.

[414] K. M. Baines, J. A. Cooke, *Organometallics* **1992**, *11*, 3487–3488.

[415] S. M. I. Al-Rafia, A. C. Malcolm, R. McDonald, M. J. Ferguson, E. Rivard, *Angew. Chem. Int. Ed.* **2011**, *50*, 8354–8357.

[416] P. O'Leary, J. R. Thomas, H. F. Schaefer, B. J. Duke, B. O'Leary, *Int. J. Quantum Chem.* **1995**, *56*, 593–604.

[417] A. J. Boone, D. H. Magers, J. Leszczyński, *Int. J. Quantum Chem.* **1998**, *70*, 925–932.

[418] A. Jana, V. Huch, D. Scheschkewitz, *Angew. Chem. Int. Ed.* **2013**, *52*, 12179–12182.

[419] K. Abersfelder, D. Güclü, D. Scheschkewitz, *Angew. Chem. Int. Ed.* **2006**, *45*, 1643–1645.

[420] K. Abersfelder, H. Zhao, A. J. P. White, C. Präsang, D. Scheschkewitz, *Z. Anorg. Allg. Chem.* **2015**, *641*, 2051–2055.

[421] H. Zhao, L. Klemmer, M. J. Cowley, M. Majumdar, V. Huch, M. Zimmer, D. Scheschkewitz, *Chem. Commun.* **2018**, *54*, 8399–8402.

[422] D. Nieder, V. Huch, C. B. Yildiz, D. Scheschkewitz, *J. Am. Chem. Soc.* **2016**, *138*, 13996–14005.

[423] C. Ortega-Moo, J. Cervantes, M. A. Mendez-Rojas, K. H. Pannell, G. Merino, *Chem. Phys. Lett.* **2010**, *490*, 1–3.

[424] J. A. Gámez, M. Hermann, G. Frenking, *Z. Anorg. Allg. Chem.* **2013**, *639*, 2493–2501.

[425] V. Y. Lee, R. Kato, M. Ichinohe, A. Sekiguchi, *J. Am. Chem. Soc.* **2005**, *127*, 13142–13143.

[426] Y. Ito, V. Y. Lee, H. Gornitzka, C. Goedecke, G. Frenking, A. Sekiguchi, *J. Am. Chem. Soc.* **2013**, *135*, 6770–6773.

[427] V. Y. Lee, Y. Ito, O. A. Gapurenko, R. M. Minyaev, H. Gornitzka, A. Sekiguchi, *J. Am Chem. Soc.* **2020**, *142*, 16455−16460

[428] M. Kosa, M. Karni, Y. Apeloig, *J. Chem. Theory Comput.* **2006**, *2*, 956–964.

[429] B. Pintér, A. Olasz, K. Petrov, T. Veszprémi, *Organometallics* **2007**, *26*, 3677–3683.

[430] S. Ishida, T. Iwamoto, C. Kabuto, M. Kira, *Nature* **2003**, *421*, 725–727.

[431] T. Iwamoto, H. Masuda, C. Kabuto, M. Kira, *Organometallics* **2005**, *24*, 197–199.

[432] T. Iwamoto, T. Abe, C. Kabuto, M. Kira, *Chem. Commun.* **2005**, 5190–5192.

[433] H. Tanaka, S. Inoue, M. Ichinohe, M. Driess, A. Sekiguchi, *Organometallics* **2011**, *30*, 3475–3478.

[434] T. Sugahara, T. Sasamori, N. Tokitoh, *Angew. Chem. Int. Ed.* **2017**, *56*, 9920–9923.

[435] T. Veszprémi, K. Petrov, C. T. Nguyen, *Organometallics* **2006**, *25*, 1480–1484.

[436] A. Sekiguchi, M. Tsukamoto, M. Ichinohe, *Science* **1997**, *275*, 60–62.

[437] K. McNeice, V. Y. Lee, A. Sekiguchi, *Organometallics* **2011**, *30*, 4796–4797.

[438] A. Sekiguchi, Y. Ishida, N. Fukaya, M. Ichinohe, N. Takagi, S. Nagase, *J. Am. Chem. Soc.* **2002**, *124*, 1158–1159.

[439] A. Jana, M. Majumdar, V. Huch, M. Zimmer, D. Scheschkewitz, *Dalton Trans.* **2014**, *43*, 5175–5181.

[440] K. Leszczyńska, K. Abersfelder, M. Majumdar, B. Neumann, H.-G. Stammler, H. S. Rzepa, P. Jutzi, D. Scheschkewitz, *Chem. Commun.* **2012**, *48*, 7820–7822.

[441] K. Leszczyńska, K. Abersfelder, A. Mix, B. Neumann, H.-G. Stammler, M. J. Cowley, P. Jutzi, D. Scheschkewitz, *Angew. Chem. Int. Ed.* **2012**, *51*, 6785–6788.

[442] H. Zhao, K. Leszczyńska, L. Klemmer, V. Huch, M. Zimmer, D. Scheschkewitz, *Angew. Chem. Int. Ed.* **2018**, *57*, 2445–2449.

[443] A. Jana, I. Omlor, V. Huch, H. S. Rzepa, D. Scheschkewitz, *Angew. Chem. Int. Ed.* **2014**, *53*, 9953–9956.

[444] M. J. Cowley, V. Huch, H. S. Rzepa, D. Scheschkewitz, *Nat. Chem.* **2013**, *5*, 876–879.

[445] D. Nieder, C. B. Yildiz, A. Jana, M. Zimmer, V. Huch, D. Scheschkewitz, *Chem. Commun.* **2016**, *52*, 2799–2802.

[446] M. Ichinohe, N. Fukaya, A. Sekiguchi, *Chem. Lett.* **1998**, 1045–1046.

[447] A. Sekiguchi, N. Fukaya, M. Ichinohe, *Phosphorus. Sulfur. Silicon Relat. Elem.* **1999**, *150*, 59–68.

[448] A. Sekiguchi, N. Fukaya, M. Ichinohe, Y. Ishida, *Eur. J. Inorg. Chem.* **2000**, 1155–1159.

[449] M. M. Olmstead, L. Pu, R. S. Simons, P. P. Power, *Chem. Commun.* **1997**, 1595–1596.

[450] A. Jana, V. Huch, M. Repisky, R. J. F. Berger, D. Scheschkewitz, *Angew. Chem. Int. Ed.* **2014**, *53*, 3514–3518.

[451] Y. Li, K. C. Mondal, J. Labben, H. Zhu, B. Dittrich, I. Purushothaman, P. Parameswaran, H. W. Roesky, *Chem. Commun.* **2014**, *50*, 2986–2989.

[452] K. C. Mondal, S. Roy, B. Dittrich, D. M. Andrada, G. Frenking, H. W. Roesky, *Angew. Chem. Int. Ed.* **2016**, *55*, 3158–3161.

[453] G. Trinquier, C. Jouany, *J. Phys. Chem. A* **1999**, *103*, 4723–4736.

[454] J. L. Buechele, E. Weitz, F. D. Lewis, *J. Am. Chem. Soc.* **1981**, *103*, 3588–3589.

[455] K. A. Nguyen, M. S. Gordon, *J. Am. Chem. Soc.* **1995**, *117*, 3835–3847.

[456] S. Sakai, *Chem. Phys. Lett.* **2000**, *319*, 687–694.

[457] R. Koch, T. Bruhn, M. Weidenbruch, *J. Mol. Struct. THEOCHEM* **2004**, *680*, 91–97.

[458] R. Koch, T. Bruhn, M. Weidenbruch, *J. Mol. Struct. THEOCHEM* **2005**, *714*, 109–115.

[459] T. Kudo, S. Nagase, *J. Phys. Chem.* **1992**, *96*, 9189–9194.

[460] S. Masamune, Y. Kabe, S. Collins, D. J. Williams, R. Jones, *J. Am. Chem. Soc.* **1985**, *107*, 5552–5553.

[461] R. Jones, D. J. Williams, Y. Kabe, S. Masamune, *Angew. Chem. Int. Ed.* **1986**, *25*, 173–174.

[462] K. Ueba-Ohshima, T. Iwamoto, M. Kira, *Organometallics* **2008**, *27*, 320–323.

[463] T. Nukazawa, T. Iwamoto, *J. Am. Chem. Soc.* **2020**, *142*, 9920–9924.

[464] C. B. Yildiz, K. I. Leszczyńska, S. González-Gallardo, M. Zimmer, A. Azizoglu, T. Biskup, C. W. M. Kay, V. Huch, H. S. Rzepa, D. Scheschkewitz, *Angew. Chem. Int. Ed.* **2020**, *59*, 15087−15092.

[465] N. Wiberg, W. Hochmuth, H. Nöth, A. Appel, M. Schmidt-Amelunxen, *Angew. Chem. Int. Ed.* **1995**, *35*, 1333–1334.

[466] H. H. Karsch, G. Baumgartner, S. Gamper, *J. Organomet. Chem.* **1993**, *462*, 3–5.

[467] H.-X. Yeong, H.-W. Xi, Y. Li, S. B. Kunnappilly, B. Chen, K.-C. Lau, H. Hirao, K. H. Lim, C. W. So, *Chem. - A Eur. J.* **2013**, *19*, 14726–14731.

[468] H. X. Yeong, S. H. Zhang, H. W. Xi, J. D. Guo, K. H. Lim, S. Nagase, C. W. So, *Chem. - A Eur. J.* **2012**, *18*, 2685–2691.

[469] V. Y. Lee, K. Takanashi, T. Matsuno, M. Ichinohe, A. Sekiguchi, *J. Am. Chem. Soc.* **2004**, *126*, 4758–4759.

[470] K. Takanashi, V. Y. Lee, M. Ichinohe, A. Sekiguchi, *Eur. J. Inorg. Chem.* **2007**, 5471–5474.

[471] V. Y. Lee, K. Takanashi, M. Ichinohe, A. Sekiguchi, *Angew. Chem. Int. Ed.* **2004**, *43*, 6703–6705.

[472] V. Y. Lee, M. Ichinohe, A. Sekiguchi, *J. Am. Chem. Soc.* **2002**, *124*, 9962–9963.

[473] “Cluster Definiton Oxford Dictionary,” can be found online under https://www.oxfordlearnersdictionaries.com/definition/american_english/cluster_1, **2020**.

[474] F. A. Cotton, *Q. Rev. Chem. Soc.* **1966**, *20*, 389–401.

[475] C. Schenk, A. Schnepf, *Dalton Trans.* **2006**, *3*, 5400–5404.

[476] A. Sekiguchi, C. Kabuto, H. Sakurai, *Angew. Chem. Int. Ed. Engl.* **1989**, *28*, 55–56.

[477] A. Sekiguchi, T. Yatabe, H. Kamatani, C. Kabuto, H. Sakurai, *J. Am. Chem. Soc.* **1992**, *114*, 6260–6262.

[478] A. Schnepf, H. Schnöckel, *Angew. Chem. Int. Ed.* **2002**, *41*, 3532–3554.

[479] A. Schnepf, R. Köppe, *Angew. Chem. Int. Ed.* **2003**, *42*, 911–913.

[480] A. Schnepf, *Angew. Chem. Int. Ed.* **2003**, *42*, 2624–2625.

[481] A. Schnepf, C. Drost, *Dalton Trans.* **2005**, *3*, 3277–3280.

[482] W. Carrillo-Cabrera, R. Cardoso Gil, M. Somer, Ö. Persil, H. G. von Schnering, *Z. Anorg. Allg. Chem.* **2003**, *629*, 601–608.

[483] A. F. Richards, M. Brynda, M. M. Olmstead, P. P. Power, *Organometallics* **2004**, *23*, 2841–2844.

[484] V. Y. Lee, Y. Ito, O. A. Gapurenko, A. Sekiguchi, V. I. Minkin, R. M. Minyaev, H. Gornitzka, *Angew. Chem. Int. Ed.* **2015**, *54*, 5654–5657.

[485] A. F. Richards, H. Hope, P. P. Power, *Angew. Chem.* **2003**, *115*, 4205–4208.

[486] J. Helmer, A. Hepp, F. Lips, *Dalton Trans.* **2020**, *49*, 11843−11850.

[487] K. Koch, A. Schnepf, H. Schnöckel, *Z. Anorg. Allg. Chem.* **2006**, *632*, 1710–1716.

[488] F. Henke, C. Schenk, A. Schnepf, *Dalton Trans.* **2011**, *40*, 6704–6710.

[489] C. Schenk, F. Henke, M. Neumaier, M. Olzmann, H. Schnöckel, A. Schnepf, *Z. Anorg. Allg. Chem.* **2010**, *636*, 1173–1182.

[490] C. Schenk, A. Schnepf, *Chem. Commun.* **2009**, *09*, 3208–3210.

[491] O. Kysliak, A. Schnepf, *Z. Anorg. Allg. Chem.* **2019**, *645*, 335–339.

[492] O. Kysliak, T. Kunz, A. Schnepf, *Eur. J. Inorg. Chem.* **2017**, *2017*, 805–810.

[493] O. Kysliak, A. Schnepf, *Dalton Trans.* **2016**, *45*, 2404–2408.

[494] O. Kysliak, C. Schrenk, A. Schnepf, *Chem. - A Eur. J.* **2016**, *22*, 18787–18793.

[495] A. Sekiguchi, Y. Ishida, Y. Kabe, M. Ichinohe, *J. Am. Chem. Soc.* **2002**, *124*, 8776–8777.

[496] A. Schnepf, *Chem. Commun.* **2007**, *4*, 192–194.

[497] C. Schenk, F. Henke, A. Schnepf, *Angew. Chem. Int. Ed.* **2013**, *52*, 1834–1838.

[498] C. Schenk, A. Schnepf, *Chem. Commun.* **2008**, *3*, 4643–4645.

[499] C. Schenk, A. Kracke, K. Fink, A. Kubas, W. Klopper, M. Neumaier, H. Schnöckel, A. Schnepf, *J. Am. Chem. Soc.* **2011**, *133*, 2518–2524.

[500] M. W. Hull, S. C. Sevov, *Angew. Chem.* **2007**, *119*, 6815–6818.

[501] M. W. Hull, S. C. Sevov, *Inorg. Chem.* **2007**, *46*, 10953–10955.

[502] M. W. Hull, S. C. Sevov, *J. Am. Chem. Soc.* **2009**, *131*, 9026–9037.

[503] C. B. Benda, J. Q. Wang, B. Wahl, T. F. Fässler, *Eur. J. Inorg. Chem.* **2011**, 4262–4269.

[504] F. Li, S. C. Sevov, *Inorg. Chem.* **2012**, *51*, 2706–2708.

[505] O. Kysliak, C. Schrenk, A. Schnepf, *Inorg. Chem.* **2015**, *54*, 7083–7088.

[506] K. Mayer, L. J. Schiegerl, T. Kratky, S. Günther, T. F. Fässler, *Chem. Commun.* **2017**, *53*, 11798–11801.

[507] C. Schenk, A. Schnepf, *Angew. Chem. Int. Ed.* **2007**, *46*, 5314–5316.

[508] C. Schenk, F. Henke, G. Santiso-Quinones, I. Krossing, A. Schnepf, *Dalton Trans.* **2008**, 4372–4386.

[509] F. Henke, C. Schenk, A. Schnepf, *Dalton Trans.* **2009**, *9226*, 9141–9145.

[510] M. M. Bentlohner, W. Klein, Z. H. Fard, L. A. Jantke, T. F. Fässler, *Angew. Chem.Int. Ed.* **2015**, *54*, 3748–3753.

[511] O. Kysliak, C. Schrenk, A. Schnepf, *Inorg. Chem.* **2017**, *56*, 9693–9697.

[512] S. Frischhut, M. M. Bentlohner, W. Klein, T. F. Fässler, *Inorg. Chem.* **2017**, *56*, 10691–10698.

[513] A. Nienhaus, R. Hauptmann, T. F. Fässler, *Angew. Chem. Int. Ed.* **2002**, *41*, 3213–3215.

[514] A. Ugrinov, S. C. Sevov, *J. Am. Chem. Soc.* **2002**, *124*, 10990–10991.

[515] M. S. Denning, J. M. Goicoechea, *J. Chem. Soc. Dalton Trans.* **2008**, *3*, 5882–5885.

[516] A. Ugrinov, S. C. Sevov, *Inorg. Chem.* **2011**, *42*, 5789–5791.

[517] K. Abersfelder, A. Russell, H. S. Rzepa, A. J. P. White, P. R. Haycock, D. Scheschkewitz, *J. Am. Chem. Soc.* **2012**, *134*, 16008–16016.

[518] P. Willmes, K. Leszczyńska, Y. Heider, K. Abersfelder, M. Zimmer, V. Huch, D. Scheschkewitz, *Angew. Chem. Int. Ed.* **2016**, *55*, 2907–2910.

[519] Y. Heider, N. E. Poitiers, P. Willmes, K. I. Leszczyńska, V. Huch, D. Scheschkewitz, *Chem. Sci.* **2019**, *10*, 4523–4530.

[520] Y. Heider, P. Willmes, V. Huch, M. Zimmer, D. Scheschkewitz, *J. Am. Chem. Soc.* **2019**, *141*, 19498–19504.

[521] N. E. Poitiers, L. Giarrana, K. I. Leszczyńska, V. Huch, M. Zimmer, D. Scheschkewitz, *Angew. Chem. Int. Ed.* **2020**, *59*, 8532–8536.

[522] N. E. Poitiers, V. Huch, M. Zimmer, D. Scheschkewitz, *Chem. - A Eur. J.* **2020**, DOI 10.1002/chem.202003180.

[523] N. E. Poitiers, L. Giarrana, V. Huch, M. Zimmer, D. Scheschkewitz, *Chem. Sci.* **2020**, *11*, 7782−7788.

[524] N. E. Poitiers, V. Huch, M. Zimmer, D. Scheschkeiwtz, *Chem. Commun.* **2020**, *56*, 10898-

10901.

[525] D. Nied, W. Klopper, F. Breher, *Angew. Chem. Int. Ed.* **2009**, *48*, 1411–1416.

[526] D. Nied, P. Oña-Burgos, W. Klopper, F. Breher, *Organometallics* **2011**, *30*, 1419–1428.

[527] Y. Heider, D. Scheschkewitz, *Dalton Trans.* **2018**, *47*, 7104–7112.

[528] Y. Guo, Z. Xia, J. Liu, J. Yu, S. Yao, W. Shi, K. Hu, S. Chen, Y. Wang, A. Li, M. Driess, W. Wang, *J. Am. Chem. Soc.* **2019**, *141*, 19252–19256.

[529] S. Nagase, T. Kudo, *Organometallics* **1987**, *6*, 2456–2458.

[530] P. von Ragué Schleyer, R. Janoschek, *Angew. Chem. Int. Ed. Engl.* **1987**, *26*, 1267–1268.

[531] S. Nagase, M. Nakano, T. Kudo, *J. Chem. Soc. Chem. Commun.* **1987**, 60–62.

[532] R. S. Grev, H. F. Schaefer III, *J. Am. Chem. Soc.* **1987**, *109*, 6569–6577.

[533] W. W. Schoeller, T. Dabisch, T. Busch, *Inorg. Chem.* **1987**, *26*, 4383–4389.

[534] S. Nagase, T. Kudo, *Organometallics* **1988**, *7*, 2534–2536.

[535] D. B. Kitchen, J. E. Jackson, L. C. Allen, *J. Am. Chem. Soc.* **1990**, *112*, 3408–3414.

[536] S. Nagase, *Acc. Chem. Res.* **1995**, *28*, 469–476.

[537] A. S. Ivanov, A. I. Boldyrev, *J. Phys. Chem. A* **2012**, *116*, 9591–9598.

[538] D. Nieder, PhD Thesis, Saarland University (Germany), **2017**.

[539] L. Klemmer, Master Thesis, Saarland University (Germany), **2016**.

[540] Yvonne Kaiser, Master Thesis, Saarland University (Germany), **2016**.

[541] Y. Heider, Master Thesis, Saarland University (Germany), **2016**.

[542] R. Cheng, B. Li, J. Wu, J. Zhang, Z. Qiu, W. Tang, S. L. You, Y. Tang, Z. Xie, *J. Am. Chem. Soc.* **2018**, *140*, 4508–4511.

Supporting Information

An anionic heterosiliconoid with two germanium vertices (SI)

Electronic Supplementary Information

for

An Anionic Heterosiliconoid with two Germanium Vertices

Lukas Klemmer,[a] Volker Huch,[a] Anukul Jana[b] and David Scheschkewitz*[a]

[a] *Krupp-Chair of General and Inorganic Chemistry, Saarland University, 66123 Saarbrücken, Germany. E-mail: scheschkewitz@mx.uni-saarland.de*
[b] *Tata Institute of Fundamental Research Hyderabad, Gopanpally, Hyderabad-500107, India.*

Experimental Details and Analytical Data

General Considerations

All reactions were carried out under a protective argon atmosphere using Schlenk techniques or a gloveboxe. *n*-Pentane, benzene, and 1,2-dimethoxyethane (DME) were refluxed with sodium/benzophenone and distilled prior to use under argon. *n*-Hexane, toluene, diethyl ether (Et_2O), and tetrahydrofuran (THF) were taken directly from a solvent purification system (Innovative Technology PureSolv MD7). Deuterated benzene was refluxed over potassium and distilled prior to use under argon. Deuterated THF-d_8 was refluxed over Na/K alloy and condensed *in vacuo*. NMR spectra were recorded at 300 K on a Bruker Avance III 300 (^{1}H: 300.13 MHz, ^{7}Li{^{1}H}: 116.59 MHz, ^{29}Si{^{1}H}: 59.6 MHz) and a Bruker Avance III HD 400 (^{1}H: 400.13 MHz, ^{13}C{^{1}H}: 100.61 MHz ^{29}Si{^{1}H}: 79.5 MHz). ^{1}H, ^{13}C{^{1}H}, and ^{29}Si{^{1}H} chemical shifts are reported relative to $SiMe_4$. ^{7}Li{^{1}H} chemical shift was referenced to aqueous solution of LiCl. Solid state CP/MAS NMR spectra were measured on a Bruker AV400WB spectrometer. Powdered samples were packed in a 4 mm o.d. zirconia rotor. Diameter of the Probe is 89 mm with spinning speed of 13 KHz. ^{29}Si{^{1}H} CP MAS experiment was performed using ^{1}H 90° pulse for 3.3 μs, with contact time 5 ms, CPD Spinal64 as decoupling scheme, and a recycle delay of 3 s. UV/vis spectra were acquired on a Shimadzu UV-2600 or a PerkinElmer Lambda 35 spectrometer using quartz cells with a path length of 1 mm. Silicon tetrachloride was boiled over magnesium and distilled prior to use under argon. Lithium/naphthalene was freshly prepared from lithium granules and naphthalene prior to use. 1,3,3,4,6,6-hexakis(2,4,6-triisopropylphenyl)-1,3,4,6-tetrasila-2,5-digerma-tricyclo[3.1.0.0^{2,4}]-hexane-2,5-diyl **1** was synthesized according to our published procedure.[S1]

Synthesis of 2,2,4,5,5-pentakis(2,4,6-triisopropylphenyl)-1,2,4,5-tetrasila-3,6-digermatetracyclo[2.2.0.0^{1,3}.0^{3,6}]hexan-6-yllithium 2Li·(THF)$_2$

At −80 °C, a solution of Li/$C_{10}H_8$ in THF (1.0 mL, 1.06 M, 2.2 eq.) is added dropwise to a suspension of dismutational Si_4Ge_2 isomer **1** (766 mg, 0.23 mmol) in 15 mL of dry Et_2O and the resulting blue-green reaction mixture is stirred for 1 hour at −80 °C before thawing up to room temperature overnight. The reaction mixture is dried *in vacuo* and the resulting solid extracted with 30 mL of benzene. The filtrate is dried *in vacuo* once again to give a bright orange solid, which is freed from naphthalene *in vacuo* at 65°C for 2 hours. The remaining solid is dissolved in about 15 mL of *n*-hexane and concentrated to about 5 mL. After storing the resulting solution overnight at 0°C, anionic siliconoid **2Li**·(THF)$_2$ is isolated as orange block-shaped single crystals.

Yield: 369 mg (47%).

^{1}H NMR (400.13 MHz, 300 K, benzene-d_6, TMS): *Due to the presence of two rotamers in solution (61:39) and solid state (64:36), two overlapping sets of signals arise. A detailed integration and assignment of the signals was therefore not possible*. δ = 7.30, 7.29 (each broad s, partially overlapping, altogether 1H, Tip-*H*), 7.13-7.06

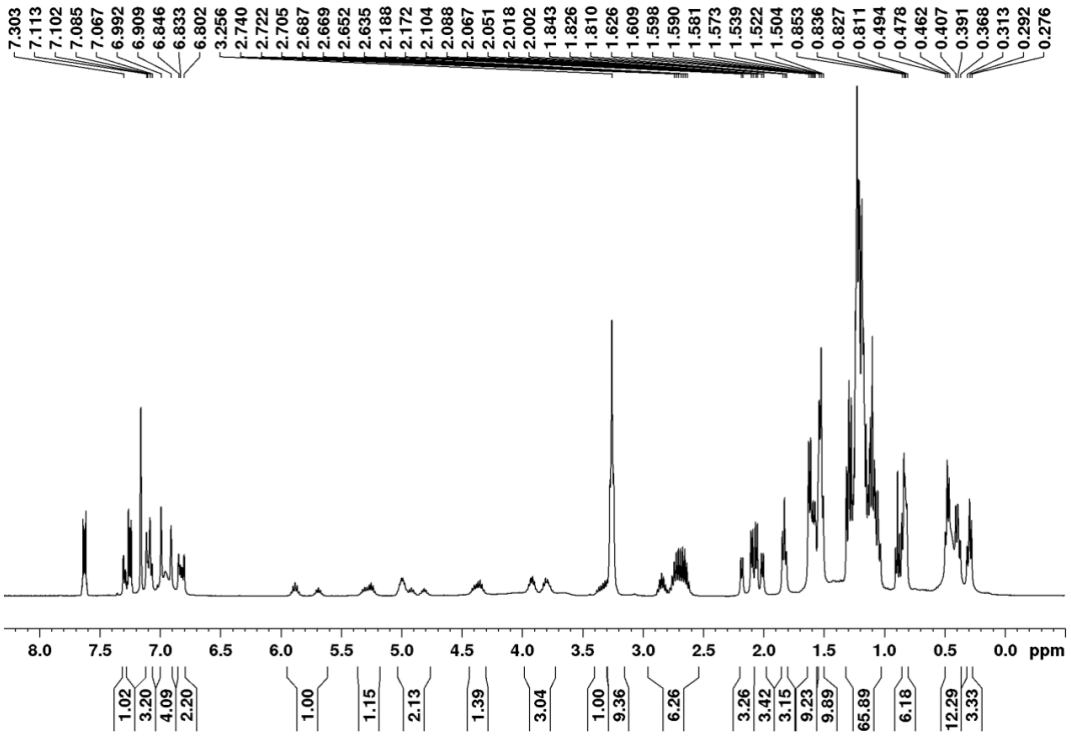

Figure S1: ^{1}H NMR spectrum of **2Li**·(THF)$_2$ in [D$_6$]-benzene at 300 K.

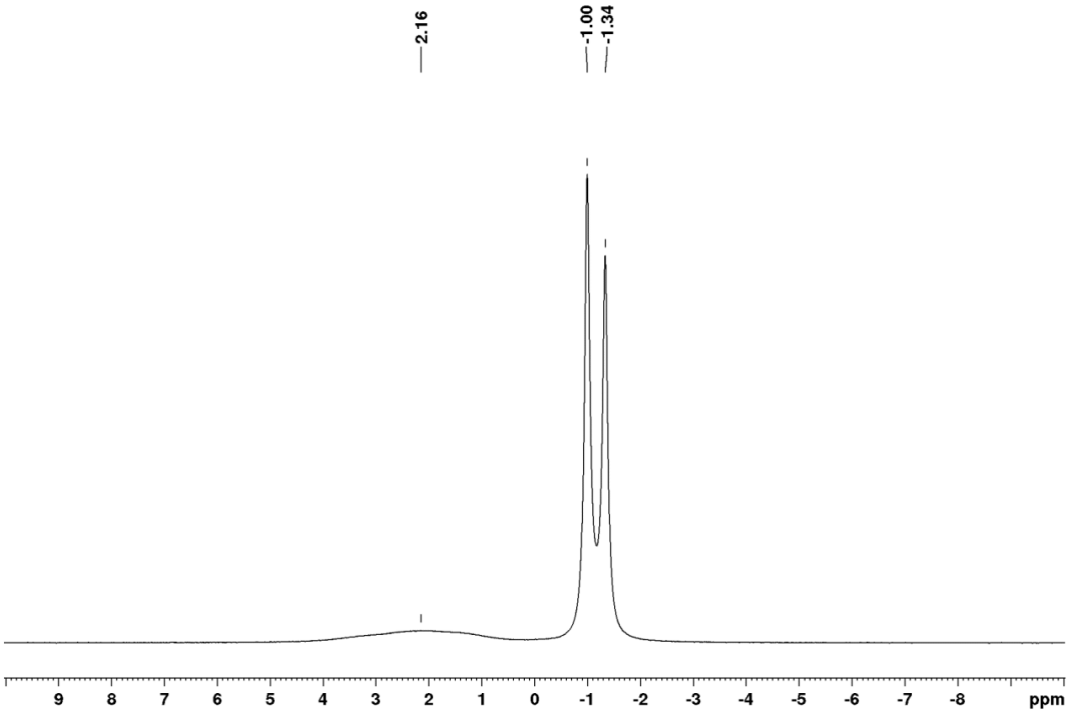

Figure S2: ^{7}Li{^{1}H} NMR spectrum of **2Li**·(THF)$_2$ in [D$_6$]-benzene at 300 K.

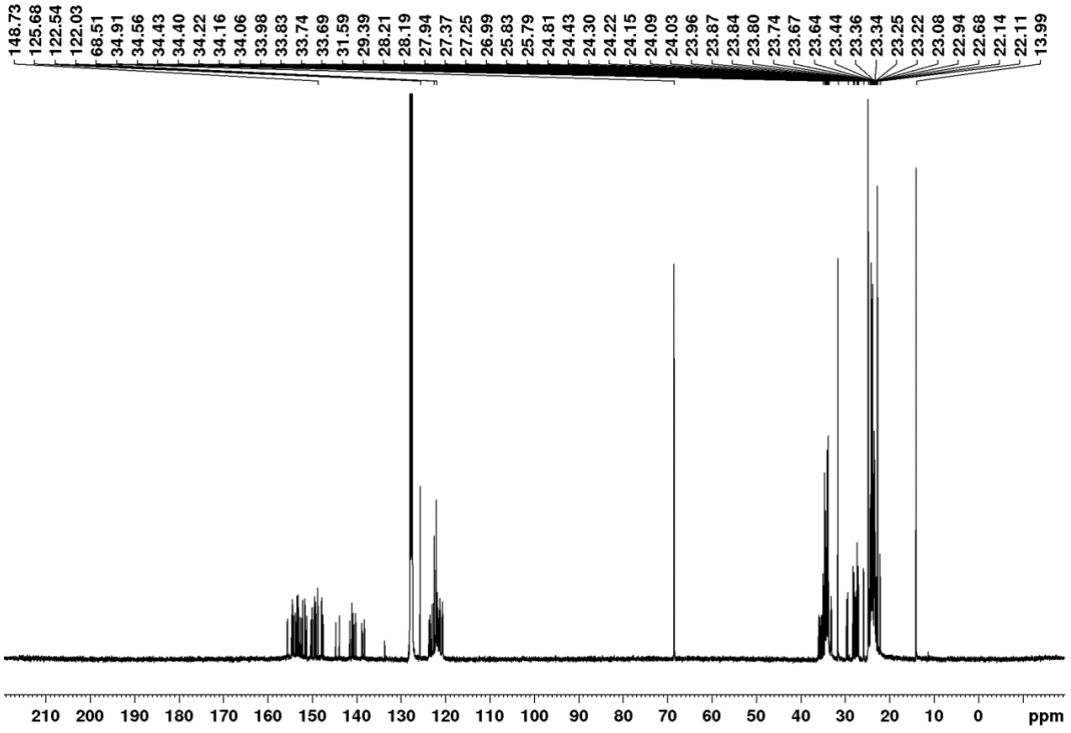

Figure S3: $^{13}C\{^{1}H\}$ NMR spectrum of **2Li**·$(THF)_2$ in $[D_6]$-benzene at 300 K.

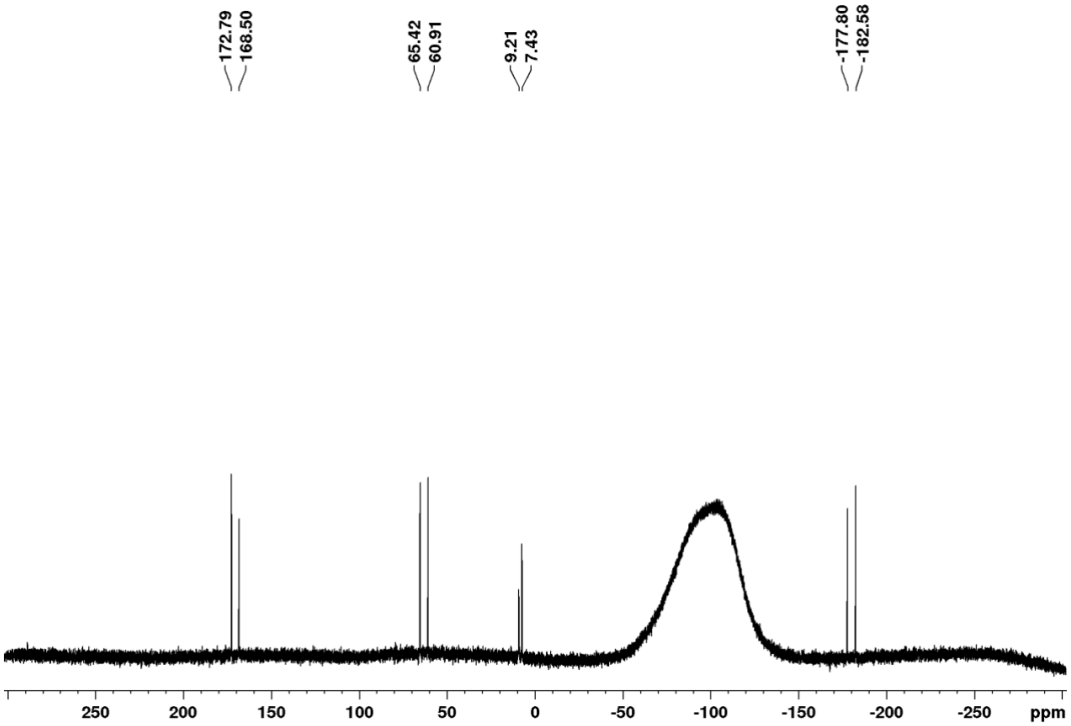

Figure S4: $^{29}Si\{^{1}H\}$ NMR spectrum of **2Li**·$(THF)_2$ in $[D_6]$-benzene at 300 K.

Synthesis of 2,2,4,5,5-pentakis(2,4,6-triisopropylphenyl)-1,2,4,5-tetrasila-3,6-digermatetracyclo[2.2.0.0^{1,3}.0^{3,6}]hexan-6-yllithium 2[Li(DME)$_3$]

a) **2Li**·(THF)$_2$ (201.6 mg, 0.14 mmol) is dissolved in 3 mL of dry dme and then dried *in vacuo* for 1 hour. This dissolving-drying cycle is repeated two more times before 5 mL of dry hexane are added to the remaining dark red sticky solid. Drying once more *in vacuo* affords **2**[Li(DME)$_3$] in quantitative yield as dark red powder.
b) At −80 °C a solution of Li/$C_{10}H_8$ in thf (0.48 mL, 0.92 M, 2.2 eq.) is added dropwise to a suspension of dismutational isomer **1** (289 mg, 0.20 mmol) in 5 mL of dry Et_2O and the resulting blue-green reaction mixture is stirred for 1 hour at −80 °C before thawing up to room temperature overnight. After that all the volatilities are removed *in vacuo*. The resulting solid is extracted with 10 mL benzene and the filtrate is dried. Subsequently the obtained solid is dissolved in 1 mL of dme and then dried again. This dissolving-drying cycle is repeated two more times before 4 mL of *n*-hexane are added. Storage of the resulting solution at 0 °C overnight leads to the formation of **2**[Li(DME)$_3$] as dark red, block-shaped single crystals of X-Ray quality.
Yield: 201 mg (64%).
^{1}H NMR (400.13 MHz, 300 K, thf-d_8, TMS): *Due to the presence of two rotamers in solution (56:44) and solid state (55:45), two overlapping sets of signals arise. A detailed integration and assignment of the signals was therefore not possible*. δ = 6.97, 6.96 (each broad s, partially overlapping, altogether 1H, Tip-*H*), 6.87 (broad s, 2H, Tip-*H*), 6.74, 6.72, 6.71, 6.69 (each broad s, partially overlapping, altogether 3H, Tip-*H*), 6.60 (broad s, 4H, Tip-*H*), 5.96-5.63 (m, 1H, Tip-^{i}Pr-C*H*), 5.24-5.00 (m, 1H, Tip-^{i}Pr-C*H*), 5.00-4.50 (m, 2H, Tip-^{i}Pr-C*H*), 4.44-4.13 (m, 2H, Tip-^{i}Pr-C*H*), 3.86-3.55 (m, overlapping with thf-d8 signal, 4H, Tip-^{i}Pr-C*H*), 3.44 (s, 8H, dme-CH_2), 3.28 (s, 12H, dme-CH_3), 3.22-3.06 (m, 1H, Tip-^{i}Pr-C*H*), 2.81-2.56 (m, 5H, Tip-^{i}Pr-C*H*), 1.91, 1.88 (each d, altogether 3H, Tip-^{i}Pr-CH_3), 1.67-1.57 (m, 3H, Tip-^{i}Pr-CH_3), 1.47-1.39 (m, 3H, Tip-^{i}Pr-CH_3), 1.35-1.06 (m, overlapping with hexane signals, 60H, Tip-^{i}Pr-CH_3), 0.71-0.60 (m, 3H, Tip-^{i}Pr-CH_3), 0.52-0.41 (m, 6H, Tip-^{i}Pr-CH_3), 0.24-0.05 (m, overlapping with signal of grease, 9H, Tip-^{i}Pr-CH_3), −0.07 (br, 6H, Tip-^{i}Pr-CH_3) ppm.
^{7}Li{^{1}H} NMR (116.59 MHz, 300 K, thf-d_8, Li^+ aq): δ = 0.77 (very broad), −0.55 (s) ppm.
^{7}Li SPE/MAS NMR (155.6 MHz, 300 K, 13 kHz): δ = −1.55 (s) ppm.
^{13}C{^{1}H} NMR (100.61 MHz, 300 K, thf-d_8, TMS): δ = 155.63, 155.19, 154.88, 154.75, 154.69, 154.42, 154.23, 153.88, 153.66, 153.49, 153.16, 152.71, 152.58, 152.19, 152.05, 151.94, 151.87, 151.37, 149.13, 148.37, 147.70, 147.65, 147.54, 147.38, 147.28, 147.20, 146.41, 146.35, 145.57, 145.44, 145.00, 144.62, 144.43, 144.01, 143.92, 143.58, 142.53 (Tip-Ar-*C*H), 134.35 ($C_{10}H_8$), 128.31 (Tip-Ar-*C*H), 126.23 ($C_{10}H_8$), 122.60, 122.41, 122.38, 122.28, 122.14, 121.77, 121.71, 121.27, 121.00, 120.84, 120.57, 120.47, 120.38, 120.28, 120.12 (Tip-Ar-*C*), 72.48 (dme-*C*H$_2$), 58.65 (dme-*C*H$_3$), 35.85, 36.63, 35.16, 35.02, 35.00, 34.80, 34.70, 34.61, 34.43, 33.87, 33.81, 33.76, 33.32, 33.19, 33.03, 32.36, 30.13, 29.94, 28.84, 28.72, 28.29, 27.81, 27.72, 27.66, 27.58, 27.26, 26.44 (Tip-^{i}Pr-*C*H), 25.58, 25.38, 25.18, 24.55, 24.42, 24.35, 24.32, 24.29, 24.27, 24.21, 24.07, 23.97, 23.81, 23.04, 22.15, 22.08 (Tip-^{i}Pr-*C*H$_3$) ppm.
^{29}Si{^{1}H} NMR (79.5 MHz, 300 K, thf-d_8, TMS): *Due to the presence of two rotamers in solution two sets of signals arise which are assigned according to their distinct*

intensities. Major rotamer: δ = 171.4 (br, *privo*-Si), 36.1 (s, *ligato*-Si), 5.6 (s, *remoto*-Si), −181.1 (s, *nudo*-Si) ppm. *Minor rotamer:* δ = 172.4 (br, *privo*-Si), 37.2 (s, *ligato*-Si), 6.2 (s, *remoto*-Si), −183.9 (s, *nudo*-Si) ppm.

^{29}Si CP/MAS NMR (79.5 MHz, 300 K, 13 kHz, TMS): δ = 168.3 (br, *privo*-Si), 42.9 (br, *ligato*-Si), 41.0 (br, *ligato*-Si), 3.6 (br, *remoto*-Si), 2.6 (br, *remoto*-Si), −180.9 (s, *nudo*-Si), −185.4 (s, *nudo*-Si) ppm.

UV/vis (*n*-hexane): λ_{max} (ε) = 373 nm (9206 L*mol^{-1}cm^{-1}), 324 nm (8946 L*mol^{-1}cm^{-1}).

m.p.: .167°C (decomp.).

Elemental analysis: calc. for $C_{87}H_{145}Ge_2LiO_6Si_4$ (1551.65): C, 67.34; H, 9.42; N 0.00: Found: C, 49.43; H, 10.16; N, 0.00. *Note: Tetrel carbide formation is a plausible reason for unsatisfying agreement between observed and theoretical value.*

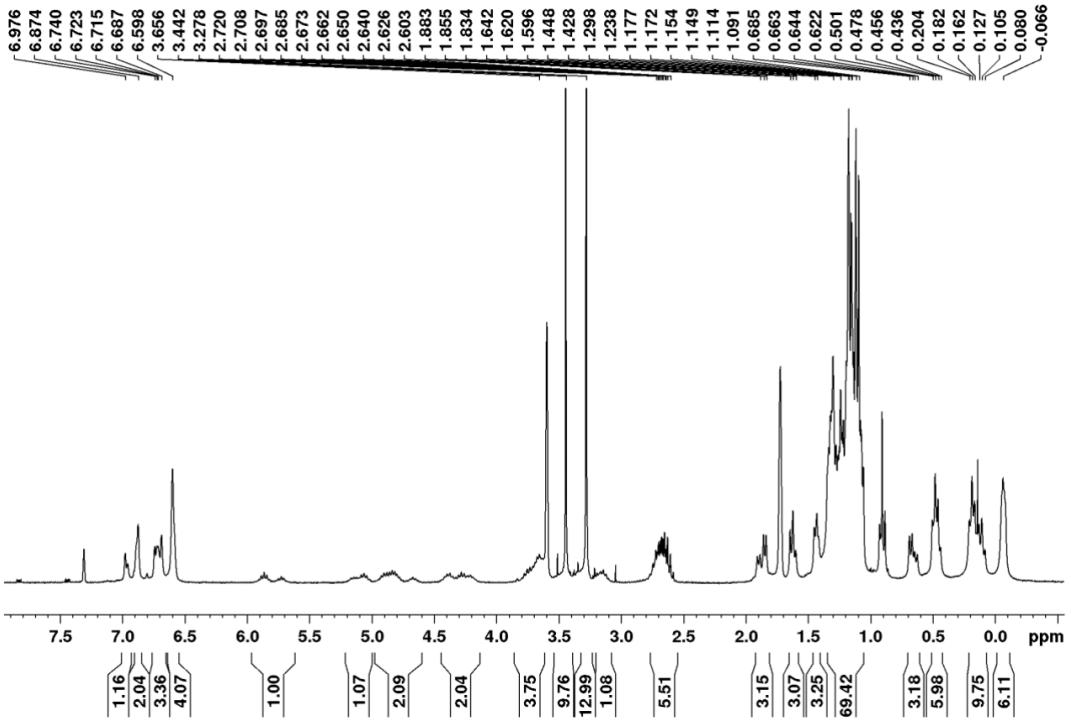

Figure S5: ^{1}H NMR spectrum of **2**[Li(DME)$_3$] in thf-d$_8$ at 300 K.

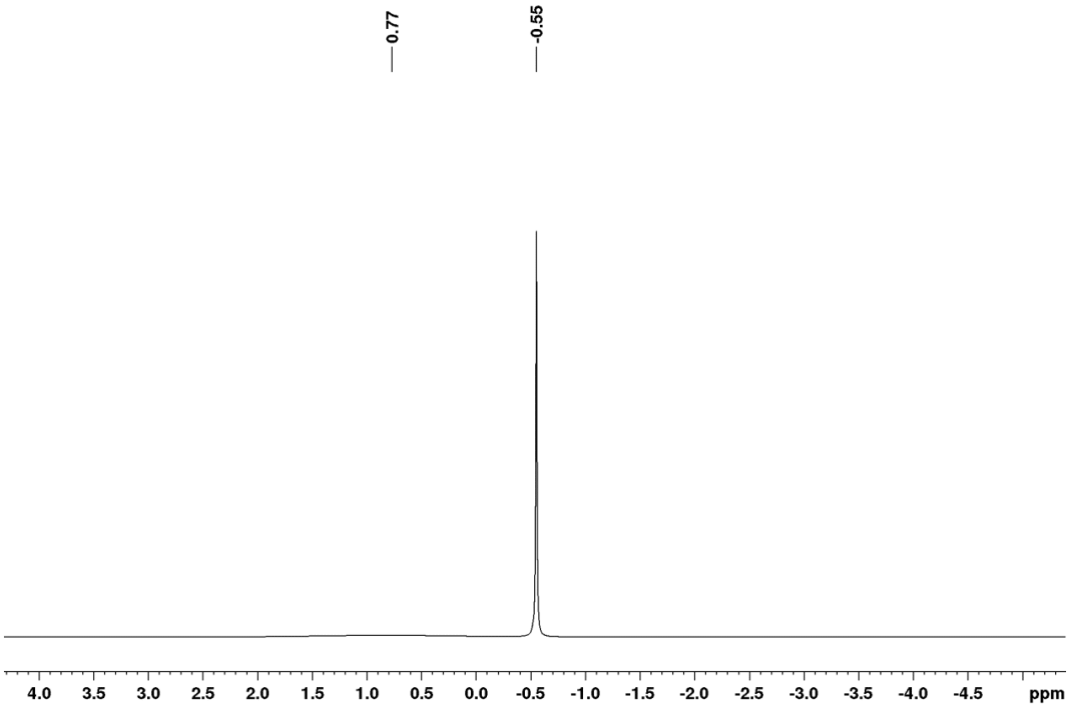

Figure S6: $^{7}Li\{^{1}H\}$ NMR spectrum of **2**[Li(DME)$_3$] in thf-d$_8$ at 300 K.

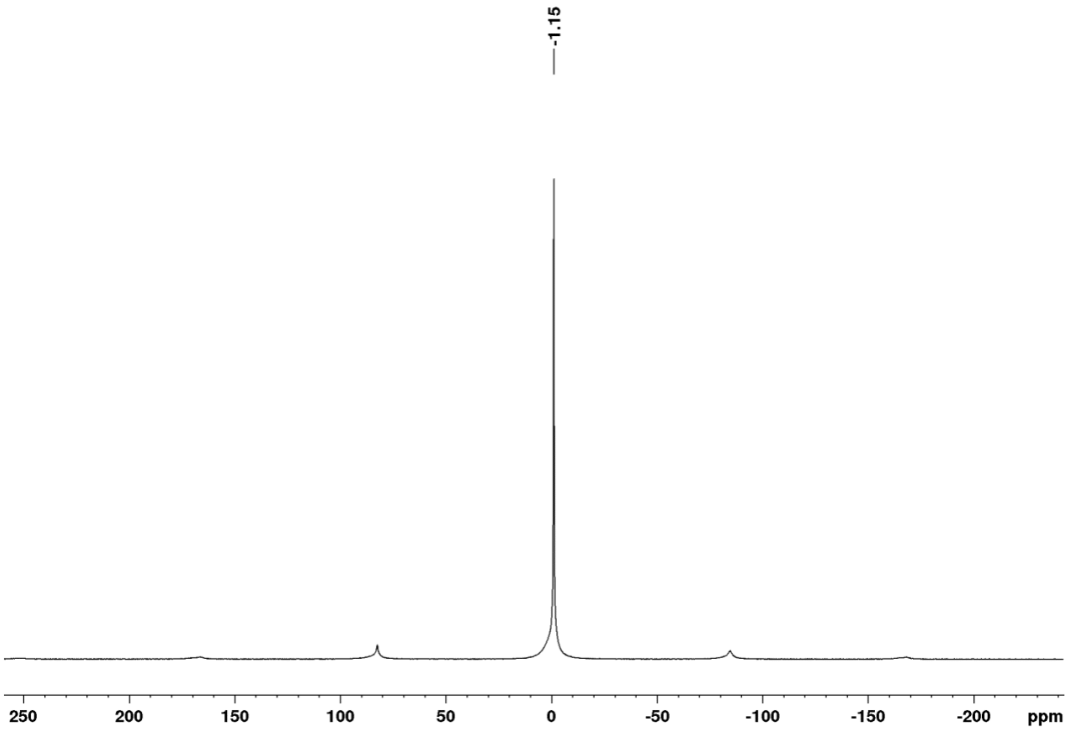

Figure S7: ^{7}Li SPE/MAS NMR spectrum of **2**[Li(DME)$_3$].

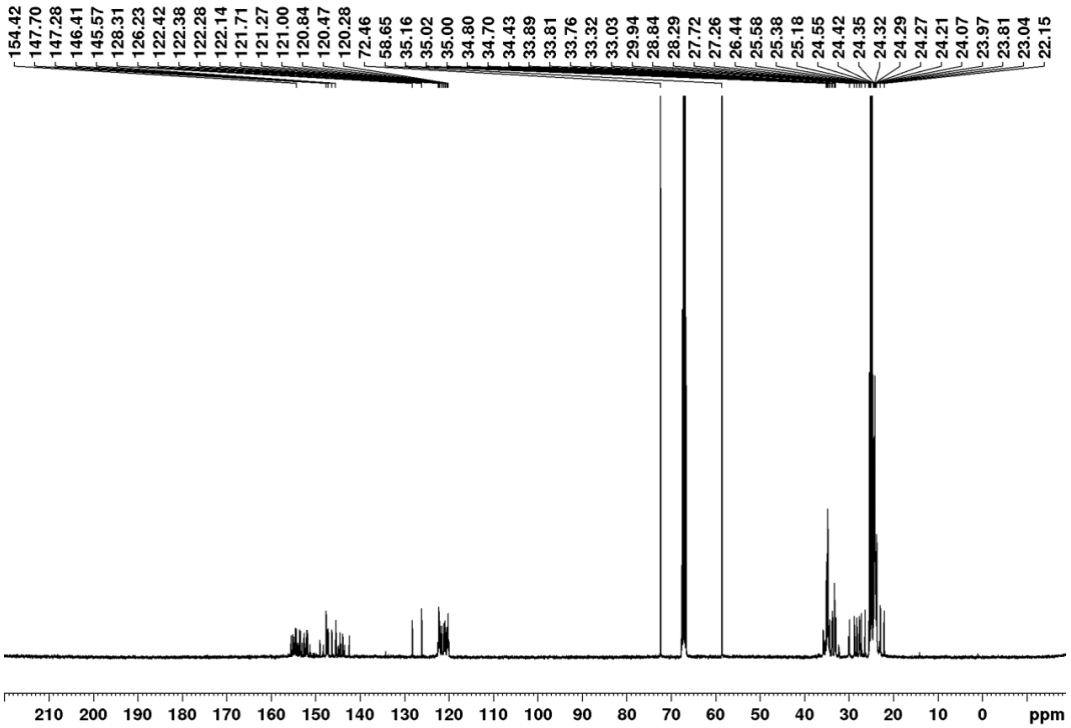

Figure S8: $^{13}C\{^{1}H\}$ NMR spectrum of **2**[Li(DME)$_3$] in thf-d$_8$ at 300 K.

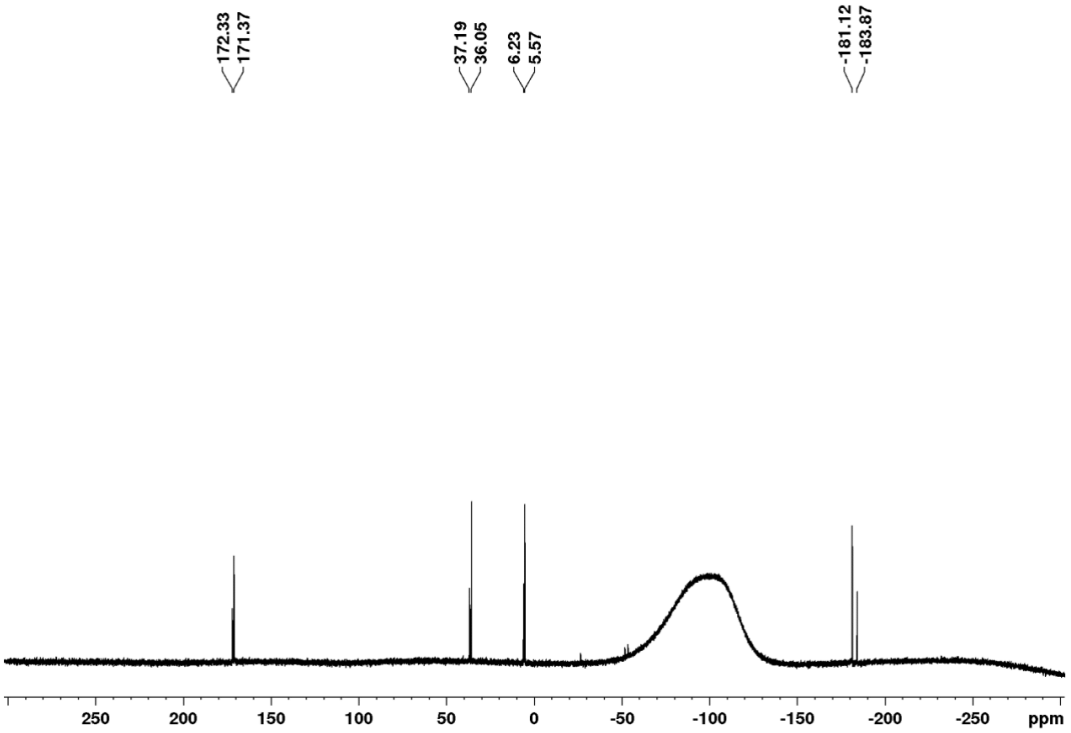

Figure S9: $^{29}Si\{^{1}H\}$ NMR spectrum of **2**[Li(DME)$_3$] in thf-d$_8$ at 300 K.

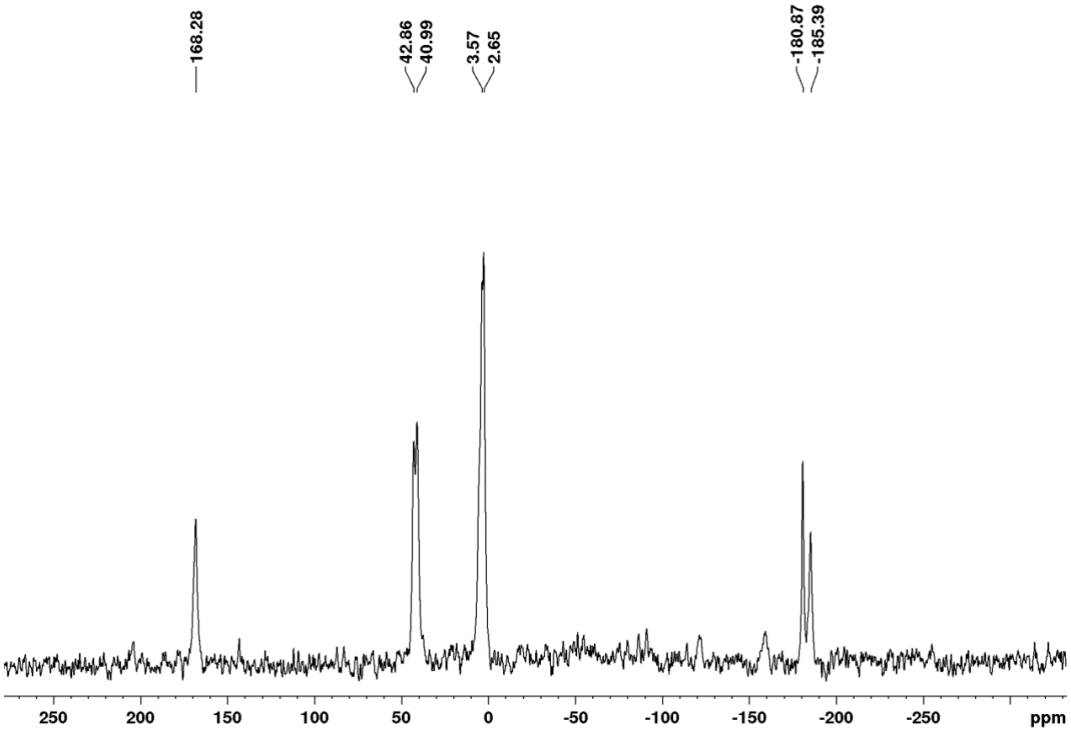

Figure S10: ^{29}Si CP/MAS NMR spectrum of **2**[Li(DME)$_3$].

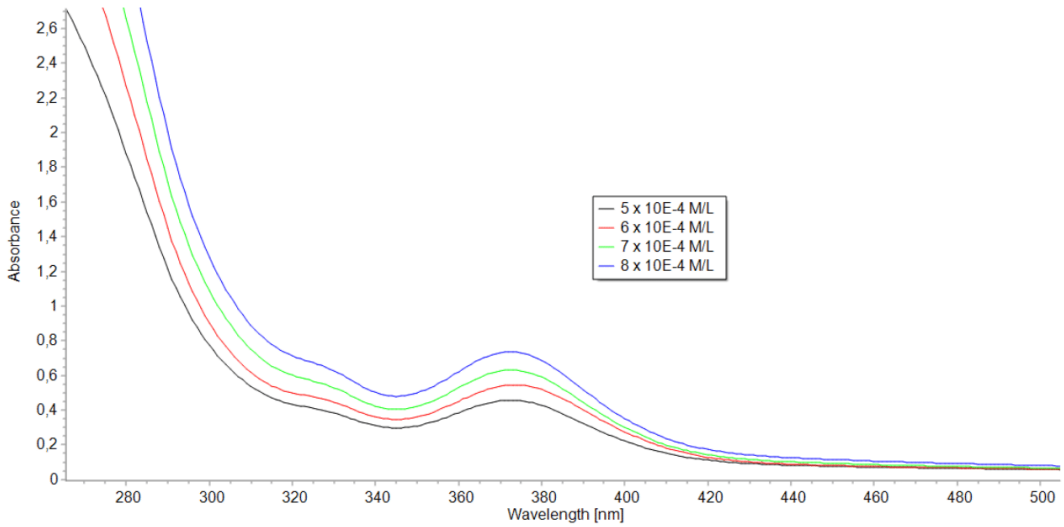

Figure S11: UV/vis spectra of **2**[Li(DME)$_3$] in *n*-hexane at different concentrations (5×10^{-4} molL^{-1} - 8×10^{-4} molL^{-1}).

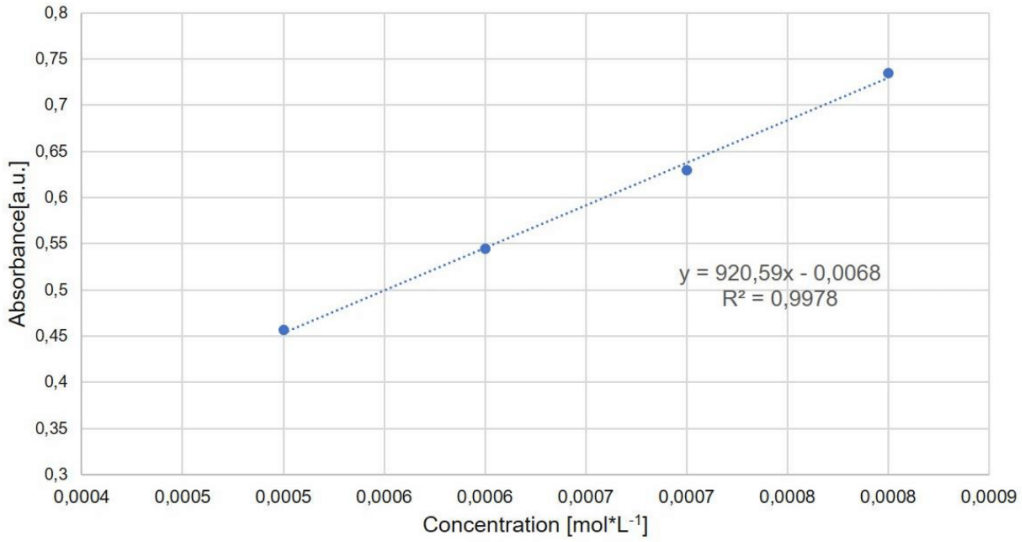

Figure S12: Linear regression of **2**[Li(DME)$_3$] at λ = 373 nm.

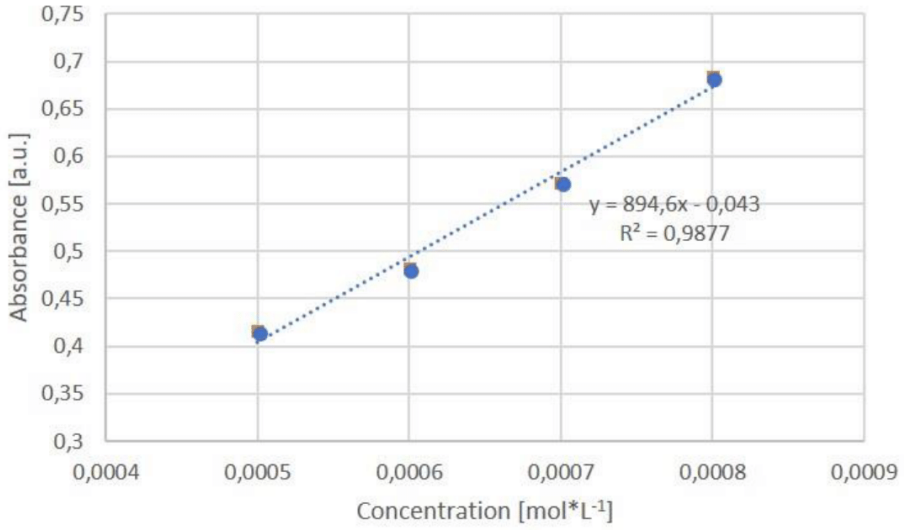

Figure S13: Linear regression of **2**[Li(DME)$_3$] at λ = 324 nm.

2,2,4,5,5-pentakis(2,4,6-triisopropylphenyl)-6-(trichlorosilyl)-1,2,4,5-tetrasila-3,6-digermatetracyclo[2.2.0.0^{1,3}.0^{3,6}]hexane 12

Anionic benzpolarenide **2Li**·(THF)$_2$ (272 mg, 0.18 mmol, co-crystallized with 0.41 eq. thf, 0.36 eq. $C_{10}H_8$) is dissolved in 10 mL of toluene and neat silicon tetrachloride (22.8 µl, 33.7 mg, 1.1 eq.) is added at room temperature. The reaction mixture is

stirred overnight at room temperature. The now red reaction mixture is dried *in vacuo* and the resulting solid is extracted with 10 mL of *n*-hexane. Removal of *n*-hexane from the resulting filtrate *in vacuo* gives trichlorosilyl-substituted benzpolarene **12** as red sticky oil.

^{1}H NMR (300.13 MHz, 233 K, thf-d_8, TMS): δ = 7.38 - 6.38 (m, 10H, Tip-*H*), 4.75, 4.51, 4.25, 3.93, 3.59 (masked by thf-d_8), 3.34, 3.19, 3.08, 2.76 (each br., altogether 15H, Tip-^{i}Pr-C*H*), 1.65 - 0.97 (br. m, overlapping with *n*-hexane, 72H, Tip-^{i}Pr-CH_3), 0.59 - −0.25 (br. m, 18H, Tip-^{i}Pr-CH_3) ppm.

^{29}Si{^{1}H} NMR (79.5 MHz, 300 K, benzene-d_6, TMS): δ = 201.6 (br., *privo-Si*), 49.4 (br., *remoto-Si*), 27.6 (br., *Si*Cl$_3$), 11.3 (br., *ligato-Si*), −218.6 (br., *nudo-Si*) ppm.

^{29}Si{^{1}H} NMR (79.5 MHz, 223 K, thf-d_8, TMS): *Due to the presence of two rotamers in solution two sets of signals (ratio 68:32) arise which are assigned based on their relative intensities. Major rotamer:* δ = 202.9 (s, *privo-Si*), 47.7 (s, *remoto-Si*), 27.2 (s, *Si*Cl$_3$), 11.4 (s, *ligato-Si*), −222.9 (s, *nudo-Si*) ppm. *Minor rotamer:* δ = 204.6 (s, *privo-Si*), 49.3 (s, *remoto-Si*), 26.2 (s, *Si*Cl$_3$), 12.1 (s, *ligato-Si*), −225.0 (s, *nudo-Si*) ppm.

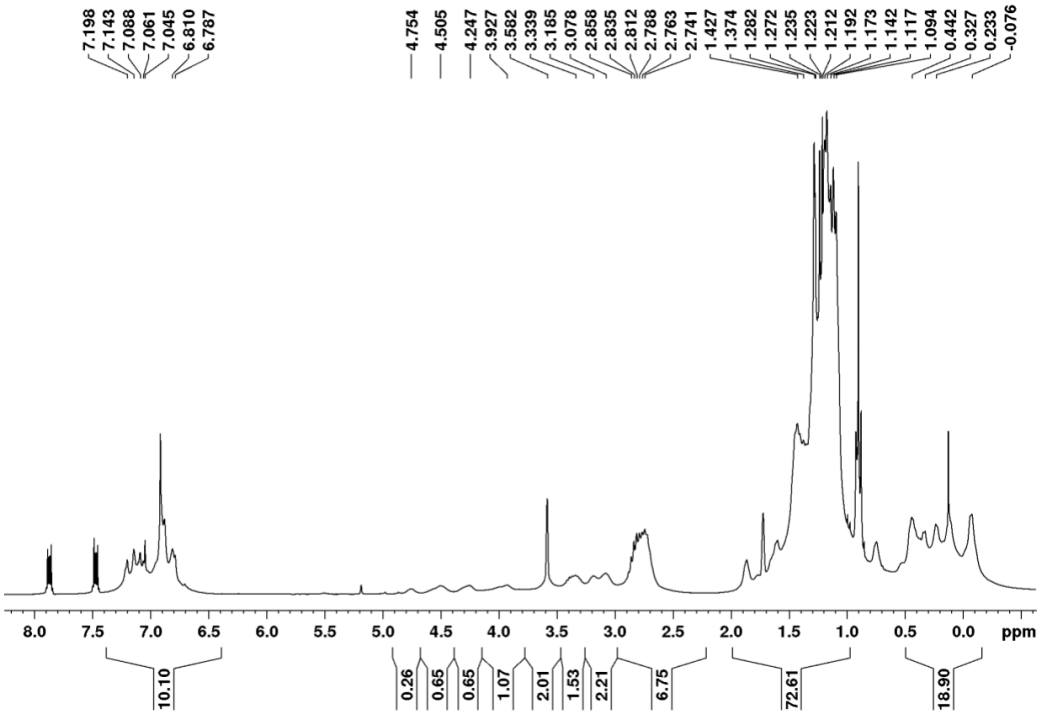

Figure S14: ^{1}H NMR spectrum of **12** in [D_8]-thf at 233 K.

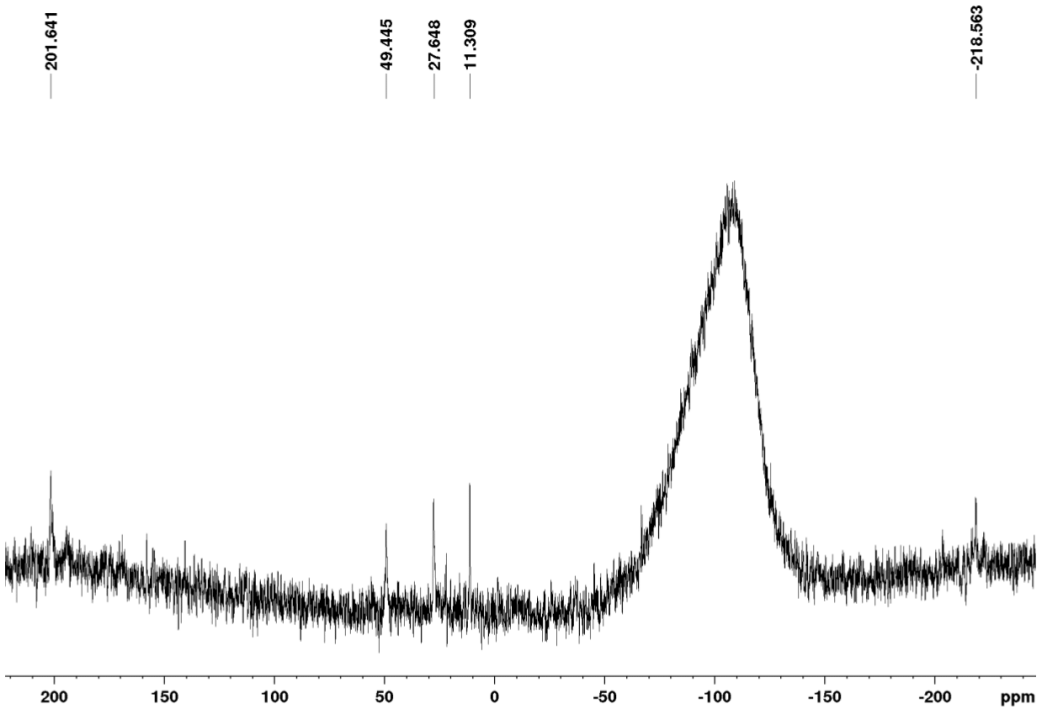

Figure S15: $^{29}Si\{^{1}H\}$ NMR spectrum of **12** in $[D_6]$-benzene at 300 K.

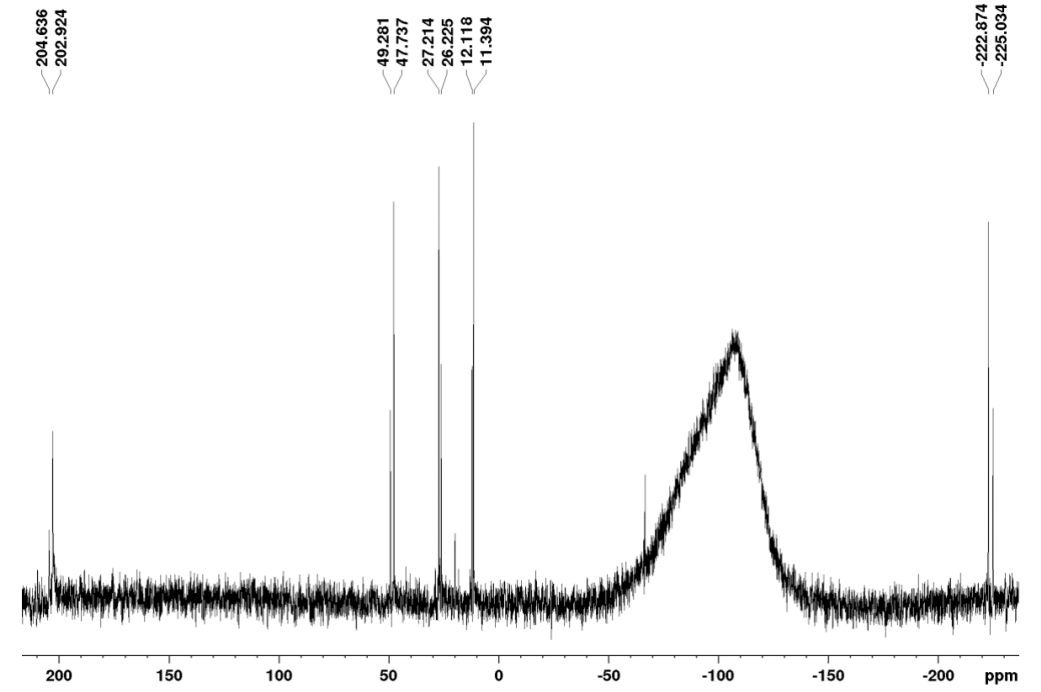

Figure S16: $^{29}Si\{^{1}H\}$ NMR spectrum of **12** in $[D_8]$-thf at 223 K.

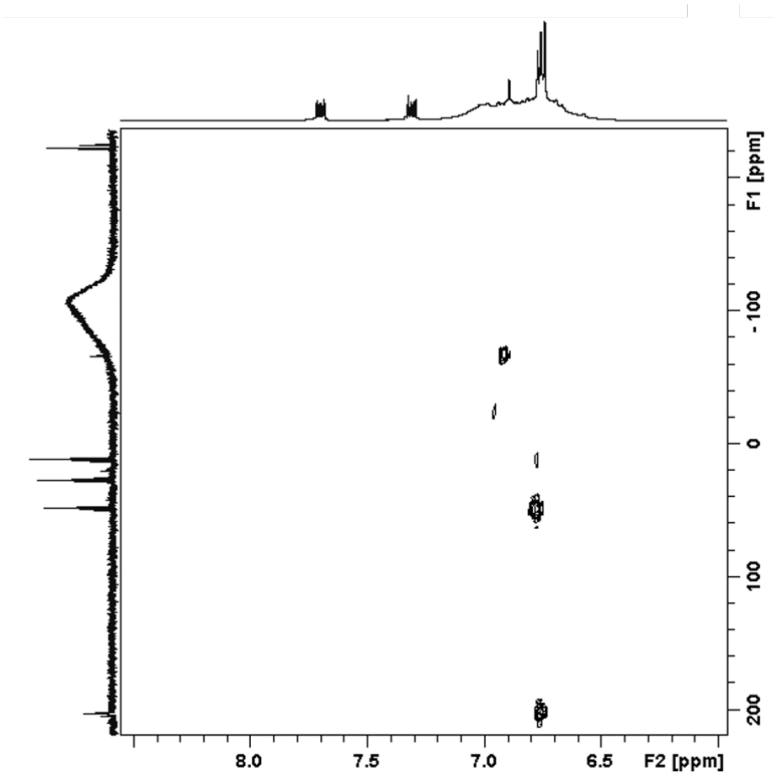

Figure S17: 2D- $^{29}Si/^{1}H$ NMR spectrum of **12** in $[D_6]$-benzene at 300 K.

Molecular structures of of **2Li**·$(THF)_2$ and **2**[$Li(DME)_3$]

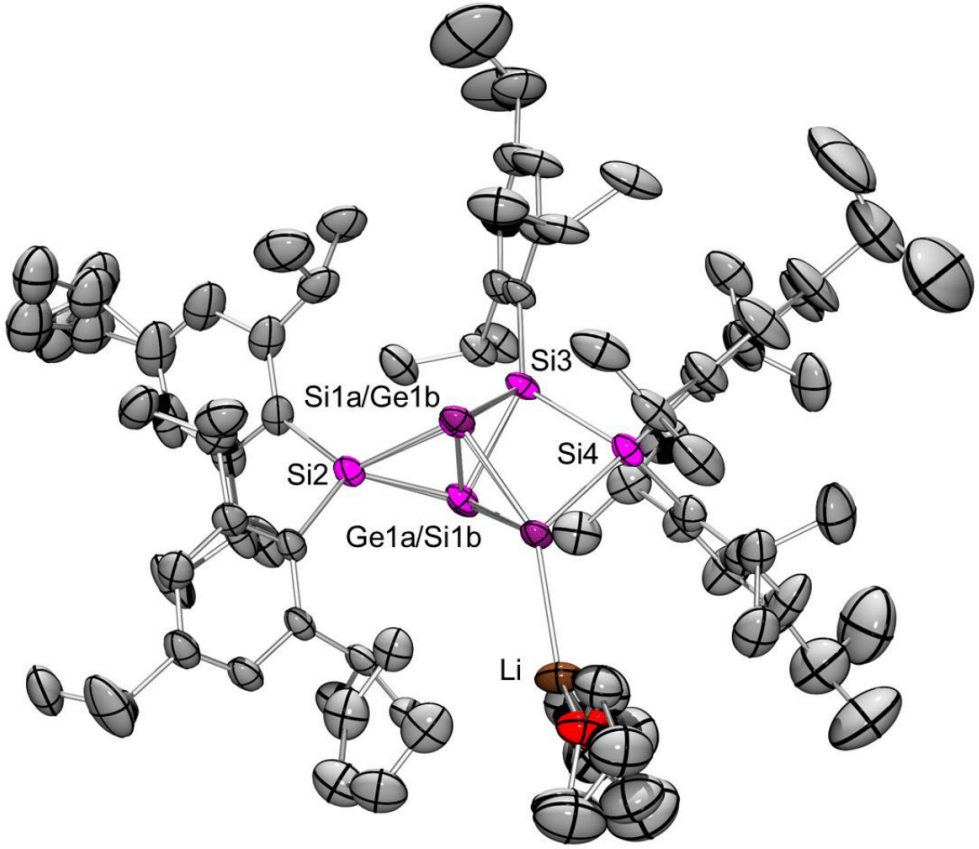

Figure S18: Molecular structure of **2Li**·$(THF)_2$ in the solid state (thermal ellipsoids at 50 % probality level; hydrogen atoms are omitted for clarity). Selected interatomic distances (Å): Si1a···Ge1a 2.670(8), Si1a–Si2 2.344(8), Si1a–Si3 2.347(8), Si1a–Ge2 2.432(8), Ge1a–Si2 2.454(2), Ge1a–Si3 2.428(2), Ge1a–Ge2 2.557(2), Si1b···Ge1b 2.656(9), Si1b–Si2 2.344(9), Si1b–Si3 2.341(9), Si1b–Ge2 2.456(8), Ge1b–Si2 2.457(5), Ge1b–Si3 2.438(6), Ge1b–Ge2 2.496(5), Si3–Si4 2.3470(17), Ge2–Si4 2.458(1), Ge2–Li 2.594(8).

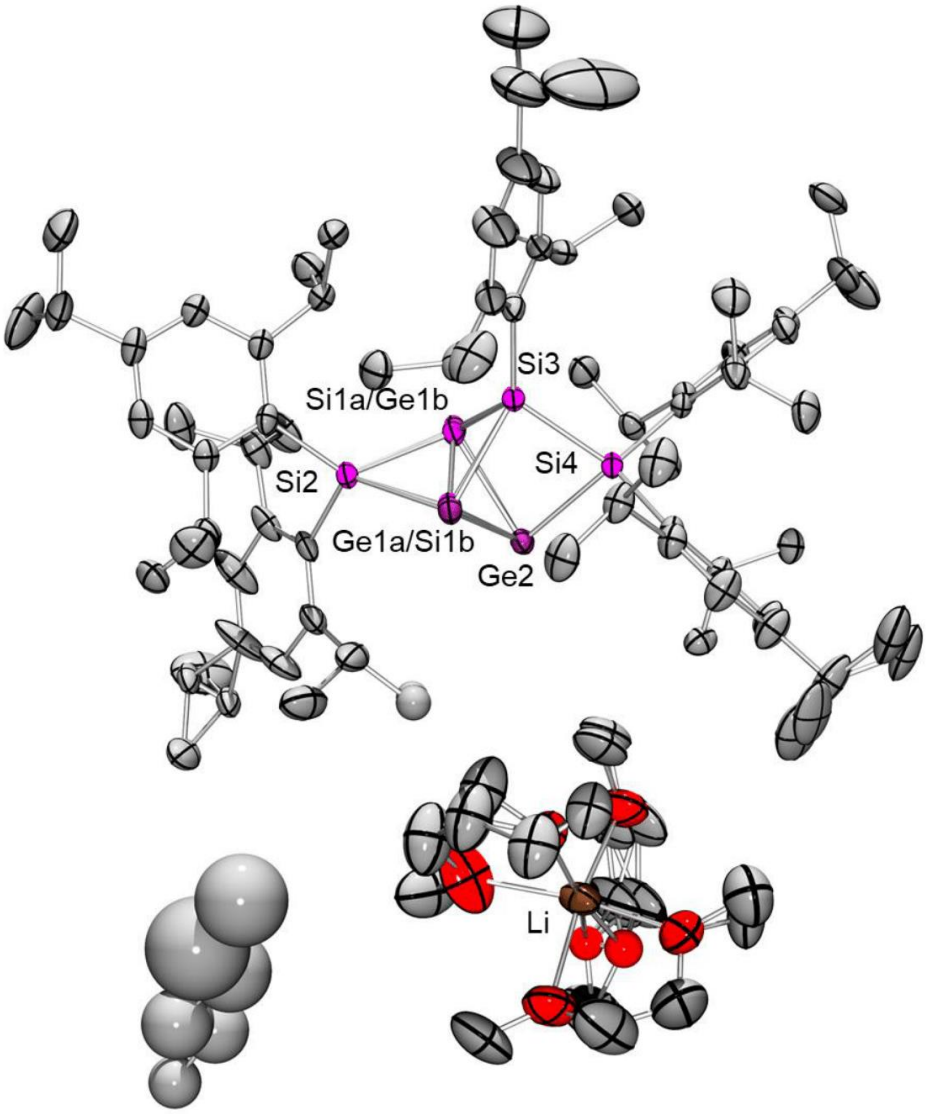

Figure S19: Molecular structures of the minor isomer (45 %) of **2**[Li(DME)$_3$] in the solid state (thermal ellipsoids at 50 % probality level; hydrogen atoms are omitted for clarity). Selected interatomic distances (Å): Si1a···Ge1a 2.674(7), Ge2···Li 7.607 (9), Si1a–Si2 2.339(8), Si1a–Si3 2.343(8), Si1a–Ge2 2.467(8), Ge1a–Si2 2.450(3), Ge1a–Si3 2.414(3), Ge1a–Ge2 2.559(2), Si1b···Ge1b 2.669(7), Si1b–Si2 2.343(9), Si1b–Si3 2.340(9), Si1b–Ge2 2.470(8), Ge1b–Si2 2.447(4), Ge1b–Si3 2.430(4), Ge1b–Ge2 2.530(4), Si3–Si4 2.344 (1), Ge2–Si4 2.4800(9).

Crystallographic data and structure refinement

Table S1: Crystal data and structure refinement for **2Li**·$(THF)_2$ (CCDC 1921154).

Identification code	sh3748	
Empirical formula	C83 H131 Ge2 Li O2 Si4, 0.75(C10 H8)	
Formula weight	1521.47	
Temperature	152(2) K	
Wavelength	0.71073 Å	
Crystal system	Monoclinic	
Space group	C2/c	
Unit cell dimensions	a = 38.5015(14) Å	α= 90°.
	b = 25.0063(10) Å	β= 119.264(2)°.
	c = 25.1216(9) Å	γ = 90°.
Volume	21099.8(14) $Å^3$	
Z	8	
Density (calculated)	0.958 Mg/m^3	
Absorption coefficient	0.652 mm^{-1}	
F(000)	6552	
Crystal size	0.473 x 0.352 x 0.264 mm^3	
Theta range for data collection	1.015 to 27.167°.	
Index ranges	-47<=h<=49, -32<=k<=32, -30<=l<=32	
Reflections collected	93773	
Independent reflections	23385 [R(int) = 0.0501]	
Completeness to theta = 25.242°	100.0 %	
Absorption correction	Semi-empirical from equivalents	
Max. and min. transmission	0.7455 and 0.7060	
Refinement method	Full-matrix least-squares on F^2	
Data / restraints / parameters	23385 / 505 / 998	
Goodness-of-fit on F^2	1.732	
Final R indices [I>2sigma(I)]	R1 = 0.0707, wR2 = 0.2217	
R indices (all data)	R1 = 0.1206, wR2 = 0.2086	
Extinction coefficient	n/a	
Largest diff. peak and hole	1.165 and -0.603 e.$Å^{-3}$	

Table S2: Crystal data and structure refinement for **2**[Li(DME)$_3$] (CCDC 1921153).

Identification code	sh3772	
Empirical formula	C75 H115 Ge2 Si4, C12 H30 O6 Li, C6 H14	
Formula weight	1637.67	
Temperature	142(2) K	
Wavelength	0.71073 Å	
Crystal system	Monoclinic	
Space group	$P2_1/c$	
Unit cell dimensions	a = 16.0399(10) Å	α= 90°.
	b = 33.650(3) Å	β= 113.728(3)°.
	c = 19.5422(14) Å	γ = 90°.
Volume	9656.1(12) Å^3	
Z	4	
Density (calculated)	1.127 Mg/m^3	
Absorption coefficient	0.719 mm^{-1}	
F(000)	3552	
Crystal size	0.399 x 0.354 x 0.180 mm^3	
Theta range for data collection	1.210 to 27.235°.	
Index ranges	-19<=h<=20, -43<=k<=43, -25<=l<=25	
Reflections collected	88152	
Independent reflections	21451 [R(int) = 0.0602]	
Completeness to theta = 25.242°	99.9 %	
Absorption correction	Semi-empirical from equivalents	
Max. and min. transmission	0.7455 and 0.6684	
Refinement method	Full-matrix least-squares on F^2	
Data / restraints / parameters	21451 / 286 / 1060	
Goodness-of-fit on F^2	1.273	
Final R indices [I>2sigma(I)]	R1 = 0.0699, wR2 = 0.1800	
R indices (all data)	R1 = 0.0966, wR2 = 0.1956	
Extinction coefficient	n/a	
Largest diff. peak and hole	1.770 and -0.806 e.Å^{-3}	

Theoretical Details and Optimized Structures

All Computations were performed using the Gaussian09 program package.[S2] Optimization of molecular structures was carried out at the BP86-D3/def2SVP level of theory, employing the third generation of Grimme's dispersion correction.[S3-S5] Presence of local minima were verified using frequency analyses at the BP86 /def2SVP level of theory. Pictures of molecular structures were plotted with ChemCraft.[S6]

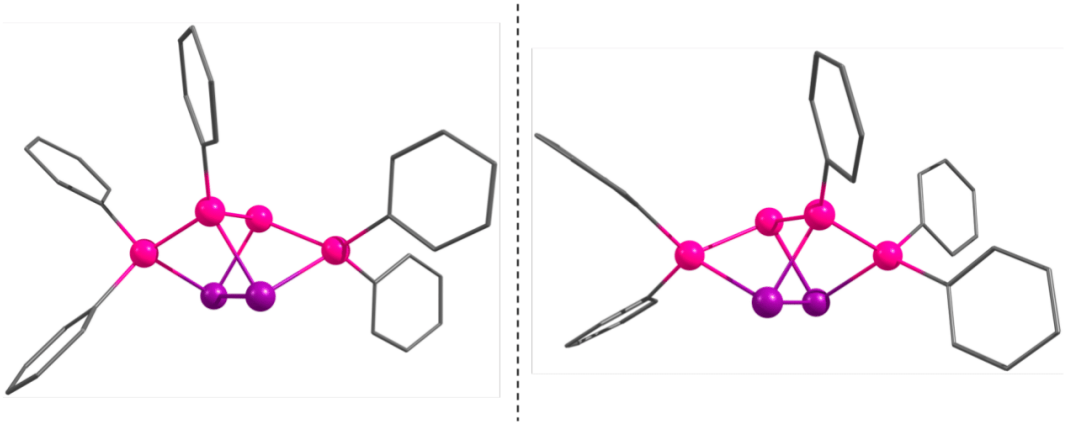

Figure **S1**: Stuctural comparison of the optimized structures of the enantiomeric forms of anionic benzpolarenide **2** (left) and **2'** (right). Hydrogen atomes and isopropyl-carbon atoms are omitted for clarity.

Table S1: Atomic coordinates of optimized benzpolarenide **2**.

C	-5.420873000	-4.751616000	5.073388000
C	-7.196704000	-3.021944000	4.492489000
C	-6.153260000	-4.012771000	3.935042000
C	-5.182188000	-3.314124000	2.989121000
C	-4.301934000	-2.319927000	3.448366000
C	-5.142912000	-3.622913000	1.620956000
C	-1.416431000	-1.239001000	4.059587000
C	-3.294444000	0.471444000	4.052781000
C	-3.430727000	-1.624079000	2.587312000
C	-2.524417000	-0.571280000	3.222669000
C	-4.276761000	-2.962246000	0.725216000
C	-5.974595000	0.255246000	1.319115000
C	-3.413090000	-1.920516000	1.189555000
C	-3.961688000	-4.888416000	-0.908769000
C	3.404226000	-4.295315000	2.034399000
C	-0.448868000	2.850850000	4.355483000
C	-4.324229000	-3.400735000	-0.740023000
C	-5.673950000	-3.049027000	-1.394895000
C	2.378998000	-5.104961000	-0.147970000
C	-4.770542000	0.927178000	0.628317000
C	2.976431000	-3.902289000	0.608198000
C	4.409001000	-0.661172000	3.717430000
C	-4.765126000	2.451666000	0.855105000
C	-0.037686000	2.299760000	2.978221000
C	1.493330000	2.166804000	2.893630000
C	-4.701421000	0.539964000	-0.851504000
C	4.783963000	-0.799668000	2.229218000
C	-0.592947000	3.098725000	1.797359000
C	-3.660843000	-0.284120000	-1.389666000
C	6.118519000	-1.540253000	2.030381000
C	-5.725268000	1.022762000	-1.689142000
C	4.093571000	-3.245925000	-0.200389000
C	5.232526000	-4.034566000	-0.471693000
C	-0.767687000	4.490927000	1.940361000
C	-0.894787000	2.475014000	0.548248000
C	-8.249452000	0.835303000	-3.535570000
C	-3.670168000	-0.533745000	-2.795582000
C	-5.752724000	0.758058000	-3.069202000
C	4.753379000	0.558217000	1.527333000
C	4.023531000	-1.908582000	-0.699548000
C	-1.249495000	5.297122000	0.895747000
C	-3.110748000	-2.572224000	-4.245007000
C	6.307324000	-3.573185000	-1.246389000
C	-2.819763000	7.298199000	0.829192000
C	7.557904000	-4.421496000	-1.449858000
C	-4.706242000	-0.011392000	-3.599346000
C	-2.575330000	-1.336573000	-3.498178000
C	-1.416554000	3.283995000	-0.511746000
C	-6.850997000	1.326058000	-3.961531000
C	-1.377222000	6.807391000	1.063409000
C	3.773870000	0.884128000	0.539262000
C	5.708513000	1.515852000	1.925809000
C	-1.582341000	4.669003000	-0.316868000
C	-6.787152000	2.867193000	-4.008235000
C	8.771479000	-3.781365000	-0.742762000
C	-1.762398000	2.712040000	-1.890552000

C	7.851974000	-4.683994000	-2.940184000
C	5.078416000	-1.465553000	-1.557847000
C	-3.089757000	3.228946000	-2.475141000
C	6.193152000	-2.288655000	-1.806495000
C	3.724162000	2.233957000	0.064174000
C	5.730443000	2.810540000	1.385684000
C	-1.744204000	-0.438314000	-4.432396000
C	-0.375641000	7.547111000	0.151413000
C	6.206379000	5.060227000	2.465674000
C	2.054390000	4.115577000	-0.353365000
C	4.713014000	3.148789000	0.477064000
C	2.625925000	2.775642000	-0.859002000
C	6.806594000	3.817325000	1.777274000
C	-0.608270000	2.959727000	-2.880176000
C	5.022352000	-0.116794000	-2.269075000
C	6.199073000	0.805829000	-1.906189000
C	4.875184000	-0.300506000	-3.791999000
C	3.100086000	2.923152000	-2.319914000
C	7.668061000	4.212095000	0.559517000
H	-6.137002000	-5.303492000	5.720452000
H	-7.942821000	-3.538690000	5.134808000
H	-4.683961000	-5.476623000	4.670518000
H	-4.866562000	-4.038548000	5.720582000
H	-6.701314000	-4.776307000	3.336830000
H	-6.707122000	-2.236681000	5.107502000
H	-7.737531000	-2.509343000	3.670351000
H	-4.297886000	-2.064552000	4.521521000
H	-3.816037000	0.010478000	4.918834000
H	-1.843839000	-1.764679000	4.941572000
H	-5.817752000	-4.407058000	1.236102000
H	-0.686496000	-0.485816000	4.427543000
H	-2.599050000	1.233000000	4.456578000
H	-4.055389000	0.995806000	3.441806000
H	-0.858072000	-1.980150000	3.452145000
H	-5.969774000	0.456049000	2.411029000
H	-4.706440000	-5.556358000	-0.424072000
H	2.541477000	-4.719059000	2.590778000
H	-5.952830000	-0.844433000	1.182240000
H	-6.510041000	-3.604456000	-0.916893000
H	-0.212626000	2.110312000	5.148405000
H	-2.966088000	-5.097787000	-0.466003000
H	-6.933011000	0.638651000	0.905780000
H	-1.533496000	3.078297000	4.406079000
H	-2.021860000	-0.031166000	2.389896000
H	1.485988000	-5.490617000	0.387207000
H	4.210881000	-5.060517000	2.028737000
H	3.772550000	-3.419503000	2.605174000
H	4.393432000	-1.656573000	4.211719000
H	-3.919881000	-5.158693000	-1.985996000
H	-4.808186000	2.679009000	1.941807000
H	0.102250000	3.782337000	4.609482000
H	-5.884107000	-1.963587000	-1.309427000
H	-3.846604000	0.547209000	1.106494000
H	3.111924000	-5.936291000	-0.246005000
H	-5.669235000	-3.306535000	-2.475378000
H	-0.450067000	1.271761000	2.884399000
H	3.401533000	-0.209786000	3.823039000
H	-3.537489000	-2.836126000	-1.280375000
H	1.883557000	1.555300000	3.734704000

H	2.155906000	-3.160519000	0.708931000
H	5.133127000	-0.021371000	4.266275000
H	2.050471000	-4.806126000	-1.163779000
H	-5.636973000	2.949655000	0.378011000
H	6.065617000	-2.564649000	2.455178000
H	5.286056000	-5.054362000	-0.052734000
H	-3.839557000	2.914264000	0.458917000
H	3.987528000	-1.423998000	1.775390000
H	-6.522518000	1.644480000	-1.246875000
H	-8.502175000	1.189934000	-2.513570000
H	1.988728000	3.160682000	2.932682000
H	-0.510358000	4.975707000	2.896288000
H	1.804799000	1.670962000	1.955998000
H	6.956706000	-1.009036000	2.531424000
H	-8.297036000	-0.273209000	-3.523945000
H	-3.667288000	-3.246943000	-3.564502000
H	-3.534213000	6.770254000	1.493963000
H	7.366747000	-5.406359000	-0.966083000
H	6.361492000	-1.633727000	0.952976000
H	-9.035449000	1.212488000	-4.225375000
H	-1.879459000	-1.702396000	-2.712119000
H	-1.108267000	7.042435000	2.118507000
H	-6.978493000	3.301412000	-3.003575000
H	6.466059000	1.241109000	2.680264000
H	8.561903000	-3.615983000	0.334177000
H	-2.270449000	-3.152633000	-4.681666000
H	-2.907742000	8.390183000	1.017504000
H	-3.916107000	3.163269000	-1.743151000
H	-1.874484000	1.612668000	-1.770939000
H	9.676106000	-4.421653000	-0.831065000
H	-3.794464000	-2.291816000	-5.075679000
H	6.982287000	-5.155222000	-3.442736000
H	-3.140647000	7.113024000	-0.217995000
H	-4.697978000	-0.212826000	-4.684867000
H	5.605063000	4.773767000	3.353007000
H	8.731029000	-5.353163000	-3.062626000
H	-7.545806000	3.282678000	-4.706773000
H	1.789253000	4.067619000	0.719597000
H	-6.661776000	0.949992000	-4.992852000
H	-5.784410000	3.214710000	-4.331343000
H	-1.972086000	5.277531000	-1.149128000
H	1.790442000	2.042135000	-0.845767000
H	-3.379303000	2.604799000	-3.346064000
H	9.009994000	-2.792379000	-1.189419000
H	-1.332022000	0.427314000	-3.877890000
H	7.473939000	3.313611000	2.513281000
H	0.662159000	7.201954000	0.338335000
H	-0.415935000	8.646233000	0.313726000
H	-3.014453000	4.282322000	-2.823512000
H	8.076287000	-3.737916000	-3.477807000
H	-0.886683000	-1.001509000	-4.857729000
H	7.000248000	-1.907702000	-2.454907000
H	0.309816000	2.430741000	-2.557858000
H	4.094970000	0.386712000	-1.928765000
H	-2.355240000	-0.046581000	-5.275214000
H	1.127138000	4.367128000	-0.905457000
H	7.003878000	5.761477000	2.794342000
H	-0.600524000	7.354205000	-0.919415000
H	5.535863000	5.614250000	1.774538000

H	6.283679000	0.924553000	-0.807418000
H	2.768061000	4.955911000	-0.497541000
H	-0.870979000	2.594739000	-3.895692000
H	4.681798000	4.173469000	0.072462000
H	-0.379806000	4.045103000	-2.955912000
H	3.976261000	-0.906237000	-4.028957000
H	7.163310000	0.406241000	-2.289550000
H	3.279121000	1.940280000	-2.796644000
H	5.759300000	-0.814742000	-4.227184000
H	8.107682000	3.315965000	0.074857000
H	2.335761000	3.451006000	-2.926943000
H	6.052389000	1.814740000	-2.345382000
H	8.495014000	4.893931000	0.854340000
H	4.041986000	3.511138000	-2.372924000
H	7.055569000	4.735781000	-0.205213000
H	4.774067000	0.683919000	-4.298079000
Si	-2.331829000	-1.029607000	-0.167687000
Si	0.715942000	-1.174471000	1.047732000
Ge	-0.424566000	-2.624815000	-0.701772000
Si	-0.647450000	0.584966000	0.219064000
Si	2.699662000	-0.584939000	-0.148527000
Ge	0.706500000	-0.410464000	-1.596547000

Table S2: Atomic coordinates of optimized benzpolarenide **2'**.

C	5.572685000	-4.704764000	-4.953861000
C	7.311764000	-2.957109000	-4.316711000
C	6.265023000	-3.962746000	-3.792875000
C	5.261752000	-3.278042000	-2.870691000
C	4.381322000	-2.293833000	-3.350222000
C	5.194783000	-3.586361000	-1.503625000
C	1.527579000	-1.241315000	-4.072605000
C	3.363244000	0.504174000	-3.956845000
C	3.481842000	-1.607518000	-2.510644000
C	2.581260000	-0.565662000	-3.173259000
C	4.303915000	-2.932277000	-0.627436000
C	5.994632000	0.293581000	-1.194795000
C	3.437875000	-1.901320000	-1.111926000
C	3.968580000	-4.852798000	1.010790000
C	-3.392124000	-4.304103000	-1.870702000
C	0.467896000	2.865782000	-4.326680000
C	4.331407000	-3.365415000	0.840487000
C	5.672564000	-3.009467000	1.510682000
C	-2.394617000	-5.104196000	0.330631000
C	4.773437000	0.961343000	-0.530216000
C	-2.976402000	-3.905466000	-0.443048000
C	-4.439047000	-0.689751000	-3.621365000
C	4.763080000	2.484645000	-0.764433000
C	0.041418000	2.318936000	-2.952560000
C	-1.491563000	2.195002000	-2.876966000
C	4.679120000	0.579920000	0.949405000
C	-4.800319000	-0.809601000	-2.128256000
C	0.591940000	3.115184000	-1.767416000
C	3.640313000	-0.258215000	1.468078000
C	-6.132444000	-1.548267000	-1.908205000
C	5.680101000	1.078654000	1.804988000
C	-4.094411000	-3.229344000	0.346348000
C	-5.236911000	-4.008374000	0.629878000

C	0.761416000	4.508743000	-1.903280000
C	0.890403000	2.486393000	-0.520169000
C	8.163323000	0.908113000	3.722725000
C	3.631827000	-0.514572000	2.873320000
C	5.682571000	0.819756000	3.186190000
C	-4.761611000	0.557407000	-1.444479000
C	-4.019950000	-1.881842000	0.816694000
C	1.232362000	5.311334000	-0.851082000
C	3.116903000	-2.515802000	4.391554000
C	-6.311453000	-3.527662000	1.392895000
C	2.791163000	7.320802000	-0.760052000
C	-7.567847000	-4.364893000	1.605757000
C	4.640336000	0.031236000	3.696479000
C	2.550231000	-1.353607000	3.555321000
C	1.399454000	3.291817000	0.548440000
C	6.753447000	1.406745000	4.099269000
C	1.353528000	6.823179000	-1.009441000
C	-3.775204000	0.892566000	-0.465800000
C	-5.715812000	1.512869000	-1.849589000
C	1.558932000	4.678778000	0.361139000
C	6.689284000	2.948341000	4.117199000
C	-8.771184000	-3.735064000	0.872285000
C	1.740938000	2.713227000	1.925439000
C	-7.877141000	-4.590858000	3.098887000
C	-5.072745000	-1.420195000	1.667740000
C	3.042236000	3.263573000	2.537645000
C	-6.191307000	-2.234124000	1.930379000
C	-3.719318000	2.247409000	-0.007254000
C	-5.731147000	2.814103000	-1.324962000
C	1.610232000	-0.466392000	4.390777000
C	0.339854000	7.552447000	-0.102377000
C	-6.209105000	5.056020000	-2.421287000
C	-2.049045000	4.131871000	0.386371000
C	-4.708040000	3.159962000	-0.425622000
C	-2.615838000	2.795401000	0.905587000
C	-6.807509000	3.818684000	-1.721444000
C	0.568125000	2.910545000	2.904081000
C	-5.009954000	-0.062501000	2.360248000
C	-6.185789000	0.858419000	1.990119000
C	-4.859396000	-0.226603000	3.885332000
C	-3.082186000	2.956785000	2.367898000
C	-7.665110000	4.222959000	-0.504032000
H	6.312529000	-5.245543000	-5.583288000
H	8.080535000	-3.461367000	-4.942074000
H	4.833784000	-5.440408000	-4.574496000
H	5.027696000	-3.995693000	-5.613203000
H	6.805126000	-4.722757000	-3.183061000
H	6.829486000	-2.173480000	-4.939588000
H	7.824337000	-2.443461000	-3.477317000
H	4.400095000	-2.037886000	-4.423151000
H	3.929823000	0.064077000	-4.805426000
H	2.004465000	-1.726753000	-4.952427000
H	5.868699000	-4.363330000	-1.103072000
H	0.791832000	-0.497358000	-4.447989000
H	2.667807000	1.255648000	-4.380264000
H	4.086296000	1.037305000	-3.309378000
H	0.966607000	-2.018211000	-3.514577000
H	6.009308000	0.489331000	-2.287561000
H	4.720738000	-5.521946000	0.539191000

H	-2.525477000	-4.733561000	-2.416640000
H	5.977132000	-0.805586000	-1.053065000
H	6.516159000	-3.563427000	1.044441000
H	0.232370000	2.126709000	-5.121207000
H	2.979497000	-5.065663000	0.555267000
H	6.942646000	0.684947000	-0.765283000
H	1.555030000	3.083363000	-4.367465000
H	2.030313000	-0.047420000	-2.357747000
H	-1.500668000	-5.502237000	-0.193858000
H	-4.203537000	-5.064367000	-1.869499000
H	-3.748841000	-3.427574000	-2.447922000
H	-4.417237000	-1.692241000	-4.100925000
H	3.911932000	-5.116834000	2.088831000
H	4.827933000	2.707693000	-1.850911000
H	-0.072411000	3.802146000	-4.585981000
H	5.880966000	-1.923572000	1.426412000
H	3.861601000	0.571971000	-1.024168000
H	-3.133434000	-5.929620000	0.434017000
H	5.656115000	-3.265781000	2.591331000
H	0.446610000	1.287869000	-2.855261000
H	-3.437385000	-0.229294000	-3.742990000
H	3.537776000	-2.800574000	1.369617000
H	-1.879408000	1.577037000	-3.714540000
H	-2.148685000	-3.172556000	-0.541868000
H	-5.174657000	-0.065718000	-4.173206000
H	-2.070627000	-4.795215000	1.345062000
H	5.621548000	2.990450000	-0.271646000
H	-6.082470000	-2.577272000	-2.322236000
H	-5.293223000	-5.035824000	0.230335000
H	3.826543000	2.943107000	-0.389878000
H	-3.999234000	-1.428430000	-1.674023000
H	6.477681000	1.709416000	1.376428000
H	8.445489000	1.243317000	2.701735000
H	-1.979999000	3.191807000	-2.929177000
H	0.507700000	4.996839000	-2.858564000
H	-1.812733000	1.709926000	-1.936307000
H	-6.975840000	-1.023145000	-2.406997000
H	8.210100000	-0.200462000	3.733056000
H	3.790426000	-3.157246000	3.787908000
H	3.514407000	6.799968000	-1.420908000
H	-7.377502000	-5.361783000	1.146944000
H	-6.365349000	-1.630150000	-0.827705000
H	8.929708000	1.297635000	4.427661000
H	1.924827000	-1.803723000	2.753222000
H	1.092549000	7.062557000	-2.065575000
H	6.911165000	3.365916000	3.111793000
H	-6.478262000	1.230959000	-2.596418000
H	-8.550969000	-3.597402000	-0.206412000
H	2.290604000	-3.153655000	4.770829000
H	2.874676000	8.414112000	-0.942613000
H	3.879956000	3.242361000	1.815921000
H	1.888146000	1.620063000	1.794272000
H	-9.680615000	-4.367432000	0.968064000
H	3.692497000	-2.156392000	5.272204000
H	-7.014600000	-5.054267000	3.620678000
H	3.104045000	7.132743000	0.289056000
H	4.615179000	-0.169525000	4.781695000
H	-5.610005000	4.762418000	-3.307773000
H	-8.760583000	-5.252822000	3.228470000

H	7.427408000	3.375066000	4.830732000
H	-1.790684000	4.076274000	-0.687798000
H	6.534983000	1.049056000	5.131384000
H	5.677960000	3.302372000	4.404590000
H	1.938659000	5.285709000	1.199010000
H	-1.780432000	2.061567000	0.890912000
H	3.340689000	2.631512000	3.399592000
H	-9.007036000	-2.733783000	1.292255000
H	1.133461000	0.303633000	3.752235000
H	-7.477342000	3.309701000	-2.451552000
H	-0.694398000	7.203005000	-0.300599000
H	0.375865000	8.652664000	-0.258115000
H	2.925216000	4.306058000	2.906725000
H	-8.102060000	-3.631455000	3.611938000
H	0.795467000	-1.070746000	4.842978000
H	-6.996921000	-1.838230000	2.571698000
H	-0.324131000	2.345395000	2.571285000
H	-4.082486000	0.432283000	2.009246000
H	2.157981000	0.052056000	5.208481000
H	-1.119435000	4.389089000	0.931290000
H	-7.007534000	5.754502000	-2.753553000
H	0.556079000	7.354612000	0.969329000
H	-5.536936000	5.615871000	-1.736475000
H	-6.278000000	0.958922000	0.890234000
H	-2.763463000	4.971809000	0.528728000
H	0.836609000	2.551846000	3.920045000
H	-4.672644000	4.188962000	-0.032560000
H	0.294837000	3.985344000	2.981290000
H	-3.963218000	-0.833637000	4.129067000
H	-7.148537000	0.468541000	2.386951000
H	-3.255391000	1.979396000	2.857529000
H	-5.745009000	-0.730439000	4.329516000
H	-8.104032000	3.330612000	-0.011799000
H	-2.317491000	3.495296000	2.964601000
H	-6.032949000	1.873932000	2.411391000
H	-8.492328000	4.903524000	-0.801098000
H	-4.026293000	3.541348000	2.418512000
H	-7.049732000	4.751248000	0.255205000
H	-4.752548000	0.764046000	4.378022000
Si	2.333389000	-1.009649000	0.226789000
Ge	-0.730728000	-1.227499000	-1.178236000
Ge	0.429408000	-2.596461000	0.779342000
Si	0.652409000	0.588009000	-0.233122000
Si	-2.697275000	-0.575676000	0.212589000
Si	-0.680533000	-0.428602000	1.452710000

References

S1 A. Jana, V. Huch, M. Repisky, R. J. F. Berger and D. Scheschkewitz, *Angew. Chem. Int. Ed.*, 2014, **53**, 3514.

S2 Gaussian 09, Revision A.02, M. J. Frisch, G. W. Trucks, H. B. Schlegel, G. E. Scuseria, M. A. Robb, J. R. Cheeseman, G. Scalmani, V. Barone, G. A. Petersson, H. Nakatsuji, X. Li, M. Caricato, A. Marenich, J. Bloino, B. G. Janesko, R. Gomperts, B. Mennucci, H. P. Hratchian, J. V. Ortiz, A. F. Izmaylov, J. L. Sonnenberg, D. Williams-Young, F. Ding, F. Lipparini, F. Egidi, J. Goings, B. Peng, A. Petrone, T. Henderson, D. Ranasinghe, V. G. Zakrzewski, J. Gao, N. Rega, G. Zheng, W. Liang, M. Hada, M. Ehara, K. Toyota, R. Fukuda, J. Hasegawa, M. Ishida, T. Nakajima, Y. Honda, O. Kitao, H. Nakai, T. Vreven, K. Throssell, J. A. Montgomery, Jr., J. E. Peralta, F. Ogliaro, M. Bearpark, J. J. Heyd, E. Brothers, K. N. Kudin, V. N. Staroverov, T. Keith, R. Kobayashi, J. Normand, K. Raghavachari, A. Rendell, J. C. Burant, S. S. Iyengar, J. Tomasi, M. Cossi, J. M. Millam, M. Klene, C. Adamo, R. Cammi, J. W. Ochterski, R. L. Martin, K. Morokuma, O. Farkas, J. B. Foresman and D. J. Fox, *Gaussian Inc.*, Wallingford CT, 2016.

S3 a) J. P.Perdew, *Phys. Rev. B*, 1986, **33**, 8822; b) A. D. Becke, *Phys. Rev. A*, 1988, **38**,3098.

S4 a) A. Horn, H. Horn, R. Ahlrichs, *J. Chem. Phys.*, 1992, **97**, 2571; b) A. Schäfer, C. Huber, R. Ahlrichs, *J. Chem. Phys*., 1994, **100**, 5829; c) F. Weigend, R. Ahlrichs, *Phys. Chem. Chem. Phys*., 2005, **18**, 3297; d) F. Weigend, *Phys. Chem. Chem. Phys*., 2006, **9**, 1057.

S5 S. Grimme, J. Antony, S. Ehrlich, H. Krieg, *J. Chem. Phys*., 2010, **132**, 154104.

S6 Chemcraft - graphical software for visualization of quantum chemistry computations. https://www.chemcraftprog.com

Persistent digermenes with acyl and α-chlorosilyl functionalities (SI)

CHEMISTRY
A European Journal

Supporting Information

Persistent Digermenes with Acyl and α-Chlorosilyl Functionalities

Lukas Klemmer[+], Yvonne Kaiser[+], Volker Huch, Michael Zimmer, and David Scheschkewitz*[a]

chem_201902553_sm_miscellaneous_information.pdf

Table of contents

NMR-, IR and UV/vis spectra

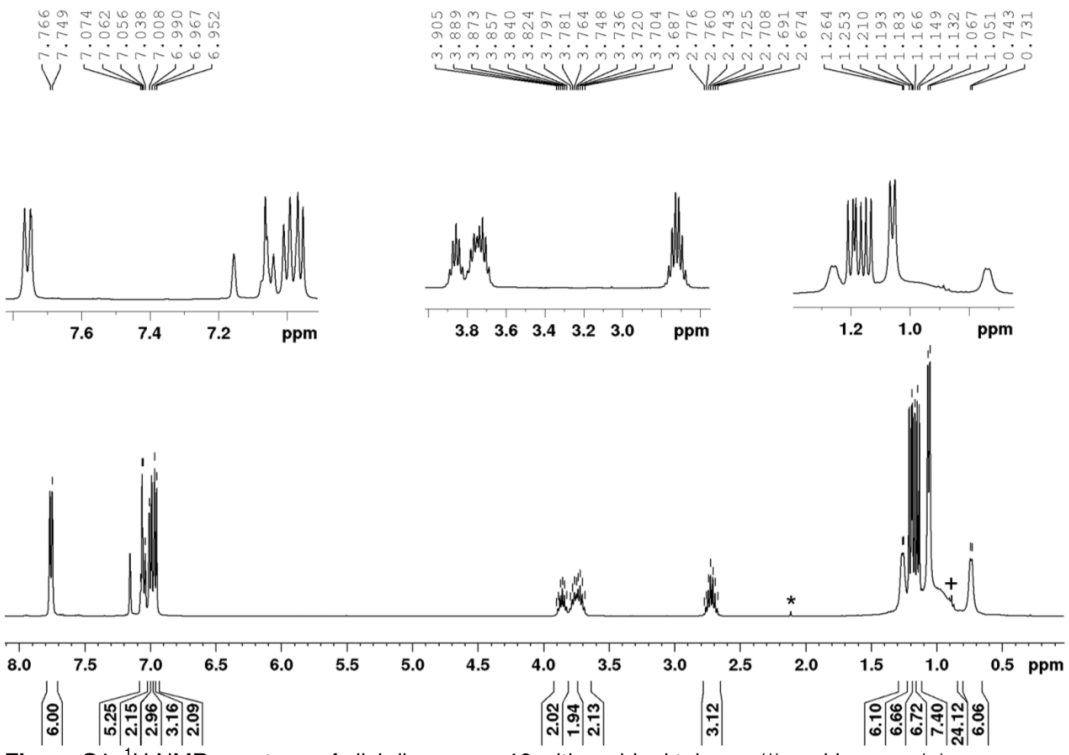

Figure S1: ^{1}H NMR spectrum of silyl digermene **10** with residual toluene (*) and hexane (+).

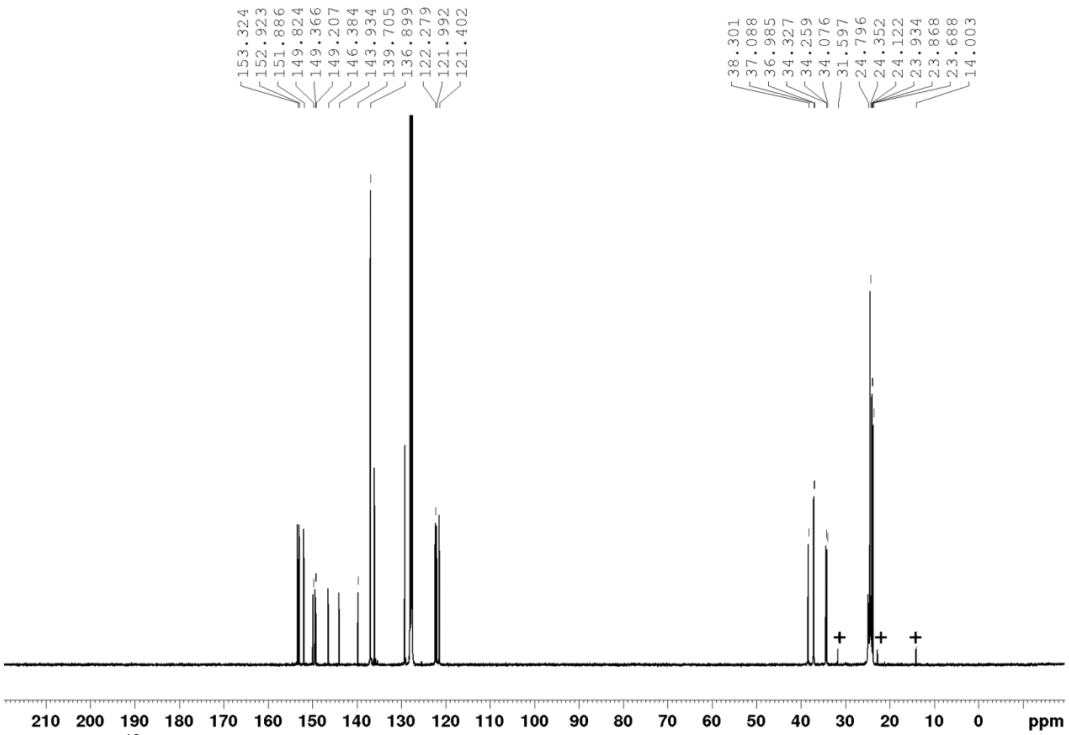

Figure S2: ^{13}C NMR spectrum of silyl digermene **10** with residual hexane (+).

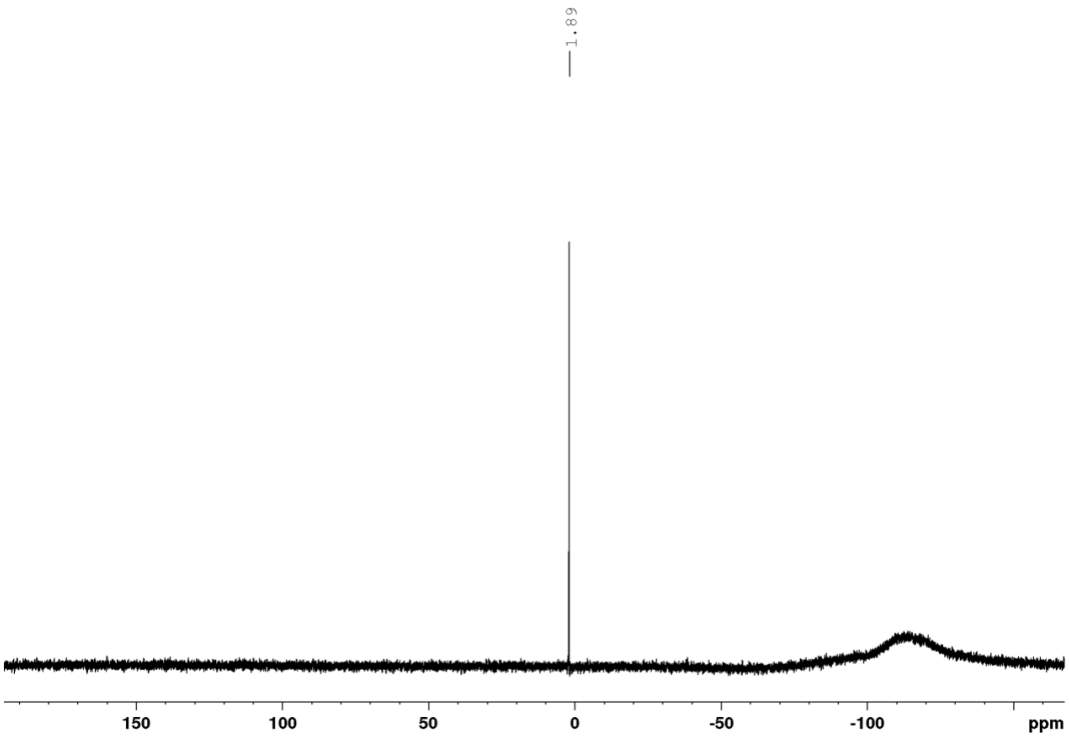

Figure S3: ^{29}Si NMR spectrum of silyl digermene **10**.

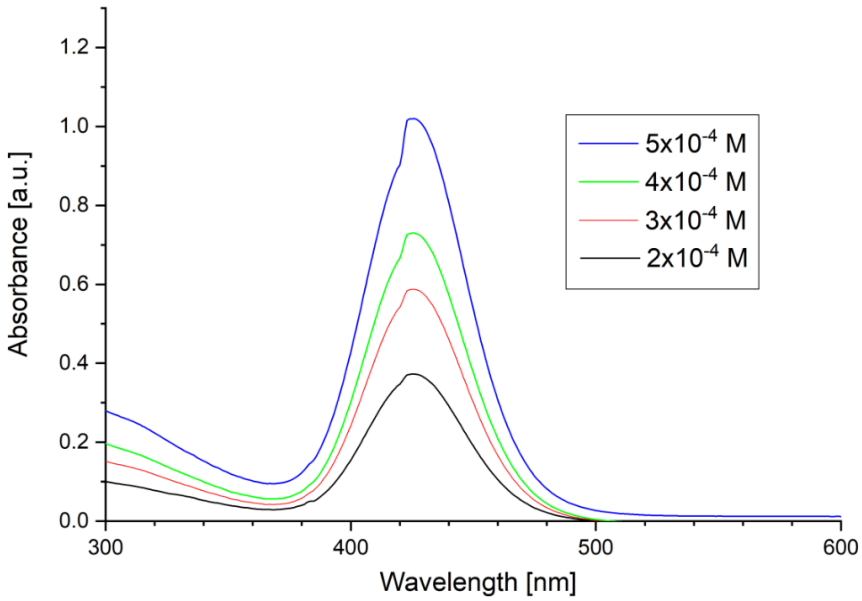

Figure S4: UV/vis spectra of **10** in hexane at different concentrations ($2\cdot10^{-4}$ - $5\cdot10^{-4}$ mol L^{-1}).

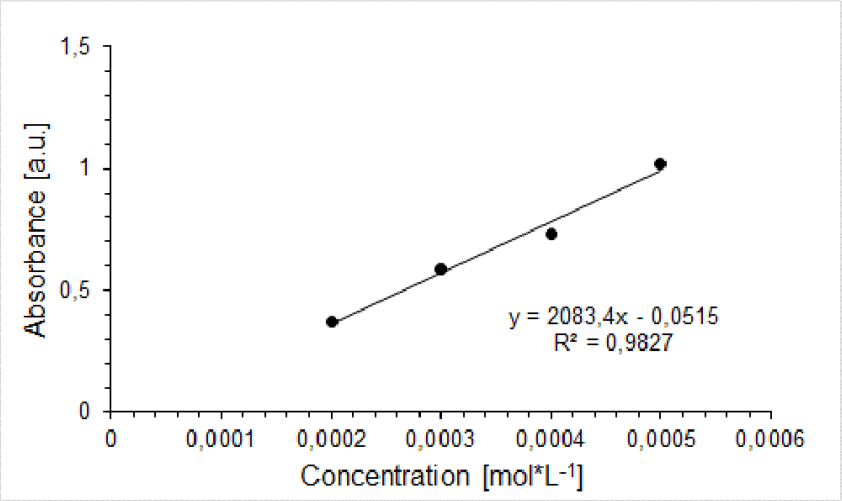

Figure S5: Determination of ε (20834 L mol^{-1} cm^{-1}) by linear regression of absorbance (λ = 426 nm) of **10** against concentration.

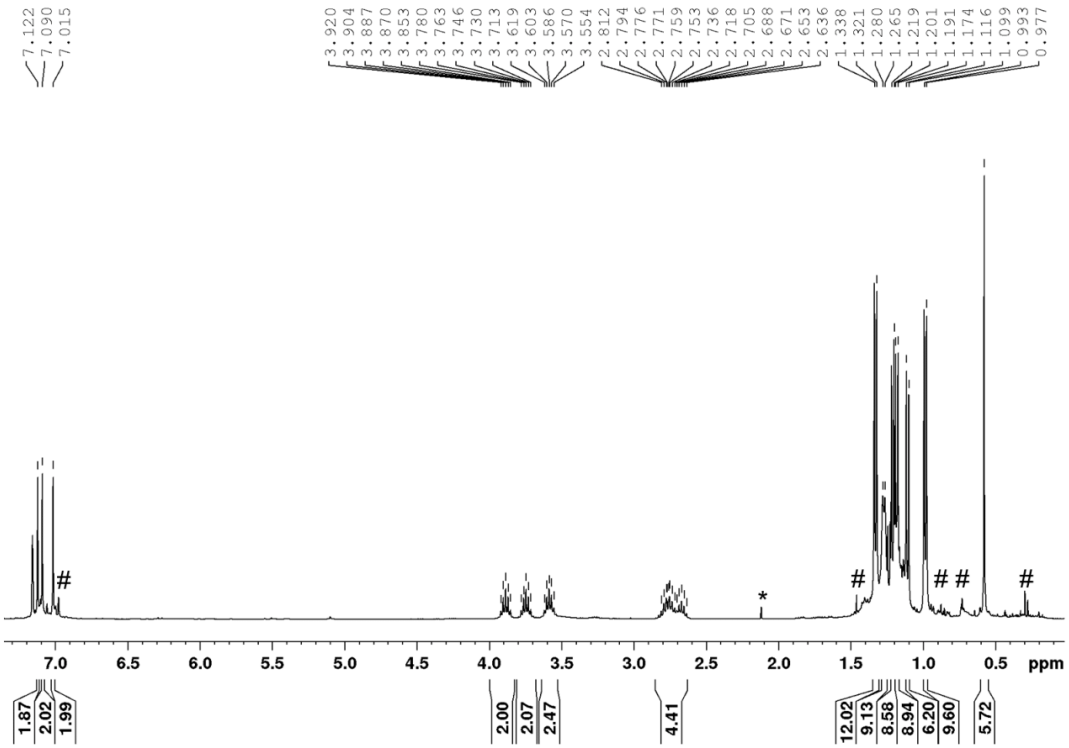

Figure S6: ^{1}H NMR spectrum of chlorosilyl digermene **11a** with residual toluene (*) and unidentified impurities (#).

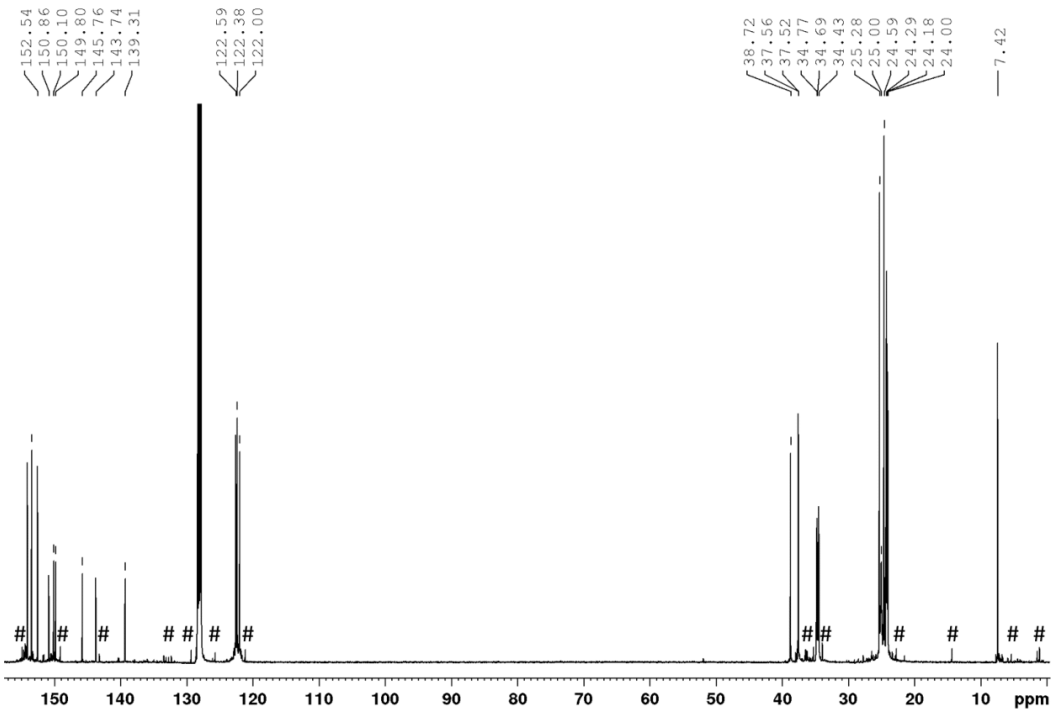

Figure S7: ^{13}C NMR spectrum of chlorosilyl digermene **11a** with residual unidentified impurities (#).

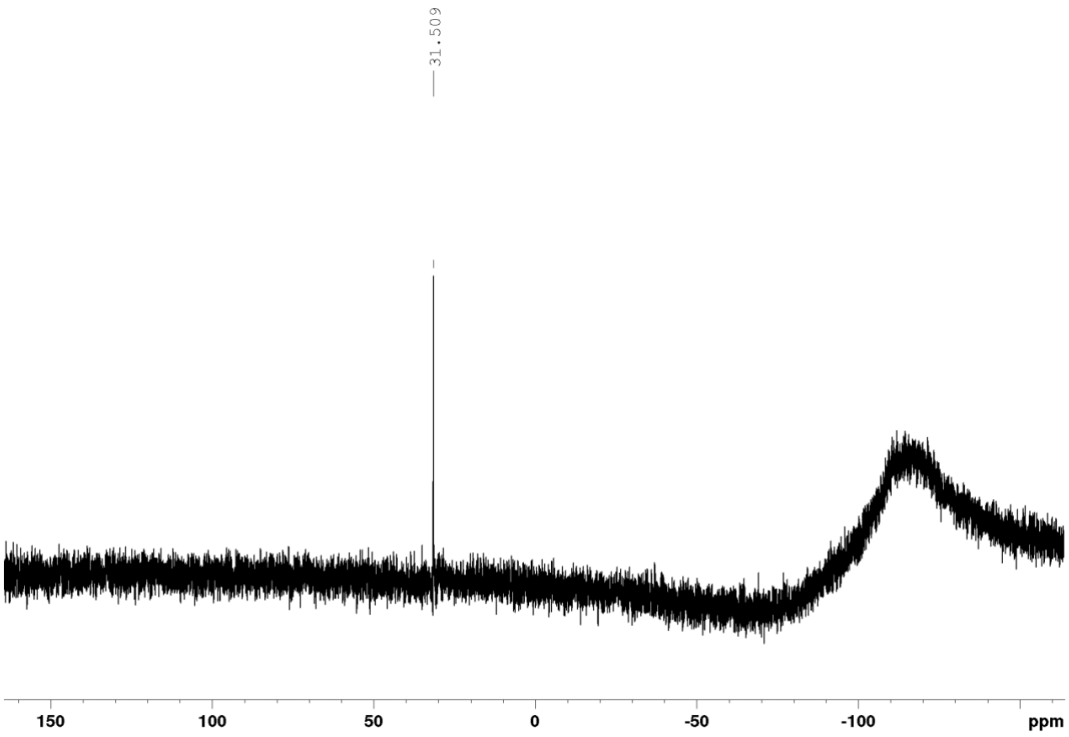

Figure S8: ^{29}Si NMR spectrum of chlorosilyl digermene **11a**.

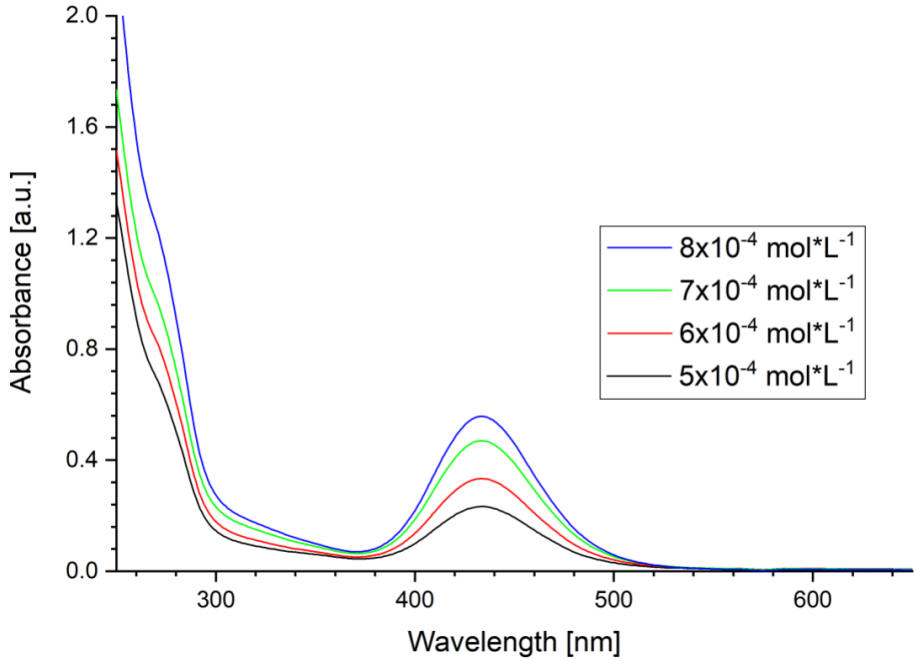

Figure S9: UV/vis spectra of **11a** in hexane at different concentrations ($5 \cdot 10^{-4}$ - $8 \cdot 10^{-4}$ mol L^{-1}).

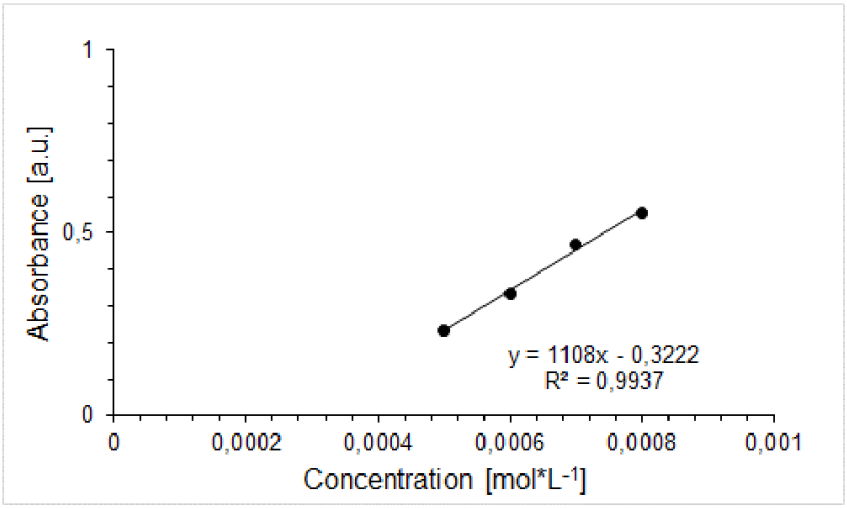

Figure S10: Determination of ε (11080 L mol^{-1} cm^{-1}) by linear regression of absorbance (λ = 435 nm) of **11a** against concentration.

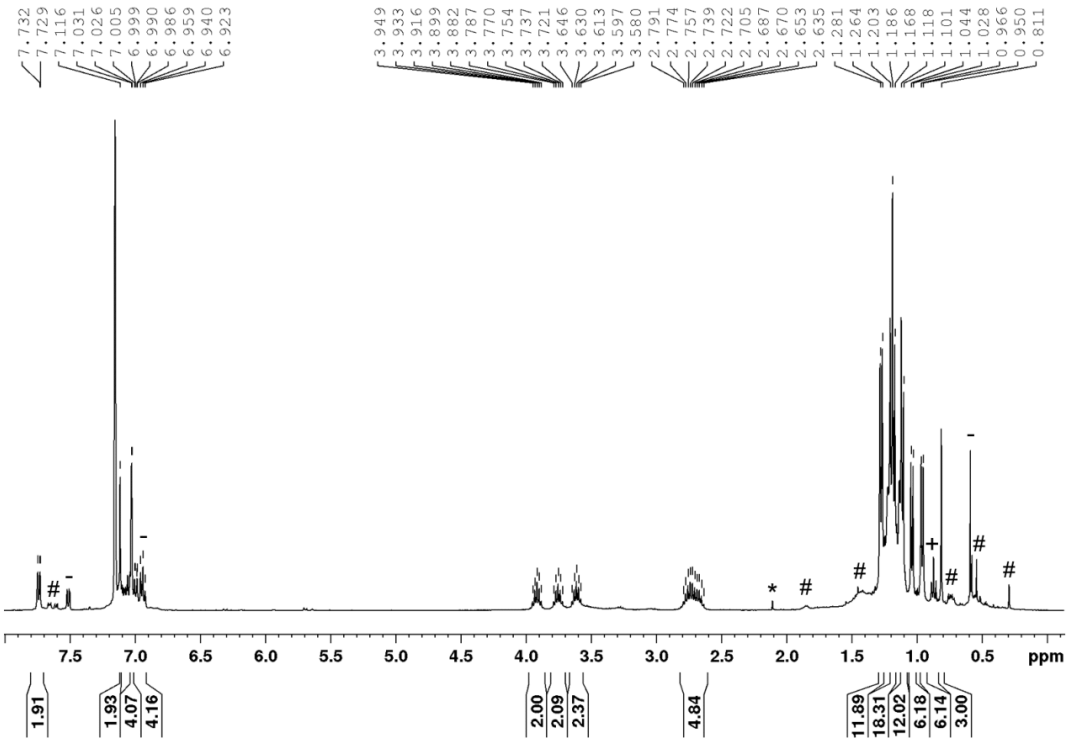

Figure S11: ^{1}H NMR spectrum of chlorosilyl digermene **11b** with residual toluene (*), hexane (+), $MePhSiCl_2$ (-) and unidentified impurities (#).

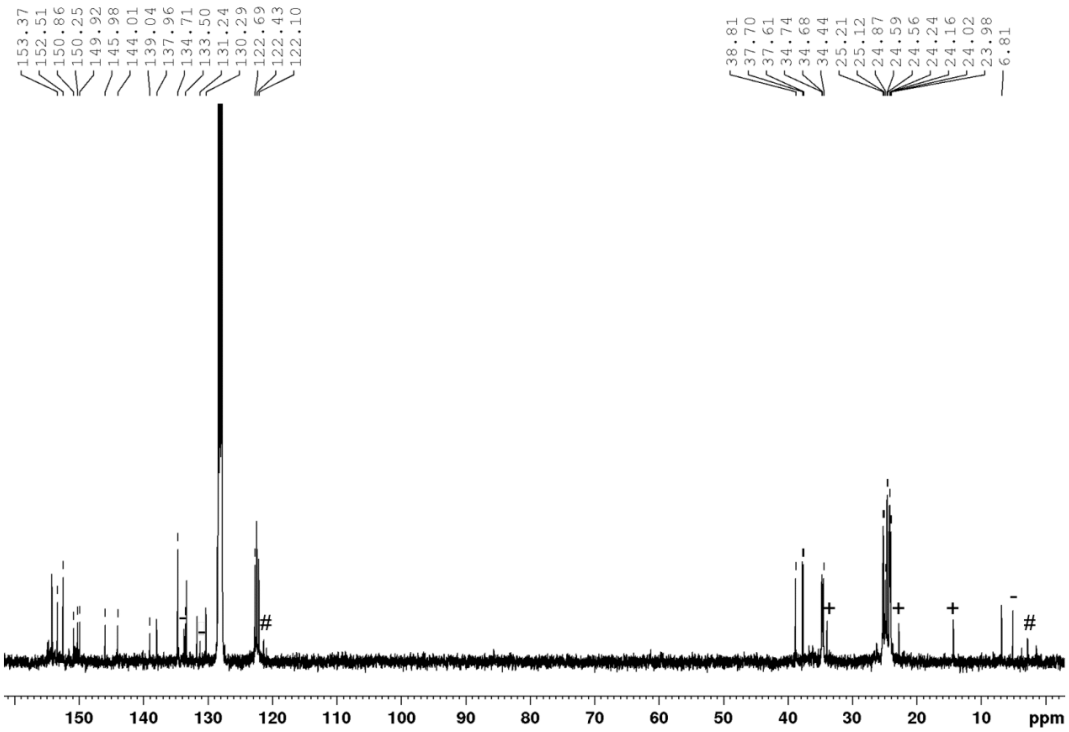

Figure S12: ^{13}C NMR spectrum of chlorosilyl digermene **11b** with residual hexane (+), $MePhSiCl_2$ (-) and unidentified impurities (#).

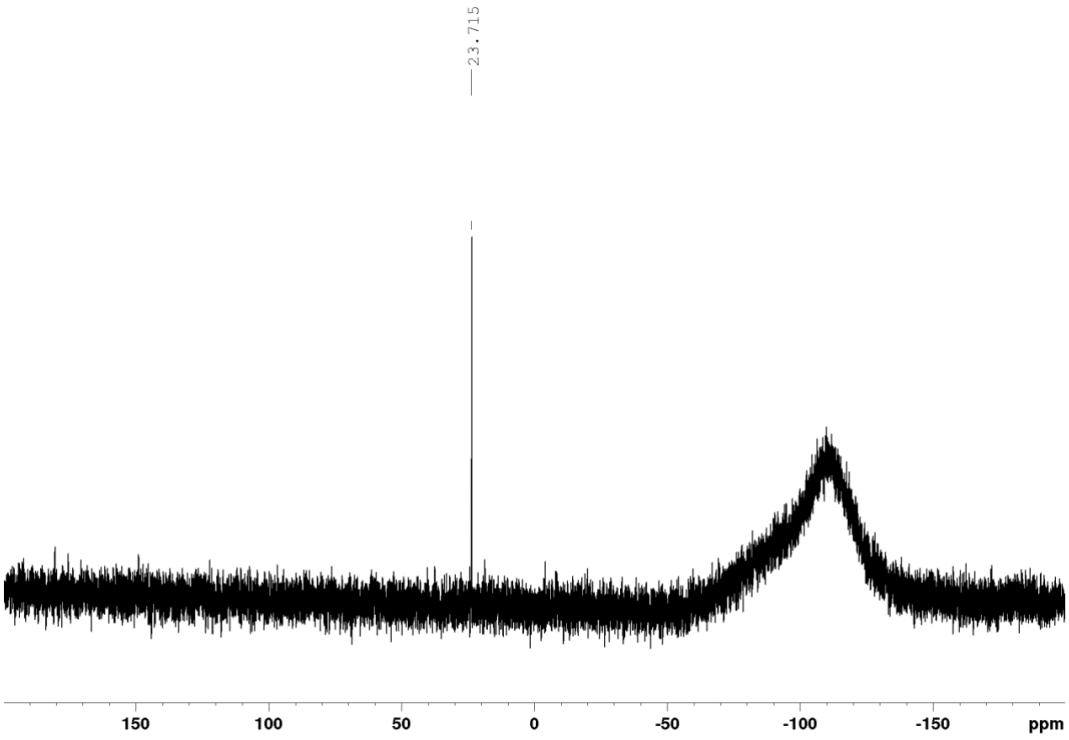

Figure S13: ^{29}Si NMR spectrum of chlorosilyl digermene **11b**.

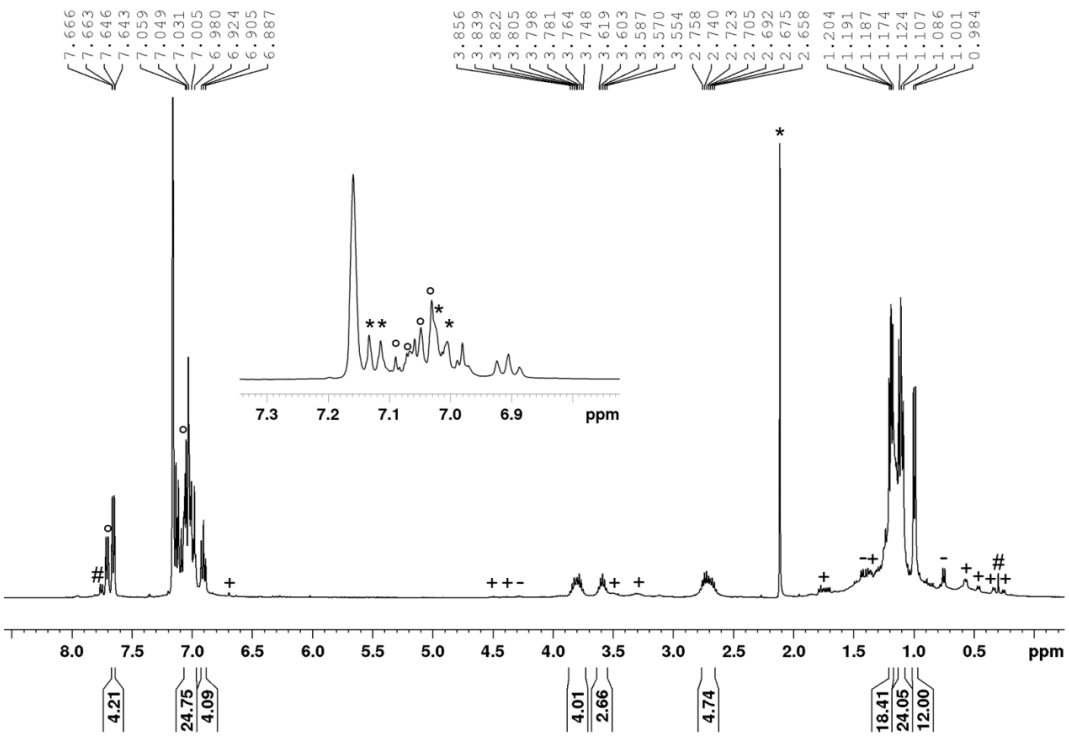

Figure S14: ^{1}H NMR spectrum of chlorosilyl digermene **11c** with residual toluene (*), Tip_4-Digermene (-), Tetragermabutadiene (+), $Ph2SiCl_2$ (°) and unidentified impurities (#).

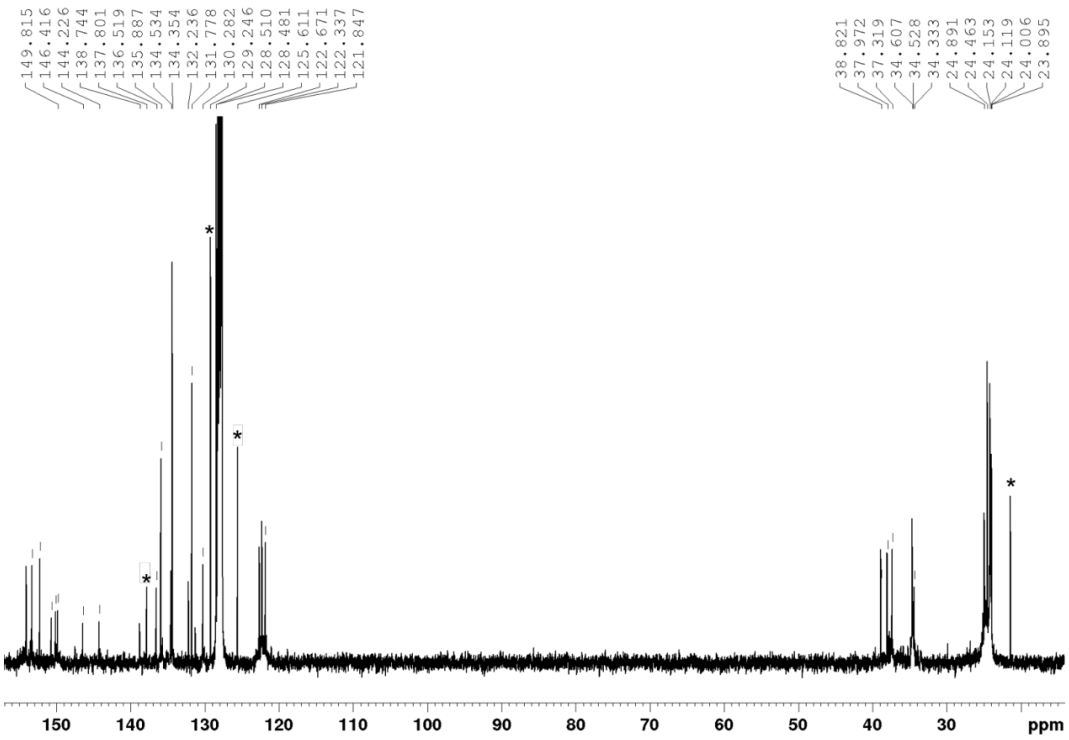

Figure S15: ^{13}C NMR spectrum of chlorosilyl digermene **11c** with residual toluene (*).

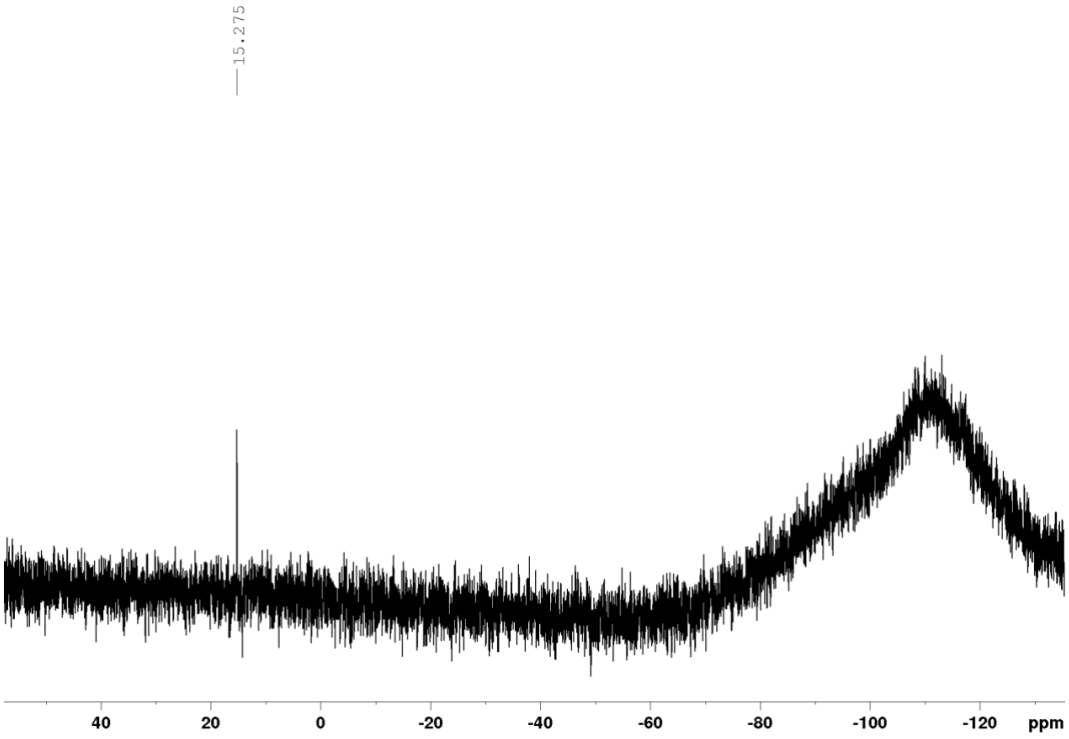

Figure S16: ^{29}Si NMR spectrum of chlorosilyl digermene **11c**.

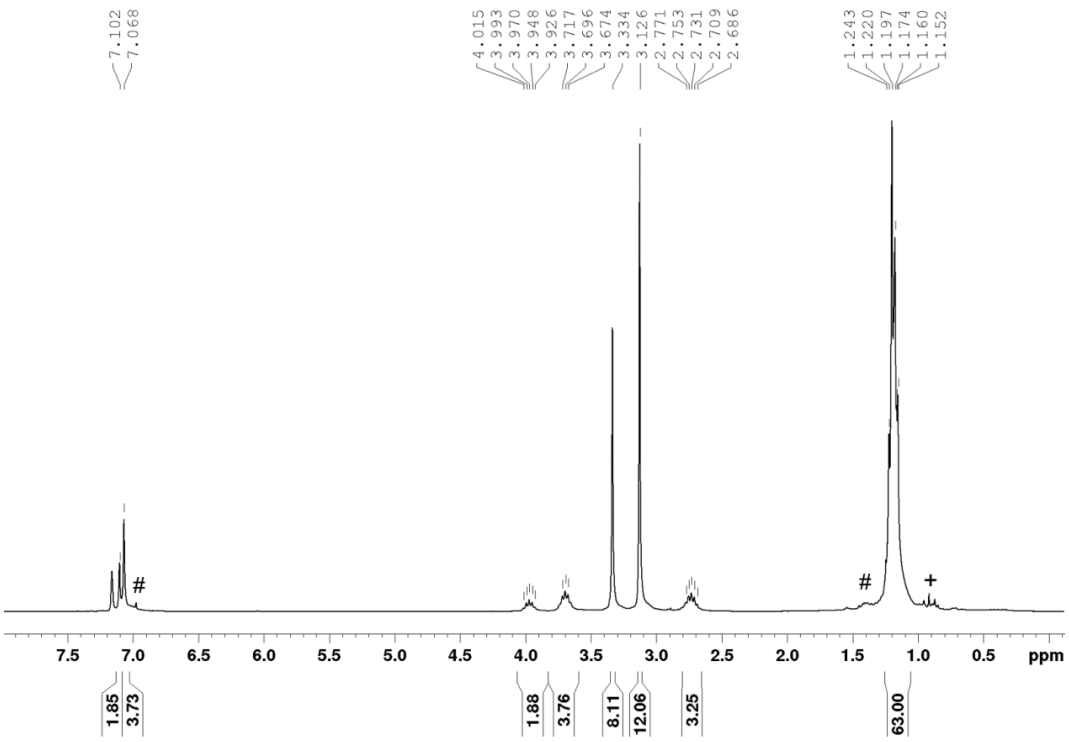

Figure S17: ^{1}H NMR spectrum of acyl digermene **13a** with residual hexane (+) and unidentified side products (#).

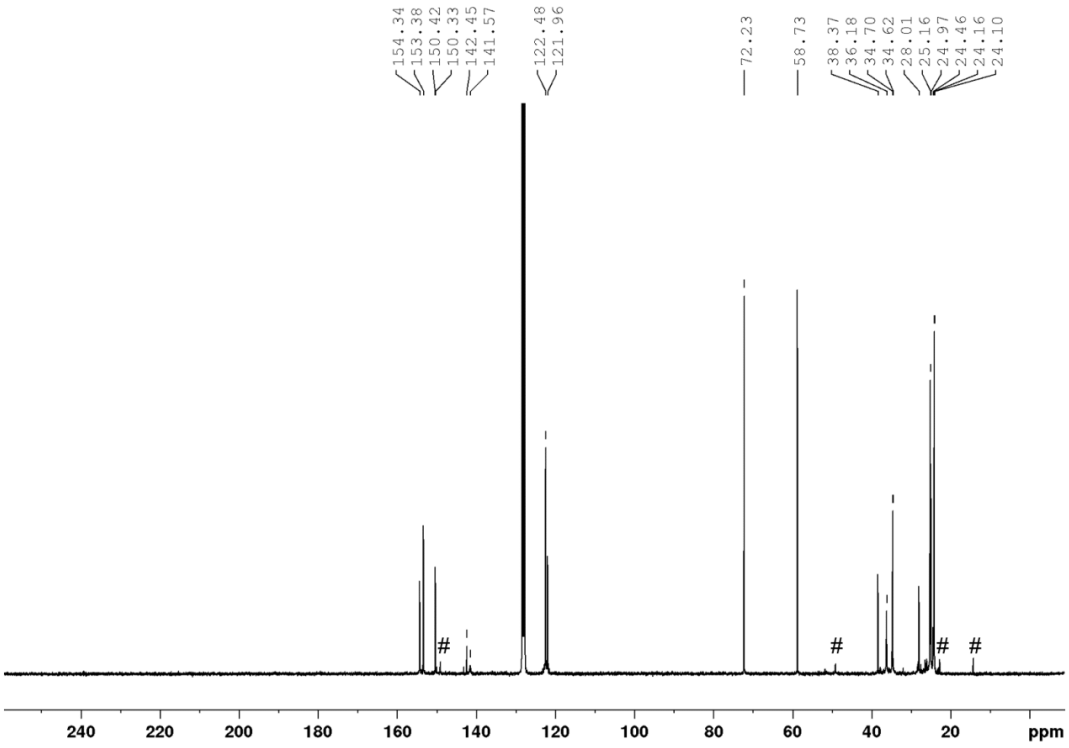

Figure S18: ^{13}C NMR spectrum of acyl digermene **13a** with residual unidentified side products (#).

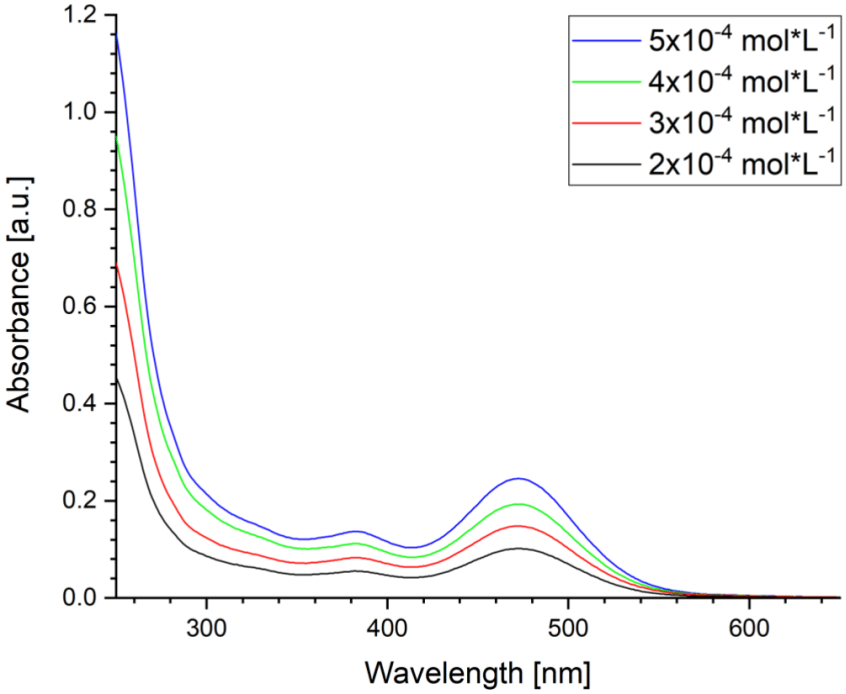

Figure S19: UV/vis spectra of **13a** in hexane at different concentrations ($2 \cdot 10^{-4}$ - $5 \cdot 10^{-4}$ mol L^{-1}).

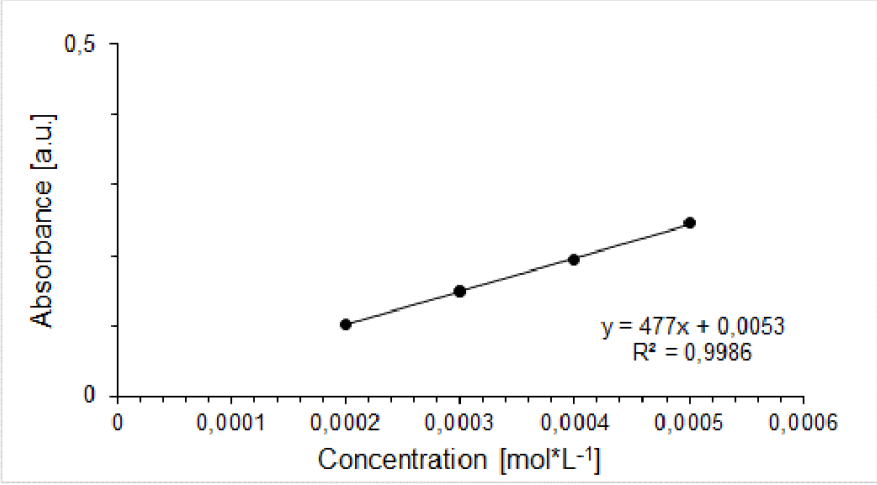

Figure S20: Determination of ε (4770 L mol^{-1} cm^{-1}) by linear regression of absorbance (λ = 472 nm) of **13a** against concentration.

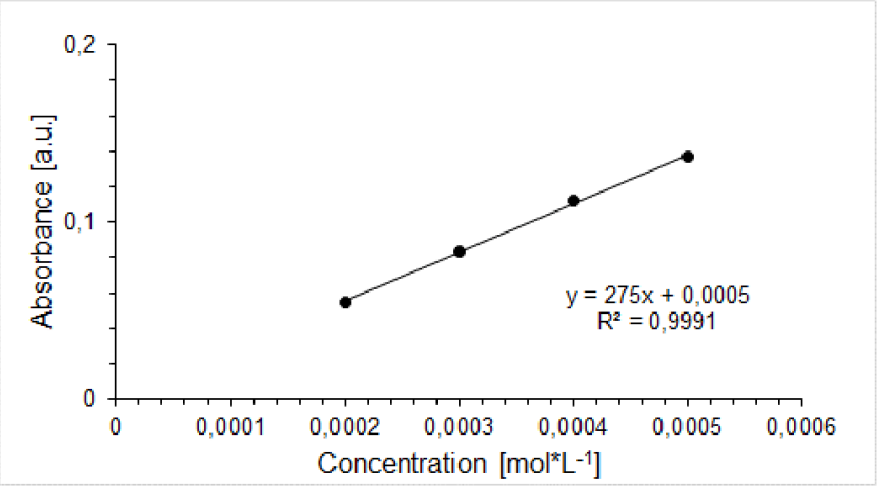

Figure S21: Determination of ε (2750 L mol^{-1} cm^{-1}) by linear regression of absorbance (λ = 383 nm) of **13a** against concentration.

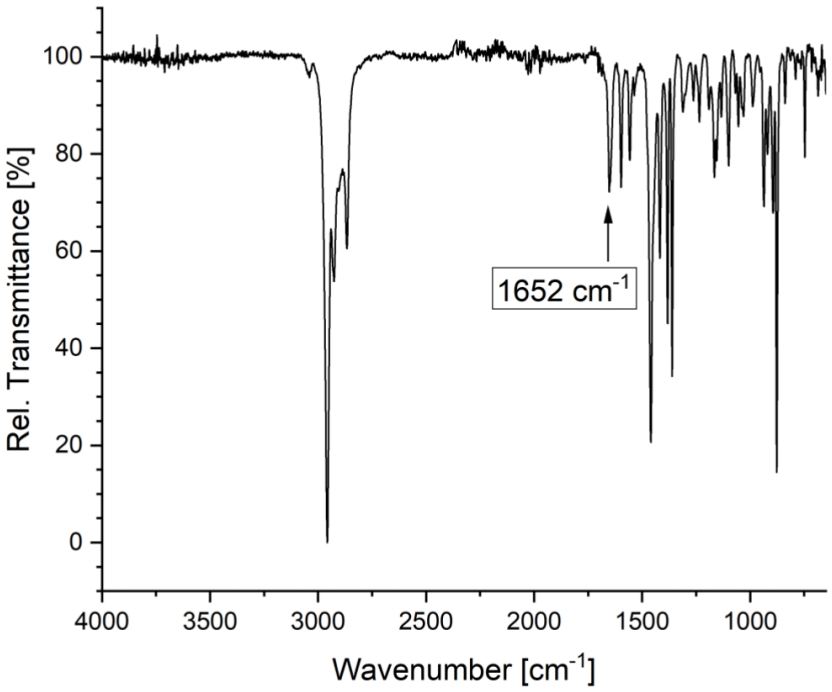

Figure S22: Infrared spectrum of acyl digermene **13a** (powder).

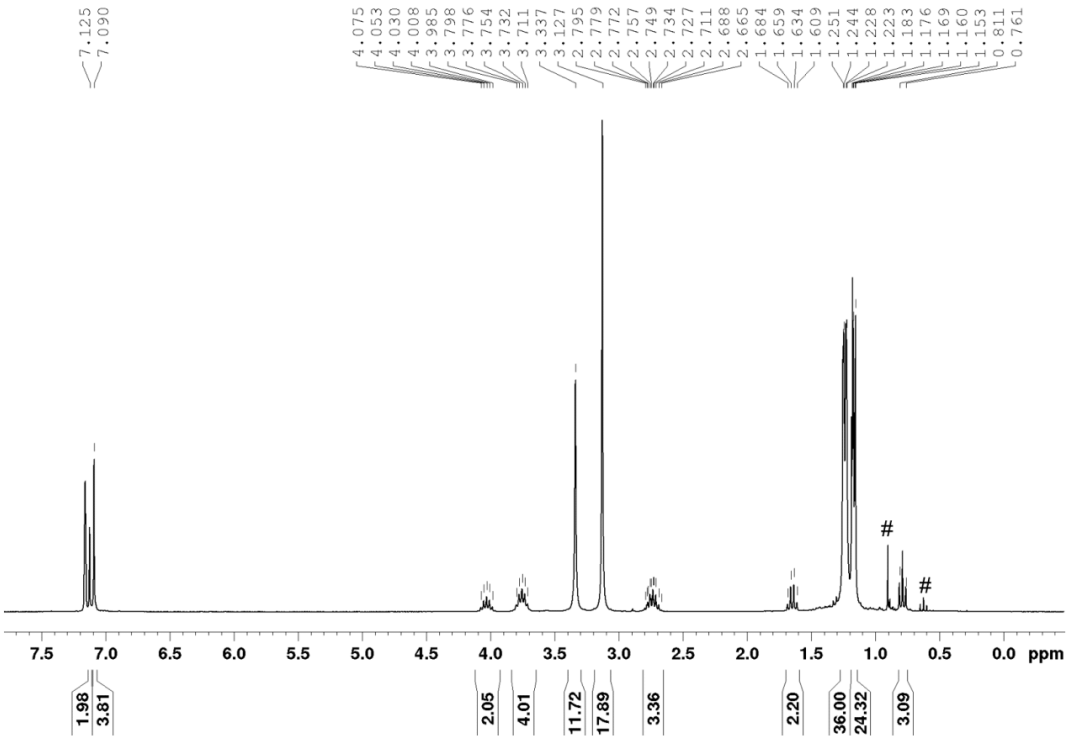

Figure S23: ^{1}H NMR spectrum of acyl digermene **13b** with residual unidentified side products.

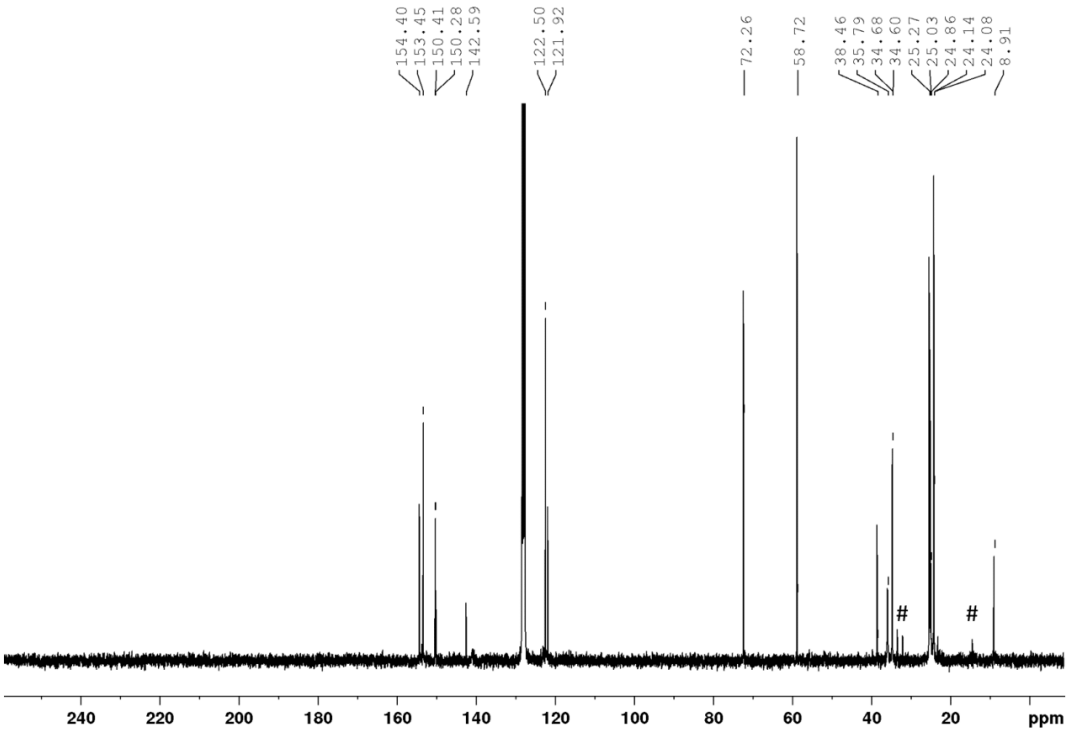

Figure S24: ^{13}C NMR spectrum of acyl digermene **13b** with residual unidentified impurities (#).

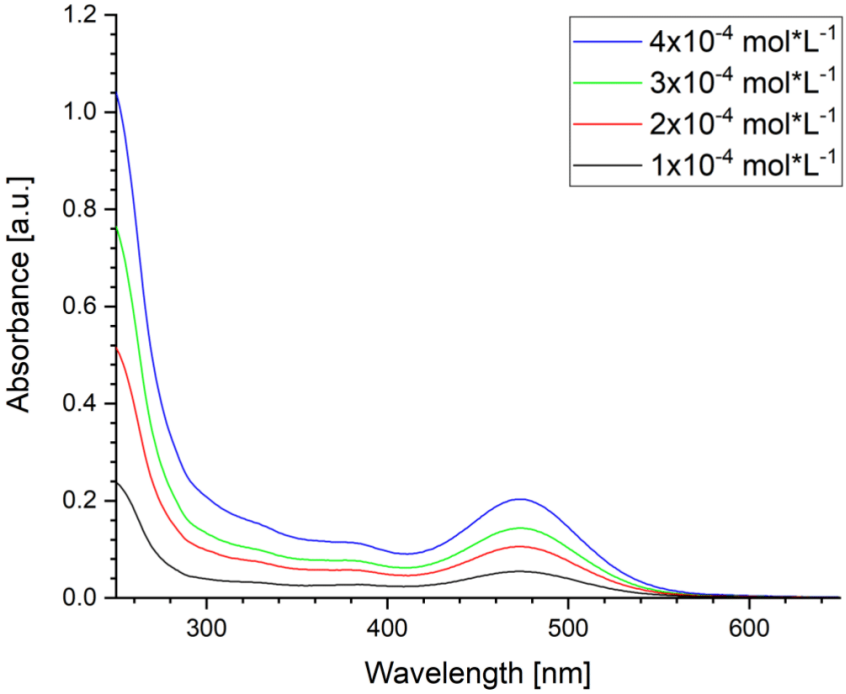

Figure S25: UV/vis spectra of **13b** in hexane at different concentrations ($1 \cdot 10^{-4}$ - $4 \cdot 10^{-4}$ mol L^{-1}).

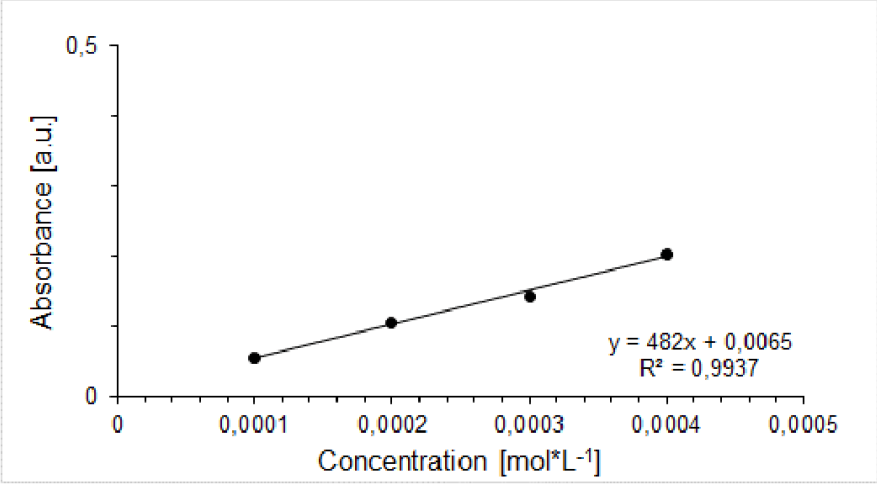

Figure S26: Determination of ε (4820 L mol^{-1} cm^{-1}) by linear regression of absorbance (λ = 474 nm) of **13b** against concentration.

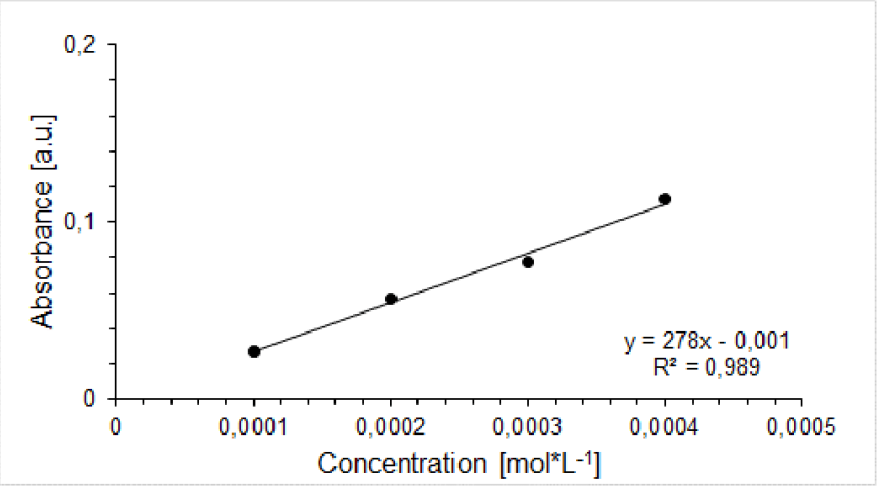

Figure S27: Determination of ε (2780 L mol^{-1} cm^{-1}) by linear regression of absorbance (λ = 382 nm) of **13b** against concentration.

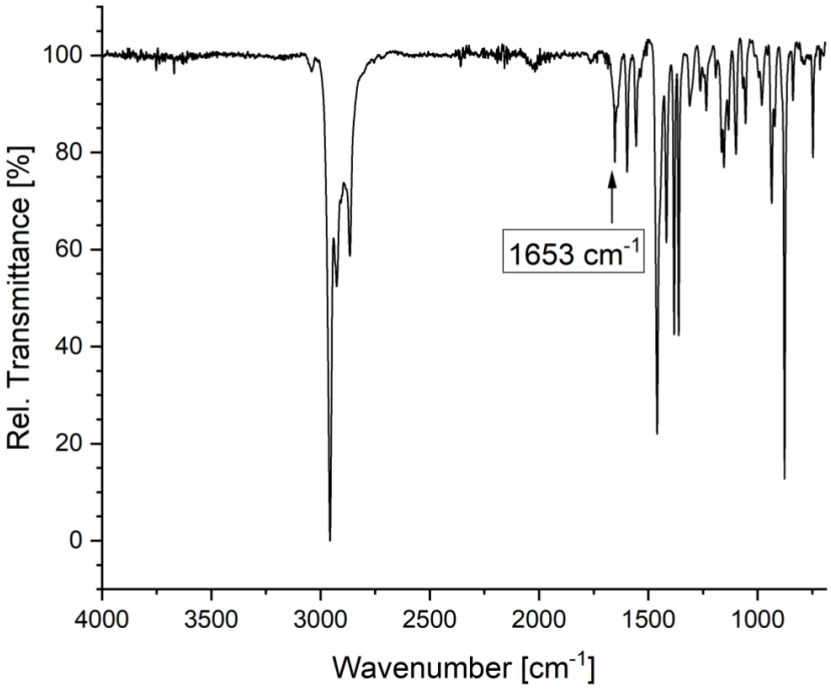

Figure S28: Infrared spectrum of acyl digermene **13b** (powder).

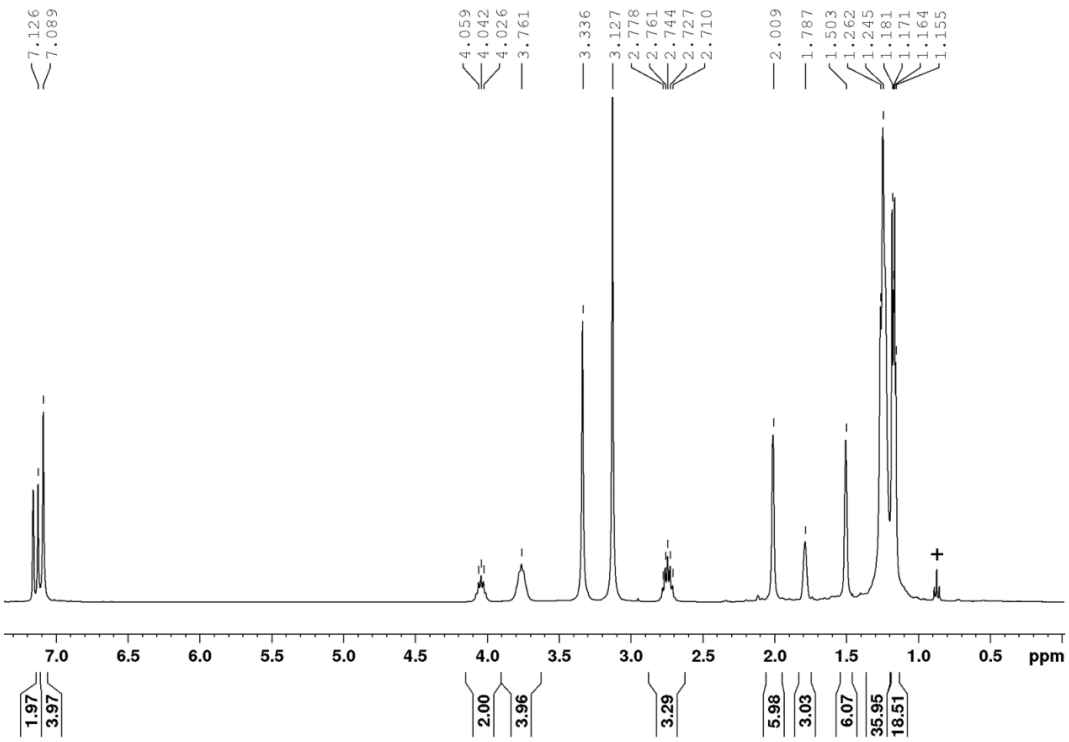

Figure S29: ^{1}H NMR spectrum of Acyldigermene **13c** with residual hexane (+).

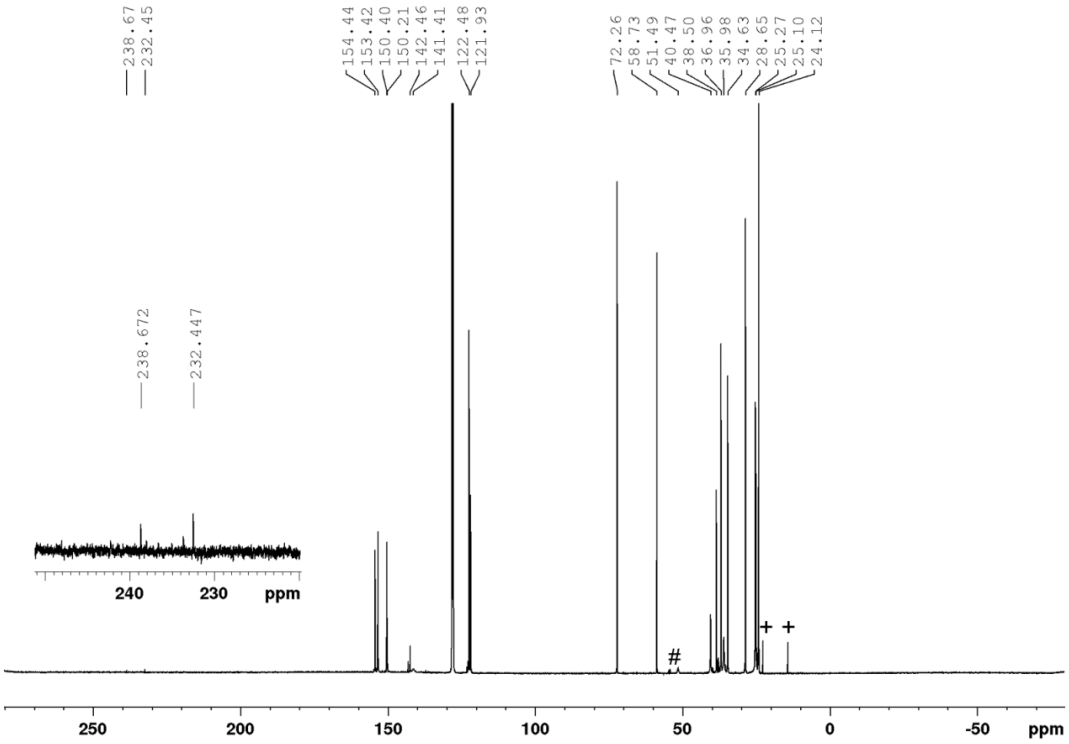

Figure S30: ^{13}C NMR spectrum of acyl digermene **13c** with residual hexane (+) and unidentified impurities (#).

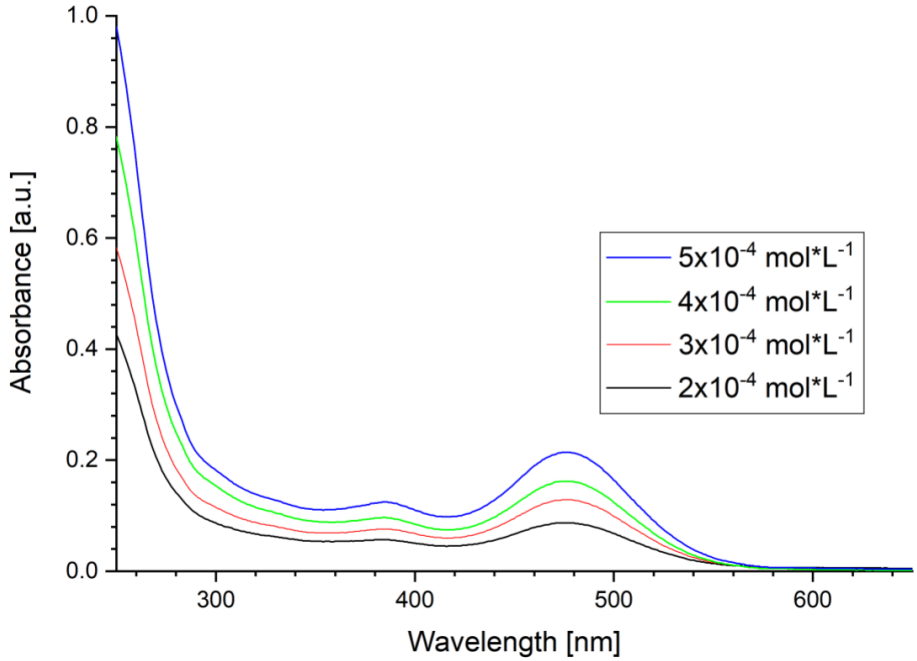

Figure S31: UV/vis spectra of **13c** in hexane at different concentrations ($2 \cdot 10^{-4}$ - $5 \cdot 10^{-4}$ mol L^{-1}).

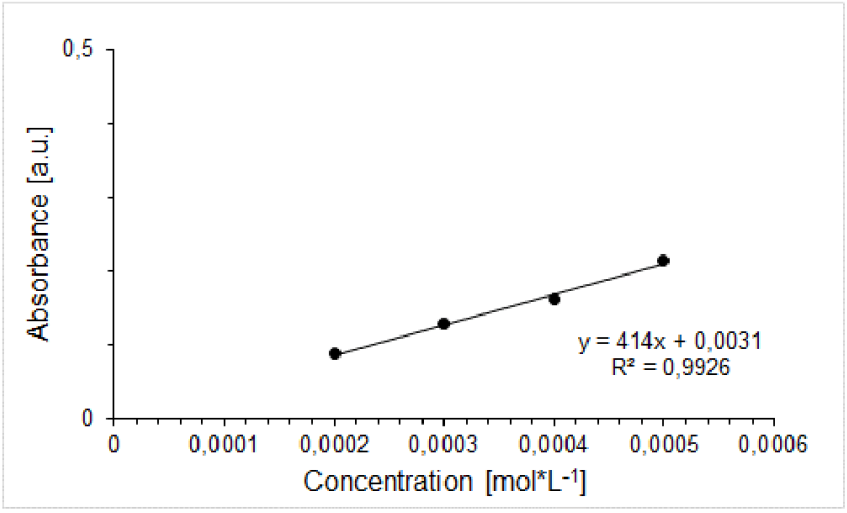

Figure S32: Determination of ε (4140 L mol^{-1} cm^{-1}) by linear regression of absorbance (λ = 476 nm) of **13c** against concentration.

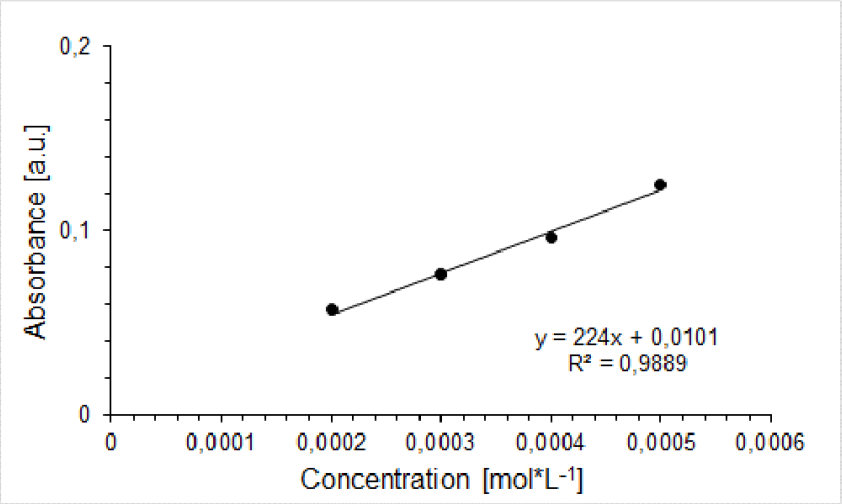

Figure S33: Determination of ε (2240 mol L^{-1} cm^{-1}) by linear regression of absorbance (λ = 386 nm) of **13c** against concentration.

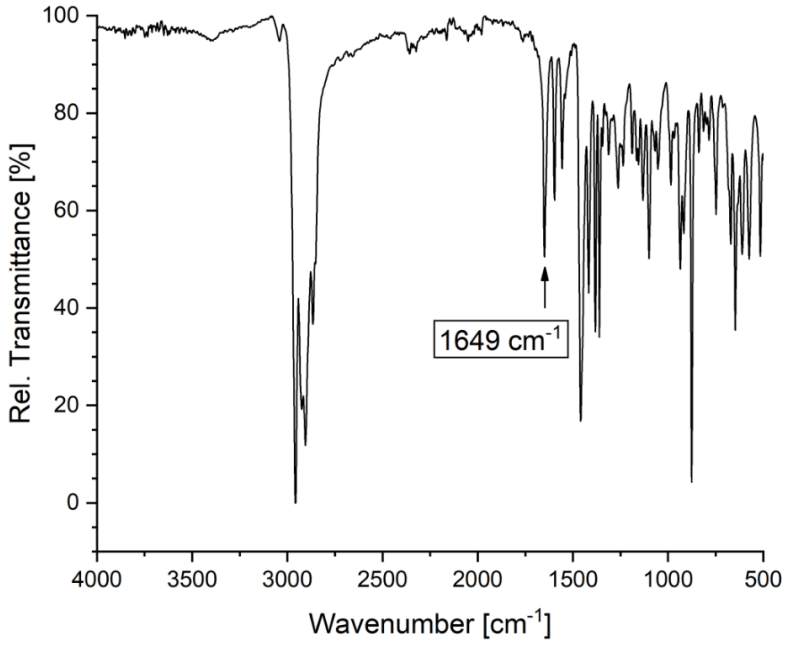

Figure S34: Infrared spectrum of acyl digermene **13c** (powder).

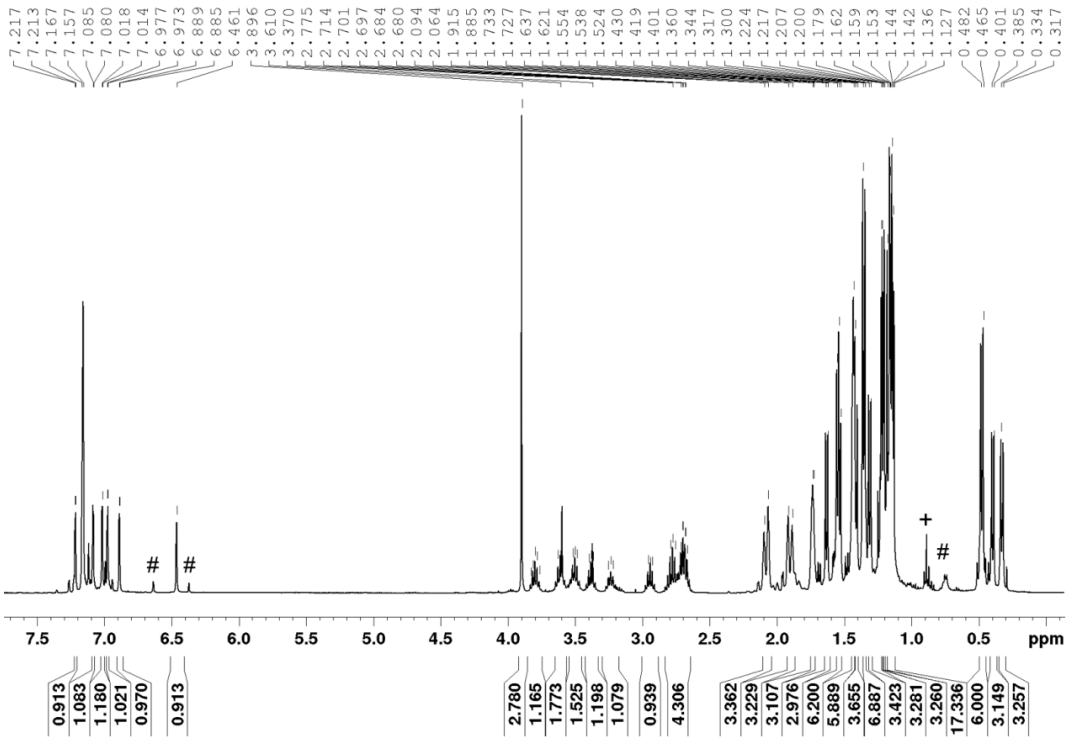

Figure S35: ^{1}H NMR spectrum of acyl digermane **15** with residual hexane (+) and unidentified impurities (#).

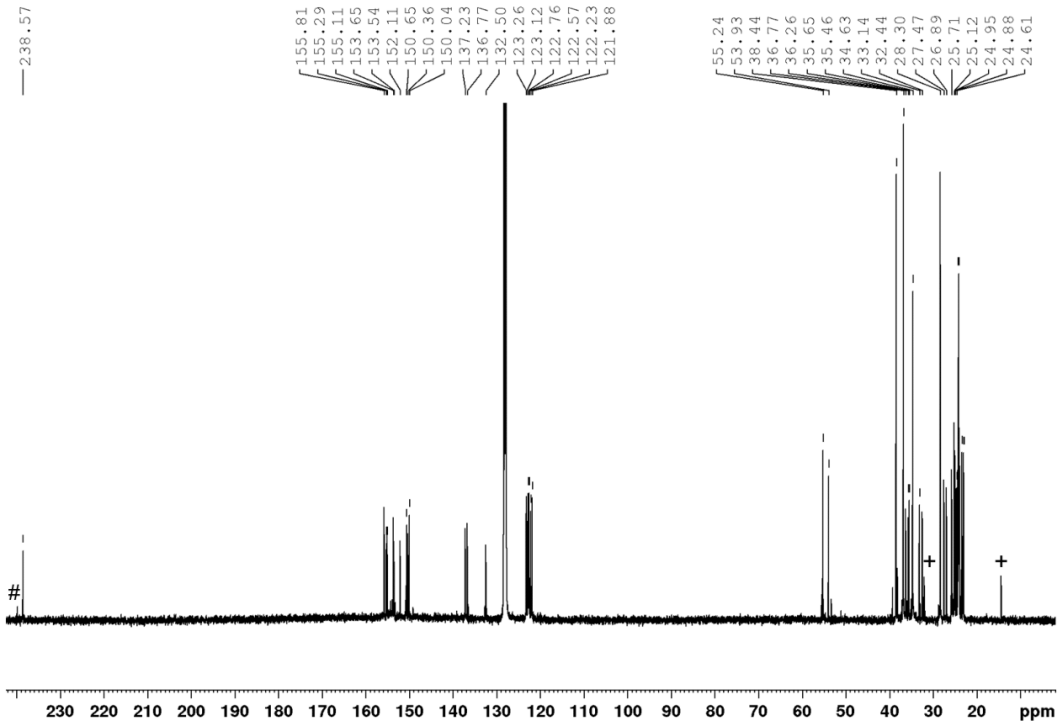

Figure S36: ^{13}C NMR spectrum of acyl digermane **15** with residual hexane (+) and unidentified impurities (#).

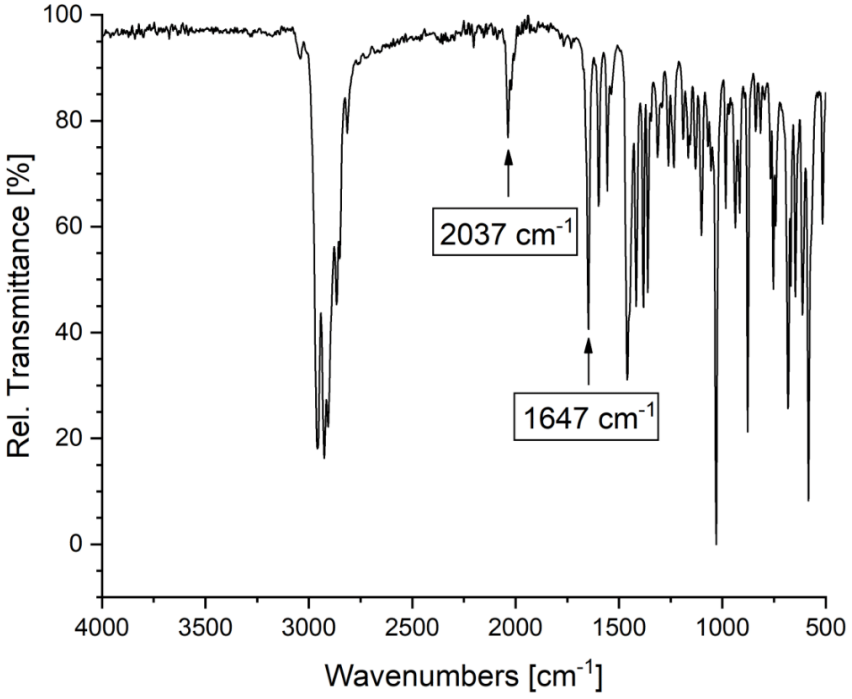

Figure S37: Infrared spectrum of acyl digermane **15** (powder).

Crystallographic Data and Refinement

Table S1: Crystal data and structure refinement for **10** (CCDC 1920322).

Identification code	sh3862	
Empirical formula	C63 H84 Ge2 Si	
Formula weight	1014.57	
Temperature	132(2) K	
Wavelength	0.71073 Å	
Crystal system	Triclinic	
Space group	P-1	
Unit cell dimensions	a = 11.5903(8) Å	α= 78.086(4)°.
	b = 12.3404(9) Å	β= 80.574(6)°.
	c = 22.2077(19) Å	γ = 69.062(4)°.
Volume	2888.6(4) $Å^3$	
Z	2	
Density (calculated)	1.166 Mg/m^3	
Absorption coefficient	1.097 mm^{-1}	
F(000)	1080	
Crystal size	0.311 x 0.073 x 0.028 mm^3	
Theta range for data collection	1.884 to 27.965°.	
Index ranges	-15<=h<=15, -14<=k<=16, -29<=l<=29	
Reflections collected	50869	
Independent reflections	13605 [R(int) = 0.0655]	
Completeness to theta = 25.242°	99.2 %	
Absorption correction	Semi-empirical from equivalents	
Max. and min. transmission	0.7456 and 0.6394	
Refinement method	Full-matrix least-squares on F^2	
Data / restraints / parameters	13605 / 9 / 625	
Goodness-of-fit on F^2	1.012	
Final R indices [I>2sigma(I)]	R1 = 0.0476, wR2 = 0.0877	
R indices (all data)	R1 = 0.0922, wR2 = 0.1015	
Extinction coefficient	n/a	
Largest diff. peak and hole	0.954 and -0.730 $e.Å^{-3}$	

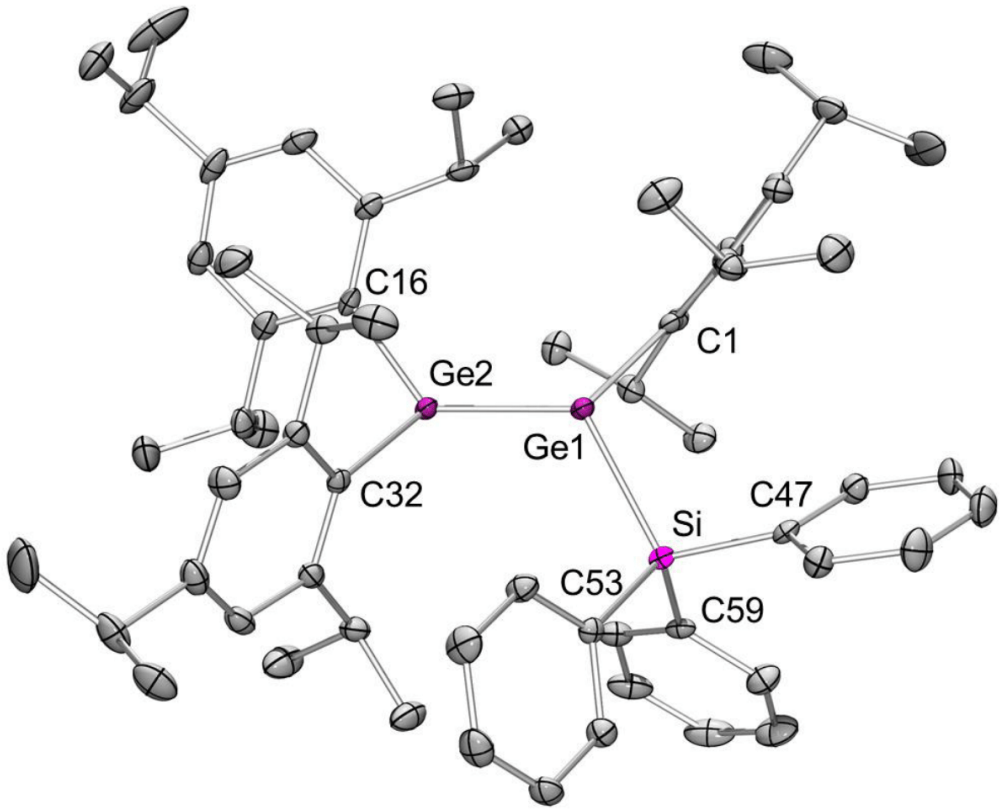

Figure S38: Molecular structure of silyl digermene **10** (carbon-bonded hydrogens omitted for clarity; thermal ellipsoids at 50% probability). Selected bond lengths (in Å) and -angles (in °): Ge1-Ge2 2.3279(4), Ge1-Si 2.3984(8), Ge1-C1 1.973(3), Ge2-C16 1.997(3), Ge2-C32 1.985(3), Si-C47 1.868(3), Si-C53 1.875(3), Si-C59 1.885(3), Ge2-Ge1-Si 119.09(8), Σ°(Ge1) 346.53, Σ °(Ge2) 345.24, θ(Ge1) 23.71, θ(Ge2) 21.29, τ 13.58.

Table S2: Crystal data and structure refinement for **15** (CCDC 1920323).

Identification code	sh3822	
Empirical formula	C57 H88 Ge2 O2 x 0.5(C6 H14)	
Formula weight	993.53	
Temperature	152(2) K	
Wavelength	0.71073 Å	
Crystal system	Monoclinic	
Space group	$P2_1/n$	
Unit cell dimensions	a = 16.8029(17) Å	α= 90°.
	b = 9.6893(9) Å	β= 102.400(6)°.
	c = 35.869(4) Å	γ = 90°.
Volume	5703.6(10) $Å^3$	
Z	4	
Density (calculated)	1.157 Mg/m^3	
Absorption coefficient	1.092 mm^{-1}	
F(000)	2140	
Crystal size	0.520 x 0.155 x 0.060 mm^3	
Theta range for data collection	1.162 to 30.624°.	
Index ranges	-24<=h<=22, -13<=k<=12, -51<=l<=50	
Reflections collected	66950	
Independent reflections	17402 [R(int) = 0.0639]	
Completeness to theta = 25.242°	100.0 %	
Absorption correction	Semi-empirical from equivalents	
Max. and min. transmission	0.7461 and 0.6954	
Refinement method	Full-matrix least-squares on F^2	
Data / restraints / parameters	17402 / 93 / 628	
Goodness-of-fit on F^2	1.017	
Final R indices [I>2sigma(I)]	R1 = 0.0556, wR2 = 0.1120	
R indices (all data)	R1 = 0.0995, wR2 = 0.1261	
Extinction coefficient	n/a	
Largest diff. peak and hole	1.085 and -0.679 $e.Å^{-3}$	

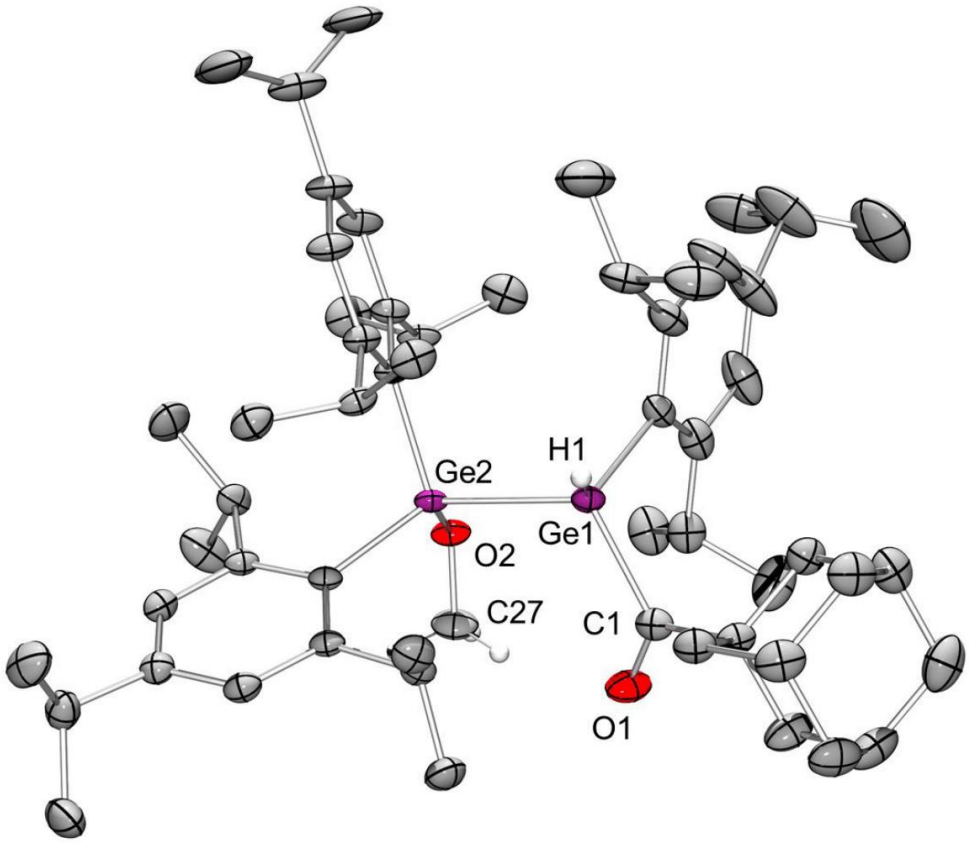

Figure S39: Molecular structure of acyl digermane **15** (carbon-bonded hydrogens omitted for clarity; thermal ellipsoids at 50% probability). Selected bond lengths (in Å) and -angles (in °): Ge1-Ge2 2.4694(5), Ge1-C1 2.041(3), C1-O1 1.215(3), Ge2-O2 1.8189(17), Ge1-C1-O1 118.7(2).

Theoretical Details

Computations were carried out with the Gaussian09 program package.[S1] Structural optimizations and frequency analyses were performed at the BP86/def2-SVP level of theory[S2,S3] including the dispersion correction by Grimme[S4] whereas single-point energy determination was carried out at the M06-2X(D3)/def2-TZVPP level of theory.[S5] For TD-DFT and population analysis (including natural bond orbital analysis) M06-2X(D3)/def2-SVP was employed.[S6] Pictures of minimum structures and Kohn-Sham orbitals were displayed with ChemCraft[S7] and simulated UV/vis data was processed using GaussSum[S8] and Origin 2018.[S9]

Optimized structures

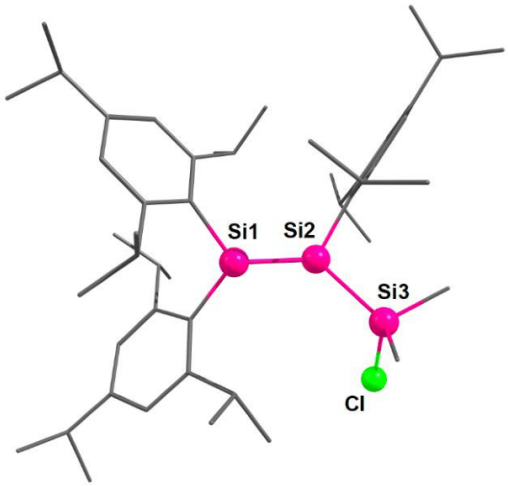

Si1-Si2	2.20156
Si2-Si3	2.35122
Si3-Cl	2.12065
°Σ (Si1)	357.144
°Σ (Si2)	348.571
Si1-Si2-Si3-Cl	82.729

Figure S40: Optimized structure of α-chlorosilyl disilene **6a** and selected bondlengths [Å] and -angles [°].

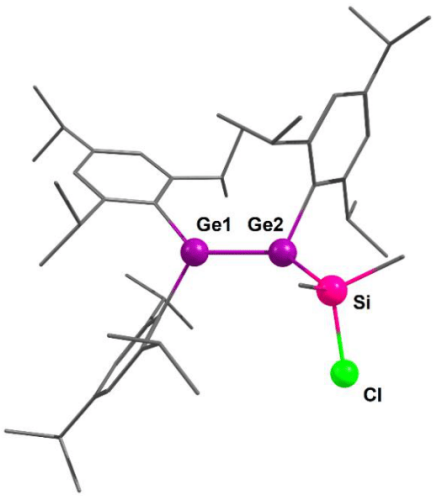

Ge1-Ge2	2.33824
Ge2-Si	2.41924
Si-Cl	2.12148
°Σ (Ge1)	349.531
°Σ (Ge2)	334.150
Ge1-Ge2-Si-Cl	90.682

Figure S41: Optimized structure of α-chlorosilyl disilene **11a** and selected bond lengths [Å] and angles [°].

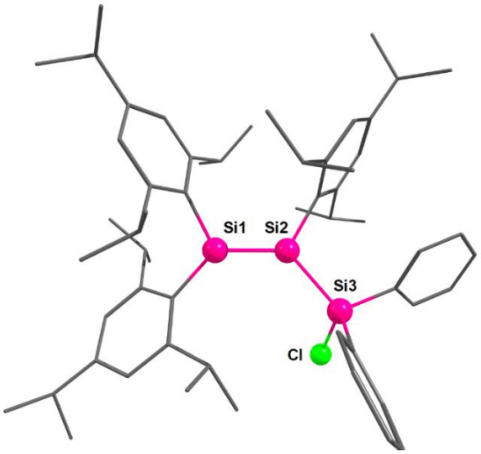

Si1-Si2	2.17853
Si2-Si3	2.33684
Si3-Cl	2.11906
°Σ (Si1)	359.888
°Σ (Si2)	356.393
Si1-Si2-Si3-Cl	66.380

Figure S42: Optimized structure of α-chlorosilyl disilene **6b** and selected bond lengths [Å] and angles [°].

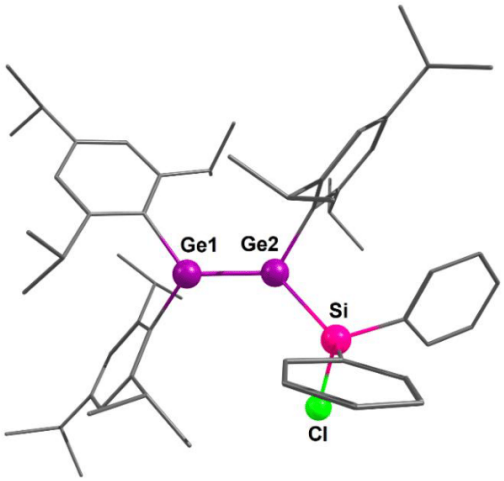

Ge1-Ge2	2.35442
Ge2-Si	2.42969
Si-Cl	2.12201
°Σ (Ge1)	346.781
°Σ (Ge2)	336.382
Ge1-Ge2-Si-Cl	72.516

Figure S43: Optimized structure of α-chlorosilyl disilene **11b** and selected bond lengths [Å] and angles [°].

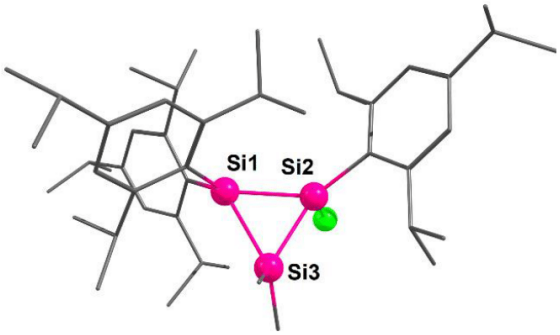

Si1-Si2	2.35873
Si2-Si3	2.33615
Si3-Si1	2.39877
Si3-Si1-Si2	58.811
Si1-Si2-Si3	61.450
Si2-Si3-Si1	59.739

Figure S44: Optimized structure of cyclotrisilane **7a** and selected bond lengths [Å] and angles [°].

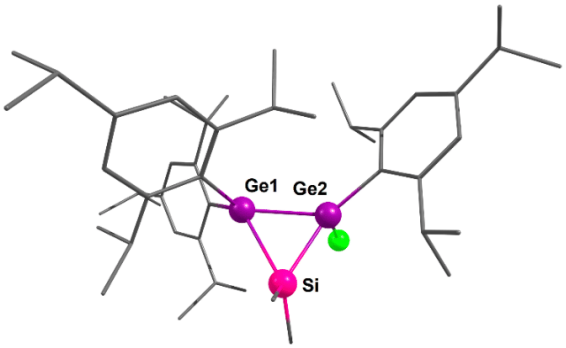

Ge1-Ge2	2.47151
Ge2-Si	2.40365
Si-Ge1	2.45461
Si-Ge1-Ge2	58.409
Ge1-Ge2-Si	60.444
Ge2-Si-Ge1	61.147

Figure S45: Optimized structure of cyclotrisilane **12a** and selected bond lengths [Å] and angles [°].

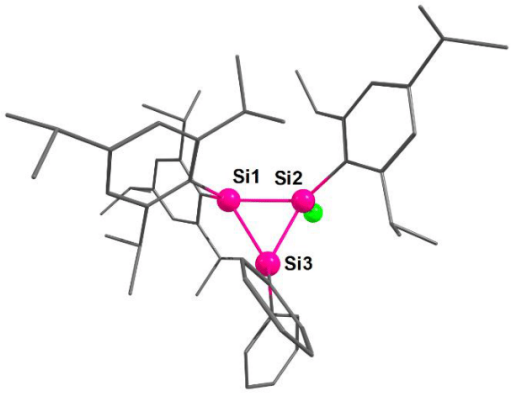

Si1-Si2	2.37014
Si2-Si3	2.35689
Si3-Si1	2.41296
Si3-Si1-Si2	59.035
Si1-Si2-Si3	61.388
Si2-Si3-Si1	59.576

Figure S46: Optimized structure of cyclotrisilane **7b** and selected bond lengths [Å] and angles [°].

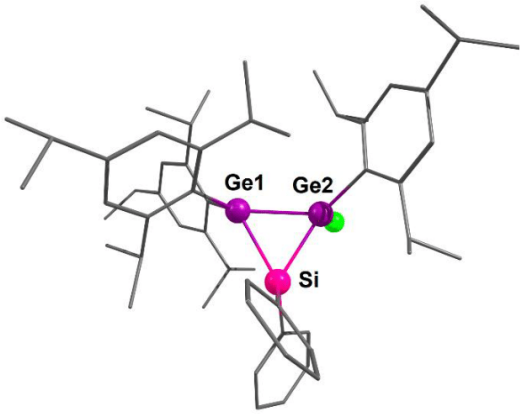

Ge1-Ge2	2.47834
Ge2-Si	2.42160
Si-Ge1	2.47231
Si-Ge1-Ge2	58.569
Ge1-Ge2-Si	60.591
Ge2-Si-Ge1	60.840

Figure S47: Optimized structure of cyclotrisilane **12b** and selected bond lengths [Å] and angles [°].

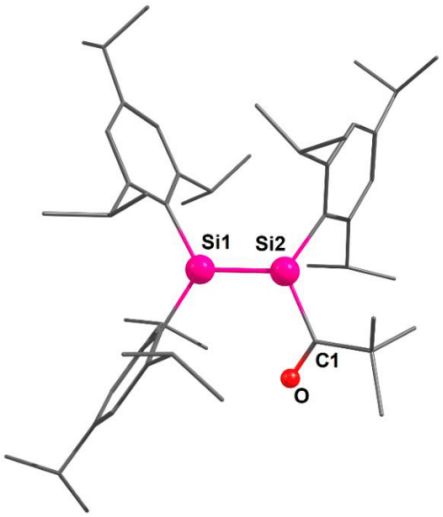

Si1-Si2	2.17445
Si2-C1	1.94286
C1-O	1.23163
°Σ (Si1)	359.745
°Σ (Si2)	358.437
Si1-Si2-C1-O	28.862

Figure S48: Optimized structure of acyldisilene **2a** and selected bond lengths [Å] and angles [°].

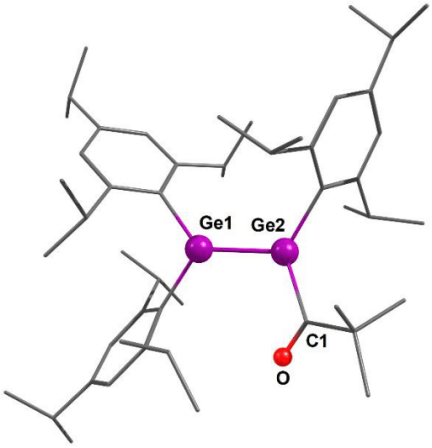

Ge1-Ge2	2.31620
Ge2-C1	2.05576
C1-O	1.22021
°Σ (Ge1)	352.038
°Σ (Ge2)	343.497
Ge1-Ge2-C1-O	51.681

Figure S49: Optimized structure of acyldigermene **13a** and selected bond lengths [Å] and angles [°].

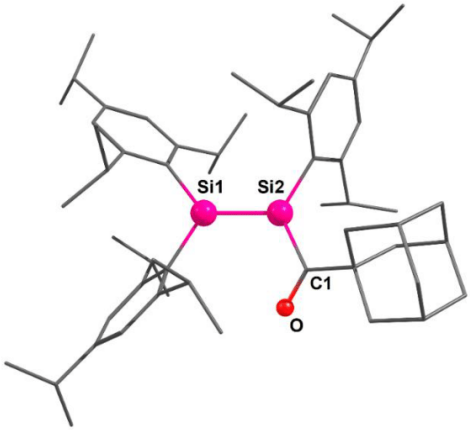

Si1-Si2	2.18092
Si2-C1	1.94573
C1-O	1.22943
°Σ (Si1)	358.881
°Σ (Si2)	357.075
Si1-Si2-C1-O	38.985

Figure S50: Optimized structure of acyldisilene **2c** and selected bond lengths [Å] and angles [°].

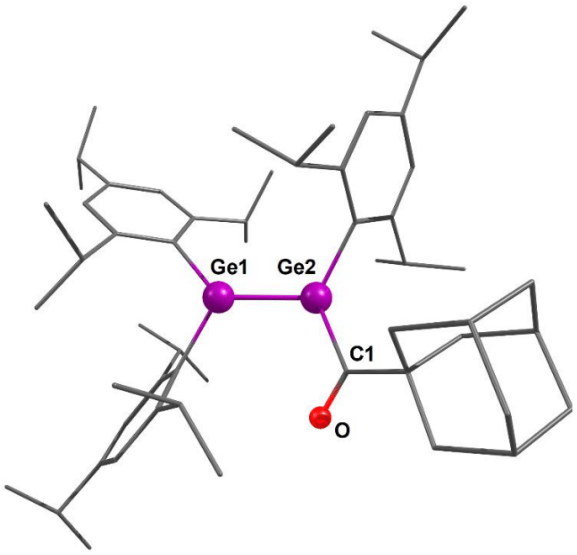

Ge1-Ge2	2.31900
Ge2-C1	2.05797
C1-O	1.22106
°Σ (Ge1)	351.622
°Σ (Ge2)	341.715
Ge1-Ge2-C1-O	51.635

Figure S51: Optimized structure of s-cis-acyldigermene **13c** and selected bond lengths [Å] and angles [°].

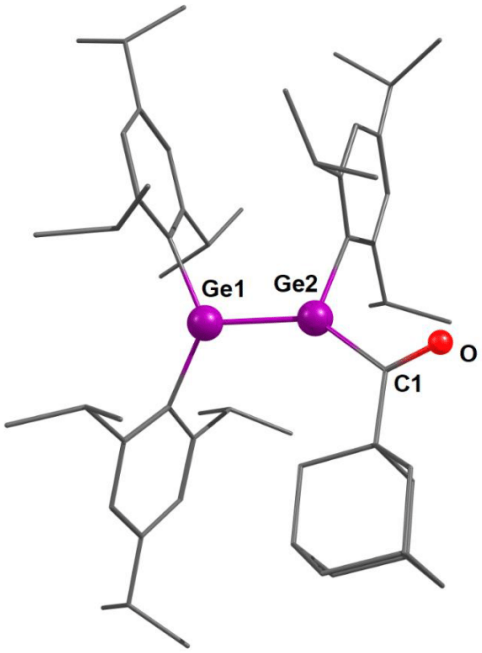

Ge1-Ge2	2.31443
Ge2-C1	2.03095
C1-O	1.22557
°Σ (Ge1)	354.416
°Σ (Ge2)	355.496
Ge1-Ge2-C1-O	149.129

Figure S52: Optimized structure of s-trans-acyldigermene **13c** and selected bond lengths [Å] and angles [°].

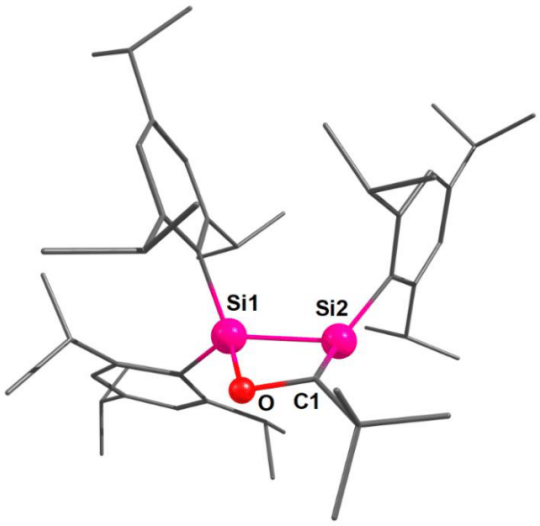

Si1-Si2	2.33147
Si2-C1	1.82136
C1-O	1.38906
O-Si1	1.79312
Si1-Si2-C1	71.715
Si2-C1-O	107.335
C1-O-Si1	100.920
O-Si1-Si2	76.889
Si1-Si2-C1-O	13.656

Figure S53: Optimized structure of cyclic Brook silene **3a** and selected bond lengths and angles.

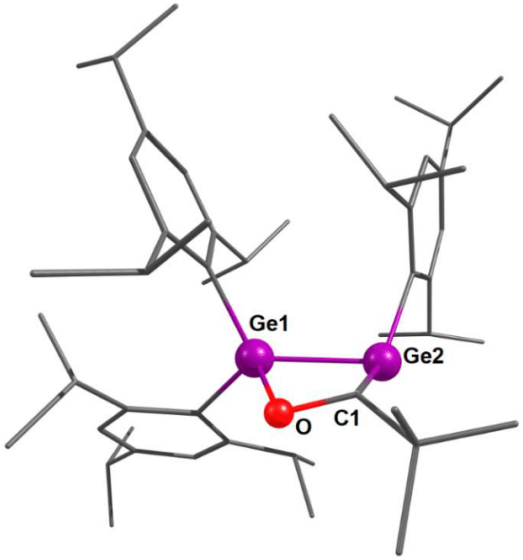

Ge1-Ge2	2.48449
Ge2-C1	1.97765
C1-O	1.32298
O-Ge1	2.00454
Ge1-Ge2-C1	70.590
Ge2-C1-O	109.923
C1-O-Ge1	101.413
O-Ge1-Ge2	73.995
Ge1-Ge2-C1-O	16.511

Figure S54: Optimized structure of cyclic Brook germene **14a** and selected bond lengths and angles.

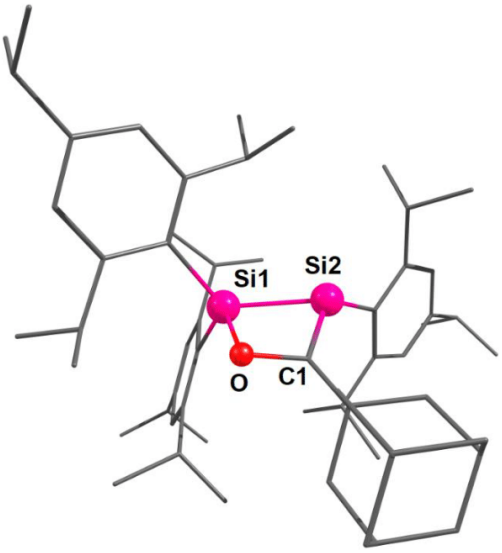

Si1-Si2	2.33749
Si2-C1	1.81918
C1-O	1.38301
O-Si1	1.79844
Si1-Si2-C1	71.567
Si2-C1-O	108.164
C1-O-Si1	100.857
O-Si1-Si2	76.887
Si1-Si2-C1-O	12.330

Figure S55: Optimized structure of cyclic Brook silene **3c** and selected bond lengths and angles.

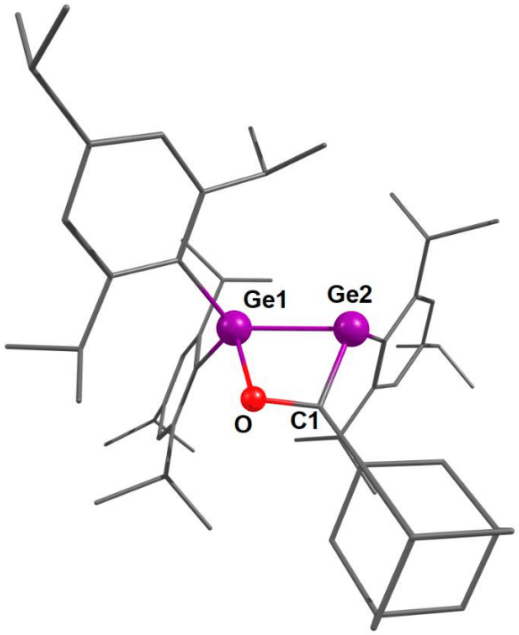

Ge1-Ge2	2.48935
Ge2-C1	1.96876
C1-O	1.32131
O-Ge1	2.00384
Ge1-Ge2-C1	70.447
Ge2-C1-O	110.585
C1-O-Ge1	101.228
O-Ge1-Ge2	73.933
Ge1-Ge2-C1-O	16.016

Figure S56: Optimized structure of cyclid Brook germene **14c** and selected bond lengths and angles.

Thermodynamic & Spectroscopic Data

a) conformers of **13c**

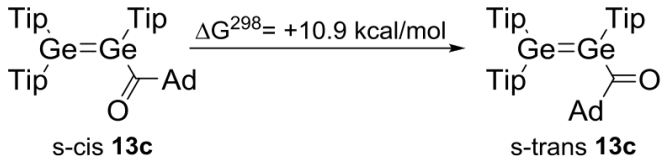

s-cis **13c** s-trans **13c**

b) cyclizations of α-chloro ditetrenes

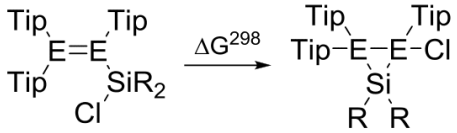

6a, 7a: E = Si, R = Me
6b, 7b: E = Si, R = Ph
11a, 12a: E = Ge, R = Ph
11c, 12c: E = Ge, R = Ph

Compound	ΔG298 [kcal/mol]
6a	-17.9
6b	-16.9
11a	-2.5
11c	-3.1

c) cyclizations of acyl ditetrenes

2a, 3a: E = Si, R = *t*Bu
2b, 3b: E = Si, R = 1-Ad
13a, 14a: E = Ge, R = *t*Bu
13c, 14c: E = Ge, R = 1-Ad

Compound	ΔG298 [kcal/mol]
2a	-7.6
2b	-5.1
13a	+2.6
13c	+0.02

Scheme S1: Calculated Free Gibbs Enthalpies for the isomerization of **13c** and the cyclization of **6a**,**b**, **11a**,**c**, **2a**,**b** and **13a**,**c** at the M06-2X(D3)/def2-TZVPP//BP86-D3/def2-SVP level of theory.

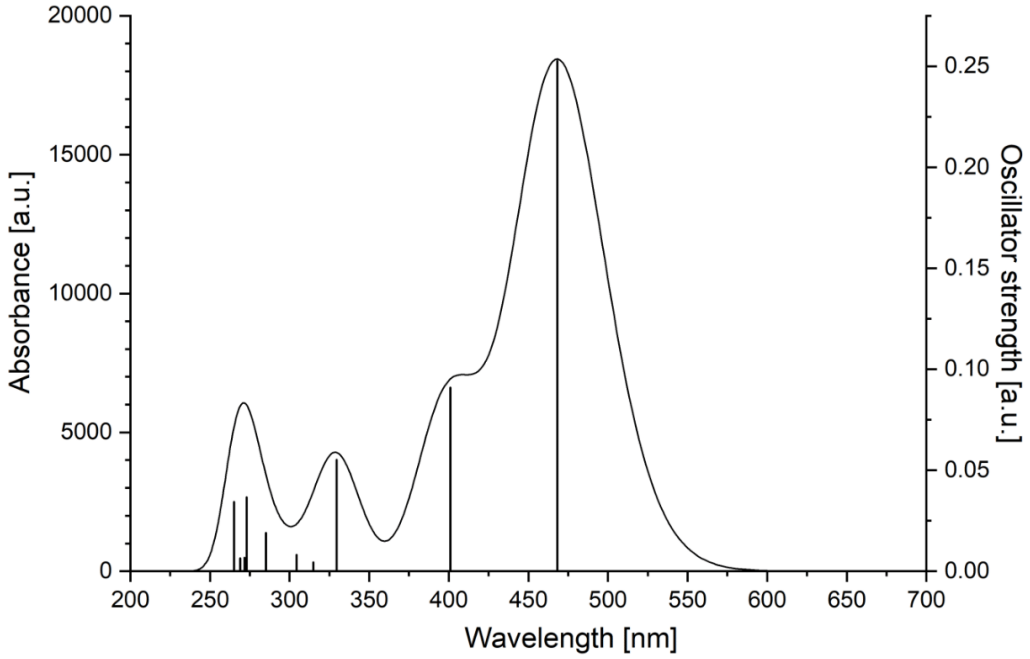

Figure S57: Simulated electronic transitions and UV/vis spectrum of s-cis **13c** at the M06-2X-D3/def2-SVP//BP86-D3/def2-SVP level of theory.

Atomic coordinates of optimized structures

Table S3: Atomic coordinates of **2a**.

6	2.294331000	3.888923000	-2.302512000
6	0.721813000	2.167693000	-3.335302000
6	1.389304000	2.671594000	-2.039672000
6	-2.996379000	-0.725371000	-3.555144000
6	0.297409000	-4.308371000	-1.475158000
6	-0.409939000	4.112798000	-1.027323000
6	-2.447011000	6.449509000	1.022719000
6	-2.307593000	5.643748000	-0.282862000
6	0.335612000	2.920603000	-0.964252000
6	3.405591000	-1.890466000	-2.692585000
6	-3.688341000	5.254629000	-0.855816000
8	1.830213000	-3.263546000	0.103776000
6	-1.445630000	4.397259000	-0.122546000
6	0.766387000	-3.180166000	-0.511240000
6	3.875880000	0.473662000	-3.475683000
6	-2.492894000	-0.085120000	-2.246557000
6	3.207331000	-0.390300000	-2.389916000
6	-2.821792000	1.419434000	-2.190682000
6	0.037444000	1.946130000	0.038533000
6	-3.016308000	-0.835086000	-1.022172000
6	-7.368860000	-1.576848000	-0.486765000
6	-1.705328000	3.453019000	0.884971000
6	-4.398583000	-0.795002000	-0.753251000
6	3.696170000	-0.074173000	-0.976290000
6	-1.001092000	2.237334000	0.981378000
6	-2.154943000	-1.565902000	-0.149694000
6	2.811639000	0.136758000	0.121103000
6	-4.961302000	-1.439971000	0.362602000
6	5.087588000	-0.067385000	-0.741367000
6	-6.438495000	-1.286727000	0.705865000
6	-2.716632000	-2.256068000	0.972054000
6	-4.102324000	-2.171221000	1.202933000
6	-2.479425000	-4.409063000	2.344110000
6	-1.384850000	1.297020000	2.121012000
6	-1.854007000	-3.055952000	1.954779000
6	3.356010000	0.267089000	1.436235000
6	5.637021000	0.119037000	0.537215000
6	-2.897595000	1.016521000	2.175034000
6	-6.695891000	0.118756000	1.293062000
6	-0.874266000	1.835136000	3.472973000
6	7.603703000	-1.026291000	1.658757000
6	2.214365000	-1.185183000	3.126096000
6	4.748395000	0.268410000	1.619866000
6	7.146936000	0.134215000	0.750756000
6	2.428856000	0.267371000	2.648828000
6	-1.506297000	-2.236081000	3.213782000
6	7.625120000	1.495733000	1.296195000
6	2.866279000	1.192246000	3.794178000
1	3.115377000	3.618066000	-2.998614000
1	1.738567000	4.728304000	-2.771505000
1	1.478604000	1.945876000	-4.115428000
1	0.023235000	2.931260000	-3.738428000
1	2.749091000	4.262390000	-1.362460000
1	-2.546548000	-0.221397000	-4.436648000
1	0.140332000	1.241882000	-3.145978000
1	-0.193111000	4.840237000	-1.826597000
1	-1.454757000	6.720919000	1.438033000

1	-1.803498000	6.296720000	-1.030589000
1	2.959099000	-2.158754000	-3.673941000
1	2.050445000	1.864209000	-1.662772000
1	-2.739159000	-1.803605000	-3.604903000
1	-4.314852000	6.153521000	-1.038408000
1	-4.100682000	-0.640761000	-3.645976000
1	-3.017709000	7.385497000	0.847126000
1	3.397810000	0.297480000	-4.461977000
1	-4.233957000	4.594997000	-0.147639000
1	-3.582601000	4.700123000	-1.810948000
1	2.949169000	-2.518915000	-1.905959000
1	4.487059000	-2.141959000	-2.733383000
1	-2.343898000	1.955953000	-3.035990000
1	-2.992282000	5.873515000	1.800380000
1	2.111068000	-0.194316000	-2.412207000
1	-1.381632000	-0.185121000	-2.231223000
1	4.952851000	0.226856000	-3.587985000
1	-3.916298000	1.598951000	-2.257093000
1	3.805663000	1.554879000	-3.244223000
1	-7.238618000	-0.828283000	-1.296885000
1	-5.052763000	-0.219275000	-1.427860000
1	-8.433104000	-1.537232000	-0.172890000
1	-2.456735000	1.877480000	-1.250989000
1	-7.172152000	-2.579611000	-0.918738000
1	5.774950000	-0.225640000	-1.589232000
1	-2.505576000	3.657400000	1.613387000
1	-2.817969000	-4.977966000	1.455019000
1	-0.874964000	0.328240000	1.923368000
1	7.273853000	-2.005715000	1.255658000
1	1.878557000	-1.831565000	2.288002000
1	-3.284062000	0.693856000	1.189642000
1	-0.889770000	-3.270762000	1.443566000
1	-3.355757000	-4.277587000	3.013927000
1	0.206644000	2.075190000	3.435823000
1	-1.741648000	-5.030006000	2.893781000
1	-4.534637000	-2.677686000	2.081597000
1	-3.470590000	1.913746000	2.492783000
1	7.618607000	-0.014008000	-0.246823000
1	-1.411098000	2.766238000	3.754503000
1	1.433478000	0.634169000	2.292397000
1	-7.754992000	0.235134000	1.607095000
1	-6.473737000	0.904037000	0.539130000
1	-6.046313000	0.309944000	2.171835000
1	8.710200000	-1.043211000	1.753514000
1	3.166931000	-1.605583000	3.513521000
1	1.458543000	-1.227472000	3.938571000
1	7.182418000	-0.925328000	2.681737000
1	-3.118099000	0.210374000	2.902696000
1	-1.037487000	1.089815000	4.280375000
1	5.154222000	0.370670000	2.638653000
1	-0.943668000	-1.318745000	2.951843000
1	-2.426792000	-1.936819000	3.758373000
1	-0.874658000	-2.831398000	3.905782000
1	7.319520000	2.326977000	0.627986000
1	3.017093000	2.233652000	3.442418000
1	8.731209000	1.517721000	1.394884000
1	2.100234000	1.202550000	4.596904000
1	7.194756000	1.696971000	2.300378000
1	3.813792000	0.847607000	4.260098000
14	0.912199000	0.245022000	0.001640000
14	-0.269288000	-1.542622000	-0.368012000

6	-0.106172000	-3.679419000	-2.826350000
1	-0.938519000	-2.952833000	-2.705386000
1	0.744934000	-3.142182000	-3.291287000
1	-0.448544000	-4.468417000	-3.529621000
6	1.441529000	-5.319959000	-1.663157000
1	1.111335000	-6.156007000	-2.314519000
1	2.325746000	-4.840746000	-2.129936000
1	1.767786000	-5.734035000	-0.688549000
6	-0.931979000	-5.004848000	-0.843873000
1	-0.682391000	-5.445227000	0.143180000
1	-1.778642000	-4.301395000	-0.708655000
1	-1.278487000	-5.825702000	-1.507274000
1	-6.667590000	-2.031316000	1.501382000

Table S4: Atomic coordinates of **2b.**

6	4.291345000	-0.336812000	-2.193219000
6	2.656624000	0.710654000	-3.843269000
6	2.916388000	0.333990000	-2.371650000
6	-3.005952000	0.726329000	-3.286430000
6	-2.852630000	-2.904703000	0.238008000
6	3.505171000	2.677471000	-1.662052000
6	5.194909000	5.295589000	0.083425000
6	4.248430000	5.056828000	-1.112024000
6	2.728226000	1.525385000	-1.435639000
6	0.688219000	-4.516589000	-1.106239000
6	3.413332000	6.313860000	-1.428514000
8	-0.689539000	-3.063691000	1.327794000
6	3.371098000	3.832934000	-0.874675000
6	-1.534322000	-2.344295000	0.798341000
6	1.717196000	-3.116947000	-2.947425000
6	-1.950662000	1.090819000	-2.222049000
6	1.256198000	-3.129992000	-1.475348000
6	-0.933519000	2.115074000	-2.760464000
6	1.790055000	1.501007000	-0.357349000
6	-2.604103000	1.568333000	-0.925580000
6	-5.981942000	4.473956000	-1.016090000
6	2.405342000	3.816405000	0.147474000
6	-3.441706000	2.699961000	-0.982783000
6	2.362748000	-2.709070000	-0.505121000
6	1.612538000	2.686590000	0.423451000
6	-2.404413000	0.916079000	0.328871000
6	2.286411000	-1.537664000	0.305482000
6	-4.096273000	3.210330000	0.152828000
6	3.506039000	-3.527888000	-0.408986000
6	-4.905260000	4.500374000	0.085964000
6	-3.118453000	1.382364000	1.476484000
6	-3.940232000	2.518897000	1.367243000
6	-4.382576000	0.360348000	3.447539000
6	0.588848000	2.802882000	1.550938000
6	-3.006796000	0.679682000	2.831774000
6	3.329303000	-1.266983000	1.242914000
6	4.566508000	-3.245907000	0.469080000
6	-0.539068000	3.785099000	1.175500000
6	-3.959417000	5.710073000	-0.077144000
6	1.235878000	3.180777000	2.898095000
6	5.959191000	-4.817289000	1.893840000
6	3.269471000	-0.516486000	3.668092000
6	4.446691000	-2.119106000	1.304115000
6	5.803707000	-4.135229000	0.519299000
6	3.263070000	-0.072147000	2.193099000
6	-2.125652000	1.470087000	3.816972000
6	7.073497000	-3.348727000	0.133166000

6	4.355615000	0.970501000	1.891576000
1	4.369136000	-1.246723000	-2.823942000
1	5.107442000	0.356037000	-2.490532000
1	2.697861000	-0.190794000	-4.490766000
1	3.418878000	1.423353000	-4.222609000
1	4.460380000	-0.639380000	-1.141189000
1	-2.521001000	0.273703000	-4.176946000
1	1.661183000	1.182156000	-3.965791000
1	4.241854000	2.678066000	-2.483080000
1	5.813857000	4.398383000	0.290037000
1	4.879330000	4.838160000	-2.002845000
1	-0.200177000	-4.749867000	-1.732298000
1	2.136997000	-0.415047000	-2.097703000
1	-3.746245000	-0.000744000	-2.891876000
1	4.071675000	7.177673000	-1.660426000
1	-3.568296000	1.619792000	-3.632057000
1	5.875066000	6.151596000	-0.111987000
1	0.881032000	-3.405204000	-3.619073000
1	2.777506000	6.603281000	-0.564947000
1	2.743685000	6.144365000	-2.296603000
1	0.380389000	-4.549397000	-0.044111000
1	1.436048000	-5.318394000	-1.285914000
1	-0.465793000	1.744211000	-3.696885000
1	4.620223000	5.525199000	1.006027000
1	0.431651000	-2.388368000	-1.373055000
1	-1.384286000	0.163381000	-1.979566000
1	2.544970000	-3.837899000	-3.116661000
1	-1.420947000	3.085687000	-2.993649000
1	2.075122000	-2.118082000	-3.262882000
1	-5.526973000	4.410068000	-2.027349000
1	-3.573005000	3.213756000	-1.949224000
1	-6.595050000	5.399309000	-0.989307000
1	-0.124189000	2.304431000	-2.026765000
1	-6.661008000	3.604726000	-0.896988000
1	3.579285000	-4.425336000	-1.046584000
1	2.267368000	4.720180000	0.763005000
1	-5.046719000	-0.152234000	2.723163000
1	0.123015000	1.800488000	1.677957000
1	5.050671000	-5.395408000	2.160176000
1	2.458805000	-1.247755000	3.864424000
1	-1.025286000	3.494009000	0.223567000
1	-2.488264000	-0.293123000	2.649001000
1	-4.900860000	1.282701000	3.785228000
1	2.007979000	2.444238000	3.199435000
1	-4.266362000	-0.294606000	4.336225000
1	-4.467994000	2.893934000	2.260206000
1	-0.151863000	4.820649000	1.063324000
1	5.659431000	-4.936572000	-0.239965000

1	1.719524000	4.179451000	2.856203000
1	2.275901000	0.419607000	2.025283000
1	-4.524619000	6.666130000	-0.060771000
1	-3.412057000	5.653810000	-1.042236000
1	-3.201927000	5.736769000	0.733027000
1	6.826781000	-5.510772000	1.897013000
1	4.233455000	-0.992726000	3.947193000
1	3.122521000	0.356366000	4.339339000
1	6.127177000	-4.067537000	2.696259000
1	-1.325107000	3.794180000	1.958028000
1	0.470498000	3.220938000	3.701166000
1	5.251132000	-1.892451000	2.023354000
1	-1.098699000	1.587700000	3.421012000
1	-2.542504000	2.483849000	3.997533000
1	-2.057144000	0.948309000	4.794629000
1	6.958200000	-2.863578000	-0.857956000
1	4.302317000	1.312275000	0.838078000
1	7.959718000	-4.017024000	0.094012000
1	4.241760000	1.862848000	2.541964000
1	7.289169000	-2.549675000	0.874168000
1	5.368166000	0.548597000	2.068711000
14	0.981298000	-0.176282000	0.060224000
14	-1.112957000	-0.454979000	0.601378000
6	-2.912837000	-2.618010000	-1.289253000
1	-2.834750000	-1.524647000	-1.468394000
1	-2.038495000	-3.088644000	-1.789743000
6	-2.948824000	-4.430244000	0.469836000
1	-2.077032000	-4.929712000	-0.001436000
1	-2.879783000	-4.643907000	1.557900000
6	-4.063490000	-2.207406000	0.919720000
1	-4.021924000	-2.381754000	2.017117000
1	-4.012705000	-1.110705000	0.757843000
1	-5.426687000	4.610057000	1.063573000
6	-4.234426000	-3.159061000	-1.876113000
1	-4.259476000	-2.945973000	-2.967608000
6	-4.271358000	-4.970724000	-0.117028000
1	-4.327176000	-6.067894000	0.055917000
6	-5.384584000	-2.751541000	0.335031000
1	-6.237556000	-2.243682000	0.836889000
6	-4.316240000	-4.683945000	-1.635511000
1	-5.253575000	-5.090313000	-2.076111000
1	-3.469511000	-5.195324000	-2.144847000
6	-5.424047000	-2.457874000	-1.181895000
1	-6.383963000	-2.814322000	-1.616406000
1	-5.374648000	-1.360112000	-1.357777000
6	-5.467018000	-4.275552000	0.572973000
1	-6.426042000	-4.674609000	0.174187000
1	-5.455401000	-4.491874000	1.664214000

Table S5: Atomic coordinates of **3a.**

6	-1.441390000	4.053810000	2.773453000
6	0.967732000	3.321479000	3.006211000
6	-0.398757000	2.989578000	2.373535000
6	4.219429000	1.012647000	2.140833000
6	0.947478000	-0.959833000	4.265070000
6	0.069489000	3.970768000	0.102766000
6	-0.279334000	5.485484000	-3.248197000
6	0.655224000	5.187277000	-2.059795000
6	-0.261974000	2.825914000	0.856120000
6	-4.731065000	2.038854000	1.763342000
6	2.127236000	5.073065000	-2.512072000
8	-0.796984000	-0.198903000	2.716013000
6	0.240825000	3.938920000	-1.290558000
6	0.459947000	-0.776680000	2.841698000
6	-3.498892000	2.944514000	-0.282071000
6	3.169131000	0.921381000	1.015826000
6	-3.578125000	1.815277000	0.762046000
6	3.152509000	2.202026000	0.160893000
6	-0.430693000	1.580647000	0.183619000
6	3.375298000	-0.334965000	0.172773000
6	7.224437000	-1.233094000	-1.896098000
6	0.088459000	2.700169000	-1.938790000
6	4.457210000	-0.357431000	-0.727916000
6	-3.675240000	0.431340000	0.125074000
6	-0.225824000	1.525828000	-1.230782000
6	2.514001000	-1.474399000	0.248808000
6	-2.693020000	-0.581396000	0.334926000
6	4.711193000	-1.450168000	-1.578147000
6	-4.818995000	0.152480000	-0.652771000
6	5.856494000	-1.414398000	-2.584016000
6	2.768946000	-2.596072000	-0.597130000
6	3.853583000	-2.559409000	-1.495073000
6	2.621018000	-5.142250000	-0.406008000
6	-0.332513000	0.216885000	-2.021319000
6	1.855472000	-3.821752000	-0.604137000
6	-2.971126000	-1.908742000	-0.142047000
6	-5.042431000	-1.109715000	-1.218637000
6	0.961630000	-0.085901000	-2.804579000
6	5.615695000	-0.328800000	-3.654241000
6	-1.579559000	0.193149000	-2.926028000
6	-7.158603000	-2.480751000	-1.563586000
6	-2.236430000	-3.373572000	1.765676000
6	-4.120601000	-2.132843000	-0.920374000
6	-6.243201000	-1.371617000	-2.120047000
6	-2.091414000	-3.094716000	0.252354000
6	0.978762000	-3.849907000	-1.870958000
6	-5.787106000	-1.686978000	-3.560174000

6	-2.318083000	-4.378836000	-0.556900000
1	-1.554083000	4.087123000	3.877517000
1	-1.141052000	5.069997000	2.441431000
1	0.885852000	3.403300000	4.109769000
1	1.362723000	4.287026000	2.624503000
1	-2.437020000	3.841576000	2.338330000
1	4.029237000	1.895521000	2.787923000
1	1.712436000	2.536981000	2.777065000
1	0.208363000	4.933609000	0.622805000
1	-1.335857000	5.564799000	-2.919059000
1	0.586169000	6.044573000	-1.352676000
1	-4.608548000	3.009862000	2.288637000
1	-0.729236000	2.017379000	2.792887000
1	4.206578000	0.107803000	2.782082000
1	2.464917000	6.002390000	-3.018311000
1	5.244396000	1.114172000	1.723686000
1	0.003207000	6.438130000	-3.743823000
1	-3.338192000	3.926254000	0.209809000
1	2.256438000	4.230979000	-3.225196000
1	2.796782000	4.881698000	-1.648297000
1	-4.759310000	1.234056000	2.526196000
1	-5.717460000	2.058933000	1.253681000
1	2.869821000	3.077752000	0.778817000
1	-0.225594000	4.685252000	-4.016680000
1	-2.643515000	1.839208000	1.357034000
1	2.169592000	0.823419000	1.494273000
1	-4.438150000	3.013202000	-0.870862000
1	4.147001000	2.417120000	-0.285240000
1	-2.659247000	2.780334000	-0.986249000
1	7.400636000	-2.021489000	-1.135777000
1	5.116964000	0.523630000	-0.781585000
1	7.290428000	-0.250118000	-1.382865000
1	2.413556000	2.124807000	-0.660455000
1	8.048880000	-1.276162000	-2.638878000
1	-5.561746000	0.949307000	-0.825084000
1	0.234405000	2.641554000	-3.029458000
1	3.250115000	-5.107275000	0.506964000
1	-0.448711000	-0.619627000	-1.292041000
1	-7.491631000	-2.247961000	-0.531295000
1	-1.986301000	-2.480072000	2.373033000
1	1.844764000	-0.103342000	-2.134279000
1	1.167831000	-3.707928000	0.273431000
1	3.286477000	-5.365750000	-1.267123000
1	-2.504225000	0.348019000	-2.334639000
1	1.913445000	-5.992320000	-0.308130000
1	4.034701000	-3.419468000	-2.161728000
1	1.143218000	0.671524000	-3.595923000
1	-6.837444000	-0.430662000	-2.153341000

1	-1.524298000	0.990465000	-3.697472000
1	-1.032274000	-2.787862000	0.092616000
1	6.414428000	-0.346571000	-4.425758000
1	5.609008000	0.684518000	-3.199051000
1	4.639024000	-0.474311000	-4.160031000
1	-8.060347000	-2.603731000	-2.199908000
1	-3.280709000	-3.667401000	2.006426000
1	-1.559131000	-4.195478000	2.079112000
1	-6.635723000	-3.460393000	-1.535846000
1	0.893387000	-1.074836000	-3.302934000
1	-1.667370000	-0.783016000	-3.447491000
1	-4.316664000	-3.142535000	-1.308568000
1	0.343534000	-2.942334000	-1.936639000
1	1.604692000	-3.888996000	-2.787871000
1	0.310008000	-4.734763000	-1.873818000
1	-5.146050000	-0.876425000	-3.963741000
1	-2.226768000	-4.205233000	-1.648754000
1	-6.659852000	-1.811423000	-4.235814000
1	-1.562661000	-5.139382000	-0.270464000
1	-5.198008000	-2.628344000	-3.593692000
1	-3.316441000	-4.825176000	-0.360135000
14	-0.945234000	-0.092834000	0.932178000
14	0.886349000	-1.504851000	1.227609000
6	1.248264000	0.422410000	4.894103000
1	2.072413000	0.930057000	4.354897000
1	0.353520000	1.075199000	4.856446000
1	1.549509000	0.305940000	5.956788000
6	-0.164846000	-1.669357000	5.079483000
1	0.161989000	-1.817810000	6.130563000
1	-1.095703000	-1.068339000	5.077663000
1	-0.397021000	-2.660826000	4.638293000
6	2.226595000	-1.819053000	4.257420000
1	2.020867000	-2.834859000	3.859184000
1	3.013491000	-1.358004000	3.624609000
1	2.633326000	-1.925579000	5.284746000
1	5.867453000	-2.400459000	-3.100820000

Table S6: Atomic coordinates of **3b.**

6	-0.210140000	6.364747000	-3.332775000
6	2.127660000	5.662194000	-2.597869000
6	0.637965000	5.749782000	-2.202339000
6	6.192622000	2.620577000	3.080244000
6	0.123875000	4.382884000	-1.766446000
6	-0.180578000	4.114539000	-0.421810000
6	0.398960000	2.805739000	2.351484000
6	-2.056242000	3.456493000	1.972718000
6	-0.001372000	3.326175000	-2.684904000
6	2.953760000	2.131674000	-1.091243000
6	6.095594000	1.083878000	3.173790000
6	-0.583133000	2.834601000	0.002101000
6	-0.862414000	2.614836000	1.488235000
6	4.476796000	0.771220000	1.223015000
6	4.789403000	0.566883000	2.580385000
6	7.317297000	0.403319000	2.522304000
6	-0.397727000	2.026635000	-2.309612000
6	3.038777000	0.614897000	-0.834176000
6	4.098525000	-0.053276000	-1.732328000
6	-0.700382000	1.766969000	-0.937721000
6	3.280966000	0.306390000	0.642208000
6	3.857314000	-0.127141000	3.370022000
6	0.947061000	0.728326000	-4.017937000
6	-1.447087000	1.352787000	-4.534717000
6	-0.452562000	0.970467000	-3.418773000
6	1.191411000	-0.453382000	4.912210000
6	2.348434000	-0.410778000	1.455820000
6	-2.525320000	0.323738000	4.251802000
6	2.648612000	-0.614963000	2.836461000
6	-4.681964000	1.470512000	-2.421652000
6	1.681978000	-1.349658000	3.762898000
6	-2.207632000	-0.526983000	3.007061000
6	-2.935792000	-0.048581000	0.535766000
6	-3.756242000	0.365129000	-1.879646000
6	-3.251497000	-0.360619000	1.896584000
6	-4.006079000	0.061282000	-0.403483000
6	-7.559786000	0.342943000	2.800720000
6	-4.596734000	-0.564523000	2.263170000
6	2.268489000	-2.679398000	4.270164000
6	0.303594000	-1.777188000	-0.779041000
6	-5.333919000	-0.158550000	0.013486000
6	-5.654801000	-0.476219000	1.342463000
6	-2.034993000	-2.016738000	3.365242000
6	-3.830344000	-0.919534000	-2.729699000
6	1.270046000	-2.522249000	-2.979127000
6	-7.098290000	-0.711758000	1.773885000
6	2.103225000	-3.520456000	-0.817018000

6	0.857150000	-2.949568000	-1.540246000
6	3.078357000	-4.275989000	-3.016830000
6	1.836998000	-3.728732000	-3.756957000
6	2.673540000	-4.726120000	-1.595138000
6	-7.302857000	-2.143778000	2.309529000
6	-0.217614000	-4.073624000	-1.652352000
6	0.759885000	-4.831974000	-3.851657000
6	1.595366000	-5.829947000	-1.690454000
6	0.353406000	-5.279743000	-2.429474000
1	0.146419000	7.386155000	-3.583334000
1	2.533376000	6.663218000	-2.857169000
1	0.562773000	6.423917000	-1.319461000
1	-1.279223000	6.431832000	-3.044043000
1	2.736936000	5.240223000	-1.772440000
1	-0.149604000	5.756629000	-4.260213000
1	2.263208000	5.002319000	-3.481370000
1	5.318884000	3.108716000	3.558850000
1	7.114096000	2.990586000	3.577622000
1	-0.082401000	4.926461000	0.318638000
1	0.771841000	3.850314000	2.300157000
1	-1.863057000	4.542088000	1.842506000
1	6.226301000	2.956119000	2.021948000
1	3.910485000	2.643415000	-0.851452000
1	0.240003000	3.515981000	-3.743581000
1	2.717177000	2.337073000	-2.155129000
1	0.179023000	2.578435000	3.416204000
1	6.093846000	0.811481000	4.253175000
1	-2.255139000	3.279076000	3.050188000
1	2.151174000	2.595628000	-0.484030000
1	1.215669000	2.132763000	2.017696000
1	5.191930000	1.321424000	0.588937000
1	-2.973055000	3.198740000	1.403905000
1	8.261634000	0.741501000	2.999047000
1	5.112672000	0.358890000	-1.543404000
1	7.381107000	0.648271000	1.440695000
1	1.346927000	1.646837000	-4.497481000
1	3.868114000	0.114045000	-2.805734000
1	-1.159316000	1.549979000	1.627206000
1	-1.104069000	2.245478000	-5.099610000
1	-2.688012000	1.386150000	3.980386000
1	4.084319000	-0.290745000	4.437525000
1	7.258266000	-0.700819000	2.612845000
1	0.739347000	0.480501000	4.520099000
1	2.022668000	-0.166426000	5.591159000
1	2.050011000	0.179126000	-1.095162000
1	1.664346000	0.414830000	-3.237761000
1	-4.616348000	2.388250000	-1.802107000
1	-1.687273000	0.275580000	4.976704000

1	4.143207000	-1.148210000	-1.559045000
1	-2.450721000	1.584616000	-4.129101000
1	0.915103000	-0.067026000	-4.791065000
1	-3.436195000	-0.030728000	4.778187000
1	-4.403914000	1.737085000	-3.462720000
1	0.428079000	-0.978084000	5.524948000
1	-1.553410000	0.520722000	-5.262212000
1	-1.227191000	-0.180847000	2.617081000
1	-0.791532000	0.014783000	-2.971784000
1	-2.722463000	0.757984000	-1.963985000
1	-5.743915000	1.147899000	-2.446214000
1	-7.431497000	1.371834000	2.406270000
1	0.789448000	-1.610948000	3.138348000
1	3.166556000	-2.510773000	4.902585000
1	-6.973569000	0.268681000	3.741454000
1	2.029686000	-1.716958000	-2.913837000
1	-4.827044000	-0.812721000	3.311777000
1	-1.291734000	-2.145935000	4.180005000
1	2.872733000	-2.724321000	-0.713066000
1	-8.630205000	0.201622000	3.061352000
1	-6.150566000	-0.084454000	-0.723476000
1	1.523433000	-3.231844000	4.881210000
1	2.569499000	-3.327691000	3.421534000
1	-3.595280000	-0.699833000	-3.792579000
1	-2.994269000	-2.460140000	3.706868000
1	0.384967000	-2.098892000	-3.498532000
1	3.864704000	-3.490725000	-2.959470000
1	-7.732486000	-0.597696000	0.865963000
1	-1.682396000	-2.591067000	2.483467000
1	1.819909000	-3.826014000	0.215123000
1	-4.847907000	-1.363434000	-2.686374000
1	-3.102671000	-1.669769000	-2.361543000
1	2.125690000	-3.397092000	-4.778868000
1	3.565093000	-5.118653000	-1.058807000
1	-6.707902000	-2.315782000	3.231918000
1	3.514626000	-5.130691000	-3.579939000
1	-1.118162000	-3.666945000	-2.158781000
1	-8.369317000	-2.324660000	2.561480000
1	-0.528294000	-4.375397000	-0.628196000
1	-6.988967000	-2.901394000	1.562451000
1	-0.129407000	-4.449909000	-4.400320000
1	1.311415000	-6.173980000	-0.671447000
1	1.150140000	-5.699269000	-4.429261000
1	2.000612000	-6.714504000	-2.230383000
1	-0.424546000	-6.071997000	-2.495072000
8	-0.918306000	-1.298054000	-1.214898000
14	-1.144358000	0.105484000	-0.113092000
14	0.658120000	-1.034438000	0.843177000

Table S7: Atomic coordinates of **6a.**

6	2.814136000	6.294912000	-0.013648000
6	1.023594000	6.564568000	-1.807695000
6	1.361882000	5.973613000	-0.423702000
6	-0.880959000	2.508106000	3.066390000
6	-6.879775000	2.428528000	-0.265062000
6	0.153258000	3.936476000	0.526891000
6	1.094047000	4.474128000	-0.366951000
6	-3.641136000	-0.162991000	3.908689000
6	-2.555218000	2.588340000	1.150519000
6	-1.169484000	2.092029000	1.610740000
6	-0.088291000	2.551682000	0.634829000
6	-6.925435000	0.910321000	0.010617000
6	1.778605000	3.578782000	-1.209494000
6	2.922201000	2.205954000	2.356786000
6	-4.953572000	-0.092407000	1.277856000
6	-3.059709000	-0.969491000	2.733796000
6	-7.825327000	0.181185000	-1.006446000
6	-5.515953000	0.330705000	0.060183000
6	-3.632892000	-0.574249000	1.367406000
6	0.660949000	1.651339000	-0.178715000
6	1.572413000	2.189821000	-1.141031000
6	-3.199809000	-2.483432000	3.003029000
6	2.503937000	0.193743000	3.878158000
6	2.426090000	0.750576000	2.443061000
6	-4.721784000	0.249650000	-1.098325000
6	-2.848846000	-0.671350000	0.177400000
6	-3.408023000	-0.255915000	-1.066010000
6	3.845683000	1.321734000	-1.893256000
6	2.324325000	1.296827000	-2.127524000
6	-2.075881000	1.116595000	-2.714082000
6	3.141462000	-0.164037000	1.451514000
6	1.956771000	1.624858000	-3.587493000
6	4.527980000	-0.364362000	1.604774000
6	-2.596548000	-0.291127000	-2.359549000
6	2.448172000	-0.831774000	0.397897000
6	5.258308000	-1.217325000	0.759932000
6	-3.354569000	-0.934233000	-3.534351000
6	6.767445000	-1.371020000	0.908738000
6	7.500748000	-0.836906000	-0.339571000
6	-3.339948000	-3.968834000	-0.509198000
6	3.165466000	-1.750673000	-0.424213000
6	4.549174000	-1.917668000	-0.233512000
6	7.171633000	-2.825854000	1.221343000
6	2.473088000	-2.593909000	-1.491382000
6	3.047038000	-2.384891000	-2.905291000
6	-0.926871000	-3.917437000	-2.360541000
6	2.502410000	-4.082911000	-1.090119000

1	2.987770000	7.391656000	0.010182000
1	1.160494000	7.666687000	-1.812208000
1	0.687492000	6.453322000	0.320844000
1	3.047598000	5.883033000	0.989655000
1	-0.025278000	6.343827000	-2.093961000
1	-0.875532000	3.612321000	3.184667000
1	-0.413110000	4.629671000	1.171439000
1	3.538318000	5.855921000	-0.732699000
1	-7.898632000	2.870380000	-0.240543000
1	-6.253622000	2.953480000	0.485550000
1	1.682939000	6.143754000	-2.596654000
1	-2.603121000	3.698120000	1.147868000
1	-1.659142000	2.104165000	3.746256000
1	-3.637320000	0.926713000	3.703354000
1	-3.045473000	-0.342050000	4.827499000
1	0.100180000	2.127834000	3.413499000
1	-4.687070000	-0.459273000	4.137892000
1	-3.352958000	2.212426000	1.821958000
1	-6.445140000	2.635970000	-1.266296000
1	2.331545000	2.865054000	3.026548000
1	-5.568962000	-0.019329000	2.188633000
1	-2.790996000	2.227244000	0.129820000
1	-8.862670000	0.575749000	-0.969216000
1	-7.373125000	0.765874000	1.019839000
1	2.498152000	3.974294000	-1.944932000
1	2.827379000	2.600312000	1.325212000
1	3.987923000	2.284251000	2.660986000
1	-1.188050000	0.980684000	1.584320000
1	1.909202000	0.823587000	4.573624000
1	-1.965537000	-0.749265000	2.687046000
1	-2.833360000	-2.737884000	4.019844000
1	1.347975000	0.746001000	2.167494000
1	-7.861295000	-0.908988000	-0.803898000
1	-4.261979000	-2.799153000	2.927169000
1	3.549035000	0.177276000	4.253940000
1	-7.456822000	0.318509000	-2.045308000
1	4.262361000	2.326934000	-2.117398000
1	-5.136701000	0.597349000	-2.058505000
1	-1.428836000	1.519896000	-1.908260000
1	2.109026000	-0.841952000	3.924204000
1	-2.919213000	1.824649000	-2.862933000
1	2.289172000	2.645573000	-3.871817000
1	4.092979000	1.071673000	-0.842620000
1	-2.605983000	-3.085652000	2.284955000
1	5.062420000	0.166772000	2.410567000
1	0.860085000	1.570374000	-3.742519000
1	4.360706000	0.588008000	-2.547496000
1	1.975135000	0.250295000	-1.953761000

1	-1.480442000	1.094187000	-3.651726000
1	2.444033000	0.909639000	-4.283796000
1	7.075229000	-0.742796000	1.774796000
1	-4.207739000	-0.309207000	-3.874377000
1	7.220530000	0.215953000	-0.549348000
1	-1.698770000	-0.918673000	-2.155375000
1	-3.739945000	-3.921935000	0.522079000
1	-3.868147000	-3.199780000	-1.111390000
1	-3.760488000	-1.929920000	-3.258371000
1	8.602339000	-0.884643000	-0.206171000
1	-2.679889000	-1.066556000	-4.406254000
1	3.007531000	-1.320501000	-3.211952000
1	1.407197000	-2.264465000	-1.515092000
1	7.244529000	-1.436756000	-1.238892000
1	6.652493000	-3.201680000	2.126751000
1	-3.555302000	-4.972898000	-0.931627000
1	8.266443000	-2.904525000	1.390132000
1	5.094334000	-2.616075000	-0.889663000
1	-1.583149000	-3.310580000	-3.019437000
1	0.121900000	-3.623163000	-2.549769000
1	4.105600000	-2.714792000	-2.968732000
1	6.915047000	-3.505206000	0.380740000
1	2.472136000	-2.975552000	-3.649692000
1	2.035677000	-4.241782000	-0.098606000
1	-1.049931000	-4.988198000	-2.627835000
1	3.546871000	-4.458459000	-1.045263000
1	1.952987000	-4.709206000	-1.823523000
14	-1.476420000	-3.646487000	-0.569499000
14	0.674851000	-0.255480000	-0.022108000
14	-1.122167000	-1.487823000	0.292432000
17	-0.557144000	-5.124796000	0.641570000

Table S8: Atomic coordinates of **6b.**

6	-4.193339000	6.098126000	1.133101000
6	-2.080447000	6.302605000	2.546247000
6	-2.661781000	5.922506000	1.168470000
6	-0.609897000	3.341690000	-3.227218000
6	5.323180000	4.792998000	0.392371000
6	-1.393454000	4.289873000	-0.325938000
6	-2.246341000	4.512016000	0.767878000
6	2.384081000	0.759188000	-3.750319000
6	1.303332000	3.677398000	-1.607985000
6	0.002802000	2.895740000	-1.884680000
6	-0.977637000	3.000666000	-0.717316000
6	5.756233000	3.337809000	0.122909000
6	-2.676268000	3.390037000	1.500379000
6	-4.066950000	2.138521000	-2.187099000
6	4.370183000	1.663698000	-1.212547000
6	3.168759000	-0.017901000	-2.674220000
6	6.713441000	2.819674000	1.216353000
6	4.556398000	2.411098000	-0.037522000
6	3.286275000	0.781581000	-1.372937000
6	-1.461048000	1.869358000	0.006172000
6	-2.296296000	2.083539000	1.147016000
6	4.523178000	-0.504603000	-3.217383000
6	-3.439407000	0.543598000	-4.083585000
6	-3.294054000	0.865840000	-2.583785000
6	3.610968000	2.262716000	0.992851000
6	2.322053000	0.657034000	-0.324104000
6	2.489506000	1.418399000	0.872217000
6	-4.309730000	0.691777000	1.825020000
6	-2.797073000	0.920051000	2.003541000
6	0.973609000	2.738572000	2.436766000
6	-3.671688000	-0.324247000	-1.706130000
6	-2.403816000	1.060440000	3.485658000
6	-4.974684000	-0.848410000	-1.813039000
6	1.522805000	1.349686000	2.055465000
6	-2.749267000	-0.909048000	-0.786197000
6	-5.400057000	-1.949302000	-1.050972000
6	2.177629000	0.649841000	3.264019000
6	-6.825909000	-2.478560000	-1.156013000
6	-7.577782000	-2.316645000	0.181588000
6	-3.154061000	-2.056187000	-0.036975000
6	-4.465349000	-2.544778000	-0.184491000
6	-6.859896000	-3.940039000	-1.647431000
6	-2.218333000	-2.792107000	0.918630000
6	-2.760300000	-2.859009000	2.358808000
6	-1.892626000	-4.203022000	0.391548000
1	-4.478120000	7.146479000	1.363476000
1	-2.328542000	7.353165000	2.807946000

1	-2.225292000	6.616922000	0.415704000
1	-4.604376000	5.837511000	0.136117000
1	-0.976704000	6.191160000	2.559113000
1	-0.916989000	4.408779000	-3.194535000
1	-1.028270000	5.163025000	-0.892234000
1	-4.690347000	5.445225000	1.881890000
1	6.204206000	5.467780000	0.434973000
1	4.640213000	5.160825000	-0.400756000
1	-2.492244000	5.650838000	3.346168000
1	1.126838000	4.774238000	-1.618498000
1	0.133552000	3.231508000	-4.044668000
1	1.349964000	0.976730000	-3.415948000
1	2.319335000	0.171465000	-4.689990000
1	-1.500813000	2.743831000	-3.498643000
1	2.883938000	1.724039000	-3.980764000
1	2.061739000	3.450219000	-2.384200000
1	4.788504000	4.881507000	1.361950000
1	-3.718522000	3.013317000	-2.774605000
1	5.106847000	1.765948000	-2.024952000
1	1.740942000	3.406053000	-0.628919000
1	7.615463000	3.462838000	1.295457000
1	6.310307000	3.324692000	-0.842625000
1	-3.325302000	3.536791000	2.379620000
1	-3.923659000	2.375413000	-1.113622000
1	-5.155195000	2.015304000	-2.373493000
1	0.277407000	1.822855000	-1.978076000
1	-3.077033000	1.391379000	-4.702966000
1	2.569658000	-0.930492000	-2.438159000
1	4.366284000	-1.249820000	-4.024310000
1	-2.210446000	1.061965000	-2.410801000
1	7.043785000	1.782909000	0.998457000
1	5.114865000	0.328436000	-3.654451000
1	-4.498977000	0.360819000	-4.361006000
1	6.216443000	2.812126000	2.209854000
1	-4.885319000	1.568506000	2.191709000
1	3.743413000	2.835371000	1.925438000
1	0.487794000	3.231554000	1.571582000
1	-2.855721000	-0.359396000	-4.356294000
1	1.775986000	3.408820000	2.812906000
1	-2.866766000	1.954410000	3.953993000
1	-4.566529000	0.530263000	0.759100000
1	5.130025000	-0.980600000	-2.423083000
1	-5.687373000	-0.381308000	-2.513516000
1	-1.304297000	1.147985000	3.599403000
1	-4.646433000	-0.201273000	2.391418000
1	-2.274924000	0.002647000	1.639619000
1	0.213223000	2.653158000	3.240037000
1	-2.739344000	0.173116000	4.062766000

1	-7.350146000	-1.855528000	-1.915249000
1	3.035566000	1.237973000	3.654175000
1	-7.570147000	-1.260500000	0.521320000
1	0.657860000	0.727213000	1.736258000
1	2.555920000	-0.358250000	2.995165000
1	-8.634729000	-2.644215000	0.086609000
1	1.447694000	0.526776000	4.092656000
1	-2.977280000	-1.851106000	2.765261000
1	-1.264200000	-2.219118000	0.950983000
1	-7.106626000	-2.928905000	0.979893000
1	-6.330964000	-4.051160000	-2.616112000
1	-7.906008000	-4.288635000	-1.779963000
1	-4.770290000	-3.423899000	0.406337000
1	-3.697004000	-3.453149000	2.414893000
1	-6.371346000	-4.620846000	-0.918246000
1	-2.014986000	-3.344437000	3.021635000
1	-1.443508000	-4.162540000	-0.619870000
1	-2.809146000	-4.828962000	0.336702000
1	-1.170578000	-4.710301000	1.063093000
14	1.793560000	-2.773598000	-0.268811000
14	-1.136940000	0.039890000	-0.434673000
14	0.933083000	-0.623344000	-0.579988000
17	1.130901000	-4.124786000	-1.760653000
6	1.354801000	-3.529734000	1.411147000
6	0.875116000	-2.734157000	2.474927000
6	1.564872000	-4.910712000	1.638806000
6	0.615608000	-3.298299000	3.736674000
6	1.294973000	-5.479115000	2.894387000
6	0.821704000	-4.672559000	3.947098000
1	0.677471000	-1.662377000	2.306390000
1	1.926010000	-5.550702000	0.816860000
1	0.240524000	-2.661435000	4.553616000
1	1.453920000	-6.557633000	3.054762000
1	0.610611000	-5.118852000	4.932112000
6	3.682611000	-2.698406000	-0.410389000
6	4.396784000	-1.799163000	0.419275000
6	4.413553000	-3.519485000	-1.298833000
6	5.797389000	-1.718481000	0.356475000
6	5.817269000	-3.451188000	-1.351354000
6	6.511763000	-2.547418000	-0.527881000
1	3.858330000	-1.135855000	1.114743000
1	3.876578000	-4.217938000	-1.960695000
1	6.330507000	-1.000362000	0.999520000
1	6.370658000	-4.100145000	-2.048990000
1	7.610626000	-2.485056000	-0.578446000

Table S9: Atomic coordinates of **7a.**

6	-2.703964000	6.164805000	-1.067253000
6	-1.585343000	6.684269000	1.163603000
6	-1.467539000	5.927813000	-0.174816000
6	1.706780000	2.276802000	-2.386714000
6	6.985040000	1.563301000	-1.758056000
6	-0.073425000	3.812135000	-0.477874000
6	-1.221960000	4.437653000	0.033138000
6	2.020760000	-1.320477000	-3.590319000
6	2.656529000	2.222789000	-0.038167000
6	1.450789000	1.858341000	-0.927738000
6	0.157199000	2.426624000	-0.345805000
6	6.848745000	0.027502000	-1.835976000
6	-2.146638000	3.636842000	0.729234000
6	-2.227824000	1.680870000	-2.708452000
6	4.490171000	-0.934098000	-1.925533000
6	2.183930000	-1.955904000	-2.200391000
6	8.091855000	-0.677609000	-1.258681000
6	5.557186000	-0.427071000	-1.165472000
6	3.262402000	-1.300499000	-1.337989000
6	-0.798977000	1.622763000	0.340203000
6	-1.953931000	2.254345000	0.903151000
6	2.472694000	-3.469239000	-2.320737000
6	-1.373067000	-0.424670000	-3.849444000
6	-1.673320000	0.257710000	-2.500615000
6	5.386861000	-0.316934000	0.228931000
6	3.088519000	-1.130015000	0.065946000
6	4.176959000	-0.653161000	0.861007000
6	-4.342987000	1.368923000	0.896584000
6	-3.017627000	1.472229000	1.675952000
6	5.027237000	0.447305000	3.037173000
6	-2.598742000	-0.604625000	-1.641141000
6	-3.237613000	2.033219000	3.093934000
6	-3.857305000	-0.951458000	-2.173987000
6	4.050515000	-0.539990000	2.381186000
6	-2.233145000	-1.072113000	-0.343446000
6	-4.766916000	-1.764710000	-1.478297000
6	4.148586000	-1.939569000	3.027126000
6	-6.147048000	-2.072527000	-2.048046000
6	-7.254674000	-1.459984000	-1.165220000
6	0.680918000	1.124827000	3.440834000
6	-3.112837000	-1.966602000	0.336912000
6	-4.359689000	-2.280908000	-0.234639000
6	-6.363190000	-3.585255000	-2.254735000
6	-2.745006000	-2.623247000	1.665070000
6	-3.684589000	-2.205035000	2.811533000
6	-0.200418000	-1.824653000	4.059230000
6	-2.657998000	-4.155319000	1.528418000

1	-2.844339000	7.246733000	-1.275685000
1	-1.702267000	7.775522000	0.993618000
1	-0.581189000	6.332530000	-0.713463000
1	-2.606574000	5.633026000	-2.036062000
1	-0.687164000	6.525390000	1.795138000
1	1.883865000	3.368760000	-2.483483000
1	0.667858000	4.431245000	-1.010366000
1	-3.628027000	5.794485000	-0.574066000
1	7.889139000	1.912726000	-2.300374000
1	6.098996000	2.066916000	-2.196895000
1	-2.468428000	6.340998000	1.743590000
1	2.791598000	3.324859000	0.008785000
1	2.610867000	1.762632000	-2.774366000
1	1.779140000	-0.242410000	-3.520841000
1	1.203605000	-1.819801000	-4.147188000
1	0.850006000	2.015429000	-3.041180000
1	2.939395000	-1.429162000	-4.204129000
1	3.589015000	1.768531000	-0.431336000
1	7.071876000	1.898664000	-0.702503000
1	-1.501882000	2.309507000	-3.265308000
1	4.627846000	-1.052469000	-3.012396000
1	2.518117000	1.856659000	0.999888000
1	9.006116000	-0.381631000	-1.815002000
1	6.773162000	-0.250166000	-2.911396000
1	-3.053985000	4.103928000	1.146433000
1	-2.435818000	2.181129000	-1.742803000
1	-3.172009000	1.655125000	-3.293394000
1	1.357605000	0.750594000	-0.919373000
1	-0.605777000	0.144599000	-4.414206000
1	1.210414000	-1.843602000	-1.665166000
1	1.659068000	-3.980313000	-2.877414000
1	-0.703368000	0.343256000	-1.962571000
1	7.992754000	-1.781006000	-1.316416000
1	3.425883000	-3.638301000	-2.866214000
1	-2.280706000	-0.482958000	-4.486594000
1	8.252375000	-0.408853000	-0.192890000
1	-4.801320000	2.371237000	0.754704000
1	6.221723000	0.063212000	0.835915000
1	4.980798000	1.447039000	2.557453000
1	-0.999969000	-1.457729000	-3.700288000
1	6.078963000	0.092057000	2.989305000
1	-3.687884000	3.048263000	3.070572000
1	-4.187258000	0.915331000	-0.102057000
1	2.554556000	-3.940880000	-1.322294000
1	-4.144814000	-0.566576000	-3.166672000
1	-2.281510000	2.103063000	3.651704000
1	-5.070196000	0.733850000	1.444807000
1	-2.632055000	0.437876000	1.807869000

1	4.778195000	0.571267000	4.111587000
1	-3.927800000	1.379498000	3.668472000
1	-6.204253000	-1.584509000	-3.047127000
1	5.149567000	-2.384325000	2.841608000
1	-7.106521000	-0.367925000	-1.036591000
1	3.024373000	-0.163676000	2.583104000
1	0.847826000	1.873769000	2.641233000
1	-0.155278000	1.485859000	4.076304000
1	3.389761000	-2.633814000	2.609148000
1	-8.258289000	-1.626138000	-1.611165000
1	3.992478000	-1.881465000	4.125353000
1	-3.684274000	-1.104900000	2.953942000
1	-1.727098000	-2.270995000	1.923675000
1	-7.255724000	-1.918681000	-0.153332000
1	-5.572828000	-4.019909000	-2.900586000
1	1.592440000	1.058929000	4.072263000
1	-7.347806000	-3.783713000	-2.728599000
1	-5.038720000	-2.954361000	0.314038000
1	-1.178166000	-1.582441000	4.525328000
1	-0.246985000	-2.848292000	3.636635000
1	-4.732166000	-2.517381000	2.614352000
1	-6.343440000	-4.130537000	-1.287258000
1	-3.370855000	-2.675104000	3.767245000
1	-1.954613000	-4.436473000	0.719521000
1	0.581596000	-1.805529000	4.847503000
1	-3.648733000	-4.603893000	1.300815000
1	-2.291259000	-4.608409000	2.473828000
14	0.233146000	-0.570315000	2.701460000
14	-0.713756000	-0.287506000	0.515707000
14	1.362520000	-1.365342000	0.817309000
17	0.856247000	-3.452604000	0.864877000

Table S10: Atomic coordinates of **7b.**

6	1.824917000	-5.720351000	3.632221000
6	0.406991000	-4.327719000	5.228164000
6	0.571681000	-4.833410000	3.780008000
6	-1.927895000	-3.713249000	-0.799351000
6	-6.668872000	-2.530487000	-1.228671000
6	-0.428782000	-3.537075000	1.823390000
6	0.583518000	-3.676644000	2.787165000
6	-1.748835000	-1.934693000	-4.085547000
6	-2.880612000	-1.871786000	0.655053000
6	-1.625463000	-2.389596000	-0.074414000
6	-0.446257000	-2.478026000	0.892602000
6	-6.652944000	-1.325520000	-2.196514000
6	1.601242000	-2.704728000	2.815466000
6	2.035232000	-3.816547000	-1.017814000
6	-4.236317000	-0.836704000	-2.812468000
6	-1.851536000	-0.482215000	-3.594658000
6	-7.920742000	-0.467366000	-2.039686000
6	-5.356158000	-0.546028000	-2.009246000
6	-2.986368000	-0.228289000	-2.602143000
6	0.590641000	-1.502307000	0.933799000
6	1.619365000	-1.619781000	1.920776000
6	-1.995918000	0.484777000	-4.791668000
6	1.524814000	-3.011361000	-3.375857000
6	1.690881000	-2.599827000	-1.898981000
6	-5.208004000	0.415607000	-0.995688000
6	-2.836430000	0.692543000	-1.517670000
6	-3.972050000	1.038178000	-0.727821000
6	4.117428000	-1.159008000	1.703825000
6	2.734760000	-0.584021000	2.060702000
6	-4.547443000	1.645004000	1.696646000
6	2.715095000	-1.472747000	-1.760261000
6	2.708920000	0.091487000	3.445408000
6	4.027462000	-1.725857000	-2.210233000
6	-3.921706000	2.103017000	0.367796000
6	2.391701000	-0.186567000	-1.231395000
6	5.031050000	-0.744030000	-2.188287000
6	-4.557345000	3.412626000	-0.143727000
6	6.455362000	-1.058553000	-2.631109000
6	7.445715000	-0.903087000	-1.458128000
6	3.377058000	0.844073000	-1.286332000
6	4.671297000	0.542553000	-1.749473000
6	6.880739000	-0.206920000	-3.844367000
6	3.083120000	2.283323000	-0.880282000
6	3.914522000	2.741376000	0.330893000
6	3.236906000	3.250169000	-2.069343000
1	1.773628000	-6.596695000	4.312465000
1	0.336188000	-5.176754000	5.940638000

1	-0.315868000	-5.460610000	3.538639000
1	1.932746000	-6.092683000	2.592749000
1	-0.506672000	-3.707299000	5.335368000
1	-2.254317000	-4.507591000	-0.095826000
1	-1.237604000	-4.286107000	1.801378000
1	2.747949000	-5.155689000	3.883724000
1	-7.575797000	-3.154063000	-1.378348000
1	-5.775697000	-3.172812000	-1.373092000
1	1.273147000	-3.703479000	5.534763000
1	-3.177968000	-2.566721000	1.469491000
1	-2.752119000	-3.564990000	-1.527669000
1	-1.605160000	-2.641362000	-3.246594000
1	-0.889104000	-2.044394000	-4.775401000
1	-1.041390000	-4.091785000	-1.348562000
1	-2.653248000	-2.247544000	-4.648251000
1	-3.731180000	-1.768816000	-0.048387000
1	-6.660406000	-2.180444000	-0.174295000
1	1.234019000	-4.582710000	-1.072306000
1	-4.353377000	-1.561484000	-3.634233000
1	-2.701451000	-0.878837000	1.111736000
1	-8.825132000	-1.058240000	-2.294392000
1	-6.643503000	-1.728434000	-3.234707000
1	2.404155000	-2.786782000	3.566492000
1	2.155492000	-3.527660000	0.044438000
1	2.980307000	-4.292465000	-1.355542000
1	-1.364999000	-1.638212000	-0.852350000
1	0.699836000	-3.745294000	-3.487498000
1	-0.891661000	-0.239481000	-3.079569000
1	-1.132945000	0.385003000	-5.483300000
1	0.705969000	-2.202481000	-1.570273000
1	-7.891903000	0.424348000	-2.699085000
1	-2.924334000	0.257922000	-5.358553000
1	2.448393000	-3.483680000	-3.771867000
1	-8.048995000	-0.112449000	-0.995072000
1	4.420530000	-1.960518000	2.411394000
1	-6.077496000	0.680539000	-0.375085000
1	-4.039760000	0.742143000	2.093001000
1	1.297041000	-2.132245000	-4.011708000
1	-5.630033000	1.418766000	1.593276000
1	2.961730000	-0.621523000	4.258715000
1	4.115568000	-1.581694000	0.678287000
1	-2.044039000	1.538060000	-4.454295000
1	4.279911000	-2.728902000	-2.593422000
1	1.701979000	0.506217000	3.662331000
1	4.889392000	-0.361738000	1.737970000
1	2.531758000	0.223727000	1.326710000
1	-4.445933000	2.439657000	2.462507000
1	3.445251000	0.922092000	3.487715000

1	6.470911000	-2.126143000	-2.946779000
1	-5.635549000	3.271029000	-0.372704000
1	7.145613000	-1.531121000	-0.594161000
1	-2.850840000	2.318021000	0.570239000
1	-4.058448000	3.761419000	-1.071493000
1	8.473148000	-1.195423000	-1.762388000
1	-4.472386000	4.214879000	0.619671000
1	3.718811000	2.107050000	1.219210000
1	2.016744000	2.323144000	-0.582792000
1	7.485739000	0.150411000	-1.107780000
1	6.176161000	-0.334227000	-4.691799000
1	7.896787000	-0.490845000	-4.191654000
1	5.426555000	1.345551000	-1.764079000
1	5.003121000	2.696343000	0.114034000
1	6.905440000	0.873646000	-3.588091000
1	3.661337000	3.786052000	0.603408000
1	2.625757000	2.915153000	-2.931026000
1	4.294723000	3.327933000	-2.400422000
1	2.896438000	4.265627000	-1.776903000
14	-0.089937000	1.880997000	0.998958000
14	0.752463000	-0.005375000	-0.247781000
14	-1.091764000	1.254812000	-1.040442000
6	-1.038966000	1.498474000	2.606741000
6	-1.220791000	0.212224000	3.169474000
6	-1.636269000	2.601675000	3.271612000
6	-1.979187000	0.033646000	4.339771000
6	-2.385734000	2.424839000	4.446224000
6	-2.565589000	1.137198000	4.982396000
1	-0.762164000	-0.665652000	2.696735000
1	-1.511725000	3.618838000	2.865243000
1	-2.104035000	-0.980721000	4.751355000
1	-2.837743000	3.299066000	4.942124000
1	-3.158321000	0.996459000	5.900427000
6	0.725288000	3.574421000	1.245112000
6	1.428139000	3.805099000	2.454303000
6	0.707968000	4.600282000	0.271130000
6	2.093277000	5.020963000	2.682478000
6	1.380946000	5.814357000	0.495556000
6	2.074899000	6.028213000	1.700153000
1	1.454265000	3.021432000	3.229476000
1	0.176079000	4.442075000	-0.679373000
1	2.635527000	5.180561000	3.628341000
1	1.359978000	6.600443000	-0.276382000
1	2.600923000	6.980490000	1.874584000
17	-0.264397000	2.541112000	-2.543399000

Table S11: Atomic coordinates of **11a.**

6	3.105990000	6.263216000	0.355741000
6	1.564205000	6.740960000	-1.617089000
6	1.696675000	6.060630000	-0.239959000
6	-0.919178000	2.551279000	2.911197000
6	-6.780676000	2.742008000	-0.574988000
6	0.319466000	4.048732000	0.512014000
6	1.341495000	4.579008000	-0.292576000
6	-3.893803000	0.167188000	3.880848000
6	-2.489945000	2.782536000	0.917672000
6	-1.148168000	2.216820000	1.424441000
6	0.004332000	2.673518000	0.532859000
6	-6.932209000	1.252433000	-0.199592000
6	2.035863000	3.692884000	-1.137658000
6	2.947742000	2.136392000	2.374555000
6	-5.070967000	0.206446000	1.195151000
6	-3.281597000	-0.696194000	2.764027000
6	-7.846643000	0.512232000	-1.195459000
6	-5.565219000	0.590127000	-0.064062000
6	-3.784364000	-0.345824000	1.358236000
6	0.763344000	1.786198000	-0.279251000
6	1.757320000	2.314153000	-1.154732000
6	-3.470195000	-2.195799000	3.081246000
6	2.381085000	0.100603000	3.813349000
6	2.399438000	0.697139000	2.392427000
6	-4.738945000	0.390321000	-1.183987000
6	-2.969910000	-0.558910000	0.207818000
6	-3.458773000	-0.190227000	-1.076686000
6	4.030715000	1.386618000	-1.843462000
6	2.520881000	1.429736000	-2.139918000
6	-2.010292000	1.003312000	-2.771376000
6	3.135644000	-0.215214000	1.413470000
6	2.222733000	1.825898000	-3.599271000
6	4.504922000	-0.474273000	1.629438000
6	-2.621965000	-0.346728000	-2.345803000
6	2.484306000	-0.828714000	0.308004000
6	5.245285000	-1.330090000	0.795290000
6	-3.392645000	-1.010339000	-3.501330000
6	6.735832000	-1.555694000	1.023749000
6	7.565104000	-1.028115000	-0.165589000
6	-3.415414000	-3.980009000	-0.375292000
6	3.201574000	-1.738702000	-0.516094000
6	4.566740000	-1.967912000	-0.260013000
6	7.054415000	-3.034595000	1.321883000
6	2.532514000	-2.501575000	-1.658445000
6	3.197265000	-2.254556000	-3.025887000
6	-1.032190000	-3.839205000	-2.294166000
6	2.462714000	-4.006492000	-1.330346000

1	3.345619000	7.343073000	0.456430000
1	1.764597000	7.830529000	-1.540524000
1	0.967776000	6.546801000	0.446827000
1	3.188301000	5.792539000	1.357036000
1	0.546862000	6.604133000	-2.037855000
1	-0.888499000	3.647674000	3.085155000
1	-0.251738000	4.737698000	1.157109000
1	3.881656000	5.804468000	-0.294169000
1	-7.768832000	3.247967000	-0.613747000
1	-6.143102000	3.276974000	0.158756000
1	2.289176000	6.320832000	-2.346344000
1	-2.499096000	3.892758000	0.954612000
1	-1.740502000	2.138172000	3.531854000
1	-3.852752000	1.248294000	3.635830000
1	-3.345471000	0.008683000	4.832342000
1	0.033743000	2.124504000	3.283376000
1	-4.956416000	-0.094909000	4.071568000
1	-3.332352000	2.407922000	1.533374000
1	-6.304961000	2.851569000	-1.573051000
1	2.345042000	2.794795000	3.034493000
1	-5.711499000	0.367870000	2.076745000
1	-2.687046000	2.467727000	-0.126539000
1	-8.859017000	0.968173000	-1.216870000
1	-7.416988000	1.205496000	0.801597000
1	2.821577000	4.086683000	-1.803176000
1	2.916122000	2.564076000	1.352316000
1	3.998934000	2.170377000	2.732329000
1	-1.212051000	1.110955000	1.345678000
1	1.771329000	0.732640000	4.493700000
1	-2.181563000	-0.499788000	2.759832000
1	-3.133123000	-2.428198000	4.113365000
1	1.339338000	0.742161000	2.060776000
1	-7.953627000	-0.558390000	-0.925001000
1	-4.538604000	-2.484573000	2.989005000
1	3.403405000	0.038050000	4.242832000
1	-7.441015000	0.559171000	-2.228519000
1	4.495898000	2.382641000	-2.003580000
1	-5.099526000	0.703116000	-2.177542000
1	-1.393357000	1.440669000	-1.960025000
1	1.949825000	-0.921547000	3.810583000
1	-2.805320000	1.737150000	-3.024603000
1	2.601192000	2.844868000	-3.826293000
1	4.223960000	1.078609000	-0.796523000
1	-2.881303000	-2.837916000	2.393630000
1	5.017121000	0.010314000	2.478044000
1	1.131142000	1.818110000	-3.797921000
1	4.544888000	0.663265000	-2.509878000
1	2.131701000	0.390230000	-2.021177000

1	-1.359593000	0.881142000	-3.663778000
1	2.712163000	1.121869000	-4.305427000
1	7.020860000	-0.962668000	1.921803000
1	-4.204679000	-0.360380000	-3.890868000
1	7.347533000	0.041869000	-0.362541000
1	-1.769459000	-1.013281000	-2.090825000
1	-3.773090000	-3.990825000	0.672975000
1	-3.974060000	-3.186023000	-0.914991000
1	-3.856750000	-1.966510000	-3.181094000
1	8.653426000	-1.132604000	0.029949000
1	-2.710782000	-1.223450000	-4.351516000
1	3.235100000	-1.175018000	-3.274634000
1	1.484081000	-2.120719000	-1.725767000
1	7.335067000	-1.593148000	-1.094131000
1	6.466150000	-3.406371000	2.185761000
1	-3.639148000	-4.963678000	-0.839303000
1	8.132637000	-3.168958000	1.551646000
1	5.120155000	-2.664100000	-0.911752000
1	-1.749423000	-3.298757000	-2.945763000
1	-0.017671000	-3.444690000	-2.488653000
1	4.238453000	-2.640173000	-3.047277000
1	6.816483000	-3.681416000	0.450679000
1	2.635539000	-2.772643000	-3.831572000
1	1.901646000	-4.189768000	-0.392747000
1	-1.053506000	-4.917339000	-2.559157000
1	3.482086000	-4.430878000	-1.210033000
1	1.959890000	-4.571950000	-2.142783000
14	-1.563107000	-3.619321000	-0.490197000
32	0.658044000	-0.212209000	-0.215189000
32	-1.190155000	-1.447904000	0.509088000
17	-0.562384000	-5.091715000	0.663624000

Table S12: Atomic coordinates of **11c.**

6	-5.732472000	5.242322000	0.139456000
6	-4.368394000	6.012062000	2.150449000
6	-4.316000000	5.460999000	0.711108000
6	-0.629616000	3.429960000	-2.631492000
6	5.468200000	4.785465000	1.305205000
6	-2.332598000	4.121963000	-0.175177000
6	-3.485399000	4.185787000	0.623018000
6	2.927577000	2.618259000	-3.689879000
6	0.746862000	3.954231000	-0.548359000
6	-0.310586000	3.026409000	-1.179099000
6	-1.559092000	2.948995000	-0.304992000
6	5.857351000	3.503282000	0.540924000
6	-3.844126000	3.030469000	1.341105000
6	-4.032964000	1.542827000	-2.405804000
6	4.227061000	2.369650000	-1.061726000
6	2.693731000	1.370954000	-2.815786000
6	6.954604000	2.716261000	1.286513000
6	4.639324000	2.630990000	0.255556000
6	3.103346000	1.569038000	-1.351787000
6	-1.971202000	1.773107000	0.384537000
6	-3.105975000	1.836479000	1.246703000
6	3.384970000	0.146170000	-3.449281000
6	-2.709630000	-0.017202000	-3.944173000
6	-3.006116000	0.397873000	-2.490762000
6	3.885332000	2.072375000	1.303652000
6	2.386346000	0.968381000	-0.276912000
6	2.777403000	1.234736000	1.066934000
6	-4.946811000	0.138585000	1.681651000
6	-3.554290000	0.648624000	2.096325000
6	1.041929000	1.709212000	2.841688000
6	-3.414873000	-0.796433000	-1.631504000
6	-3.471322000	0.963869000	3.602815000
6	-4.586559000	-1.506660000	-1.967458000
6	2.023250000	0.667474000	2.268101000
6	-2.656914000	-1.213075000	-0.503949000
6	-5.024995000	-2.618832000	-1.228123000
6	2.945971000	0.094142000	3.357039000
6	-6.314842000	-3.346652000	-1.590759000
6	-7.361090000	-3.217410000	-0.464044000
6	-3.068225000	-2.352325000	0.242287000
6	-4.240924000	-3.032591000	-0.134635000
6	-6.057518000	-4.823193000	-1.953924000
6	-2.263839000	-2.879546000	1.429121000
6	-3.085226000	-3.038193000	2.721207000
6	-1.549621000	-4.193772000	1.062869000
1	-6.313237000	6.188983000	0.141384000
1	-4.923892000	6.973062000	2.186786000

1	-3.810801000	6.223506000	0.076454000
1	-5.690511000	4.861651000	-0.901816000
1	-3.348780000	6.184145000	2.552267000
1	-1.050270000	4.455830000	-2.691379000
1	-2.023450000	5.027557000	-0.723740000
1	-6.296871000	4.500932000	0.744457000
1	6.350618000	5.443399000	1.453447000
1	4.694043000	5.359904000	0.756187000
1	-4.883430000	5.303162000	2.833340000
1	0.382099000	5.002172000	-0.492592000
1	0.288549000	3.411378000	-3.251900000
1	2.555998000	3.543403000	-3.204340000
1	2.409011000	2.506212000	-4.664535000
1	-1.363700000	2.738226000	-3.090506000
1	4.005525000	2.765966000	-3.913579000
1	1.683961000	3.942894000	-1.140712000
1	5.057773000	4.544290000	2.308949000
1	-3.678872000	2.432631000	-2.966981000
1	4.804651000	2.813494000	-1.888383000
1	1.008368000	3.623102000	0.476127000
1	7.859232000	3.341567000	1.441659000
1	6.274931000	3.812221000	-0.443774000
1	-4.729166000	3.058908000	1.997932000
1	-4.198745000	1.851336000	-1.353672000
1	-5.010553000	1.238464000	-2.836850000
1	0.131535000	2.009415000	-1.216264000
1	-2.339684000	0.851387000	-4.529534000
1	1.595323000	1.168387000	-2.810945000
1	3.124508000	0.058499000	-4.525212000
1	-2.046639000	0.781955000	-2.078595000
1	7.254881000	1.810886000	0.719226000
1	4.488711000	0.225614000	-3.358625000
1	-3.618619000	-0.400859000	-4.454208000
1	6.601217000	2.383074000	2.285441000
1	-5.724972000	0.905078000	1.883161000
1	4.176355000	2.284177000	2.345015000
1	0.321585000	2.052728000	2.071551000
1	-1.937166000	-0.812853000	-3.979309000
1	1.585578000	2.601216000	3.220919000
1	-4.188705000	1.760900000	3.891132000
1	-4.975564000	-0.108982000	0.601662000
1	3.089745000	-0.798383000	-2.954469000
1	-5.184337000	-1.179414000	-2.835190000
1	-2.454057000	1.308017000	3.882142000
1	-5.222164000	-0.776565000	2.245588000
1	-2.828284000	-0.177481000	1.917584000
1	0.457381000	1.279247000	3.683176000
1	-3.712958000	0.063465000	4.206620000

1	-6.730031000	-2.845348000	-2.493977000
1	3.553243000	0.881305000	3.852694000
1	-7.554986000	-2.153262000	-0.216991000
1	1.408434000	-0.175598000	1.890821000
1	3.636611000	-0.667109000	2.939316000
1	-8.323222000	-3.688203000	-0.757581000
1	2.344587000	-0.405173000	4.143841000
1	-3.589910000	-2.095775000	3.011449000
1	-1.475290000	-2.114618000	1.633226000
1	-7.011564000	-3.718444000	0.463888000
1	-5.313692000	-4.912242000	-2.772067000
1	-6.995330000	-5.320203000	-2.280944000
1	-4.557865000	-3.911184000	0.450861000
1	-3.867456000	-3.819030000	2.613636000
1	-5.666823000	-5.389703000	-1.081838000
1	-2.426403000	-3.348208000	3.559515000
1	-0.909901000	-4.069685000	0.168398000
1	-2.291439000	-4.991133000	0.842855000
1	-0.905687000	-4.544274000	1.896330000
14	2.199995000	-2.440812000	-0.290650000
32	-1.159979000	-0.050353000	0.137068000
32	0.986138000	-0.391197000	-0.769190000
17	1.302421000	-4.039497000	-1.359048000
6	2.328111000	-2.935393000	1.535123000
6	1.262781000	-2.738250000	2.440561000
6	3.520394000	-3.524493000	2.020781000
6	1.368377000	-3.126888000	3.784927000
6	3.635562000	-3.905628000	3.369724000
6	2.559493000	-3.710486000	4.253607000
1	0.340634000	-2.249031000	2.091006000
1	4.372221000	-3.681501000	1.339143000
1	0.522827000	-2.960707000	4.471587000
1	4.572806000	-4.357280000	3.732698000
1	2.651995000	-4.006761000	5.310787000
6	3.956691000	-2.251009000	-0.970967000
6	4.811453000	-1.278782000	-0.393323000
6	4.428255000	-2.988692000	-2.081267000
6	6.088110000	-1.037829000	-0.925817000
6	5.709099000	-2.752290000	-2.610127000
6	6.538252000	-1.770359000	-2.039025000
1	4.476914000	-0.685822000	0.471978000
1	3.778242000	-3.749185000	-2.543177000
1	6.727936000	-0.265576000	-0.470419000
1	6.059543000	-3.334734000	-3.477374000
1	7.537613000	-1.576850000	-2.460964000

Table S13: Atomic coordinates of **12a.**

6	-2.830630000	6.229698000	-1.128107000
6	-1.727194000	6.785340000	1.101318000
6	-1.596111000	6.014631000	-0.227774000
6	1.675552000	2.374766000	-2.340537000
6	7.071535000	1.727850000	-1.852904000
6	-0.171521000	3.914263000	-0.490623000
6	-1.335291000	4.529507000	-0.000662000
6	2.091654000	-1.216217000	-3.642021000
6	2.566093000	2.355170000	0.034042000
6	1.388254000	1.970623000	-0.883850000
6	0.076952000	2.533553000	-0.336828000
6	6.932321000	0.192363000	-1.923110000
6	-2.258709000	3.725920000	0.694125000
6	-2.259508000	1.699509000	-2.753776000
6	4.595393000	-0.823546000	-2.006138000
6	2.311919000	-1.896358000	-2.280768000
6	8.172582000	-0.512343000	-1.338155000
6	5.641304000	-0.265355000	-1.252880000
6	3.373303000	-1.214463000	-1.418535000
6	-0.881122000	1.735276000	0.345592000
6	-2.051025000	2.346671000	0.885239000
6	2.664389000	-3.389677000	-2.455279000
6	-1.359571000	-0.401508000	-3.873173000
6	-1.710163000	0.275893000	-2.534584000
6	5.453834000	-0.112940000	0.135834000
6	3.201455000	-1.025173000	-0.021988000
6	4.251328000	-0.474919000	0.768617000
6	-4.433235000	1.454895000	0.852037000
6	-3.115690000	1.552893000	1.645595000
6	4.963402000	0.811619000	2.886981000
6	-2.667471000	-0.583582000	-1.707420000
6	-3.341308000	2.102557000	3.066983000
6	-3.903648000	-0.943193000	-2.284624000
6	4.095912000	-0.302029000	2.280499000
6	-2.366524000	-1.027856000	-0.390221000
6	-4.840000000	-1.746316000	-1.612412000
6	4.325246000	-1.649454000	2.998319000
6	-6.183950000	-2.089361000	-2.246049000
6	-7.349881000	-1.482117000	-1.438127000
6	0.658762000	0.946205000	3.616746000
6	-3.281157000	-1.879012000	0.291359000
6	-4.496338000	-2.219211000	-0.332711000
6	-6.359708000	-3.610061000	-2.432118000
6	-2.986731000	-2.457078000	1.672542000
6	-4.069275000	-2.110498000	2.711539000
6	-0.271606000	-2.054993000	3.947693000
6	-2.725269000	-3.973544000	1.597012000

1	-2.979981000	7.307726000	-1.350055000
1	-1.854717000	7.873310000	0.918315000
1	-0.711407000	6.422186000	-0.767000000
1	-2.724218000	5.687496000	-2.090149000
1	-0.830092000	6.643020000	1.738352000
1	1.849891000	3.466493000	-2.445409000
1	0.567824000	4.537081000	-1.021712000
1	-3.753609000	5.857099000	-0.634620000
1	7.977934000	2.071701000	-2.394868000
1	6.188346000	2.231338000	-2.297401000
1	-2.609145000	6.439448000	1.681539000
1	2.677353000	3.459237000	0.091245000
1	2.589617000	1.859494000	-2.702483000
1	1.800300000	-0.154467000	-3.522746000
1	1.286389000	-1.731433000	-4.202471000
1	0.833911000	2.101812000	-3.009602000
1	3.001087000	-1.253081000	-4.277933000
1	3.517396000	1.922683000	-0.337554000
1	7.157527000	2.070494000	-0.799635000
1	-1.520844000	2.328779000	-3.293012000
1	4.741907000	-0.962716000	-3.089714000
1	2.408215000	1.980345000	1.066473000
1	9.090585000	-0.216679000	-1.888567000
1	6.859981000	-0.090644000	-2.997310000
1	-3.177215000	4.186441000	1.094260000
1	-2.487792000	2.198101000	-1.791542000
1	-3.190601000	1.674979000	-3.359303000
1	1.304546000	0.862204000	-0.867092000
1	-0.580655000	0.176694000	-4.412214000
1	1.345642000	-1.846032000	-1.726936000
1	1.866601000	-3.916618000	-3.019916000
1	-0.760090000	0.362885000	-1.962041000
1	8.073630000	-1.615739000	-1.396007000
1	3.617161000	-3.500488000	-3.016420000
1	-2.245202000	-0.468337000	-4.539663000
1	8.324851000	-0.243402000	-0.271129000
1	-4.890269000	2.457797000	0.711373000
1	6.266985000	0.319344000	0.738079000
1	4.828839000	1.771086000	2.346012000
1	-0.979526000	-1.430523000	-3.712488000
1	6.044613000	0.556899000	2.869843000
1	-3.780996000	3.122328000	3.049373000
1	-4.264907000	1.007802000	-0.148097000
1	2.775299000	-3.889335000	-1.473049000
1	-4.149663000	-0.580163000	-3.296698000
1	-2.386984000	2.158078000	3.630338000
1	-5.167984000	0.816408000	1.386094000
1	-2.731991000	0.516917000	1.771648000

1	4.687598000	0.974077000	3.949647000
1	-4.040788000	1.450066000	3.631558000
1	-6.196215000	-1.622829000	-3.256871000
1	5.367094000	-2.000782000	2.840281000
1	-7.230446000	-0.384912000	-1.325026000
1	3.036340000	-0.015926000	2.458256000
1	0.857753000	1.753167000	2.882528000
1	-0.183408000	1.273699000	4.263509000
1	3.643412000	-2.435952000	2.612393000
1	-8.323757000	-1.677403000	-1.935261000
1	4.153843000	-1.551906000	4.091541000
1	-4.224386000	-1.014382000	2.785260000
1	-2.045264000	-1.983033000	2.014189000
1	-7.399439000	-1.920134000	-0.418331000
1	-5.529001000	-4.040827000	-3.027965000
1	1.556037000	0.813419000	4.258117000
1	-7.314901000	-3.838561000	-2.950611000
1	-5.201406000	-2.874063000	0.205273000
1	-1.264548000	-1.870829000	4.409545000
1	-0.299073000	-3.022508000	3.406684000
1	-5.048009000	-2.571292000	2.459414000
1	-6.377784000	-4.135112000	-1.453431000
1	-3.778909000	-2.484867000	3.716080000
1	-1.881887000	-4.191292000	0.911810000
1	0.488922000	-2.121056000	4.754171000
1	-3.622347000	-4.520158000	1.234695000
1	-2.464248000	-4.375486000	2.599251000
14	0.193678000	-0.672715000	2.735380000
32	-0.774491000	-0.252524000	0.519262000
32	1.423523000	-1.350979000	0.784751000
17	0.959086000	-3.549378000	0.701250000

Table S14: Atomic coordinates of **12c.**

6	-1.890880000	6.027359000	3.247021000
6	-0.589393000	4.783124000	5.050735000
6	-0.660913000	5.148023000	3.554043000
6	1.936695000	3.709814000	-0.878047000
6	6.494018000	2.815937000	-1.341682000
6	0.391869000	3.710422000	1.728904000
6	-0.635575000	3.907917000	2.667422000
6	1.766841000	1.780935000	-4.105642000
6	2.853259000	1.940679000	0.687839000
6	1.612022000	2.434213000	-0.080958000
6	0.427725000	2.590552000	0.871629000
6	6.655862000	1.486615000	-2.114683000
6	-1.644277000	2.929766000	2.755895000
6	-2.075179000	3.828938000	-1.108459000
6	4.284599000	0.852832000	-2.751468000
6	1.932078000	0.351792000	-3.566159000
6	7.963872000	0.777567000	-1.726126000
6	5.403382000	0.637677000	-1.921157000
6	3.063950000	0.183492000	-2.553260000
6	-0.606350000	1.622525000	0.972883000
6	-1.644939000	1.786624000	1.934737000
6	2.132721000	-0.651820000	-4.723577000
6	-1.548511000	2.917877000	-3.426123000
6	-1.737635000	2.572964000	-1.934881000
6	5.287807000	-0.305392000	-0.886595000
6	2.956122000	-0.718848000	-1.454105000
6	4.078644000	-0.984857000	-0.626111000
6	-4.140970000	1.302475000	1.740997000
6	-2.754445000	0.751774000	2.120551000
6	4.610331000	-1.481965000	1.831855000
6	-2.774711000	1.462294000	-1.760668000
6	-2.721398000	0.133389000	3.531335000
6	-4.086251000	1.706558000	-2.219954000
6	4.046626000	-2.014863000	0.503376000
6	-2.469543000	0.190870000	-1.198000000
6	-5.093562000	0.728872000	-2.168812000
6	4.759946000	-3.308031000	0.056368000
6	-6.512259000	1.031506000	-2.638614000
6	-7.525861000	0.885015000	-1.484862000
6	-3.450611000	-0.838584000	-1.210796000
6	-4.743466000	-0.544733000	-1.685219000
6	-6.908985000	0.163372000	-3.850210000
6	-3.157311000	-2.261678000	-0.749215000
6	-3.974102000	-2.657666000	0.493694000
6	-3.330180000	-3.276079000	-1.894685000
1	-1.873808000	6.961084000	3.848289000
1	-0.541384000	5.696636000	5.680462000

1	0.248023000	5.742268000	3.308410000
1	-1.927249000	6.304835000	2.173498000
1	0.303743000	4.162825000	5.271070000
1	2.279417000	4.536027000	-0.220464000
1	1.193729000	4.464840000	1.664690000
1	-2.833901000	5.491039000	3.486169000
1	7.362249000	3.487886000	-1.510591000
1	5.573321000	3.352592000	-1.650749000
1	-1.484521000	4.206533000	5.367288000
1	3.145889000	2.672123000	1.471435000
1	2.756197000	3.505175000	-1.597916000
1	1.586907000	2.507691000	-3.290678000
1	0.904592000	1.827898000	-4.800026000
1	1.055159000	4.072275000	-1.446135000
1	2.657809000	2.116906000	-4.676782000
1	3.712027000	1.795988000	0.002139000
1	6.414856000	2.620845000	-0.250834000
1	-1.264305000	4.582642000	-1.189275000
1	4.379231000	1.566440000	-3.586033000
1	2.656831000	0.973214000	1.190873000
1	8.839949000	1.399464000	-2.004011000
1	6.714098000	1.734691000	-3.199108000
1	-2.458972000	3.057989000	3.488018000
1	-2.204193000	3.586174000	-0.035516000
1	-3.012347000	4.301866000	-1.471596000
1	1.347904000	1.643422000	-0.818309000
1	-0.715558000	3.639588000	-3.558858000
1	0.978674000	0.083367000	-3.054576000
1	1.277292000	-0.610810000	-5.430233000
1	-0.761451000	2.180107000	-1.576809000
1	8.061649000	-0.204823000	-2.232292000
1	3.061333000	-0.412557000	-5.285132000
1	-2.462857000	3.379177000	-3.855375000
1	8.025729000	0.603079000	-0.630825000
1	-4.452126000	2.128273000	2.416358000
1	6.156835000	-0.508842000	-0.243236000
1	4.056619000	-0.584415000	2.174262000
1	-1.318614000	2.010153000	-4.019821000
1	5.686147000	-1.217712000	1.752025000
1	-2.965068000	0.880485000	4.316506000
1	-4.140861000	1.685451000	0.699742000
1	2.210833000	-1.688976000	-4.343804000
1	-4.333334000	2.697480000	-2.636905000
1	-1.715126000	-0.278343000	3.757827000
1	-4.907109000	0.501384000	1.804931000
1	-2.547594000	-0.083411000	1.419550000
1	4.514344000	-2.249730000	2.625358000
1	-3.460522000	-0.691921000	3.612544000

1	-6.527042000	2.095080000	-2.967571000
1	5.835617000	-3.118252000	-0.147967000
1	-7.246688000	1.523841000	-0.621763000
1	2.981933000	-2.276799000	0.686886000
1	4.307011000	-3.713460000	-0.871909000
1	-8.547687000	1.170107000	-1.813847000
1	4.694027000	-4.087216000	0.845073000
1	-3.774462000	-1.972019000	1.342654000
1	-2.086388000	-2.293924000	-0.464001000
1	-7.570765000	-0.164718000	-1.123871000
1	-6.188743000	0.285652000	-4.685105000
1	-7.919924000	0.436423000	-4.220507000
1	-5.503858000	-1.343026000	-1.674002000
1	-5.064949000	-2.630042000	0.285140000
1	-6.930871000	-0.914300000	-3.581551000
1	-3.712901000	-3.684350000	0.821757000
1	-2.700153000	-2.997138000	-2.762798000
1	-4.386876000	-3.338508000	-2.232231000
1	-3.022560000	-4.287176000	-1.555485000
14	0.044011000	-1.917074000	1.134557000
32	-0.756076000	0.009637000	-0.192088000
32	1.162149000	-1.368705000	-0.942267000
6	1.029581000	-1.502342000	2.705396000
6	1.196668000	-0.193521000	3.219241000
6	1.659557000	-2.573543000	3.390717000
6	1.974553000	0.037626000	4.367518000
6	2.427653000	-2.343777000	4.543821000
6	2.592771000	-1.034936000	5.032813000
1	0.708168000	0.657935000	2.724926000
1	1.543323000	-3.604782000	3.018263000
1	2.090224000	1.066396000	4.744230000
1	2.905681000	-3.191581000	5.060657000
1	3.200664000	-0.853386000	5.933585000
6	-0.790520000	-3.591303000	1.411173000
6	-1.440502000	-3.820614000	2.649959000
6	-0.856458000	-4.596293000	0.416824000
6	-2.136589000	-5.017458000	2.887235000
6	-1.555683000	-5.792447000	0.654307000
6	-2.198047000	-6.005742000	1.887452000
1	-1.401215000	-3.052266000	3.440194000
1	-0.371988000	-4.434478000	-0.558903000
1	-2.638313000	-5.177866000	3.855067000
1	-1.598999000	-6.563692000	-0.131447000
1	-2.746853000	-6.943393000	2.070605000
17	0.292902000	-2.702451000	-2.532357000

Table S15: Atomic coordinates of **13a.**

6	-3.847628000	1.354825000	2.061782000
6	-1.982471000	1.783574000	3.746317000
6	-2.326156000	1.395366000	2.295146000
6	3.127634000	-0.949997000	3.533496000
6	1.486177000	-4.464793000	0.293898000
6	-1.820985000	3.669989000	1.326317000
6	-2.127543000	6.511622000	-0.817444000
6	-1.443496000	6.050808000	0.487042000
6	-1.604077000	2.278908000	1.280601000
6	-2.539267000	-4.125800000	1.529365000
6	-0.171204000	6.872045000	0.776401000
8	-0.510669000	-3.725135000	-0.886090000
6	-1.163958000	4.552508000	0.452720000
6	0.577332000	-3.432924000	-0.417287000
6	-2.806081000	-2.218671000	3.179405000
6	2.418274000	-0.253806000	2.353351000
6	-2.391517000	-2.605970000	1.744996000
6	1.919342000	1.147833000	2.754946000
6	-0.715903000	1.738397000	0.307440000
6	3.308343000	-0.210544000	1.110933000
6	7.615832000	0.857887000	1.498844000
6	-0.245999000	4.004594000	-0.462098000
6	4.556815000	0.436170000	1.225650000
6	-3.153616000	-1.812246000	0.680754000
6	0.000665000	2.620708000	-0.554322000
6	2.952061000	-0.798572000	-0.137793000
6	-2.520763000	-0.878638000	-0.184317000
6	5.471508000	0.511398000	0.160263000
6	-4.542925000	-2.016865000	0.552601000
6	6.771530000	1.297596000	0.287049000
6	3.895087000	-0.788193000	-1.207443000
6	5.129015000	-0.130875000	-1.042119000
6	4.711978000	-2.407514000	-3.010114000
6	1.043651000	2.151770000	-1.568475000
6	3.592035000	-1.456230000	-2.550862000
6	-3.271094000	-0.229418000	-1.204245000
6	-5.316543000	-1.343101000	-0.408686000
6	2.464564000	2.567343000	-1.136504000
6	6.477533000	2.812826000	0.324601000
6	0.726416000	2.623026000	-3.001077000
6	-7.314013000	-1.976940000	-1.861067000
6	-2.723367000	0.131710000	-3.650220000
6	-4.655335000	-0.469634000	-1.293399000
6	-6.828793000	-1.529737000	-0.468094000
6	-2.615869000	0.702226000	-2.222863000
6	3.244823000	-0.415717000	-3.632158000
6	-7.550450000	-0.245467000	-0.006223000

6	-3.146470000	2.144613000	-2.129333000
1	-4.330464000	0.624363000	2.743907000
1	-4.301207000	2.351103000	2.251654000
1	-2.434109000	1.063304000	4.461156000
1	-2.374434000	2.790945000	3.999996000
1	-4.088687000	1.057154000	1.022575000
1	2.424852000	-1.091272000	4.381658000
1	-0.885877000	1.796056000	3.909043000
1	-2.525107000	4.082548000	2.068567000
1	-3.055779000	5.934868000	-1.008916000
1	-2.156765000	6.230237000	1.322898000
1	-1.888246000	-4.682744000	2.237274000
1	-1.937274000	0.358792000	2.151145000
1	3.521543000	-1.945454000	3.242102000
1	-0.409871000	7.953081000	0.863648000
1	3.983798000	-0.349923000	3.908381000
1	-2.390187000	7.589882000	-0.771134000
1	-2.225688000	-2.801304000	3.925788000
1	0.574888000	6.761473000	-0.039128000
1	0.312094000	6.545668000	1.720129000
1	-2.252485000	-4.408863000	0.498852000
1	-3.583013000	-4.459417000	1.712751000
1	1.254124000	1.085222000	3.642113000
1	-1.456970000	6.365204000	-1.691097000
1	-1.311732000	-2.353900000	1.627133000
1	1.521337000	-0.858667000	2.095768000
1	-3.882854000	-2.427005000	3.354548000
1	2.765265000	1.817994000	3.018087000
1	-2.636596000	-1.143259000	3.383238000
1	7.098687000	1.081054000	2.456303000
1	4.819711000	0.909917000	2.185640000
1	8.587893000	1.394279000	1.516917000
1	1.346648000	1.627560000	1.936402000
1	7.821167000	-0.232077000	1.473368000
1	-5.047231000	-2.725156000	1.231714000
1	0.301076000	4.682709000	-1.137252000
1	4.969652000	-3.139374000	-2.217750000
1	1.020014000	1.040291000	-1.581293000
1	-6.796951000	-2.901694000	-2.189646000
1	-2.300206000	-0.892658000	-3.698536000
1	2.699675000	2.196174000	-0.119475000
1	2.676609000	-2.081632000	-2.402629000
1	5.638196000	-1.853799000	-3.272688000
1	-0.281789000	2.291418000	-3.322822000
1	4.398705000	-2.970014000	-3.914605000
1	5.845550000	-0.102740000	-1.880560000
1	2.578224000	3.672735000	-1.136844000
1	-7.086259000	-2.337985000	0.252919000

1	0.762149000	3.729297000	-3.090283000
1	-1.529352000	0.733856000	-1.983727000
1	7.417943000	3.403484000	0.350823000
1	5.884989000	3.076357000	1.226714000
1	5.890176000	3.128039000	-0.562321000
1	-8.406996000	-2.173174000	-1.853531000
1	-3.779849000	0.080882000	-3.989932000
1	-2.170057000	0.772050000	-4.369888000
1	-7.123818000	-1.194895000	-2.626574000
1	3.224132000	2.140618000	-1.823874000
1	1.466904000	2.213765000	-3.719675000
1	-5.235920000	0.047918000	-2.074693000
1	2.365472000	0.186920000	-3.328667000
1	4.093802000	0.280643000	-3.800642000
1	3.006088000	-0.907015000	-4.599003000
1	-7.216465000	0.059673000	1.006958000
1	-3.015950000	2.553277000	-1.107070000
1	-8.651473000	-0.391103000	0.018113000
1	-2.601391000	2.810616000	-2.830529000
1	-7.335658000	0.598224000	-0.696496000
1	-4.226019000	2.194420000	-2.387624000
32	-0.668657000	-0.253776000	0.166226000
32	1.132134000	-1.466159000	-0.641285000
6	1.547016000	-4.061330000	1.785502000
1	1.967269000	-3.044112000	1.914544000
1	0.536721000	-4.075319000	2.244916000
1	2.192202000	-4.771449000	2.344698000
6	0.872307000	-5.868279000	0.140801000
1	1.503187000	-6.620842000	0.658231000
1	-0.147334000	-5.904750000	0.572292000
1	0.790903000	-6.152545000	-0.928012000
6	2.899705000	-4.415584000	-0.326454000
1	2.871933000	-4.633879000	-1.414615000
1	3.381822000	-3.427033000	-0.182012000
1	3.546971000	-5.177690000	0.156465000
1	7.367054000	1.092319000	-0.631036000

Table S16: Atomic coordinates of s-cis **13c.**

6	4.438076000	-0.260233000	-2.182387000
6	2.855447000	0.841040000	-3.852738000
6	3.076593000	0.429712000	-2.384041000
6	-2.946906000	0.583994000	-3.284986000
6	-2.823968000	-2.944108000	0.241944000
6	3.677855000	2.745204000	-1.585854000
6	5.298316000	5.293552000	0.327177000
6	4.429962000	5.096629000	-0.933557000
6	2.866942000	1.603897000	-1.430514000
6	0.778662000	-4.497788000	-1.257302000
6	3.639825000	6.375435000	-1.277301000
8	-0.625940000	-3.139270000	1.248834000
6	3.517532000	3.884812000	-0.780010000
6	-1.505147000	-2.412702000	0.812844000
6	1.824947000	-3.028154000	-3.037002000
6	-1.946381000	1.003412000	-2.187574000
6	1.345801000	-3.098502000	-1.572688000
6	-0.916063000	2.012963000	-2.730265000
6	1.872151000	1.581938000	-0.411164000
6	-2.660926000	1.530415000	-0.942275000
6	-6.141311000	4.293013000	-1.342926000
6	2.490830000	3.865977000	0.181291000
6	-3.518672000	2.637865000	-1.106489000
6	2.437347000	-2.695280000	-0.577575000
6	1.657843000	2.747785000	0.382326000
6	-2.511706000	0.963450000	0.357870000
6	2.345389000	-1.533280000	0.235608000
6	-4.240509000	3.202532000	-0.039885000
6	3.580153000	-3.512874000	-0.460202000
6	-5.083393000	4.458091000	-0.234460000
6	-3.289213000	1.481395000	1.435706000
6	-4.130307000	2.589791000	1.219814000
6	-4.614918000	0.508939000	3.391804000
6	0.560511000	2.861967000	1.439376000
6	-3.224679000	0.875849000	2.840292000
6	3.354882000	-1.252845000	1.198137000
6	4.616650000	-3.227969000	0.445749000
6	-0.541679000	3.845232000	0.994798000
6	-4.175356000	5.678592000	-0.498401000
6	1.123317000	3.224549000	2.827503000
6	5.981157000	-4.797702000	1.900304000
6	3.181519000	-0.530974000	3.622856000
6	4.472794000	-2.104436000	1.282776000
6	5.855828000	-4.113328000	0.523869000
6	3.250514000	-0.066158000	2.155576000
6	-2.444180000	1.781752000	3.810515000
6	7.131947000	-3.322645000	0.168775000

6	4.363502000	0.972327000	1.924245000
1	4.521372000	-1.158338000	-2.829280000
1	5.271290000	0.426673000	-2.443589000
1	2.911359000	-0.044513000	-4.520890000
1	3.628617000	1.561622000	-4.193162000
1	4.573922000	-0.586173000	-1.132276000
1	-2.417368000	0.082970000	-4.122691000
1	1.864373000	1.319235000	-3.989188000
1	4.461286000	2.747950000	-2.362565000
1	5.886392000	4.380973000	0.555733000
1	5.115010000	4.884262000	-1.785005000
1	-0.094740000	-4.717095000	-1.908948000
1	2.286493000	-0.321737000	-2.148896000
1	-3.711394000	-0.118508000	-2.893008000
1	4.326663000	7.231461000	-1.446998000
1	-3.485122000	1.458242000	-3.708574000
1	6.004982000	6.140539000	0.197056000
1	1.003337000	-3.303763000	-3.731582000
1	2.953330000	6.658621000	-0.451211000
1	3.026023000	6.236191000	-2.190855000
1	0.449060000	-4.563529000	-0.203222000
1	1.534613000	-5.290252000	-1.443520000
1	-0.390962000	1.595719000	-3.615621000
1	4.666478000	5.514637000	1.213897000
1	0.512226000	-2.366577000	-1.454105000
1	-1.383373000	0.094555000	-1.883165000
1	2.665404000	-3.731902000	-3.215888000
1	-1.405104000	2.959227000	-3.045736000
1	2.174902000	-2.014000000	-3.311609000
1	-5.667560000	4.143043000	-2.336360000
1	-3.612675000	3.087842000	-2.108585000
1	-6.781274000	5.197606000	-1.415323000
1	-0.149183000	2.262934000	-1.969741000
1	-6.796374000	3.419264000	-1.147550000
1	3.671459000	-4.407324000	-1.099844000
1	2.331870000	4.760045000	0.805800000
1	-5.178464000	-0.124949000	2.677371000
1	0.082658000	1.862459000	1.534598000
1	5.068608000	-5.379698000	2.143504000
1	2.351778000	-1.252351000	3.770368000
1	-0.964536000	3.555741000	0.012136000
1	-2.645292000	-0.077418000	2.759390000
1	-5.226403000	1.413563000	3.594381000
1	1.886672000	2.490509000	3.157686000
1	-4.520787000	-0.045882000	4.348833000
1	-4.710150000	3.002526000	2.062740000
1	-0.149079000	4.881534000	0.910983000
1	5.731845000	-4.913868000	-0.239855000

1	1.595318000	4.229682000	2.832574000
1	2.279871000	0.437476000	1.945438000
1	-4.771723000	6.612287000	-0.578678000
1	-3.611978000	5.553077000	-1.447755000
1	-3.431457000	5.807581000	0.314669000
1	6.851041000	-5.487975000	1.922992000
1	4.124352000	-1.026295000	3.938672000
1	3.015779000	0.334714000	4.299018000
1	6.126799000	-4.049067000	2.708118000
1	-1.379979000	3.850291000	1.722084000
1	0.313656000	3.240944000	3.586500000
1	5.258697000	-1.879665000	2.022942000
1	-1.412427000	1.950084000	3.443162000
1	-2.935063000	2.773034000	3.912211000
1	-2.379300000	1.325375000	4.820754000
1	7.039075000	-2.837504000	-0.824715000
1	4.365182000	1.328993000	0.874480000
1	8.021182000	-3.987887000	0.150859000
1	4.219334000	1.856210000	2.580258000
1	7.326868000	-2.523068000	0.914907000
1	5.364346000	0.544236000	2.147157000
32	0.950695000	-0.161929000	-0.102127000
32	-1.130524000	-0.390779000	0.894818000
6	-2.863272000	-2.627623000	-1.280200000
1	-2.764084000	-1.534379000	-1.436608000
1	-1.992439000	-3.106094000	-1.779654000
6	-2.938244000	-4.474144000	0.440764000
1	-2.069474000	-4.972611000	-0.038107000
1	-2.879705000	-4.712701000	1.524542000
6	-4.026847000	-2.242435000	0.930047000
1	-3.995648000	-2.436535000	2.024811000
1	-3.957812000	-1.143913000	0.787316000
1	-5.623551000	4.640378000	0.721920000
6	-4.188680000	-3.137381000	-1.885990000
1	-4.202081000	-2.901450000	-2.972956000
6	-4.264869000	-4.983702000	-0.164589000
1	-4.337248000	-6.083178000	-0.013900000
6	-5.350161000	-2.757404000	0.324851000
1	-6.200211000	-2.248041000	0.829897000
6	-4.295501000	-4.665658000	-1.676881000
1	-5.236358000	-5.048254000	-2.130851000
1	-3.453920000	-5.180039000	-2.191654000
6	-5.372884000	-2.432189000	-1.186010000
1	-6.334468000	-2.765445000	-1.634794000
1	-5.305481000	-1.331899000	-1.337477000
6	-5.454973000	-4.284943000	0.531833000
1	-6.416473000	-4.662397000	0.118538000
1	-5.454048000	-4.523138000	1.618603000

Table S17: Atomic coordinates of s-trans **13c.**

6	-0.825623000	4.543899000	-2.323341000
6	-1.552386000	2.525539000	-3.686419000
6	-1.094767000	3.026012000	-2.305743000
6	-2.218827000	-1.734511000	-3.351281000
6	2.665900000	-2.339945000	-1.465614000
6	-3.378183000	3.074634000	-1.238991000
6	-6.143489000	4.252955000	0.711360000
6	-5.770909000	3.202616000	-0.355656000
6	-2.032673000	2.659079000	-1.156322000
6	2.589111000	2.703889000	-2.541971000
6	-6.718707000	1.986515000	-0.297268000
8	0.581291000	-3.487527000	-1.870921000
6	-4.310298000	2.782391000	-0.232483000
6	1.143456000	-2.509296000	-1.392335000
6	2.721968000	4.856266000	-1.193988000
6	-2.757845000	-0.755190000	-2.284156000
6	2.264068000	3.386127000	-1.198722000
6	-3.994801000	-0.009244000	-2.803737000
6	-1.589407000	1.948822000	-0.003797000
6	-2.980715000	-1.496502000	-0.967932000
6	-6.684590000	-3.815793000	-0.057863000
6	-3.856247000	2.072885000	0.895155000
6	-4.278135000	-1.874882000	-0.576920000
6	2.790361000	2.585977000	-0.011607000
6	-2.521127000	1.652721000	1.035917000
6	-1.880264000	-1.878182000	-0.151131000
6	1.956398000	1.691333000	0.720957000
6	-4.521624000	-2.641590000	0.579973000
6	4.141448000	2.741266000	0.356270000
6	-5.946897000	-2.977904000	1.005939000
6	-2.100583000	-2.687016000	0.998230000
6	-3.417264000	-3.061571000	1.338508000
6	-0.486976000	-4.595711000	1.316837000
6	-2.096253000	0.946721000	2.321279000
6	-0.924413000	-3.205789000	1.824469000
6	2.493297000	1.037223000	1.873499000
6	4.704999000	2.053222000	1.443233000
6	-3.216892000	0.154683000	3.010135000
6	-6.733089000	-1.696357000	1.354815000
6	-1.463144000	1.973216000	3.283421000
6	6.956551000	0.903927000	1.596305000
6	2.153064000	-1.293072000	2.852274000
6	3.854245000	1.225218000	2.194273000
6	6.176979000	2.218013000	1.805714000
6	1.675844000	0.169313000	2.832928000
6	-1.155103000	-3.195689000	3.342951000
6	6.356620000	2.754961000	3.240344000

6	1.676193000	0.762466000	4.257334000
1	-0.048033000	4.801311000	-3.073419000
1	-1.748127000	5.104006000	-2.586248000
1	-0.822954000	2.831253000	-4.465666000
1	-2.540720000	2.941984000	-3.973384000
1	-0.487585000	4.909745000	-1.332103000
1	-1.934381000	-1.192048000	-4.278471000
1	-1.626795000	1.421090000	-3.706888000
1	-3.717481000	3.623614000	-2.133600000
1	-5.477591000	5.138455000	0.653767000
1	-5.891581000	3.678248000	-1.355042000
1	2.180496000	3.288390000	-3.393434000
1	-0.131077000	2.504086000	-2.098825000
1	-1.336671000	-2.298811000	-2.986975000
1	-7.773111000	2.297562000	-0.453652000
1	-3.000390000	-2.478827000	-3.615038000
1	-7.191812000	4.596892000	0.583300000
1	2.176636000	5.428980000	-1.972391000
1	-6.662035000	1.479711000	0.689025000
1	-6.459909000	1.235270000	-1.071408000
1	2.153649000	1.683973000	-2.589925000
1	3.687322000	2.610323000	-2.679608000
1	-3.737723000	0.592875000	-3.697923000
1	-6.051253000	3.829203000	1.734197000
1	1.161402000	3.402562000	-1.085395000
1	-1.966152000	0.002858000	-2.086363000
1	3.805476000	4.956625000	-1.415736000
1	-4.798945000	-0.712038000	-3.110043000
1	2.529562000	5.336770000	-0.212885000
1	-6.804740000	-3.246334000	-1.004045000
1	-5.134758000	-1.560879000	-1.191563000
1	-7.699925000	-4.098522000	0.292566000
1	-4.399506000	0.680340000	-2.037493000
1	-6.126961000	-4.745071000	-0.294942000
1	4.782907000	3.421138000	-0.227876000
1	-4.575369000	1.831544000	1.692027000
1	-0.294539000	-4.577508000	0.225170000
1	-1.311385000	0.208866000	2.036514000
1	6.881548000	0.554732000	0.546893000
1	2.067592000	-1.749636000	1.845755000
1	-3.702241000	-0.549948000	2.306094000
1	-0.072664000	-2.504956000	1.629319000
1	-1.284872000	-5.344871000	1.509575000
1	-0.587956000	2.474689000	2.820225000
1	0.436703000	-4.934959000	1.832901000
1	-3.592734000	-3.679859000	2.234060000
1	-3.995217000	0.819441000	3.442312000
1	6.600829000	2.975568000	1.108597000

1	-2.202247000	2.759371000	3.546582000
1	0.628494000	0.166594000	2.466293000
1	-7.751143000	-1.939237000	1.726731000
1	-6.845790000	-1.045437000	0.462358000
1	-6.209920000	-1.103466000	2.133471000
1	8.031596000	1.035002000	1.841752000
1	3.214361000	-1.376201000	3.168558000
1	1.541682000	-1.896941000	3.553960000
1	6.557246000	0.095284000	2.244357000
1	-2.801595000	-0.437161000	3.851560000
1	-1.126167000	1.486253000	4.221322000
1	4.261790000	0.704760000	3.076409000
1	-1.447672000	-2.187376000	3.700063000
1	-1.949337000	-3.909482000	3.648248000
1	-0.229623000	-3.498433000	3.876232000
1	5.801685000	3.704152000	3.387737000
1	1.376935000	1.829218000	4.252386000
1	7.428967000	2.941144000	3.460475000
1	0.969091000	0.206223000	4.908263000
1	5.984590000	2.027480000	3.992833000
1	2.680817000	0.695970000	4.726569000
32	0.219913000	1.079993000	-0.093451000
32	-0.014590000	-1.208453000	-0.347591000
6	3.269612000	-3.366230000	-0.455557000
1	2.892716000	-3.149080000	0.567821000
1	2.915435000	-4.384587000	-0.723537000
6	3.175273000	-2.687965000	-2.889603000
1	2.814765000	-3.700161000	-3.168511000
1	2.736871000	-1.972209000	-3.619697000
6	3.146122000	-0.928700000	-1.083270000
1	2.704791000	-0.178235000	-1.772300000
1	2.797570000	-0.674304000	-0.062100000
1	-5.875620000	-3.593772000	1.930755000
6	4.810482000	-3.286074000	-0.488703000
1	5.225453000	-4.018177000	0.238709000
6	4.718394000	-2.614195000	-2.923501000
1	5.071118000	-2.863444000	-3.948378000
6	4.684534000	-0.846658000	-1.122659000
1	4.989071000	0.184882000	-0.843392000
6	5.306445000	-3.626078000	-1.913047000
1	6.417984000	-3.596587000	-1.946889000
1	5.000594000	-4.659857000	-2.186944000
6	5.264887000	-1.857837000	-0.109872000
1	6.375663000	-1.802167000	-0.101173000
1	4.919453000	-1.598632000	0.915213000
6	5.178506000	-1.187032000	-2.546440000
1	6.287891000	-1.116380000	-2.595778000
1	4.773735000	-0.449138000	-3.274355000

Table S18: Atomic coordinates of **14a.**

6	-1.115080000	3.991376000	3.015313000
6	1.055860000	2.747650000	3.384847000
6	-0.255172000	2.788996000	2.575747000
6	4.138855000	0.156403000	2.389025000
6	0.656382000	-1.513744000	4.265122000
6	0.561066000	3.959688000	0.500393000
6	0.772224000	5.863600000	-2.676275000
6	1.500092000	5.340192000	-1.423413000
6	0.039433000	2.780872000	1.072346000
6	-4.473536000	2.456312000	1.728927000
6	3.003582000	5.115378000	-1.695628000
8	-0.771723000	-0.335166000	2.721420000
6	0.872985000	4.068414000	-0.864817000
6	0.327351000	-1.061496000	2.842950000
6	-3.100192000	3.329496000	-0.241424000
6	3.182263000	0.483652000	1.226163000
6	-3.345629000	2.151939000	0.720731000
6	3.414508000	1.911896000	0.701539000
6	-0.169465000	1.652284000	0.232499000
6	3.279146000	-0.573739000	0.128995000
6	6.969069000	-1.013968000	-2.338519000
6	0.658421000	2.941079000	-1.678045000
6	4.318608000	-0.450052000	-0.815141000
6	-3.617083000	0.844743000	-0.018373000
6	0.155639000	1.735743000	-1.152367000
6	2.373185000	-1.670869000	0.019541000
6	-2.780560000	-0.300372000	0.095975000
6	4.482503000	-1.350504000	-1.883699000
6	-4.784602000	0.775484000	-0.809272000
6	5.556271000	-1.129097000	-2.942883000
6	2.532701000	-2.600451000	-1.051746000
6	3.577052000	-2.417861000	-1.981679000
6	2.284699000	-5.116867000	-1.463338000
6	-0.056947000	0.554106000	-2.101528000
6	1.567531000	-3.766417000	-1.284739000
6	-3.201525000	-1.532086000	-0.506260000
6	-5.166519000	-0.397422000	-1.474353000
6	1.196929000	0.243026000	-2.939434000
6	5.210065000	0.102760000	-3.807163000
6	-1.309027000	0.749850000	-2.978807000
6	-7.451127000	-1.442694000	-1.855660000
6	-2.707418000	-3.301820000	1.207549000
6	-4.374013000	-1.546788000	-1.283515000
6	-6.402434000	-0.433307000	-2.365776000
6	-2.459994000	-2.845267000	-0.247728000
6	0.616473000	-3.468244000	-2.460391000
6	-6.018272000	-0.715259000	-3.833473000

6	-2.774436000	-3.978733000	-1.234298000
1	-1.412902000	3.882944000	4.079186000
1	-0.561712000	4.949942000	2.926176000
1	0.850973000	2.742274000	4.475288000
1	1.684977000	3.635697000	3.162646000
1	-2.037224000	4.081052000	2.409029000
1	4.019145000	0.884369000	3.220223000
1	1.644095000	1.842047000	3.143307000
1	0.740634000	4.834255000	1.147950000
1	-0.309426000	6.014018000	-2.480581000
1	1.413861000	6.120149000	-0.633419000
1	-4.228262000	3.357776000	2.329255000
1	-0.817835000	1.865471000	2.821412000
1	3.949834000	-0.860184000	2.789059000
1	3.491703000	6.048221000	-2.049889000
1	5.196910000	0.192092000	2.051926000
1	1.203432000	6.831887000	-3.007039000
1	-2.844692000	4.252184000	0.319766000
1	3.149427000	4.336560000	-2.474485000
1	3.528593000	4.771279000	-0.780881000
1	-4.624039000	1.607558000	2.427337000
1	-5.440324000	2.649832000	1.217923000
1	3.163405000	2.658059000	1.480601000
1	0.865351000	5.155330000	-3.526919000
1	-2.424788000	2.004970000	1.316337000
1	2.145110000	0.434642000	1.624673000
1	-4.002780000	3.545569000	-0.851765000
1	4.474278000	2.083959000	0.416314000
1	-2.258807000	3.114520000	-0.930112000
1	7.214757000	-1.899845000	-1.717476000
1	5.012116000	0.401055000	-0.728591000
1	7.061368000	-0.114444000	-1.693257000
1	2.779480000	2.123233000	-0.181004000
1	7.734991000	-0.926782000	-3.137881000
1	-5.420019000	1.671633000	-0.909729000
1	0.902400000	2.995564000	-2.750806000
1	2.974109000	-5.319688000	-0.618265000
1	-0.234901000	-0.355690000	-1.473443000
1	-7.738167000	-1.228964000	-0.805600000
1	-2.386411000	-2.529633000	1.936934000
1	2.086607000	0.110628000	-2.293033000
1	0.934864000	-3.853106000	-0.368271000
1	2.880171000	-5.149769000	-2.400605000
1	-2.216498000	0.900967000	-2.360146000
1	1.546713000	-5.945071000	-1.515562000
1	3.680738000	-3.120981000	-2.825446000
1	1.411541000	1.055822000	-3.664916000
1	-6.862468000	0.579637000	-2.325694000

1	-1.188184000	1.637391000	-3.635810000
1	-1.369856000	-2.641125000	-0.332206000
1	5.947648000	0.238745000	-4.626691000
1	5.210022000	1.028467000	-3.192671000
1	4.200916000	0.003175000	-4.257509000
1	-8.368633000	-1.409328000	-2.480429000
1	-3.788516000	-3.496025000	1.374855000
1	-2.142323000	-4.230736000	1.430410000
1	-7.060697000	-2.482011000	-1.892661000
1	1.056586000	-0.689801000	-3.521627000
1	-1.478872000	-0.137102000	-3.624847000
1	-4.689626000	-2.486588000	-1.759816000
1	0.036924000	-2.539568000	-2.279429000
1	1.181839000	-3.332301000	-3.407109000
1	-0.107248000	-4.296225000	-2.608726000
1	-5.280876000	0.025714000	-4.204954000
1	-2.632689000	-3.661104000	-2.287724000
1	-6.911432000	-0.678872000	-4.492613000
1	-2.097576000	-4.837409000	-1.045225000
1	-5.563142000	-1.723129000	-3.939166000
1	-3.813754000	-4.355757000	-1.123824000
32	-0.894645000	-0.131724000	0.731027000
32	0.726655000	-1.970920000	1.132803000
6	1.034502000	-0.273214000	5.109889000
1	1.951708000	0.210044000	4.717812000
1	0.215206000	0.472161000	5.099340000
1	1.224299000	-0.573988000	6.161564000
6	-0.610126000	-2.182547000	4.861226000
1	-0.414651000	-2.513942000	5.902973000
1	-1.461271000	-1.473442000	4.864943000
1	-0.902563000	-3.068189000	4.259524000
6	1.826370000	-2.514829000	4.254120000
1	1.562101000	-3.436842000	3.694937000
1	2.727677000	-2.073243000	3.781813000
1	2.096577000	-2.806492000	5.290528000
1	5.545901000	-2.021320000	-3.609035000

Table S19: Atomic coordinates of **14c.**

6	-0.972932000	-5.388232000	-4.790295000
6	-3.114883000	-4.536854000	-3.702612000
6	-1.649726000	-4.968195000	-3.471967000
6	-6.298252000	-2.793070000	2.256422000
6	-0.895227000	-3.864888000	-2.739299000
6	-0.631332000	-3.962055000	-1.363456000
6	-1.185218000	-3.196695000	1.591677000
6	1.118918000	-4.243191000	1.186471000
6	-0.516832000	-2.679746000	-3.391707000
6	-3.207557000	-1.229288000	-1.612900000
6	-6.179529000	-1.339050000	2.758738000
6	-0.028995000	-2.908604000	-0.649588000
6	0.165390000	-3.080145000	0.857781000
6	-4.516555000	-0.516029000	1.003782000
6	-4.843519000	-0.723666000	2.355480000
6	-7.371606000	-0.482582000	2.285871000
6	0.094303000	-1.597115000	-2.725126000
6	-3.042612000	0.133994000	-0.913391000
6	-3.953413000	1.199772000	-1.554482000
6	0.342139000	-1.711591000	-1.325889000
6	-3.280640000	0.023462000	0.592369000
6	-3.884581000	-0.368622000	3.317087000
6	-0.870501000	0.322870000	-4.064517000
6	1.331375000	-0.703377000	-4.767856000
6	0.419352000	-0.361762000	-3.571755000
6	-1.115197000	-0.803364000	4.718153000
6	-2.326168000	0.402144000	1.584613000
6	2.479265000	-1.857229000	3.869036000
6	-2.640081000	0.190796000	2.961353000
6	4.504256000	-1.556818000	-2.766014000
6	-1.650785000	0.496546000	4.088810000
6	2.272464000	-0.603493000	2.996072000
6	2.939711000	-0.515329000	0.473018000
6	3.678850000	-0.501943000	-2.004065000
6	3.292897000	-0.536933000	1.856143000
6	3.973710000	-0.504602000	-0.506240000
6	7.550723000	-1.682411000	2.477324000
6	4.654578000	-0.510324000	2.217505000
6	-2.228996000	1.451053000	5.148985000
6	-0.068828000	1.999024000	-0.482680000
6	5.320704000	-0.467810000	-0.091800000
6	5.686434000	-0.463124000	1.263922000
6	2.282038000	0.686393000	3.838737000
6	3.858653000	0.906949000	-2.605850000
6	-0.807154000	3.377301000	-2.447432000
6	7.150803000	-0.418570000	1.688049000
6	-1.518339000	4.034756000	-0.113105000

6	-0.379018000	3.402513000	-0.950019000
6	-2.252549000	5.411308000	-2.096275000
6	-1.108459000	4.807357000	-2.941904000
6	-1.823663000	5.463915000	-0.612448000
6	7.468157000	0.863605000	2.484970000
6	0.894498000	4.295453000	-0.822484000
6	0.159832000	5.678017000	-2.801518000
6	-0.553982000	6.334587000	-0.472280000
6	0.588084000	5.725475000	-1.317651000
1	-1.505928000	-6.246969000	-5.249891000
1	-3.702846000	-5.348922000	-4.180972000
1	-1.661748000	-5.856612000	-2.800809000
1	0.083957000	-5.682941000	-4.626292000
1	-3.606574000	-4.264169000	-2.746299000
1	-0.981387000	-4.562409000	-5.533094000
1	-3.161796000	-3.645349000	-4.364298000
1	-5.453889000	-3.413449000	2.621269000
1	-7.246458000	-3.257605000	2.601217000
1	-0.928598000	-4.879791000	-0.828351000
1	-1.743305000	-4.096953000	1.258717000
1	0.723773000	-5.206844000	0.801788000
1	-6.287987000	-2.833324000	1.146236000
1	-4.256609000	-1.591712000	-1.564839000
1	-0.726613000	-2.580623000	-4.468803000
1	-2.929490000	-1.160674000	-2.683265000
1	-1.032679000	-3.283396000	2.687461000
1	-6.203984000	-1.364581000	3.871604000
1	1.245752000	-4.350275000	2.283779000
1	-2.557819000	-1.998390000	-1.151361000
1	-1.822405000	-2.309045000	1.402552000
1	-5.249950000	-0.799473000	0.230848000
1	2.117827000	-4.078049000	0.733458000
1	-8.333186000	-0.910433000	2.640752000
1	-5.025370000	0.924233000	-1.458687000
1	-7.417101000	-0.434743000	1.176938000
1	-1.468199000	-0.356753000	-4.708627000
1	-3.732999000	1.309565000	-2.637948000
1	0.653476000	-2.155356000	1.254570000
1	0.809827000	-1.339484000	-5.514091000
1	2.501748000	-2.776152000	3.249798000
1	-4.115837000	-0.539427000	4.382440000
1	-7.293959000	0.557764000	2.663274000
1	-0.629141000	-1.439914000	3.951276000
1	-1.932764000	-1.398438000	5.178282000
1	-1.989658000	0.462123000	-1.052681000
1	-1.507003000	0.630886000	-3.214737000
1	4.370702000	-2.566463000	-2.326565000
1	1.660871000	-1.957284000	4.611544000

References

[S1] Gaussian 09, Revision A.02, M. J. Frisch, G. W. Trucks, H. B. Schlegel, G. E. Scuseria, M. A. Robb, J. R. Cheeseman, G. Scalmani, V. Barone, G. A. Petersson, H. Nakatsuji, X. Li, M. Caricato, A. Marenich, J. Bloino, B. G. Janesko, R. Gomperts, B. Mennucci, H. P. Hratchian, J. V. Ortiz, A. F. Izmaylov, J. L. Sonnenberg, D. Williams-Young, F. Ding, F. Lipparini, F. Egidi, J. Goings, B. Peng, A. Petrone, T. Henderson, D. Ranasinghe, V. G. Zakrzewski, J. Gao, N. Rega, G. Zheng, W. Liang, M. Hada, M. Ehara, K. Toyota, R. Fukuda, J. Hasegawa, M. Ishida, T. Nakajima, Y. Honda, O. Kitao, H. Nakai, T. Vreven, K. Throssell, J. A. Montgomery, Jr., J. E. Peralta, F. Ogliaro, M. Bearpark, J. J. Heyd, E. Brothers, K. N. Kudin, V. N. Staroverov, T. Keith, R. Kobayashi, J. Normand, K. Raghavachari, A. Rendell, J. C. Burant, S. S. Iyengar, J. Tomasi, M. Cossi, J. M. Millam, M. Klene, C. Adamo, R. Cammi, J. W. Ochterski, R. L. Martin, K. Morokuma, O. Farkas, J. B. Foresman, and D. J. Fox, Gaussian, Inc., Wallingford CT, **2016**.

[S2] a) J. P.Perdew, *Phys. Rev. B* **1986**, *33*, 8822; b) A. D. Becke, *Phys. Rev. A* **1988**, *38*,3098.

[S3] a) A. Horn, H. Horn, R. Ahlrichs, *J. Chem. Phys.* **1992**, *97*, 2571; b) A. Schäfer, C. Huber, R. Ahlrichs, *J. Chem. Phys.* **1994**, *100*, 5829; c) F. Weigend, R. Ahlrichs, *Phys. Chem. Chem. Phys.* **2005**, *18*, 3297; d) F. Weigend, *Phys. Chem. Chem. Phys.* **2006**, *9*, 1057.

[S4] S. Grimme, J. Antony, S. Ehrlich, H. Krieg, *J. Chem. Phys.* **2010**, *132*, 154104.

[S5] Y. Zhao, D.G. Truhlar, *Theor. Chem. Acc.* **2008**, *120*, 215-241.

[S6] a) J. P. Foster, F. J. Weinhold, *J.Am.Chem.Soc.* **1980**, *102*, 7211; b) A. E. Reed, L. A. Curtiss, F. Weinhold, *Chem. Rev.* **1988**, *88*, 899.

[S7] Chemcraft - graphical software for visualization of quantum chemistry computations. https://www.chemcraftprog.com

[S8] N. M. O'Boyle, A. L. Tenderholt, K. M. Langner, *J. Comp. Chem.* **2008**, *29*, 839.

[S9] Origin (OriginLab, Northampton, MA).

Metathesis of Ge=Ge double bonds (SI)

nature portfolio

https://doi.org/10.1038/s41557-021-00639-9

Supplementary information

Metathesis of Ge=Ge double bonds

In the format provided by the authors and unedited

Supplementary Information for

Metathesis of Ge=Ge double bonds

Lukas Klemmer, Anna-Lena Thömmes, Michael Zimmer, Volker Huch, Bernd Morgenstern & David Scheschkewitz

Correspondence to: scheschkewitz@mx.uni-saarland.de

Table of Content

Materials and Methods

General:

All reactions were carried out under a protective argon atmosphere and using Schlenk techniques or a gloveboxe. Benzene and pentane were refluxed with sodium/benzophenone and distilled prior to use. Hexane, toluene and tetrahydrofuran were taken directly from a solvent purification system (Innovative Technology PureSolv MD7). Deuterated benzene was refluxed over potassium and distilled prior to use. NMR spectra were recorded at 300 K on a Bruker Avance III HD 400 (^{1}H: 400.13 MHz, ^{13}C{^{1}H}: 100.61 MHz, ^{29}Si{^{1}H}: 79.5 MHz). Chemical shifts are reported relative to $SiMe_4$. Solid state CP/MAS NMR spectra were acquired on a Bruker AV400 WB spectrometer. UV/vis spectra were measured using a Shimadzu UV-2600 spectrometer in quartz cells with a path length of 1 mm. Elemental analyses were carried out on an elementar vario Micro Cube. Dynamic light scattering (DLS) measurements were carried out by non-invasive backscattering on an ALV/CGS-3 compact goniometer system with an ALV/LSE-5003 and a multiple tau correlator at a wavelength of 632.8 nm (He–Ne Laser) and a goniometer angle of 90°. The determination of the particle size was carried out by the analysis of the correlation-function via the g2(t) method followed by a linearized number-weighting (n.w.) of the distribution function. Thermogravimetric analyses (TGA) were performed on a Netzsch Iris TG 209 C instrument in alumina crucibles with heating to 1000 °C under nitrogen, with a rate of 10 K min^{-1}. Differential scanning calorimetry was performed with a Netzsch DSC 204 F1 Phoenix calorimeter with aluminum crucibles with pierced lids under nitrogen (100 ml min^{-1}) with a heating rate of 20 K min^{-1} from −120 to 260°C and a cooling rate of 15 K min^{-1} from 260°C to −120°C. Diphenyldichlorosilane, dimethyldichlorosilane and triethylsilane were stirred over magnesium and distilled under vacuum prior to use. Lithium disilenide,[1] *o*-lithio-*N*,*N*-dimethylaniline,[2] and 2,5-dibromo-N,N,N',N'-tetramethylbenzene-1,4-diamine[3] were prepared according to literature procedures.

Synthesis of 2-(chlorodiphenylsilyl)-*N*,*N*-dimethylaniline **3b**:

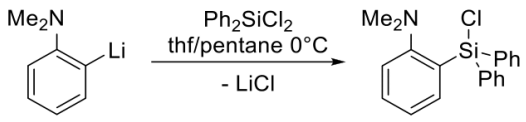

3b

o-Lithio-*N*,*N*-dimethylaniline (3.03 g, 23.8 mmol) is suspended in a mixture of 20 ml pentane and 20 ml of thf and cooled down to 0°C. Quick addition of diphenyldichlorosilane (5.0 mL, 6.04 g, 23.8 mmol, 1 eq.) at 0°C turns the reaction mixture pale-yellow accompanied by precipitation of lithium chloride. After stirring at room temperature for 2 hours, volatile components are removed in vacuo, the remaining solid is digested in 50 mL toluene and filtered. The yellow filtrate is dried in vacuo and the remaining yellow wax dissolved in 35 mL hot hexane. Crystallization at 0°C gives crude **3b** as off-white crystals which are washed with hexane and once again recrystallized from hexane at 0°C to yield 2.83 g (35%) **3b** as large colorless block-shaped crystals (**mp**: 88°C).

^{1}H NMR (400.13 MHz, C_6D_6, 300 K, TMS): δ = 8.16 (dd, ^{1}H, ^3J = 7.34 Hz, ^4J = 1.58 Hz, Me_2N-Ph-C*H*), 7.81 to 7.74 (m, 4H, Ph-C*H*), 7.23 (td, 1H, ^3J = 7.52 Hz, ^4J = 1.71 Hz, Me_2N-Ph-C*H*), 7.19 to 7.08 (m, overlapping with solvent signal, 7H, Ph-C*H* & Me_2N-Ph-C*H*), 6.97 (broad d, ^3J = 7.75 Hz, 1H, Me_2N-Ph-C*H*), 1.94 (s, 6H, N-CH_3) ppm.
^{13}C{^{1}H} NMR (100.61 MHz, C_6D_6, 300 K, TMS): δ = 161.2, 137.7 (Me_2N-Ph-*C*), 135.5 (Ph-*C*), 135.3 (Me_2N-Ph-*C*), 132.9 (Ph-*C*), 132.64 (Me_2N-Ph-*C*),130.1, 128.0 (Ph-*C*), 126.7, 122.4 (Me_2N-Ph-*C*), 46.4 (N-*C*H_3) ppm
^{29}Si{^{1}H} NMR (79.5 MHz, C_6D_6, 300 K, TMS): δ = –4.0 ppm.
Elemental analysis: Calcd. for $C_{20}H_{20}ClNSi$ (337.92): C, 71.09; H, 5.97; N, 4.15. Found: C, 70.88; H, 5.93; N, 4.11.

Synthesis of 2,5-bis(chlorodimethylsilyl)-N,N,N',N'-tetramethylbenzene-1,4-diamine **10**:

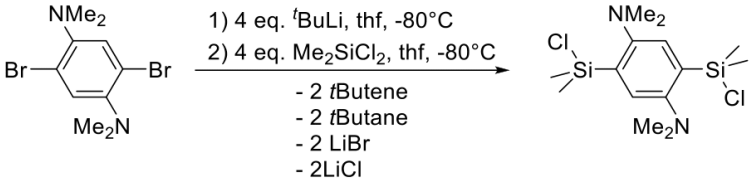

10

2,5-Dibromo-N,N,N',N'-tetramethylbenzene-1,4-diamine (1.00 g, 3.1 mmol) is dissolved in 50 mL thf and cooled down to −78°C before 1.9 M tBuLi solution in pentane (6.6 mL, 12.5 mmol, 4 eq.) is added dropwise over 5 minutes. The resulting yellow solution is allowed to reach −30°C before cooling down to −78°C again. The solution of the dilithiated arene is added *via* cannula to a −78°C cold solution of Me_2SiCl_2 (1.51 mL, 1.60 g, 12.4 mmol, 4 eq.) in 15 mL thf and the cooling bath is removed. After reaching room temperature all volatile species are removed *in vacuo* and the remaining solid is extracted with 50 mL hexane. The filtrate is then concentrated to about 10 mL and storage at −20°C results in formation of 520 mg (48%) bissilylbenzene **10** as colorless needles (**mp**: > 180 °C) suitable for X-Ray diffraction.
*Note: Compound **10** should be stored in the dark as it exhibits moderate light sensitivity over several days, indicated by a brownish color of the solid.*

^{1}H NMR (400.13 MHz, C_6D_6, 300 K, TMS): δ = 8.10 (s, 2H, Ar-*H*), 2.25 (s, 12H, N-CH_3), 0.64 (s, 12H, Si-CH_3) ppm.
^{13}C{^{1}H} NMR (100.61 MHz, C_6D_6, 300 K, TMS): δ = 158.7, 140.2, 129.2 (Ar-*C*), 46.7 (N-*C*H_3), 3.9 (Si-*C*H_3) ppm.
^{29}Si{^{1}H} NMR (79.5 MHz, C_6D_6, 300 K, TMS): δ = 14.3 ppm.
Elemental analysis: Calcd. for $C_{14}H_{26}Cl_2N_2Si_2$ (349.35): C, 48.12; H, 7.50; N, 8.02. Found: C, 48.17; H, 7.30; N, 7.48.

Synthesis of 2-(1,1-dimethyl-2,3,3-tris(2,4,6-triisopropylphenyl)trisil-2-en-1-yl)-*N*,*N*-dimethylaniline:

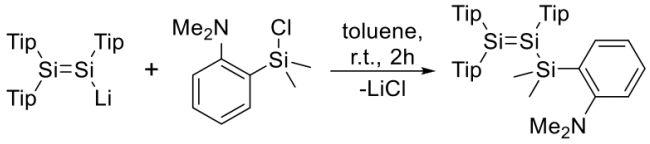

3a

Lithium disilenide (400 mg, 0.47 mmol) and 2-(chlorodimethylsilyl)-*N*,*N*-dimethylaniline **3a** (100.2 mg, 0.47 mmol, 1 eq.) are mixed as solids in a Schlenk flask and 10 mL toluene are added at room temperature. Stirring of the reaction mixture for 2 hours at room temperature is followed by removal of volatile species in vacuo. The remaining solid is digested in 10 mL hexane and filtered via cannula to remove insoluble parts. The yellow-orange filtrate is dried thoroughly to give 282 mg (70%) of silyldisilene as orange powder.

^{1}H NMR (400.13 MHz, C_6D_6, 300 K, TMS): δ = 8.20 (dd, ^{3}J = 7.41 Hz, ^{4}J = 1.41 Hz, 1H, Me_2N-Ph-*H*), 7.09 (s, 2H, Tip-*H*), 7.08 to 7.03 (m, 1H, Me_2N-Ph-*H*), 7.03 to 6.97 (m, 5H, Tip-*H* & Me_2N-Ph-*H*), 6.70 (td, ^{3}J = 7.25 Hz, ^{4}J = 1.04 Hz, 1H, Me_2N-Ph-*H*), 4.30 (sept., ^{3}J = 6.69 Hz, 2H, Tip-*i*Pr-C*H*), 4.04 (sept., ^{3}J = 6.59 Hz, 2H, Tip-*i*Pr-C*H*), 3.83 (sept., ^{3}J = 6.55 Hz, 2H, Tip-*i*Pr-C*H*), 2.81 to 2.65 (m, 3H, Tip-*i*Pr-C*H*), 2.41 (s, 6H, N-CH_3), 1.31 (br. d, ^{3}J = 6.40 Hz, 12H, Tip-*i*Pr-CH_3), 1.20 (d, ^{3}J = 6.91 Hz, 6H, Tip-*i*Pr-CH_3), 1.18 (d, ^{3}J = 6.91 Hz, 6H, Tip-*i*Pr-CH_3), 1.13 (d, ^{3}J = 6.91 Hz, 6H, Tip-*i*Pr-CH_3), 1.11 (br., 12H, Tip-*i*Pr-CH_3), 0.95 (d, ^{3}J = 6.59 Hz, 12H, Tip-*i*Pr-CH_3), 0.72 (s, 6H, Si-CH_3) ppm.
^{13}C{^{1}H} NMR (100.61 MHz, C_6D_6, 300 K, TMS): δ = 161.5 (Ph-*C*), 155.8, 154.8, 154.4, 150.7, 150.3, 150.1 (Tip-*C*), 139.4 (Ph-*C*), 136.7, 136.5, 136.3 (Tip-*C*), 132.3 (Ph-*C*), 131.0 (Ph-*C*), 125.3 (Ph-*C*), 122.3, 122.1, 121.9 (Tip-*C*), 47.1 (N-*C*H_3), 37.9, 37.5, 37.2, 34.9, 34.7, 34.5 (*i*Pr-*C*H), 24.6, 24.2, 24.2, 24.0 (*i*Pr-*C*H_3), 3.5 (Si-*C*H_3) ppm.
^{29}Si{^{1}H} NMR (79.5 MHz, C_6D_6, 300 K, TMS): δ = 98.4 (*Si*Tip_2), 52.7 (*Si*(Tip)-$SiMe_2$R), –4.9 (*Si*Me_2R) ppm.
UV/vis (hexane): λ_{max} (ε) = 413 nm (ε = 17900 L mol^{-1} cm^{-1}), 365 nm (5500 L mol^{-1} cm^{-1}).
Elemental analysis: Calcd. for $C_{55}H_{85}NSi_3$ (844.55): C, 78.22; H, 10.15; N, 1.66. Found: C, 77.52; H, 10.18; N, 1.40.

Trapping of germylene **6a** with Et_3SiH

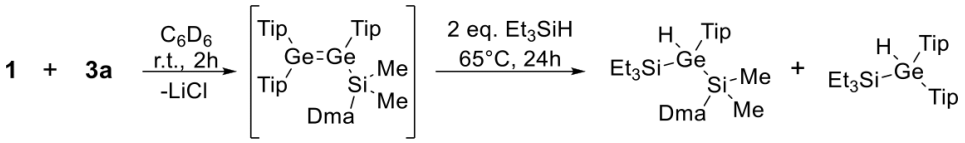

4a **7a** **9**

Digermenide **1** (50.0 mg, 49 µmol) and chlorosilane **3a** (10.4 mg, 49 µmol, 1 eq.) are mixed as solids and 0.5 ml deuterated benzene are added. After two hours at room temperature,

completion of the reaction to **4a** is confirmed by ^{1}H NMR and Et_3SiH (11.3 mg, 15.5 µl, 98 µmol, 2 eq.) is added. Heating to 65°C for 24 hours leads to a color change from dark orange to yellow and the resulting mixture is characterized NMR spectroscopically.

*Note: As two products are obtained which signals are strongly overlapping, a detailed assignment of all signals is not possible. As seen from the ^{1}H NMR spectrum, **7a** and **9** exist in a ratio of 1:1.15. Integrals from the spectrum are corrected by this factor to get integer values.*

^{1}H NMR (400.13 MHz, C_6D_6, 300 K, TMS): δ = 7.58 (dd, ^{3}J = 7.43 Hz, ^{4}J = 1.55 Hz, 1H, Dma-Aryl-*H*), 7.15 to 7.14 (m, 3H, Dma-Aryl-*H* & (**7a**)-Tip-*H*), 7.08 (s, 4H, (**9**)-Tip-*H*), 7.03 to 7.00 (m, 1H, Dma-Aryl-*H*), 6.96 (td, ^{3}J = 7.32 Hz, ^{4}J = 1.12 Hz, 1H, Dma-Aryl-*H*), 5.57 (s, 1H, (**9**)-Ge-*H*), 4.21 (s, 1H, (**7a**)-Ge-*H*), 3.42 (sept., ^{3}J = 6.77 Hz, 5H, Tip-*i*Pr-C*H* & Tip-*i*Pr-C*H*), 2.85 to 2.74 (m, 4H, Tip-*i*Pr-C*H* & Tip-*i*Pr-C*H*), 2.37 (s, 6H, Dma-N(CH_3)$_2$), 1.36 to 1.29, 1.24 to 1.20, 1.18 to 1.13, 1.09 to 1.04, 1.02 to 0.96, 0.86 to 0.82 (each m, altogether 93H, Tip-*i*Pr-CH_3, Tip-*i*Pr-CH_3, SiEt-CH_3, SiEt-CH_3), 0.73, 0.70 (each s, each 3H, altogether 6H, Si-CH_3) ppm.
^{29}Si{^{1}H} NMR (79.5 MHz, C_6D_6, 300 K, TMS): δ = 5.56 ((**7a**)-*Si*Et_3), 5.01 ((**8**)-*Si*Et_3), −11.9 (*Si*Me_2) ppm.

Trapping of Germylene **6b** with Et_3SiH

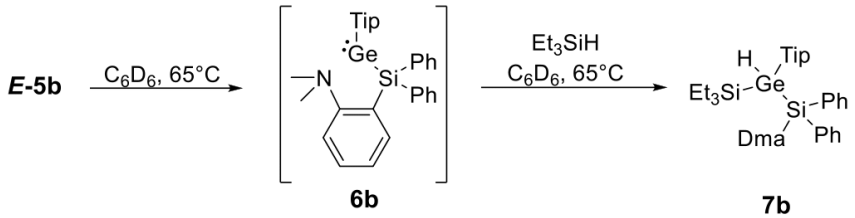

***E*-5b** (52 mg, 45 µmol) is dissolved in 0.45 mL C_6D_6 and Et_3SiH (72 µl, 52 mg, 10 eq.) is added at room temperature. Heating overnight to 65°C leads to decolorization of the reaction mixture. Drying in vacuo yields a pale-yellow residue which was subsequently characterized by NMR spectroscopy.

*Note: As an unidentified byproduct is formed which signals strongly overlap with those of **7b**, a detailed assignment of all signals is not possible. In the following, only diagnostic signals of the main product are listed.*
^{1}H NMR (400.13 MHz, C_6D_6, 300 K, TMS): δ = 4.79 (s, 1H, Ge-*H*) ppm.
^{29}Si{^{1}H} NMR (79.5 MHz, C_6D_6, 300 K, TMS): δ = 5.2 (*Si*Et_3), −12.5 (*Si*Ph_2) ppm.

Spectroscopic characterization of new compounds

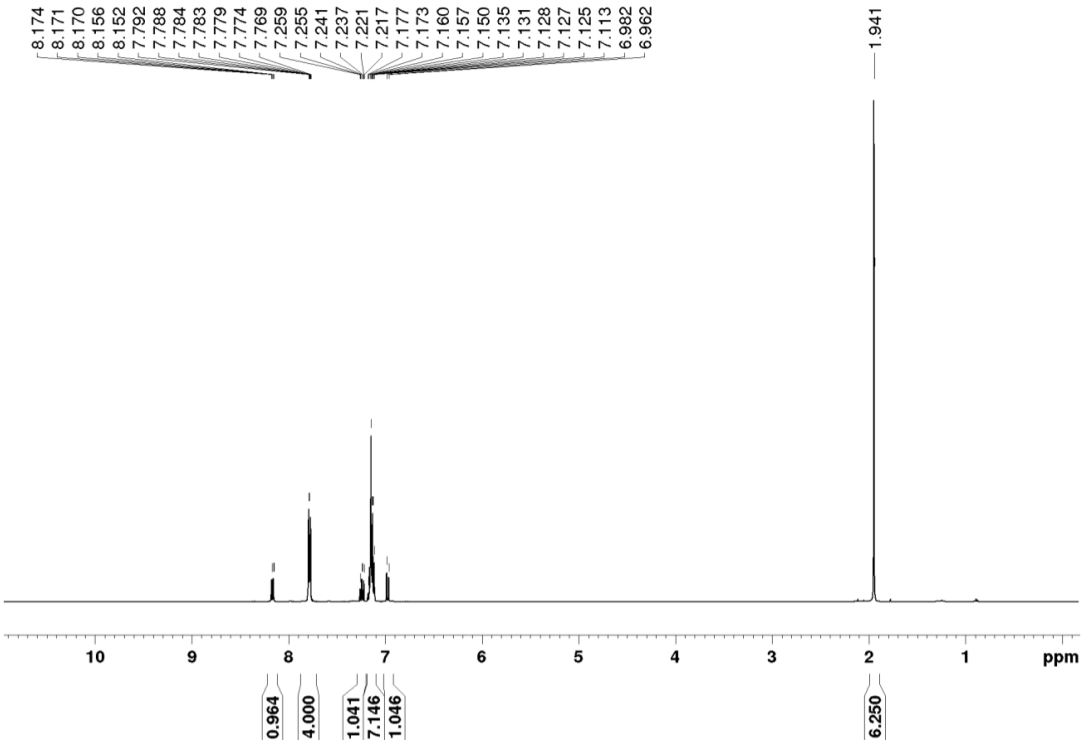

Figure 1.
^{1}H NMR of *o*-(chlorodiphenylsilyl)dimethylaniline **3b** in C_6D_6 at 300 K.

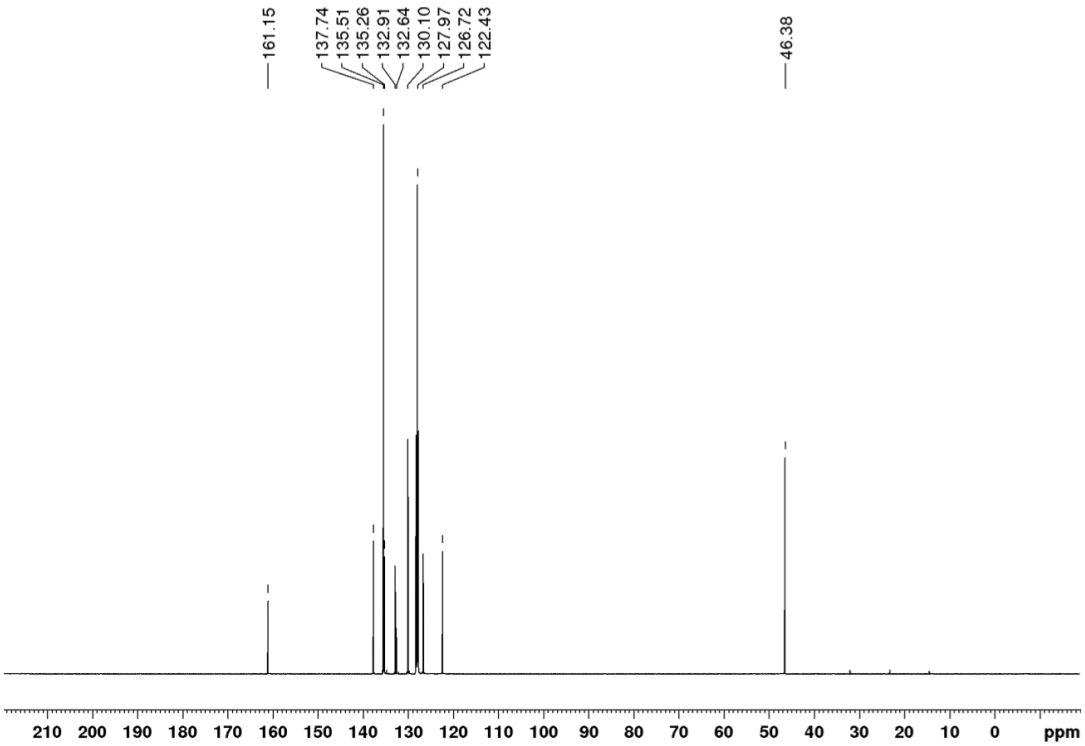

Figure 2.
$^{13}C\{^{1}H\}$ NMR of *o*-(chlorodiphenylsilyl)dimethylaniline **3b** in C_6D_6 at 300 K.

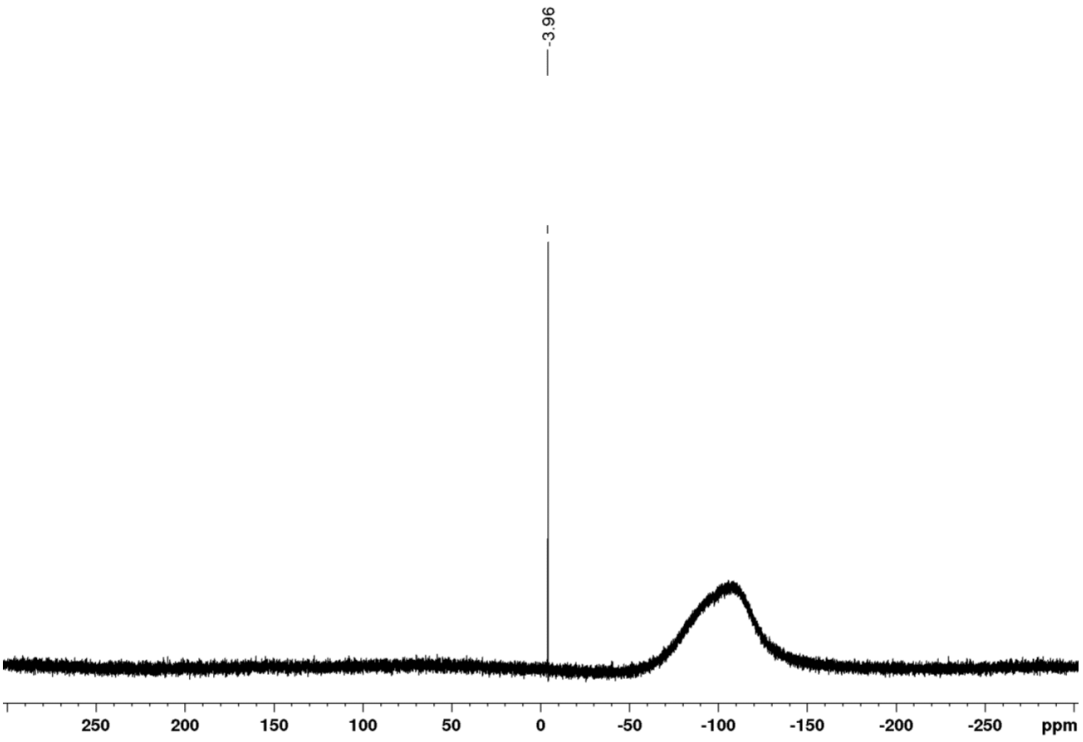

Figure 3.
$^{29}Si\{^{1}H\}$ NMR of *o*-(chlorodiphenylsilyl)dimethylaniline **3b** in C_6D_6 at 300 K.

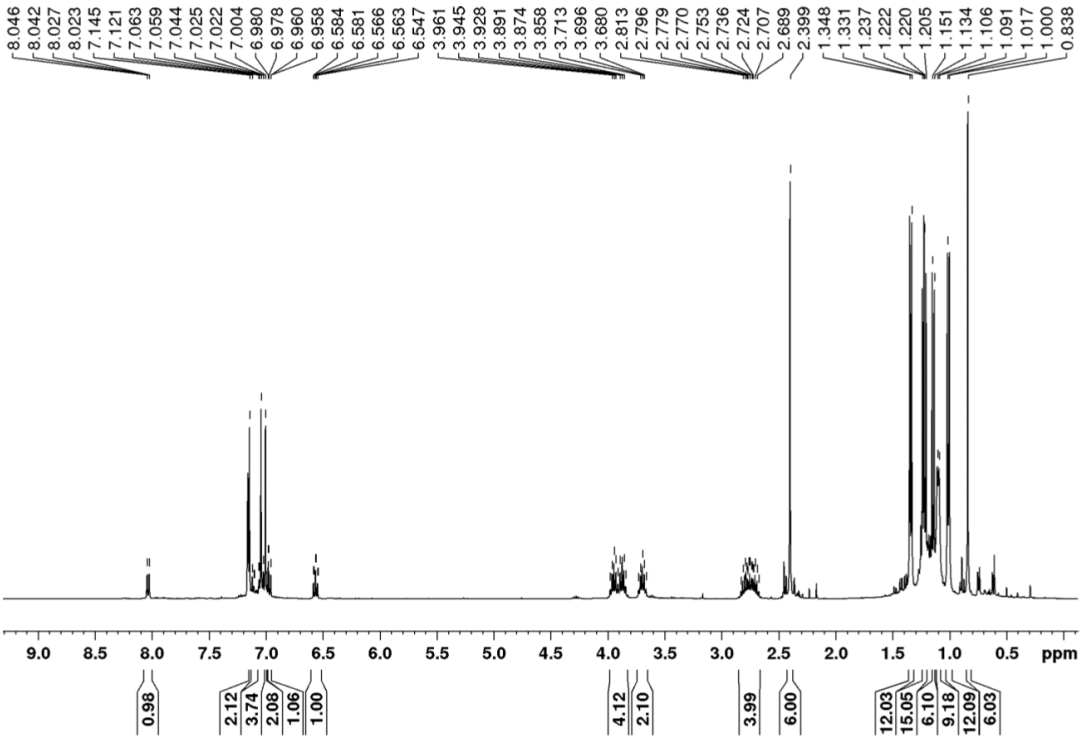

Figure 4.
^{1}H NMR of (*o*-dimethylanilino)silyldigermene **4a** in C_6D_6 at 300 K.

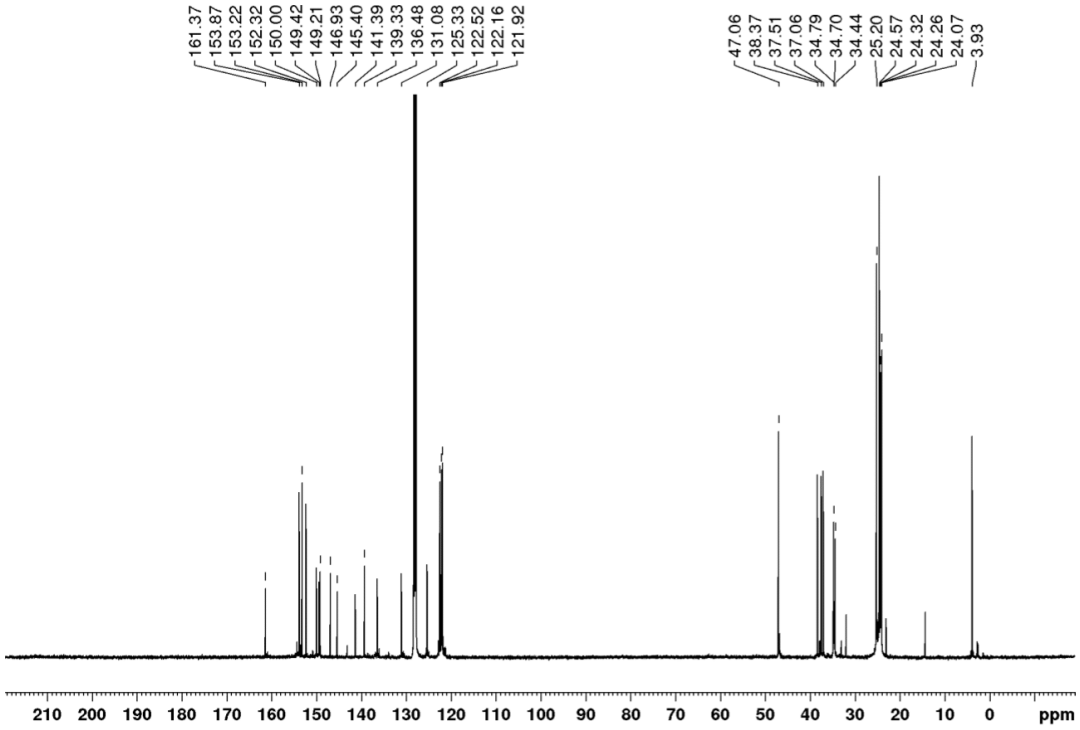

Figure 5.
$^{13}C\{^{1}H\}$ NMR of (*o*-dimethylanilino)silyldigermene **4a** in C_6D_6 at 300 K.

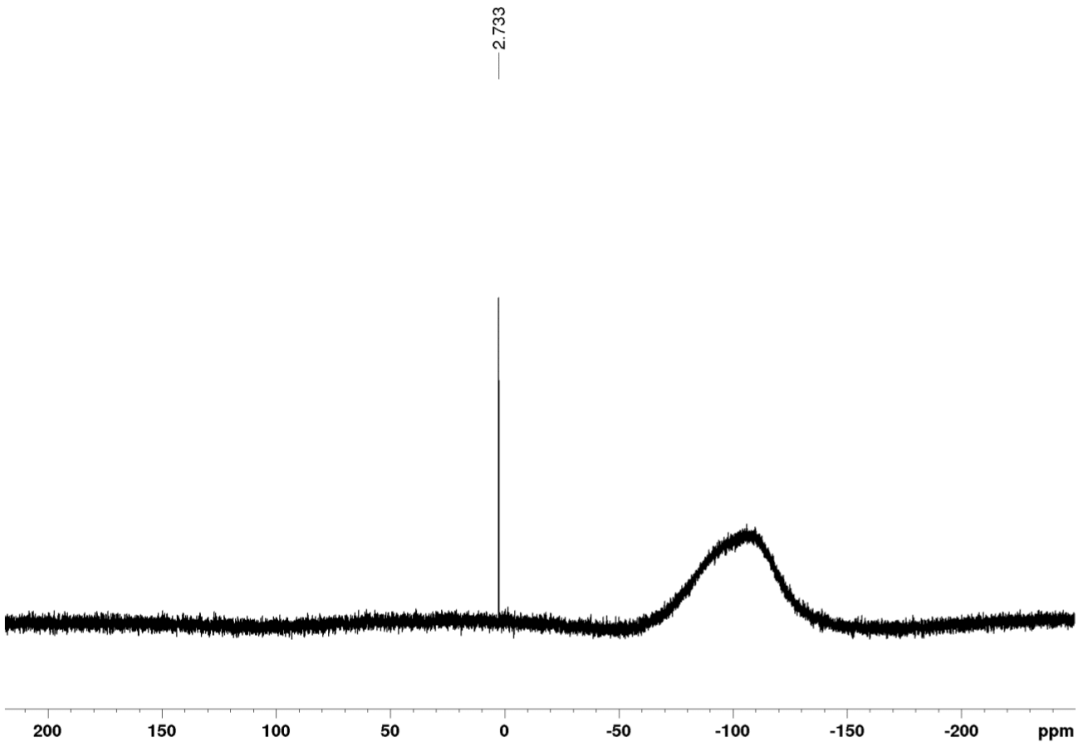

Figure 6.
$^{29}Si\{^{1}H\}$ NMR of (*o*-dimethylanilino)silyldigermene **4a** in C_6D_6 at 300 K.

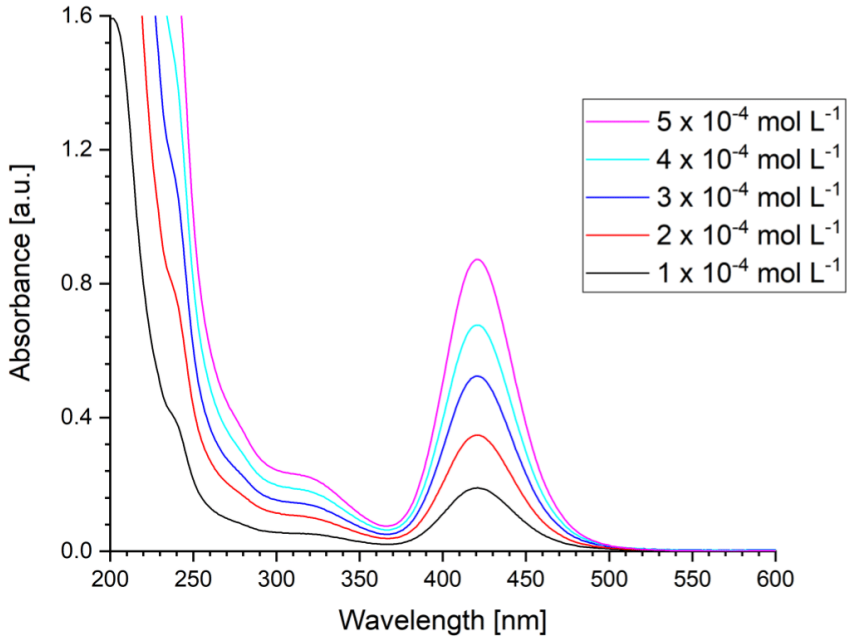

Figure 7.
UV/vis spectra of **4a** in hexane at different concentrations ($1 \cdot 10^{-4}$ to $5 \cdot 10^{-4}$ mol L^{-1}).

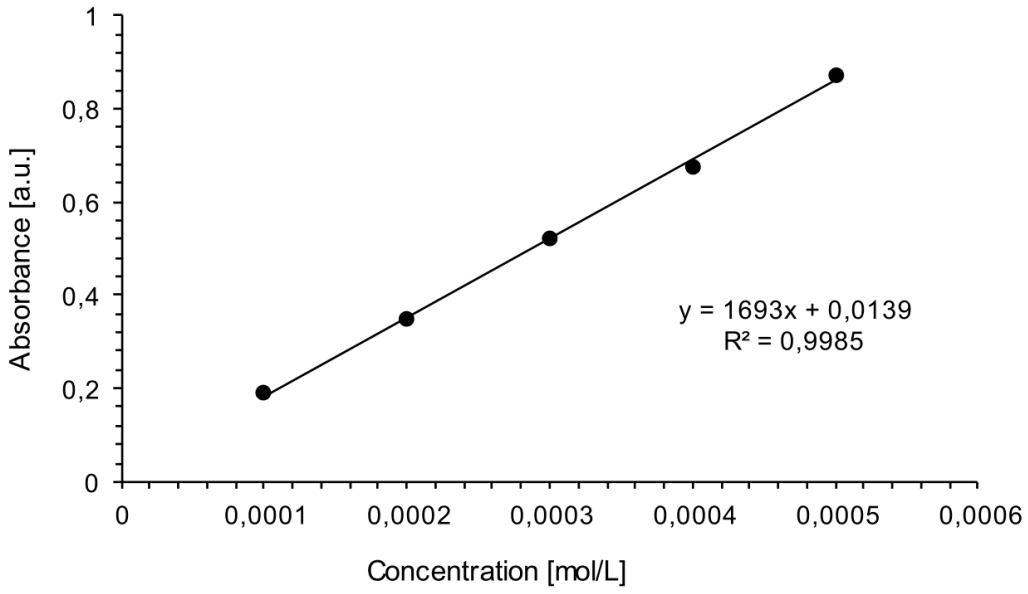

Figure 8.

Determination of ε (16900 L mol^{-1} cm^{-1}) by linear regression of absorbance (λ = 421 nm) of **4a** against concentration.

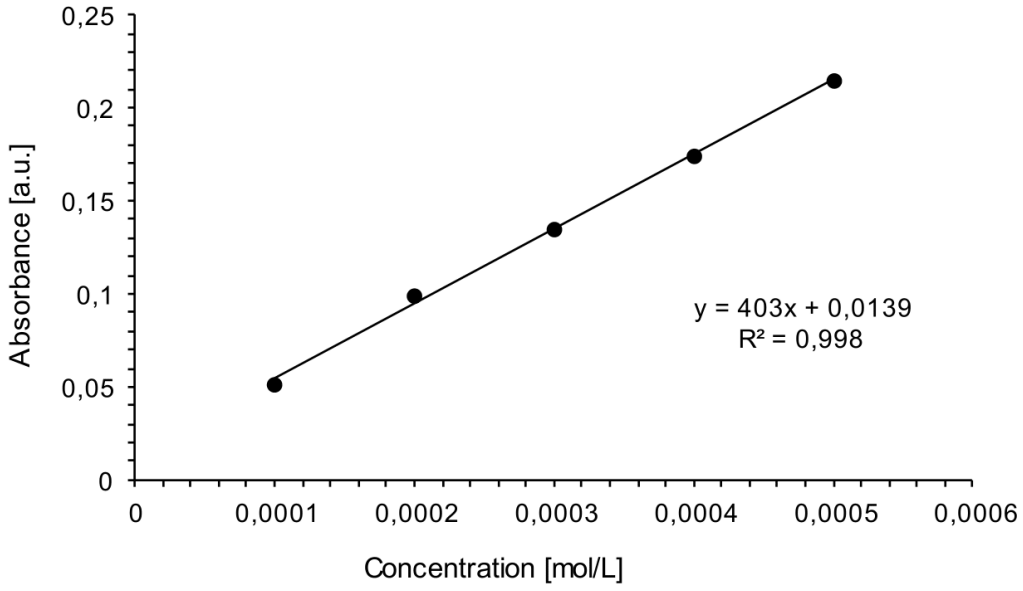

Figure 9.

Determination of ε (4000 L mol^{-1} cm^{-1}) by linear regression of absorbance (λ = 323 nm) of **4a** against concentration.

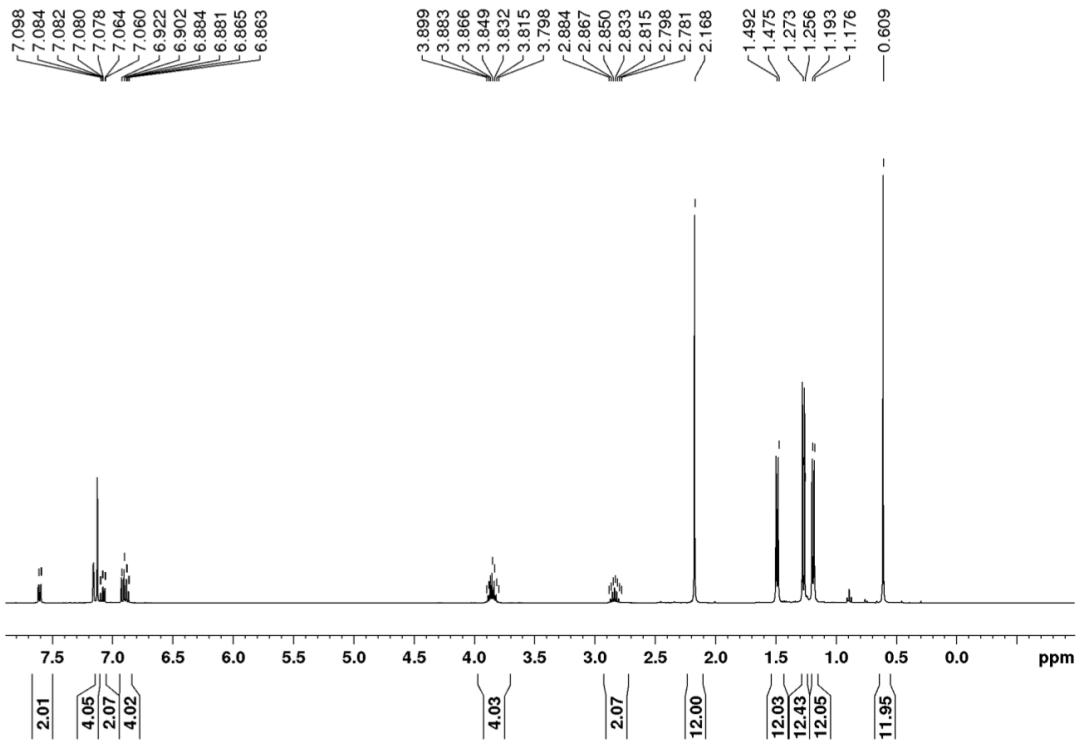

Figure 10.
^{1}H NMR spectrum bis-silylated digermene ***E*-5a** in C_6D_6 at 300 K.

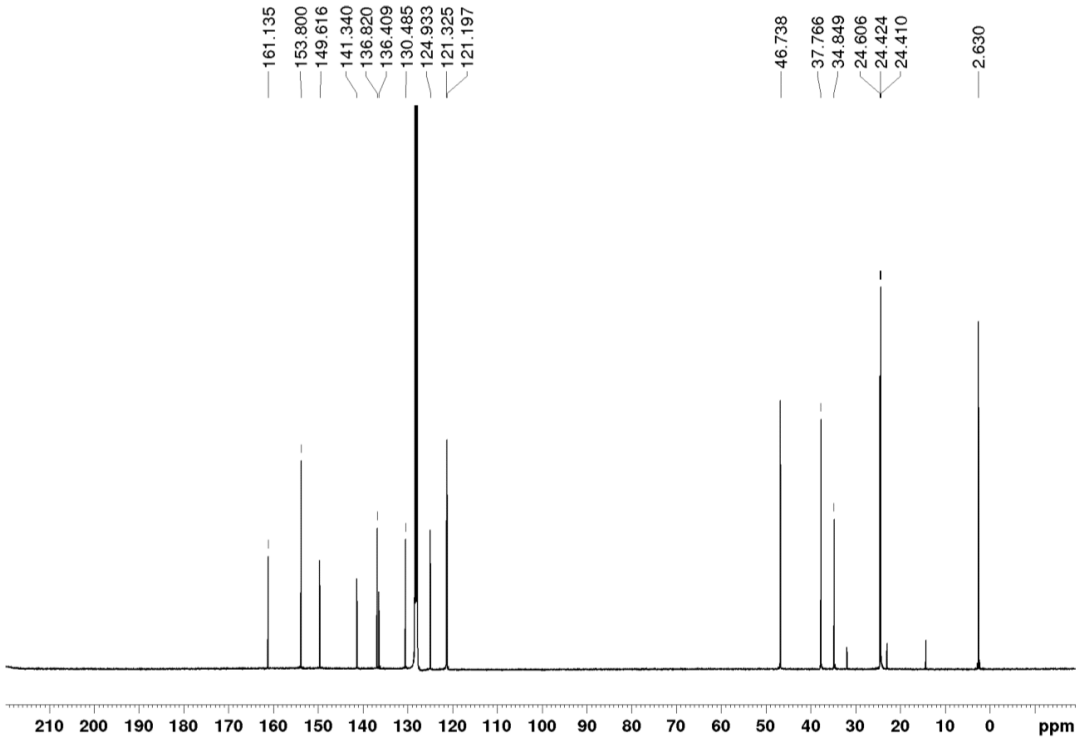

Figure 11.
$^{13}C\{^{1}H\}$ NMR spectrum bis-silylated digermene ***E*-5a** in C_6D_6 at 300 K.

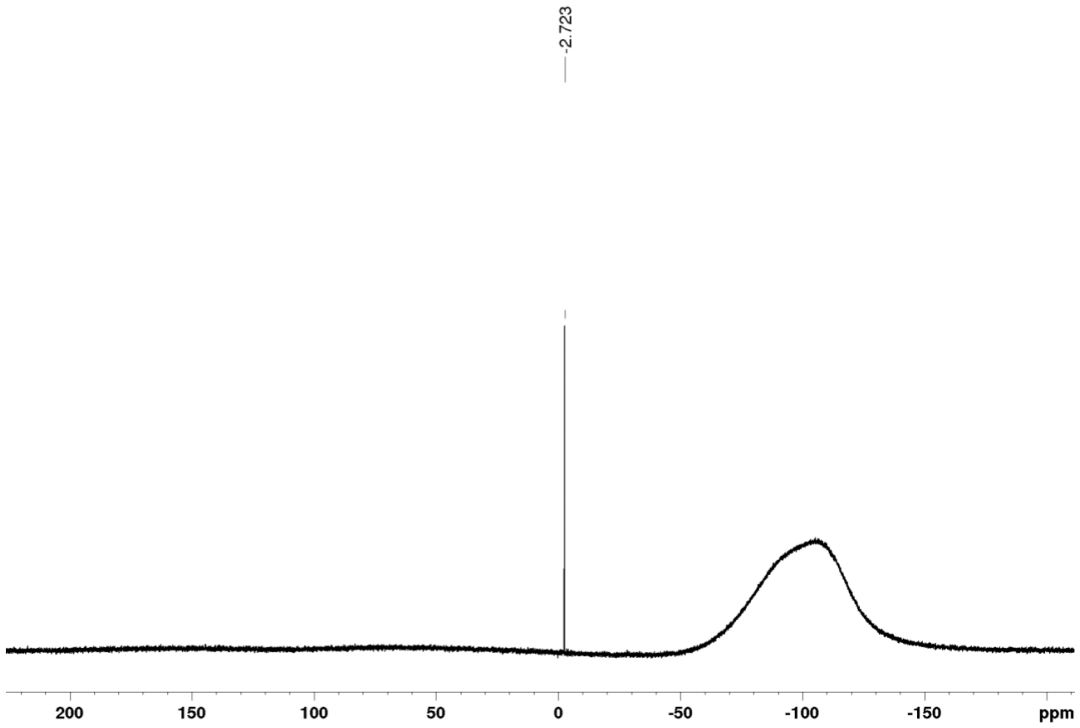

Figure 12.
$^{29}Si\{^{1}H\}$ NMR spectrum bis-silylated digermene ***E*-5a** in C_6D_6 at 300 K.

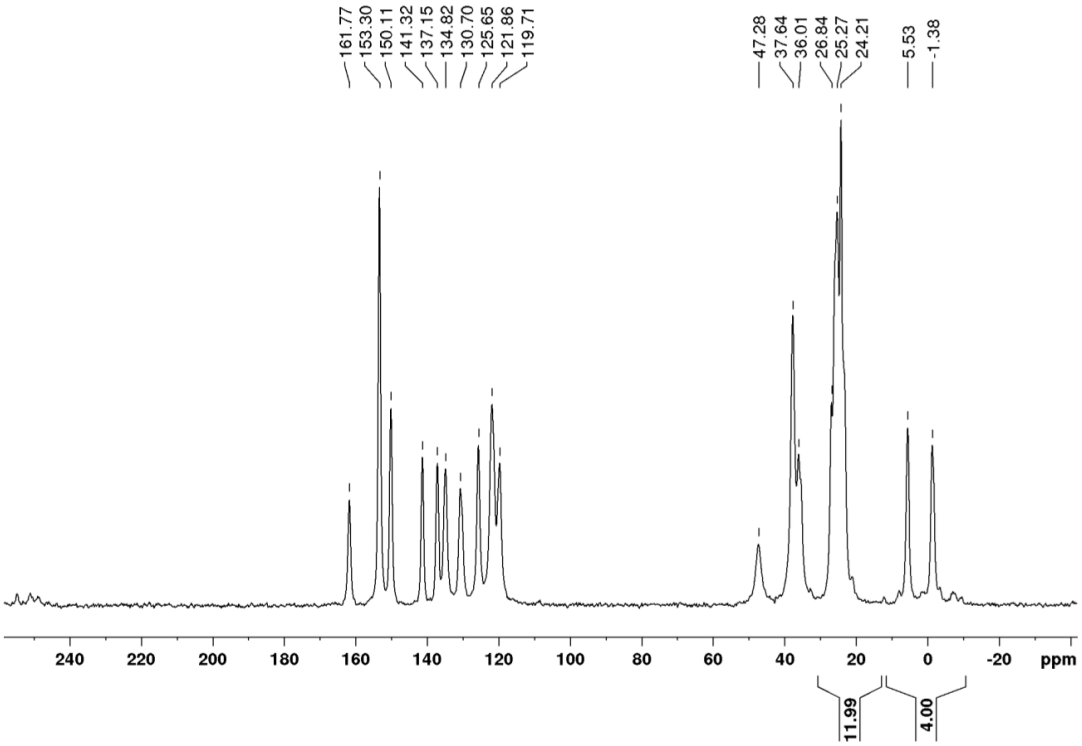

Figure 13.
$^{13}C\{^{1}H\}$ CP/MAS NMR spectrum bis-silylated digermene ***E*-5a** in C_6D_6 at 300 K.

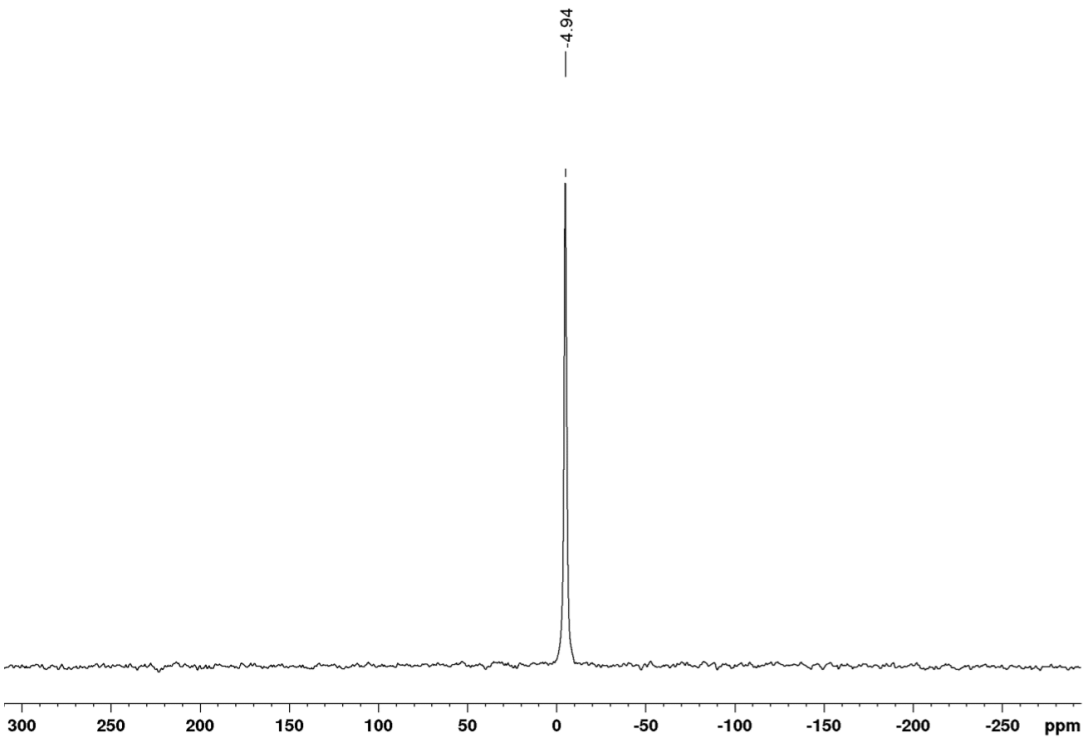

Figure 14.

$^{29}Si\{^{1}H\}$ CP/MAS NMR spectrum bis-silylated digermene ***E*-5a** in C_6D_6 at 300 K.

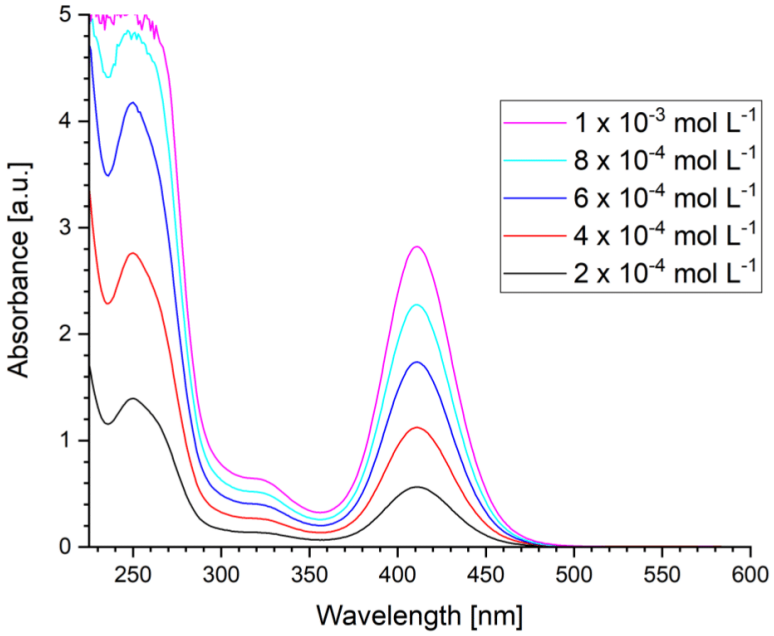

Figure 15.
UV/vis spectra of ***E*-5a** in hexane at different concentrations ($2 \cdot 10^{-4}$ to $1 \cdot 10^{-3}$ mol L^{-1}).

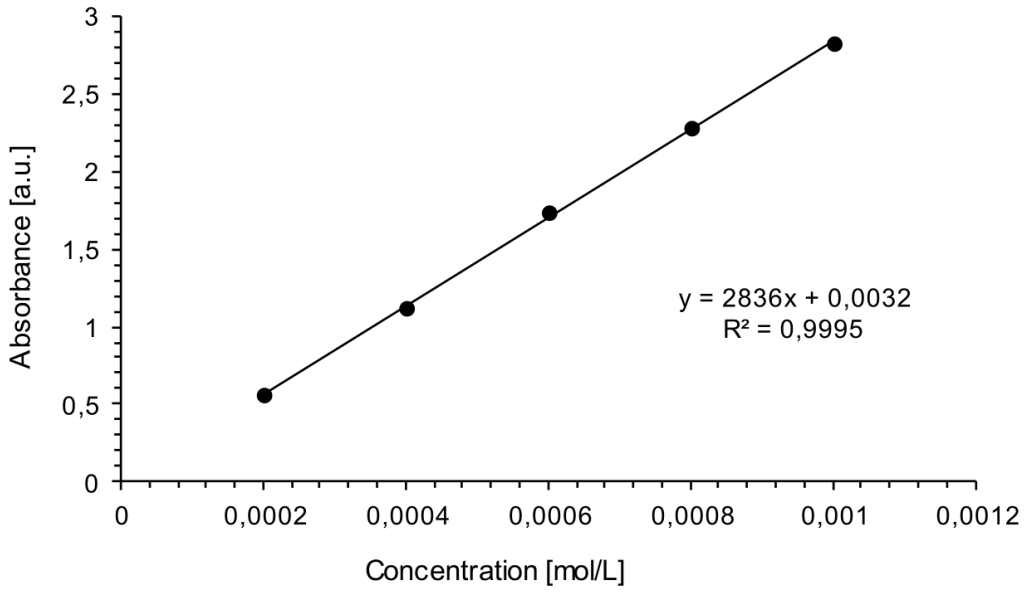

Figure 16.

Determination of ε (28400 L mol^{-1} cm^{-1}) by linear regression of absorbance (λ = 411 nm) of ***E*-5a** against concentration.

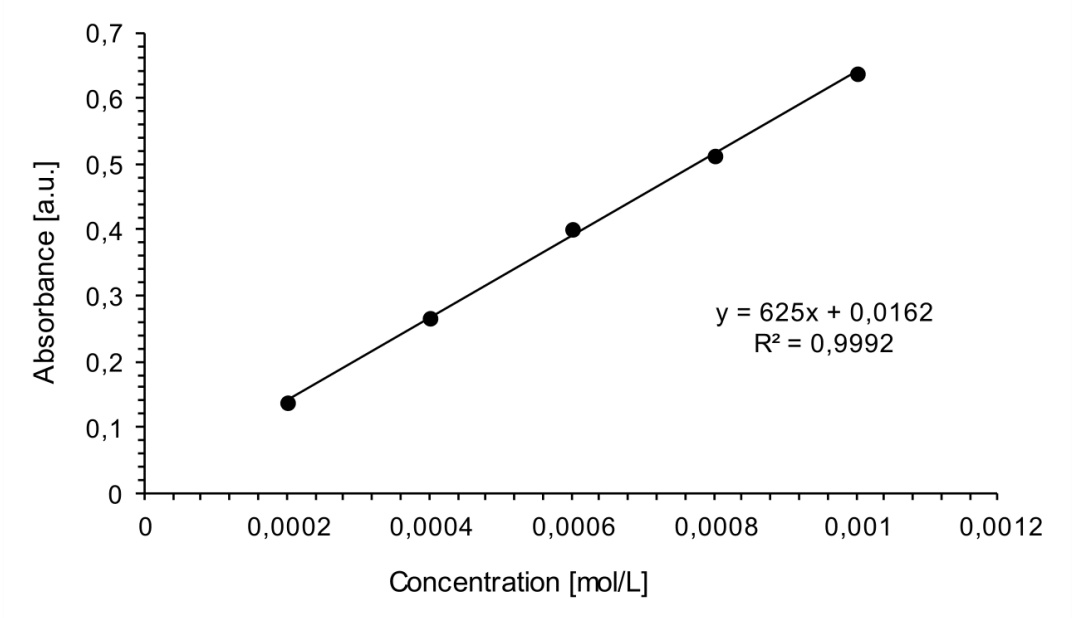

Figure 17.

Determination of ε (6300 L mol^{-1} cm^{-1}) by linear regression of absorbance (λ = 322 nm) of ***E*-5a** against concentration.

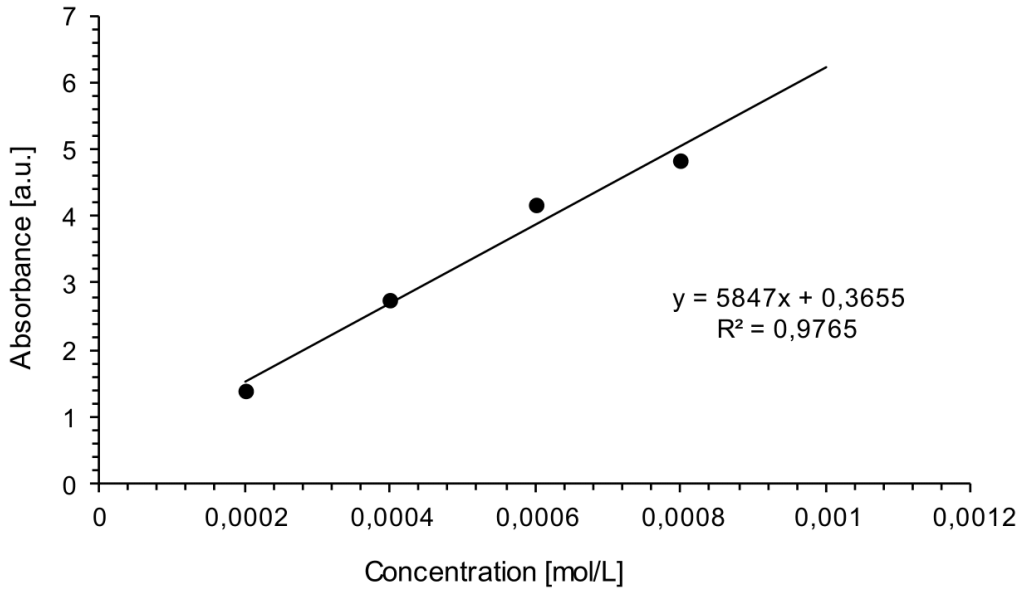

Figure 18.

Determination of ε (58500 L mol^{-1} cm^{-1}) by linear regression of absorbance (λ = 250 nm) of ***E*-5a** against concentration.

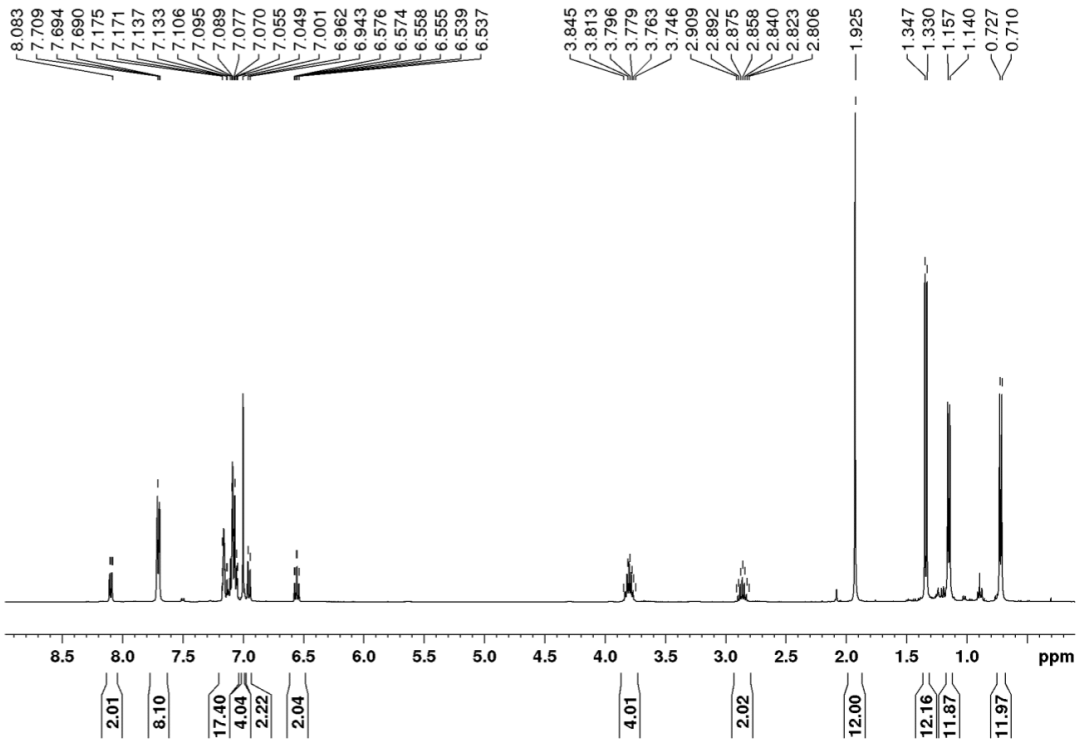

Figure 19.
^{1}H NMR spectrum bis-silylated digermene ***E*-5b** in C_6D_6 at 300 K.

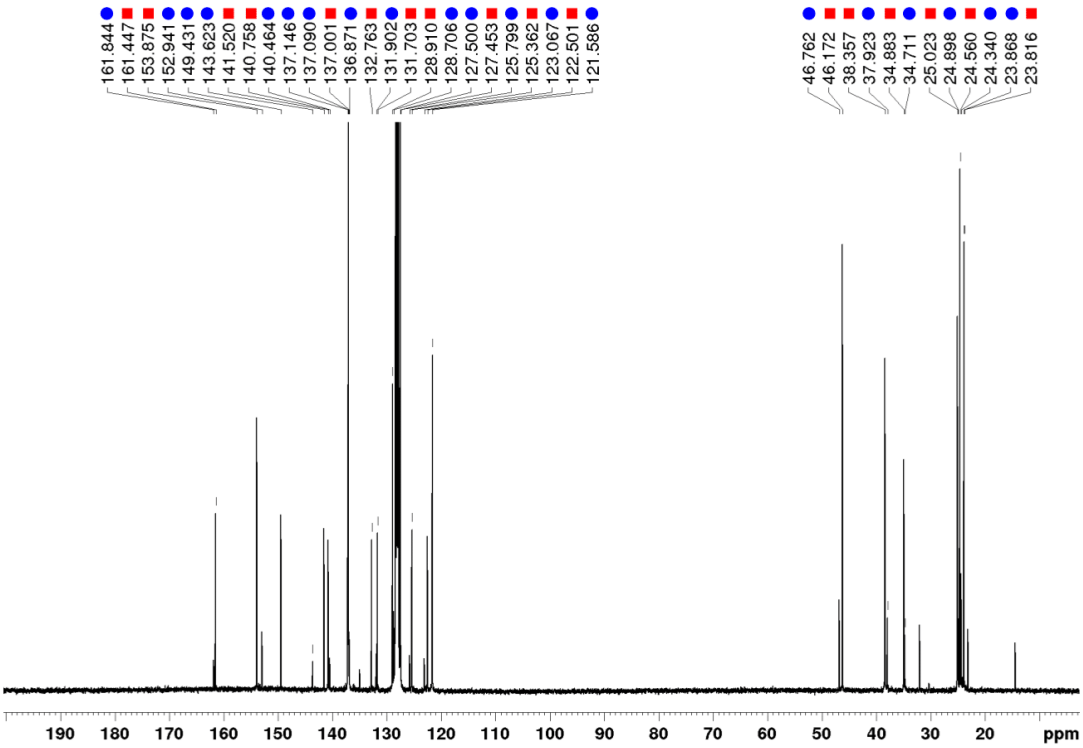

Figure 20.
$^{13}C\{^{1}H\}$ NMR spectrum bis-silylated digermene ***E*-5b** in C_6D_6 at 300 K (labelled with ■, signals of equilibirum species digermene ***Z*-5b** labelled with ●).

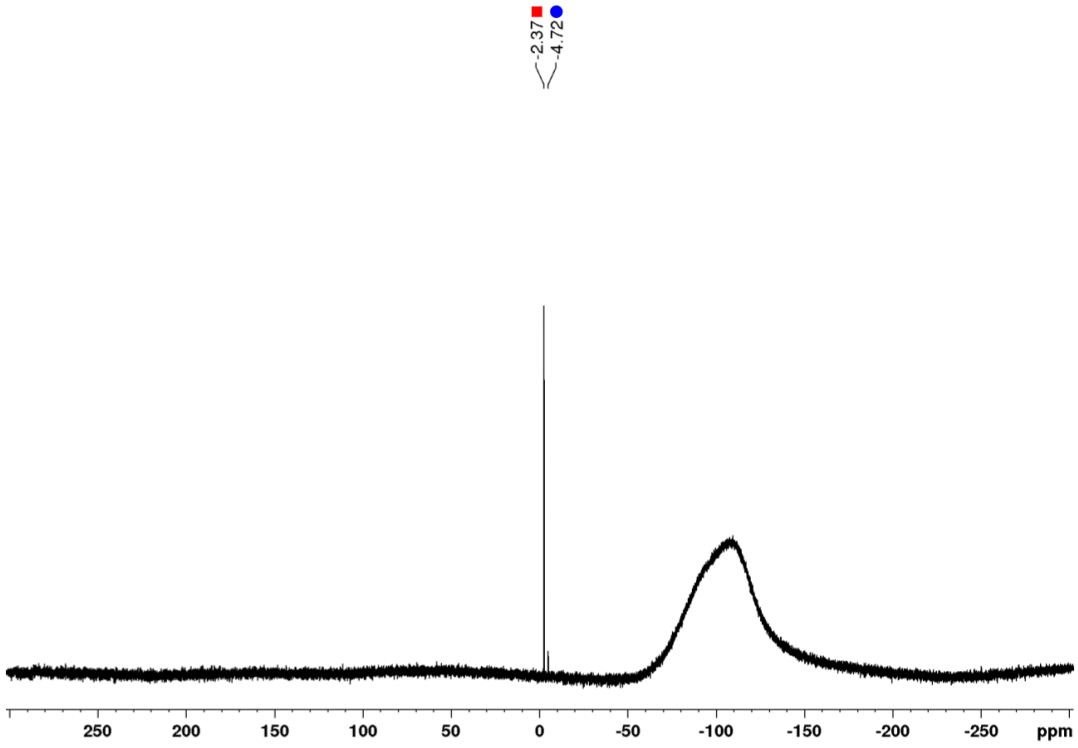

Figure 21.
$^{29}Si\{^{1}H\}$ NMR spectrum bis-silylated digermene ***E*-5b** in C_6D_6 at 300 K (labelled with ■, signals of equilibirum species digermene ***Z*-5b** labelled with ●).

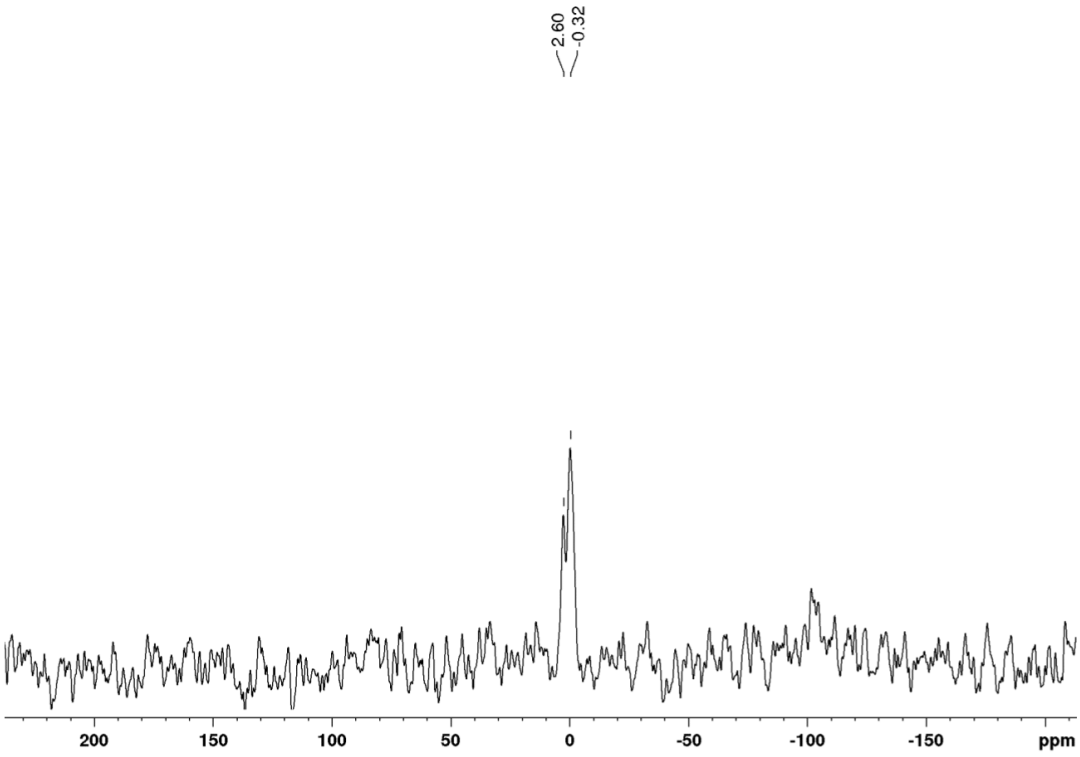

Figure 22.
^{29}Si CP/MAS NMR spectrum bis-silylated digermene ***E*-5b** at 300 K.

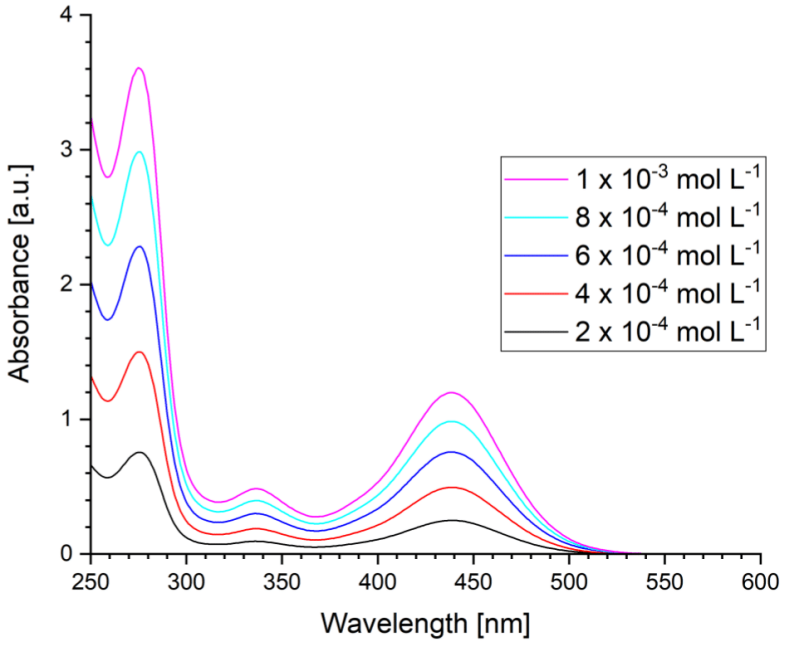

Figure 23.
UV/vis spectra of ***E*-5b** in hexane at different concentrations ($2 \cdot 10^{-4}$ to $1 \cdot 10^{-3}$ mol L^{-1}).

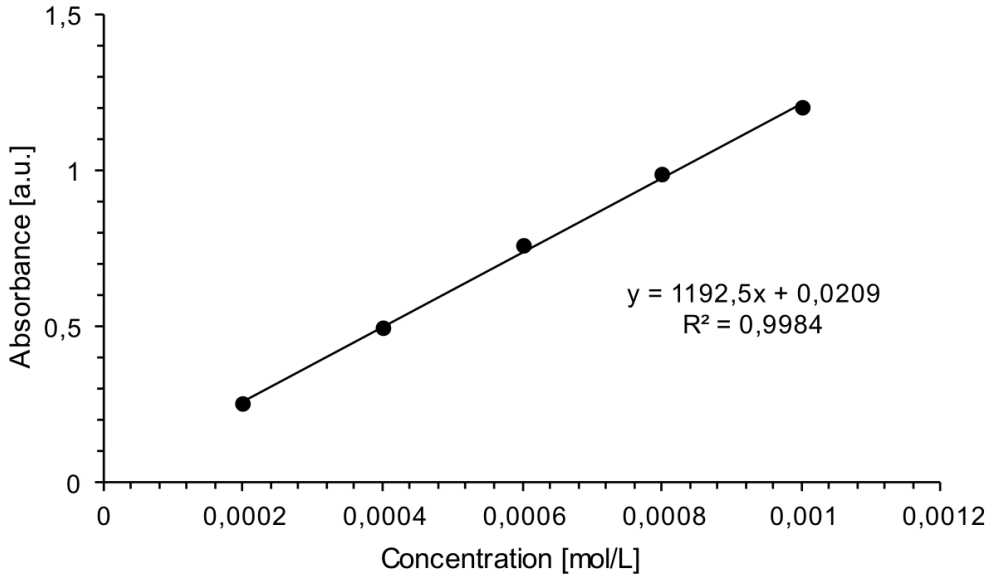

Figure 24.

Determination of ε (11900 L mol^{-1} cm^{-1}) by linear regression of absorbance (λ = 438 nm) of ***E*-5b** against concentration.

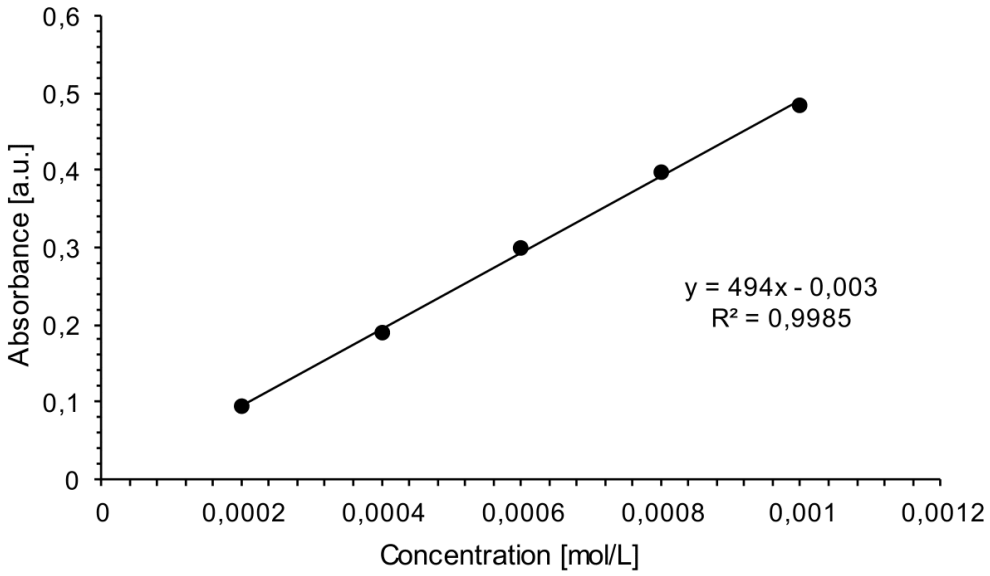

Figure 25.

Determination of ε (4900 L mol^{-1} cm^{-1}) by linear regression of absorbance (λ = 336 nm) of ***E*-5b** against concentration.

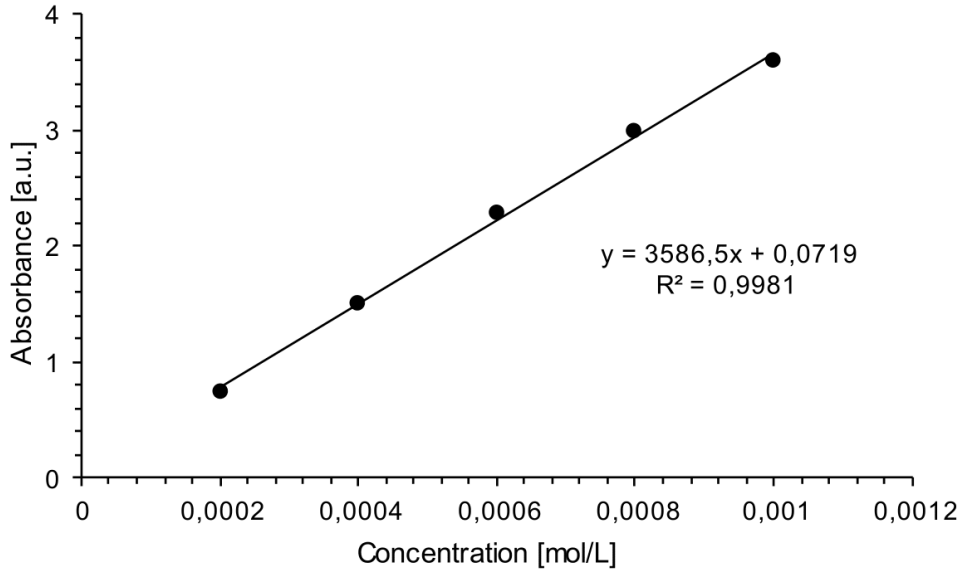

Figure 26.

Determination of ε (35900 L mol^{-1} cm^{-1}) by linear regression of absorbance (λ = 276 nm) of ***E*-5b** against concentration.

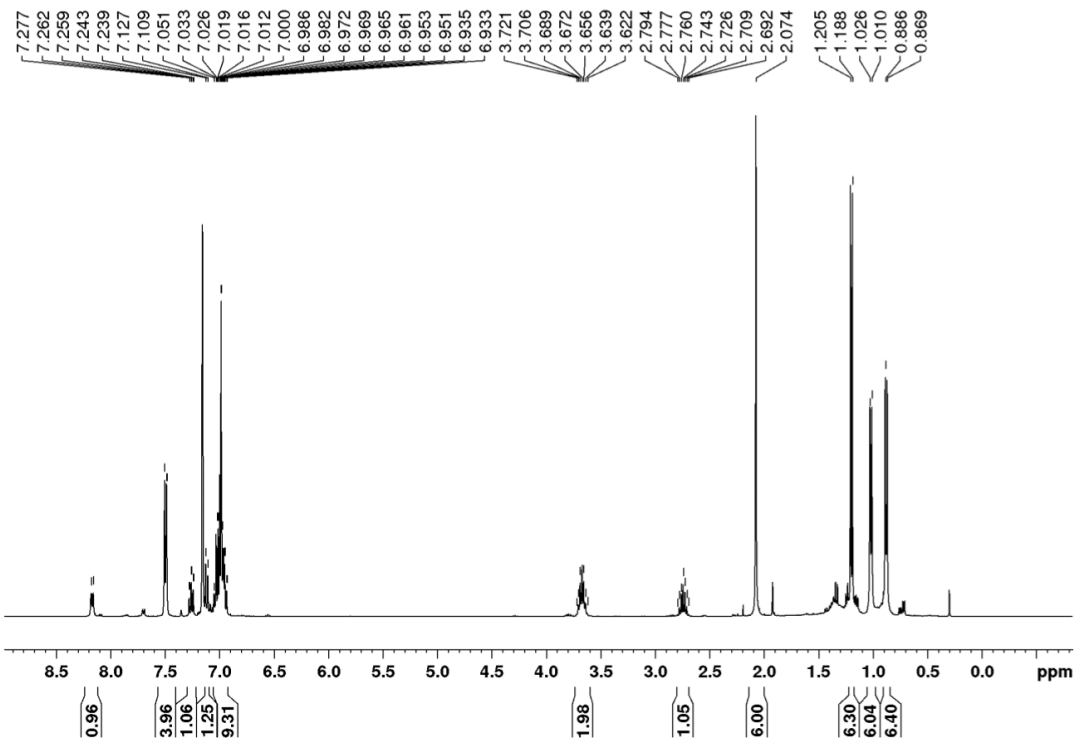

Figure 27.
^{1}H NMR of digermene ***Z*-5b** in C_6D_6 at 300 K.

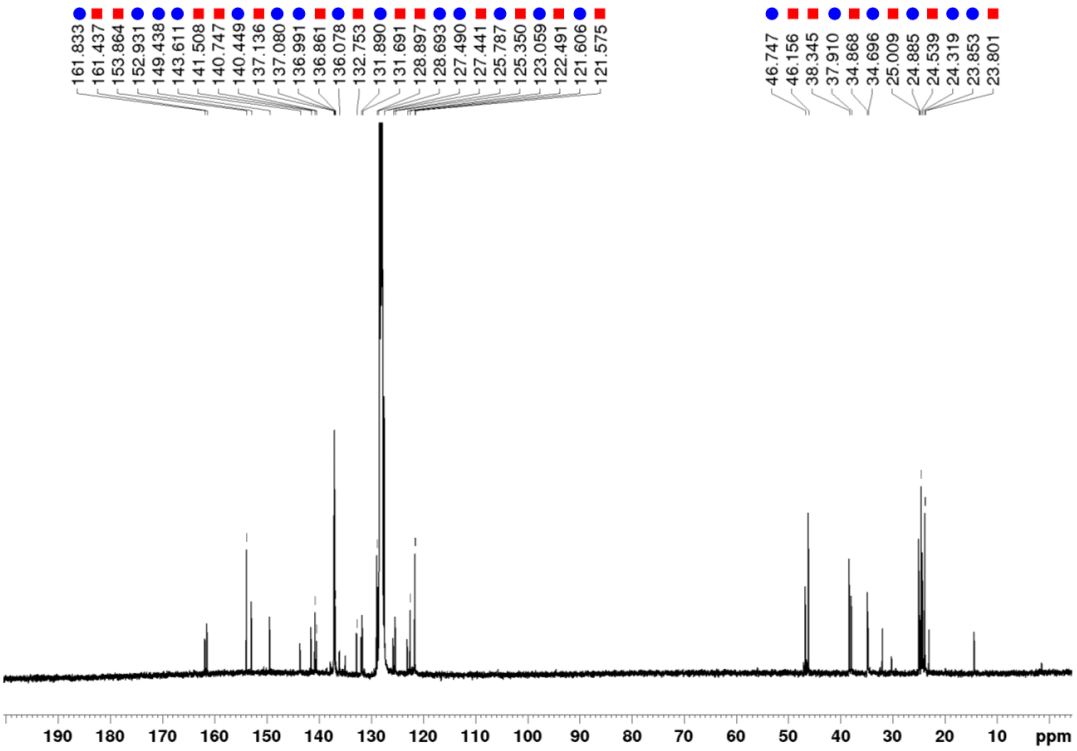

Figure 28.
$^{13}C\{^{1}H\}$ NMR of digermene ***Z*-5b** in C_6D_6 at 300 K (labelled with ●, signals of equilibrium species digermene ***E*-5b** labelled with ■).

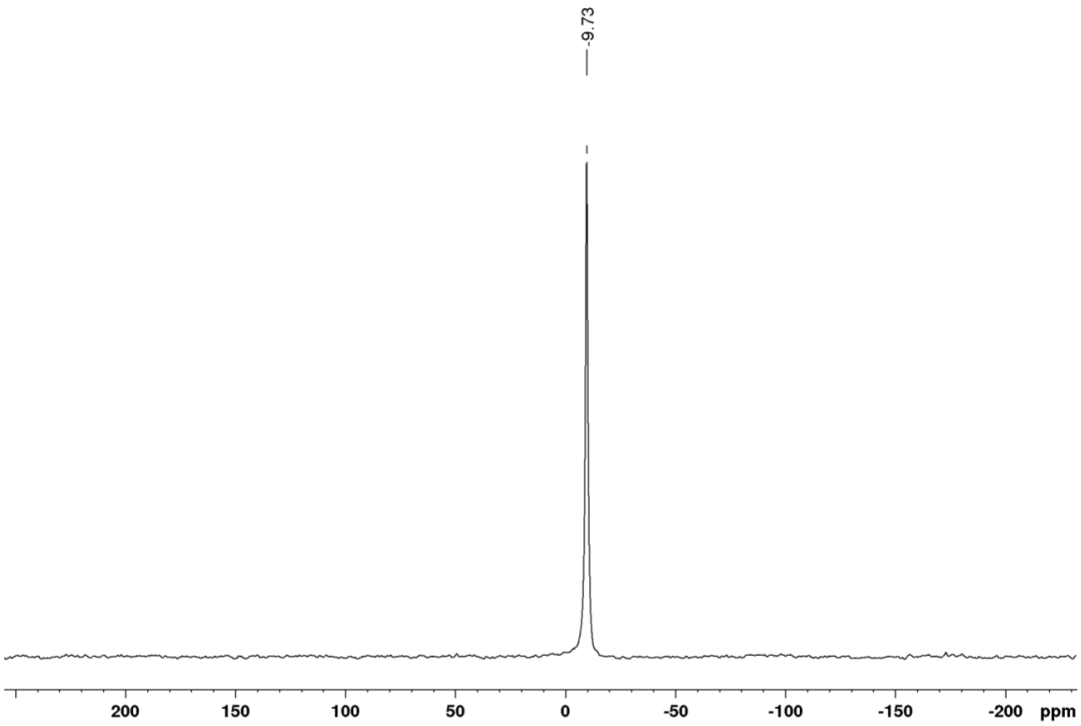

Figure 29.
^{29}Si CP/MAS NMR spectrum bis-silylated digermene **Z-5b** at 300 K.

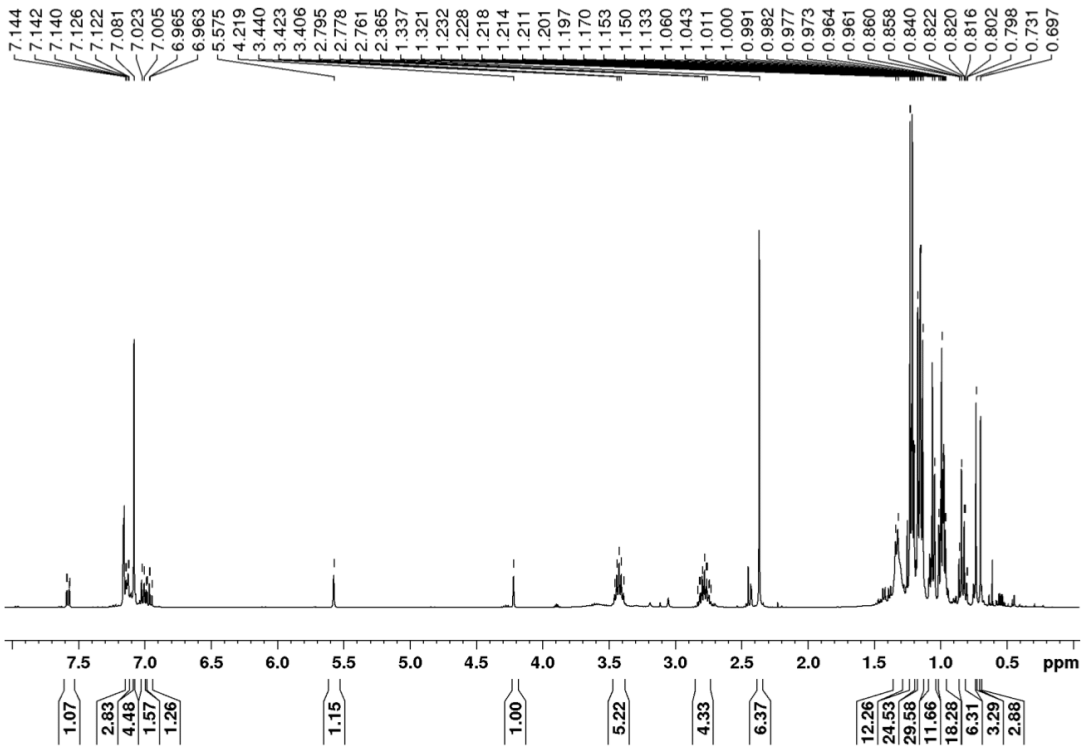

Figure 30.

^{1}H NMR in C_6D_6 at 300 K of the worked up reaction mixture of trapping germylene **6a** with Et_3SiH.

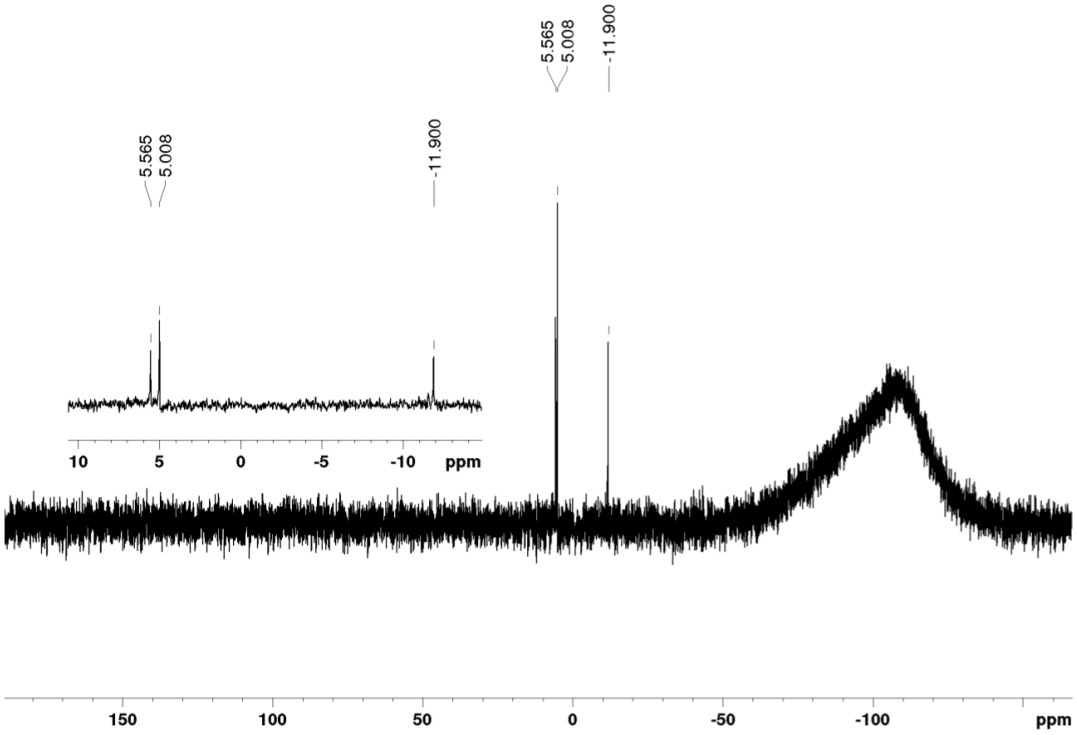

Figure 31.
^{29}Si NMR in C_6D_6 at 300 K of the worked-up reaction mixture of trapping germylene **6a** with Et_3SiH.

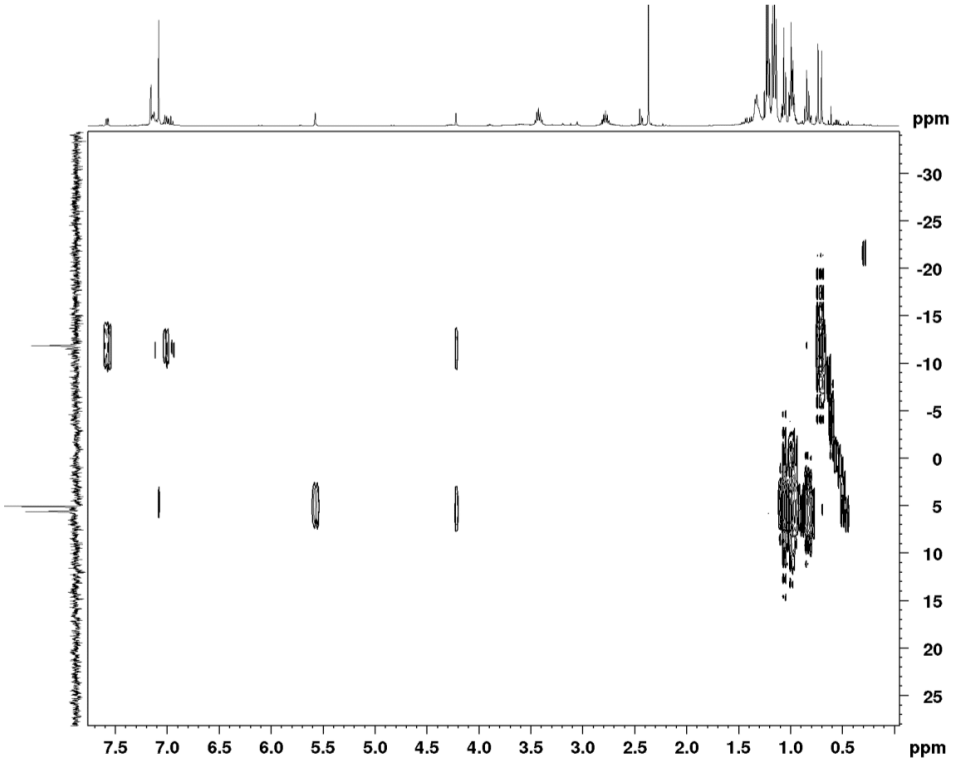

Figure 32.
$^{29}Si/^{1}H$ 2D NMR in C_6D_6 at 300 K of the worked up reaction mixture of trapping germylene **6a** with Et_3SiH.

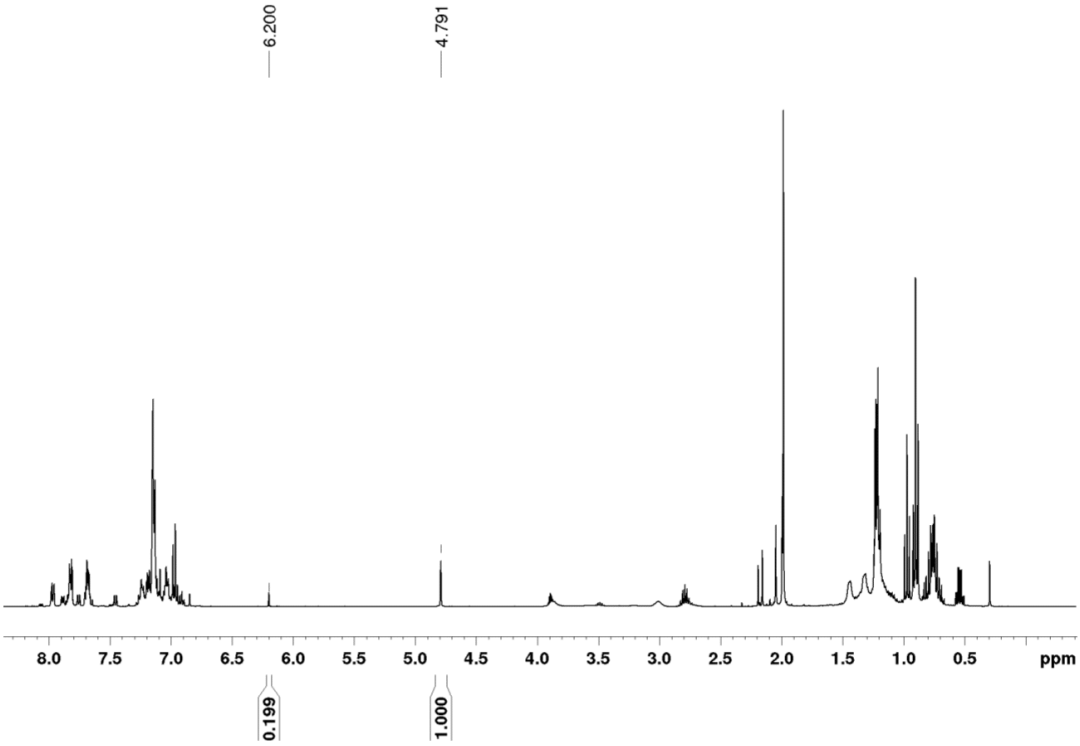

Figure 33.
^{1}H NMR in C_6D_6 at 300 K of the worked up reaction mixture of trapping germylene **6b** with Et_3SiH.

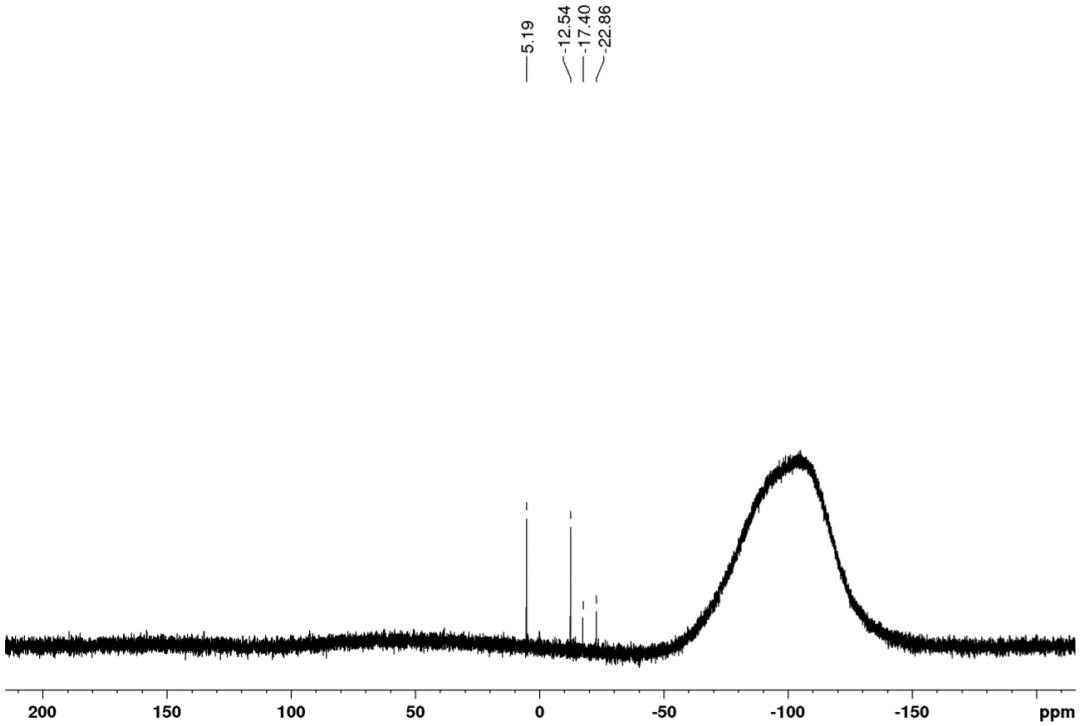

Figure 34.
^{29}Si NMR in C_6D_6 at 300 K of the worked up reaction mixture of trapping germylene **6b** with Et_3SiH.

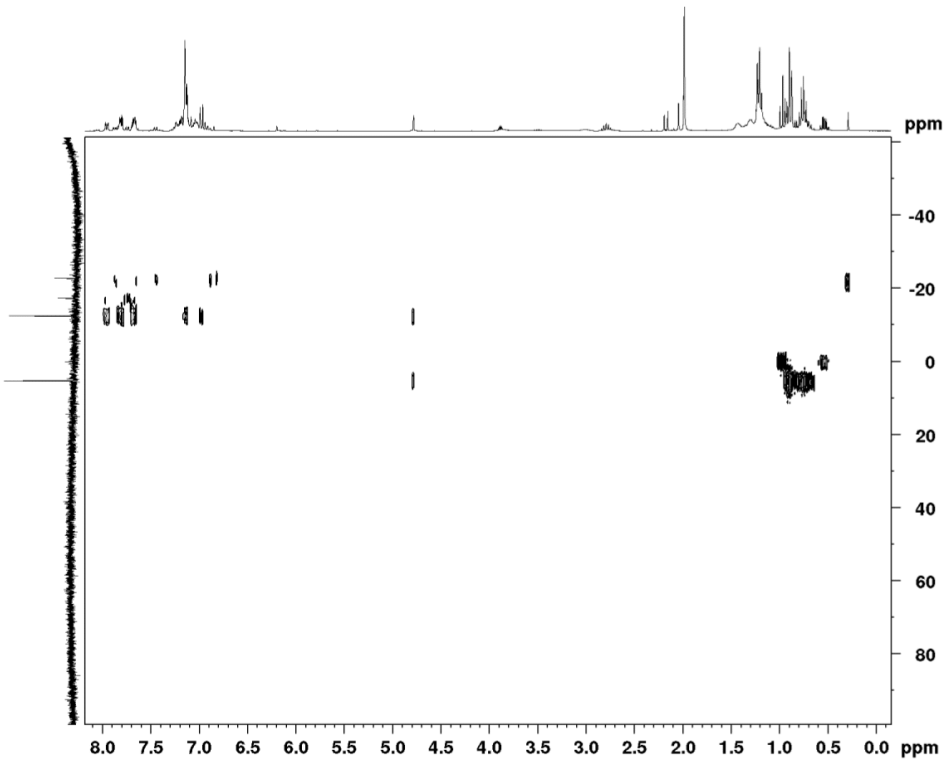

Figure 35.
$^{29}Si/^{1}H$ 2D NMR in C_6D_6 at 300 K of the worked up reaction mixture of trapping germylene **6b** with Et_3SiH.

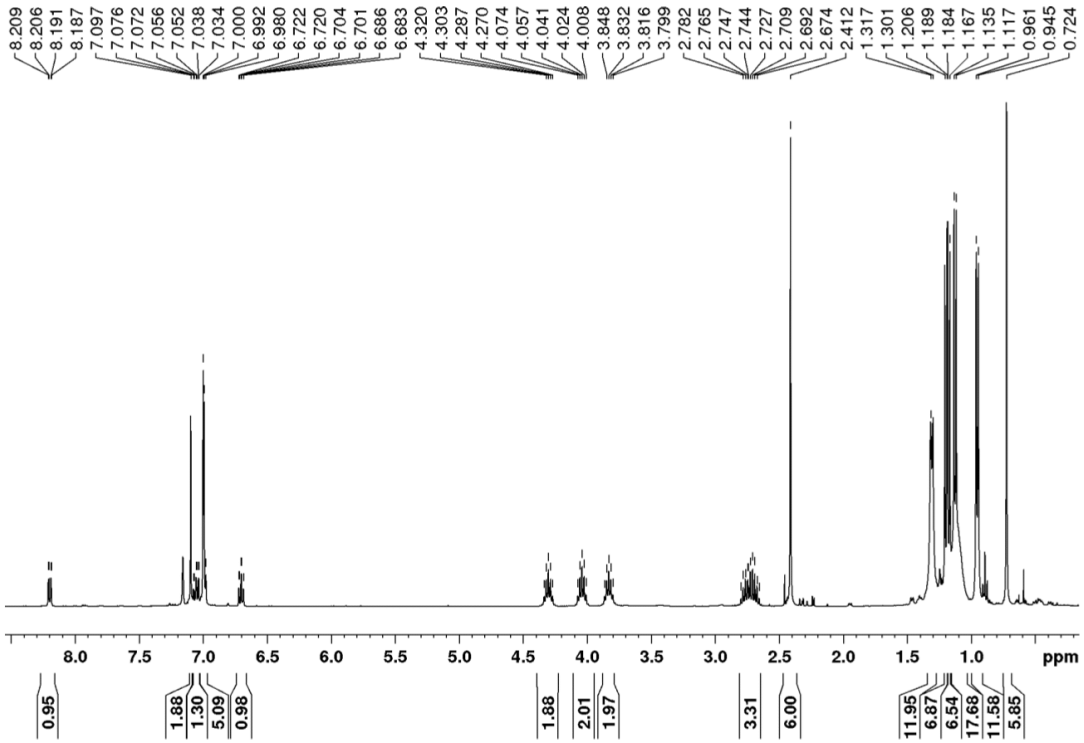

Figure 36.
^{1}H NMR of (*o*-dimethylanilino)silyldisilene in C_6D_6 at 300 K.

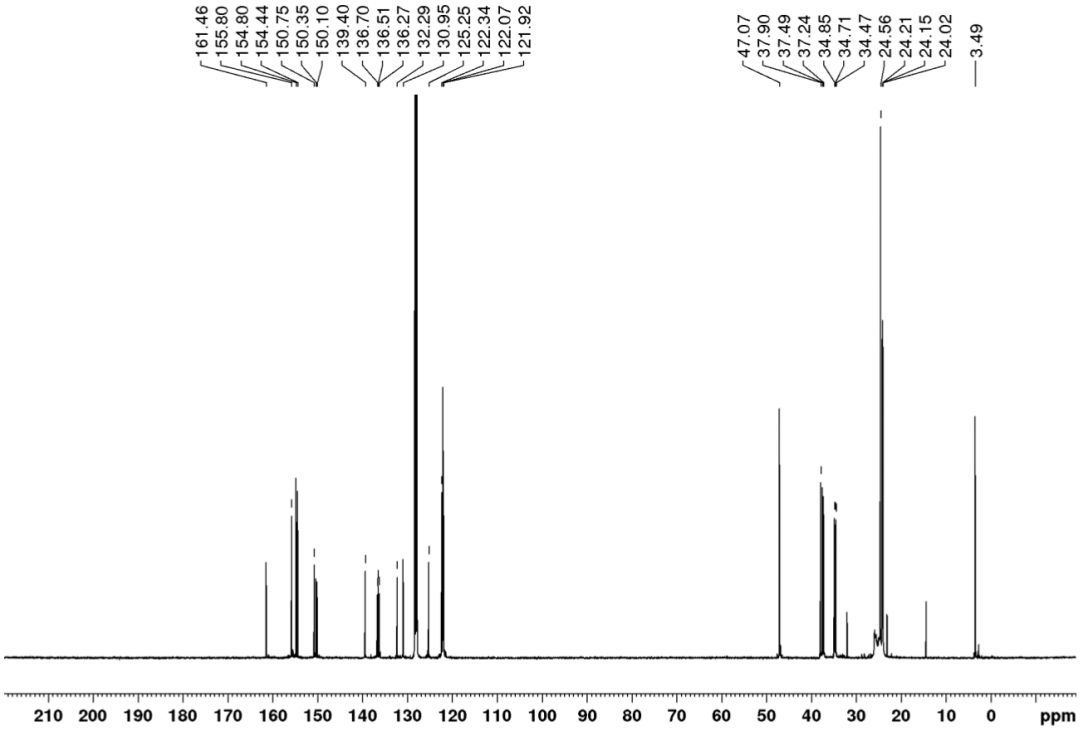

Figure 37.
$^{13}C\{^{1}H\}$ NMR of (*o*-dimethylanilino)silyldisilene in C_6D_6 at 300 K.

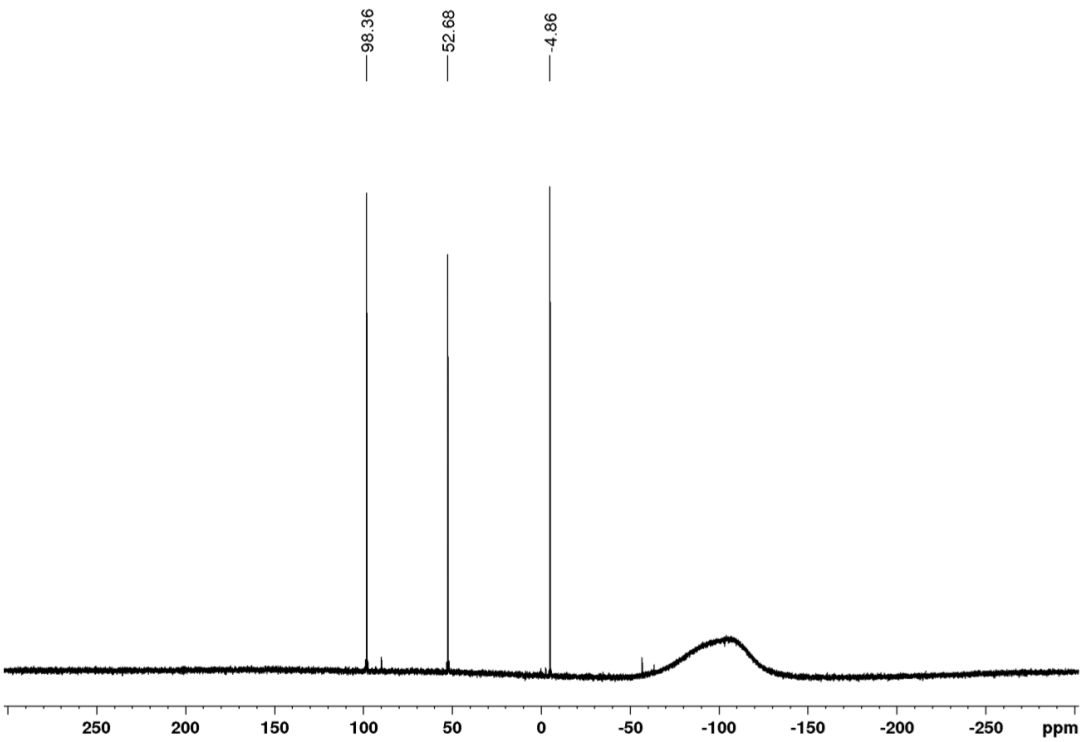

Figure 38.
$^{29}Si\{^{1}H\}$ NMR of (*o*-dimethylanilino)silyldisilene in C_6D_6 at 300 K.

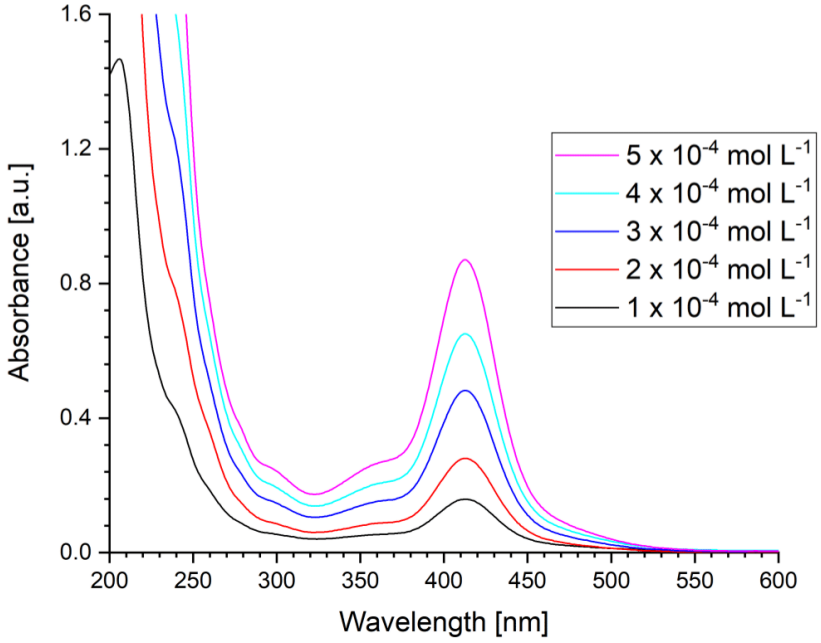

Figure 39.

UV/vis spectra of (*o*-dimethylanilino)silyldisilene in hexane at different concentrations ($1 \cdot 10^{-4}$ to $5 \cdot 10^{-4}$ mol L^{-1}).

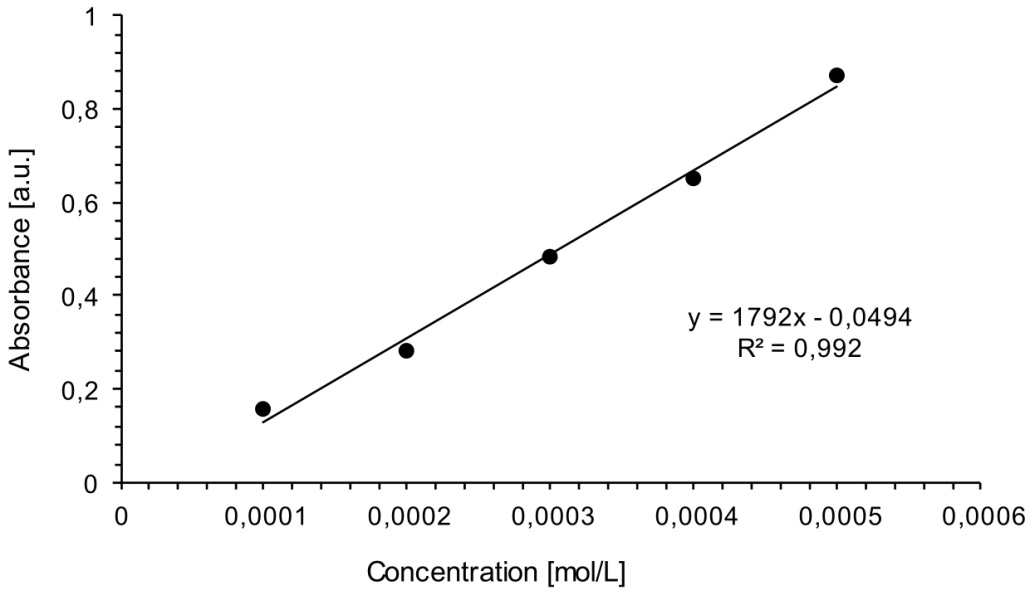

Figure 40.

Determination of ε (17900 L mol^{-1} cm^{-1}) by linear regression of absorbance (λ = 413 nm) of (*o*-dimethylanilino)silyldisilene against concentration.

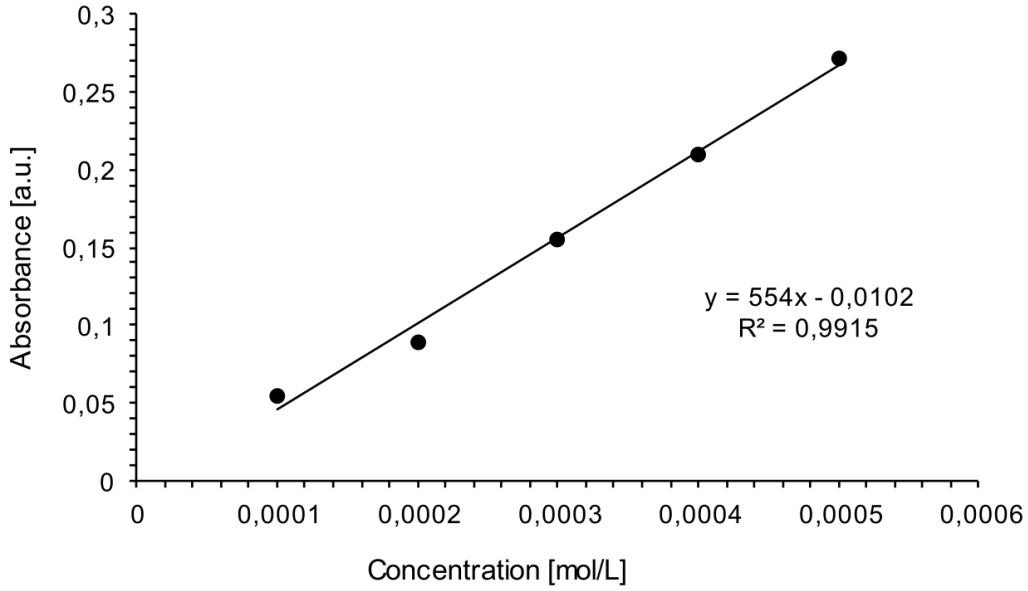

Figure 41.

Determination of ε (5500 L mol^{-1} cm^{-1}) by linear regression of absorbance (λ = 365 nm) of (*o*-dimethylanilino)silyldisilene against concentration.

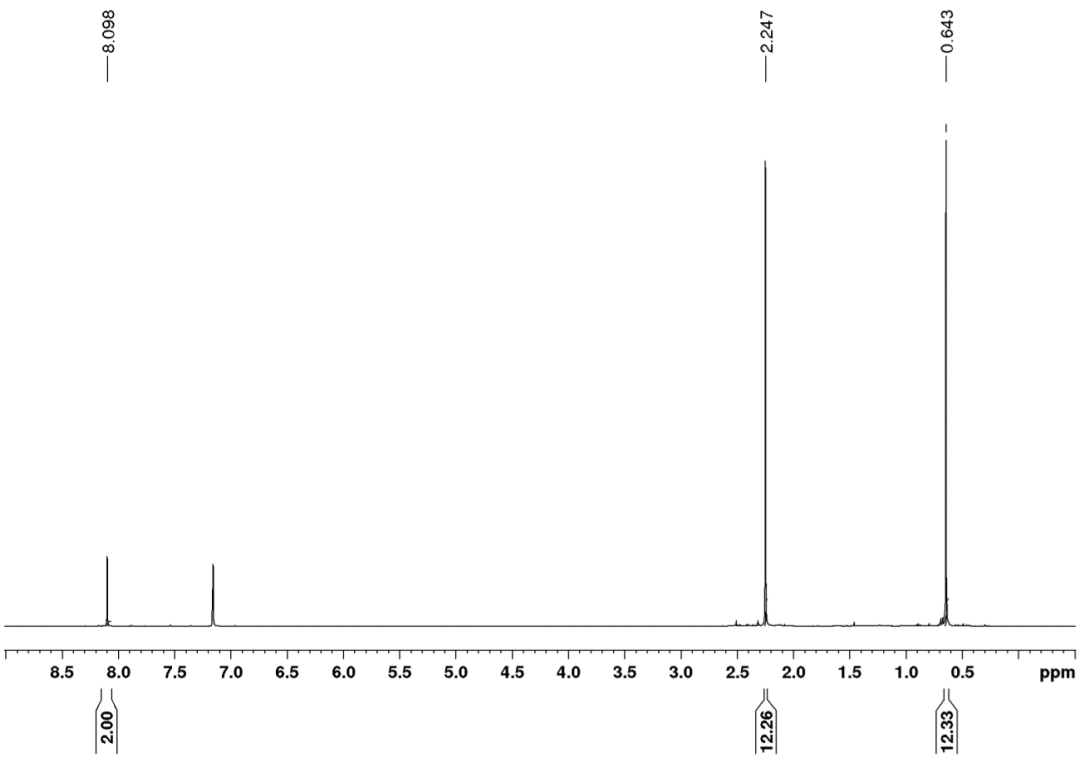

Figure 42.
^{1}H NMR of **10** in C_6D_6 at 300 K.

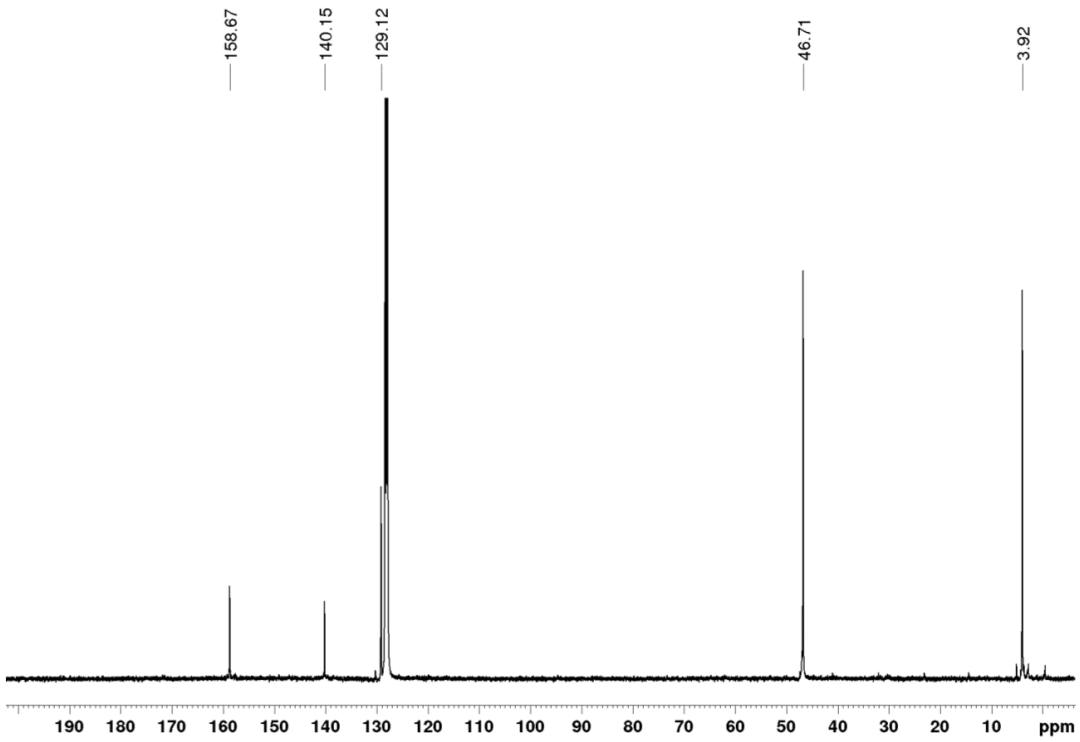

Figure 43.
$^{13}C\{^{1}H\}$ NMR of **10** in C_6D_6 at 300 K.

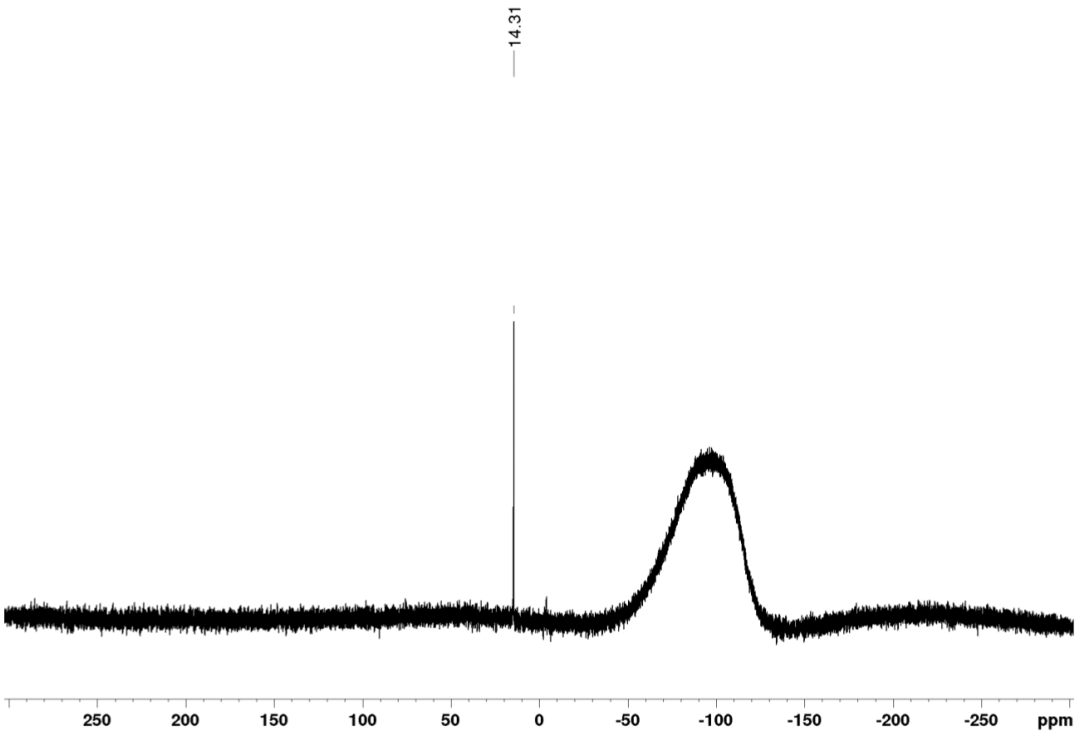

Figure 44.
$^{29}Si\{^{1}H\}$ NMR of **10** in C_6D_6 at 300 K.

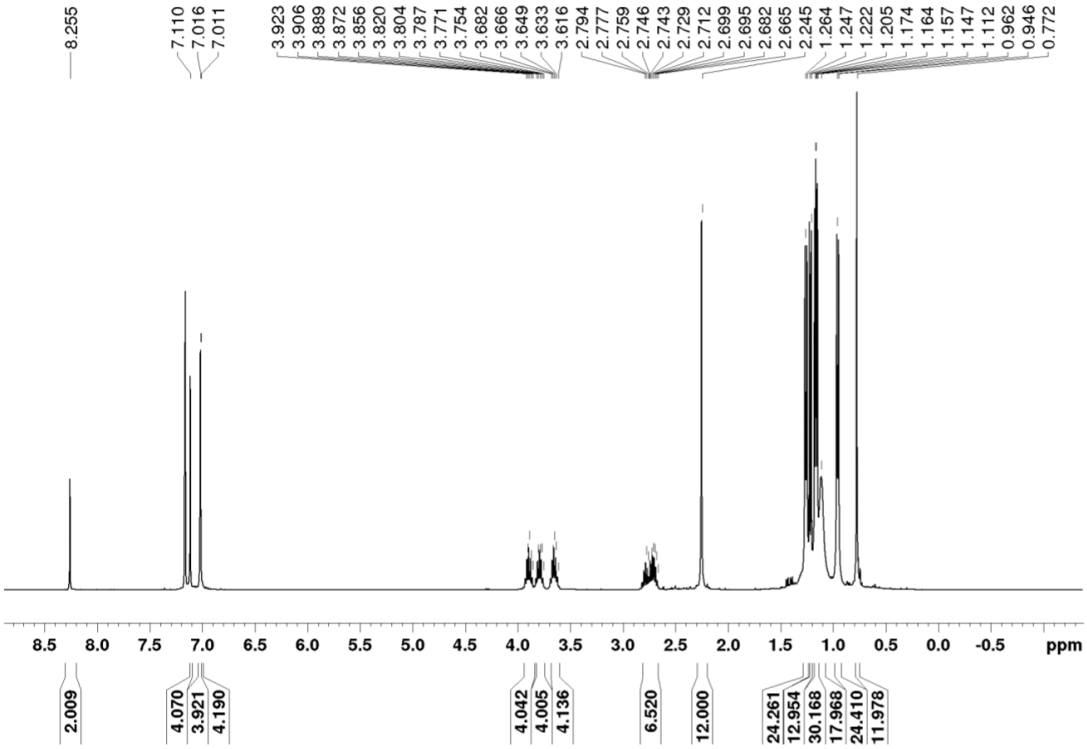

Figure 45.
^{1}H NMR of tetragermadiene **11** in C_6D_6 at 300 K.

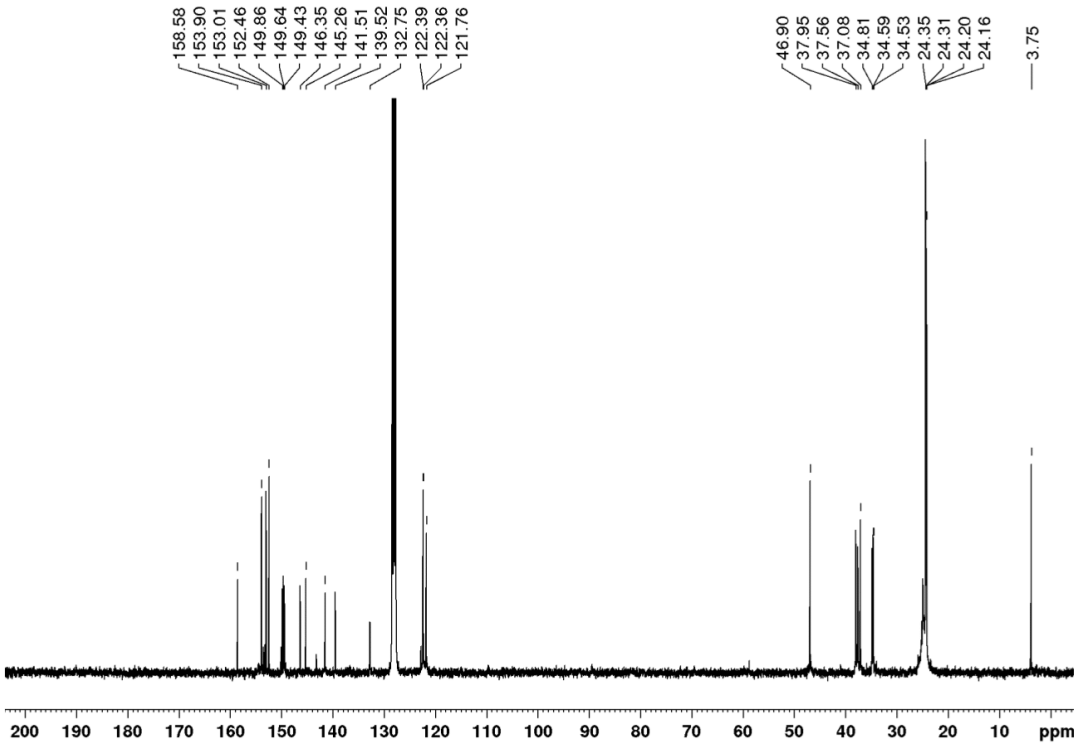

Figure 46.
$^{13}C\{^{1}H\}$ NMR of tetragermadiene **11** in C_6D_6 at 300 K.

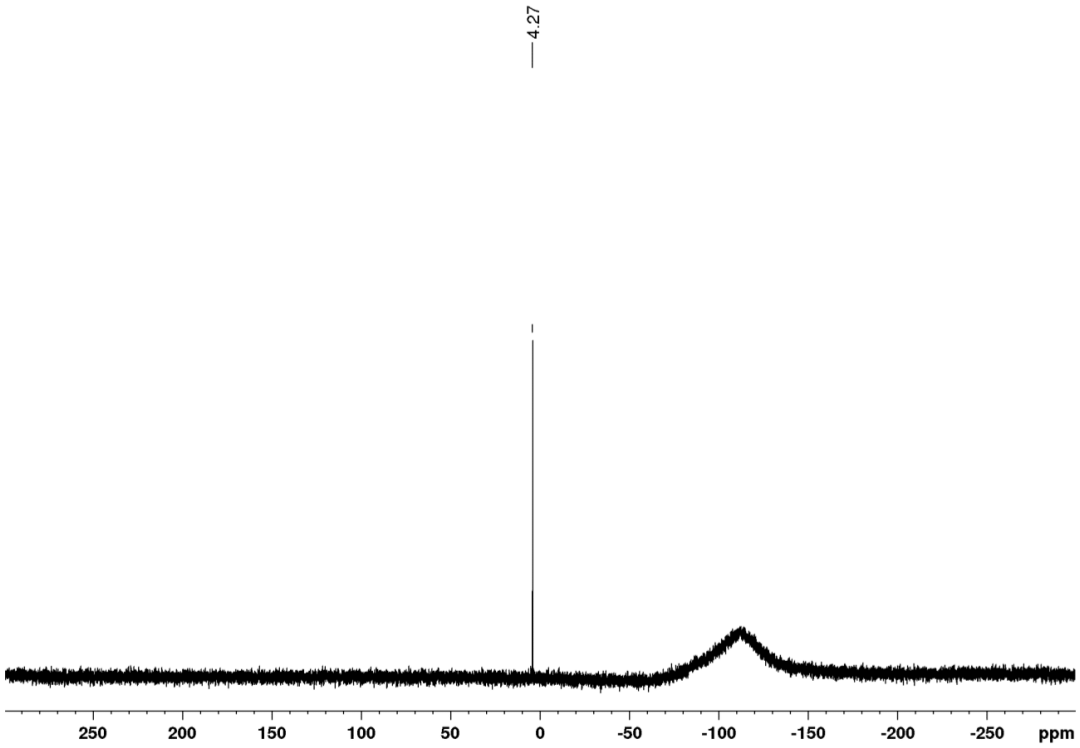

Figure 47.
$^{29}Si\{^{1}H\}$ NMR of tetragermadiene **11** in C_6D_6 at 300 K.

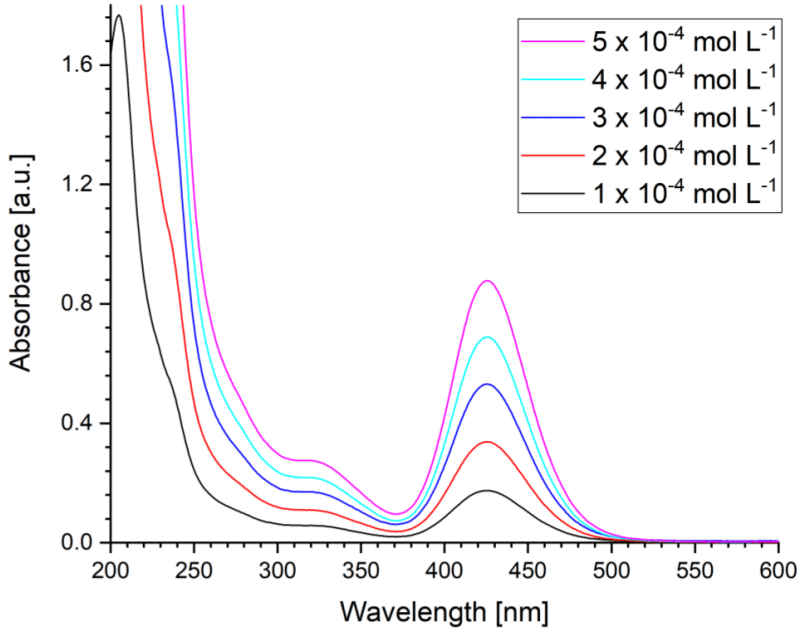

Figure 48.
UV/vis spectra of **11** in hexane at different concentrations ($1 \cdot 10^{-4}$ to $5 \cdot 10^{-4}$ mol L^{-1}).

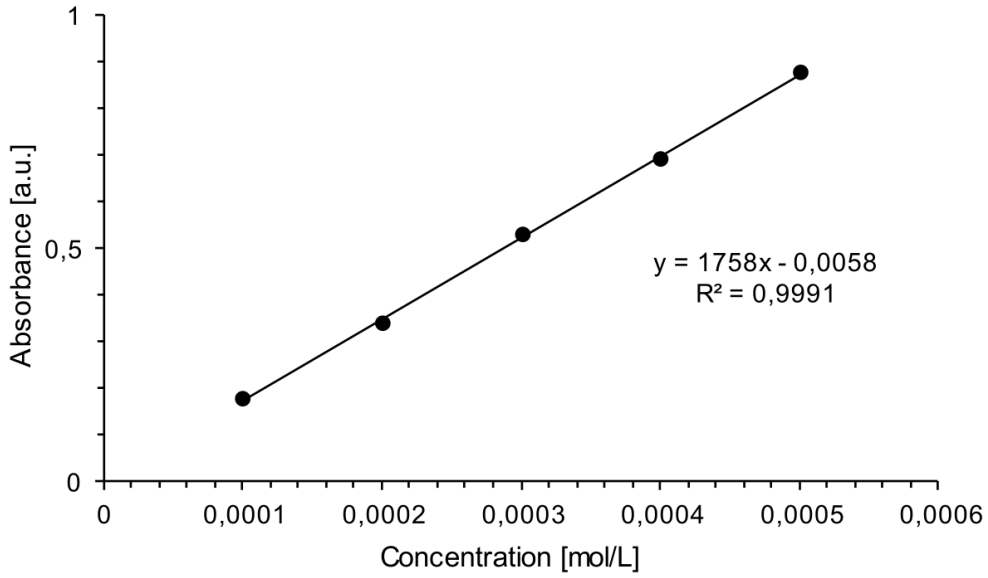

Figure 49.

Determination of ε (17600 L mol^{-1} cm^{-1}) by linear regression of absorbance (λ = 426 nm) of **11** against concentration.

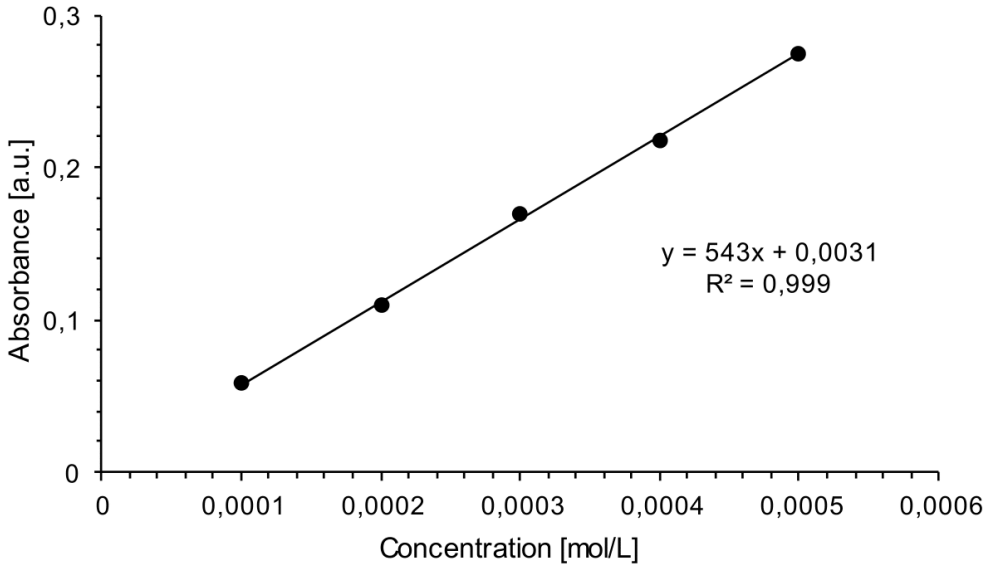

Figure 50.

Determination of ε (5400 L mol^{-1} cm^{-1}) by linear regression of absorbance (λ = 320 nm) of **11** against concentration.

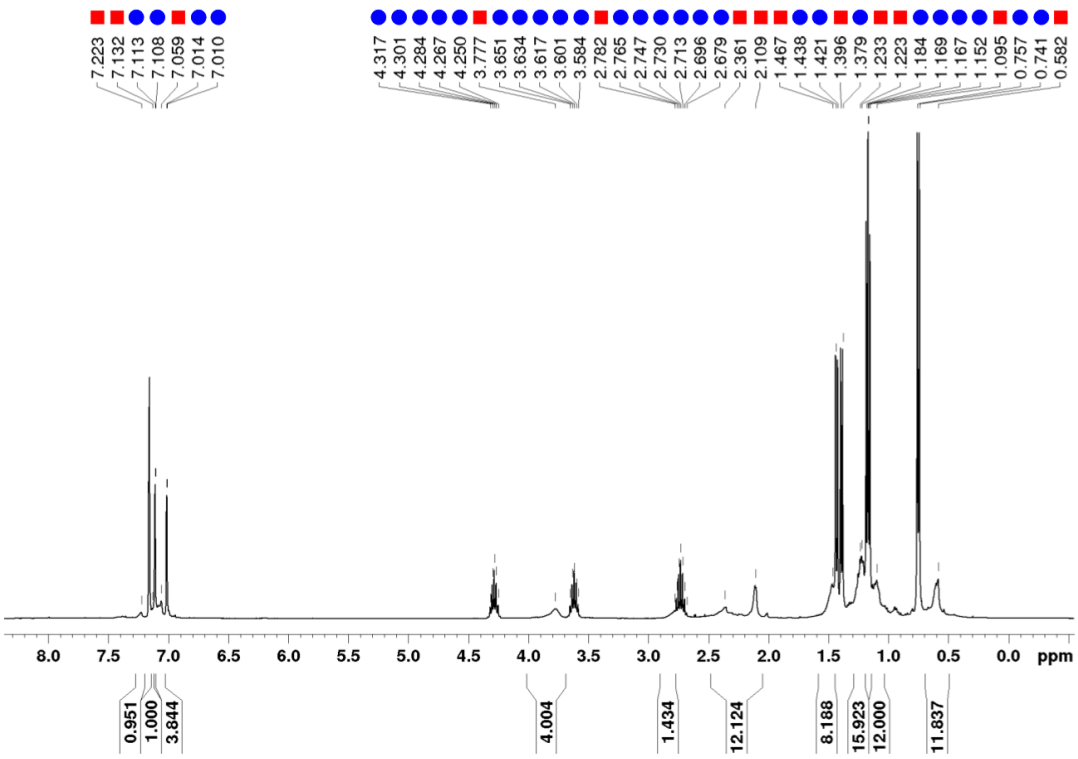

Figure 51.

^{1}H NMR of the polymerization reaction mixture for synthesis of polydigermene **P1** in C_6D_6 at 300 K (labelled with ■, signals of co-product digermene **2** with ●).

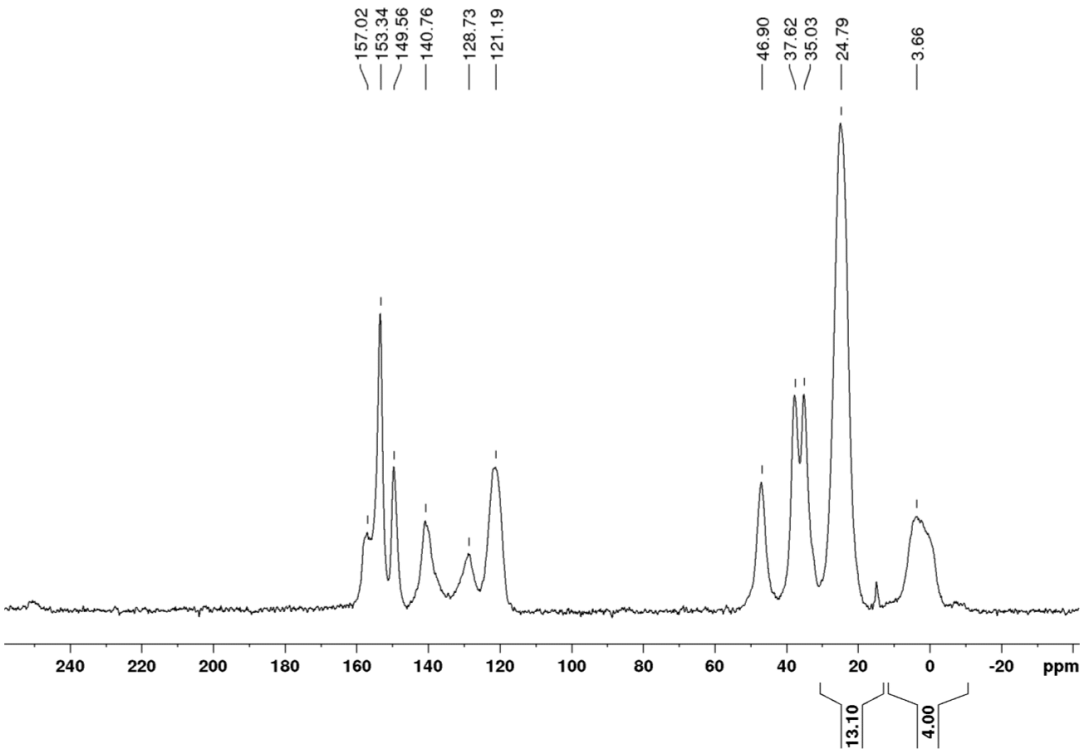

Figure 52.
^{13}C CP/MAS NMR spectrum of polydigermene **P1** at 300 K.

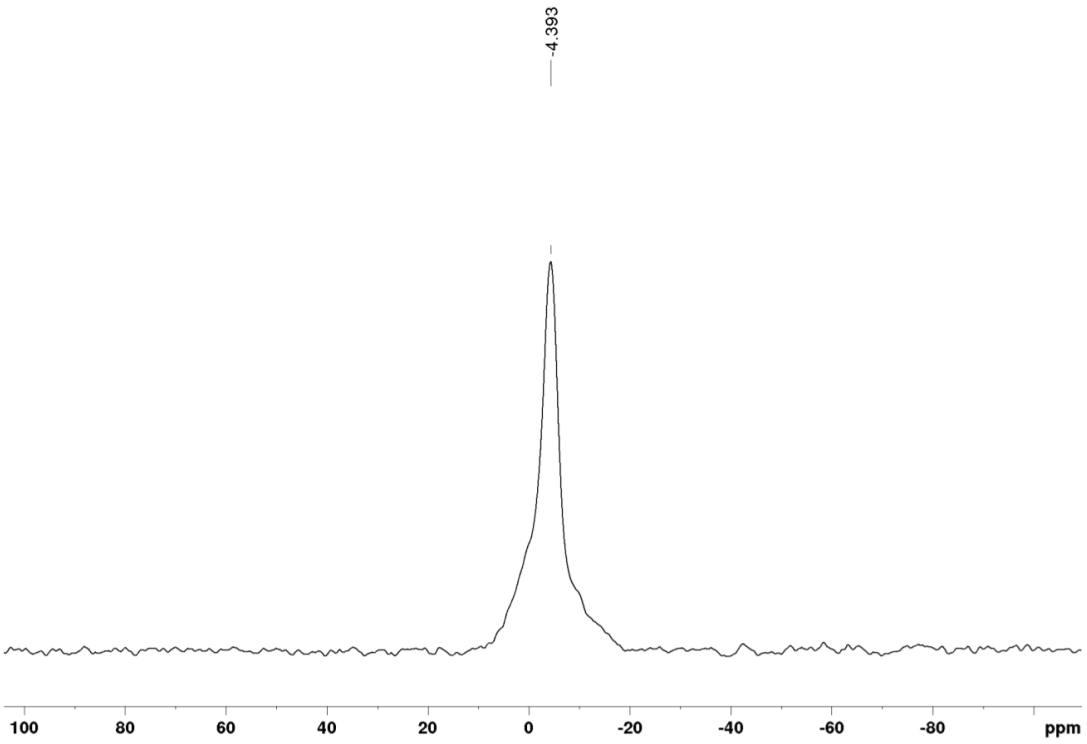

Figure 53.
^{29}Si CP/MAS NMR spectrum of polydigermene **P1** at 300 K.

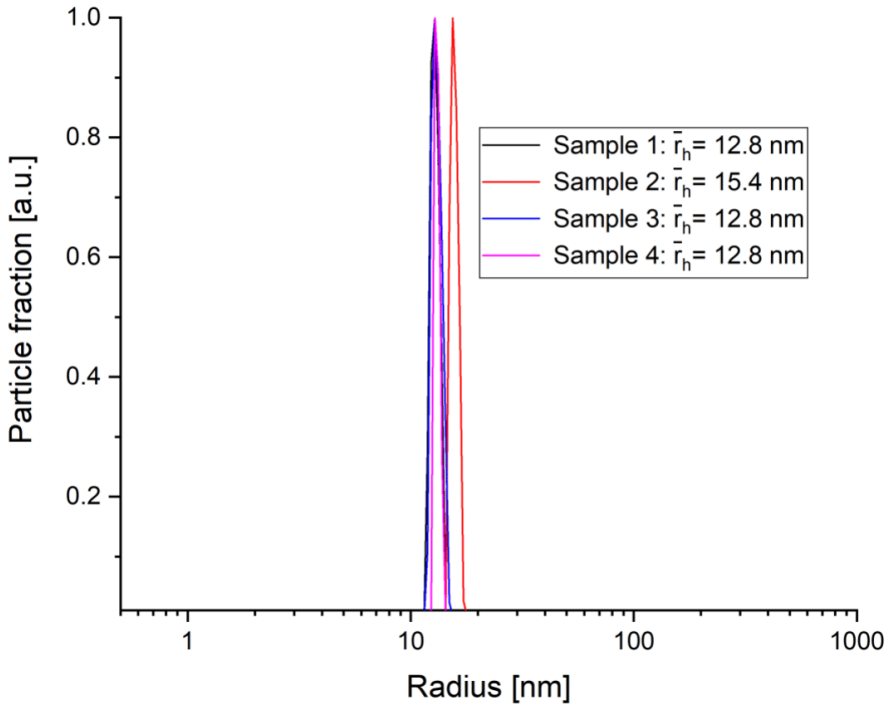

Figure 54.

Number-weighted size distribution of particles in a supernatant suspension of **P1** after centrifugation.

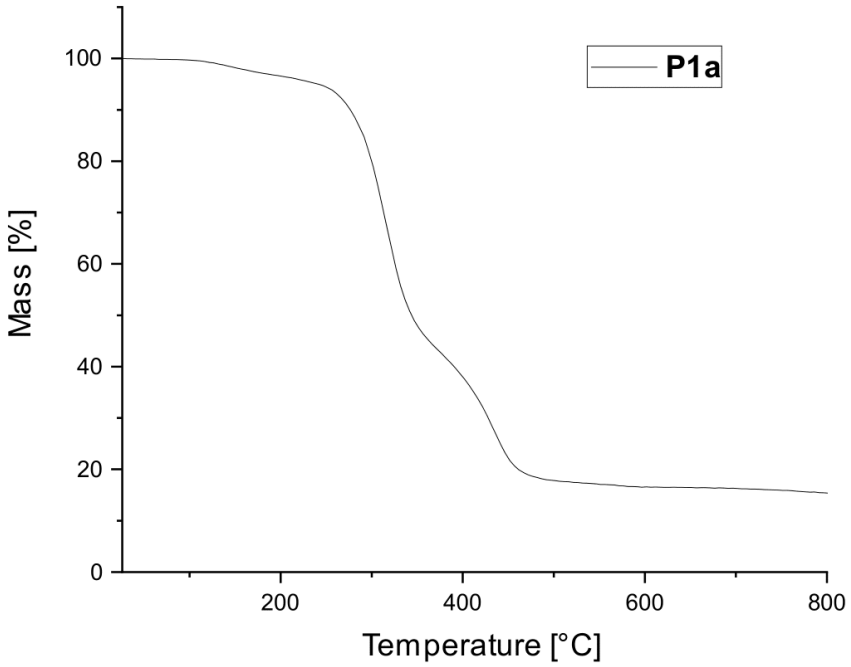

Figure 55.
TGA thermogram for polydigermene **P1**.

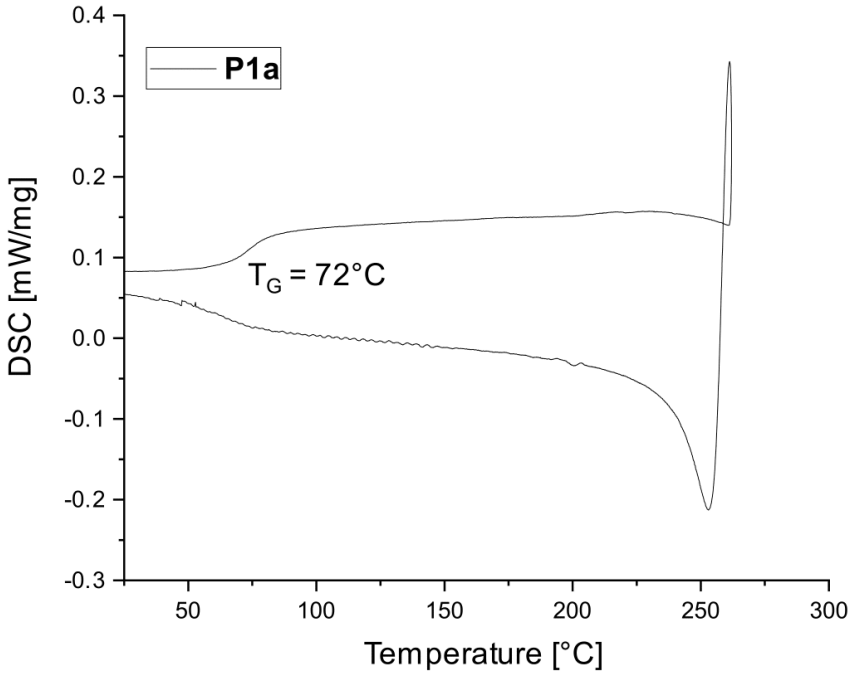

Figure 56.
DSC thermogram for polydigermene **P1** (third heating-cooling cycle).

Estimation of the degree of polymerization of polymer P1 by ^{1}H NMR spectroscopy

The acylic diene metathesis (ADMET) polymerization belongs to the step-growth polymerizations. For strictly linear polymers the Carother's equation[4] holds true:

$$\bar{X}_n = \frac{1}{1-p}$$

where $\bar{X}_n$ refers to the number-average value of the degree of polymerization and p refers to the conversion, which is in turn given by

$$p = \frac{N_0 - N_t}{N_0}$$

with N_0 for the initial number of monomer molecules and N_t for the total number of all molecules (regardless of their chain lengths) at the time t.

P_n be the n-mer in an AMDET-polymerization and P_c the co-condensate molecule that is released during the reaction. In the present case P_1 would be bisdigermene **11** and P_c would be homoleptic digermene **2**. The reaction will have to proceed on an intermediate course between two extremes: (1) a chain-growth reaction where one P_1 after another reacts to a single long chain P_n and (2) an ideal step-growth reaction where all P_1 react to P_2 which then react to P_4 and so on.
Case (1) can then be described as:

$$\begin{aligned} n\,P_1 &\rightarrow (n-2)\,P_1 + 1\,P_2 + 1\,P_c \\ &\rightarrow (n-k)\,P_1 + 1\,P_k + (k-1)\,P_c \\ &\rightarrow 0\,P_1 + 1\,P_n + (n-1)\,P_c \end{aligned}$$

and case (2) as:

$$\begin{aligned} n\,P_1 &\rightarrow (n-2)\,P_1 + 1\,P_2 + 1\,P_c \\ &\rightarrow (n-2k)\,P_1 + k\,P_2 + k\,P_c \\ &\rightarrow 0\,P_1 + \tfrac{n}{2}\,P_2 + \tfrac{n}{2}\,P_c \\ &\rightarrow 0\,P_1 + \tfrac{n}{4}\,P_4 + \tfrac{3n}{4}\,P_c \\ &\rightarrow 0\,P_1 + 1\,P_n + (n-1)\,P_c \end{aligned}$$

Assuming reaction course free of significant amounts of side-products, the stochiometric coefficients sum up to n in both cases (1) and (2), and hence every other intermediate pathway, irrespective of the completeness of conversion. It therefore follows that

$$N_0 = N_t + N_{t,c}$$

with $N_{t,c}$ as the number of molecules P_c present at time t. The formula for the conversion hence can be simplified to:

$$p = \frac{N_{t,c}}{N_0}$$

This formula allows in turn to calculate the degree of polymerization via the Carother's equation as $N_{t,c}$ can be easily determined from NMR spectroscopy.

To determine the degree of polymerization from **11** to **P1**, 40 mg of **11** (2.236 mmol) are put in an NMR tube, dissolved in 0.5 mL C_6D_6 and a ^{1}H NMR spectrum is measured immediately. The sample is then heated to 60°C in an oil bath for 44 hours. The degree of polymerization after total time t in the oil bath can then be calculated using the simplified Carother's equation from above. The spectrum before heating is used to reference the peak area of the solvent signal by integrating the septet of **11** at 3.66 ppm to a value of 4 (which corresponds to N_0) and reading off the peak area of the solvent signal (8.0700 in this case). The solvent signal peak area is then defined as this value in all subsequent spectra and integration of the septet of **2** at 4.29 ppm gives then $N_{t,c}$. In Table S1 all determined $N_{t,c}$ values as well as the according p and $\bar{X}_n$ values are listed. The table furthermore contains the weight-average degree of polymerization $\bar{X}_w$and the dispersity $Đ$ which are defined as follows:

$$\bar{X}_w = \frac{1+p}{1-p}$$

$$Đ = \frac{\bar{X}_w}{\bar{X}_n}$$

Table 1.

Conversion p and estimated maximum number and weight average degree of polymerization $\bar{X}_n$ and $\bar{X}_w$ after selected time intervals of the ADMET polymerization of **11** to **P1** determined from ^{1}H NMR spectroscopy.

Time [h]	Peak area [a.u.]	Conversion p [%]	$\bar{X}_n$	$\bar{X}_w$	Đ
0	0	0	1.00	1.00	1.00
1	0.329	8.583	1.09	1.18	1.08
2	0.6426	16.065	1.19	1.38	1.16
3	0.8414	21.035	1.27	1.53	1.21
4	1.0919	27.298	1.38	1.75	1.27
5	1.3157	32.893	1.49	1.98	1.32
20	3.1082	77.705	4.49	7.97	1.78
24	3.3954	84.885	6.62	12.23	1.84
44	3.8267	95.668	23.08	45.16	1.95

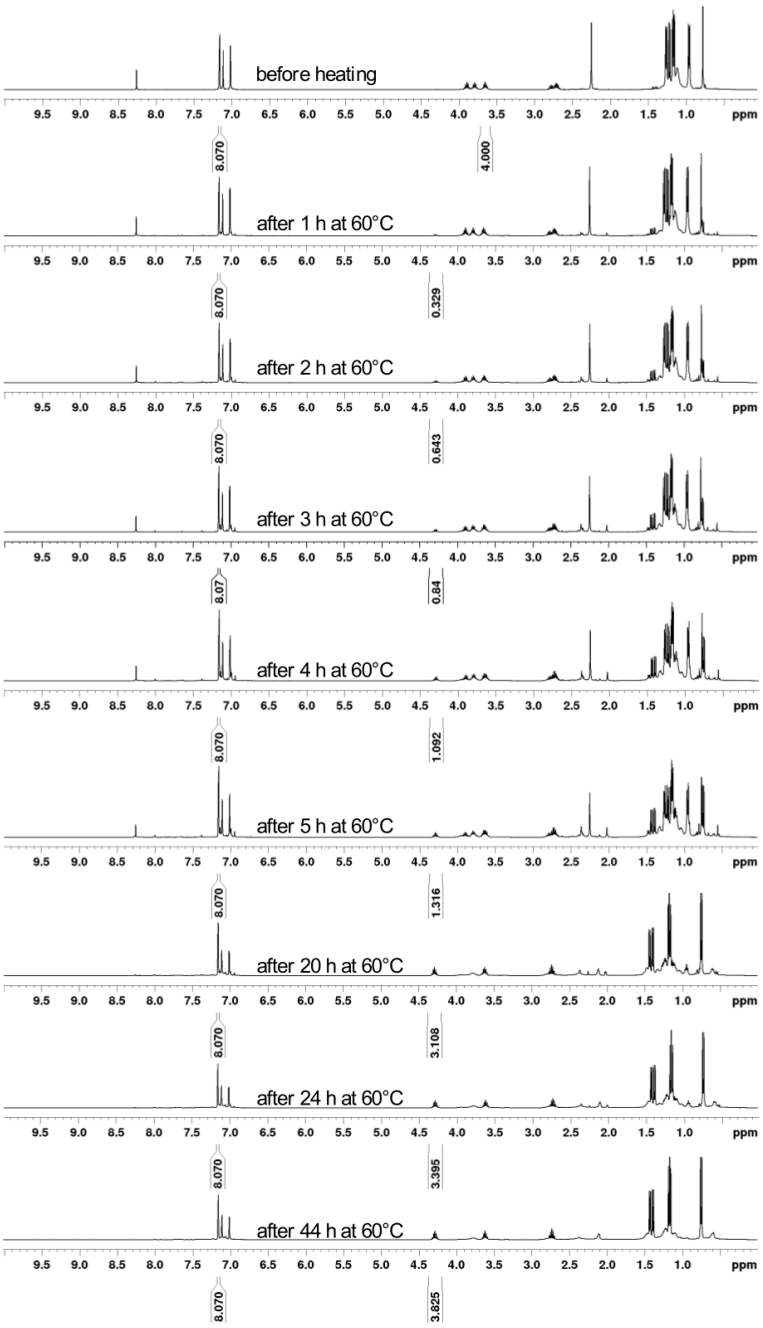

Figure 57.
Screening of polymerization to **P1** for determination of $\bar{X}_n$.

64

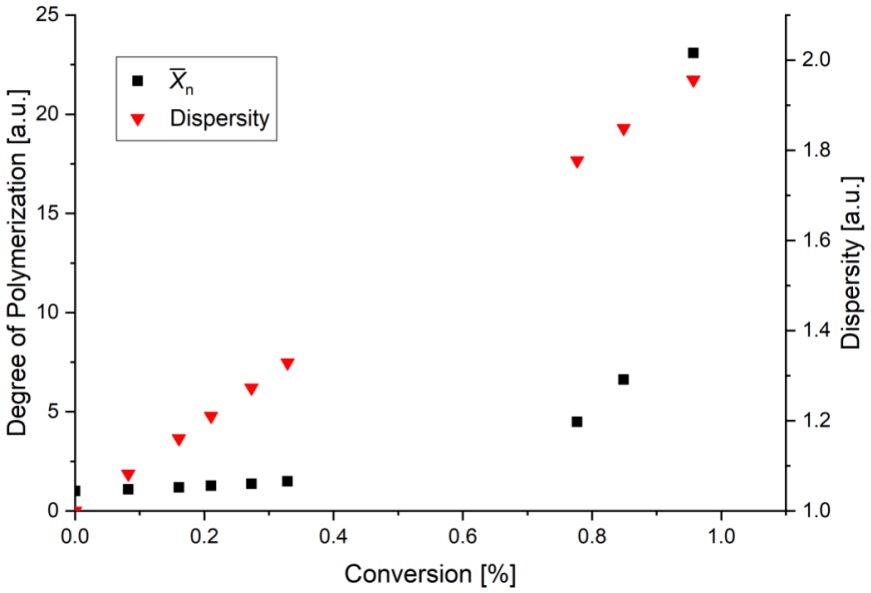

Figure 58.
Plot of number average degree of polymerization $\bar{X}_n$.and dispersity Đ against conversion.

Kinetic model for the number average degree of polymerization $\overline{X}_n$

Generally, every step of the polymerization from **11** to **P1** can be described as:

$$A_n + A_m \rightarrow A_{n+m}$$

With A_n, A_m and A_{n+m} being n-, m- and n+m-mers and B being homoleptic digermene **2**. When one now assumes that there is no reactivity difference between monomers, dimers and higher -mers, it is more convenient to describe the reaction as one where "reactive species" R and "unreactive species" U are transformed into each other. Consequently, in a normal step during the polymerization two reactive species form one reactive species and one unreactive species.

$$R + R \rightarrow R + U$$

Where R is any n-mer and U is the unreactive digermene **2**. It follows that in every step of the polymerization the number of reactive species decreases by one and the number of unreactive species increases by one as well. One can therefore model the general reaction step as

$$R \rightarrow U$$

For such unimolecular reactions, the concentration of R and U as a function of the reaction time t is described as

$$[R]_t = [R]_0 e^{-kt} \quad (1)$$
$$[U]_t = [R]_0 - [R]_0 e^{-kt} \quad (2)$$

Simultaneously, the polymerization degree $\bar{X}$ in dependence of the conversion is given by the Carother's equation[4]:

$$\bar{X} = \frac{1}{1-\frac{[U]_t}{[R]_0}} \quad (3)$$

Putting eq. (3) into eq. (3) gives then an expression for $\bar{X}$ in dependence of the time:

$$\bar{X} = \frac{1}{1-\frac{[R]_0-[R]_0 e^{-kt}}{[R]_0}} = \frac{1}{1-(1-e^{-kt})} = e^{kt} \quad (4)$$

Fitting this simple exponential law on the data acquired from ^{1}H NMR spectroscopy gives the graph in Supplementary Figure 59 with a R^2 value of 0.99701 and k = 1.99 10^{-5} s^{-1}.

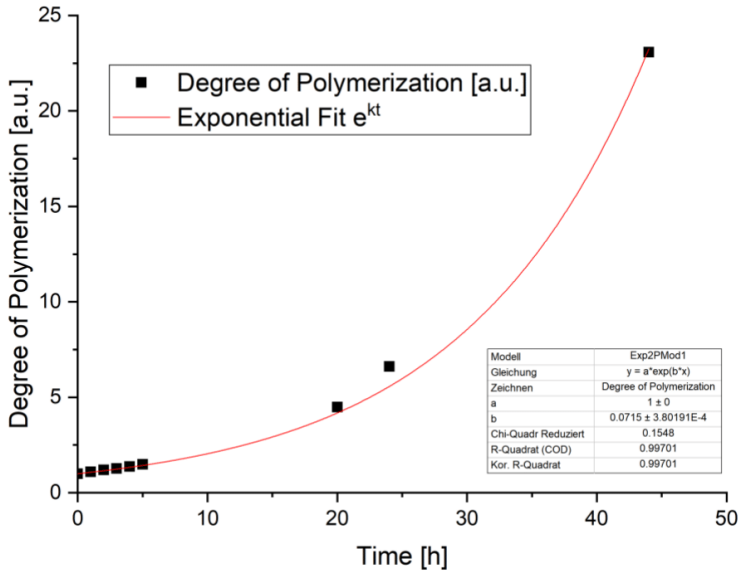

Figure 59.
Exponential fit of eq. (4) with data from Supplementary Table 1.

Crystallographic data and refinement

Crystallographic data have been deposited with the Cambridge Crystallographic Data Center as supplementary publication no. CCDC 1948744 (**3b**), 1948745 (***E*-5a**), 1948746 (***E*-5b**), 1948747 (***Z*-5b**), 1995973 (**10**) and 1995974 (**11**).These data can be obtained free of charge from The Cambridge Crystallographic Data Centre via www.ccdc.cam.ac.uk/data_request/cif

Table 2.

Selected bond lengths (in Å) and angles (in °) of symmetrically substituted digermenes ***E*-5a,b** and ***Z*-5a,b** and asymmetrically substituted α,ω-tetragermadiene **11.**

	***E*-5a**	***E*-5b**	***Z*-5b**		**11**
Ge−Ge [Å]	2.2576(5)	2.2604(6)	2.2909(6)	Ge−Ge [Å]	2.3038(4)
Ge−Si [Å]	2.3778(5)	2.387(1)	2.4014(5)	Ge−Si [Å]	2.4007(7)
Ge2−Si2 [Å]	–	2.4045(9)	–	Ge2−Si2 [Å]	–
Ge−N [Å]	4.074(1)	5.310(3)	3.597(1)	Ge−N [Å]	5.332(2)
Ge2−N2 [Å]	–	5.471(3)	–	Ge2−N2 [Å]	–
Si-N [Å]	3.1708(9)	3.002(3)	3.080(1)	Si-N [Å]	2.984(2)
Si2-N2 [Å]	–	3.199(3)	–	Si2-N2 [Å]	–
°Σ(Ge) [°]	355.1	357.2	352.3	°Σ(Ge) [°]	346.69
°Σ(Ge2) [°]	–	359.6	–	°Σ(Ge2) [°]	352.40
θ(Ge) [°]	21.5	15.25	26.0	θ(Ge) [°]	31.9
θ(Ge2) [°]	–	5.9	–	θ(Ge2) [°]	14.9
τ [°]	0.0	20.1	23.9	τ [°]	18.0

Table 3.

Crystal data and structure refinement for CCDC 1948744 (**3b**).

Identification code	sh4121	
Empirical formula	C40 H40 Cl2 N2 Si2	
Formula weight	675.82	
Temperature	152(2) K	
Wavelength	0.71073 Å	
Crystal system	Monoclinic	
Space group	I2/a	
Unit cell dimensions	a = 16.9805(11) Å	α= 90°.
	b = 8.8975(5) Å	β= 91.813(3)°.
	c = 24.2322(12) Å	γ = 90°.
Volume	3659.3(4) $Å^3$	
Z	4	
Density (calculated)	1.227 Mg/m^3	
Absorption coefficient	0.273 mm^{-1}	
F(000)	1424	
Crystal size	0.410 x 0.333 x 0.250 mm^3	
Theta range for data collection	1.682 to 30.636°.	
Index ranges	-24<=h<=24, -12<=k<=12, -34<=l<=34	
Reflections collected	72154	
Independent reflections	5656 [R(int) = 0.0291]	
Completeness to theta = 25.242°	100.0 %	
Absorption correction	Semi-empirical from equivalents	
Max. and min. transmission	0.7461 and 0.7205	
Refinement method	Full-matrix least-squares on F^2	
Data / restraints / parameters	5656 / 0 / 288	
Goodness-of-fit on F^2	1.062	
Final R indices [I>2sigma(I)]	R1 = 0.0316, wR2 = 0.0859	
R indices (all data)	R1 = 0.0367, wR2 = 0.0901	
Extinction coefficient	n/a	
Largest diff. peak and hole	0.388 and -0.250 $e.Å^{-3}$	

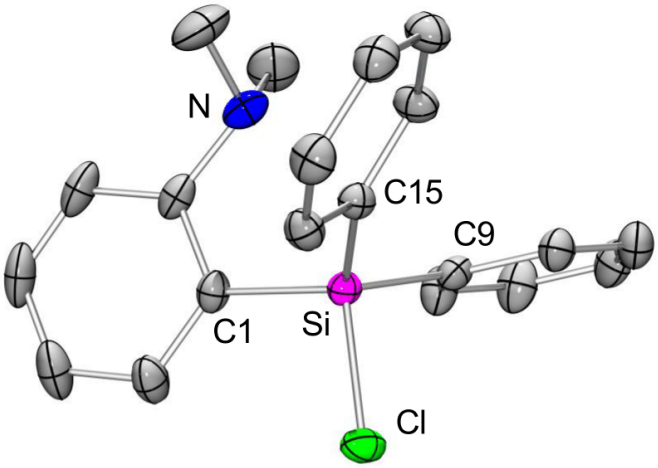

Figure 60.

Molecular structure of **3b** in the solid state (hydrogens omitted for clarity; thermal ellipsoids at 50% probability). Selected bond lengths (in Å): Si-Cl 2.1017(5), N-Si 2.8506(9), Si-C1 1.859(1), Si-C9 1.857(1), Si-C15 1.860(1).

Table 4.

Crystal data and structure refinement for CCDC 1948745 (***E*-5a**).

Identification code	sh4120	
Empirical formula	C50 H78 Ge2 N2 Si2	
Formula weight	908.50	
Temperature	152(2) K	
Wavelength	0.71073 Å	
Crystal system	Triclinic	
Space group	P-1	
Unit cell dimensions	a = 10.4649(19) Å	α= 97.181(4)°.
	b = 10.9528(18) Å	β= 107.644(4)°.
	c = 13.128(2) Å	γ = 111.201(4)°.
Volume	1289.5(4) $Å^3$	
Z	1	
Density (calculated)	1.170 Mg/m^3	
Absorption coefficient	1.244 mm^{-1}	
F(000)	484	
Crystal size	0.605 x 0.290 x 0.112 mm^3	
Theta range for data collection	2.068 to 36.405°.	
Index ranges	-17<=h<=17, -18<=k<=18, -21<=l<=21	
Reflections collected	49014	
Independent reflections	12517 [R(int) = 0.0367]	
Completeness to theta = 25.242°	100.0 %	
Absorption correction	Semi-empirical from equivalents	
Max. and min. transmission	0.7471 and 0.6420	
Refinement method	Full-matrix least-squares on F^2	
Data / restraints / parameters	12517 / 18 / 404	
Goodness-of-fit on F^2	1.025	
Final R indices [I>2sigma(I)]	R1 = 0.0316, wR2 = 0.0736	
R indices (all data)	R1 = 0.0501, wR2 = 0.0811	
Extinction coefficient	n/a	
Largest diff. peak and hole	1.342 and -0.666 $e.Å^{-3}$	

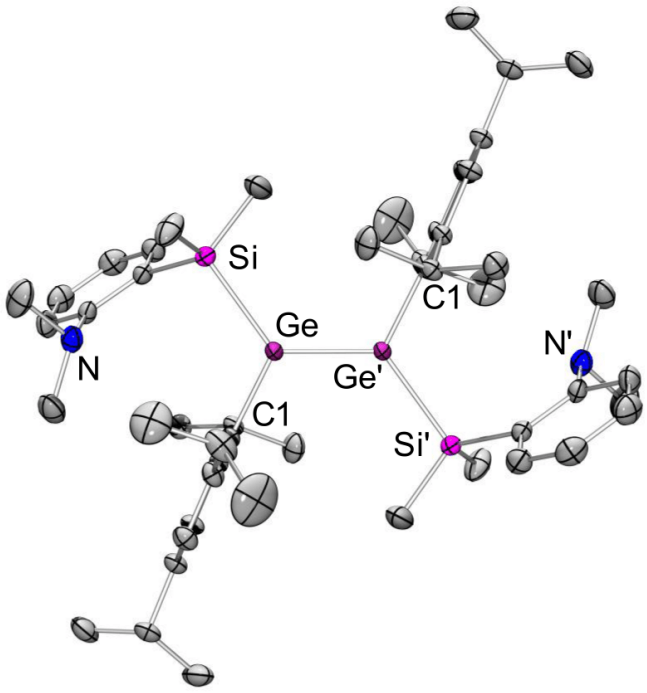

Figure 61.

Molecular structure of ***E*-5a** in the solid state (hydrogens omitted for clarity; thermal ellipsoids at 50% probability). Selected bond lengths (in Å) and angles (in °): Ge-Ge' 2.2576(5), Ge-Si 2.3778(5), Ge-C1 1.9601(9), N-Ge 4.073(1), C1-Ge-Si 116.99(4), Si-Ge-Ge' 123.42(1), Ge'-Ge-C1 114.70(3), Σ°(Ge) 355.1, θ(Ge) 21.5, τ 0.0.

Table 5.

Crystal data and structure refinement for CCDC 1948746 (***E*-5b**).

Identification code	sh4142	
Empirical formula	C70 H86 Ge2 N2 Si2	
Formula weight	1156.76	
Temperature	152(2) K	
Wavelength	0.71073 Å	
Crystal system	Triclinic	
Space group	P-1	
Unit cell dimensions	a = 10.9149(7) Å	α= 100.468(2)°.
	b = 13.8140(9) Å	β= 91.287(2)°.
	c = 22.6460(16) Å	γ = 108.258(2)°.
Volume	3177.1(4) $Å^3$	
Z	2	
Density (calculated)	1.209 Mg/m^3	
Absorption coefficient	1.025 mm^{-1}	
F(000)	1224	
Crystal size	0.567 x 0.251 x 0.104 mm^3	
Theta range for data collection	1.584 to 25.448°.	
Index ranges	-13<=h<=13, -16<=k<=16, -27<=l<=27	
Reflections collected	41281	
Independent reflections	11753 [R(int) = 0.0396]	
Completeness to theta = 25.242°	100.0 %	
Absorption correction	Semi-empirical from equivalents	
Max. and min. transmission	0.7452 and 0.6778	
Refinement method	Full-matrix least-squares on F^2	
Data / restraints / parameters	11753 / 27 / 731	
Goodness-of-fit on F^2	1.022	
Final R indices [I>2sigma(I)]	R1 = 0.0496, wR2 = 0.1123	
R indices (all data)	R1 = 0.0747, wR2 = 0.1236	
Extinction coefficient	n/a	
Largest diff. peak and hole	1.470 and -1.169 $e.Å^{-3}$	

The Alert level B in the checkcif (difference in the Hirshfeld test for Ge1 and Ge2) is related to a slight positional disorder of the Ge atoms which caused the extraordinary anisotropic displacement parameters.

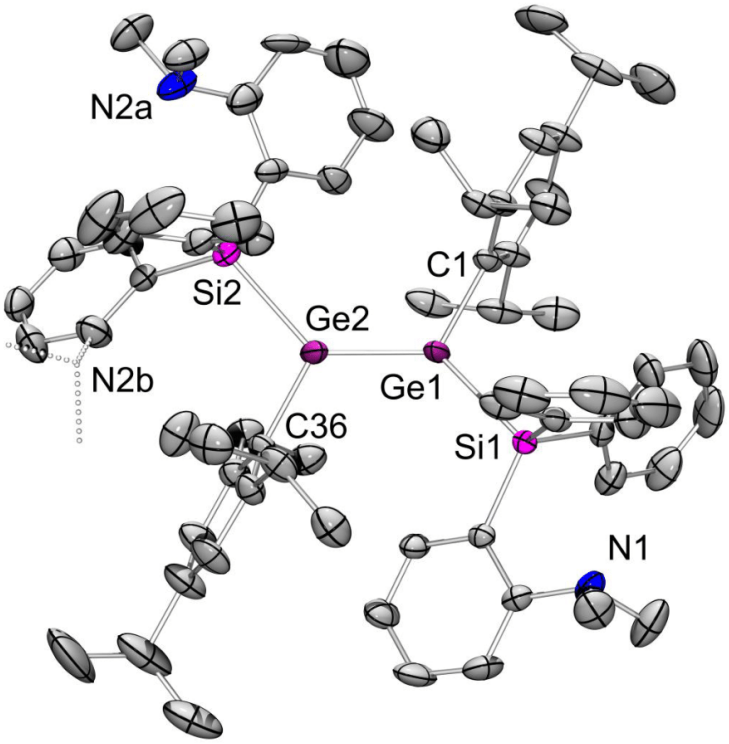

Figure 62.

Molecular structure of ***E*-5b** in the solid state (hydrogens omitted for clarity; thermal ellipsoids at 50% probability). The anilino group at Si2 is slightly disordered about two positions by rotation around Ge2-Si2 in an occupation ratio of N2a to N2b of 0.854 to 0.146. The minor position is shown with dashed bonds and without thermal ellipsoids. The Alert level B in the checkcif (difference in the Hirshfeld test for Ge1 and Ge2) is related to this rotational disorder. Unresolved disorder at Ge2 but not Ge1 is adversely affecting the physical plausibility of the thermal ellipsoids at these atoms. Selected bond lengths (in Å) and angles (in °): Ge1-Ge2 2.2604(6), Ge1-Si1 2.387(1), Ge2-Si2 2.4045(9), Ge-C1 1.980(4), Ge2-C36 1.976(4), N1-Ge1 5.310(3), N2a-Ge2 5.471(3), C1-Ge1-Si1 109.4(1), Si1-Ge1-Ge2 127.23(3), Ge2-Ge1-C1 120.4(1), C36-Ge2-Si2 109.9(1), Si2-Ge2-Ge1 130.92(3), Ge1-Ge2-C36 118.6(1), Σ°(Ge1) 357.2, Σ°(Ge2) 359.6, θ(Ge1) 15.2, θ(Ge2) 5.9, τ 20.1.

Table 6.
Crystal data and structure refinement for CCDC 1948747 (**Z-5b**).

Identification code	sh4147	
Empirical formula	C70 H86 Ge2 N2 Si2	
Formula weight	1156.76	
Temperature	152(2) K	
Wavelength	0.71073 Å	
Crystal system	Monoclinic	
Space group	C2/c	
Unit cell dimensions	a = 20.8248(6) Å	α= 90°.
	b = 13.2686(6) Å	β= 112.992(3)°.
	c = 24.3799(9) Å	γ = 90°.
Volume	6201.4(4) $Å^3$	
Z	4	
Density (calculated)	1.239 Mg/m^3	
Absorption coefficient	1.050 mm^{-1}	
F(000)	2448	
Crystal size	0.270 x 0.253 x 0.180 mm^3	
Theta range for data collection	1.815 to 34.321°.	
Index ranges	-32<=h<=32, -21<=k<=20, -38<=l<=38	
Reflections collected	98559	
Independent reflections	12930 [R(int) = 0.0418]	
Completeness to theta = 25.242°	100.0 %	
Absorption correction	Semi-empirical from equivalents	
Max. and min. transmission	0.7467 and 0.7054	
Refinement method	Full-matrix least-squares on F^2	
Data / restraints / parameters	12930 / 0 / 515	
Goodness-of-fit on F^2	1.030	
Final R indices [I>2sigma(I)]	R1 = 0.0297, wR2 = 0.0712	
R indices (all data)	R1 = 0.0443, wR2 = 0.0764	
Extinction coefficient	n/a	
Largest diff. peak and hole	0.475 and -0.235 $e.Å^{-3}$	

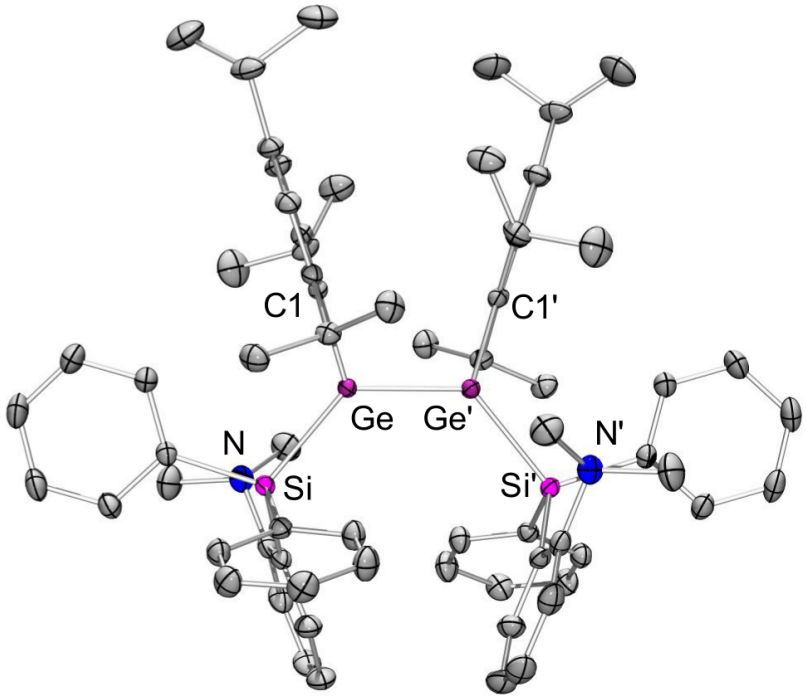

Figure 63.

Molecular structure of ***Z*-5b** in the solid state (hydrogens omitted for clarity; thermal ellipsoids at 50% probability). Selected bond lengths (in Å) and angles (in °): Ge-Ge' 2.2909(6), Ge-Si 2.4014(5), Ge-C1 1.987(1), N-Ge 3.597(1), C1-Ge-Si 114.58(3), Si-Ge-Ge' 129.78(2), Ge'-Ge-C1 107.90(3), Σ°(Ge) 352.3, θ(Ge) 26.0, τ 23.9.

Table 7.

Crystal data and structure refinement for CCDC 1995973 (**10**).

Identification code	sh4197	
Empirical formula	C14 H26 Cl2 N2 Si2	
Formula weight	349.45	
Temperature	133(2) K	
Wavelength	0.71073 Å	
Crystal system	Triclinic	
Space group	P-1	
Unit cell dimensions	a = 6.3961(7) Å	α= 62.274(3)°.
	b = 9.0974(9) Å	β= 89.152(4)°.
	c = 9.4554(10) Å	γ = 81.605(4)°.
Volume	480.91(9) $Å^3$	
Z	1	
Density (calculated)	1.207 Mg/m^3	
Absorption coefficient	0.456 mm^{-1}	
F(000)	186	
Crystal size	0.209 x 0.133 x 0.076 mm^3	
Theta range for data collection	2.438 to 27.870°.	
Index ranges	-7<=h<=8, -11<=k<=11, -12<=l<=12	
Reflections collected	6676	
Independent reflections	2265 [R(int) = 0.0543]	
Completeness to theta = 25.242°	99.5 %	
Absorption correction	Semi-empirical from equivalents	
Max. and min. transmission	0.7456 and 0.6790	
Refinement method	Full-matrix least-squares on F^2	
Data / restraints / parameters	2265 / 0 / 143	
Goodness-of-fit on F^2	1.086	
Final R indices [I>2sigma(I)]	R1 = 0.0576, wR2 = 0.1463	
R indices (all data)	R1 = 0.0812, wR2 = 0.1606	
Extinction coefficient	n/a	
Largest diff. peak and hole	0.457 and -0.662 $e.Å^{-3}$	

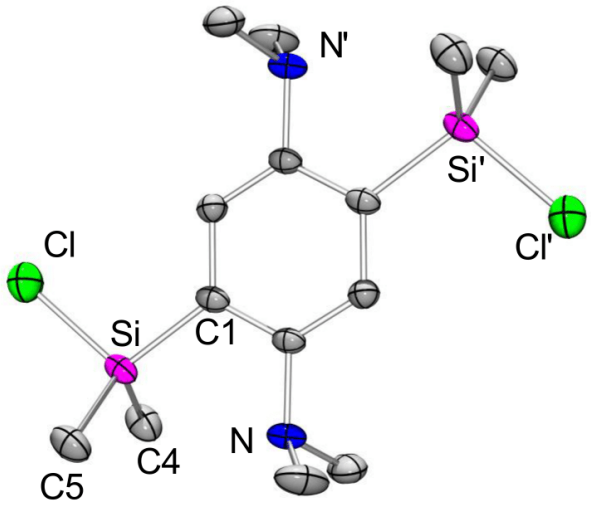

Figure 64.

Molecular structure of **10** in the solid state (hydrogens omitted for clarity; thermal ellipsoids at 50% probability). Selected bond lengths (in Å): Si-Cl 2.080(2), N-Si 2.893(4), Si-C1 1.872(3), Si-C4 1.849(4), Si-C5 1.850(4).

Table 8.

Crystal data and structure refinement for CCDC 1995974 (**11**).

Identification code	4222_a	
Empirical formula	C110 H170 Ge4 N2 Si2	
Formula weight	1867.01	
Temperature	130(2) K	
Wavelength	0.71073 Å	
Crystal system	Triclinic	
Space group	P-1	
Unit cell dimensions	a = 10.8632(5) Å	α= 87.664(2)°.
	b = 12.8566(6) Å	β= 88.582(2)°.
	c = 20.2422(9) Å	γ = 73.687(2)°.
Volume	2710.8(2) $Å^3$	
Z	1	
Density (calculated)	1.144 Mg/m^3	
Absorption coefficient	1.164 mm^{-1}	
F(000)	1000	
Crystal size	0.175 x 0.174 x 0.095 mm^3	
Theta range for data collection	2.185 to 27.978°.	
Index ranges	-14<=h<=14, -16<=k<=16, -26<=l<=26	
Reflections collected	82972	
Independent reflections	12976 [R(int) = 0.0730]	
Completeness to theta = 25.242°	99.9 %	
Absorption correction	Semi-empirical from equivalents	
Max. and min. transmission	0.7456 and 0.6685	
Refinement method	Full-matrix least-squares on F^2	
Data / restraints / parameters	12976 / 573 / 724	
Goodness-of-fit on F^2	1.043	
Final R indices [I>2sigma(I)]	R1 = 0.0446, wR2 = 0.1086	
R indices (all data)	R1 = 0.0690, wR2 = 0.1205	
Extinction coefficient	n/a	
Largest diff. peak and hole	1.453 and -0.557 $e.Å^{-3}$	

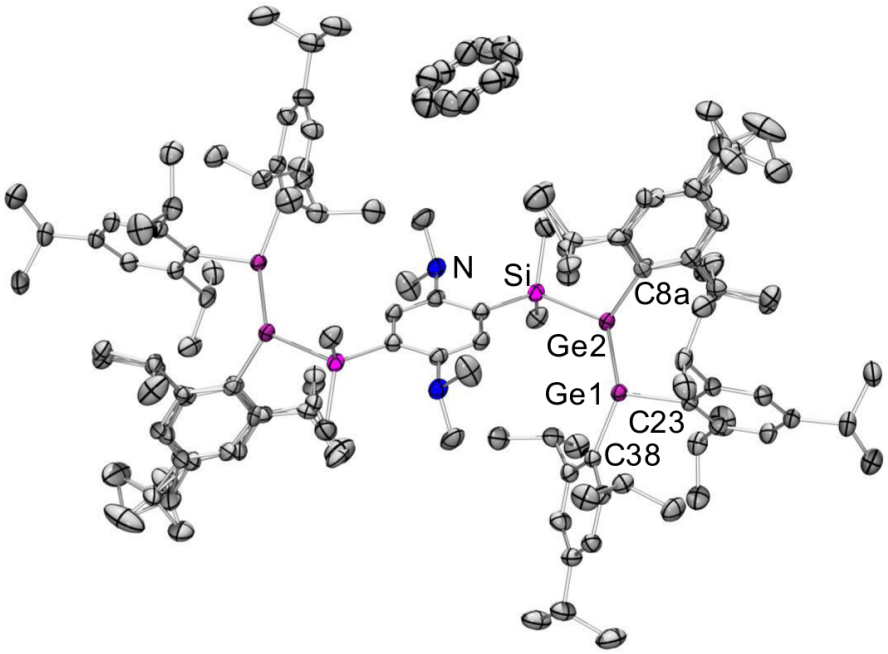

Figure 65.

Molecular structure of **11** in the solid state (hydrogens omitted for clarity; thermal ellipsoids at 50% probability). Selected bond lengths (in Å) and angles (in °): Ge1-Ge2 2.3038(4), Ge2-Si 2.4007(7), Ge2-C8a 1.982(9), Ge1-C23 1.978(2), Ge1-C38 1.986(2), N-Si 2.984(2), N-Ge2 5.332(2), Ge2-Ge1-C23 110.34(7), C23-Ge1-C38 105.7(1), C38-Ge1-Ge2 130.65(7), Si-Ge2-C8a 109.4(5), C8a-Ge2-Ge1 113.5(5), Ge1-Ge2-Si 129.50(2), °Σ(Ge1) 346.69, °Σ(Ge2) 352.40, θ(Ge1) 31.9, θ(Ge2) 24.9, τ 18.0.

DFT-Calculations

General:

Structural optimizations and frequency analysis were carried out at the BP86/def2-SVP level of theory including D3 dispersion correction by Grimme,[5-10] using the Gaussian 16 program package.[11] Optimized structures are plotted using ChemCraft 1.8.[12] Single-Point energies were determined at the M06-2X/def2-TVPP level of theory. [7, 8, 13] Population analysis was carried out using the NBO 3.1 program package[14] at the M06-2X/def2-SVPP level of theory.[7, 8, 13]

Optimized Structures

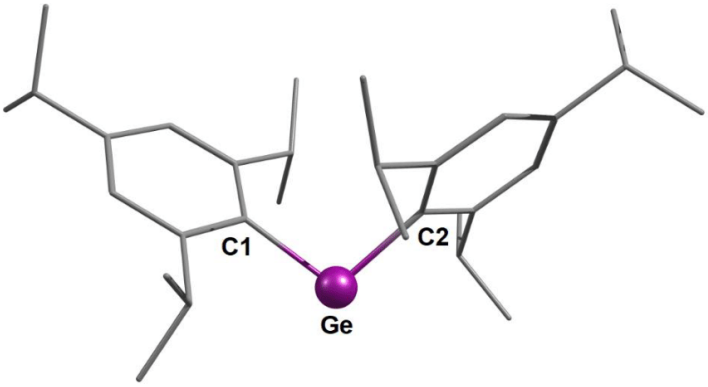

Ge-C1	2.0358
Ge-C2	2.0360
C1-Ge-C2	101.318

Figure 66.
Optimized structure of Tip_2Ge **8** and selected bond lengths [Å] and -angles [°] (E_{M062X} = −3247.79664710 Hartree).

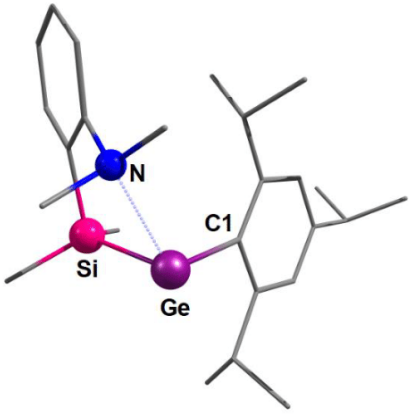

Ge-C1	2.0775
Ge-Si	2.4761
C1-Ge-Si	88.857
N-Ge	2.4662

Figure 67.
Optimized structure of germylene **6a** and selected bond lengths [Å] and -angles [°] (E_{M062X} = −3397.32437623 Hartree).

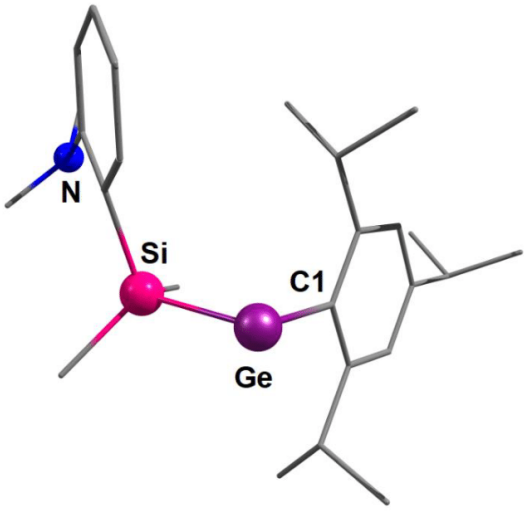

Ge-C1	2.0148
Ge-Si	2.5043
C1-Ge-Si	91.499

Figure 68.
Optimized structure of germylene **6a'** without donor-stabilization and selected bond lengths [Å] and -angles [°] (E_{M062X} = −3397.30477642 Hartree).

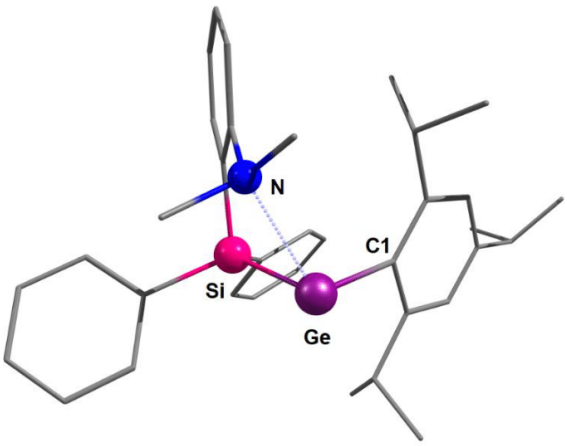

Ge-C1	2.0747
Ge-Si	2.4807
C1-Ge-Si	89.840
N-Ge	2.5137

Figure 69.
Optimized structure of germylene **6b** and selected bond lengths [Å] and -angles [°] (E_{M062X} = −3780.78793638 Hartree).

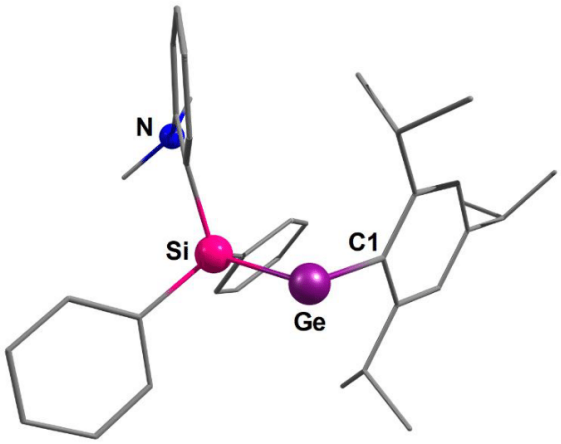

Ge-C1	2.0102
Ge-Si	2.5061
C1-Ge-Si	94.839

Figure 70.
Optimized structure of germylene **6b'** without donor-stabilization and selected bond lengths [Å] and -angles [°] (E_{M062X} = −3780.76970888 Hartree).

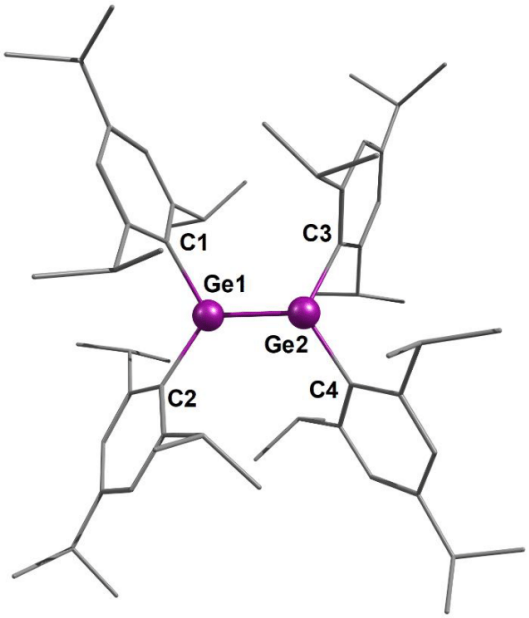

Ge1-Ge2	2.2986
C1-Ge1-C2	115.683
C3-Ge2-C4	115.871
°Σ (Ge1)	350.603
°Σ (Ge2)	350.466

Figure 71.
Optimized structure of digermene **2** and selected bond lengths [Å] and -angles [°] (E_{M062X} = −6495.67416568 Hartree).

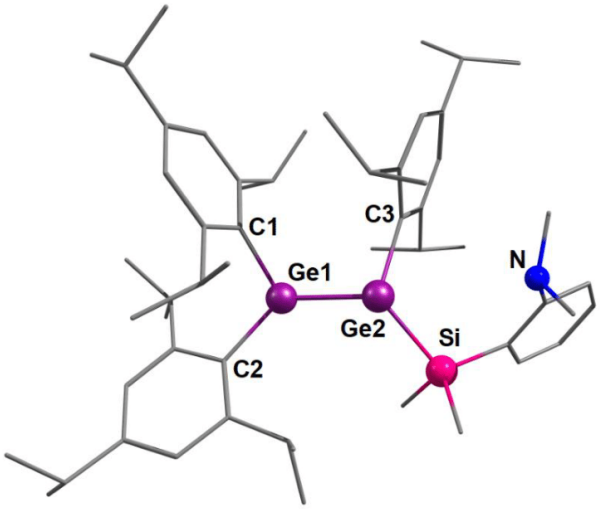

Ge1-Ge2	2.3512
Ge2-Si	2.4290
C1-Ge1-C2	104.449
C3-Ge2-Si	116.164
°Σ (Ge1)	343.228
°Σ (Ge2)	342.284

Figure 72.
Optimized structure of digermene **4a** and selected bond lengths [Å] and -angles [°] (E_{M062X} = −6645.19417181 Hartree).

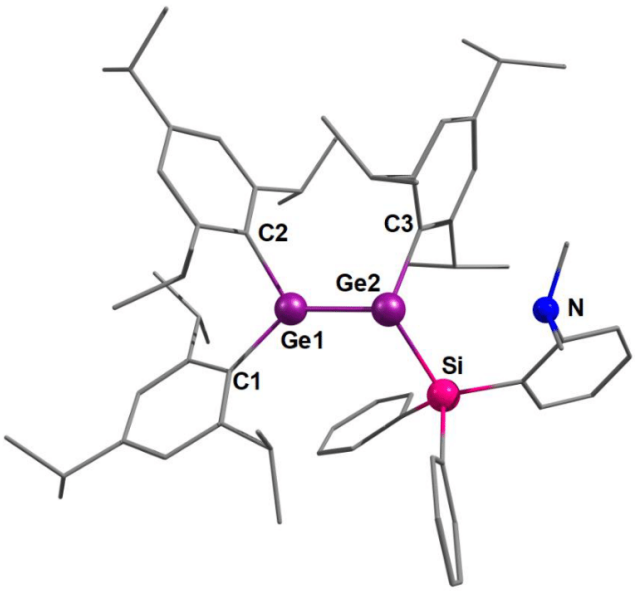

Ge1-Ge2	2.3451
Ge2-Si	2.4250
C1-Ge1-C2	104.929
C3-Ge2-Si	118.717
°Σ (Ge1)	348.729
°Σ (Ge2)	338.343

Figure 73.
Optimized structure of digermene **4b** and selected bond lengths [Å] and -angles [°(E_{M062X} = −7028.65515836 Hartree).

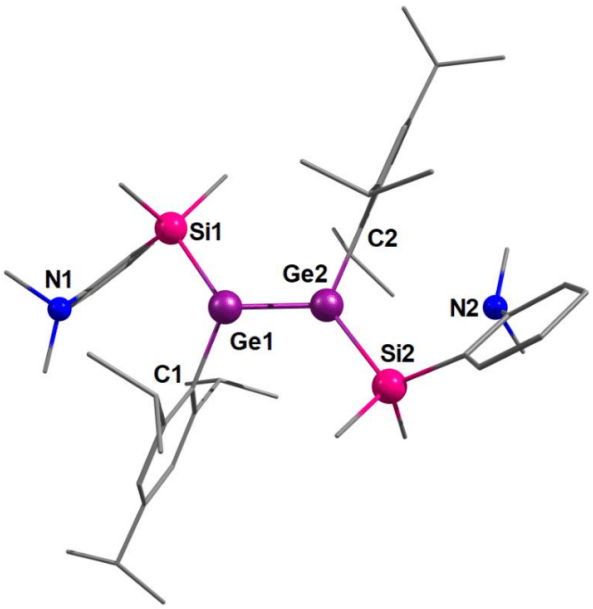

Ge1-Ge2	2.2982
Ge1-Si1	2.4011
Ge2-Si2	2.4002
C1-Ge1-Si1	117.867
C2-Ge2-Si2	119.826
°Σ (Ge1)	348.420
°Σ (Ge2)	353.257

Figure 74.
Optimized structure of digermene ***E*-5a** and selected bond lengths [Å] and -angles [°] (E_{M062X} = −6794.71695624 Hartree).

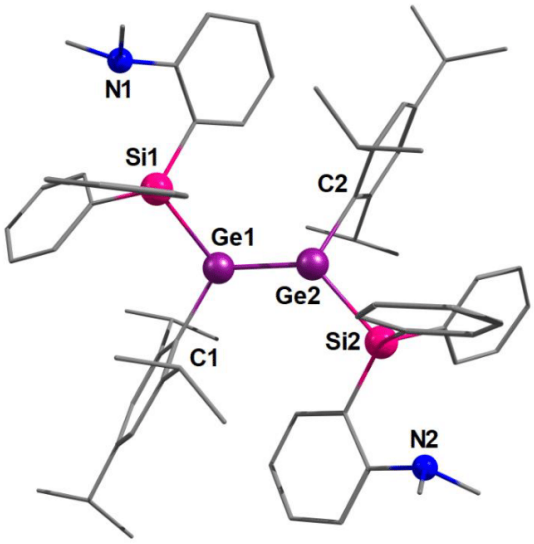

Ge1-Ge2	2.3005
Ge1-Si1	2.3996
Ge2-Si2	2.3998
C1-Ge1-Si1	110.679
C2-Ge2-Si2	108.375
°Σ (Ge1)	346.254
°Σ (Ge2)	355.753

Figure 75.
Optimized structure of digermene ***E*-5b** and selected bond lengths [Å] and -angles [°] (E_{M062X} = −7561.63164096 Hartree).

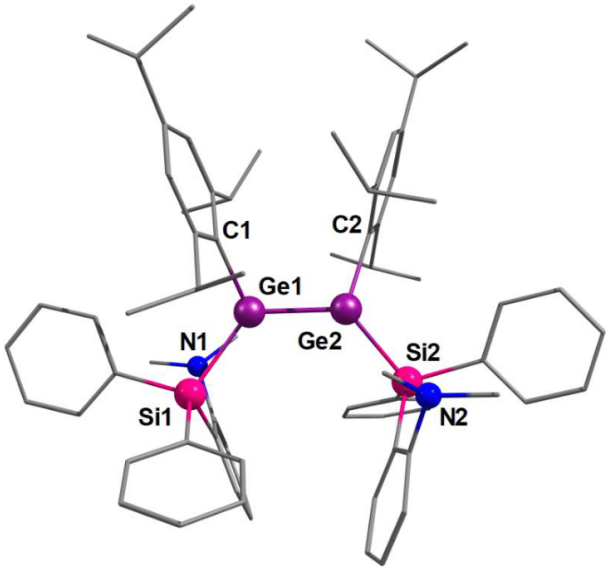

Ge1-Ge2	2.3007
Ge1-Si1	2.4038
Ge2-Si2	2.4059
C1-Ge1-Si1	115.529
C2-Ge2-Si2	115.494
°Σ (Ge1)	350.731
°Σ (Ge2)	350.669

Figure 76.
Optimized structure of digermene ***E*-5b** and selected bond lengths [Å] and -angles [°] (E_{M062X} = −7561.63164096 Hartree).

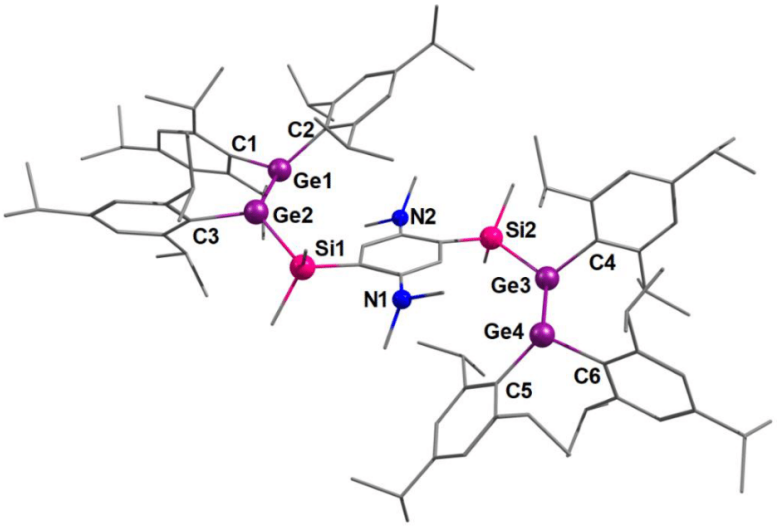

Ge1-Ge2	2.3232
Ge3-Ge4	2.3249
Ge2-Si1	2.4322
Ge3-Si2	2.4220
C1-Ge1-C2	118.230
C3-Ge2-Si1	116.389
C4-Ge3-Si2	110.760
C5-Ge4-C6	108.329
°Σ (Ge1)	348.969
°Σ (Ge2)	356.873
°Σ (Ge3)	345.934
°Σ (Ge4)	343.991

Figure 77.
Optimized structure of digermene **11** and selected bond lengths [Å] and -angles [°].

NBO analysis:

Table 9.
Natural charges and atomic Ge-Ge double bond contributions in **2**, **4a,b**, ***E*-5a,b** and **11** according to NBO analysis.

	Natural charge Ge1 (G4)	Natural charge Ge2 (Ge3)	Ge1 & Ge2 contribution Ge-Ge σ-bond	Ge1 & Ge2 contribution Ge-Ge π-bond
2	0.819	0.823	0.501 & 0.499	0.498 & 0.502
4a	0.880	0.318	0.532 & 0468	0.439 & 0.561
4b	0.971	0.256	0.523 & 0.577	0.399 & 0.601
***E*-5a**	0.293	0.376	0.498 & 0.502	0.526 & 0.474
***E*-5b**	0.287	0.403	0.495 & 0.505	0.537 & 0.463
***Z*-5b**	0.369	0.376	0.500 & 0.500	0.502 & 0.498
11	0.777 (0.855)	0.356 (0.333)	0.497 & 0.503 (0.499 & 0.501)	0.521 & 0.479 (0.517 & 0.483)

Table 10.
Donor-Acceptor strengths in germylenes **6a,b** according to Second-Order Perturbation Theory Analysis.

	Donor	Acceptor	ΔE [kcal mol^{-1}]
6a	N-lone-pair	Ge-p*	45.6
6b	N-lone-pair	Ge-p*	41.7

Thermodynamic Data

Table 11.
Calculated free enthalpies between involved species during metathesis.

	R = Me	R = Ph
ΔG_{Diss}	+ 62.9	+59.1
ΔG_{Stab}	−17.0	−15.7
ΔG_{Dim1}	−28.6	−28.6
ΔG_{Dim2}	−41.2	−36.1
ΔG_{Dim3}	−24.3	−20.3
$\Delta G_{cis\text{-}trans}$	--	−2.3
ΔG_{Met}	−6.9	−5.2

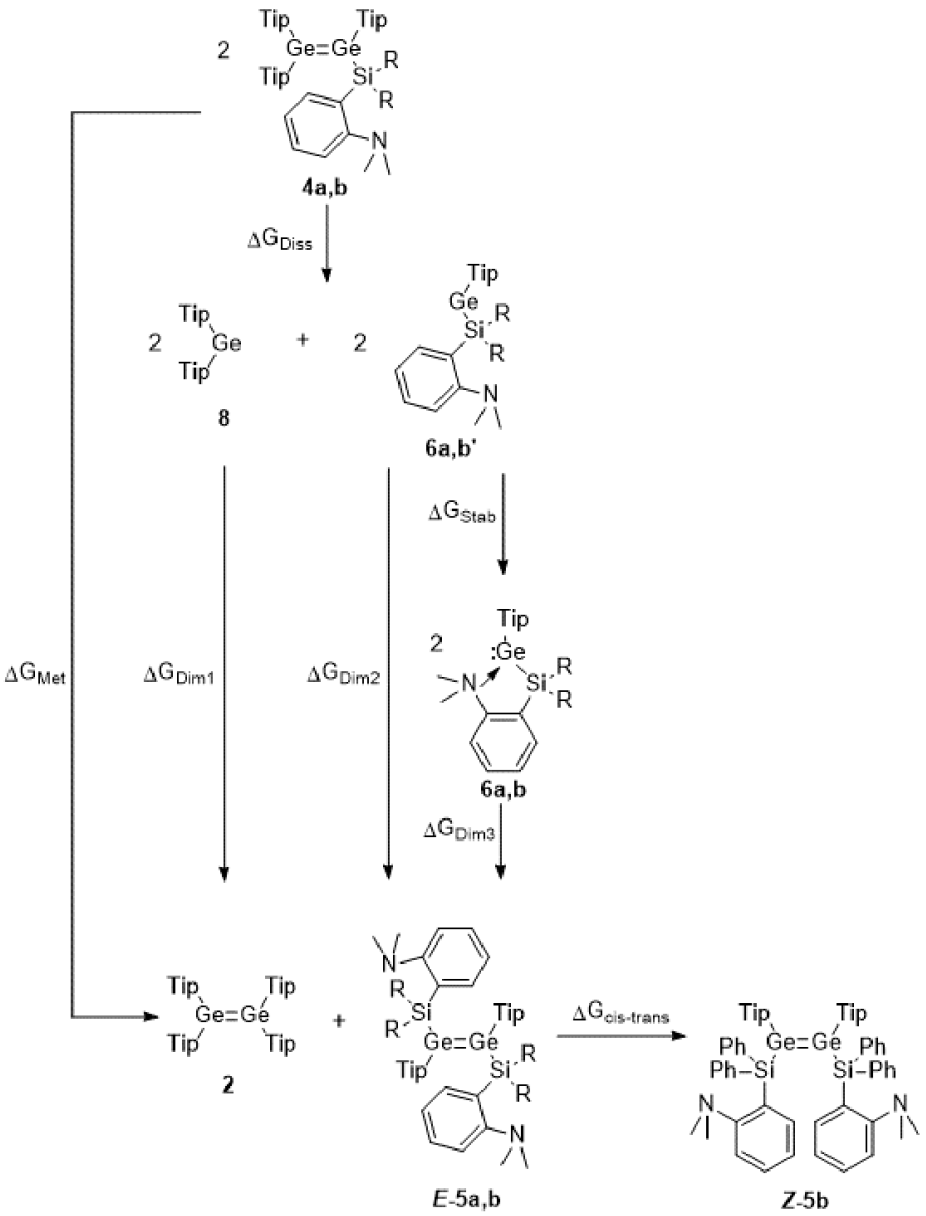

Figure S78

Calculated free reaction enthalpies (in kcal mol^{-1}) for the metathesis of **4a,b** to **2** and ***E*-5a,b** at 298 K at the (M06-2X/def2-TZVPP//BP86(D3)/def2-SVP) level of theory.

.

References

1. Scheschkewitz, D. A silicon analogue of vinyllithium: structural characterization of a disilenide. *Angew. Chem. Int. Ed.* **43**, 2965−2967 (2004).

2. Chernichenko, K. et al. Replacing C_6F_5 groups with Cl and H atoms in frustrated Lewis pairs: H_2 additions and catalytic hydrogenations. *Dalton Trans.* **46**, 2263−2269 (2017).

3. Doornbos, T. & Strating, J. The complete N-alkylation of 1,4-diamino-2,5-dibromobenzene and of 1,4-diamino-2,5-dimethoxybenzene. *Org. Prep. Proc.* **4**, 287−303 (1969).

4. Carothers, W. H. Polymers and Polyfunctionality. *Trans. Faraday Soc.* **32**, 39−49 (1936).

5. Becke, A. D. Density-functional exchange-energy approximation with correct asymptotic-behavior. *Phys. Rev. A* **38**, 3098−3100 (1988).

6. Perdew, J. P. Density-functional approximation for the correlation energy of the inhomogeneous electron gas. *Phys. Rev. B* **33**, 8822−8824 (1986).

7. Schaefer, A., Horn, H. & Ahlrichs, R. Fully optimized contracted Gaussian-basis sets for atoms Li to Kr. *J. Chem. Phys.* **97**, 2571−2577 (1992).

8. Weigend, F. & Ahlrichs, R. Balanced basis sets of split valence, triple zeta valence and quadruple zeta valence quality for H to Rn: Design and assessment of accuracy. *Phys. Chem. Chem. Phys.* **7**, 3297−3305 (2005).

9. Weigend, F. Accurate Coulomb-fitting basis sets for H to Rn. *Phys. Chem. Chem. Phys.* **8**, 1057−1065 (2006).

10. Grimme, S., Antony, J., Ehrlich, S. & Krieg, H. A consistent and accurate ab initio parameterization of density functional dispersion correction (DFT-D) for the 94 elements H-Pu. *J. Chem. Phys*. **132**, 154104 (2010).

11. Gaussian 16, Revision D.01, Frisch, M. J.; Trucks, G. W.; Schlegel, H. B.; Scuseria, G. E.; Robb, M. A.; Cheeseman, J. R.; Scalmani, G.; Barone, V.; Petersson, G. A.; Nakatsuji, H.; Li, X.; Caricato, M.; Marenich, A. V.; Bloino, J.; Janesko, B. G.; Gomperts, R.; Mennucci, B.; Hratchian, H. P.; Ortiz, J. V.; Izmaylov, A. F.; Sonnenberg, J. L.; Williams-Young, D.; Ding, F.; Lipparini, F.; Egidi, F.; Goings, J.; Peng, B.; Petrone, A.; Henderson, T.; Ranasinghe, D.; Zakrzewski, V. G.; Gao, J.; Rega, N.; Zheng, G.; Liang, W.; Hada, M.; Ehara, M.; Toyota, K.; Fukuda, R.; Hasegawa, J.; Ishida, M.; Nakajima, T.; Honda, Y.; Kitao, O.; Nakai, H.; Vreven, T.; Throssell, K.; Montgomery, J. A., Jr.; Peralta, J. E.; Ogliaro, F.; Bearpark, M. J.; Heyd, J. J.; Brothers, E. N.; Kudin, K. N.; Staroverov, V. N.; Keith, T. A.; Kobayashi, R.; Normand, J.; Raghavachari, K.; Rendell, A. P.; Burant, J. C.; Iyengar, S. S.; Tomasi, J.; Cossi, M.; Millam, J. M.; Klene, M.; Adamo, C.; Cammi, R.; Ochterski, J. W.; Martin, R. L.; Morokuma, K.; Farkas, O.; Foresman, J. B.; Fox, D. J. Gaussian, Inc., Wallingford CT, 2016.

12. Chemcraft - graphical software for visualization of quantum chemistry computations. https://www.chemcraftprog.com

13. Zhao, Y. & Truhlar, D. G. The M06 suite of density functionals for main group thermochemistry, thermochemical kinetics, noncovalent interactions, excited states, and transition elements: two new functionals and systematic testing of four M06-class functionals and 12 other functionals. *Theor. Chem. Acc.* **120**, 215−241 (2008).

14. NBO Version 3.1, Glendening, E. D., Reed, A. E., Carpenter, J. E. & Weinhold, F.

Curriculum Vitae

Personal Data

Date of Birth:	May 21st 1993
Birthplace:	Saarbrücken
Nationality:	German
E-Mail:	lukasklemmer@yahoo.de

Academic Education

01/2017-03/2021 **PhD**, Krupp-Chair for General and Inorganic Chemistry, Prof. Dr. David Scheschkewitz, Saarland University, Saarbrücken, Germany.

04/2015-09/2016 **Master of Science in Chemistry** (Final grade: 1.2), Saarland University, Saarbrücken, Germany.

Master thesis: “Reactivity of a Digermenide towards Heavy Group 14 Chlorides” (Grade: 1.0).

09/2014-12/2014 **Language Stay**, Aoyama Gakuin University, Tokyo, Japan.

09/2011-08/2014 **Bachelor of Science in Chemistry** (Final grade: 2.1), Saarland University, Saarbrücken, Germany.

Bachelor thesis: “Vergleichende Untersuchung mikroskaliger Ultraschallkontrastmittel“ (Grade: 2.0).

School Education

08/2003-07/2011 **Abitur**, Marienschule, Saarbrücken, Germany (Final grade: 1.7).

Occupation

01/2017-12/2020 **Scientific Assistant**, Krupp-Chair for General and Inorganic Chemistry, Saarland University, Saarbrücken, Germany.

01/2015-09/2016 **Student Associate**, Krupp-Chair for General and Inorganic Chemistry, Saarland University, Saarbrücken, Germany.

05/2013-09/2014 **Student Associate**, In-vitro-culture Technology, Fraunhofer Institute for Biomedical Technology, St. Ingbert, Germany.

Awards

09/2019 *Chemical Science* award for best oral presentation “Metathesis of Digermenes” at ICCOC-GTL-16 conference in Saitama, Japan.

05/2017 GDCh-award for “Outstanding achievements in the Master‘s program of chemistry of the Saarland university.

Publications

- N. M. Obeid, L. Klemmer, D. Maus, M. Zimmer, J. Jeck, I. Bejan, A. J. P. White, V. Huch, G. Jung, D. Scheschkewitz, (Oligo)aromatic species with one or two conjugated Si=Si bonds: near-IR emission of anthracenyl-bridged tetrasiladiene. *Dalton Trans*. **2017**, *46*, 8839−8848.
- D. Nieder, L. Klemmer, Y. Kaiser, V. Huch, D. Scheschkewitz, Isolation and reactivity of a digerma analogue of vinyllithiums: a lithium digermenide. *Organometallics* **2018**, *37*, 632−635.
- D. Mandal, D. Dhara, A. Maiti, L. Klemmer, V. Huch, M. Zimmer, H. S. Rzepa, D. Scheschkewitz, A. Jana, Mono- and dicoordinate Germanium(0) as a Four-Electron Donor. *Chem. Eur. J.* **2018**, *24*, 2873−2878.
- H. Zhao, K. Leszczyńska, L. Klemmer, V. Huch, M. Zimmer, D. Scheschkewitz, Disilenyl silylene reactivity of a cyclotrisilene. *Angew. Chem. Int. Ed.* **2018**, *57*, 2445−2449; *Angew. Chem.* **2018**, *130*, 2470−2474.
- H. Zhao, L. Klemmer, M. J. Cowley, M. Majumdar, V. Huch, M. Zimmer, D, Scheschkewitz, phenylene-bridged cross-conjugated 1,2,3-trisilacyclopenta-dienes. *Chem. Commun*. **2018**, *54*, 8399−8402.
- H. Zhao, L. Klemmer, M. J. Cowley, V. Huch, M. Zimmer, D, Scheschkewitz, Reactivity of a peraryl cyclotrisilene (c-Si_3R_4) toward chalcogens. *Z. Anorg. Allg. Chem.* **2018**, *644*, 999−1005.
- A.-C. Andres, J. Beckmann, L. Klemmer, S. Muth, D. Scheschkewitz, M. Springborg, Structure and stability of propellane-like $E_2E'_2E''_2H_6$. *J. Mol. Model*. **2018**, *24*:190.
- A. Maiti, D. Mandal, I. Omlor, D. Dhara, L. Klemmer, V. Huch, M. Zimmer, D. Scheschkewitz, A. Jana, Equilibrium coordination of NHCs to Si(IV) species

and donor exchange in donor-acceptor stabilized Si(II) and Ge(II) compounds. *Inorg. Chem.* **2019**, *58*, 4071−4075.

- Y. Heider, P. Willmes, D. Mühlhausen, L. Klemmer, M. Zimmer, V. Huch, D. Scheschkewitz, A three-membered cyclic phosphasilene. *Angew. Chem. Int. Ed.* **2019**, *58*, 1939−1944; *Angew. Chem.* **2019**, *131*, 1958−1964.
- L. Klemmer, Y. Kaiser, V. Huch, M. Zimmer, D. Scheschkewitz, Persistent digermenes with acyl and α-chlorosilyl functionalities. *Chem. Eur. J.* **2019**, *25*, 12187−12195.
- L. Klemmer, V. Huch, A. Jana, D. Scheschkewitz, An anionic heterosiliconoid with two germanium vertices. *Chem. Commun*. **2019**, *55*, 10100−10103.
- L. Klemmer, A.-L. Thömmes, M. Zimmer, V. Huch, B. Morgenstern, D. Scheschkewitz, Metathesis of Ge=Ge double bonds. *Nat. Chem.* **2021**, https://doi.org/10.1038/s41557-021-00639-9.

Language

German (native speaker)

English (busines fluent)

French (Basic skills)

Japanese (Basic skills)